NOTICE

The quality of this microform is heavily dependent upon the quality of the original thesis submitted for microfilming. Every effort has been made to ensure the highest quality of reproduction possible.

If pages are missing, contact the university which granted the degree.

Some pages may have indistinct print especially if the original pages were typed with a poor typewriter ribbon or if the university sent us an inferior photocopy.

Reproduction in full or in part of this microform is governed by the Canadian Copyright Act, R.S.C. 1970, c. C-30, and subsequent amendments.

AVIS

La qualité de cette microforme dépend grandement de la qualité de la thèse soumise au microfilmage. Nous avons tout fait pour assurer une qualité supérieure de reproduction.

S'il manque des pages, veuillez communiquer avec l'université qui a conféré le grade.

La qualité d'impression de certaines pages peut laisser à désirer, surtout si les pages originales ont été dactylographiées à l'aide d'un ruban usé ou si l'université nous a fait parvenir une photocopie de qualité inférieure.

La reproduction, même partielle, de cette microforme est soumise à la Loi canadienne sur le droit d'auteur, SRC 1970, c. C-30, et ses amendements subséquents.

THE UNIVERSITY OF ALBERTA

LATE CENOZOIC GEOLOGY OF THE NORTHERN ROCKY MOUNTAIN TRENCH, BRITISH COLUMBIA

by

PETER T. BOBROWSKY

A THESIS

SUBMITTED TO THE FACULTY OF GRADUATE STUDIES AND RESEARCH

IN PARTIAL FULFILMENT OF THE REQUIREMENTS FOR THE DEGREE

OF DOCTOR OF PHILOSOPHY

DEPARTMENT OF GEOLOGY

EDMONTON, ALBERTA

SPRING, 1989

ISBN 0-315-52922-9

THE UNIVERSITY OF ALBERTA

RELEASE FORM

NAME OF AUTHOR: PETER THEODORE BOBROWSKY

TITLE OF THESIS: LATE CENOZOIC GEOLOGY OF THE NORTHERN ROCKY MOUNTAIN TRENCH, BRITISH COLUMBIA

DEGREE: DOCTOR OF PHILOSOPHY IN GEOLOGY

YEAR THIS DEGREE WAS GRANTED: SPRING 1989

Permission is hereby granted to THE UNIVERSITY OF ALBERTA LIBRARY to reproduce single copies of this thesis and to lend or sell such copies for private, scholarly or scientific research purposes only.

The author reserves other publication rights, and neither the thesis nor extensive extracts from it may be printed or otherwise reproduced without the author's written permission.

(SIGNED) P.T. Bobrowsky

PERMANENT ADDRESS:

#407 - 2341

HARBOUR ROAD, N. SAANICH

B.C. V8L 3K8

DATE: 12 Dec 1988

THE UNIVERSITY OF ALBERTA

FACULTY OF GRADUATE STUDIES AND RESEARCH

The undersigned certify that they have read, and recommend to the Faculty of Graduate Studies and Research for acceptance, a thesis entitled LATE CENOZOIC SEDIMENTOLOGY AND STRATIGRAPHY OF THE NORTHERN ROCKY MOUNTAIN TRENCH, BRITISH COLUMBIA submitted by PETER T. BOBROWSKY in partial fulfilment of the requirements for the degree of DOCTOR OF PHILOSOPHY in GEOLOGY

Dr. N.W. Rutter (Supervisor)

Dr. F. Bachhuber (External Examiner)

Dr. S.G. Pemberton

Dr. T. Moslow

Dr. B.E. Nesbitt

Dr. I. Campbell

Date: Nov 12, 1988

ABSTRACT

Detailed sedimentological analysis of unconsolidated sediments along the Finlay River in the northern Rocky Mountain Trench was undertaken as part of a stratigraphic study of the Quaternary of northeastern British Columbia. Fifteen sediment types were identified and classified within four broad textural groups: diamicton, gravel, sand, and fines. The diamicton group consists of: 1) structureless diamicton; 2) diamicton with clastic intrabeds; and, 3) stratified diamicton. Gravels are represented by the following sediment types: 1) massive gravels; 2) normal/inverse graded gravels; 3) stratified gravels; 4) disrupted gravels; and, 5) inclined gravels. The sand group consists of: 1) structureless and graded sands; 2) horizontally laminated sands; 3) trough-cross stratified sands; 4) planar cross-stratified sands; and, 5) ripple laminated sands. Fines are represented by two sediment types, silt and clay.

Paleomagnetic samples (discontinuous suite) were removed from several bluff exposures. Analysis of these samples indicates normal polarity was in existence during their deposition (late Pleistocene). Fossils retrieved from the study area include one trace fossil (annelid burrow), several freshwater snail shells, and numerous wood fragments (Picea sp.). C14 dating of the wood specimens provided a number of dates ranging from circa 15,000 to 40,000 years B.P. The C14 dates correlate well with the amino-acid racemization values obtained from the same samples.

The results of this study indicate that the northern Rocky Mountain Trench was glaciated twice during the Quaternary. The penultimate glaciation was probably pan-provincial, owes its source area to the coastal mountains of B.C., and extended eastward across the Rocky Mountains into the foothills region. The timing and duration of this glaciation could not be established, but definitely occurred before 44,000 years B.P. A nonglacial interval starting before 44,000 years B.P. and ending approximately 15,000 years B.P. followed the penultimate glaciation. Pollen data from this interval indicate a northern boreal environment typified the area (dominated by black and white spruce). The second and final glaciation began approximately 15,000 years ago, ended before 10,000 years B.P. and corresponds to the Late Wisconsinan. This glaciation was localized in extent and probably consisted of a confined valley glacier, whose furthest eastward progression is marked by the Portage Mountain moraine. This study concludes that an extensive ice-free-corridor was in existence throughout the Quaternary.

ACKNOWLEDGEMENTS

My appreciation and recognition for total support in this endeavor go firstly to my parents John and Tekla Bobrowsky. Financial support during tenure of this study was provided by NSERC (Postgraduate Scholarships to me and research grants to N.W. Rutter), the Alberta Heritage Trust Fund (Ralf Steinhauer Award of Distinction), the Geological Society of America (student research award), the Boreal Institute for Northern Studies (research grants to me and L. Leslie), and several indirect consulting projects. Logistical support was graciously given by Dennis Macks and colleagues in Mackenzie (air, food and other support), as well as Dome Petroleum and their affiliated corporations (access to Finbow Camp).

Human resources which assisted in the completion of this study include: L. Leslie, Art, Al, J. Blaxley, B. Ward, and especially Jennifer Gibbs in the field; J. Albanese and Jerry (Tech Services) for prompt photographic reproduction; Ted Evans for paleomagnetic instruction (and patience); D. Arnold, R. Gardiner, G. Lyons, K. Mikels, I. Moffat, and Harvey for laboratory work, and N. Catto and J. Kulig for editorial elegance and speed. Thanks to Odie for field protection.

I am very grateful to my committee members: I. Campbell, T. Moslow, B. Nesbitt, and G. Pemberton for serving on this committee, offering their expertise, and thus contributing to the successful completion of this study. Bruce and George grudgingly provided access to their laser printers. Special thanks to my external examiner Fred Bachhuber for his time, effort, and academic contributions to this study.

Moral support was unselfishly and continuously provided by my sisters Jeannine and Mary and my nieces Natalya and Kate.

Final sincere thanks go to Nat Rutter for suggesting persual of this degree, the project area, and for providing both logistical and financial support. As supervisor and very good friend he made my tenure much more enjoyable and productive. Pax.

Table of Contents

List of Tables

List of Figures

List of Plates

I. Introduction

A. GENERAL STATEMENT

This study provides information concerning the Quaternary geologic history of the northern Rocky Mountain Trench of British Columbia. Emphasis is placed on the determination of the origins, timing, duration, and extent of several glacial advances. Ancillary results provide information on local and regional paleoenvironments and geochronology. The purpose of this chapter is to provide pertinent background information for the area. This chapter outlines the: 1) study objectives; 2) location; 3) climate; 4) soils; 5) flora; 6) fauna; 7) bedrock geology; 8) physiography; 9) history; 10) paleoenvironments; and, 11) previous geologic work and geologic history for the northern Rocky Mountain Trench and surrounding area. This final section includes comments on various models and theories of glaciation in British Columbia.

B. OBJECTIVES

The Finlay River region of the Rocky Mountain Trench represents a geographic and temporal gap in the understanding of the Quaternary history of northern British Columbia. Several large cutbank exposures occur along the river and contain a variety of Quaternary glacial and nonglacial deposits. Moreover, an airstrip recently constructed by Dome Petroleum has provided access to the area which was previously difficult to access without excessive logistical support. Quaternary geologic studies recently completed to the north, east, and south of the region suggest that the Finlay River area may have acted as a 'depot' for several ice sources; thus, the extent and direction of glacial ice advances in the region can only be resolved in the proposed study area.

The major purposes of this study are to: 1) interpret the Quaternary geologic history in the area between 56°55' N and 57°25' N, and 124°45' W and 125°39' W,

using stratigraphic and sedimentological data from cutbank exposures along the Finlay River; 2) determine the nature, extent and association of subsurface glacial, interglacial, and Holocene surficial deposits present in the area delimited by 56°0' N to 58°0' N and 124°0' W to 127°0' W; 3) collect and interpret information pertinent to the regional paleoenvironmental and geochronologic history; and, 4) redefine the Quaternary geologic history of the northern Cordillera of B.C..

C. LOCATION

The study area is located in the northern Rocky Mountain Trench and areas of northeastern British Columbia adjacent to the Trench (Figure 1). Regionally, this area encloses 6600 km^2 of land and covers all of the 1:250,000 Ware (94F) map sheet and the northern part of the 1:250,000 Mesilinka River (93C) map sheet. On a 'local' scale, this study was restricted to accessible river cut bluffs exposed along the central reach of the Finlay River, which flows southeast along the Rocky Mountain Trench. Usable sections were encountered from south of the native community of Fort Ware to the northern tip of the artificially dammed Williston Lake (Figure 1) in an area of approximately 240 km^2. The 'central' position of the study area is occupied by the Finbow airstrip which lies 256 km north-northwest of the town of Mackenzie, 300 km west-northwest of Fort St. John and 230 km southwest of Fort Nelson (Figure 1).

D. CLIMATE

The present climate of the north central Rocky Mountain Trench is continental with cool summers and long, cold winters. The Omineca Mountains to the west create a partial rain shadow effect along the edge of the wide valley. Weather conditions shift rapidly during the summer days with a mean daily temperature of 13.6° C in July (Environment Canada 1984). The study area is humid and frequently cloud covered throughout most of the year. Snow was observed at higher elevations near Finbow in

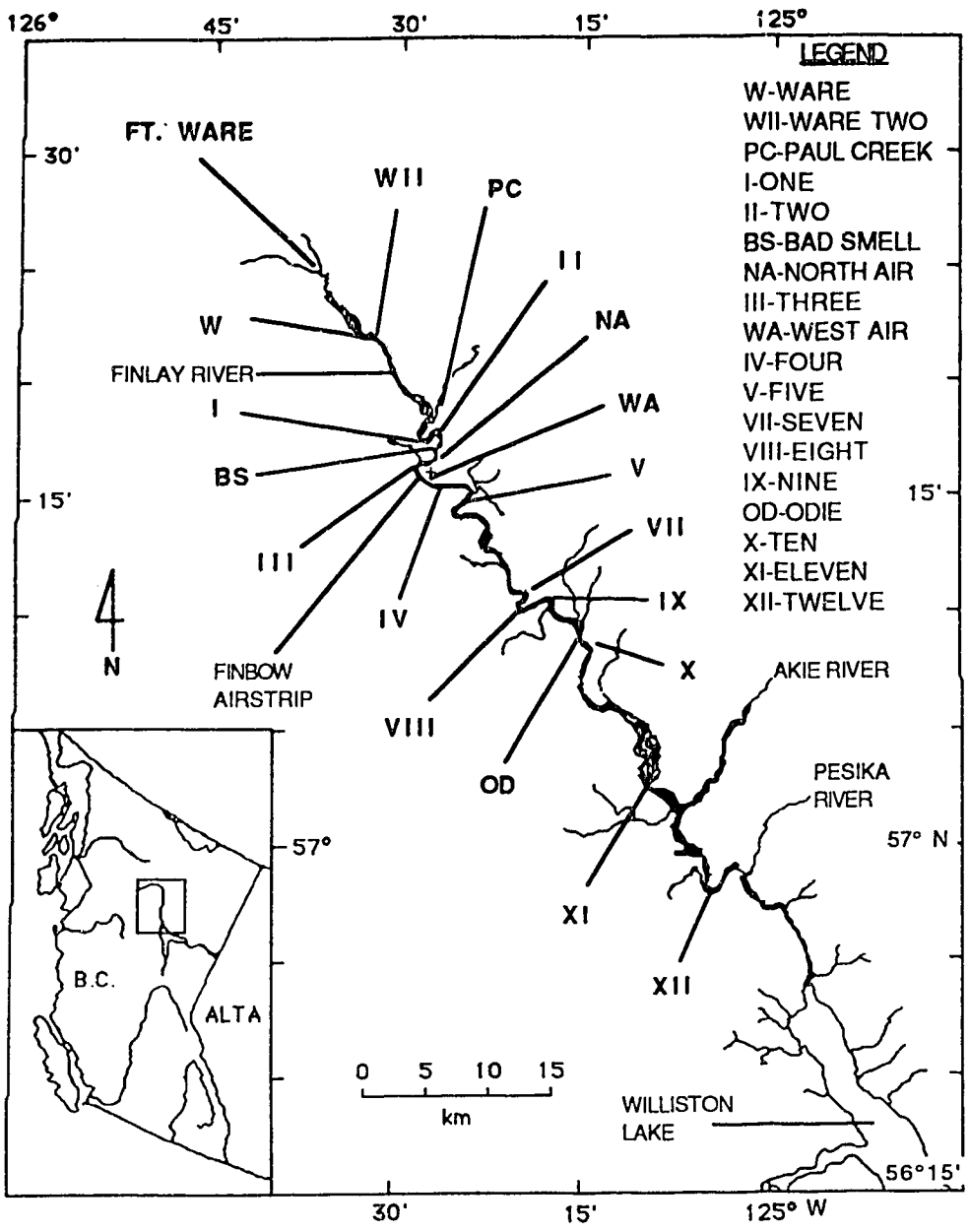

Figure 1. Map of study area illustrating location of primary sections along the Finlay River discussed in this study. Note alpha numeric codes for actual section names.

late August of 1984. Summary climatic data from Environment Canada (1984) for the community of Fort Ware at the northern end of the study area are given in Table 1.

E. SOILS

At lower elevations, the common soil type encountered is a Grey Luvisol, whereas at higher elevations Humo-Ferric Podzols are common (Young and Alley 1981). Brunisols, Podzols, and Gleysols are also found at low and intermediate elevations, with Regosols and Cryosols appearing at intermediate to higher elevations (Figure 2). The developed soils are commonly acidic on volcanic and plutonic bedrock and neutral to slightly acidic over limestones and other sedimentary rocks. Regionally, the soil temperature class is Cold Cryoboreal, with a mean annual soil temperature of 2°-8° C and 120-180 growing season days over 5°C (Lavkulich and Valentine 1981).

F. FLORA

According to Rowe (1977) the entire region lies at the northern end of the Interior Subalpine Forest area of British Columbia (see Plate 1). The high mountainous areas on either side of the Trench, above the tree line (approximately 1750 m), lie within the Tundra Forest Region. Vegetation in the Subalpine Region consists of white spruce (Picea glauca) and black spruce (Picea mariana), and rarely Engelmann spruce (Picea engelmannii) and tamarack (Larix laricina). At higher elevations alpine fir (Abies lasiocarpa) is common and to the west various cedars (Thuja sp.) and hemlocks (Tsuga sp.). Krajina (1965) includes Mertens cassiope (Cassiope mertensiana) and crowberry (Empetrum nigrum) in the alpine community.

Toward the southern part of the area, willow (Salix), lodgepole pine (Pinus contorta), paper birch (Betula papyrifera), and balsam poplar (Populus balsamifera) become much more common. At intermediate elevations, Krajina (1965) includes cranberry/blueberry (Vaccinium sp.) and bunchberry (Cornus canadensis). On

Table 1. Meteorological data for Ware, British Columbia. Compiled from Environment Canada (1984).

MEAN DAILY MAXIMUM JULY TEMPERATURE	21° C
MEAN DAILY MINIMUM JULY TEMPERATURE	6.2° C
MEAN DAILY JULY TEMPERATURE	13.6° C
MEAN DAILY MAXIMUM JANUARY TEMPERATURE	-15.2° C
MEAN DAILY MINIMUM JANUARY TEMPERATURE	-24.4° C
MEAN DAILY JANUARY TEMPERATURE	-19.9° C
EXTREME MAXIMUM TEMPERATURE	33.3° C (JUNE)
EXTREME MINIMUM TEMPERATURE	-48.3° C (JAN)
JULY DEGREE DAYS ABOVE 18° C	1.2
JULY DEGREE DAYS ABOVE 10° C	120
JULY DEGREE DAYS BELOW 18° C	132
TOTAL FROST FREE DAYS	45
LAST FROST (SPRING)	27 JUNE
FIRST FROST (FALL)	12 AUGUST
MEAN ANNUAL WIND SPEED FROM WEST	5.5 km/h
MEAN ANNUAL RAINFALL	301 mm
TOTAL NUMBER OF RAINFALL DAYS	60
GREATEST RAINFALL IN 24 HOURS	34 mm (JULY)
MEAN ANNUAL SNOWFALL	186 mm
TOTAL NUMBER OF SNOWFALL DAYS	47
GREATEST SNOWFALL IN 24 HOURS	21 mm (DEC)
MEAN ANNUAL PRECIPITATION	493 mm

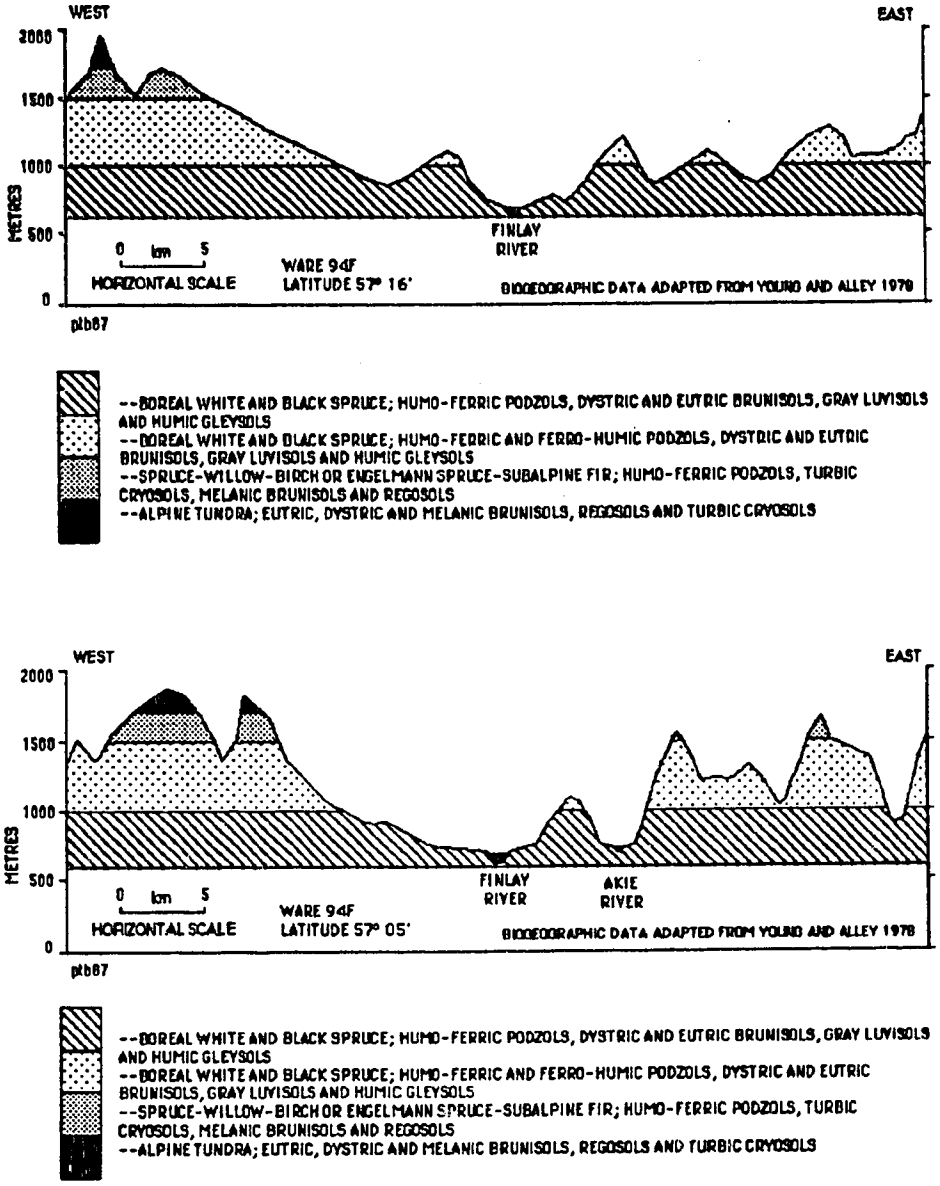

Figure 2. Physiographic cross sections across the Finlay River of northeastern British Columbia. Illustrates changes in soils, vegetation and relief. Both figures adapted from Young and Alley 1978.

Plate 1. General view of study area to north. Photo shows Finlay River, north end of Section II and spruce dominated vegetation.

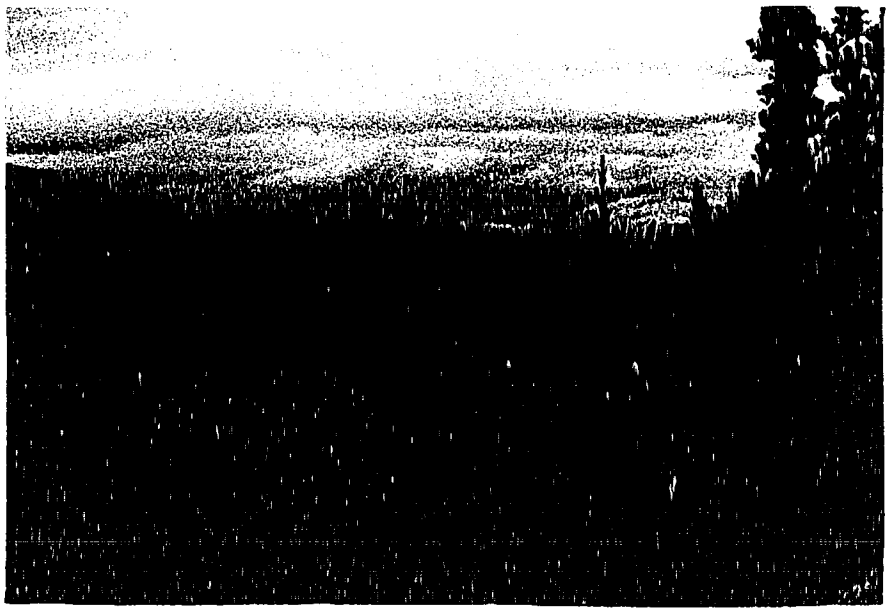

poorly drained soils, bog areas develop within which the major peat moss is Sphagnum fuscum. All of the above taxa are typical residents for an area marked by a northern continental climate where winters are both cold and long. Furthermore, forest fires in the summer months are extremely common, thus maintaining most of the vegetative communities at this early successional stage (Jones and Annas 1981).

G. FAUNA

Regionally, northeastern British Columbia supports a diverse group of animal species. A considerable variety of small mammals such as shrews and voles are known to inhabit the area. Notable larger mammals include bighorn sheep (Ovis canadensis), mountain goat (Oreamnos americanus), moose (Alces alces) and mule deer (Odocoileus hemionus). Smaller carnivores such as the wolf (Canis lupus) and coyote (Canis latrans) are rare, while larger omnivores such as the black bear (Ursus americanus) and grizzly bear (Ursus horribilis) are very common. Economically hunted species include short-tailed weasel (Mustela erminea), fisher (Martes pennanti) and marten (Martes americana). Other trapped fur-bearers include beaver (Castor canadensis), fox (Vulpes sp.), lynx (Felis lynx), wolverine (Gulo gulo), mink (Mustela vison) and muskrat (Ondatra zibethicus) (Irish 1969).

Larger avifauna which varies seasonally include ptarmigan (Lagopus sp.), spruce grouse (Canachites canadensis), ruffed grouse (Bonasa umbellus), Canada goose (Branta canadensis) and numerous ducks (Anatidae). Ichthyofauna includes northern pike (Esox lucius), Arctic grayling (Thymallus arcticus), Dolly Varden (Salvelinus malma), rainbow trout (Salmo gairdneri), and Rocky Mountain whitefish (Prosopium williamsoni).

H. BEDROCK GEOLOGY

The study area borders two distinct geologic belts; the Omineca Crystalline Belt to the west and the Rocky Mountain Belt to the east (Monger et al. 1972). Unfortunately, mapping of the bedrock geology in this area has been temporally sporadic during the last several decades, so that a detailed bedrock map has yet to be published. Dolmage's (1928) original map for the study area has been modified considerably, and the synthesis of Gabrielse et al. (n.d.) remains incomplete as an Open File Report. Further information can be found in Tipper et al. (1981) and Jackson (1976). Most of the bedrock in the region structurally parallels the north-northwest oriented Rocky Mountain Trench. In general, folded and faulted sedimentary rocks (Paleozoic and Mesozoic clastics) predominate east of the Finlay River in the Rocky Mountains and low grade metamorphics and igneous rocks west of the river in the Omineca Mountains (Rutter and Taylor 1968; Gabrielse 1971). A thick undifferentiated assemblage of Late Cretaceous and Tertiary sandstones, shales, conglomerates, coal, and acid tuff occur in the broad Rocky Mountain Trench (see Figure 3 and Table 2).

Proterozoic quartzites, basic lavas, shales, conglomerates, and carbonates occur in the far northern part of the study region with Proterozoic gneiss, quartzites, and schists bordering the Trench north of Ware (Evenchick 1984). Proterozoic clastics, basalts, and diamictites fringe the east side of the Finlay River and extend far to the west. Non-fossiliferous Cambrian and Devonian carbonates and shales are a minor component in the west, but dominate the eastern lithology of the Muskwa Ranges in the Rocky Mountains, with rare outcrops of Devonian and Mississippian clastics occurring in the north-central area (Gabrielse et al. 1977). Devonian to Triassic basalts, andesites, rhyolites, ultramafics, and cherts are patchily distributed along the west side of the map sheet west of the Finlay Range and Russel Range. This area also contains numerous small outcroppings of diorite, monzonite, syenite, basaltic volcanics, and gabbro (Triassic-Jurassic). Early Cretaceous granites, granodiorites, and quartz

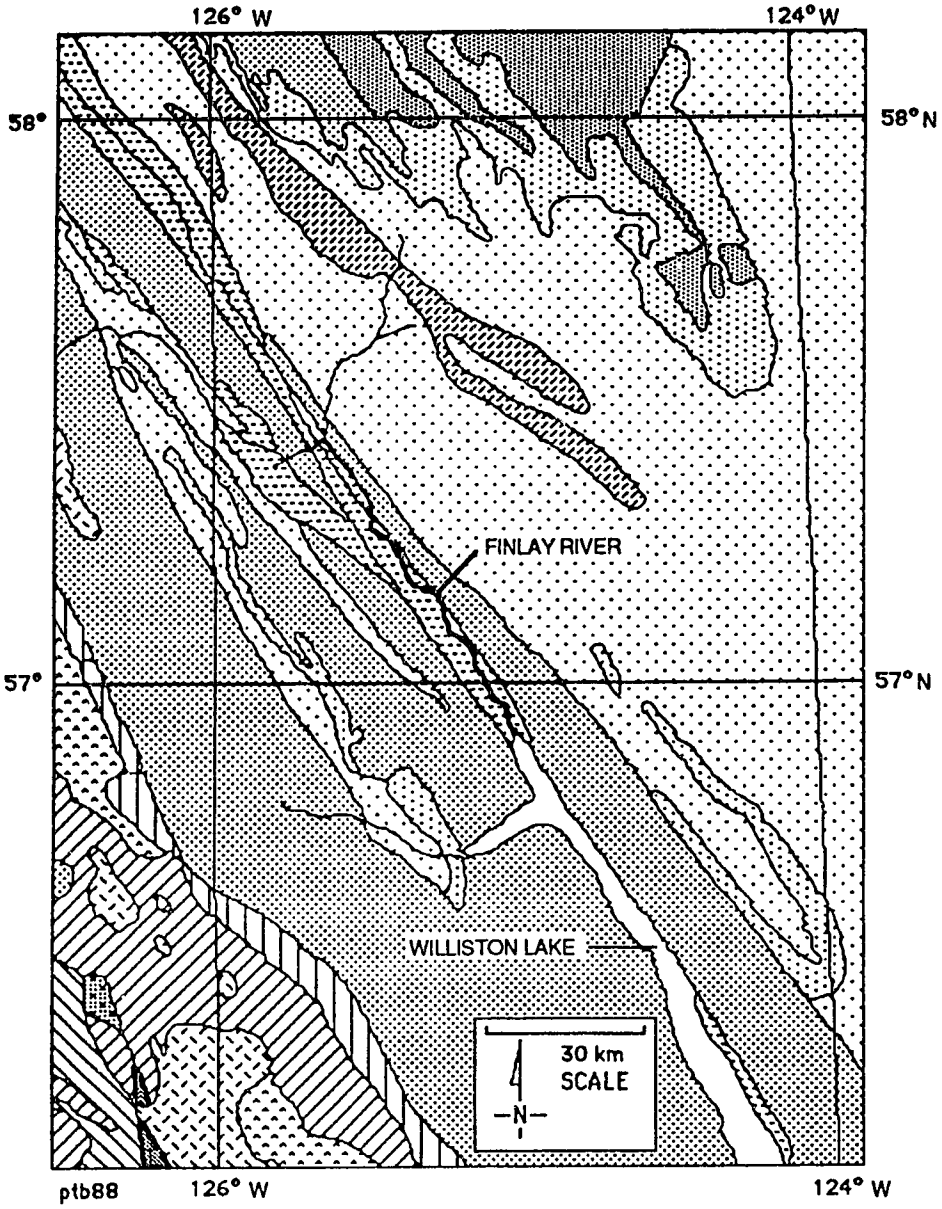

Figure 3. Generalized bedrock geology map of northeastern British Columbia adapted from Tipper et al. (1981). Legend appears on following page.

BEDROCK LEGEND (MODIFIED AFTER TIPPER ET AL. 1981)

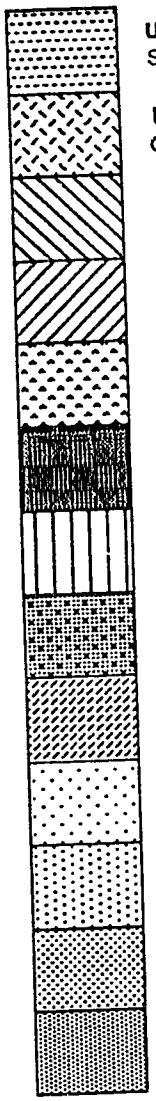

UPPER CRETACEOUS-OLIGOCENE
SANDSTONE, SHALE, CONGLOMERATE, COAL, ACID TUFF

LOWER CRETACEOUS
QUARTZ MONZONITE, GRANITE, GRANODIORITE

LOWER AND MIDDLE JURASSIC
INTERMEDIATE FLOWS, TUFFS, LOCAL BASALT, RHYOLITE, SANDSTONE, SHALE

UPPER TRIASSIC-LOWER JURASSIC
AUGITE PORPHYRY, BASALTIC VOLCANICS, SILTSTONE, SHALE,
LIMESTONE, CONGLOMERATE

UPPER TRIASSIC-LOWER JURASSIC
DIORITE, MONZONITE, SYENITE, QUARTZ DIORITE, MINOR PYROXENITE,
GRANODIORITE

MISSISSIPPIAN-TRIASSIC
CHERT, ARGILLITE, CARBONATE, BASALT, ASSOCIATED DIABASE,
GABBRO, ULTRAMAFICS

DEVONIAN-TRIASSIC
UPPER: BASALT, DIABASE, LOCAL GABBRO, ULTRAMAFICS
LOWER: CHERT, ARGILLITE, SANDSTONE, CONGLOMERATE, LIMESTONE

MISSISSIPPIAN-TRIASSIC
BASALT, ANDESITE, RHYOLITE, TUFF, CARBONATE,ARGILLITE, CHERT

DEVONIAN-MISSISSIPPIAN
SANDSTONE, SHALE, PEBBLE CONGLOMERATE

CAMBRIAN-DEVONIAN
CARBONATE, SHALE

PROTEROZOIC-CAMBRIAN
SANDSTONE, SILTSTONE, SHALE, PEBBLE CONGLOMERATE

PROTEROZOIC
SANDSTONE, SILTSTONE, SHALE, DIAMICTITE, LIMESTONE, BASALT
IRON FORMATION, PEBBLE CONGLOMERATE

PROTEROZOIC
QUARTZITE, SHALE, BASIC LAVAS, CARBONATE, CONGLOMERATE

Table 2. Groups, Formations and lithology of bedrock in northeastern B.C.

STRATIFIED ROCKS WEST OF THE NORTHERN ROCKY MOUNTAIN TRENCH

CRETACEOUS/ TERTIARY	SIFTON FM	CONGLOMERATE, SHALE, SILTSTONE COAL, DACITIC VOLCANICS
	BROTHERS PEAK FM	CONGLOMERATE, TUFF, SILTSTONE, SHALE, SANDSTONE
	TANGO CREEK FM	CONGLOMERATE, SHALE, SILTSTONE, SANDSTONE
MIDDLE/UPPER JURASSIC	BOWSER LAKE GRP	SHALE, SILTSTONE, PEBBLE CONGLOMERATE
	'TOODOGGONE'	DACITE, LATITE, RHYOLITE, TUFF, BRECCIA, FLOWS
LOWER JURASSIC	HAZELTON GRP	VOLCANIC CONGLOMERATE, BRECCICA, LAHAR, FELDSPAR PORPHYRY DYKES
TRIASSIC	TAKLA GRP	PLAGIOCLASE PORPHYRY, AUGITE PORPHYRY, TUFF
PERMIAN	ASITKA GRP	CHERT, ARGILLITE, LIMESTONE, PHYLLITE, TUFF, SCHIST
PENNSYLVANIAN/ PERMIAN	'LAY RANGE ASSEMBLAGE'	TUFF, LIMESTONE
CAMBRIAN/ ORDOVICIAN	KECHIKA GRP	LIMESTONE, PHYLLITE, SHALE
LOWER CAMBRIAN	ATAN GRP	LIMESTONE, SILTSTONE, DOLOMITE, QUARTZITE, SANDSTONE, CONGLOMERATE
PROTEROZOIC/ LOWER CAMBRIAN	UNDIVIDED	MICA SCHIST, PHYLLITE, QUARTZITE, LIMESTONE
UPPER PROTEROZOIC	STELKUZ FM	SILTSTONE, SHALE, SANDSTONE, LIMESTONE
	ESPEE FM	LIMESTONE, DOLOMITE
	TSAYDIZ FM	PHYLLITE
	SWANNELL FM	SANDSTONE, SILTSTONE, SHALE, CONGLOMERATE, LIMESTONE, KYANITE GRADE METAMORPHICS

STRATIFIED ROCKS EAST OF THE NORTHERN ROCKY MOUNTAIN TRENCH

CRETACEOUS/ TERTIARY	SIFTON FM	CONGLOMERATE, SANDSTONE, SHALE, COAL
UPPER TRIASSIC		SILTSTONE, LIMESTONE
DEVONIAN/ MISSISSIPPIAN		ARGILLITE, SLATE, SHALE, CONGLOMERATE, LIMESTONE
MIDDLE DEVONIAN	DUNEDIN FM	LIMESTONE
LOWER DEVONIAN		SANDSTONE, DOLOMITE, BRECCIA
ORDOVICIAN/SILURIAN DEVONIAN	ROAD RIVER FM	SHALE, SILTSTONE, SANDSTONE
CAMBRIAN/ORDOVICIAN	KECHIKA GRP	LIMESTONE, SHALE
MIDDLE CAMBRIAN		LIMESTONE
LOWER CAMBRIAN	ATAN GRP	LIMESTONE, SANDSTONE
PROTEROZOIC/ UPPER CAMBRIAN	MISINCHINKA GRP	SLATE, PHYLLITE, SCHIST, SILTSTONE, CONGLOMERATE, LIMESTONE, DIAMICTITE
	GATAGA FM	MUDSTONE, SILTSTONE, SANDSTONE

GRANITIC ROCKS

EOCENE	DACITE, GRANITE, QUARTZ MONZONITE, GNEISS, GRANODIORITE
CRETACEOUS	QUARTZ MONZONITE, GNEISS
MIDDLE JURASSIC	GRANODIORITE
LOWER JURASSIC	QUARTZ MONZONITE, GRANODIORITE, GNEISS

ULTRABASIC ROCKS

UPPER TRIASSIC	DUNITE, PERIDOTITE, GABBRO, CLINOPYROXENITE

monzonites intrude the older deposits west of the Finlay Ranges. The bedrock within the Trench itself ranges from Oligocene clastics in the south (Hopkins et al. 1972) to Pliocene conglomerates of the Sifton Formation in the north (Gabrielse et al. 1977).

On a provincial scale, the bedrock geology and mineral deposits west of the Rocky Mountains to the Pacific Ocean are discussed by Armstrong (1946). From Ware northwards, bedrock information is provided by Hedley and Holland (1941). South of the study area, a detailed bedrock map has recently been completed for the Parsnip map sheet (93) by Tipper et al. (1979). Eastwards into the Rocky Mountains, Irish (1969) synthesized the bedrock geology of the Halfway River map area (94/B) and Macqueen and Thompson (1978) discussed carbonate hosted lead-zinc deposits east of the Finlay River. Most recent discussion on economic geology centres on areas to the north and northeast of this study area (eg. Morrow et al. 1978; Goodwin and Sinclair 1982).

I. PHYSIOGRAPHY

The study area covers parts of the Interior System and Eastern System of the Canadian Cordilleran Subdivision (see Figure 4) (Bostock 1970). The most prominent feature here is the north-northwest trending Rocky Mountain Trench which marks the transition between the two larger systems. In northeastern B.C. the Rocky Mountains occupy the Eastern System, and the Cassiar Mountains and Omineca Mountains the northern end of the Interior System. From the Finlay area, the Trench extends south to northern Montana and north to the Yukon border for a combined length of approximately 1600 km and total area of 5000 km^2 (Slaymaker and McPherson 1977). Seismic studies have revealed that this broad structural lineament is steep sided, ranging from 1000-2000 m in depth and averaging 5-13 km in width (Leech 1966). Although the area between 56° and 58° N has not been properly mapped, Leech (1966) concluded that the entire Trench is presently not seismically active, nor is

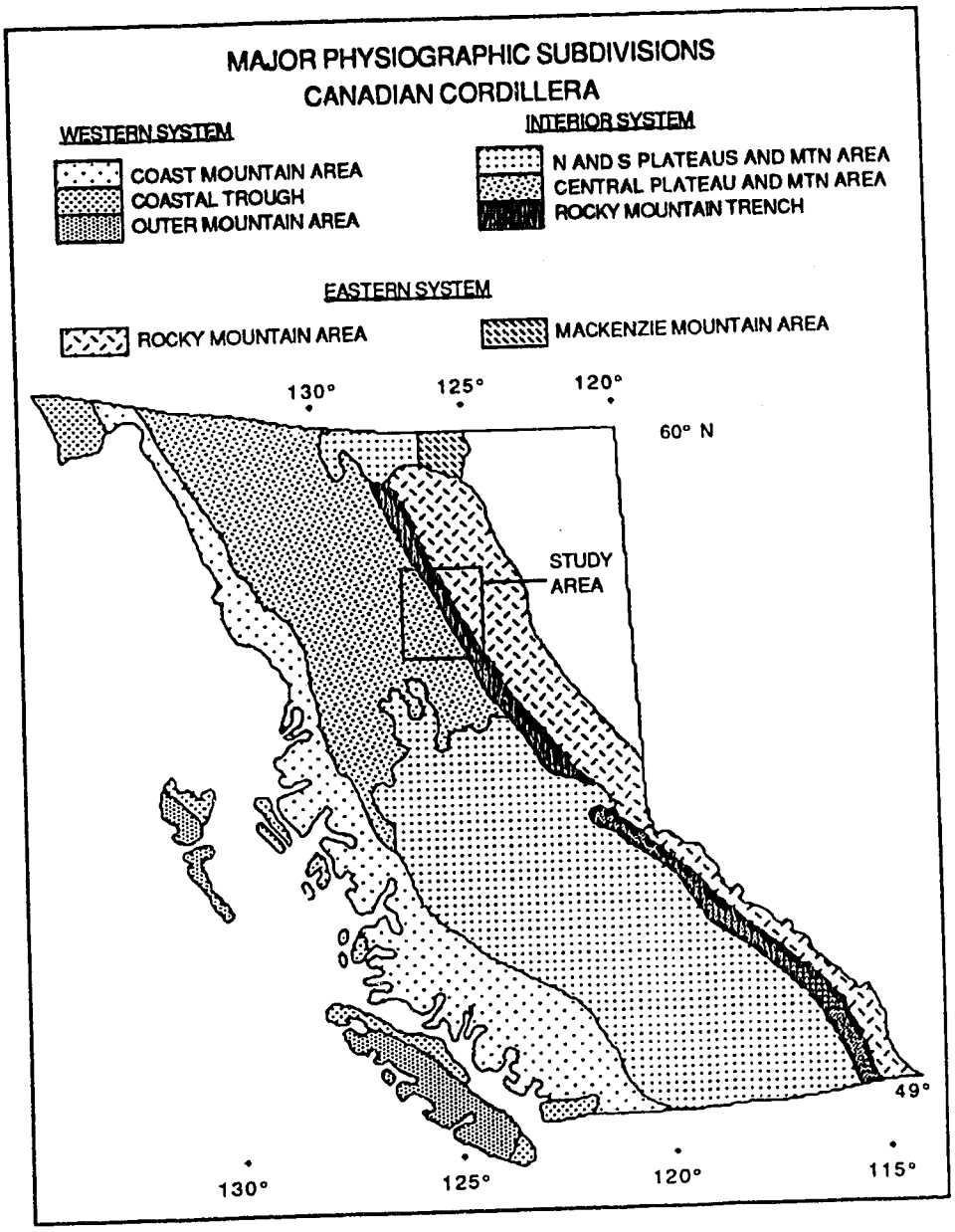

Figure 4. Physiographic subdivisions of the Canadian Cordillera and location of the study area (modified after Holland 1976).

there any indication of earlier volcanism or igneous intrusions. Initiated sometime in the early Tertiary (possibly Paleocene) from down-faulting, the Rocky Mountain Trench is filled with mid- to late-Tertiary bedrock and a thick accumulation of Quaternary deposits (see Plate 1) (Leech 1966).

Directly to the east, the Trench is bordered by the Muskwa Range of the Rocky Mountains ranging in width from 50 to 70 km and extending 260 km in length from the Peace River north to the Liard River. Near Sifton Pass the Muskwa Ranges contain the Tochieka Range and to the south the Truncate and Akie Ranges. The highest peak in the Muskwa Range is Mount Churchill (3200 m) in the far north, and the highest peak in the study area is Mount Lloyd George (2917 m).

The west side of the Trench is bordered by the Finlay Range of the Omineca Mountains, which locally encompass the Cormier Range and Russel Range. Peaks generally vary from 1800-2100 m; notable peaks include McGraw Peak (2219 m), Mount Balourdet (2209 m), Mount Russel (2174 m), and Barrier Peak (2103 m). The Finlay Range grade into the Sifton Range north of the Finlay River and parallel the larger, western Swannell Range.

A contour map of the study area (Figure 5) shows the higher elevations in the Finlay Range contrast with the lower elevations along the western margin of the Muskwa Range. High peaks in the latter occur some distance from the Trench. Both ranges are sharp and serrate at elevations over 1800 m, and evidence for cirque and alpine glaciation is common (Holland 1976). Although most peaks show evidence of glaciation during a maximum advance, surficial evidence for the latest event of glacial erosion and deposition is restricted to lower elevations (cf. Leslie 1988). The end result of the above physiographic configuration is a marked cross-valley asymmetry. Figure 2 (top and bottom) provides cross sectional views along latitudes 57°16' and 57°06' N. Biogeographic data has been imprinted over these sections. Both figures illustrate the smooth, but steep gradient of the slope towards the west from the Finlay

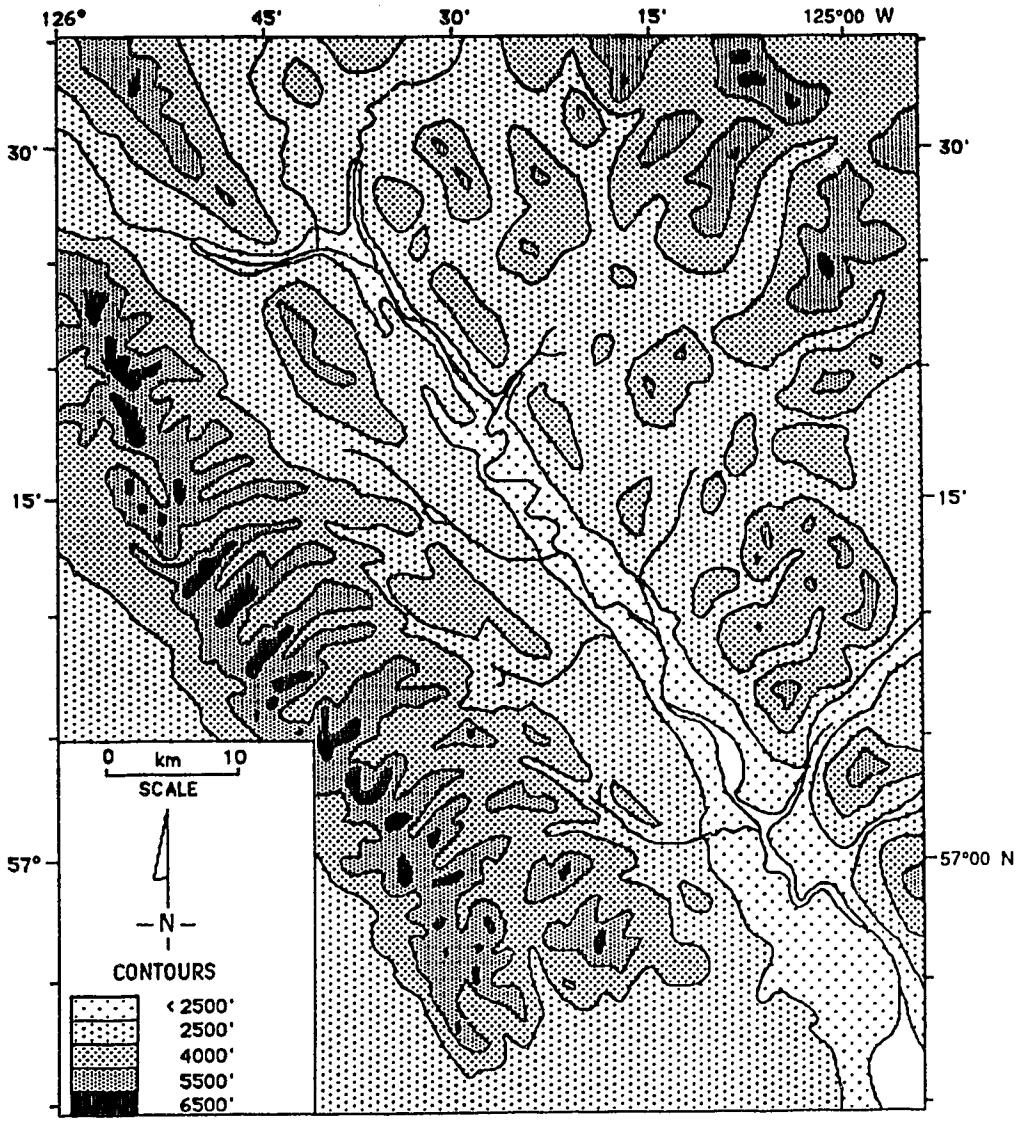

Figure 5. Contour map of study area, northern Rocky Mountain Trench, British Columbia. Elevations from NTS Ware 94F (1977).

River and the lower undulating relief towards the east. Moreover, each cross-section indicates the altitudinal zonation of soils and vegetation in the Trench. The lowest elevation in the study area lies at 665 m, marking the flood line of Williston Lake.

Several rivers, streams and lakes drain the study area into the Peace River system (Figure 1). The Finlay River represents the central drainage arm through the northern Trench with an average flow of 700 m^3/sec. This river originates at Thutade Lake in the Omineca Mountains, strikes east across the Finlay Ranges and then flows southeast down the Trench to Finlay Forks; draining 42,496 km^2 (Holland 1976). At this junction the river combines with the northwest-flowing Parsnip River, and turns due east across the Rocky Mountains down the preglacial Peace River Canyon (Beach and Spivak 1943, Dolmage and Campbell 1963). From Thutade Lake water flows a total of 3800 km to the mouth of the Mackenzie River in the Beaufort Sea (Rich 1955). Major rivers draining the Rocky Mountains include the Kwadacha, Akie, and Ospika Rivers. Minor streams on this side of the valley include Paul, Del, and Ospika Creeks. The Omineca Mountains are primarily drained by the Mesilinka, Ignenika and Omineca Rivers, as well as Stelkuz, McGraw, and Tsaydiz Creeks. From Sifton Pass (transition to the Liard River drainage) south, drainage occurs via the Fox River.

J. HISTORY

Evidence for prehistoric occupation in the northern Rocky Mountain Trench has yet to be discovered. Prehistoric evidence in the Peace River region between the W.A.C. Bennett Dam and the Alberta border has been intensively explored (Spurling 1980). According to Fladmark (1983), certain archaeologists continue to support the belief of an extensive 'ice-free-corridor' in that area; a critical point in arguments of human migration into North America during the Wisconsinan. This interest in the 'ice-free-corridor' has resulted in the successful discovery and partial excavation of the Charlie Lake Cave near Fort St. John. Archaeological excavations at this site nave uncovered

evidence for a long range of temprally sporadic human occupation beginning about 10,500 years B.P. based on an association of Clovis points with datable materials (Fladmark et al. 1988). The postglacial butchered faunal assemblage at the Charlie Lake Cave site indicates big game hunting activity in the wake of Laurentide ice retreat.

Documented historic occupation begins with the Fur Trade, when in 1793 Sir Alexander Mackenzie was the first white explorer to cross the 120th meridian into the Peace River Country of British Columbia (Bowes 1963). Shortly thereafter, John Finlay (Northwest Company) explored the Finlay and Parsnip Rivers in 1797. Subsequent noteworthy exploration of the Finlay River occurred in 1824 by Samuel Black, 1872 by Captain Butler, and in 1875 by Alfred R. C. Selwyn (Rich 1955; Selwyn 1877). Gold rush 'fever' occurred three times; once on the Parsnip River in 1861, on the Omineca River in 1870, and lastly on the Igenika River in 1908 (Bowes 1963). MacGregor suggested that in the 1870's some 2000 miners were gold panning between Fort St. John and Hudson Hope (cited in Irish 1969). Associated with the gold rush were a series of pack-trails which extended from just west of Fort St. John, up the Peace and Halfway Rivers, across a few low divides and up the Finlay River (Irish 1969).

In 1968 the British Columbia Hydro and Power Authority completed construction of the W.A.C. Bennett Dam near Hudson Hope. This large hydroelectric development project, and activity associated with construction of a second possible dam site near Fort St. John, has contributed significantly to the economic base of the Peace District. Construction of the W.A.C. Bennett dam resulted in the development of Williston Lake which flooded the Peace, Parsnip, and Finlay Rivers to an elevation of 665 m a.s.l. (Dolmage and Campbell 1963).

K. PALEOENVIRONMENTS

Paleoclimatic data for the region are lacking. Inferential paleoenvironmental conditions are, however, proposed based on the interpretation of fossil vertebrate and floral remains recovered within or adjacent to the study area. Fossil soils have yet to be identified in the study area, but weathering zones developed in Pleistocene sediments are known to occur in abundance in the northern Rocky Mountain Trench and elsewhere in the vicinity (Clague 1981). The most detailed analysis and description of paleosols from northeastern British Columbia was undertaken in conjunction with archaeological investigations of postglacial sediments in the Fort St. John area (Valentine et al. 1980). Unfortunately, this isolated study adds little to the problem of understanding paleosol distribution and genesis in the northern Rocky Mountain Trench.

Plant assemblages from fossil localities in the mountainous areas of British Columbia are generally rare. Hopkins et al. (1972) reported on a palynomorph and spore assemblage suggestive of subtropical conditions with wet summers and dry winters from an Oligocene outcrop on the Parsnip River of the northern Rocky Mountain Trench. A variety of plant remains including Sequoia are common in Tertiary deposits of the Sifton Formation of the northern Rocky Mountain Trench (Hedley and Holland 1941). More detailed palynological suites of Miocene and Pliocene age are known from near Quesnel, further to the south (Mathews and Rouse 1963; Rouse and Mathews 1979), as well as in the southern Rocky Mountain Trench (Clague 1974). All of these assemblages are dominated by coniferous palynomorphs (~ 90%) such as Picea and Pinus, but do include southern broadleaf elements such as Ulmus, in association with Metasequoia and Sequoia.

Quaternary deposits containing pollen are infrequently recorded in northeastern British Columbia. Rutter (1976) recovered pollen from a clay sample in highly oxidized sands and gravels along the Parsnip River. This nonglacial suite contained 64% Pinus, 21% Picea, 9% Abies, 3% Polypodiacea, 1% Alnus, 0.5% Betula, 0.5%

Lycopodium, 0.5% Cyperaceae and 0.5% Poaceae, and tends to reflect a cool boreal forest environment existing sometime during the late Quaternary. A Mid-Wisconsinan pollen sample dated between 34,000 ± 690 years B.P. (GSC-1754) and 43,800 ± 1830 years B.P. (GSC-1687) from silts at Babine Lake, B.C. is dominated by Betula (32.2%), Poaceae (16%), Artemisia (12%), Tubuliflorae (9.4%) and Salix (6.4%) with a host of other trees, shrubs, herbs and aquatics indicative of a cool shrub tundra environment (Harington et al. 1974). East of the study area, White and Mathewes (1982) recovered a short core from Fiddler's Pond covering the last 7250 years, west of Fort St. John near the Halfway River. An older and longer postglacial pollen suite from Spring Lake and Boone Lake east of Dawson Creek was described by White and Mathewes (1986). Beginning at 11,760 ± 260 years B.P. (SFU-223) a poplar-willow-sage-grass-sedge zone is replaced by a spruce and pine rise followed in turn by a spruce decline and birch rise at about 8,700 years B.P..

Faunal remains have yet to be discovered in the study area; supporting Harington's (1978) contention that mountainous environments are not conducive to fossil vertebrate preservation. A suite of fossil localities from surrounding areas do, however, provide insight into the animal communities which existed through much of the late Quaternary. The nearest fossil locality to the study area occurs at Finlay Forks, on the east side of the Parsnip River, where the skull of a mountain sheep (Ovis canadensis) was retrieved from ice contact gravels some three metres below ground surface (Rutter et al. 1972). This find is dated at 9,280 ± 200 years B.P. (GSC-1497).

Eastwards, a number of fossils occur in Tertiary, Mid-Wisconsinan and postglacial sediments of the Peace River district. Reimchen and Rutter (1972) reported a single Pliohippus sp. tooth (Tertiary?) from sands and gravels from the Dawson Creek map sheet. A mammoth tusk from the Portage Mountain moraine (I-2244A) and a mammoth tooth from gravels near Taylor, B.C. (GSC-2034) are known,

both representing the Mid-Wisconsinan (Mathews 1978, 1980). Churcher and Wilson (1979) summarized the postglacial vertebrate fauna found east of Fort St. John in Alberta, and included woolly mammoth (Mammuthus primigenius), squirrel (Citellus sp.), horse (Equus cf. E. nirobrarensis) and bison (Bison sp.) in the Mid-Wisconsinan assemblage and woolly mammoth (Mammuthus primigenius), Mexican half-ass (Equus cf. E. conversidens), horse (Equus sp. (E. nirobrarensis?)), camelid (Camelops sp. or Hemiauchenia sp.), wapiti (Cervus canadensis), musk-ox (Ovibos moschatus), and three types of bison (Bison b. athabascae, B. occidentalis, B. b. bison) in the postglacial record. According to these authors, the recovered fossils indicate a fauna adapted to an aspen-poplar parkland or plains environment, but not a closed boreal forest. More recently, a lengthy Holocene suite of vertebrate fossils dating back ca. 11,000 years B.P. have been excavated at Charlie Lake Cave near Fort St. John, B.C. (Fladmark et al. 1988).

South of the study area, a mountain goat (Oreamnos sp.) is recorded from Sangamonian sediments near Quesnel Forks (Harington 1978) and a Columbian mammoth (Mammuthus columbi) associated with shrub tundra vegetation in Mid-Wisconsinan silts was found at Babine Lake (Harington et al. 1974). Harington (1978) listed the following Pleistocene taxa for the Cariboo district: Columbian mammoth (Mammuthus columbi), woolly mammoth (Mammuthus primigenius), ground sloth (Megalonyx sp.), moose (Alces sp.) wild ass (Equus (Asinus) sp.), mule deer (Odocoileus hemionus), deer (Odocoileus sp.), caribou (Rangifer sp.), and bison (Bison sp.). As in the case of the Albertan Peace River district fauna discussed above, all of these forms are common open parkland elements. The oldest known invertebrate faunal assemblages are postglacial in age and consist of unidentified snail shells recovered near Dawson Creek, B.C. (Reimchen and Rutter 1972).

L. PREVIOUS GEOLOGIC WORK AND GEOLOGIC HISTORY

The earliest geologic exploration of the Finlay River area was in 1875 by Alfred R. C. Selwyn (Geological Survey of Canada) when on July 9th of that year he passed through Finlay Forks on his way to Igenika (Selwyn 1877). As part of the general mapping expedition, Selwyn formally named Portage Mountain near Hudson's Hope. George M. Dawson (Geological Survey of Canada) and R. G. McConnell explored the geology of the upper Peace River valley in 1879 while traveling from Port Simpson to Edmonton. As a result of this trip, Dawson modified some of his earlier statements regarding glaciation in British Columbia. Originally, Dawson (1878) believed that the inception of glacial ice began in the northwest corner of the province as a result of moisture supply off the warm Japanese current in conjunction with the prevailing westerlies. Furthermore, he believed that during the Pleistocene a land depression in excess of 3000' (914 m), and up to a maximum depression of 5270' (1606 m) occurred in the north. This depression permitted the influx of 'prairie ocean water' up the Peace River valley; thereby, both fueling and floating large isolated ice masses. Resultant 'boulder-clay" sediments were thought to represent debris from pan-provincial floating icebergs. Approximately a decade after his trip through the Peace District, Dawson (1888) reiterated his belief in a major northwestern ice centre for the Cordilleran; specifically, the northern Coast Mountains, but also acknowledged the existence of local ice centres in the Rocky Mountains which may have flowed off the eastern margin onto the Interior Plains. Dawson's (1890) major contribution at this time was his belief in two Cordilleran glacial events; what he saw was an early extensive glaciation and a second minor glaciation.

McConnell (1896) returned to the Finlay River in 1893, and provided the earliest documentation of the Pleistocene geology in the region. McConnell suggested the stratigraphic history consisted of stratified sands and gravels overlain by "boulder-clay" which in turn were covered by additional stratified sands and gravels.

McConnell's expedition met with personal trouble, and desertion by two of his men consequently led to the naming of Deserter's Canyon at the head of Williston Lake.

Somewhat later, Tyrrell (1919) in his discussion of glaciation south of Quesnel, disputed Dawson's earlier claims of thick and extensive glacial ice. Tyrrell proposed that thin local ice masses existed in the province, none of which reached a 6000' (1829 m) thickness over valleys. Johnston (1926) supported Tyrrell by citing evidence for glacial ice limits at 6500' (1981 m) elevations in the Cariboo Mountains, 5500' (1676 m) in the Dease Lake area, and 4500' (1372 m) near Williams Lake. As the maximum glaciation had only attained an elevation of 6500' (1981 m), ice thickness over valleys would have been in the order of 3000' (914 m). Johnston did, however, accept Dawson's two glacial hypothesis but emphasized the existence of a long interglacial between the two glaciations. Finally, a major issue in Johnson's thesis centred on the character of the ice lying between the Cariboo and Cassiar districts. Johnston abandoned the term Cordilleran Glacier in favor of the "Cordilleran system of intermontane, piedmont and valley glaciers" for glacial ice in the area.

In a 1934 discussion of glaciation in British Columbia, Kerr renewed the hypothesis of a Pleistocene ice centre in the northwest corner of the province. Prevailing westerlies coupled with the high humidity and precipitation in the area were recognized as creating ideal conditions for an ice centre. Additionally, Kerr created an hierarchical classification of glaciation types, based on evidence in the Coast Mountains: 1) Alpine Glaciation; 2) Intense Alpine Glaciation; 3) Mountain Ice Sheet; and 4) Continental Ice Sheet. He envisioned ice expanding from the ice centre in the northwest through the four types of glaciation. In the process, glacial ice apparently traveled southeast across the Stikine, Finlay and Parsnip Rivers. In contrast to Johnson and Tyrrell, but in support of Dawson, Kerr suggested maximum ice heights in excess of 10,000' (3048 m) and an axial ice thickness of 5000' (1524 m) in the Stikine valley. In the Omineca River valley, several examples of multiple till strata

interbedded with sands and gravels were recognized by Kerr (1934), who could not decide if the tills represented different advances or pulses of a single advance.

Shortly thereafter, a new and unique interpretation was offered by Hedley and Holland (1941) who proposed the main Cordilleran ice centre lay in the Cassiar Mountains. At approximately the same time, but further to the east, Beach and Spivak (1943) observed Laurentide erratics as far west of Fort St. John as Coal Creek, Johnson Creek and Lynx Creek near Hudson Hope, B.C.. They complemented this evidence for a Laurentide glacial advance by suggesting that the Portage Mountain Moraine stretching from Bull Mountain north to Portage Mountain represented the terminal position of the last Cordilleran advance.

The cyclical nature of the argument continued with Armstrong and Tipper (1948), who also believed the main ice centre in B.C. was in the Coast Mountains, but further suggested localized accumulation centres existed in the Omineca and Rocky Mountains. Observations by these authors indicated maximum ice elevations of 6000' (1829 m) in the Nechako Plain and less than 5000' (1524 m) in the Omineca Mountains. Evidence for two Cordilleran advances was recognized in the area, with the first advance considered the most erosive. The second advance apparently carried less sediment and simply reworked existing glacial sediments. The second advance also had a dominant flow to the east but did not cross the Rocky Mountains. Rather, the flow became obstructed by ice moving off the Rocky Mountains with subsequent diversion north down the Parsnip valley.

Mathews (1954) offered new evidence for the extent of ice advances by both the Cordilleran and Laurentide glaciers. Mathews recognized till of Cordilleran provenance overlying till of Laurentide provenance approximately 24 km west of Fort St. John. Moreover, Mathews (1955) offered an explicit account of Pleistocene glaciation in B.C by defining the position of the Cordilleran ice divide based on erratics and surface features. This ice divide stretched from the Cariboo Mountains westward to the Coastal

Mountains and then northwards through the Babine Range, Skeena and Cassiar Mountains, terminating in the vicinity of 131° W longitude and 64° N latitude. Elevation of the ice surface may have dropped from roughly 9000' (2743 m) in the south to 6000' (1829 m) in the north.

Tipper (1971b) provided more accurate Late Wisconsinan ice limits for central B.C. indicating elevations of 4500' (1371 m) near Prince George and approximately 3500' (1066 m) along the Parsnip River. He further suggested that the Rocky Mountains provided a substantial barrier during the last advance, hence diverting flow in the area north down the Parsnip valley where local surface topography is "characteristic of a terminal moraine area" (Tipper 1971b:747). Tipper felt an earlier extensive glaciation was responsible for particular distributions of erratics observed over much of the province. In the Williston Lake area, Rutter (1977) indicated glacial flow generally to the east from a main ice centre further west, with localized flow down the Finlay, Parsnip, and Peace Rivers. Mathews (1980) documented ice elevations in northern B.C. at 2515 m at Sentinel Peak and 2160 m at Mt. St. George and suggested most erratics range in elevation between 1770 and 2010 m.

The dilemma arising from the above evidence is that of correlating the extensive ice movements to specific events. The glacial advance responsible for the wide distribution of western provenance erratics to the east has never been proven to be either of Late Wisconsinan age or some earlier Cordilleran glaciation. The intensity of glaciation in the northern Cordillera near the study area is debatable as Irish (1969) argued that the extent of glaciation in the Rocky Mountains north of the Peace River was less intense relative to the rest of the province.

Nonetheless, by 1972 it was believed that the Cordilleran and Laurentide ice sheets coalesced near Fort St. John sometime during the Late Wisconsinan (Mathews 1972). Unfortunately, the precise number of Late Wisconsinan Cordilleran glaciations

remained equivocal. For instance, Dolmage and Campbell (1963), reported finding "three till layers" of unspecified age, in a 570' (174 m) drill hole 28 miles (45 km) east of Finlay Forks. Five years later, Rutter (1968) recognized four Cordilleran tills. The upper three were considered to be Late Wisconsinan (Rutter 1976, 1977). Rutter's published reviews of the presumed ice sheet coalescence (Cordilleran and Laurentide), suggested that an intensive Cordilleran glaciation corresponding to the Early Portage Mountain Advance occurred during the Late Wisconsinan (Figure 6) (Rutter 1977, 1981). The Late Portage Mountain Advance (and time equivalent ice to the north) coalesced with the main Late Wisconsinan advance of the Laurentide Inlandsis along a suture beginning southeast of Fort St. John and continuing north by northwest to the Yukon-Northwest Territories-British Columbia geopolitical junction (Figure 6).

Although some authors still believe in a Late Wisconsinan coalescence of Cordilleran and Laurentide ice in the Fort St. John area (cf. Mathews 1978, 1980), a general paucity of finite radiocarbon dates, in particular dates underlying tills, hinders the adequate interpretation of Quaternary stratigraphy of northeastern British Columbia. Table 3 lists all the critical radiocarbon dates for northeastern British Columbia, including finite and infinite dates for the late Quaternary. Dates itemized are in years before present and are taken from numerous sources (Clague 1980; Leslie 1988; Lowdon et al. 1971; Mathews 1978; Rutter 1978). The most obvious implication of the list is the hiatus of dated materials between approximately 10 and 26 ka. This gap corresponds to the commonly defined temporal limits for the Cordilleran Late Wisconsinan glaciation (Fulton 1984a). Late Quaternary dates over much of the province reflect the similar absence of datable materials at this time of provincially endemic ice cover (Fulton 1969; Clague 1980).

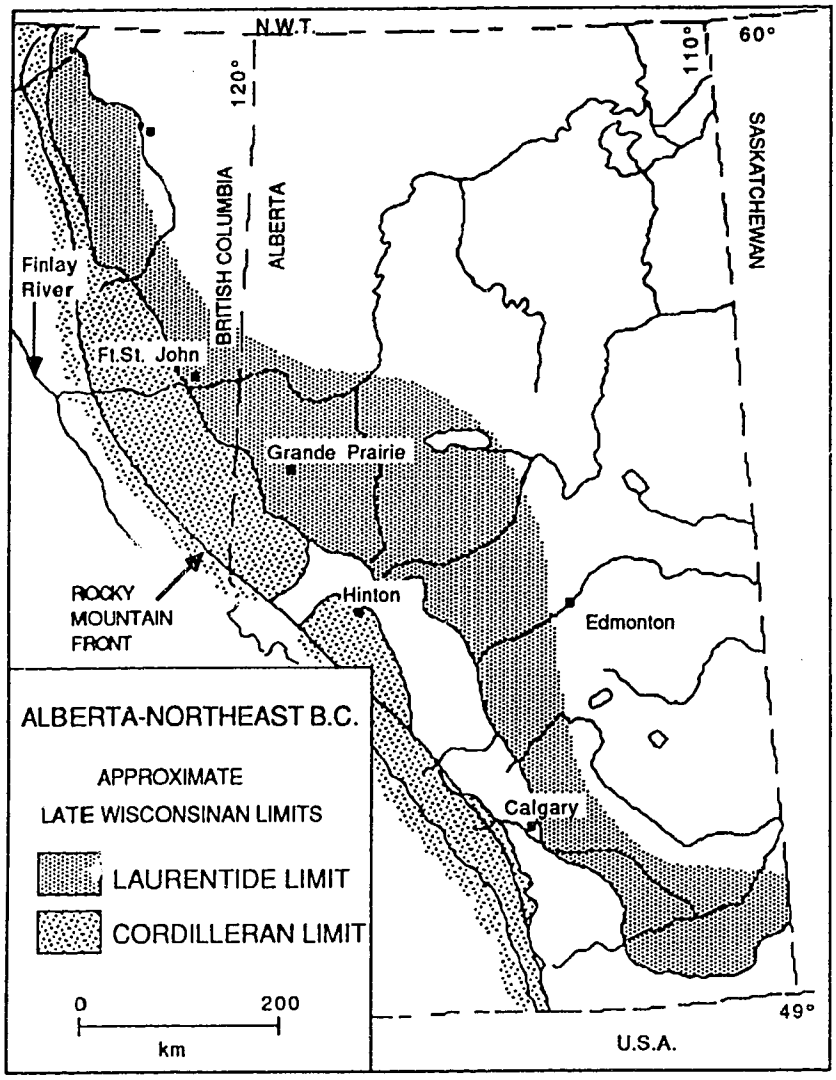

Figure 6. Possible Late Wisconsinan limits, Alberta and northeastern British Columbia (modified with permission after Rutter 1984).

Table 3. Previously published ^{14}C dates, laboratory numbers, location and material types for the late Quaternary in northeastern British Columbia and northwestern Alberta (data from numerous sources indicated).

DATE	LAB. NO.	LOCATION			MATERIAL
510 ± 40	GSC-4080	57° 11' N	125° 17' W	Finlay	charcoal [b]
520 ± 140	GSC-927	57° 11' N	125° 17' W	Finlay	charcoal [c]
660 ± 90	AECV-393C	56° 58' N	125° 04' W	Finlay	charcoal [b]
840 ± 140	GSC-944	57° 11' N	125° 17' W	Finlay	charcoal [c, f]
3,440 ± 60	GSC-4082	57° 14' N	125° 14' W	Finlay	charcoal [b]
4,090 ± 90	GSC-4109	57° 09' N	125° 16' W	Finlay	charcoal [b]
4,830 ± 150	AECV-392C	57° 09' N	125° 17' W	Finlay	charcoal [b]
5,780 ± 110	AECV-391C	57° 08' N	125° 15' W	Finlay	charcoal [b]
7,470 ± 140	GSC-1069	56° 10' N	124° 07' W	Ospika	wood [a, e]
7,480 ± 150	GSC-1161	56° 10' N	124° 07' W	Ospika	peat [a, e]
9,280 ± 200	GSC-1497	55° 48' N	123° 38' W	Finlay	bighorn skull [g, a]
9,960 ± 170	GSC-1548	55° 59' N	120° 15' W	Dawson	snail shells [d, a]
10,100 ± 90	GSC-2036	55° 47' N	125° 05' W	Omineca	marl [a]
10,400 ± 170	GSC-1654	55° 59' N	120° 16' W	Dawson	snail shells [d, a]
25,800 ± 320	GSC-2859	56° 01' N	122° 07' W	Portage Mt	mammoth tusk [e, a, x]
25,940 ± 380	GSC-573	56° 18' N	124° 21' W	Finlay	plants (subtill) [c, e, a]
27,400 ± 580	GSC-2034	56° 09' N	124° 43' W	Taylor	mammoth tooth apatite [d, e]
27,400 ± 850	I-4878	55° 43' N	117° 38' W	Watino	wood and peat (subtill) [e]
43,800 ± 1830	GSC-1687	55° 00' N	126° 14' W	Babine	wood a
> 28,000	GSC-1057	57° 22' N	125° 31' W	Finlay	wood [c, f, a]
> 40,000	I-2259	56° N	122° W	Peace	charcoal (subtill) [a]
> 41,000	GSC-841	57° 22' N	125° 31' W	Finlay	peat (subtill) [c, f]
> 44,000	GSC-837	57° 10' N	125° 20' W	Finlay	wood (subtill) [c, f, a]

Superscript Notation:
a-Clague 1980
b-Leslie 1988
c-Lowdon et al. 1971
d-Mathews 1978
e-Mathews 1980
f-Rutter 1976
g-Rutter et al. 1972
x- orginal date of 11, 600 ybp (I-2244A), redated as 7,670 ± 170 ybp (Mathews 1978) now dated as 25,800 ± 320 ybp (GSC-2859)

M. TERMINOLOGY AND DEFINITIONS

In anticipation of possible misunderstanding of the terms and phrases used throughout this study, a few elaborative comments and definitions are provided in the following discussion. Most terms are self evident in the general sense, but several require minor clarification in the case of inconsistent usage by several authors.

The nongenetic term diamicton is used to denote any unlithified, poorly sorted mixture of gravel, sand, silt and clay (Flint et al. 1960a, 1960b). Harland et al.'s (1966) introduction of the term 'diamict' in their review paper is in the same sense as defined above and has been strongly promoted by Eyles et al. (1983), but their unwarranted truncation of the original term diamicton has generally met with criticism (Kemmis and Hallberg 1984).

Powell's (1984) etymological conclusions indicate that Latin derived roots be joined by the letter 'i', and Greek roots by the letters 'io'; hence, most compound terms used in this study appear as glacimarine, glacifluvial, glacilacustrine, etc. rather than the often seen glaciomarine, glaciofluvial, and glaciolacustrine.

Throughout the last few decades, considerable attention has been directed towards the term 'till' (Dreimanis and Lundqvist 1984). Unfortunately, the level of academic discussion has become unnecessarily pedantic (eg. Dreimanis 1983). A suite of descriptive, genetic and nongenetic terms appear in the literature, ranging from paratills and orthotills to ablation flow tills and leeside tills (Dreimanis 1976, Harland et al. 1966). In this study, till is used in the genetic sense to define a "sediment deposited directly from ice that has not undergone subsequent disaggregation and resedimentation" (Lawson 1979a, p. 634). Although sediment can be transported in ice in one of three positions; supraglacially, englacially and basally, the position of deposition can differ and includes proglacial, lateral-ice contact, supraglacial and subglacial (Shaw 1986). In this study sediment deposited in a subglacial position is confidently interpreted relative to two processes of deposition; meltout and lodgment,

from which the terms meltout till and lodgment till are derived and used here (Haldorsen 1982). Regardless of the position of transportation, and deposition, glacial sediment deposited by flow or glacial sediment subsequently resedimented is not recognized as till. Thus, deposits such as subaquatic flow tills (Evenson et al. 1977), and supraglacial flow tills (Haldorsen 1982), are not recognized as till but constitute varieties of sediment gravity flows. Sedimentary structures and petrologic properties used in the identification of tills and till types are presented in the appropriate sections of Chapter 3.

The terminology surrounding mass movement processes and the classification of their associated deposits has also attracted considerable attention (eg. Hampton 1972; Postma 1986). In this study, the inclusive phrase 'sediment gravity flow' is used to describe deposits of diamicton whose genesis is interpreted not to be directly glacial in origin but gravity dominated. For this reason, deposits such as supraglacial flow tills are here defined as glacigenic sediment gravity flows instead of flow tills (Broster and Hicock 1985). All deposits classified as sediment gravity flows derive their nature directly from a gravity driven force, rather than interstitial fluid motion (Nardin et al. 1979). Moreover, depending on the mechanics of behavior (plastic vs. viscous fluid) involved during flow, these deposits can be further genetically separated into debris flows (grain flows, modified grain flows and cohesive debris flows) and fluidal flows (liquefied flows, fluidized flows, and turbidity currents) (Lowe 1976, 1982). Specific characteristics and sedimentary structures used in identifying ancient deposits within these types are discussed in Chapter 3. Figure 7 provides a schematic representation of sediment gravity flows and deposits following the classification of Shultz (1984).

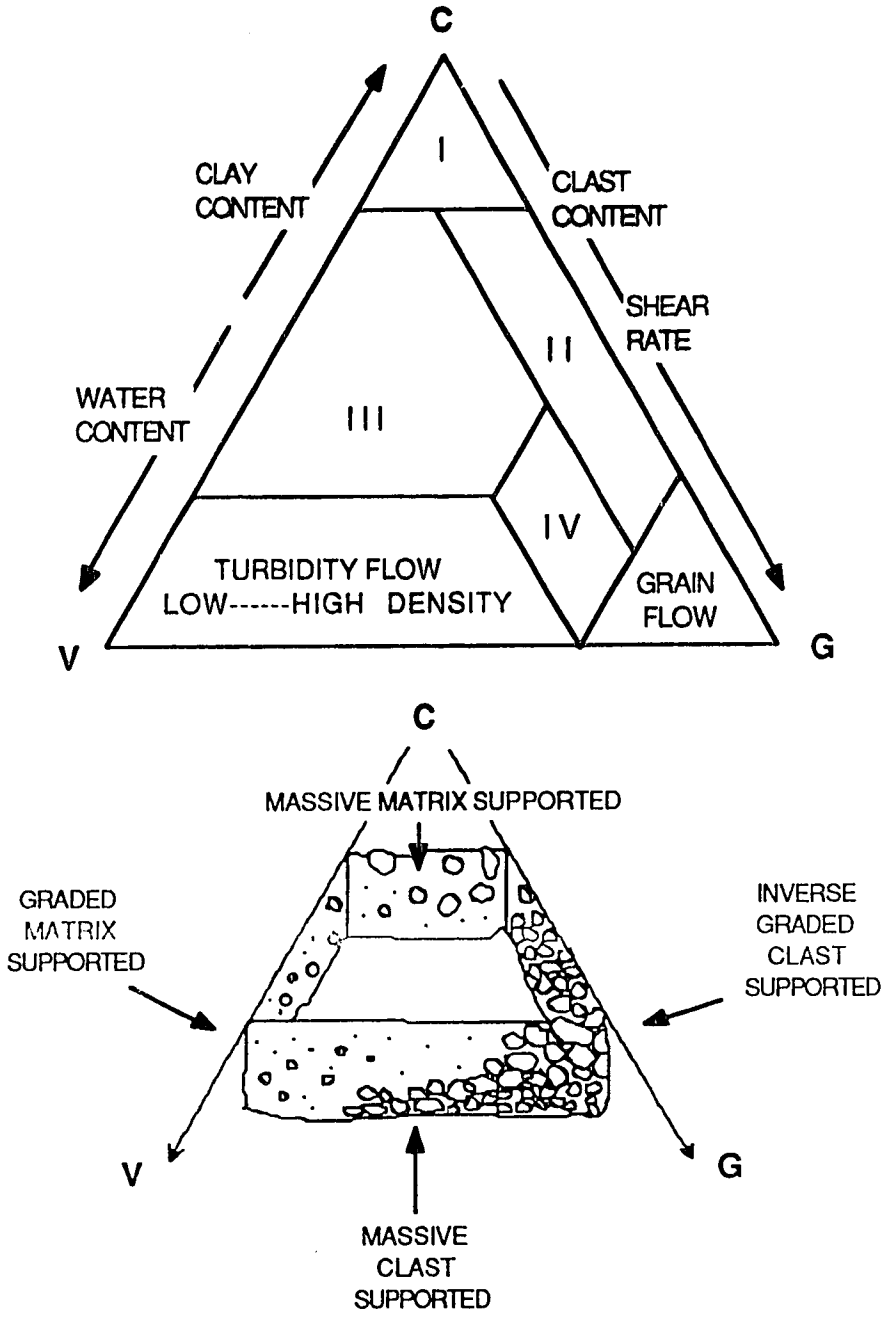

Figure 7. Top is ternary classification of sediment flows. Types I to IV after Shultz (1984) indicated in diagram. C=cohesive-plastic, V=viscous, and G=granular-collisional behaviors. Bottom is schematic of deposit associations. Both figures modified after Shultz (1984).

II. Methodology and Theory

A. GENERAL STATEMENT

The field geology component of this study began in the summer of 1983 and was completed in the summer of 1985. The initial field season consisted of a one week, two-man field reconnaissance to establish the number of sections available for study in the area and to assess conditions for future camp set-up; since periodic camp servicing or departure would not be possible in the following years. The majority of the time devoted to field mapping, description and data collection occurred in the summer of 1984 with a two-man crew and in 1985 a 'clean-up' operation was completed by another two-man field crew. During the latter two seasons, the two man crews were part of a larger four man regional project. Most sections designated for further study were initially identified in the field during the field reconnaissance of 1983. Subsequent addition of localities examined as part of the research occurred during the summer of 1984 (see Figure 1). Further localities were not recognized during the final season. The following sections outline the particular methods and theoretical assumptions used in both the field and laboratory stages of study.

B. FIELD METHODS AND THEORY

Parts of 3 field seasons were spent in the study area describing section localities and collecting samples for further laboratory work. Time spent at any particular locality varied as a function of size of exposed face (several lateral metres to kilometres), extent of slope wash and other sediment masking, accessibility to exposures (vertical versus sloping faces), encountered complexity of sediments and imposed detail of sampling, all within the general time restraint of the field season length. The discussion that follows consists of two parts detailing: 1) standard data collection; and 2) ancillary data collection. The first part describes in detail the

techniques and methods commonly employed in Quaternary field investigations (see for example Fenton and Dreimanis 1976; Karrow 1976; May and Dreimanis 1976) in light of this particular study. The second part expands on the sampling of 'atypical' materials ultimately destined for laboratory analysis involving determination of paleomagnetic grain anisotropy, and paleoecological interpretations based on pollen, seeds, and insects. Both parts include comments regarding the theoretical assumptions and justifications surrounding choice of the methods.

The theoretical premise of this study rests on a stratigraphic approach using lithostratigraphic units as a base for analysis as defined in the North American Stratigraphic Code: "A lithostratigraphic unit is a defined body of (sediment)... which is distinguished and delimited on the basis of lithic characteristics and stratigraphic position" (North American Commission on Stratigraphic Nomenclature 1983, p.855). This traditional approach differs from the mnemonic lithofacies code approach adopted by some glacial and sedimentary geologists (see Eyles and Eyles 1983).

i) Standard Data Collection

Examination and description at each section followed a fairly systematic framework. An initial foot traverse along the base of the section and top of the scree slopes provided a cursory outline of the number of lithostratigraphic units present, as well as their vertical and lateral extent. A first approximation section drawing was then completed for each locality. Detailed information was then logged onto the general sketch as research progressed. The style of information collection is detailed below. Following the arguments of Malde (1983) panoramic photographs were then taken of the section faces at point positions approximating the section sketches. These photos were later used to improve the original field drawings. A number of samples were taken and eventually processed in the laboratory.

ii) Section Descriptions

During description of sections, the following information was recorded: 1) gross form or nature of outcrop and contained units; 2) number of defined units, including average thickness; 3) lateral extent and shape of units; 4) types and shapes of beds within units; 5) primary structures in beds; 6) unit contacts; and, 7) secondary structures and features. To clarify the above, the nature of the outcrop dealt with ground level observations of such features as active slumping, vertical exposures requiring rope manoeuvres, tabular vs. hummocky surface, and whether or not the basal parts of the sections continued below water surface or lay over exhumed eroded bedrock surfaces. This information proved important in time-tabling further work and equipment (eg. climbing equipment), and in the case of the final observations correlating surface morphology to underlying sediments.

Where possible section unit thickness was determined by measuring down a series of logging spots with a metred tape or by measuring off portions of climbing ropes. Section data used were the uppermost surface of each bluff in metres above sea level. The stratigraphic units were determined visually, provided a first order division of analysis, and permitted organization of further subdivisions at detailed scales (beds within units). Lateral extent and shape of these section units could be easily established through observations from across the river. This information was essential in correlating smaller scale observations; for example, when on a rope, to the appropriate section unit defined.

Data were collected at the scale of depositional beds. Shape of individual beds was noted (tabular, plano-convex, etc.) as was horizontal and vertical extent (bed width and thickness). Other descriptive documentation included nature and orientation of primary structures and features (grading, laminations, inclusions, types of deformation, and paleocurrent orientation) and nature of contacts (straight, wavy, inclined, gradational, sharp erosive). Paleocurrent estimation was determined from

cross bed orientations (Dott 1973). In this regard, estimates were based on visual assessment of trough cross bed truncation ad modum DeCelles et al. (1983). Secondary and post-depositional structures and features were also recorded including weathering features, oxidation, folding, and faulting. When present, body and trace fossils were described and, where possible, collected.

iii) General Sampling

A total of 550 samples including pebbles, bulk sediment, and organic remains were collected for further analysis during all three years of field work. Each sample was accorded a progressive number consisting of three parts. The first three letters provide an acronym to the collector's name (PTB), the following two numbers define the year of collection (84) and the final number(s) after the hyphen define the individual sample identification. A sample diary or log-book was maintained for the samples with cross referenced information such as collection date, locality, unit, type of sample, and associated photographs. Pebble sample collection is discussed below. Bulk sediment samples were also recovered for further laboratory work. In this case, dried sediment was usually cleared from the face until a fresh exposure could be described and sampled. Following the Munsell color determination approximately 1-2 kilograms of sediment was excavated from a particular point. Occasionally, systematic suites of samples over a vertical part of each section were retrieved for compositional analysis. The sampling interval varied for each of these, hence, details for each case are included in the appropriate discussion of section descriptions.

iv) Texture, Roundness, Sorting and Color

A variety of other deposit attributes were systematically recorded for the units as discussed in many field method manuals (cf. Compton 1962; Singer and Janitzky 1986). For example, diagnostic color (Munsell Soil Color Charts 1975) was

determined using the method of modern pedologists (Dumanski 1978). As a secondary characteristic color is important in providing indirect indications of sediment deposition and diagenesis. For example, highly oxidized sediments indicate exposure to fully aerated conditions, whereas dark muds can be the product of deposition in reducing conditions (Reineck and Singh 1980). Induration and nature of cementation was qualitatively assessed for all deposits, as this information often provides insight into post-depositional processes of sediment diagenesis such as ground water percolation. For instance, leaching of calcium carbonate from a carbonate rich, late glacial diamicton may explain the prematurely lithified nature of underlying coeval gravels.

In the field, grain size was determined by providing percentage estimates of clay, silt, sand, and gravel constituents. These estimates were then verified by laboratory analysis. Sediment sorting and clast roundness descriptions complimented the grain size descriptions. Roundness determination involved an estimation of the average roundness of clasts greater than granule size (> 4 mm) according to Powers' (1953) gradational categories. The roundness of clasts provides insight into the transport history and depositional mechanisms of the sediments (Barrett 1980; Boulton 1978), and in certain cases is entirely independent of lithology (Dowdeswell et al. 1985). In the sand and silt size fraction, lithology has been shown to influence shape of particles as much as transport mechanisms (Kennedy and Ehrlich 1985; Perttunen and Hirvas 1982). True shape (particle geometry) analysis as defined by Williams (1966) was not performed, as all glacigenic clasts continue to show the wide variability (eg. pentagonal, quadrangular, triangular, etc.) determined by Wentworth (1936).

v) Pebble Fabrics

One field technique extremely useful in assessing sediment genesis and paleoflow direction is the measurement of pebble fabric orientation. Paleoflow data has been

gleaned from disc shaped clasts in fluvial deposits (Rust 1972), prolate, blade and plate shaped clasts in glacigenic deposits (Lawson 1979a), as well as from waterlogged wood specimens in flume experiments (Macdonald and Jefferson 1985). Fabric data has also proven to be very useful in genetic studies of diamictons (Dowdeswell et al. 1985). Clast dips change from near horizontal at the base of lodgment tills to higher angles up unit (Dowdeswell and Sharp 1986), a feature also observed in other sediments such as lahars and sediment flows, and thought to represent basal shear forces active during deposition (Lindsay 1970; Major and Voight 1986). Dips are apparently greater in debris flows than in lodgment tills (Rappol 1985); and pebble trends may parallel ice flow direction in lodgment tills and be both parallel and transverse to flow in meltout tills (Mark 1974). In very rare instances, reorientation of a fabric may occur in certain diamictons (eg. Nielsen 1982). Finally, fabric strengths (eigenvalues) may be related to the genesis of various deposits (eg. Dowdeswell et al. 1985). Because of the value afforded by fabric analysis, diamictons and certain clast-supported gravels were examined for internal pebble fabric information.

The shape of clasts may control to a certain extent the resultant fabric orientation and vector strength. An early study investigating pebble shape on fabric strength in tills using Zingg's (1935) four classes indicates parallel a-axis orientations were strongest in rods, less so with blades and poor with discs and spheres (Drake 1974). Mills (1977a), however, argued that no statistical relationship exists between size or shape and orientation in basal tills. Paleocurrent inferences in gravels are best estimated by imbrication direction which is favored with rods, blades and disc shaped pebbles (Hein 1984). For this reason, clasts examined for fabric data in this study were rod, blade, and disc shaped in both matrix-supported diamictons and clast-supported sediments.

The number of clasts measured during fabric analysis by researchers ranges considerably. Actual numbers include 10 (Young 1969), 25 (Domack and Lawson 1985), 50 (Dowdeswell et al. 1985), 100 (Drake 1974) or even 1000 (Glen et al. 1957). A commonly used, and acceptable range appears to be 25-50 clasts per sampling location. Clast size used by others has also been quite variable. For example, Dowdeswell and Sharp (1986) used a wide selection of stones 2-50 cm in length, while Harrison (1957) preferred a restricted range of 4-8 cm. Finally, the axial ratios of clasts measured by past researchers is far more variable than both of the preceding aspects of sample size and clast size. A few examples include a/b ratio of > 2/1 (Domack and Lawson 1985), a/b ≥ 1.7/1 (Drake 1974), a/b > 3/2 and c/b > 2/3 (Dowdeswell et al. 1985), and a/b ≥ 1.4/1 (Mills 1977a; Rappol 1985).

In this study, a total of 50 clasts ranging in size from 3-15 cm in length (a-axis) with a/b ratios of at least 3/2 and b > c axes were measured at each diamicton sampling location. For the gravels, clasts ranged in size from 5-25 cm, displayed a/b axis ratios of > 3/2 and b ≈ c axes. In both cases, the trend (azimuth) from 0° north (corrected in the laboratory for magnetic declination) and plunge from a horizontal plane were determined with a Brunton compass (equipped with inclinometer) for the clasts at 60 sampling locations; seven of these samples are related to the work of Leslie (1988) and are hereafter designated PTB84-L1 to L7. Measurement of the orientation of pebble imbrication of the b-c plane for gravels accompanied the a-axis measurements.

Vertical and lateral sampling position in a deposit appears to significantly affect both orientation and vector strength. In one case, pebbles in lodgment tills showed lower dip angles, stronger S1 values and more closely paralleled ice flow directions the lower the position of the fabric location (Dowdeswell and Sharp 1986). Examination of the data presented by May et al. (1980) on stratified "tills" also suggests that S1 eigenvalues decrease up through a depositional unit and further suggests that S1 values

increase with larger clasts (+5 cm vs. < 0.6 cm). Major and Voight (1986) identified increased S1 eigenvalues progressing downwards through lahars near Mt. St. Helens. Such spatial constraints in fabric analysis were suggested by Harrison (1957) who considered three vertical feet and 750 horizontal feet as maximum distances over which fabric would not be significantly discrepant. Given the above results the location of pebble fabric stations was accurately recorded. In the case of a single fabric station, pebble fabrics were obtained as low as possible in the unit. In certain situations multiple stations were selected up through the unit. Similarly, each sampling station was restricted in area to 1.0 m^2 in size (cf. Visser et al. 1986; Giardino and Vitek 1985) given the aberrant results obtained from larger sampling areas (eg. Van Loon 1983).

vi) Pebble Lithologies

The identification of pebble lithologies has traditionally been used in provenance studies of glacial and nonglacial sediments (eg. Shilts 1981) and other studies of transport mechanisms (Rappol 1984). In the Peace River Region of Alberta and British Columbia, the presence of Shield granites documenting a Laurentide ice source and Interior volcanics documenting a Cordilleran ice source has been a key element in stratigraphic interpretations for several separate studies (eg. Mathews 1980; Liverman in preparation). As discussed in Chapter 1, the study area overlies Tertiary aged metamorphics, is bounded to the east by carbonates and to the west by volcanics and other metamorphics. Petrologic analysis of deposits in the study area should therefore indicate sediment pathways relative to these lithologic provenances (cf. Bridgland 1986). Mineralogy and geochemistry are functionally dependent on sediment size and have proven to be very useful and precise in studies of glacigenic provenance related to drift prospecting. In this study, pebble lithologies provided the necessary

provenance information, were easy to obtainable and were therefore preferred to geochemical and mineralogical methods.

Pebble lithologies were determined for the various units at each locality. When possible a total of 50 clasts greater than 3 centimetres in maximum dimension were randomly collected and split in the field for identification. A total of 96 pebble samples were obtained for the lithologic analysis. All samples were retained and returned to the laboratory for verification.

vii) Ancillary Data Collection

Several ancillary studies to those listed above were undertaken in the study area. These studies include collection of samples for paleomagnetic and paleoecological analyses. The least problematic in this regard was the collection of wood remains for carbon-14 and amino-acid dating and indirectly paleoecology. Where present, larger in situ fossil wood fragments were photographed and the surrounding matrix described in detail. The wood fragments were not treated with preservative but wrapped dry in plastic and a protective covering of tin foil. Small wood remains were retrieved from the soil matrix by dry or wet sieving or a combination of both using a 1.00 mm sieve (Tyler Equivalent No. 18). Packaging of smaller fragments was also in plastic and protective tin foil. All wood samples were kept dry and cool to limit bacterial and fungal growth.

A total of 75 bulk samples were collected for potential pollen, seed, and insect analysis with the aim of documenting, both regional and local paleoenvironmental conditions in the northern Rocky Mountain Trench. Many of these samples were collected in conjunction with sampling for sedimentological analysis and are thus represented by the same sample. In the case of pollen data, however, individual samples collected were smaller, each sample ultimately ranging in mass from 200 to 500 grams. Again, sample intervals varied according to the peculiarities of the unit

sampled. These variations are documented in the appropriate chapters that follow. Sample numbering procedures followed that described above for the standard data collection. As in the case of wood remains, pollen samples were kept as cool and dry as possible in the field. Upon return to the laboratory, all samples were promptly stored in a freezer.

A number of units were chosen for paleomagnetic analysis. It was anticipated that these data could assist in resolving questions of deposit age and event dating, as well as provide a unique record of changing magnetic conditions through time (Tarling 1971; McElhinny 1973). Paleomagnetic sampling in soft sediment requires initial cleaning of the face to obtain a vertical profile. Plastic paleomagnetic cubes (2 x 2 x 2 cm) marked with a hole and an orientation arrow are then driven into the exposed face with a low percussion hammer (see Figure 8). Care was taken to maintain a relatively flat cube implantation. Four cubes per horizon are required for statistical accuracy (Figure 8). Field data recording included measuring the orientation of the three primary axes for each cube with a Brunton compass. Correspondence of the X, Y and Z axes to the cube, as well as methods of measuring (+ or -) follows geophysical convention and is illustrated in the top two drawings of Figure 8. Cube labelling consists of a conventional five part alphanumeric designation commonly used by geophysicists for paleomagnetic study (for example 4C2B04) (W.G.E. Evans, Department of Physics, University of Alberta, personal communication 1984). The first number refers to the last digit in the year of sampling, in the example given the number 4 represents 1984. The year of sampling is followed by a lettered section identification established on a study by study basis. Again, in the example given the letter C refers to Section Two. The section designation is in turn followed by a unit identification, here the second unit is sampled. Finally, sampling horizons were assigned defining letters, such as B for the second horizon and the four cubes within

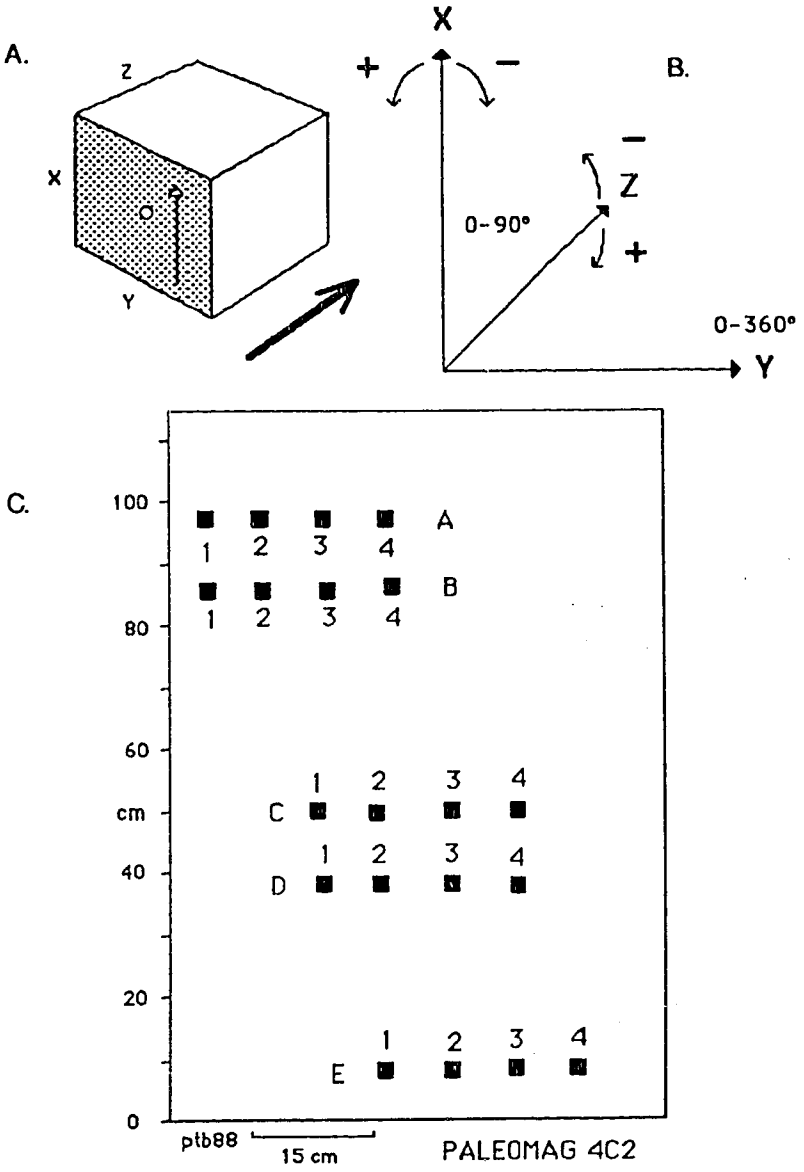

Figure 8. A) Shows orientation of paleomagnetic cube for sampling; B) indicates angular deviation conventions used for three axes; and C) shows arrangement of paleomagnetic cubes in section face at location 4C2 of paleomagnetic analysis. Similar four cube per layer, five horizon sampling strategy employed at all locations.

each horizon were then sequentially numbered 01 to 04. For further clarification, the bottom of Figure 8 provides an example of the sampled surface at Section Two.

C. LABORATORY METHODS AND THEORY

The laboratory analysis for this study began in the fall of 1984. The following explains in detail the laboratory methods and techniques employed in this research. Discussion centres on: 1) photo panoramic assembly; 2) amino acid racemization; 3) radiocarbon dating; 4) pollen analysis; 5) determination of carbonate and organic matter; 6) wood identification, seed and insect identification; 7) grain size analysis (hydrometer and sieving); 8) paleomagnetic analysis; and 10) statistical methods.

i) Panoramas

All film was initially processed at a commercial laboratory. Black and white prints were then developed in the darkroom facility of the Department of Geology. Following darkroom development of the 8.5 x 11 panoramic plates, photo composites were assembled for each section by the technical staff at the University of Alberta Photo Services Division. The results as final panoramas for several of the sections are shown as Plate 2 through Plate 4. Detailed section drawings based on these panoramic composites were then drawn with continued reference to the original field section drawings. Complimentary section drawings accompany these plates and are given in Appendix 16. Note that specific logging locations are also marked on each of the section drawings.

ii) Amino Acid Racemization

Upon return to the University of Alberta, all organic remains were placed into freezer storage. The twenty-nine organic samples were first examined for their amino acid racemization ratios in the Department of Geology, Amino Acid Laboratory.

Plate 2. Top photograph illustrates panorama of Section VIII. Section VIII is 78 m high and 750 m long. Bottom photograph illustrates panorama of Section V. Section V is 53 m high and 750 m long.

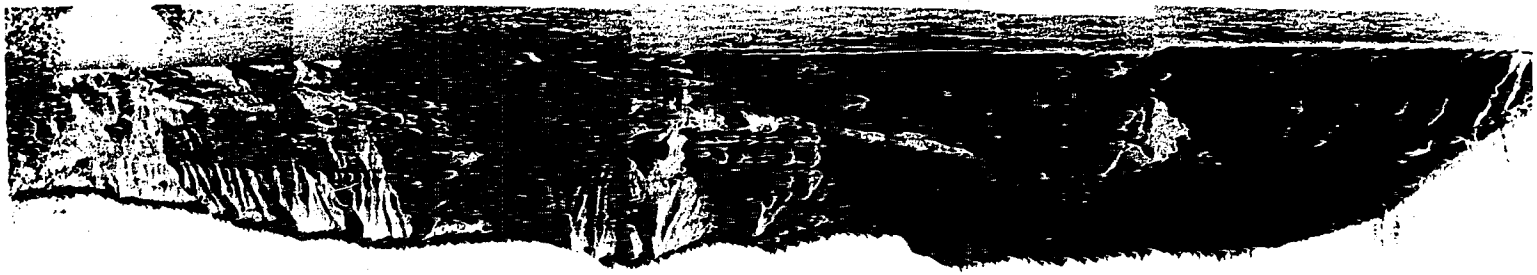

Plate 3. Panoramic views of Section IX, north and south ends of section. Section is 111 m high and 1300 m long.

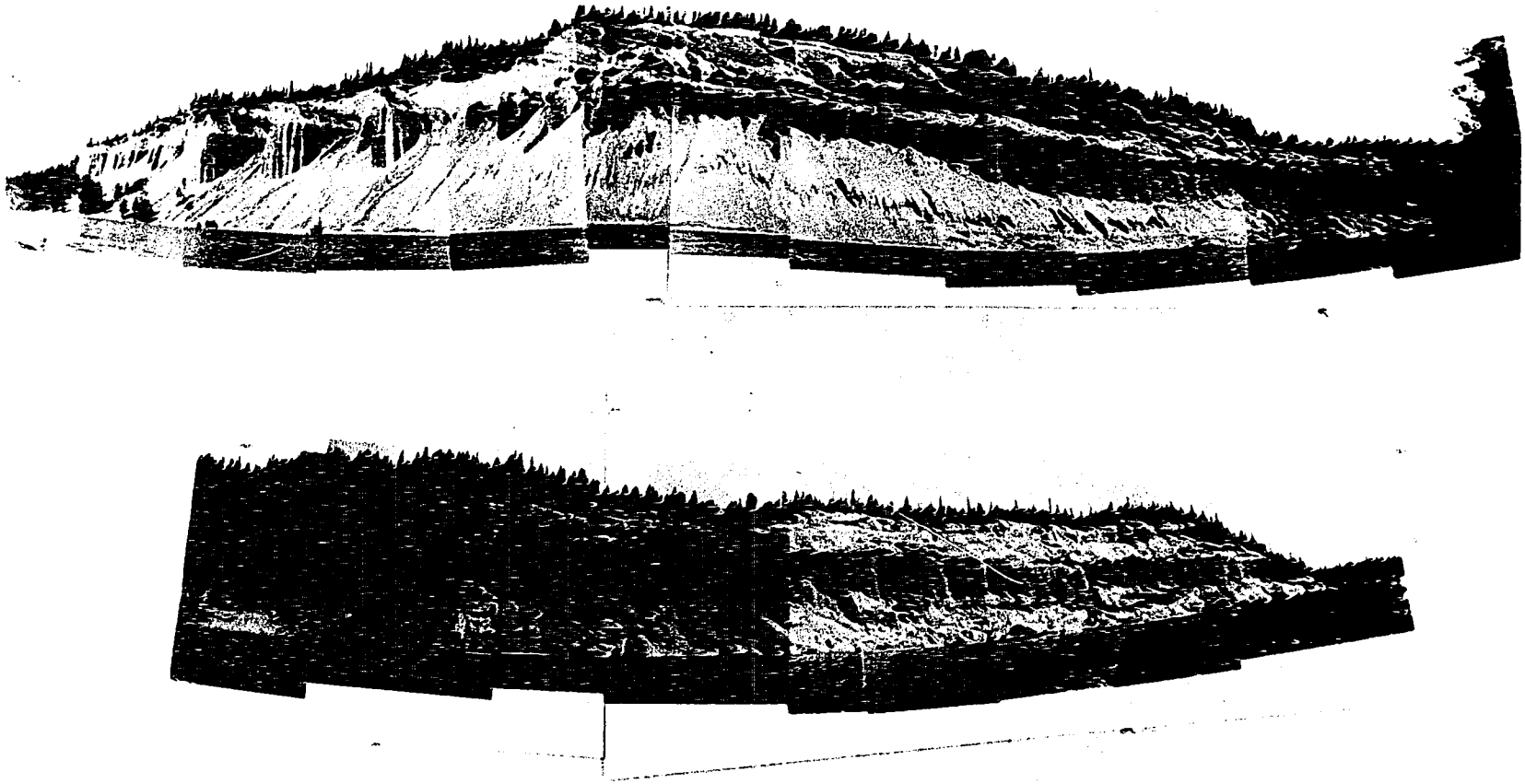

Plate 4. Panoramic views of Section X, north and south ends of section. Section is 78 m high and 1100 m long.

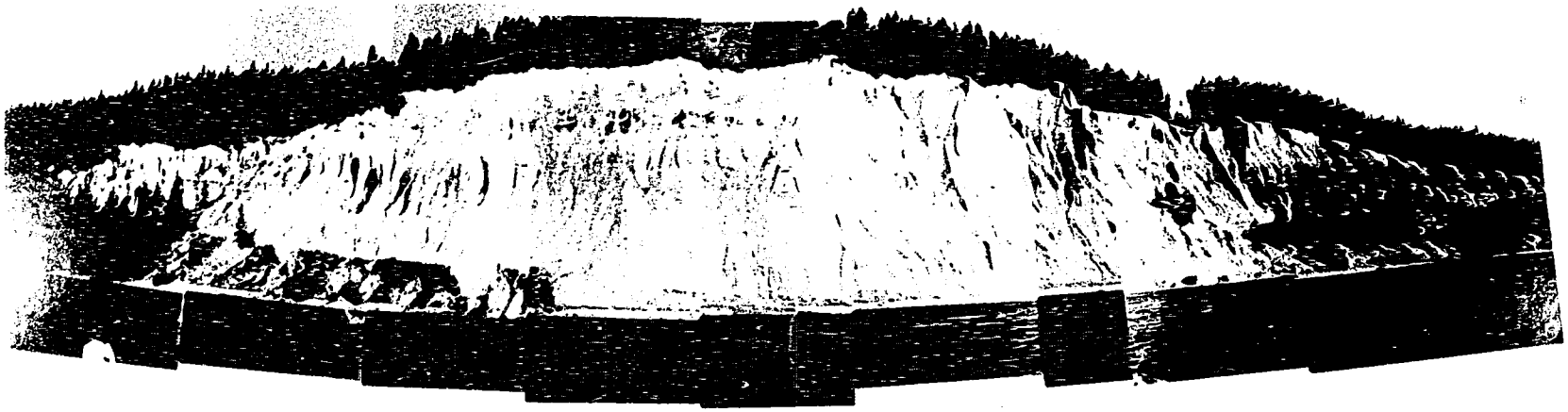

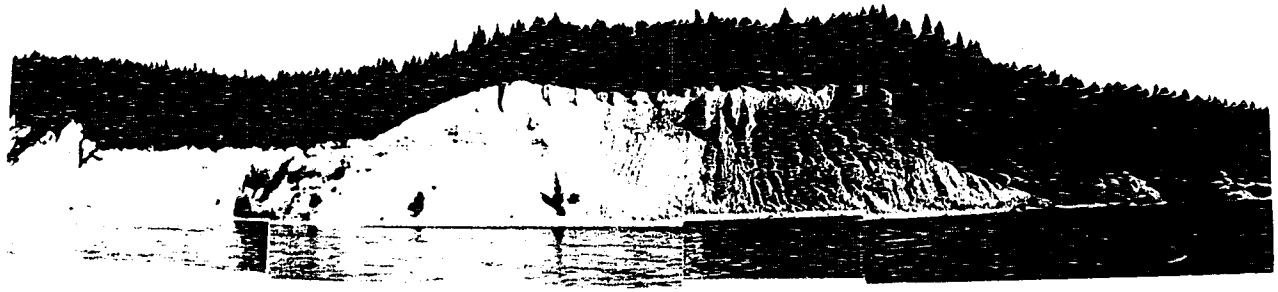

Appendix 17 provides an account of the technique employed for the analysis (G. Lyons, Department of Geology, University of Alberta, personal communication 1988). Briefly, portions of the individual samples were first cleaned, crushed and sonicated with HCl. Samples were then hydrolized for 24 hours at 108° C. Following this and acid removal, samples were concentrated through centrifuging and desalted with Dowex resin. Amino acids in a dry state were then esterified with isopropanol and acylated with a PFPA and methylene chloride mixture. The involatile DL-amino acids were then analyzed with a gas chromatograph and the D/L ratio of aspartic acid was determined with a flame ionization detector. Each sample was subjected to three independent runs to lessen the statistical spread of the best estimate.

iii) Radiocarbon Dating

Following the amino acid racemization study, 27 wood, 'lignitized wood', and organic silt samples were submitted to the Alberta Environmental Centre, Geochronology Section, Radiocarbon and Tritium Laboratory in Vegreville, Alberta for ^{14}C dating. All wood samples were given a pretreatment of HCl to remove carbonates and further cleaned with NaOH to remove all mobile humic acids. The organic sediment received the HCl pretreatment, but not the NaOH pretreatment. Samples at this laboratory were assessed relative to 1950 A.D. and a half life of 5568 years. Only certain samples were δ13C corrected relative to the standard P.D.B of -25% (L.D. Arnold, Alberta Environment, personal communication 1987). An additional two wood samples were submitted to IsoTrace Laboratory, University of Toronto for ^{14}C dating. Both samples at this laboratory were analyzed by accelerator mass spectrometry (AMS) twice on two different occasions and both were corrected for fractionation to a base of -25% (R.P. Beukens, IsoTrace Laboratory, personal communication 1987).

iv) Pollen Analysis

All pollen samples were placed into immediate cold storage upon return to the University of Alberta. Representative unit samples from the original 75 were then treated for pollen concentration at the University of Alberta, Department of Anthropology, Paleoenvironmental Laboratory. Appendix 18 provides a detailed procedural account of the technique employed for the analysis. Briefly, samples were pretreated with HCl to remove carbonates and mixed with a heavy liquid ($ZnBr_2$) and vacuum filtered to concentrate the pollen. Samples were then soaked in an HF bath to dissolve the silicates. Sediment colloids were then removed by repeated HCl baths. Samples were next subjected to acetolysis using a mixture of H_2SO_4 and acetic anhydride. Following several types of rinses, samples were mixed with silicone oil and stored in a glass vial. Where present, palynological identification was accomplished by referral to published illustrative keys and an extensive herbarial comparative collection housed in the Paleoenvironmental Laboratory.

v) Carbonate and Organic Matter

In the early 1960s and 1970s soil survey studies and surficial mapping projects attempted to characterize glacigenic sediments according to particular "till sheets" (eg. Gross and Moran 1971, Steiger and Holowaychuk 1971). Grain size analysis, calcite/dolomite ratios and calcium carbonate equivalents were routinely determined with the aim of identifying these individual "till sheets" (Dreimanis 1962). The premise in these studies was that these parameters in tills typified unique parent materials and thus different source areas. If sediment genesis is considered in such characterization, the basic premise remains valid. For example, in the Finlay River area, Cambrian and Devonian carbonates dominate the lithology east of the river, whereas metamorphics and igneous rocks occur to the west. The carbonate composition of diamictons from these two sources areas would therefore provide different analytical

signatures for the same type of deposit in the absence of any external modifying factors. The gasometric technique outlined by Dreimanis (1962) has since been shown to be extremely unreliable (cf. Catto 1988). An alternative method of quantifying carbonate content was therefore selected with the aim of documenting intraunit vertical variation as well as interunit characterization. The assumption in both cases is that parent material, transportation pathways, depositional mechanisms and post-depositional diagenetic affects will be reflected in the sediments.

Percent concentration of carbonate and organic carbon was determined using a modified version of the loss on ignition method as reviewed by Dean (1974) and McKeague (1978). All samples were first oven dried overnight at 100° C in preweighed crucibles. Dry, weighed sample were then transferred to a muffle furnace and heated to 550° C for one hour; the calculated weight difference reflecting the percent of organic carbon. All samples were again heated in the muffle furnace to 850° C overnight; the weight difference in this case reflecting the amount of CO_2 evolved from the carbonate fraction in the sample. The end result of this procedure provides percentage estimates of the total water, organic matter and carbonate content in the varying samples.

The experimental studies of Dean (1974) indicated the method is statistically reliable after comparison with several other methods including gas chromatography with a Hewlett-Packard C-N-H analyzer, gasometry with a LECO analyzer, and atomic absorption.

vi) Wood, Seed and Insect Identification

Portions of wood not destroyed by amino-acid analysis or radiocarbon dating were submitted to Sergio Cevallos-Ferriz (Department of Botany, University of Alberta) for identification. Following paraffin embedding (Johansen 1940), sections were cut and studied using radial, tangential, and transverse orientations. The woody taxa

represented were identified by quantification of features including: vertical and horizontal resin canals, the presence of spiral thickening on tracheids, types of tracheid pitting, and features of the cross-field pits (Greguss 1955).

Bulk samples collected for seed and insect analysis were first water sieved through a Tyler #230 mesh (0.0625 mm) sieve. The washed material was then sorted under 20X magnification using a binocular microscope. Recovered materials were placed in closed vials containing 90% ethyl alcohol. All samples were sent to Dr. John V. Matthews Jr. (Terrain Sciences Division, Geological Survey of Canada, Ottawa) for identification.

vii) Particle Size Analysis

As reviewed by Blatt et al. (1980) grain size analyses are primarily performed for the following reasons: 1) provides a basic description with some attempted precision; 2) particular distributions may reflect certain environmental conditions of deposition; and, 3) grain size distributions may reflect both sediment transportation histories and depositional mechanisms.

Grain size parameters are frequently used in a number of ways to distinguish between deposits such as till and alluvial fan sediments or beach sand and river sands (Landim and Frakes 1968; Blatt et al. 1980). The transportation history of sediment may be further assessed within a single genetic category as exemplified by Nickling (1983) on transportation modes of aeolian sediments.

Bulk samples of sediment were analyzed by hydrometer analysis, sieving, or both to determine the percentage constituents of various grain sizes. Samples containing noticeable amounts of silt and clay (> 10%) were treated by both methods as detailed in A.S.T.M. (1964). Bulk sediments containing low amounts of fines were only sieved. Briefly, the method of hydrometer analysis requires an initial soaking of exactly 50.00 grams of sediment (finer than 2.0 mm) in a 125 ml solution of 4% calgon overnight.

The sample is then placed in a 1000 ml graduated cylinder to which distilled water is added to the one litre mark. Following a thorough mixing, the changing density of the liquid sediment is then determined periodically over a 24 hour period by inserting a hydrometer tube into the cylinder and measuring the progressively deepening cylinder scale reading.

Following hydrometer analysis the sediment is emptied in its entirety into a #230 mesh (0.0625 mm sieve) and rinsed with water. The retained sediment is then oven dried overnight, weighed and sieved. Sieving involves a 15 minute mechanical agitation with a RoTap shaker of a stacked series of sieves through which the oven dried sediment is separated. In this study, the following sieves were commonly used: #18 mesh (1.0 mm), #35 mesh (0.50 mm), #60 mesh (0.25 mm), #120 mesh (0.125 mm), and #230 mesh (0.0625). Retained fractions on each sieve size were weighed and a percentage of total was calculated. Temperature, time elapsed, hydrometer reading, control hydrometer reading and various sieve percentages recorded are entered into the GRAIN.SIZE program on MTS at the University of Alberta. This program translates the density readings and takes into account the fluctuating conditions of recording such as temperature, time and sieve sizes and then estimates the percentage composition of the constituent particles. Textural terminology used in this study follows that of Shepard (1954).

viii) Paleomagnetic Analysis

During the deposition of fine grained sediments, ferric particles tend to align themselves with the geomagnetic field prevalent at the time of deposition. These sediments, therefore, possess a detrital remanent magnetization (DRM), which is one of several forms of natural remanent magnetism (NRM) (McElhinny 1973).

The analysis of various sediments obtained from sections along the Finlay River was performed to identify the NRM field which existed during the Quaternary. The 148

paleomagnetic plastic cubes obtained from the study area were sealed with clear tape and stored in a magnetic free locker in the Department of Physics, University of Alberta. Remanences of the 148 cubes were measured in the Department of Physics using a Digico balanced fluxgate spinner magnetometer. Analytical spin time varied depending on the intensity of magnetization of each of the cubes but most commonly required 30 seconds per orientation. Technical procedure for cube rotation allows each of the 3 orthogonal components to be measured 4 times. The magnetometer automatically determines the mean intensities based on the calculation of variance within the 4 values.

The calculated mean magnetic trend and plunge of each cube was therefore generated by the Digico computer. Mean values of each of the four cubes along a single horizon were then averaged using spherical statistics to provide a single horizon value. Fisherian confidence intervals (95%) were also determined for each horizon (McElhinny 1973).

D. STATISTICAL METHODS

Reference to descriptive statistical values in this study such as mean, and standard deviation follow commonly used parametrical assumptions and procedures (Cheeney 1983). Parametric statistics for moisture content, organic matter, carbonate content and total carbon consist of sample means and standard deviations. A different suite of statistical procedures accompany other analyses. As such some discussion should be devoted to the statistical analyses surrounding spherical distributions (fabric and paleomagnetic data) and the lognormal grain size data.

i) Grain Size Statistics

The evaluation and comparison of the textural character of sediments can be accomplished by visual assessment of cumulative grain size curves. Some researchers

believe that slope breaks in cumulative distribution curves can be related to transportation mechanisms (Visher 1969; Eschner and Kirchner 1984). This initial qualitative assessment can be further complimented by quantitative descriptors. In this study, statistical parameters of grain size distributions were quantified and derived using the graphic statistics of Folk (1974) which rely on extrapolation from a cumulative curve based on the phi (Ø) scale of Krumbein. Following the laboratory analysis of grain size described above, a computer generated cumulative curve was then used to derive graphic statistics; a more precise method than hand drawn visual extrapolation. The graphic configuration of the grain size curves follows Kurtz and Anderson (1979) and the methodology of Johnson et al. (1984), with an upper textural limit of 14Ø.

The descriptive statistics generated include measures of central tendency (Md=median and Mz=mean), a measure of uniformity (Si=sorting of the sediment), a measure of skewness (Ski=degree of asymmetry) and a measure of peakedness (Kg=kurtosis). Calculated measures and the equations employed, as well the terminological classification of values are explained in Appendix 7.

Graphic statistics can also be used in bivariate illustrations to characterize genetically different regimes (eg. Landim and Frakes 1968). Textural data (percent sand, silt and clay) and graphic statistical data can also presented as vertical compositional figures in the style of pollen diagrams to illustrate changes with depth in various lithostratigraphic units (Kemmis et al. 1981). Vertical variations of compositional parameters have proven to be extremely important in elucidating transportational and depositional mechanisms of tills and other diamictons (cf. Gross and Moran 1971; Szabo and Angle 1983; Broster 1986).

ii) Fabric Statistics

The analysis of fabric data can involve a two-dimensional evaluation of azimuthal values only or a three dimensional stereographic evaluation of both trend and plunge. Directional data on a horizontal plane is statistically manipulated using circular distributions (Cheeney 1983). Results are usually presented in the form of a rose diagram. Unfortunately, the method of analysis is severely biased depending on whether data is treated as bidirectional (each point is replicated at its polar opposite) or unidirectional prior to statistical analysis. Figure 9 illustrates this problem with six examples. The figures and statistical data along the left indicate bidirectionally generated rose diagrams. The same data is then treated unidirectionally, circular statistics are once again calculated and presented numerically and graphically along the right. The top number is the sample number, next is the statistically determined mean vector trend, followed by the vector strength, standard deviation about the mean vector and finally the significance in terms of the Rayleigh probability factor. The largely discrepant values indicate the inappropriateness of two-dimensional analysis for fabric studies. At best, rose diagrams can be used to offer an immediate visual indication of the pattern of data distribution only.

Two-dimensional analyses also fail to account for the plunge or dip of clasts which, as noted earlier, offer additional insight into sediment genesis. A suitable alternative to the above method is the analysis of spherical distributions which assess both trend and plunge. The method of 3-D eigenvector analysis is now used (Cheeney 1983). Initially three mutually orthogonal eigenvectors (V1, V2 and V3) whose sum equals N are generated from a cosine squared matrix (Mark 1973). Corresponding normalized eigenvalues or "latent roots of the matrix" (S1, S2 and S3) are calculated by simple division (S1=V1/N, S2=V2/N and S3=V3/N) and provide information on the strength and pattern of orientation (Anderson and Stephens 1972). In general clustered distributions are described by $S1 > S2 \approx S3$, whereas girdled distributions

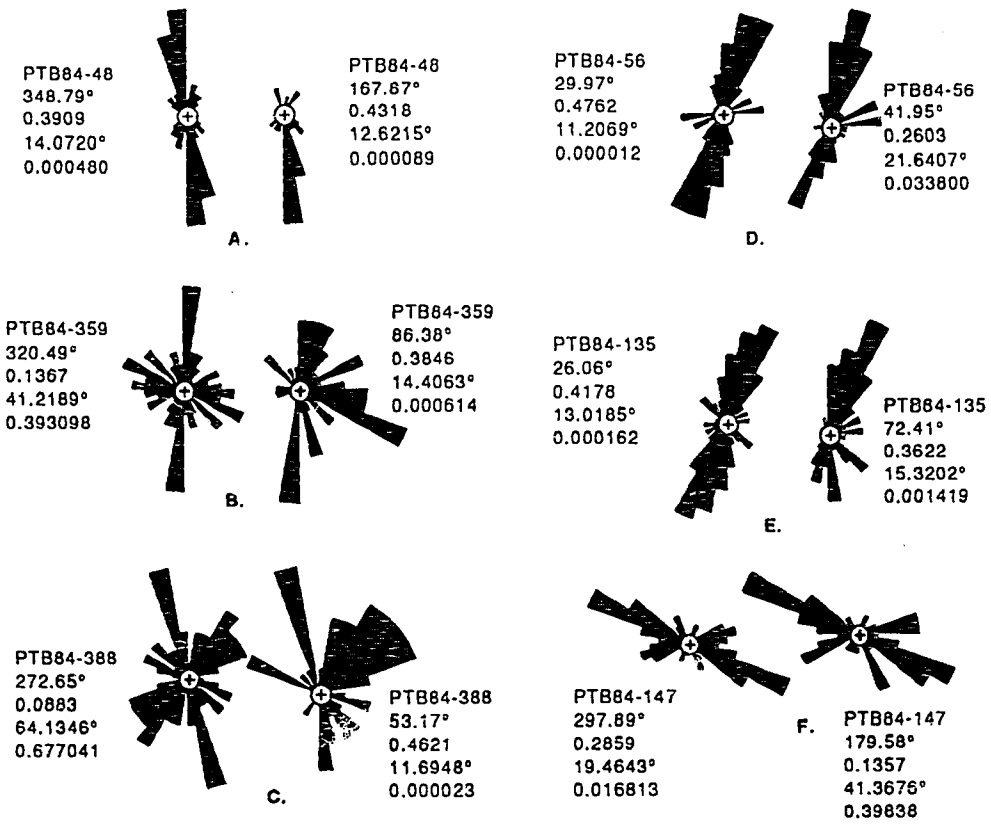

Figure 9. Two dimensional rose diagrams of pebble fabrics. Six different samples lettered A to F are shown. Paired samples show bidirectional calculations on left and unidirectional calculations on right. All sample statistics based on ungrouped data. Text consists of sample number followed by mean direction, mean resultant length, standard error about the mean and Rayleigh test of uniformity. Note discrepancy in values. See text for further explanation.

are described by S1 ≈ S2 > S3 (Woodcock 1977). Uniform distributions are defined by S1 ≈ S2 ≈ S3 (Giardino and Vitek 1985).

The eigenvalues can be assessed for significance by testing for randomness using the null hypothesis of a uniform distribution and the alternative hypothesis for an equatorial distribution. Anderson and Stephens (1972) provided critical values for varying sample sizes for both S1 and S3 eigenvalues in their Table 1. In this study sample size is always n = 50 so the following critical values are used:

S1 > 0.484	S3 < 0.198	99% CI
S1 > 0.471	S3 < 0.207	97.5% CI
S1 > 0.460	S3 < 0.216	95% CI
S1 > 0.447	S3 < 0.227	90% CI

A second method of assessing the significance of eigenvalues requires the S1/S3 ratio. Table 1 in Woodcock and Naylor (1983) provided critical values for testing the ratio for randomness at varying sample sizes. Again, at a consistent sample size of n = 50, the following critical values are used:

> 2.35	99% CI
> 2.21	97.5% CI
> 2.073	95% CI
> 1.923	90% CI

Evaluation and comparison of fabric statistics has been greatly facilitated by the adoption of numerous methods of graphic data presentation. Several graphic techniques are presently in use by glacial geologists including: 1) a bivariate graph comparing S1 to S3 with means, ranges and standard deviations illustrated for different facies (Dowdeswell et al. 1985; Rappol 1985); 2) a logarithmic two-axis ratio plot of normalized eigenvalues (S1/S2 and S2/S3) which defines girdled and clustered distributions (Woodcock 1977; Giardino and Vitek 1985); 3) a triangular plot derived from a ternary diagram comparing all three eigenvalues as girdles and clusters (Mills

1977a, 1977b; Levson 1986); 3) frequency diagrams tabulating a-axis dip angles (Dowdeswell and Sharp 1986; Rappol 1985) or cumulative probability distributions of a-axis dip angles (Domack and Lawson 1985) for genetic patterning; 4) unidirectional format (Lineback 1971) or bidirectional format (Ramsden and Westgate 1971) 2-D rose diagrams illustrating raw azimuthal values of the clasts; 5) 3-D Schmidt equal-area stereographic projections indicating the statistically preferred trend and plunge with accompanying contour lines demarcating decreasing concentrations (Mills 1984; Nielsen 1982); 6) a bivariate graph comparing mean vector trends to vector strength for each sampling locality as a means of recognizing directional clusters as well as unimodal and polymodal distributions (Lawson 1979a, 1979b; Shaw 1982).

A number of these graphic techniques are used in this study. Figures 10 and 11 illustrate the suggested templates for the logarithmic two-axis ratio plot of normalized eigenvalues and the triangular plot of normalized eigenvalues. In the following chapter fabric results are plotted on these two figures to assess the girdling and clustering characteristics of various samples. Two dimensional figures are repeatedly used for graphic purposes in section drawings. Three dimensional Schmidt equal-area projections are also used for fabric data, but are restricted to illustrations in the appendix. Bivariate vector trends vs. vector strength graphs are not illustrated in this chapter, appear where required in the remaining part of the thesis and are essentially self explanatory.

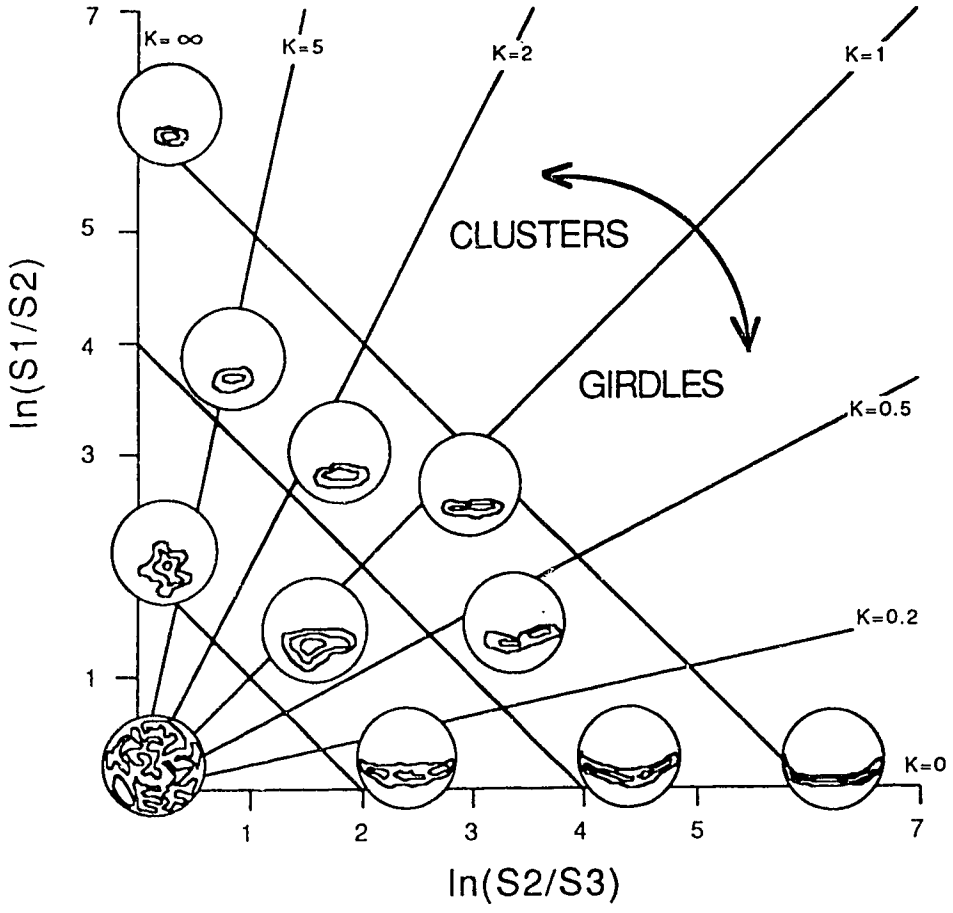

Figure 10. Logarithmic two-axis ratio plot of normalized eigenvalues S1, S2, S3 (after Woodcock 1977, Figure 1). Examples of fabric shapes.

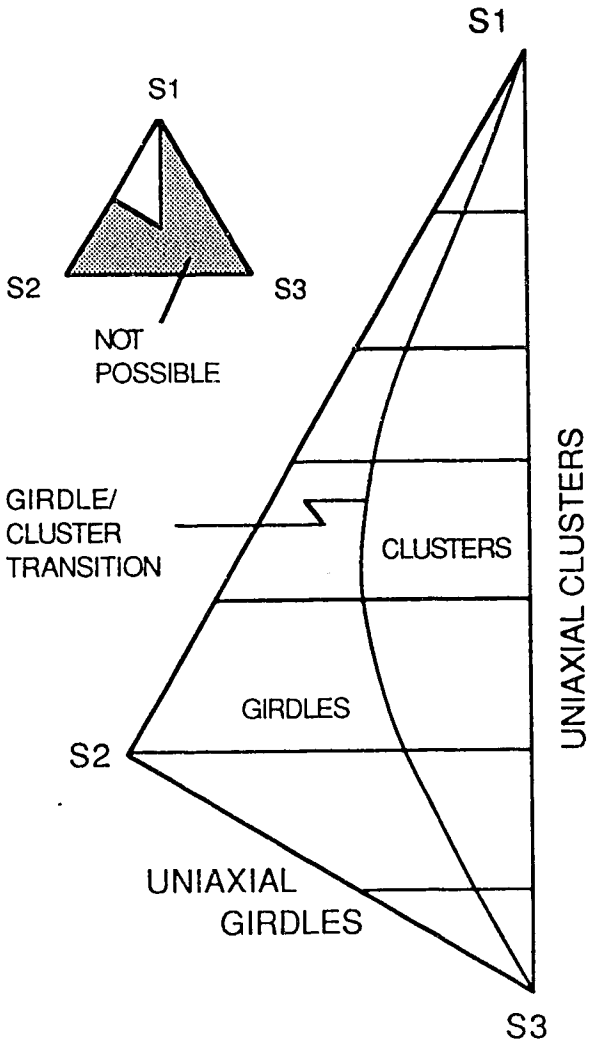

Figure 11. Triangular plot of normalized eigenvalues S1, S2, S3 (after Woodcock 1977, Figure 2). Illustration indicates position of girdled and clustered pebble fabric results. This template is used for 3-D generated results from the Finlay Rive

III. Results and Interpretation

A. GENERAL STATEMENT

Derivation of a composite Quaternary stratigraphic and geologic history for the northern Rocky Mountain Trench involved the detailed field description and laboratory methods outlined in the previous chapter. Discussion of the geologic history for the region will be facilitated with a review of the numerous sediment types identified. This chapter provides a base for the stratigraphic and chronologic chapters by outlining: 1) the descriptive format of the study results; 2) a summary of the field and laboratory data according to broad sediment types; and 3) genetic interpretations for the sediment types within each lithostratigraphic unit (sediment type or sediment type association). These data are then used in generating the geologic history for the area.

B. FORMAT

Each of the 18 sections examined along the Finlay River displays a complex suite of sediment associations. A detailed unit by unit description of the sediment associations at each section is avoided in the presentation of results (see below). Instead, the primary purpose of this chapter is to summarize all of the primary field and laboratory data provided in the appendices according to sediment types and broad lithostratigraphic units.

i) Raw Data

Field and laboratory data for each sample number are given in Appendices 1-18. Pebble counts in the field involved the separation of clasts into 38 rock types. Appendix 1 lists pebble lithology data for the 94 split samples as summarized into utilitarian categories of igneous, metamorphic, and sedimentary (the latter divided into carbonate and siliciclastics).

Appendix 2 provides the results of hydrometer analysis according to phi class. Cumulative textural curves are then given for these samples in Appendix 3. Appendix 4 further summarizes the textural data according to the Wentworth classes of sand, silt, and clay. Best estimate phi values generated from the cumulative curves and used in the determination of the various graphic statistics are presented in Appendix 5. The graphic statistics calculated from these phi values are summarized in Appendix 6. Graphic statistical measures, equations, and terminological classifications are detailed in Appendix 7. Raw data for unconsolidated nondiamicton samples sieved in this study are given as Appendix 8. Appendix 9 contains graphic presentations of these tabulated data for nondiamicton samples. Appendix 10 itemizes the percentage moisture content, organic matter content, carbonate content, and total carbon.

The trend and plunge (corrected for magnetic declination) for all 60 fabric localities discussed in this study are given in Appendix 11. Three-dimensional, Schmidt equal area stereo projections follow in Appendix 12. A tabulated summary of the mean trend, plunge, and computed normalized eigenvalues (S1, S2, and S3) of these fabrics is given in Appendix 13. Appendix 14 lists the statistical transformations and accompanying significance values used for fabric drawings (two ratio plot of normalized eigenvalues, ternary plot of normalized eigenvalues and mean vector trend vs. S1 strength graph).

The paleomagnetic data for all 148 samples generated by spin magnetometer analyses are summarized by horizon (mean of four samples) in Appendix 15.

The location and analytical data pertaining to each river section (bluff) are given in Appendix 16. Appendix 16 provides the following information for each river section: 1) a section drawing of the primary bluff face described, location of the samples and 2-D pebble fabric histograms; 2) a compositional diagrams for the units; 3) variation in pebble lithologies in individual units; 4) textural data in the form of ternary diagrams for all diamictons and histograms for all other unconsolidated

sediments; and, 5) a composite stratigraphic column with a description of each unique lithostratigraphic unit at the various sections.

Appendix 17 provides a procedural account of the method of amino acid racemization analysis used for organic remains. Appendix 18 provides a procedural account of the method of pollen analysis used in this study.

ii) Results

The separation of geological sections into different analytical units has been performed in a number of ways. In this study, objective field and laboratory criteria were used to classify the various sediments into groups and types, as a variation of the 'facies analytical approach' as discussed by Reading (1978), Walker (1984), and Shaw (1987). For the purposes of discussion, the field and laboratory results are provided according to 4 large textural groupings: diamicton, gravels, sands, and fines (silt and clay). Each grouping is further subdivided into sediment types, in the manner of facies subdivisions. A total of 15 sediment types are recognized. The diamicton group consists of: 1) structureless diamicton; 2) diamicton with clastic intrabeds; and, 3) stratified diamicton. Gravels are represented by the following sediment types: 1) massive gravels; 2) normal/inverse graded gravels; 3) stratified gravels; 4) disrupted gravels; and, 5) inclined gravels. The sand group consists of: 1) structureless and graded sands; 2) horizontally laminated sands; 3) trough-cross stratified sands; 4) planar cross-stratified sands; and, 5) ripple laminated sands. Fines are represented by two sediment types, silt and clay.

Each of the resulting 15 sediment types is either solely or partly representative of a broad lithostratigraphic unit. A lithostratigraphic unit can therefore contain one or more sediment type. Depending on the state and preservation of individual units, a mixture of sediment associations may be represented. This approach, recently used by Von Brunn and Gravenor (1983), is preferred to a discussion of formally defined

facies as it: 1) limits the number of potential sediment types to discuss; and, 2) addresses the question of lithostratigraphic units directly.

To expedite information presentation and minimize repetition, sections and units are frequently abbreviated. Location of the sections is given in Figure 1 of Chapter 1. Section abbreviations follow those defined in Figure 1 which uses capitalized Roman numerals or letters. Lithostratigraphic units within each section are consecutively numbered and placed in brackets. For example, unit five at Section West Air and unit nine at Section Ten are presented as follows: W.A.(5) and X(9).

In the discussion of the sediment types that follows, the sedimentary features observed are described with reference to specific sections and lithostratigraphic units. To enable a visual picture of the location and association of the various units to be made, schematic composite stratigraphic columns and the primary lithostratigraphic units for the 18 sections are given in Figure 12.

C. DIAMICTON

In this study, all poorly sorted, matrix-supported sediments containing varying proportions of gravel, sand, silt, and clay were classified within the inclusive and nongenetic grouping termed "diamictons" (Flint et al. 1960a, 1960b). The strict definition of diamicton may also include clast-supported sediments (bedrock equivalent being paraconglomerates), but in the present case, such deposits were assigned within various types of gravels. The term diamict as suggested by Eyles et al. (1983) is a misusage, and the correct term diamicton is required (Kemmis and Hallberg 1984).

Subdivision of diamictons depends entirely on: 1) diversity of the sediments under study; and, 2) objectives of the research. The stratigraphic emphasis of the present research and exceptional variety of sediments encountered favors subdivision of the diamictons into three types. Three primary diamicton types will be described: 1) structureless (massive); 2) massive with clastic intrabeds; and 3) stratified

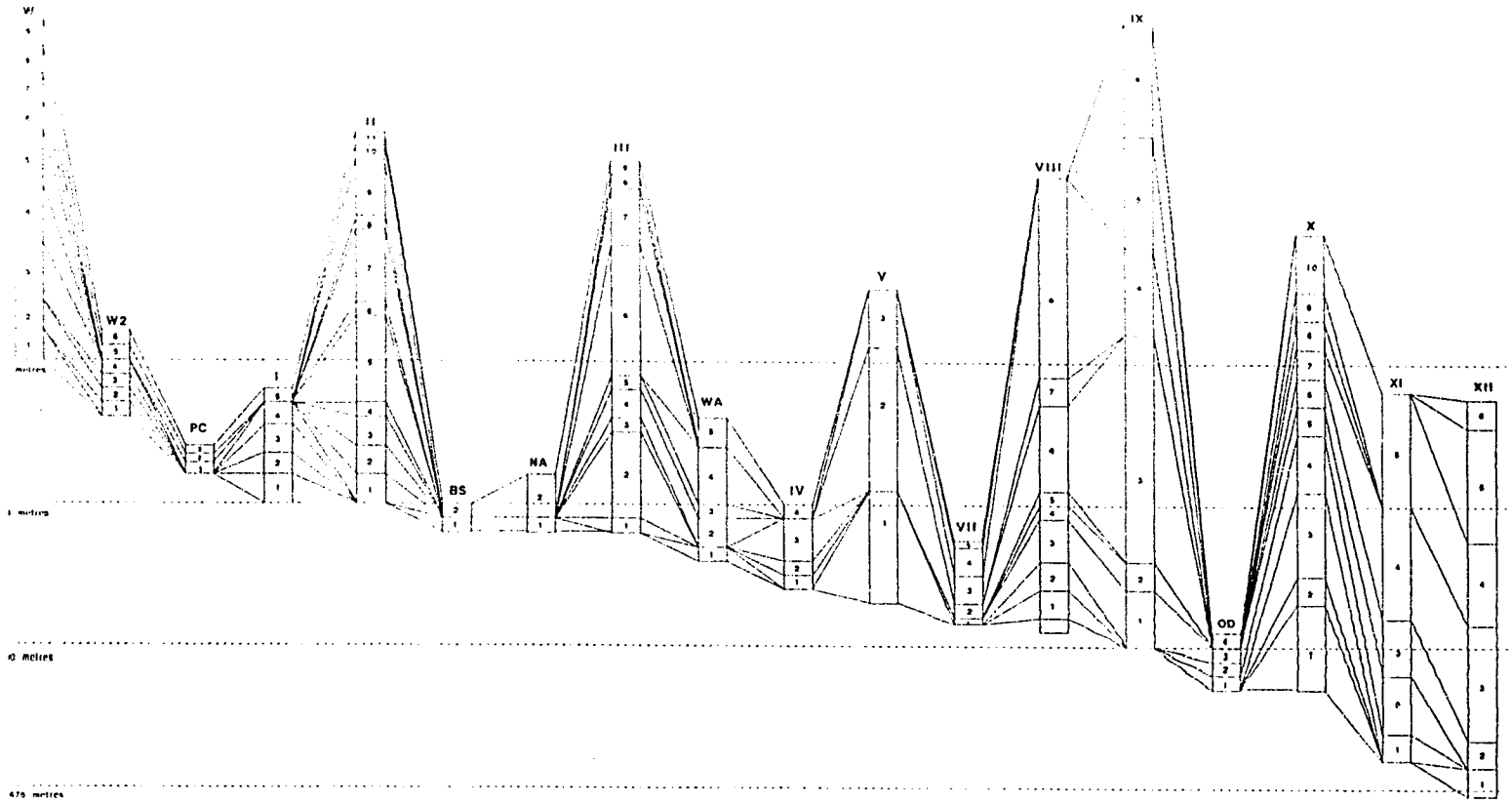

Figure 12. North-south cross-section along the Finlay River of northeastern British Columbia. Section codes defined in Figure 1. Up-stream to left. Lithostratigraphic units numbered in each column.

diamictons. Each sediment type displays considerable variability reflecting subtle facies variations. The sediment genesis interpretation that follows each descriptive category attempts to account for this variability.

i) Structureless (Massive) Diamicton

Description

The most common type of diamicton represented in the region, occurring at 11 sections, is structureless diamicton [W(5), WII(2), II(1 and 8), III(7), V(3), VII(3), VIII(8), OD(1), X(10), XI(1 and 5), and XII(4)] (Figure 12 and Plate 5). These diamictons range in thickness from 2.5-39.0 m. The low end of this range reflects thickness estimates of diamictons outcropping along the water's edge and are, therefore, minimum values. As such, an average thickness for all of these deposits cannot be confidently offered. The average thickness of subaerially exposed structureless diamictons is 17 m.

Pebble content varies from 10-35%, averaging approximately 25%. Striations and faceting (basal and upper surfaces) are common on most lithologically soft clasts. Distributions of the clasts within the units appears to be random, although in one case a clast-free zone approximately 1.5 m thick was observed in mid-unit at Section Ware (5). Lithologically, igneous, metamorphic, and sedimentary clasts are all present in differing proportions (Figure 13). Sedimentary clasts predominate, with carbonates more abundant than siliciclastics. There is minor spatial variation between and within sections. Average clast size is in the pebble range, although cobbles and rarely boulders are also present. Differences in clast content and size are evident locally. Clasts are predominantly subrounded.

A ternary plot of the textural variation within the structureless diamictons is based on 87 samples (Figure 14). All values tend to cluster centrally relative to the three grain sizes. Each value represents a mean estimate for the unit within that

Plate 5. Structureless diamicton. Pick for scale.

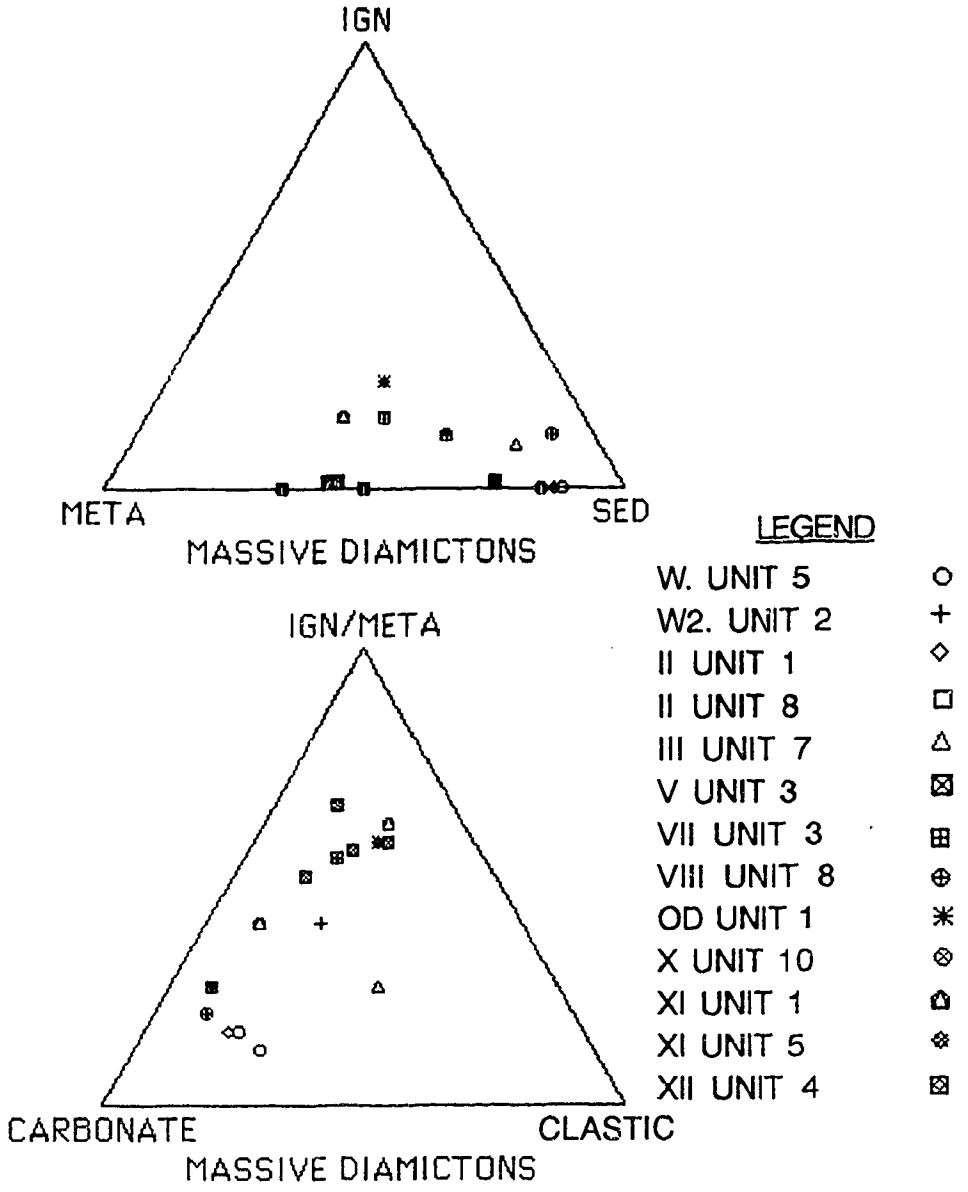

Figure 13. Ternary diagrams illustrating variation in pebble lithologies for various massive diamictons. IGN = igneous, META = metamorphic, and SED = sedimentary clasts. See text.

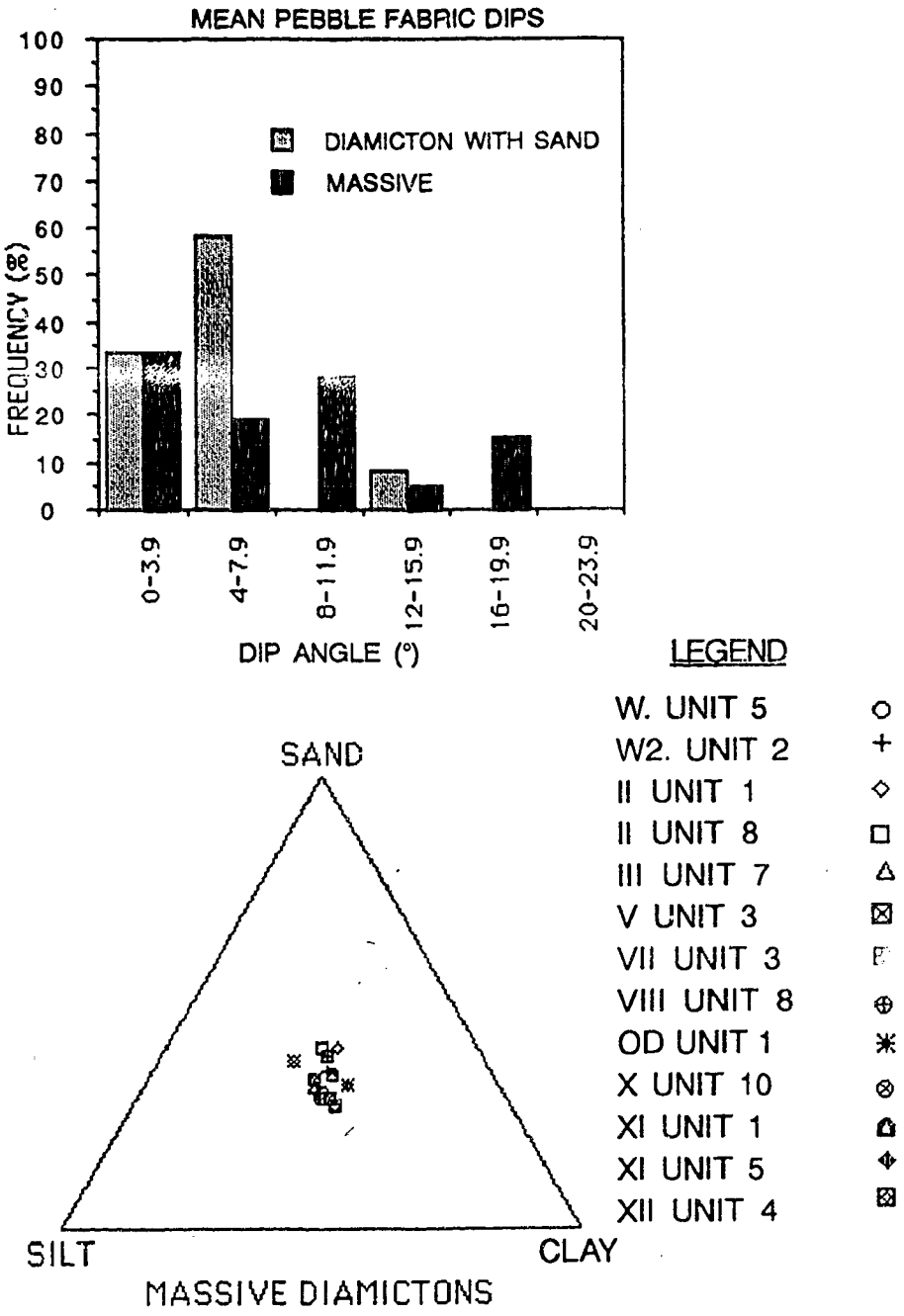

Figure 14. Ternary diagram illustrating textural variation in various massive diamictons and histogram of dip angles in massive diamictons and diamictons with clastic intrabeds. See text.

particular section. Minimum, maximum, mean, and standard deviation estimates for all compositional parameters (texture, graphic statistics, and loss on ignition) are given in Table 4. Texturally, samples range from 20-58% sand, 20-50% silt, and 17-47% clay. Average values are 32 ± 7% sand, 35 ± 5% silt, and 33± 7% clay.

Total carbon in the samples ranges from approximately 6.0% to 23.6%, averaging 11.6%. This consists of a minor organic fraction (0.6-2.3%) and a greater inorganic component (4.8%-22.3%). Calculated moisture content is consistently low (0.1-0.8%) in all samples, but these small differences contribute to the observed color variations. In complete exposures, there is a general decrease in the percent total carbonate and total carbon vertically through the unit (Figure 15).

When possible, pebble fabrics were determined within exposures of the massive diamictons. Three-dimensional stereo projections of these fabrics are given in Appendix 12. A total of 21 fabric sites were selected for total of 1050 measured clasts. A two-axis ratio plot and ternary plot of normalized eigenvalues for the 3-D values illustrates the results of these measurements (Figure 16). The two-axis ratio plot indicates particular fabrics range from moderately clustered to moderately girdled. Strength associations between the three eigenvalues also show considerable range (Figure 16). S1 values range from 0.476 to 0.904, averaging 0.644. A plot of S1 vector strengths against mean vector trends based on 3-D analysis indicates bipolar clusters trending NW and SE, paralleling the trend of Finlay valley (Figure 16). Pebbles dip up and down valley (a-axis imbrication), parallel the valley orientation, and provide fairly strong fabric results (eignevalues).

Diamictons in this group rarely display horizontal parting structures, jointing, and fracturing. Where evident, these structures occur in the upper 2-3 m of complete unit exposures. This zone of parting also corresponds to a noticeable but gradational change in color which differs from the remaining part of the unit. Most of the

Table 4. Summary of various compositional parameters for structureless diamicton samples (top) and diamicton with clastic intrabed samples (bottom).

STRUCTURELESS	MIN	MAX	MEAN	S.D.	N
Modal grain size (Ø)	2.65	7.75	6.10	0.89	85
Mean grain size (Ø)	4.15	7.25	6.11	0.68	85
Sorting (Ø)	3.09	5.10	4.08	0.32	85
Skewness	-0.19	0.48	0.02	0.11	85
Kurtosis	0.73	1.16	0.92	0.09	85
Sand (%)	20	58	32	6.8	85
Silt (%)	20	50	35	6.7	85
Clay (%)	17	47	33	6.8	85
Moisture (%)	0.13	0.76	0.28	0.12	71
Organic Matter (%)	0.61	2.29	1.22	0.28	71
Carbonate (%)	4.80	22.78	10.46	3.24	71
Total Carbon (%)	5.98	23.60	11.56	3.14	71

CLASTIC INTRABEDDED	MIN	MAX	MEAN	S.D.	N
Modal grain size (Ø)	3.05	7.85	6.04	0.92	38
Mean grain size (Ø)	4.23	7.48	6.09	0.67	38
Sorting (Ø)	3.64	5.04	4.45	0.37	38
Skewness	-0.16	0.43	0.03	0.13	38
Kurtosis	0.64	1.31	0.81	0.16	38
Sand (%)	17	56	36	8.3	38
Silt (%)	20	48	30	5.9	38
Clay (%)	21	49	34	6.1	38
Moisture (%)	0.15	1.84	0.36	0.30	29
Organic Matter (%)	0.95	1.63	1.23	0.16	29
Carbonate (%)	6.58	14.50	10.73	2.30	29
Total Carbon (%)	7.60	15.57	11.83	2.24	29

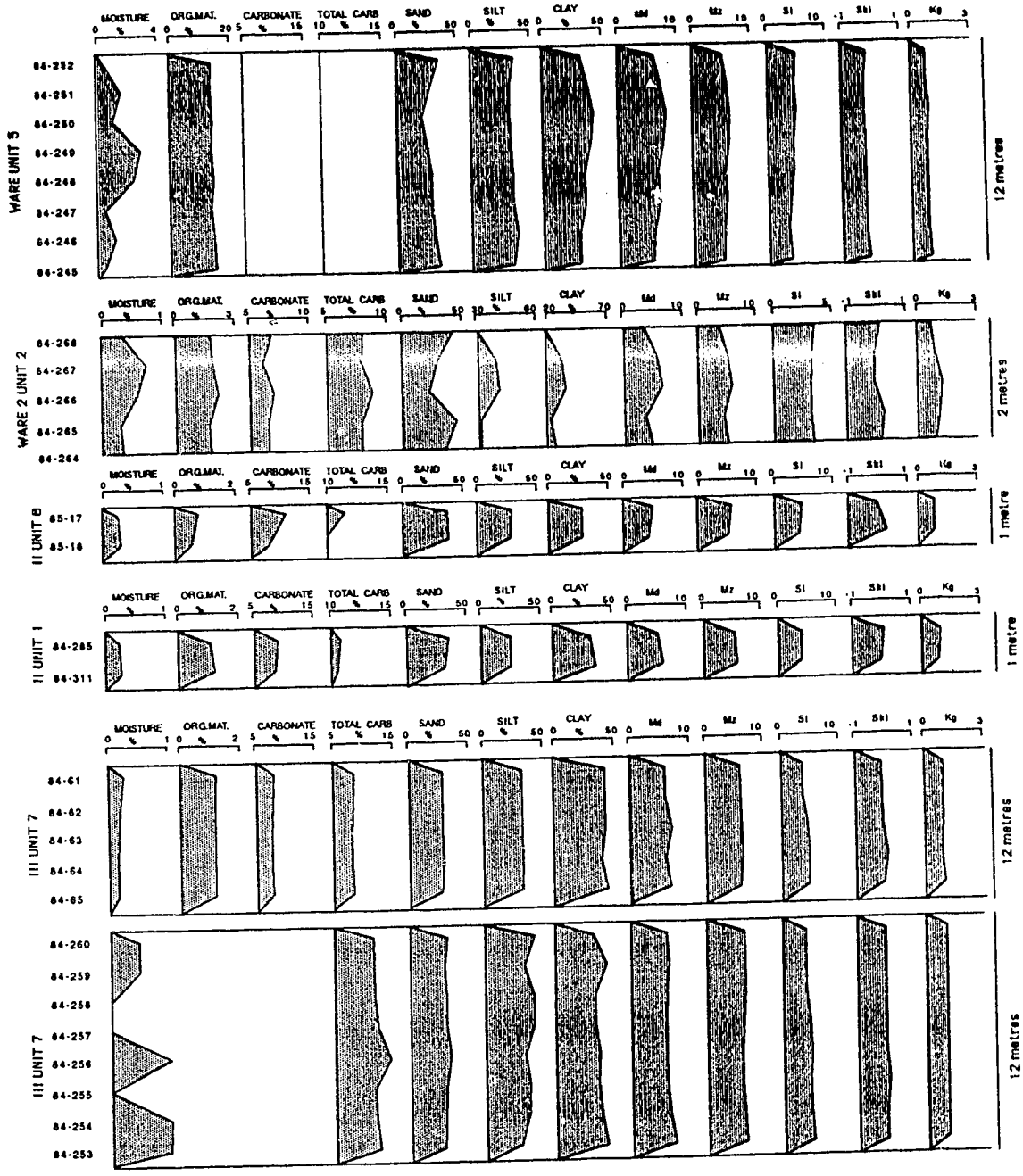

Figure 15. Compositional variation in massive diamictons. See text. Moisture content, organic matter content, carbonate content, total carbon content, sand, silt, and clay in percent. Graphic statistics shown are Md-Median, Mz-mean, Si-inclusive graphic standard deviation, Ski-inclusive graphic skewness, and Kg-kurtosis.

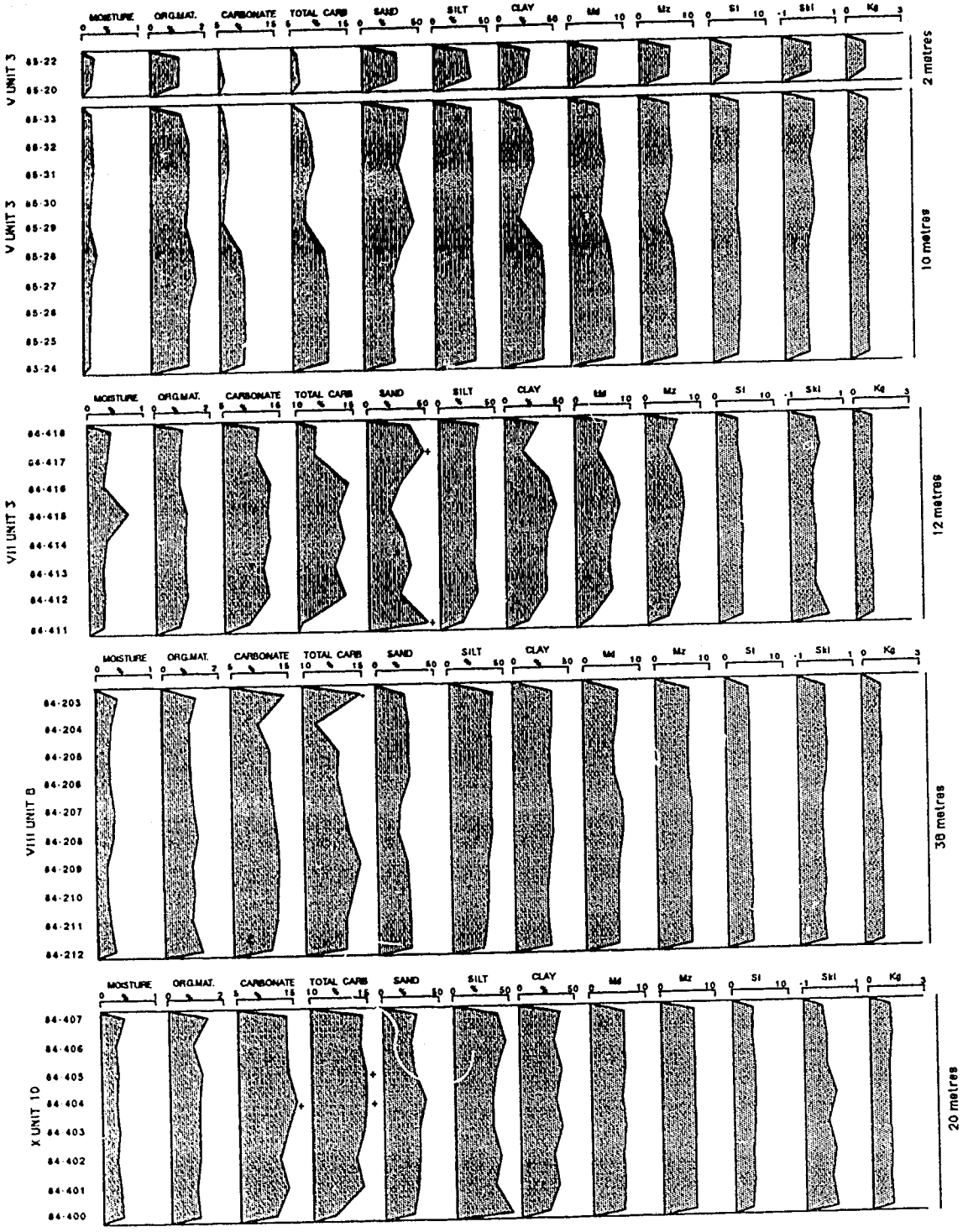

Figure 15. Continued.

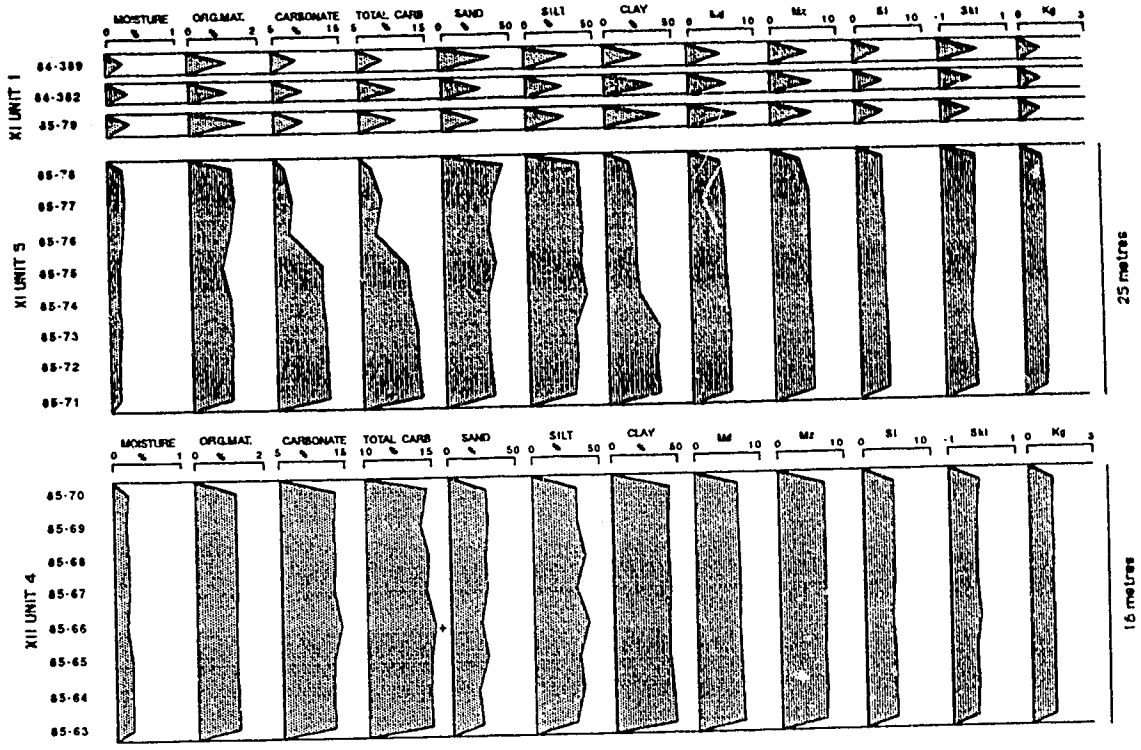

Figure 15. Continued.

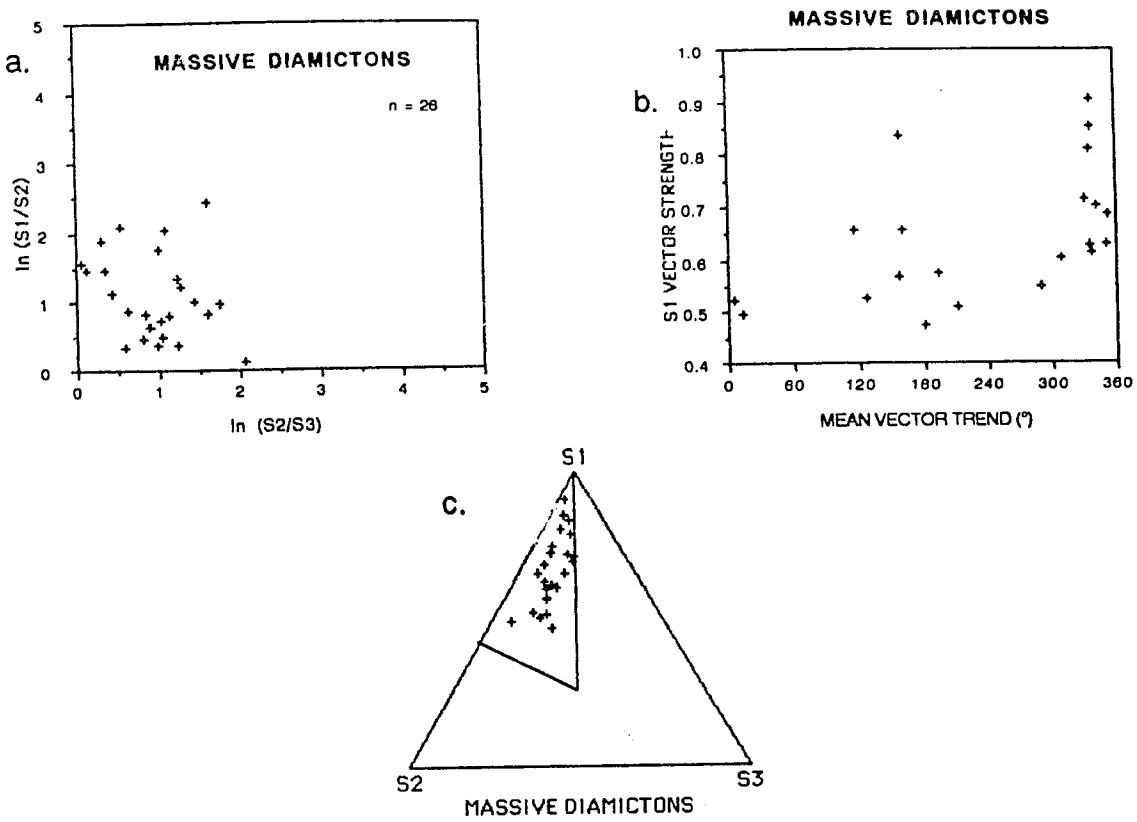

Figure 16. Structureless diamictons. A) Illustrates logarithmic two-axis ratio plot of normalized eigenvalues; B) 3-D determined pebble fabric trends compared to S1 eigenvalues; c) ternary plot of normalized eigenvalues. See text for further information.

diamictons are dark grey (eg. 10YR 4/1) in color but change to olive (eg. 5Y 4/3) within 3 m of the upper contact and within a few centimetres of the lower contact.

Basal contacts for structureless diamictons range from gradational overlying banded and stratified diamictons, to sharp, and unconformable over gravels, sand, and bedrock. Upper contacts are either gradational or sharp where massive diamictons underlie stratified gravels, sands, or diamictons.

Interpretation

Haldorsen (1982) concluded that the differentiation of till from other diamicton types is difficult, and that identifying genetic till types (eg. lodgment vs. basal meltout till) is even more difficult. Still, a genetic interpretation of an objective suite of criteria is necessary for a proper understanding of the glacial dynamics in the depositional area. Multiple criteria should be used to arrive at a proper genetic interpretation. The interpretations that follow examine as many diagnostic criteria as possible to support the final interpretation (Dowdeswell and Sharp 1986; Shaw 1987).

Sediments categorized here as structureless diamictons are interpreted to represent basal till accumulations, probably lodgment till. The hard and compact nature of the sediments supports a lodgment hypothesis (Marcussen 1975; Lawson 1979b). Shaw (1979) contended that massive till represents a former zone of uniform or slightly extending flow in glacial ice. The overconsolidated nature of the sediments indicated by the low moisture content, high clay content and compact nature, suggests an overburden of ice in the past (cf. Dowdeswell and Sharp 1986). Additionally, the high mean percentage of carbonates in the sediments is in agreement with the conclusions of Gibbard (1980) for regional lodgment till properties. Thick accumulations of till are more likely to represent lodgment than any other type of diamicton (Boulton 1976). This is especially so in temperate glaciers where

sedimentation rates can reach values as high as 3 cm/yr or 30 m/ka (Eyles et al. 1983).

The presence of bullet shaped boulders and faceted clasts indicate transportation in a basal ice position (Haldorsen 1982). The types of clasts have also been linked to lodgment processes (Boulton 1978; Krüger 1984). Clasts retrieved from the sediments in this study are very often striated on all surfaces. Striae tend to parallel the derived pebble fabrics for the specific units and many clasts show faceting of the surfaces, attributes usually ascribed to lodgment till (Boulton 1978). Low angularity (subrounded clasts) and absence of appreciable coarse sediments indicate basal rather than supraglacially transported sediments (Haldorsen 1982).

Vørren (1977) suggested that basal tills show much poorer sorting than supraglacial diamictons or stratified sediments. The mean calculated inclusive graphic standard deviation of 4.08Ø for structureless diamictons supports a basal till interpretation. Vørren (1977) further argued that basal tills tend to display near symmetrical skewness, in contrast to scattered skewness observed for supraglacial till. The range (-0.19 to 0.48) and mean (0.02 ± 0.11) skewness of the massive diamictons observed here fits Vørren's model.

The fabric data derived for these deposits strongly points towards lodgment till and not basal meltout till as a likely interpretation of the sediments. Most of the measured fabrics parallel the valley (azimuth-325°) or show a slight deviation from this trend, a characteristic associated with lodgment till by several authors (Lindsay 1968; Mark 1974; Mills 1977a; Dowdeswell and Sharp 1986) and further thought to reflect extending ice flow by others (May et al. 1980). Clast dip angles in lodgment till are usually not as steep as in basal meltout till or flow sediments (Lawson 1979a; Rappol 1985). Dip angles in lodgment essentially mimic the crystal fabric of basal ice shear zones (Hudleston 1980). In this study, the grand mean dip angle for massive diamictons is 2.10°, well within the range of 2-8° suggested by Lawson (1979a).

Drake (1974) and Boulton (1976) suggested clasts in lodgment till dip preferentially up-glacier. Clast dip to the NW supports the interpretation of lodgment till since glacial flow is assumed to have been from this direction based on clast lithology. The mean and standard deviation of the S1 eigenvalues for 21 samples is 0.644 ± 0.124 which lies within the prescribed range of 0.635-0.773 offered for lodgment till by Domack and Lawson (1985).

Boulton (1976) suggested that basal meltout tills rarely exceed 2 m in thickness. Lodgment tills, can assume considerably thicker configurations (Lawson 1979b). The thickness of the structureless diamicton deposits examined here, therefore, support a lodgment process. Stacked diamictons could account for a greater thickness, but evidence for stacking was not observed in the above mentioned cases. Some criteria used to identify basal meltout till (detailed below) are not satisfied by the structureless diamictons and the most probable interpretation remains a lodgment process.

ii) Diamicton with Clastic Intrabeds

Description

A second type of diamicton observed in the region are matrix-supported diamicton units with clastic intrabeds (Plate 6). Four sections [W(2), III(2), IV(3), and X(4)] contain diamictons identified as this sediment type (Figure 12). Diamicton units range in thickness from 4.0 to 25.0 m, averaging 9 m. Except for the clastic intrabeds, these deposits resemble the structureless diamictons. Sediments are characteristically dark grey (eg. 10YR 4/1), hard, compact, and structureless.

The clastic intrabeds occur near the base of these diamictons in all cases. At Section Ware, the intrabed consists of a single poorly sorted sand and gravel lens, which is biconvex (vertically compressed oval) in shape (1.5 m long). In the remaining three sections (III, IV, and X), the intrabeds consist of thin (3-35 cm

Plate 6. Diamicton with clastic intrabed. Photograph shows base of Unit 4 at Section X. Massive sand bed in centre of massive diamicton. Pick for scale.

thick) granular sands, moderately sorted with sharp, undulatory upper and lower contacts. These sand intrabeds range from 1 m in length at Section III to 25 m at Section IV. The sand beds are < 35 cm thick, typically massive to horizontally laminated with minor planar cross-stratification. The intrabeds are restricted to within 4 m of the basal contact in the unit.

Texturally, the diamictons at all four sections are quite similar (Figure 17). Grain size ranges are 17-56% for sand, 20-48% for silt, and 21-49% for clay (Table 4). The average textural composition of 38 samples analyzed is 36 ± 8.3% sand, 30 ± 5.9% silt, and 34 ±6.1% clay. Modal and mean grain size is fine silt (6.1Ø). These diamictons are extremely poorly sorted (4.45Ø), near symmetrical (0.03), and platykurtic (0.81). These values are not significantly different from the values derived for bulk sediments classified as structureless diamicton. An almost identical compositional signature to the massive diamictons is evident for these diamictons in terms of moisture content (0.36 ± 0.30%), organic matter (1.23 ± 0.16%), inorganic carbon (10.73 ± 2.3%) and total carbon (11.83 ± 2.24%). As evident in Figure 18, there is a slight coarsening upwards in the individual units that are thick and apparently complete or not capped by erosional contacts (Sections X and III).

Stone content ranges from 20-45%, averaging 29%. Most clasts are subangular to subrounded, small to medium pebble sized. Limestone and dolomite clasts are commonly striated, and rarely faceted. A few cobbles occur, but no boulders. Lithologically, sedimentary and metamorphic clasts predominate over igneous rocks in all the units (Figure 19). Multiple samples from a single section and single unit indicate marginal clustering of pebble types. The lower ternary plot in Figure 19 shows a down-ice increase in the percentage of siliciclastics vs. carbonates and igneous/metamorphics for three of the sections.

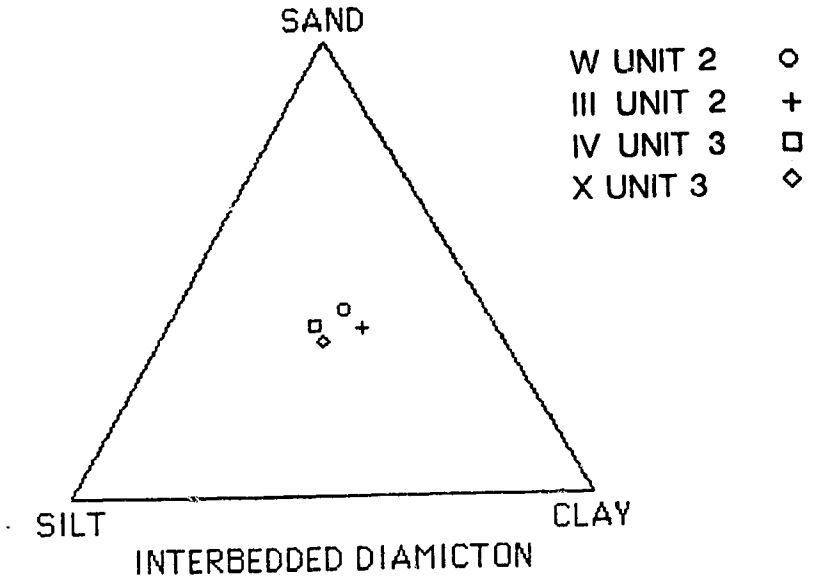

Figure 17. Ternary diagram illustrating textural variation in diamictons with clastic intrabeds at four sections.

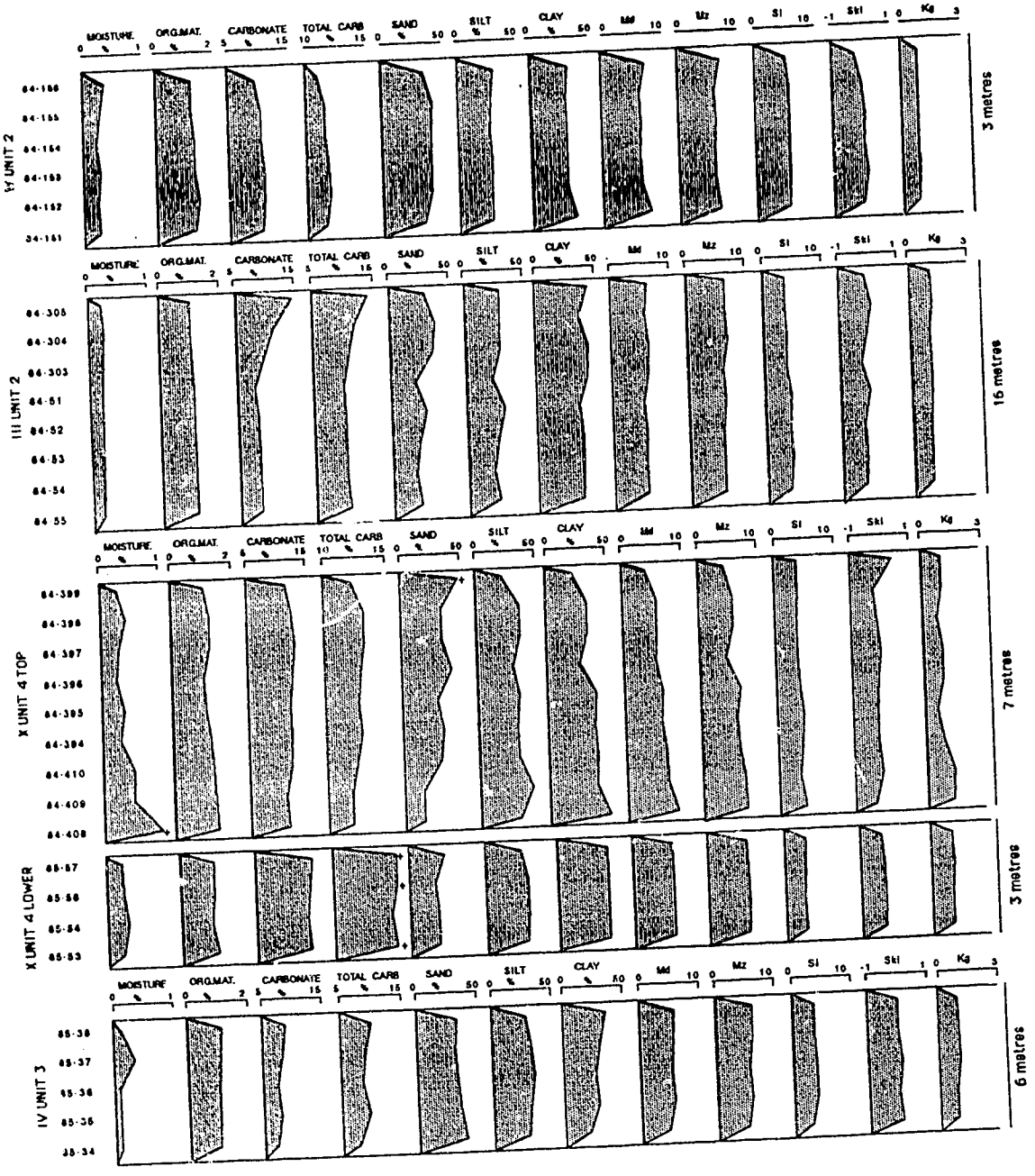

Figure 18. Compositional variation in massive diamictons with clastic intrabeds at four sections. See Figure 15 for caption detail.

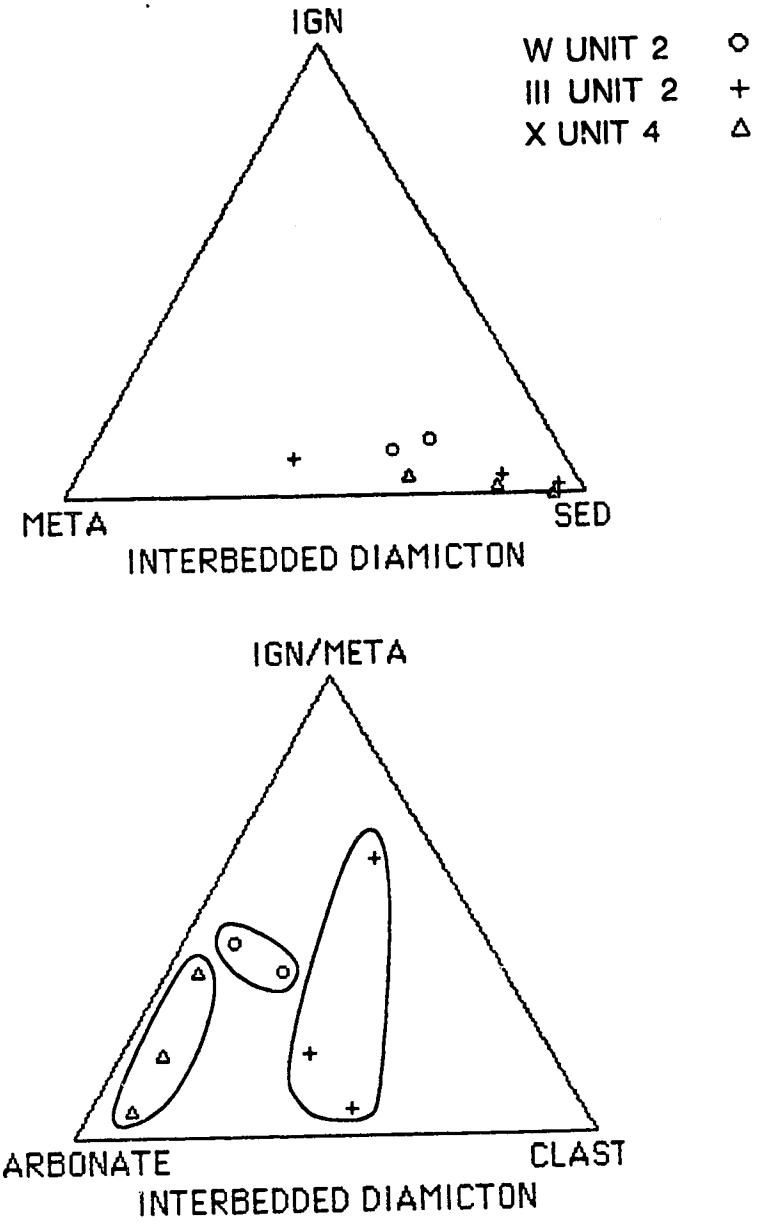

Figure 19. Pebble lithologies for diamictons with clastic intrabeds at three sections.

A total of 12 pebble fabric determinations were made. Three-dimensional stereo plots of these fabrics are given in Appendix 12. Overall, the 12 fabrics (600 clasts) displayed eigenvalues as follows: S1 (0.492-0.793), S2 (0.120-0.439), and S3 (0.045-0.183). At two sections [III(2), and X(4)], units were assumed to be complete, as the upper surfaces of the diamictons did not appear to be eroded. At these sections, fabrics were determined near the upper contacts of the units, in addition to the commonly determined basal positions. As such, the 12 fabrics can be separated into upper vs. middle and lower positions which indicate the trend upwards in any unit is a decrease in fabric strength. For instance, the S1 average at bottom vs. top for Section III is 0.755 and 0.712, and for Section X is 0.605 and 0.523. Secondly, upper fabrics cluster to the north, whereas lower fabrics show bipolar trends to the north and south. A final difference exists in the pattern of the distribution for the two positions. The top illustration in Figure 20 indicates that the basal fabrics are preferentially clustered, whereas the upper fabrics are preferentially girdled. The scattered points shown in the middle illustration of Figure 20 suggests there is no significant pattern in the interdependence of the three eigenvalues.

The basal contacts for diamictons with clastic intrabeds are gradational in all cases. The lower facies of Unit 4, Section X and the underlying Unit 1 at Section III consist of a 1-2 m thick, banded silty clay interbedded with diamicton. At sections Ware and IV, the units grade down over a distance of 1 m into clast-supported deposits. At Section W, the diamicton grades up into gravels, sand and interbedded diamicton. At the remaining three sections, the upper contact is sharp, and conformable. At Section III, diamicton is overlain by silty clays, at Section IV by terrace sediments, and at Section X by ice proximal normally graded gravels.

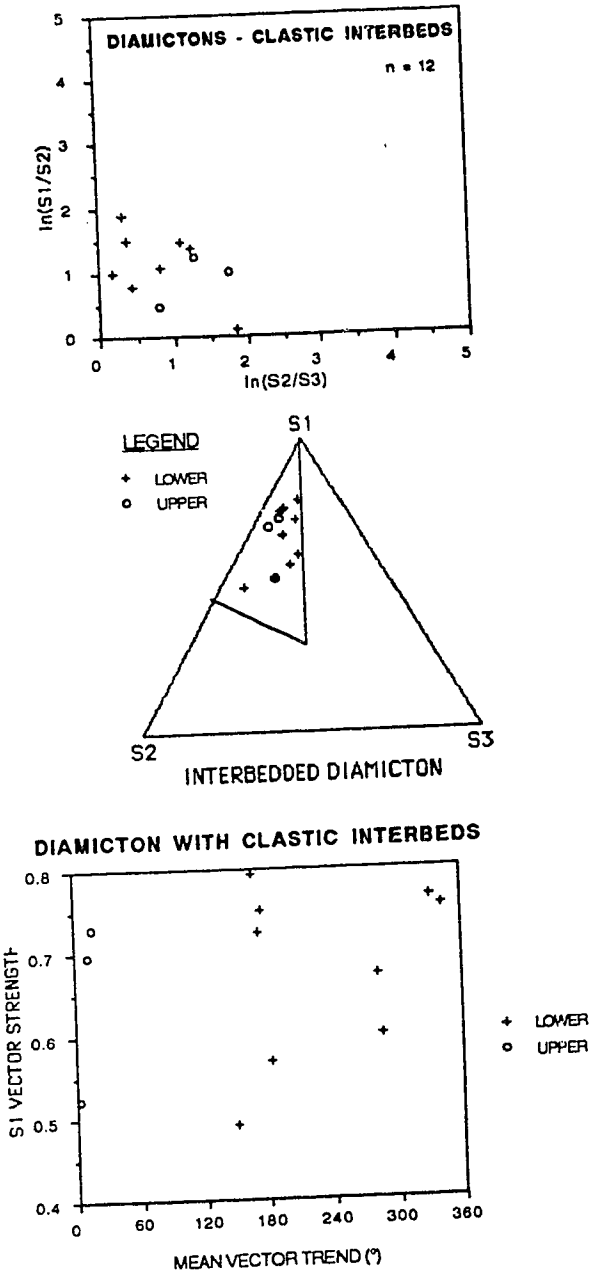

Figure 20. Pebble fabric statistics for diamictons with clastic interbeds. Top shows two-axis ratio plot of normalized eigenvalues, centre shows ternary plot of normalized eigenvalues, bottom figure shows 3-D fabric trends relative to the S1 value. N=12 samples (600 values).

Interpretation

Massive diamictons with clastic intrabeds are interpreted to represent basal tills, primarily meltout tills (cf. Haldorsen and Shaw 1982). A number of criteria support this interpretation. An original basal or englacial transportation position in ice for the sediment is inferred on the basis of clast lithology. Local lithologies predominate in the pebble counts, an indication of original basal transportation (Haldorsen 1982). The mean sorting coefficient for massive diamictons with clastic intrabeds is high (4.45Ø), and therefore similar to the value determined for the structureless diamictons. Similarly, skewness in the intrabedded diamictons (0.03 ± 0.13) is close to that determined for lodgment tills (0.02 ± 0.11). Both criteria are characteristic of basally transported ice debris (Vørren 1977).

Except for individually preserved strata, meltout till is essentially massive (Lawson 1979b). The observation of clastic intrabeds is frequently cited in the recognition of meltout till deposits (Shaw 1982), although some researchers suggest sand interbeds to be present in lodgment tills (cf. Marcussen 1975). Clastic intrabeds are assumed to represent englacial stream channels or sheets preserved during subglacial meltout within the massive matrix (cf. Shaw 1982). It is possible that the subglacial shear of sediments and bedrock that occurs during the process of lodgment is mistaken for true clastic intrabeds by some researchers (eg. Marcussen 1975). These smudging and attenuation planes which can occur along the base of a lodgment till are similar to clastic intrabeds but are not the same as those described here or in other meltout situations (eg. Levson 1986). The presence of striated clasts supports glacial ice as a transport mechanism, whereas the absence of faceted clasts precludes lodgment processes (Krüger 1979).

Fabric data provide the most conclusive collection of evidence suggesting a meltout process for sediment genesis. The mean resultant S1 eigenvalue is exceptionally high (0.794) and falls in the suggested range (0.748-0.887) for

several modern examples of meltout till observed by Lawson (1979a). Clast dips for the pebble fabrics support a meltout hypothesis. Overall, diamictons with clasts that show both up valley and down valley dips (bipolar) are attributed to meltout tills (Lawson 1979b; Dreimanis 1976). As evident in Figure 20, pebble fabric trends are both up and down valley. Lawson (1979a) proposed a range of 1-9° for average clast dip angles in meltout till deposits. In this study, diamictons with clastic intrabeds displayed comparable dip angles (1.1 to 13.2°). Shaw (1982) suggested that the S1 eigenvalue decreases in strength and changes from clustered to girdled distributions, up section through meltout till, a trend observed at all sections along the Finlay River where both upper and lower fabrics were determined. Finally, several authors have concluded that meltout till displays both parallel to flow and transverse clast orientations (Mark 1974; Boulton 1976), another attribute observed in these diamictons.

The transition at base into the banded diamicton illustrates the absence of sediment shearing and simultaneous sediment plastering during a lodgment process. The gradational transition into these banded diamictons suggests a continuous in situ accumulation of diamicton as would be the case with a meltout process.

The average thickness of 9 m for these diamictons exceeds the diagnostic limit of 2 m by Boulton (1978). Two explanations for this discrepancy include: 1) the upper few metres of sediment assigned to this lithostratigraphic deposit were deposited under different conditions; or more likely, 2) Boulton's 2 m thickness is perhaps artificial and does not take into account depositional sediment dynamics or different basal conditions such as subglacial cavities.

iii) Stratified Diamictons

Description

A third group of diamictons are classified as stratified diamictons. Although all examples are poorly sorted deposits, they share the unique characteristic of some form of internal "stratification", either visually observable or texturally quantifiable (Table 5). A second shared attribute is the divergent pebble fabric orientation compared to the diamictons discussed previously. Figure 21 provides the 2-D fabrics and 3-D statistics calculated from clasts in representative deposits. S1 eigenvalues range from 0.544 to 0.760. Mean trends do not appear to favor any particular direction, either parallel or perpendicular to the main valley orientation (Figure 22). They also show a tendency for girdled pebble fabrics rather than the uniaxial clusters common in the preceding diamictons. The sediments can be separated into three subtypes: 1) transitional; 2) banded; and, 3) normally and inversely graded diamictons.

Transitional Diamictons

Transitional diamictons are those diamictons which visually appear massive, but following laboratory analysis can be shown to be texturally and randomly heterogeneous (see ternary plot in Figure 26) (Plate 7). Examples of transitional diamictons can be found at five sections [O.D.(2), WII(3), VIII(4), IX(4), and X(8)] (Figure 12). Figure 23 illustrates the compositional variation in some of these sediments as a function of depth. All five examples are extremely loose, very poorly to extremely poorly sorted accumulations. Clast content is relatively low (10-20%), with striated pebbles occurring at Sections WII, O.D., and IX. Section VIII(4) and Section IX(4) are both silt dominated (61% and 50%, respectively), whereas Section X(8) is fairly equitable in grain size distribution, Section O.D.(2) is sand dominated (43%), and Section WII(3) is clay rich (47%). The fluctuating textural variation in

Table 5. Summary of various compositional parameters for stratified diamicton samples; according to banded, transitional, and graded categories. Min-minimum, Max-maximum, S.D.-standard deviation, and N-sample size. Moist-moisture content, O.M.-organic matter content, Carb.-carbonate content, and Total-total carbon content (all in percent). Md-graphic median, Mz-graphic mean, Si-inclusive graphic standard deviation, Ski-inclusive graphic skewness, and Kg-kurtosis.

		MIN	MAX	MEAN	S.D.	N
TRANSITIONAL (VIII UNIT 4)	SAND	1	36	15.05	10.46	19
	SILT	33	78	61.32	14.90	19
	CLAY	5	66	23.63	19.90	19
	MOIST.	0.32	1.95	0.94	0.38	19
	O.M.	1.74	11.94	4.75	2.59	19
	CARB.	2.35	7.79	4.50	1.40	19
	TOTAL	6.51	14.00	9.06	1.90	19
	Md.	4.30	8.70	6.20	1.35	19
	Mz	4.50	9.15	6.39	1.42	19
	Si	1.89	2.86	2.25	0.33	19
	Ski	-0.28	0.53	0.18	0.19	19
	Kg	0.92	2.13	1.45	0.41	19
TRANSITIONAL (IX UNIT 4)	SAND	8	19	12.86	3.53	7
	SILT	38	76	49.86	14.19	7
	CLAY	9	51	37.29	15.3	7
	MOIST.	0.19	0.48	0.31	0.1	7
	O.M.	1.43	2.29	1.81	0.29	7
	CARB.	4.80	22.83	9.76	6.06	7
	TOTAL	6.20	24.35	11.39	6.04	7
	Md	5.20	8.05	6.97	1.15	7
	Mz	5.37	8.63	7.55	1.17	7
	Si	1.79	4.16	3.31	0.74	7
	Ski	-0.01	0.59	0.17	0.21	7
	Kg	0.97	1.48	1.13	0.17	7
TRANSITIONAL (X UNIT 8)	SAND	30	34	32	2.83	2
	SILT	28	30	29	1.41	2
	CLAY	38	40	39	1.41	2
	MOIST.	0.27	0.28	0.27	0.01	2
	O.M.	1.16	1.18	1.17	0.02	2
	CARB.	11.56	12.81	12.19	0.88	2
	TOTAL	12.61	13.82	13.21	0.85	2
	Md	6.55	6.85	6.70	0.21	2
	Mz	6.23	6.53	6.38	0.21	2
	Si	4.52	4.67	4.59	0.10	2
	Ski	-0.08	-0.07	-0.07	0.01	2
	Kg	0.72	0.75	0.73	0.03	2

Table 5. Continued.

TRANSITIONAL (W2 UNIT 2)	SAND	15	28	20.29	5.28	7
	SILT	28	37	32.57	3.36	7
	CLAY	43	55	47.14	4.45	7
	MOIST	0.26	0.69	0.43	0.17	7
	O.M.	1.38	2.56	2.10	0.46	7
	CARB.	5.18	8.26	6.80	1.20	7
	TOTAL	7.35	9.71	8.76	0.86	7
	Md	7.20	8.35	7.64	0.44	7
	Mz	6.62	8.37	7.54	0.58	7
	Si	3.76	4.90	4.30	0.45	7
	Ski	-0.16	0.00	-0.09	0.06	7
	Kg	0.67	1.20	0.95	0.19	7
BANDED (W2 UNIT 1, III UNIT 1)	SAND	0	17	9.31	5.62	13
	SILT	23	60	39.92	8.92	13
	CLAY	35	68	51.77	8.43	13
	MOIST	0.26	0.60	0.43	0.12	13
	O.M.	1.47	2.86	2.09	0.50	13
	CARB.	4.94	12.61	7.77	3.01	13
	TOTAL	7.02	14.17	9.71	2.60	13
	Md	7.00	9.05	8.07	0.58	13
	Mz	7.15	9.52	8.23	0.68	13
	Si	1.93	3.96	3.15	0.63	13
	Ski	-0.29	0.27	0.05	0.14	13
	Kg	0.76	1.10	0.89	0.10	13
GRADED (MULTIPLE, II UNIT 9, IX UNIT 6)	SAND	20	55	38.70	8.78	23
	SILT	29	51	35.57	6.57	23
	CLAY	15	35	25.74	5.79	23
	MOIST	0.16	0.32	0.24	0.05	23
	O.M.	0.61	1.58	0.97	0.22	23
	CARB.	6.22	12.17	9.41	1.51	23
	TOTAL	7.22	13.26	10.29	1.53	23
	Md	3.5	6.55	5.19	0.87	23
	Mz	4.05	6.80	5.43	0.69	23
	Si	3.23	4.71	4.06	0.38	23
	Ski	-0.09	0.58	0.13	0.15	23
	Kg	0.72	1.32	0.95	0.18	23

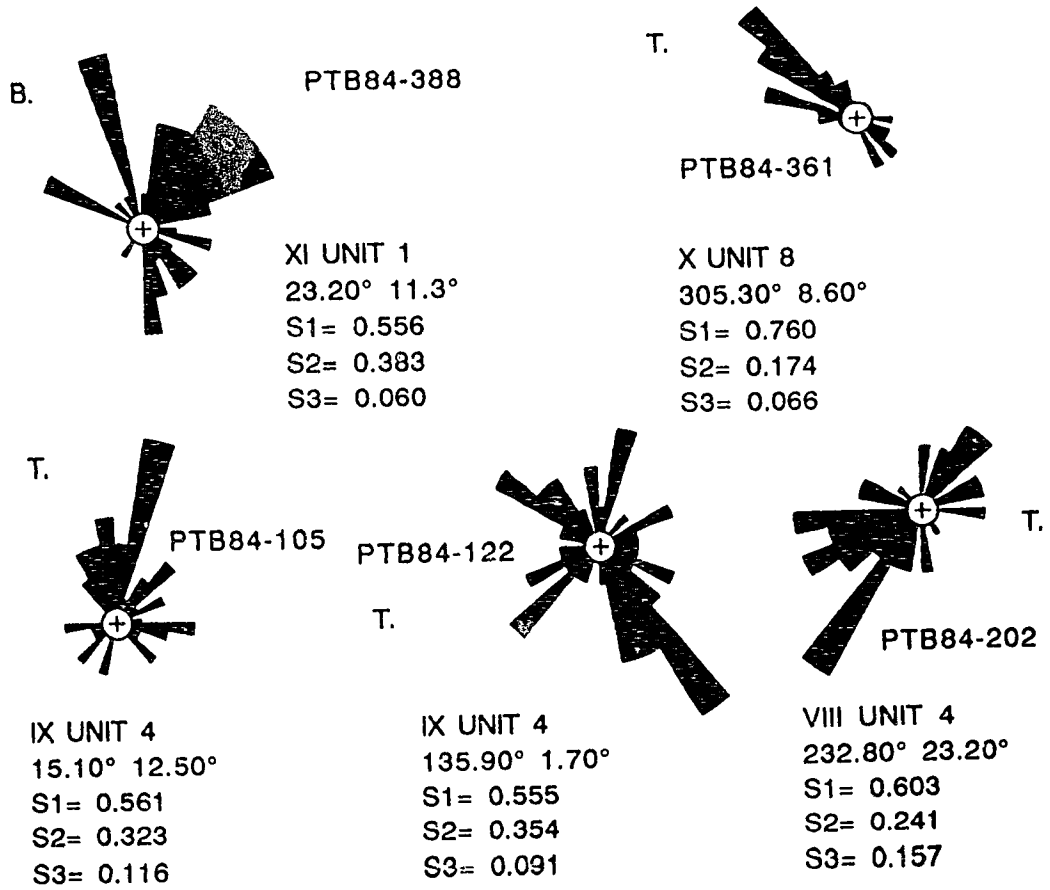

Figure 21. Pebble fabrics from several varieties of stratified diamicton for eight sections. Drawings 2-D, statistics 3-D. See text. B-banded, T-transitional, and G-graded diamictons.

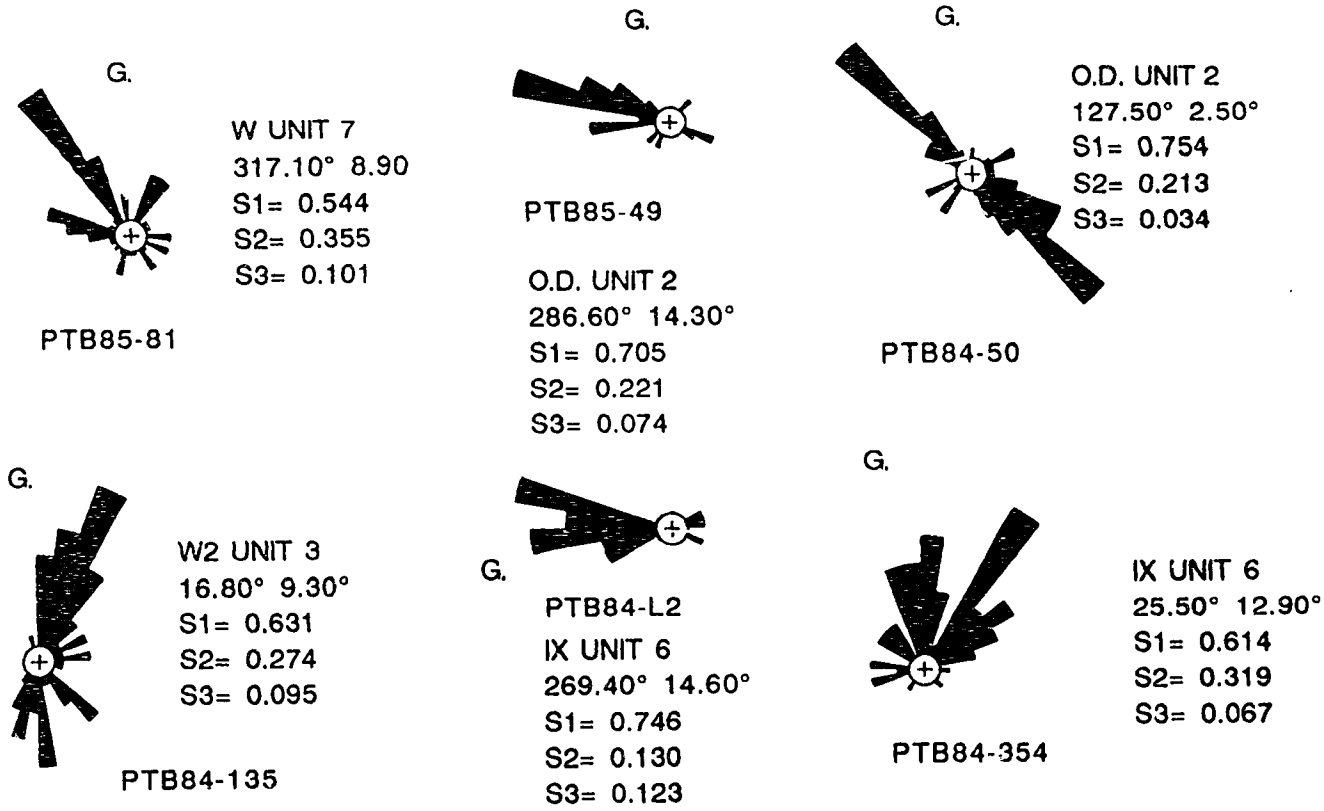

Figure 21. Continued.

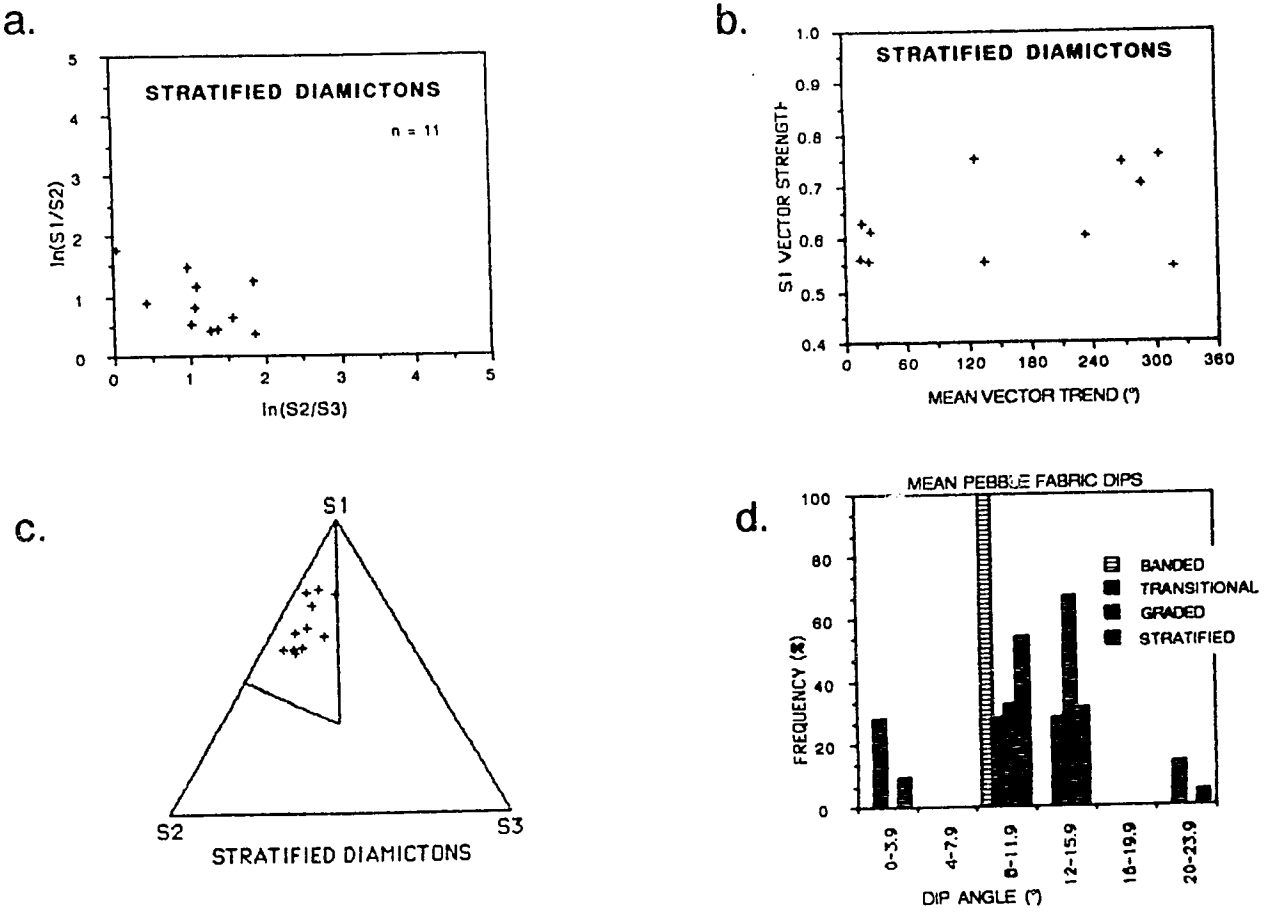

Figure 22. a) Two-axis ratio plot of normalized eigenvalues; b) 3-D pebble fabric trend vs. S1 strength; c) ternary plot of normalized eigenvalues for stratified diamictons; and, d) frequency plot of mean dip angles. See text.

Plate 7. Transitional diamicton. Photograph illustrates wood fragment within Unit 4 at Section VIII.

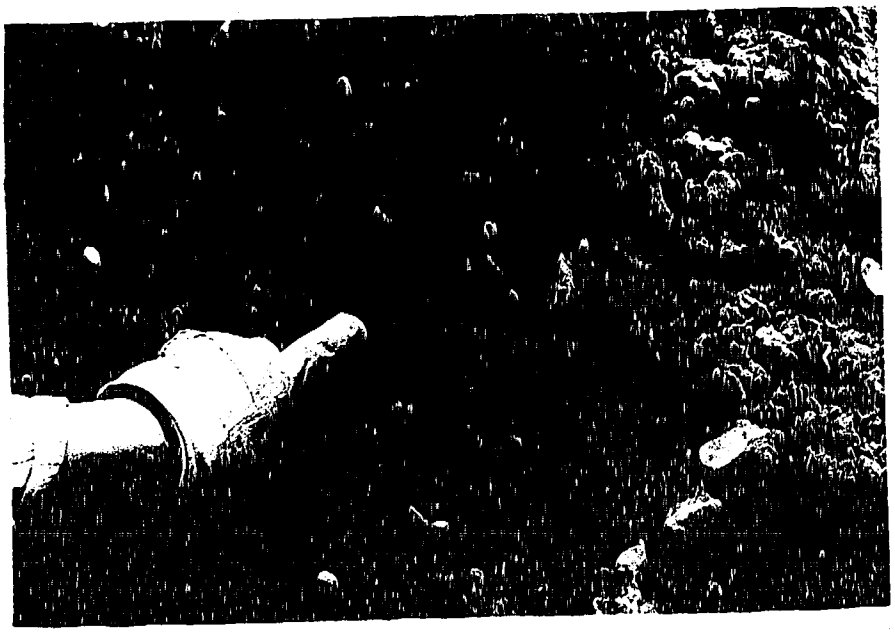

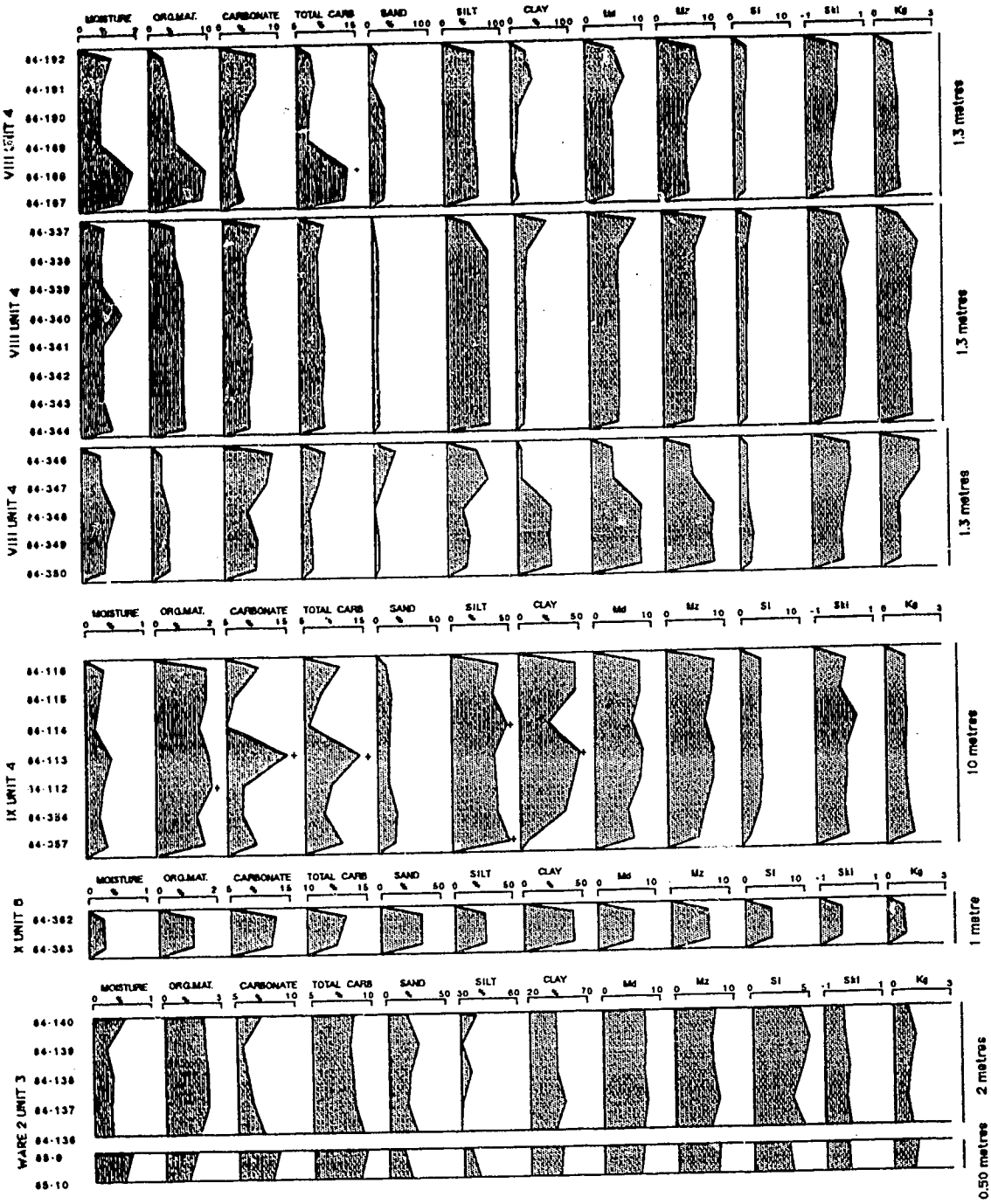

Figure 23. Compositional variation with depth and textural variation in transitional diamictons at four sections. Note changing scales along top. See text. See Figure 15 for caption detail.

the units is evident in Figure 23. Two of the diamictons (Sections VIII and X) are thin (~1 m thick), laterally short (<200 m) and rest on gravels. The stratified sediments at Section WII(3) and Section O.D.(2) are thin (2 and 4 m), and grade down into massive diamictons. At Section IX, Unit 4 is 10 m thick, laterally extensive (1300 m), and grades down into banded diamicton.

The pebble fabric at Section VIII (Unit 4) is valley transverse (232.8°) and displays a high dip angle (23.2°) and S1 eigenvalue of 0.603.. At Section IX (Unit 4) the two fabrics are valley oblique (15.1° and 135.9°) and have low S1 valuos (0.555 and 0.561). At Section O.D.(Unit 2) the mean pebble trends are oblique (286.6° and 127.5°) and show an up section increase in eigenvalues (0.705 and 0.754). At the Ware Two Section (Unit 3), the mean trend is also oblique (16.8°) with a moderate S1 value (0.631).

Paleomagnetic samples were taken from two locations in Unit 4, Section VIII (Figure 24). Equal area projections of the NRM field indicates normal polarity, with similar mean vector plunges (65°). Mean vector trends are toward the NW (322.5°) and N (2.1°) for the two localities, and both are extremely strong with S1 values of 0.945 and 0.988. Samples 4D4F-J indicate a clockwise progression of vectors up section, whereas samples 4D4A-E indicate an anti-clockwise progression of vectors up section. Several wood samples were collected from this unit and dated using ^{14}C and amino-acid racemization analysis. Radiocarbon dates are as follows: 32,750 ± 3180 years B.P. (AECV-382C), 36,510 ± 2570 years B.P. (AECV-350C), > 40,180 years B.P. (AECV-385C), > 40,330 years B.P. (AECV-381C), and > 40,400 years B.P. (AECV-383C).

Banded Diamictons

Five sections [WII(1), III(1), IX(4-base), X(4-base), and XI(1-base)] contain sediments described as banded diamictons (Table 5) (Figure 12 and Plate 8). These

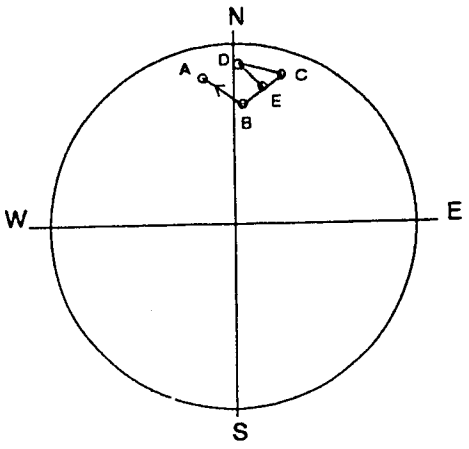

4B1A-E

SECTION W2-UNIT 1

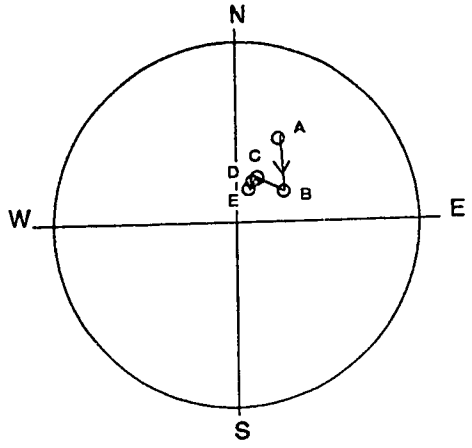

4C1A-E

SECTION II-UNIT 4

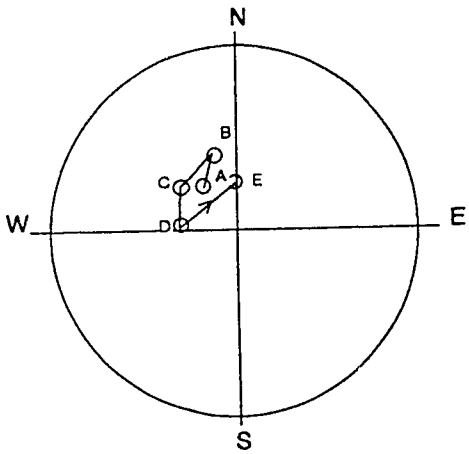

4D4A-E

SECTION VIII-UNIT 4
STATION ONE

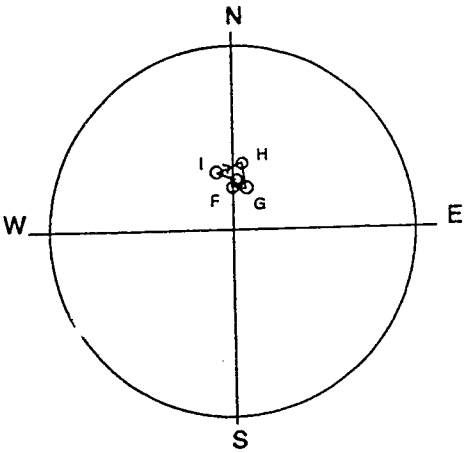

4D4F-J

SECTION VIII-UNIT 4
STATION TWO

Figure 24. Equal area projections of NRM polarity fields for samples from three sections. Letters indicate horizons and arrows illustrate progression from base to top of unit. See text for further explanation.

Plate 8. Banded diamicton. Photograph illustrates intercalated beds of pebble rich and clay-dominated diamicton in Unit 1 at Section WII. Unit underlies structureless diamicton. Pick handle for scale.

diamictons share the following characteristics: 1) all directly underlie and grade up into structureless diamictons or massive diamictons with clastic intrabeds; 2) where the lower contact is observable they overlie gravels; 3) are 2 m or less in thickness; 4) contain very few pebbles with the pebbles occurring as isolated clasts in distorted sedimentary layers or occurring as clustered stringers intercalated in a hard matrix; 5) display a low total carbon content; 6) where discernible, basal contacts are sharp, conformable, and convex down; and, 7) within each banded package, interbeds vary from 3-10 cm in thickness, and display sharp, erosive interbed contacts and flow structures. Particle size of the sediment changes up through the unit, and as in the case of transitional diamictons, no trend is apparent (Figure 25). Nonetheless, 13 samples indicate impoverished sand contents averaging 9 ± 6% sand, 40 ± 9% silt, and 51 ± 8% clay. All banded diamicton sediments are very poorly sorted (3.15Ø), near symmetrical (0.05), and platykurtic (0.89).

The single fabric associated with this type of lithostratigraphic unit provides a valley oblique mean fabric trend (23.2°) with a moderately steep dip angle (11.3°) and weak S1 value (0.556). An ungrouped, two-dimensional rose diagram illustrates the polymodal nature of the fabric (Figure 25). Paleomagnetic samples were retrieved from a single representative banded diamicton at the Ware II Section (Figure 24). All NRM determinations indicate normal polarity with the vector trend progression clockwise up section. The mean vector is to the north (5.1°) with a shallow dip (20.2°), and a strong S1 eigenvalue (0.955).

Graded Diamictons

An additional type of stratified diamicton are those matrix-supported sediments which display normal or inverse grading (Table 5) (Figure 12 and Plate 3). These diamictons are evident at three sections [II(9-base), W(7), and IX(6)] and occur either as isolated beds (Sections W, and II) or in multiple beds (Section IX). All graded

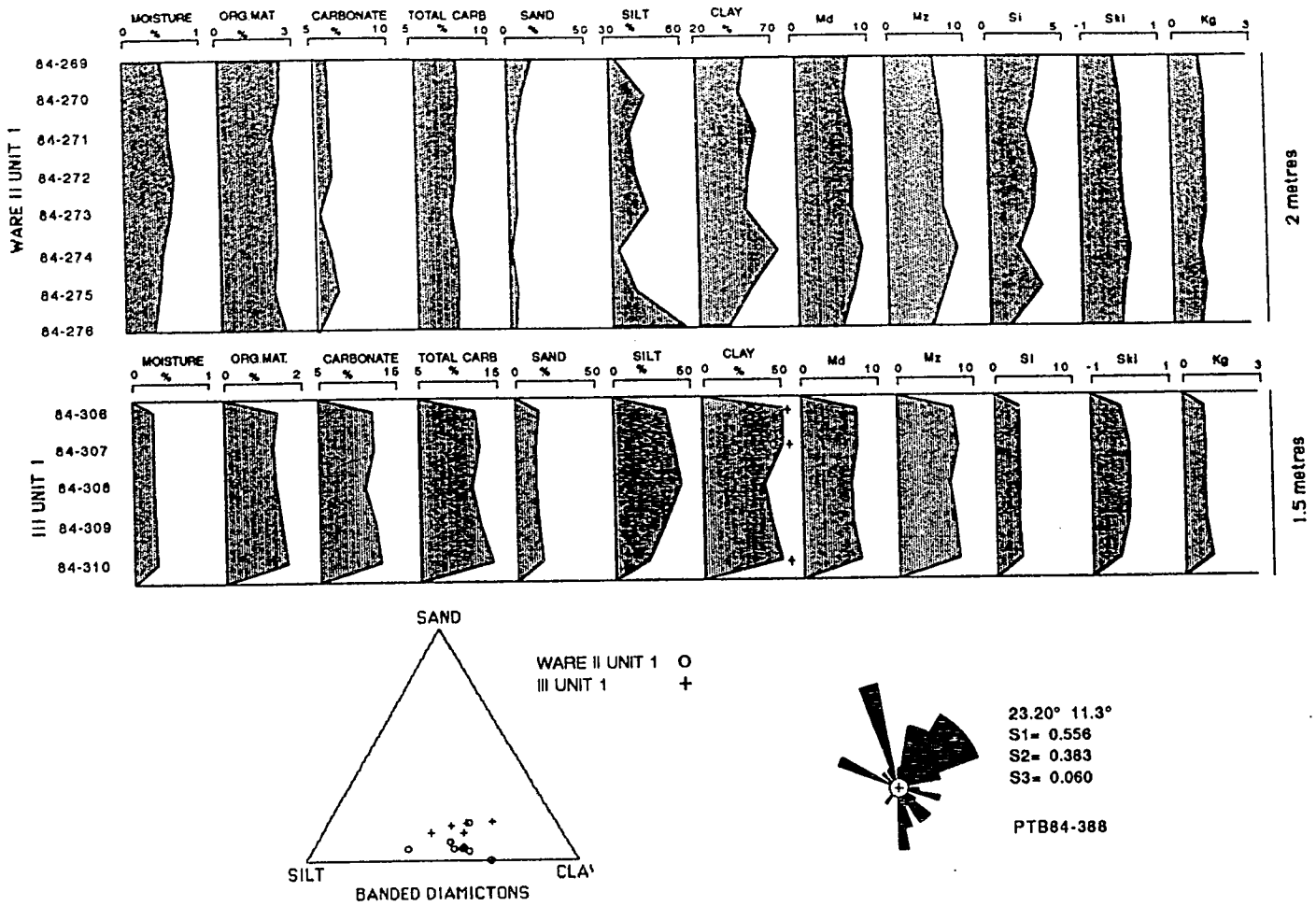

Figure 25. Compositional variation with depth and textural variation in banded diamictons at two sections. Pebble fabric from pebbly horizon within banded clay diamicton at base of Unit 1 at Section XI. Note changing scales along top. See Figure 15 for caption details.

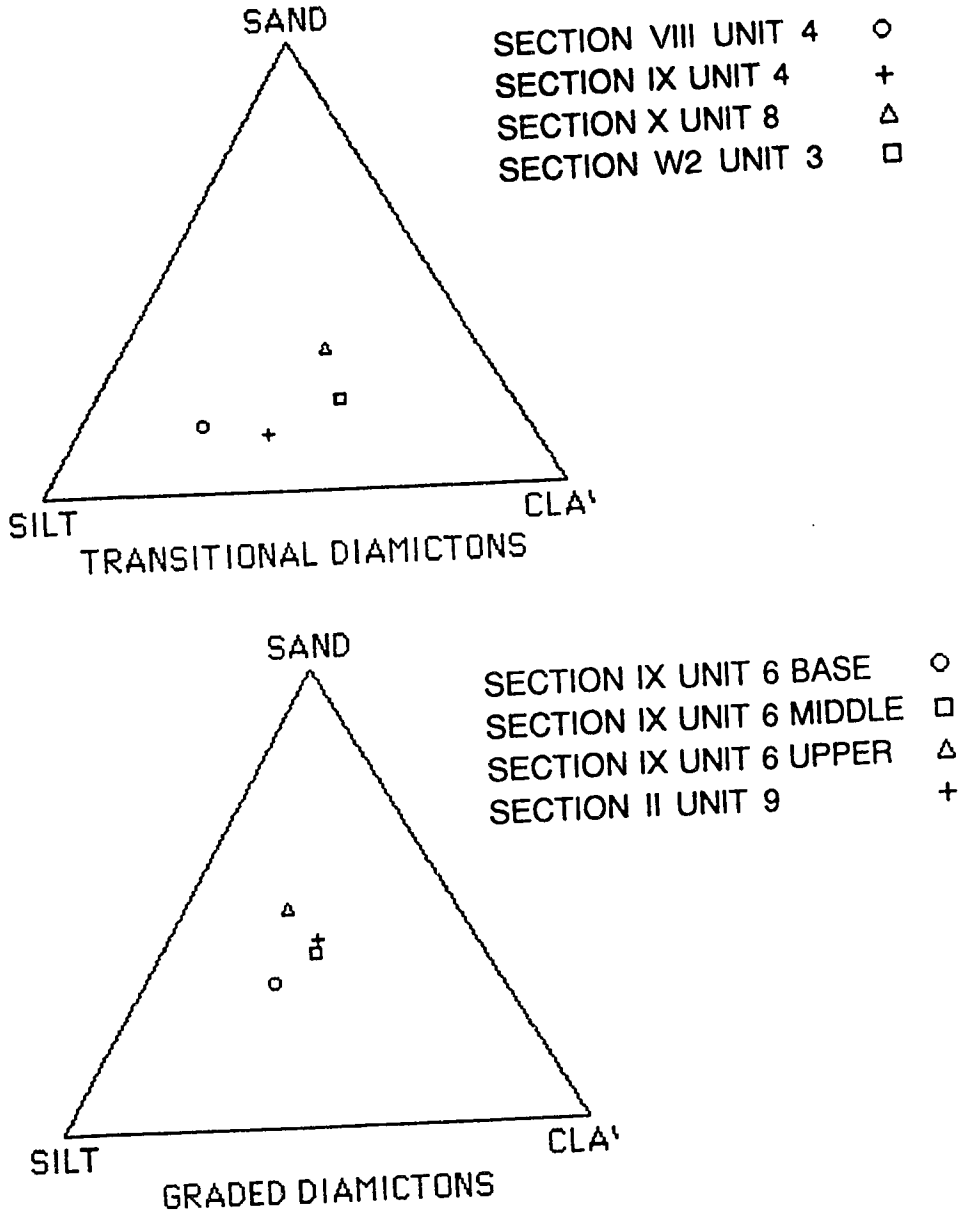

Figure 26. Ternary plots illustrating textural variation in transitional (four sections) and graded (two sections) diamictons. Note coarsening upwards in Unit 6, Section IX sediments. Compare to Figure 25 banded diamictons.

diamictons contain a moderate number of subangular to subrounded clasts (25-45%) ranging from granule to cobble in size. Faceted clasts were not observed and striated clasts were rarely present in isolated (normally graded) beds. Isolated occurrences average 1.5 m in thickness, overlie massive diamictons either gradationally or with a thin clastic wedge separating the two diamictons, and are generally loose and soft. Nine samples of isolated graded diamictons were obtained. The multiple inversely graded diamictons observed in Unit 6 at Section IX consist of several discrete beds intercalated with poorly sorted sands and gravels over a vertical height of 40 m. The maximum number of beds or their average thickness could not be determined, but 23 samples were retrieved. This multiple diamicton package overlies clastic sediments and the thick transitional diamicton described earlier.

Texturally, the isolated normally graded beds are quite coarse as evident at Sections W (Unit 7) and II (Unit 9) where averages are 48 ± 13% sand, 36 ± 16% silt, and 16 ± 4% clay. The multiple inversely graded beds are also coarse, averaging 39 ± 9% sand, 36 ± 7% silt, and 25 ± 6% clay. The gradual coarsening upward sequence at Section IX is evident both in field and laboratory observation (Figure 27). Isolated beds are very poorly sorted (3.74Ø), fine skewed (0.19), and leptokurtic (1.20). Multiple beds are extremely poorly sorted (4.06Ø), fine-skewed (0.13), and mesokurtic (0.95). Moisture content, organic carbon, inorganic carbon and total carbon is low for all graded diamictons examined (Table 5). Finally, the multiple inversely graded diamictons are intimately associated with a suite of dewatering structures and convolute laminations evident in the finer, intercalated ripple drift cross-laminated sands.

Pebble fabrics for this type of diamicton vary considerably. At section IX (6) the mean trends are oblique (269.4° and 25.5°), with steep dip angles (14.6° and 12.9°), and fairly strong S1 values (0.746 and 0.614). One fabric is strongly uniaxial, whereas the other is girdled. A similar situation is evident at Section W(7) except for

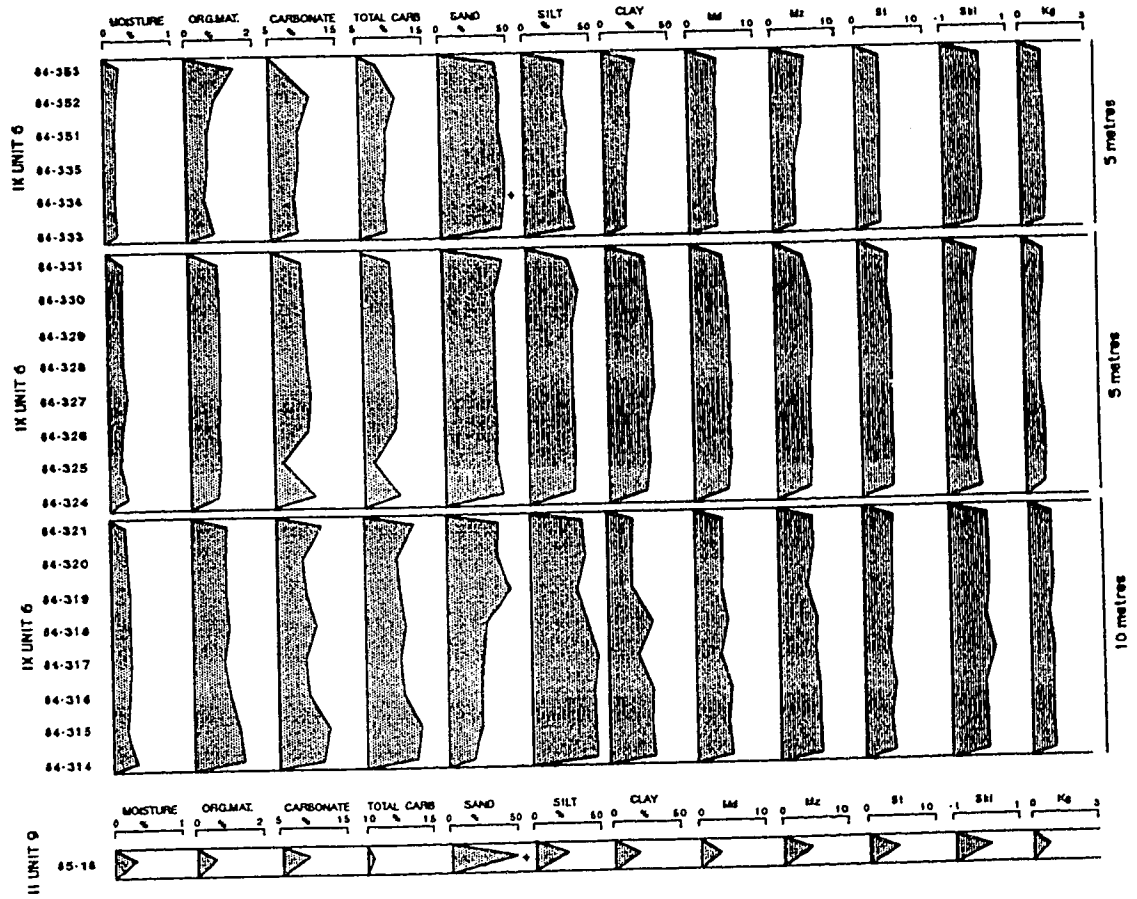

Figure 27. Compositional variation with depth for graded diamictons for two sections. Note changing scales along top and side. See Figure 15 for caption details.

the S1 eigenvalue (317.1°, 8.9°, S1= 0.544). This fabric is clearly girdled (see Figure 22). Wood was recovered from a stratified sand bed intercalated with the diamictons near the base of Unit 6 at Section IX. The resultant ^{14}C date on this wood is 29,280 ± 1230 years B.P. (AECV-352C).

Interpretation

The 13 examples of stratified diamictons examined in this study are interpreted according to the three subtypes discussed above. Three of the deposits discussed above are interpreted to represent some form of till, whereas the remaining ten deposits are all thought to be variants of sediment gravity flows.

Transitional Diamictons

The transitional stratified sediments at Sections O.D.(2) and WII (3) are interpreted to represent meltout till overlying lodgment till. The extent of basal vs. supraglacial contribution to the meltout deposits cannot be assessed in this particular study. Many of the diagnostic criteria for meltout till outlined in the previous section of massive diamictons with clastic intrabeds apply equally well to these two deposits. Several other criteria point towards a supraglacial meltout origin.

Both deposits are relatively thin, loose, and not compact. All are characteristics of basal meltout till (Dreimanis 1976). The upward coarsening of sediments at Section O.D. may indicate a transition into supraglacial meltout sediments (cf. Haldorsen 1982). At Section O.D. the S1 trend from Unit 1 to the top of Unit 2 is 0.570, 0.705 and 0.754, a trend considered indicative of a lodgment to meltout succession (Shaw 1979).

Stratigraphic position of these diamictons over sediments interpreted to be lodgment till strongly supports a meltout hypothesis for the diamictons. Section O.D.

resembles the sedimentary succession documented by Shaw (1979) for Sveg tills, in particular the upward sequence from basal massive till, to stony till and stratified till.

The interpretation of the Unit 4 Section IX diamicton is problematic. The lateral extent is at least 1800 m X 10 m, suggesting that the unit is not a matrix-supported sediment gravity flow deposit. All other attributes, such as the plunge of striated clasts, suggest a basal till deposit, but a lodgment or meltout interpretation cannot be established. The basal part of this unit is a banded diamicton commonly observed under other sediments in the area interpreted to be basal meltout tills. Similarly, this structureless unit displays a textural heterogeneity observed in other diamictons along the Finlay and interpreted to be meltout till. On the other hand, the thickness of the deposit corresponds most with other lodgment tills in the area. Both of the pebble fabrics are oblique (15.1° and 135.9°) to the valley trend, show flat to moderate dips (1.7° and 12.5°) and possess low S1 values (0.555 and 0.561), a collection of characteristics indicative of either lodgment or basal meltout.

The deposit may represent lodgment till which has undergone minor movement or destabilization in a post-depositional water saturated environment (= deformed lodgment till). Other (speculative) possibilities and variants of deformed lodgment till may occur during surge events or ice streaming. Surging of glaciers is an extremely common event in temperate and subpolar glaciers and is seen as the dominant process along the distal margins of the Laurentide glacier during the Late Wisconsinan (Clayton et al. 1985). Bruarjökull Glacier in Iceland for instance, surged five times in 350 years, providing an average periodicity of 70-100 years (Clapperton 1975). Documented surges range in length from 6-86 km on slopes ranging from 1-13.6° (McMeeking and Johnson 1986). Thick glacigenic sediment or diamicton up to 15 m is attributed to surges in many parts of North America by Clayton et al. (1985). During one documented surge the sediment (dirty ice?) in the base of the glacier dramatically increased in thickness from 1.5 to 10 m during the single event (Clapperton 1975).

The original laminar flow structure in the ice would be partially destroyed during the surge and the resultant sediments would be less compact. This would also explain the reduction in higher pebble fabric strength normally observed in either meltout or lodgment tills.

Ice streaming is also a plausible explanation for the presence of this type of diamicton. Seismic studies by Blakenship et al. (1986) indicated that in the Antarctic, ice streaming is a common process resulting in subglacial sediment deformation. Related research by Alley et al. (1986) confirmed the interpretation that up to 12 m of lodged? till undergoes deformation during ice streaming. The resultant sediment is frequently water saturated and not as dense as lodgment till. In this study, ice streaming under complete ice cover conditions or streaming via an outlet glacier may have also occurred and thus produced the deformed lodgment till.

Indirect evidence of surging (or streaming?) at this location is provided by geomorphology. The Finlay River valley does not display evidence of drumlins upstream of Section IX (Leslie 1988). Several drumlins do occur downstream of Section IX, but the greatest concentration is the drumlin field west of Section IX. Although the drumlins themselves do not necessarily indicate the presence of this type of diamicton, their development has been attributed to increased quantities of high density fluids along the ice front as occurs during surging (McCabe 1986) and ice streaming (Alley et al. 1986). Drumlinization is considered to occur in a very brief period of time and thus may be related to surging of the glacier (Dardis 1985).

The two thin and laterally restricted diamictons observed at Sections VIII (Unit 4) and X (Unit 8) are interpreted to represent isolated sediment gravity flow deposits. Both accumulations are spatially discrete and localized to a few hundred metres in length and 1.5 m in depth, with sharp basal contacts, and sheet-like form similar to most other debris flow deposits (Pierson 1981). Sediment gravity flow deposits appear massive but may show some form of random internal stratification (Nardin et

al. 1979), features which are evident at Sections VIII and X . The sediments are very poorly to extremely poorly sorted (2.25Ø and 4.59Ø), primarily matrix-supported with isolated, rare clasts. Similar features were noted in other debris flow deposits by Fisher (1971). Glacigenic flows commonly overlie either ice proximal outwash sediments or proglacial lacustrine sediments (Boulton 1970). At both Sections VIII and X the flow deposits overlie ice proximal gravels.

The two pebble fabrics are oblique (305.3°) or transverse (232.8°) to presumed glacial flow directions. Oblique and transverse fabrics were also observed in other sediment gravity flow deposits by Lawson (1979b). The presence of horizontal shear planes in sediment gravity flows are a result of internal laminar flow and, which encourages the formation of an oriented pebble fabric (Hampton 1975). Both deposits are pebble-poor, mud matrix flows, and therefore would be expected to display either parallel or transverse to flow fabrics, in contrast to sand matrix flows which typically show flow parallel fabrics (Gravenor 1986). Both fabrics show girdled distributions, typical for debris flows (Lindsay 1968). Calculated S1 values of 0.603 and 0.760 lie within or near the range for flows described by Gravenor (1986). Average S1 values, however, are generally lower for flow deposits (eg. 0.487-0.698) (Lawson 1979a; Visser 1983). The steep clast dips of 8.6° and 23.2° observed in this study, are also characteristic of sediment gravity flow deposits which show mean dip angles in the range of 2-29° (Domack and Lawson 1985; Rappol 1985). The preservation and occurrence of woody fossils in terrestrial tills is unlikely (Visser 1983) even though glaciers commonly redeposit organic materials (Gillberg 1977). The presence of wood in Unit 4 at Section VIII supports but does not discount a nontill interpretation. In summary, both deposits fulfill characteristics of Lawson's (1979b) Type III sediment flows.

According to Johnson and Rodine (1984) debris flows are highly mobile, contain 80-90% granular solids by weight, and move on slopes as low as 2-5°. Minimal water

content required to support movement of a debris flow is only 5% (Lowe 1982). Both deposits can be further classified as cohesive debris flows in Lowe's (1982) classification scheme or Type I plastic debris flows of Shultz (1984). A minimum of 5% clay content is required to maintain cohesive strength in a sediment (Postma 1986), a value which is greatly exceeded by both deposits . The random presence of clasts through both diamictons indicates dispersive pressures were a dominant supporting mechanism during transport rather than fluidal turbulence (Lowe 1979). Moreover, the presence of a moderate fabric indicates laminar flow instead of turbulent flow for the diamictons (Nardin et al. 1979).

The textural variation observed vertically through Unit 4 at Section VIII indicates poor mixing of the sediment during transportation. The presence of laminar shear (sediment heterogeneity) instead of turbulence (sediment homogeneity) during flow explains this observation. For the above reasons, fluidal flow deposits resulting from either turbidity current or fluidized flow are therefore not considered. The absence of water escape structures further eliminates the possibility of a liquefied flow type of deposit (Lowe 1982). Thus, grain flow or cohesive debris flow are the only possible depositional mechanisms. Inertial grain flows are exceptionally rare, require slopes of 18-28° and are usually < 5 cm thick (Lowe 1982). These attributes do not apply to the two diamictons under discussion. Both deposits (IX and VIII) are confidently recognized as debris flow variants, but further speculation on differences can be offered.

Unit 8 at Section X is interpreted to be a subaqueous flow deposit of limited extent, formed by cohesive freezing. The gradational contact of Unit 8 with overlying proglacial silts and sands suggests deposition by a proglacial debris flow. Also, high silt content [IX(8)] has been suggested to be indicative of subaqueous glacigenic debris flows (eg. Evenson et al. 1977). Subglacial water pulses at speeds in excess of 160 km/h have been documented in Switzerland (Iken and Bindschandler 1986). Turbid

discharges of water frequently observed along the margins of glaciers (Humphrey et al. 1986), and could be explained by such subglacial water pulses. A pronounced turbid water pulse debouching into a proglacial environment could have initiated the subaqueous debris flow responsible for the sediments evident at Section IX.

Unit 4 at Section VIII is interpreted to be a subaerial flow deposit of limited extent, also formed by cohesive freezing. The presence of abundant wood remains in the diamicton, not atypical in subaerial debris flows (Fritz and Harrison 1985), the absence of enclosing sediments suggestive of subaquatic deposition, and the superimposition over oxidized gravels (indicative of subaerial exposure) further point to a subaerial deposit.

Banded Diamictons

Banded diamictons in the Finlay River region represent subaqueous sediment gravity flow activity within a confined ice proximal environment. Small isolated catchment basins are commonly found in both ice-frontal and subglacial positions. Flame and load structures are present in the finer diamictons, as are isolated parallel lamination in siltier beds (cf. Visser 1983). The upward gradational transition into till (matrix-supported diamictons with clastic intrabeds) indicates the proximity of glacial ice during deposition of the banded diamictons. Therefore, the advancing ice either overrode the sediment pockets or subglacial deposition occurred in the depressions during the glacial advance.

The above arguments suggest that pulsating sediment wastage into small depressions occurred in the front of an ice advance or during ice advance. Subglacial deposition appears more likely for the following reasons: 1) ice proximal sedimentation in small depressions would require associated sediments to be advance outwash deposits, which are not present here; 2) ice proximal proglacial diamictons are unlikely to be preserved in advancing ice situations (Boulton 1968); 3) subglacial

cavities are a common feature beneath glaciers (Iken and Bindschadler 1986) and often act as sediment depots for resedimented glacial debris (Boulton 1970a, 1978); 4) dropstone features occur in the subglacial environment (Vivian and Bocquert 1973); and, 5) the stratigraphic position below diamictons with clastic intrabeds fits the proposed meltout genesis for the overlying sediments.

Graded Diamictons

The inversely graded multiple beds described at Section IX (Unit 6) are interpreted to represent a series of subaquatic sediment gravity flows accreting in a proglacial environment (cf. Eyles 1987). Although only the matrix-supported diamictons are discussed here, interbedding of these sediments with normally graded and inversely graded clast-supported gravity dominated flows and cross-bedded sands supports a dynamic depositional sequence similar to those observed for other ice proximal glacilacustrine deposits (Boulton 1972; Evenson et al. 1977; Eyles et al. 1987; McCabe et al. 1987). As noted by Boulton (1968), such deposits are most likely to occur in association with retreating rather than advancing glaciers. The sediment gravity flows entering a proglacial lake as density underflows reflect a continuum from distal liquefied flow deposits at depth (base of unit) to proximal cohesive debris flows at top. Basal flows with fluid escape structures, convolute bedding and homogenized sediment characterize liquefied flow deposit associations (Nardin et al. 1979). Interbedded sands displaying ripple drift cross-laminations and draped laminations have been observed in other proglacial environments (Ashley et al. 1985). The oblique pebble fabric trends and steep clast dip angles determined from Unit 6 are therefore similar to the cohesive debris flows reviewed earlier. Shultz (1984) and others (eg. Nardin et al. 1977) noted that a single sediment flow can undergo any number of changes during flow passage and thus shift from one flow type into another. Sediment deposition at any one time during this continuum would

preserve either laminar or turbulent flow characteristics. Lastly, acceptable ranges of thickness cannot be offered for subaquatic flow deposits, since Gorsline (1984) recognized turbidity current deposits (called unifites) in excess of several metres and Cas and Landis (1977) measured a single Oligocene debris flow deposit 8 m thick. All glacigenic flow deposits observed in the glacilacustrine sequence at Section IX are less than 8 m thick.

A number of processes control the textural variability observed in these sediments. First, progradation into the glacilacustrine basin evident at Section IX and concomitant infilling by sediments resulted in a gradual coarsening upwards in the sequence as each deposit represents a more proximal position to the fluvial source (Figure 26). Secondly, the low percentage of clay relative to other diamictons in the valley is a product of isolated traction currents moving along the slope of the basin (generated by incoming meltwater streams) and winnowing out of the fine fraction (cf. Eyles et al. 1985). Current flow and dewatering are indicated by the presence of deformed cross-bedded sands underlying the diamictons (Plate 9).

Isolated normally graded diamictons ubiquitously overlie massive diamictons in the study area. Typical examples include Unit 7 at Section W and the basal bed of Unit 9 at Section II. All of these sediments resemble the supraglacial flow deposits of Boulton (1968), Eyles (1979), and Haldorsen (1982). These poorly sorted sediments, with angular clasts, in a poorly compacted matrix, reflect debris flow sedimentation in a shifting ice proximal environment during deglaciation. The absence of large boulders and thick sediment layers, generally common in valley glaciation sequences (Levson 1986), reflects the great distance to valley sides in the study region and thus the paucity of supraglacial debris on the decaying or retreating ice mass.

Plate 9. Dewatering features, convolute laminae, and micro-faults in silt/clay laminations within sand bed at base of Unit 6 at Section IX.

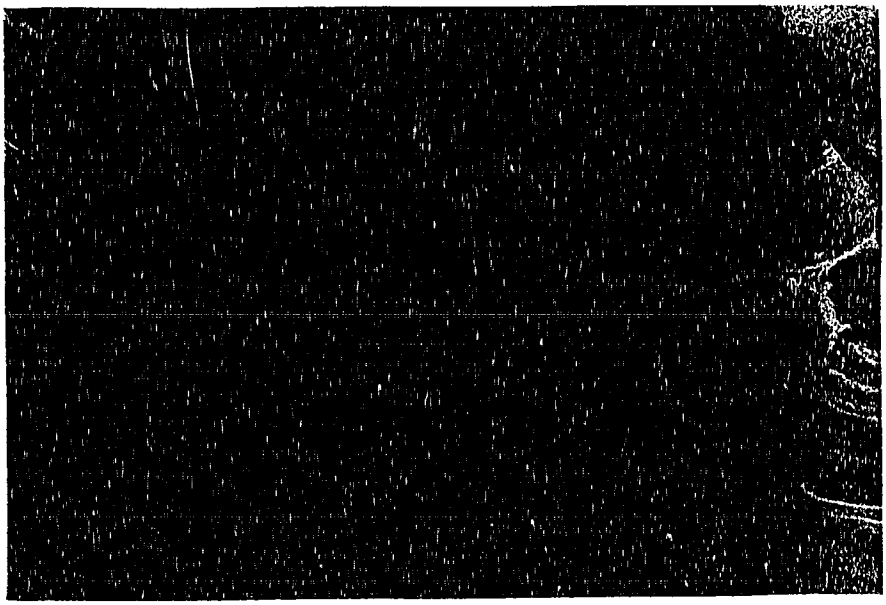

D. GRAVELS

Four sediment types grouped as gravels represent the majority of the sediment observed in the study area. Deposits classified as gravels have pebble concentrations in excess of 50% of the granular composition of the sediment. Minor constituents never exceed 50% by area (and assumed volume). Fining upward and coarsening upward sequences reflect the lithostratigraphic unit characteristics, whereas internally the unit itself may contain multiple beds of normally and/or inversely graded beds. The following five gravel types are recognized: 1) massive gravels; 2) normal and inverse graded gravels; 3) stratified gravels (with and without sand and diamicton interbeds); 4) disrupted gravels; and, 5) inclined gravels.

i) Massive Gravels

Description

Massive gravel accumulations are present at most sections examined in the study region (Plate 10). Massive gravels are never found in isolation, but occur in association with the following sediments: 1) crude, horizontally stratified gravel beds (Sections W, II, III, IV, V, VII, VIII, IX, and X); 2) normally graded gravel beds (Sections W, II, O.D., and IX); and 3) inversely graded gravel beds (Sections W, I, II, VIII, and X) (Figure 12). In the latter two situations, massive gravels typify the deposits, but grading in the unit is also an important feature indicative of separate processes. Because of this grading, normally graded and inversely graded gravel deposits are discussed separately below.

Detailed lithologs at several sections indicate similar characteristics for massive gravel beds. Thickness ranges from 0.2-5.0 m at Section III and 0.3-6.0 m at Section V. Mean thickness for these beds is 1.1 m and 2.2 m, respectively. Texturally, clasts consist of <1% boulders, 7-50% cobbles, 10-35% coarse pebbles, and 10-40% fine pebbles, with varying amounts of interstitial sand, silt, and clay as matrix. All clasts

Plate 10. Massive gravel bed at Section VIII.

are rounded to well-rounded. Imbrication is not evident and fabric is essentially unordered. Massive clast-supported beds are rarely open-worked, but more commonly are infilled with a coarse sand to granule matrix. Open-work gravels display pronounced manganese staining, whereas some matrix-filled beds display minor oxidation. Upper and basal contacts of massive gravel beds are always gradational or indistinct into other gravels. Where overlain by sands, the upper contact is conformable. The lower contact is loaded where the gravels overlie pebbly sands.

Three massive beds interbedded with horizontally stratified gravels at Section II (Unit 3) were examined for their internal pebble fabrics. The three rose diagrams in Figure 28 illustrate the 2-D trend of measured clasts in this unit. Of significance here is the moderate down valley trend and moderately strong plunge of the mean vectors in the bottom two figures and the strong transverse fabric in the upper diagram. This valley parallel and transverse trend is also apparent in the bottom illustration of Figure 30. All three fabrics are strongly girdled. S1 eigenvalues for the three fabrics are: 0.604, 0.623, and 0.474. Average sample plunges of the clasts are very steep: 14.1°, 9.4°, and 9.9°.

Interpretation

Massive clast-supported gravels represent the Type III pseudoplastic debris flow deposits (Figure 7) of Shultz (1984) or the density modified grain flows of Lowe (1982), deposited within a braided fluvial environment. Deposition occurred as clasts settled out of the bed load during mass flow or stream flood events, occasionally followed by settling of an interstitial mixture of sand, silt, and clay. Large clasts are supported during transportation by buoyancy of the granular-water mixture and turbulence (Lowe 1979). This support is due to granular interaction which causes dispersive pressures to be generated normal to the perceived shear planes through viscous or inertial contact (Shultz 1984; Nardin et al. 1979). As flow velocity is

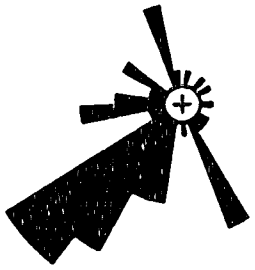

220.40° 14.10°
S1= 0.604
S2= 0.346
S3= 0.50

PTB85-92

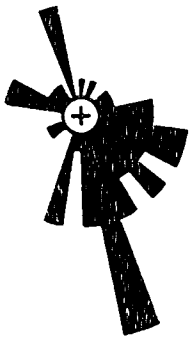

137.80° 9.40°
S1= 0.623
S2= 0.294
S3= 0.083

PTB84-39

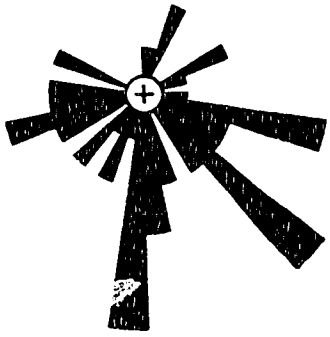

130.20° 9.90°
S1= 0.474
S2= 0.433
S3= 0.093

PTB84-39B

Figure 28. 2-D unidirectional a-axis pebble fabrics for density modified grain flows at Section II, Units 3 and 4. Sample number, trend, plunge, principal eigenvalues provided for each fabric based on 3-D calculations.

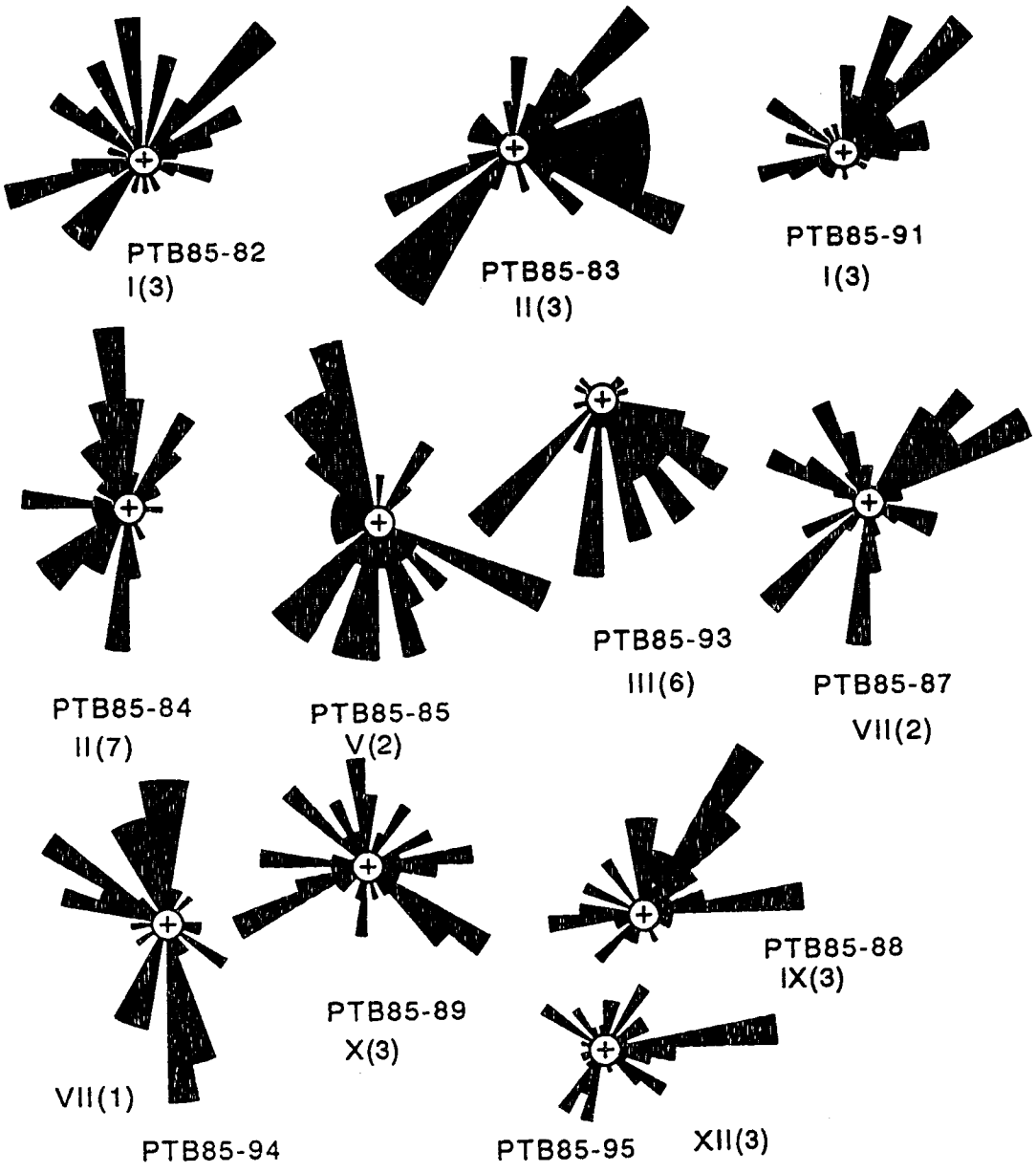

Figure 29. 2-D rose diagrams of pebble fabrics in stratified gravels from various units and sections. A-axis orientation illustrated. Sample number, section and unit shown.

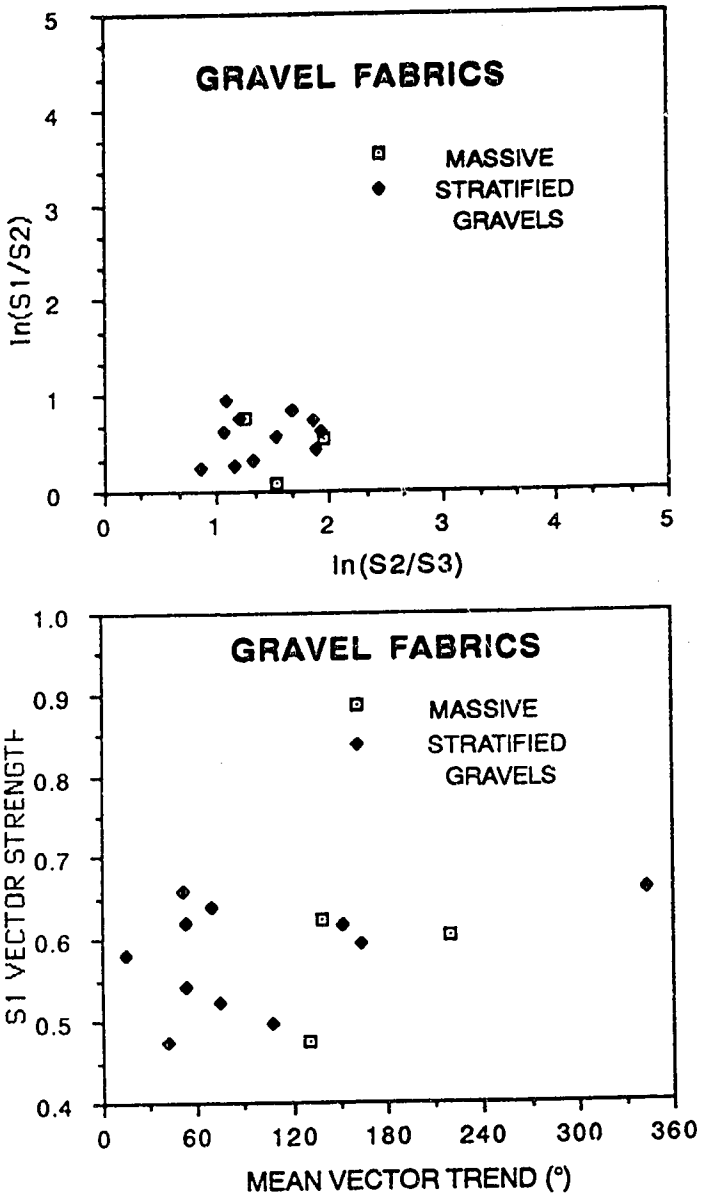

Figure 30. Top illustrates two-axis ratio plot of normalized eigenvalues; bottom illustrates 3-D pebble fabric trend vs. S1 vector strength for various types of gravel deposits. See text for further explanation.

reduced, clasts are abruptly deposited by grain to grain contact or frictional freezing. The spherical nature of the clasts precludes the development of strong clast imbrication. Nonetheless, the observed fabrics of 0.474 and 0.623 fall near or in the range of "flows" (0.525-0.606) given by Dowdeswell et al. (1985), "lahar flows" (0.424-0.642) by Major and Voight (1986), and "flows" (0.487-0.698) by Lawson (1979). The observed girdled distributions are also typical of "debris flow" sediments, according to Lindsay (1968).

Massive gravel beds in modern braided environments range in thickness from 0.25-3.75 m (Hein 1984), a range similar to that observed in these examples. The gradational contacts between massive gravel beds and other gravels indicate continuous but pulsating or fluctuating flow during a single ongoing event (Walker 1975). Intimate association of massive gravels with the normal/inversely graded gravels and crudely stratified gravels indicates proximal accumulations. The coarse braided river accumulations documented for the proximal reaches of Scott River by Boothroyd and Ashley (1975) closely resemble the deposits described here. An analogous massive gravel deposit is also located along the Lewis River of B.C., illustrating the facies association with crudely stratified gravels (Church and Gilbert 1975). Hein (1984) noted that massive gravels in combination with horizontally stratified gravels dominate the modern braided river environment (74% by frequency), concurring with the high frequency observed here.

ii) Normal/Inverse Graded Gravels

Description

Gravels displaying both a decreasing (normal grading) and increasing (inverse grading) change in clast size occur at many sections in the valley (Plate 11). Beds range in thickness from 0.25 to 7.00 m. Thin (< 1 m) isolated gravel beds displaying textural gradations are present in moderate frequency throughout the various gravel-

Plate 11. Inversely graded gravel bed at Section VIII.

and sand-dominated deposits. In the following discussion, attention is directed to the thicker (≥ 1 m) clast-supported accumulations whose textural transition dominates the composition of various lithostratigraphic units, although the genetic interpretations which follow apply equally to all thicknesses of graded beds. Pronounced normally-graded gravels are present at four sections (Sections W-Unit 6, II-Unit 9, O.D.-Unit 3, and X-Unit 5). Inversely graded gravels occur at six sections (Sections W-Unit 4, I-Unit 4, II-Unit 7, VIII-Unit 7, X-Unit 7 and X-Unit 3). As evident in this listing, normally and inversely graded gravels occur in units and sections where massive gravels are also present (Figure 12).

Normally Graded Gravels

Normally graded gravels range in thickness from 1.0-5.0 m and average 3.75 m. These gravels overlie massive diamicton (Section W) and massive diamicton with clastic intrabeds (Section X) with sharp, erosive basal contacts; or overlie stratified diamictons (Sections II and O.D.) with gradational contacts. Texturally, clasts consist of ~5% cobbles, 15-25% coarse pebbles, and 35-50% fine pebbles. Clasts are primarily subrounded to rounded in both open-work and matrix-filled gravel networks. Imbrication is poor and fabric is random at the base of units. Near the top of the units imbrication improves with b-axis dipping up-valley. Matrix ranges from 0-35% granules, 60-95% sand, and 5-17% silt and clay. Normally graded gravels grade up into horizontal and planar cross-stratified sands and silts, with isolated diamicton interbeds. Limited stacking of normally graded beds was observed.

Inversely Graded Gravels

Inversely graded gravel beds range in thickness from 2.0 to 7.0 m with an average of 5.0 m. These beds are overlain either by structureless diamicton (W, II, and VIII), massive diamicton with clastic intrabeds [X(3)], stratified diamicton [

X(7)], or postglacial sand and gravel (I). Upper contacts vary from conformable and undulatory to gradational. Pebble lithologies in the inversely graded gravel beds resemble the compositional signature of the underlying sediments and the overlying diamictons. Clasts are rounded to well-rounded and exhibit poor imbrication and fabric. The upper parts of these beds contain a high percentage of cobbles (15-25%), with coarse and fine pebbles comprising the remainder (75-85%). Most of the gravels are open-work with manganese oxide staining, but matrix-filled gravels are also present. Inversely graded gravels are underlain gradationally by horizontally stratified gravels and horizontal and planar cross-stratified sands. Stacking of inversely graded beds was not observed. Inversely graded gravels are rare relative to other gravel accumulations (< 20% by volume).

Interpretation

Normally Graded Gravels

The normally graded sediments described above typify Shultz's (1984) Type III debris flows (Figure 7) and Lowe's (1982) modified grain flows. According to these authors, clasts first settle out during plastic (Bingham) flow, and then often grade up into matrix-supported diamictons. The gravels therefore represent the short lived bedload of flood or mobile mass flow events. The normally graded beds are frequently interbedded with horizontally stratified gravels throughout the region. These fining upward sequences are normal clastic sediment response products to waning flow in the fluvial environment (cf. Miall 1977).

The fining upwards packages directly overlie diamictons of glacigenic origin. Both lodgment till and basal meltout till underlie these thick accumulations of poorly sorted gravels. These sequences are also associated with isolated glacigenic sediment gravity flow deposits, interpreted to represent cohesive debris flows moving off the melting ice mass. Therefore, the normally graded clast-supported gravels are

interpreted to represent part of a resedimented supraglacial/ice proximal braided stream package associated with valley deglaciation, similar to that documented by Boulton (1968). Lawson (1982) argued that resedimented deposits predominate in actively melting valley glacier environments.

An original supraglacial origin for the debris flow sediments is inferred on the basis of characteristics usually associated with supraglacial sediment packages including angular clasts and superposition over till. The angular oxidized clasts lacking glacial striations observed in this study point to a supraglacial origin (cf. Boulton and Eyles 1979). During sediment flow associated with active ice wastage, winnowing out of the finer fraction can occur. Rapid coarse particle sedimentation accompanied by minor sorting can follow, allowing creation of the graded texture. In the braided stream environment, normally graded gravels are rare (10%) (Hein 1984). Normally graded gravels are rare along the Finlay River supporting the braided stream hypothesis.

Inversely Graded Gravels

Inversely graded clast-supported gravels are interpreted to represent Type II or IV (Figure 7) sediment gravity flows of Shultz (1984), cohesionless debris flows of Postma (1986), or modified grain flows of Lowe (1982). These high concentration grain flows are commonly > 0.4 m thick, massive to inversely graded, clast-supported with or without interstitial fines (Lowe 1982). Oriented fabrics can develop during flow (Shultz 1984) and are usually parallel to flow and imbricate upstream (Nardin et al. 1979). Intergranular dispersive pressure in the form of inertial contact is hypothesized to be the primary support mechanism during transport of these gravels (Nardin et al. 1979; Shultz 1984). According to Walker (1975), the coarse gravel fraction is transported as a highly concentrated traction carpet along the bed with rapid frictional freezing (internal shear strength < yield strength) as velocity drops,

thereby preserving this structure. Gradual settling out of the clasts is not possible, as settling would result in normally graded sediments. The traction carpet which moves by laminar flow is further driven by an overriding turbulent flow (Lowe 1982). Gradational basal contacts are common for inversely graded debris flows (Fisher 1971). Although rare, inversely graded gravels can represent proximal accumulations. The number of inversely graded beds (out of the total) is similar to the value of 16% proposed for braided stream environments by Hein (1984). Finally, the association of these gravels with overlying diamictons interpreted as tills (Sections W, II and X-Unit 4) or glacigenic sediment gravity flow deposits (Section X-Unit 8) supports the ice proximal model.

iii) Stratified Gravels

Description

Stratified gravels represent the most ubiquitous sediment type within the northern Rocky Mountain Trench (Plate 12). This gravel type is restricted to clast-supported beds displaying crude to well-developed horizontal stratification, large and small scale trough cross-stratification and low angle planar tabular cross-bedding. Sand and/or diamicton beds are intercalated as a minor component with the stratified gravels at some locations.

Of the stratified gravels, the most common bed type observed is the crude, horizontally stratified gravels which are present at most sections (W, PC, I, II, BS, NA, III, IV, V, VII, VIII, IX, X, XI, and XII) (Figure 12). The horizontally stratified gravels range in bed thickness from 0.2-5.0 m, and average 1.6 m. Clast composition consists of 5-30% cobbles, 15-35% coarse pebbles, and 15-50% fine pebbles. Corresponding average values are 15.8% cobbles, 24.7% coarse pebbles, and 30.3% fine pebbles. The remaining particle percentage composition (29.2%) is primarily a matrix of medium sands to granules. Sediment finer than medium sands occurs in

Plate 12. Horizontally stratified gravels in Unit 3 at Section IX.

minor to trace amounts. Particle size distributions (histograms) of the matrix compositions are given for all samples in Appendix 9. Rarely, boulders occur in the basal part of a horizontally bedded gravel bed (2-5%). Both open-work and matrix-filled gravel beds are present, with the latter being less common.

Clasts are subrounded to well-rounded. Imbrication (b-axis up stream) is moderate to very good (Figure 29). The fabric results from the horizontally stratified gravels indicate that the mean a-axis trend at each sample locality is valley transverse or oblique (Figure 30). This is evident by the uniform distribution of trends between 0-180° (Figure 30). B-axis imbrication is up valley (parallel or oblique) in all examples. A second characteristic of these fabrics is the pronounced tendency for girdled distributions in the a-axis orientations. Gravels cluster towards the bottom half or girdled part of the two-axis plot (Figure 30). These patterns differ considerably from those generated by the matrix-supported diamictons which mainly show valley parallel fabrics and uniaxial clustering.

Contacts between horizontally stratified gravels and other beds vary considerably. Contacts with massive gravel beds are always gradational, but can be either gradational or sharply erosive with other types of gravel and finer sediments. Scouring is common where finer sediments are overlain by gravels. In a few cases, boulder beds were observed along the lower contacts of horizontally stratified gravel facies. Boulders occur in a single layer, lack striations on their tops, and support mixed coarse interstitial sediments. Boulder beds were observed over diamicton (Section W), on top of disrupted gravels (Section III), within disrupted gravels (Section II), at the base of disrupted gravels (Section VIII), interbedded within horizontally stratified gravels (Section V), and at the base of horizontally stratified gravels (Section WII, O.D., and XI).

Occasionally, both large and small scale trough cross-stratification were observed within the predominantly horizontally stratified gravel deposits.

Representative examples occur at Sections I (1 and 4), II (5 and 7), III (6), IV (4), V (2), VII (1), VIII (6), XI (4), and XII (3). Paleocurrent estimates based on these trough cross-beds indicate valley parallel or valley oblique flow, with no transverse flow directions. Cross-strata tend to occur randomly in small groups within particular units. Basal contacts are concave-up scour surfaces, often with finer reactivation surfaces along the contact.

Planar-tabular cross-strata were also observed in gravels at several localities including Sections I (Units 1, 3 and 4), II (Units 3, 5 and 7), III (Units 4 and 6), W.A. (Unit 2), IV (Unit 1), V (Unit 2), VII (Unit 4), VIII (Units 3,5 and 6), IX (Unit 1), O.D. (Unit 3), X (Units 1, 3 and 5), and XII (Unit 5). Frequently it was not possible to distinguish between true planar cross-strata and transverse sections through truncated trough cross-beds. Both trough cross-bedding and planar-tabular cross-bedding proportionately represent minor structures relative to the massive and horizontally stratified beds. Bed thickness was generally in the order of 0.25-1.50 m.

Sand beds also frequently occur intercalated as minor components in a predominantly gravel dominated lithostratigraphic unit. Sedimentological characteristics of these deposits are discussed in detail in the Sands section. Units with 50% or more (by frequency) pebble clast-supported beds were included within the gravel and sands lithostratigraphic unit. Units with 50% or more sand matrix-supported beds and minor gravel were included within the sands and gravel lithostratigraphic unit.

A number of small, isolated fragments of wood were retrieved from sandy interbeds within the horizontal gravel beds at three sections (W, II, and II). These isolated fragments did not provide reliable paleoflow indicators, as most fragments encountered represented fortuitous discoveries. Most fragments had suffered cellular destruction and could not be identified. Identifiable specimens were all assigned to the genus Picea and further restricted statistically to only five species within that genus

based on internal structural morphology: P. engelmannii (Engelmann spruce), P. glauca (white spruce), P. mariana (black spruce), P. rubra (red spruce) and P. sitchensis (Sitka spruce). As Sitka spruce is a coastal species limited in distribution to low elevations and red spruce is presently restricted in distribution east of the Great Lakes, neither is likely to be represented in the Finlay River valley. Engelmann spruce is present but rare, whereas both black and white spruce are quite common to the region. In the absence of a specific identification, the forest conditions at the time of burial are assumed to have been similar to that present today: namely, a boreal forest environment dominated by black and white spruce.

Geochronologic data was gleaned from the fragments through ^{14}C and amino acid analysis. The resultant time control provided the primary means of stratigraphic correlation. A date of 18,750 ± 120 years B.P. (TO-709) was obtained at Section Ware, 15,180 ± 100 years B.P. (TO-708) at Section III, and 26,800 ± 1450 years B.P. (AECV-379C) at Section II.

Interpretation

The stratified gravels recognized in this study are interpreted to represent various barforms found in a gravel-dominated braided fluvial environment. Crude, horizontally stratified gravel beds are usually considered to represent either longitudinal bars (Church and Gilbert 1975) or diagonal bars (Hein and Walker 1977). Both bar types are sheet gravels originally generated under high fluid and sediment discharge conditions, and tend to grade rapidly from one form to the other within the shifting channels of the braided river (Hein and Walker 1977). As fluid and sediment discharges drop, accelerated vertical accretion occurs over the flat incipient bars (longitudinal and diagonal) with a concomitant development of a downstream slipface or foreset. Continued aggradation under the lowered flow regime results in the

development of transverse bars whose internal stratification consists of low to moderate angle planar tabular cross-bedding (Hein and Walker 1977).

Longitudinal barforms in modern rivers range from 1-3 m in thickness, with bedforms generated by catastrophic floods reaching thicknesses of 12 m (Hein 1984), a thickness which is similar to those described in this study. Hein (1984), in her study of one braided environment, observed that massive beds predominate, followed by planar cross-stratified, horizontally stratified, and lastly trough cross-stratified beds in trace amounts. This rank order is maintained in the sections examined here, except that crude, horizontal stratified beds predominate. The transition between massive and crudely stratified beds is subjective and may account for the discrepancy noted. The thickness of transverse bars in modern environments averages 0.5-1.0 m, similar to the planar tabular beds discussed here.

Modern braided river deposits display alternating open-work and matrix-filled beds, interpreted to result from normal discharge fluctuations which either promote or inhibit sieve settling of finer particles between stacked clasts (Smith 1974). This variability is evident in all gravelly units in sections along the Finlay River.

The boulder beds observed within the stratified gravels at several sections are not boulder pavements formed by a lodgment process during glacial deposition (cf. Visser and Hall 1985), due to the absence of striae, faceting, imbrication and stratigraphic position below or within diamictons. Instead, these boulder lags likely represent winnowing of either tills or modified grain flow deposits.

iv) Disrupted Gravels

Description

This gravel type includes several examples of composite bed associations which display a variety of stratification types and bed distortion/disruption features such as faulting, folding, and tilting.

The disrupted beds are best examined at the lithostratigraphic unit scale rather than bed scale (Plate 13). Disrupted gravels consist of varying proportions of massive, horizontally stratified, normally graded, and inversely graded gravel and sand beds, all of which display considerable lateral and vertical variability in structure. Most beds are tilted or inclined, in certain cases beyond the angle of repose (~30°). Planar and curvilinear fault planes are common within and between the units. Interbed contacts show considerable change from sharply erosive to gradational. Imbricated clasts up and down valley are present. Three pebble fabrics were obtained in the upper part of Unit 3, Section II, in thick, massive in situ pebble beds interbedded with the disrupted gravels and were detailed earlier in the discussion of massive gravel beds (Figure 28). Pebble fabric orientation is valley parallel (plunge down valley) or valley transverse, and S1 values range from 0.474 to 0.623.

Disrupted beds can be found within various units at eight sections [WII(4), II(3), III(4), W.A.(2), VII(1), VIII(3), IX(1), and O.D.(3)] (Figure 12). The disrupted package is commonly in direct association with massive or stratified diamictons with the diamictons underlying the disrupted sediments (WII, II, III, and O.D.). The basal contact for the above lithostratigraphic units is either sharp and unconformable or gradational. Unit thickness ranges between 2 and 15 m and averages 6.1 m. Analysis of clast composition indicates boulders are present at only two sections, where they represent 5-10% of all clasts. Cobble frequency ranges from 5-15%, whereas the pebble fraction, generally equally distributed between large and small sizes, constitutes 45-55% of the clasts. The remaining matrix is generally dominated by the medium sand to granule size fraction (73-92%). Steeply angled faults cross cutting internal strata were observed in many localities.

Disrupted packages are commonly oxidized or contain oxidized beds. They are loose, and in certain cases fossiliferous. Small coal inclusions are the most widespread organic materials found, but datable wood fragments (mats) were also found at Section

Plate 13. Disrupted gravels. Photograph illustrates reverse faults and distorted bedding in Unit 3 at Section O.D.

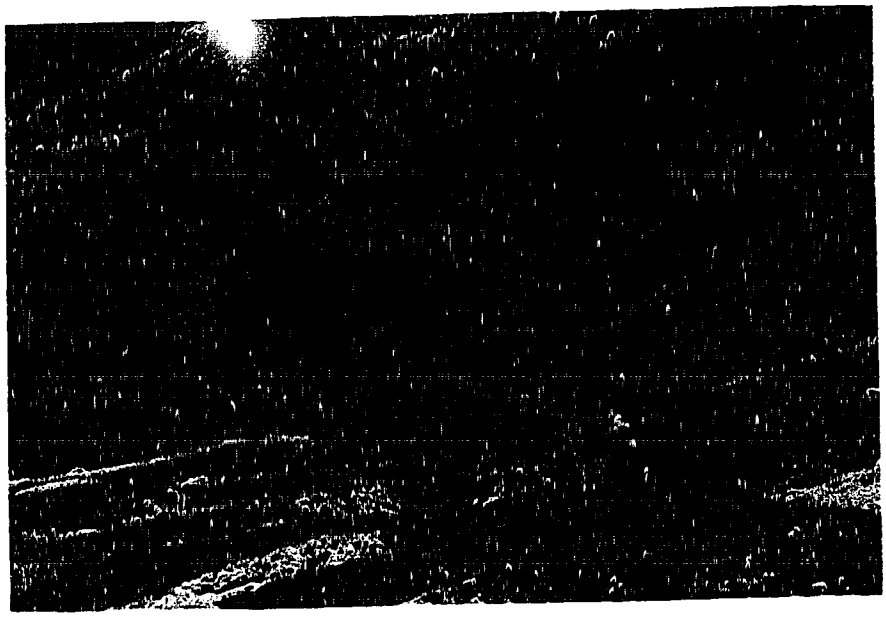

II(3). ^{14}C dates at this locality are > 40,000 years B.P. (AECV-348C), and > 40,130 years B.P. (AECV-386C). Distorted sediments at this section contain angular rip-up clasts up to 50 cm in diameter of the underlying diamicton. Several of the wood 'mats' were processed for pollen. A count of 435 degraded grains resulted in an assemblage consisting of the following: Picea (88.3%), Pinus (4.1%), Abies (3.7%), Alnus (1.1%), Cyperaceae (1.4%), and unknown (1.4%) pollen. Spores resembling a cystopteris type (bladder ferns) were very common (n=264), as was charcoal and indeterminate organic remains. The low percentage of pine indicates this taxon was extralocal and that the community was dominated by spruce with minor components of fir and alder.

Interpretation

The disrupted gravel packages are interpreted to represent an ice contact sediment complex resulting from either ice marginal or supraglacial ice stagnation accretionary processes. The coarse nature of both the clast and matrix fractions indicates selective winnowing of the fine sediments, probably by meltwater (cf. Eyles 1979). Cheel and Rust (1982) described the sediments of the ice proximal environment as an interbedded assemblage of inversely graded gravel and sand produced by sediment gravity flows, horizontal and planar cross-stratified sands, and coarse gravel. This assemblage is similar to the disordered package described above. Slumping and faulting is also common in the ice proximal environment. Boulton (1968) noted steep beds dipping up to 40° as a result of slumping in morainal front positions. Localized blocks of disintegrating ice are inferred on the basis of steeply angled normal and reverse faults which cross-cut the various waterlain strata. Such post-depositional modification in the glacifluvial environment was described by McDonald and Shilts (1975), who attributed the formation of the faults to melting of "saucer shaped" ice under the sediments. Analogous features were noted by Bobrowsky

et al. (1987b) in ice proximal successions in the pitted delta complexes of northern New Brunswick.

Stratigraphic position of the disrupted sediments over diamicton interpreted to represent meltout till adds further credence to the melting ice hypothesis. Disrupted gravels were not observed below diamicton, nor were they observed above massive diamictons interpreted as lodgment till. Ice marginal environments associated with an active steep-fronted glacier, whether advancing or rapidly retreating would tend to create a smooth topography (Drozdowski 1985). In contrast, the in situ melting of a stagnating ice mass, during which time basal meltout till could be deposited, would then be followed by supraglacial sedimentation, which tends to accentuate the underlying relief (Drozdowski 1985).

Several features of the distorted sediments match those of the valley glacier supraglacial morainic till complex of Boulton and Eyles (1979). Both successions are characterized by a basal till covered by a random interfingering of sands and gravels deposited by ephemeral streams and in crevasse fillings, ice contact scree masses, and proximal outwash. Notably lacking from the Finlay River succession are mud horizons and matrix-supported sediment gravity flow deposits. If uncovered or exposed on the surface, the distorted gravels would represent an ice-cored and kettled hummocky outwash complex.

v) Inclined Gravels

Description

Only two sections (IX-Unit 5 and XI-Unit 2) contain gravels with large, steeply inclined planar cross-beds (Figure 12 and Plate 14). The most prominent example occurs at Section IX where inclined cross-bed height approaches 40 m. These units consist of alternating beds of coarse pebble-supported and fine pebble-supported gravels in the upper half. Towards the base, beds fine to alternating fine pebble clast-

Plate 14. Inclined gravels. Photograph illustrates large scale foreset beds in Unit 5 of Section IX.

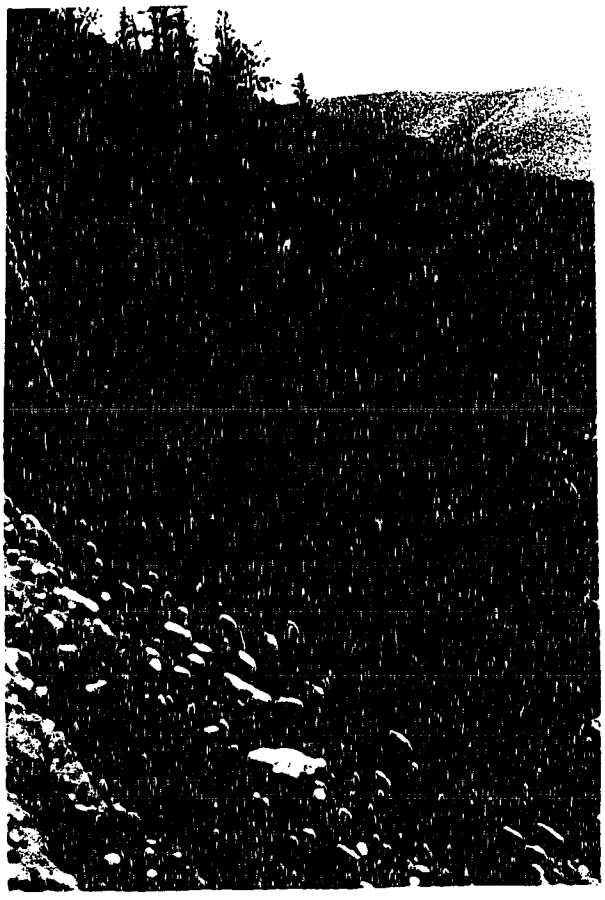

supported and coarse sand matrix-supported beds. Most individual beds display normal grading. Bed thickness measured normal to bedding planes ranges from 5-30 cm. Beds dip to the south at 25-35° from horizontal. Clasts are all rounded and well imbricated, usually with b-axis dipping slightly downstream. The upper contacts of the cross-beds are either truncated by diamicton or grade into horizontally bedded gravels. The bases of the inclined planar cross-beds grade down through 2 m into horizontally laminated silty sand beds, and minor cross laminated sands. At Section IX Unit 5 overlies a diamicton (Unit 4) and grades laterally (downstream) into a thick interbedded package of diamicton, cross-bedded sands and horizontally bedded gravels (Unit 6). Organic remains were uncovered at the top of the unit as streaked smudges, and a wood fragment ^{14}C dated at 29,280 ± 1450 years B.P. (AECV-352C) was retrieved from sediments between Units 5 and 6.

A second set of steeply inclined planar cross-beds consisting of alternating clast- and matrix-supported gravel beds occur at Section XI(2) and encompasses the entire lithostratigraphic unit. Unit thickness approaches 9 m, with individual bed thickness ranging from 5-50 cm. Both normal (common) and inverse (rare) grading is evident in the individual beds. Gravel beds also show both open and matrix-filled frameworks, whereas only matrix-filled gravels were observed at Section IX. The entire sediment package is coarse in textural composition consisting of 2% boulder lags, 10% cobbles, 30% coarse pebbles, 30% fine pebbles, and a predominantly coarse sand matrix (28%). The basal contact for the inclined gravel unit at Section XI is either indeterminate or sharply erosive overlying diamicton. The upper contact is also erosive and marked in places with a boulder lag (base of horizontally stratified gravels). The entire unit is highly oxidized and free of organic materials.

Inclined Gravels

The two examples of large inclined planar cross-beds are interpreted to represent foreset beds of fluvially dominated prograding braid deltas (cf. McPherson et al. 1987, 1988). The foresets developed along the delta front margin where meltwater debouched into a temporary proglacial lake. A rapid drop in fluid and sediment discharge would result in the deposition of bed load and, subsequently, suspended sediments, and thus cause the development of normally graded cross-stratified slip-faces at the angle of repose (Elliot 1978). Mixing of equally dense meltwater and lake water results in homopycnal flow (foreset accretion), whereas high density meltwater entering less dense proglacial lake water results in hyperpycnal flow (subaqueous fluidal and debris flows). Homopycnal flow accounts for the formation of the deltaic foresets, and hyperpycnal flow for the distal accumulation of interbedded diamictons and gravels (Unit 6) associated with the foresets at Section IX. Fluctuating meltwater discharge along the distributary channels accounts for the shifting textural patterns observed between the foreset beds (cf. Gustavson et al. 1975). At section IX the transition from foreset beds to both topset and bottomset beds is gradational and not horizontally truncated, as is evident at section XI. Such gradational transitions appear to be a rare occurrence in Quaternary glacial deltaic deposits (Bobrowsky et al. 1987b). At both localities, the delta plain is restricted in representation to the overriding foreset beds which represent rapidly shifting distributary channel deposits, essentially equivalent to the gravelly braided streams deposits discussed above (cf. Fielding 1984, 1987).

The glacial deltaic deposits described here resemble similar Pleistocene occurrences elsewhere (eg. Thomas 1984). Particularly noteworthy is the sediment complex of section IX which consists of deltaic foresets (Unit 5), coarsening upwards cycles through silty sands interbedded with glacilacustrine sand, gravel, and subaquatic diamicton (Unit 6) coupled with a topmost truncation by a subaerial cohesive gravity

flow diamicton. This sediment complex is identical to the late Pleistocene package from eastern Ireland described by McCabe et al. (1987). Moreover, the geologic composite sections of Annaloughlan and Rampark provided by these authors are similar to that compiled for section IX.

E. Sands

Sand sized particles display a widespread distribution in the study area and occur as the dominant sediment in two ways: 1) as essentially the sole grain size in a unit; or, 2) in interbedded successions with other textural units. The latter type of distribution also includes diamictons, gravel with sand interbeds, and sandy silts, all of which have been discussed above. Textural signatures of sand-dominated deposits are given in the form of histograms for each section in Appendix 16. Representative examples are illustrated below. In the discussion that follows, interpretive is given to the occurrence of sand in lithostratigraphic units characterized as either sand [II(2 and 4), VIII(2)], silty sands [W.A.(4), X(2)], sand and gravel [I(3), VII(4), VIII(5), X(3), and XII(5)], or interbedded sand, gravel, and diamicton [W(3), III(8), and IX(6)] (Figure 12). The total distribution of sand types is, however, presented in all possible combinations.

The genetic interpretation of sand beds applies equally well to sand-dominated lithostratigraphic units and units within which sand beds are a minor component. Sand is also found in all Holocene terrace gravels, and recent alluvial accumulations as the uppermost sediment type in the following sections: W, WII, I, II, III, W.A., IV, O.D. and XII. These deposits have been addressed by Leslie (1988), and are not examined here.

Sand is discussed according to the following stratified sediment types: 1) structureless and graded (with or without cobble pods); 2) horizontally laminated; 3) trough cross-stratified; 4) planar cross-stratified; and, 5) ripple drift cross-

laminated sands. These sand types occur at several sections, but only prominent associations are itemized in each description.

i) Structureless and Graded Sands

Description

Sand beds characterized as structureless and graded occur as thin beds in numerous sections or as thicker accumulations dominating entire units at a few sections (Plate 15). Thin structureless and graded sands are present as isolated beds at Sections VII(1) and X(6), and are interbedded with cross-stratified sand beds at Sections O.D.(3), X(2), and V(2). More commonly, massive sands are intimately intercalated with horizontally laminated sands (Sections I(3), II(2, 3 and 4), W.A.(4), IX(6), and X(1), and gravels (Figure 12).

Beds of massive and graded sand average 5 to 40 cm in thickness. Thicker stacked accumulations of 5 m (Section VIII) and 18 m (Section II) consist of randomly intercalated horizons of massive and horizontally laminated sands. Sorting of these beds is generally poor. In the case of isolated beds, grading is common. Contacts are generally sharp and conformable, either erosive or draped, but gradational contacts are also evident. Beds are preferentially intercalated with silt and clay laminae at Section X and gravels at Section VII. Textural signatures for single isolated massive sand beds displaying grading from these two sections are given in Figure 31. Grain size is preferentially skewed (positive) with medium to coarse sand predominating.

Thick deposits of structureless and graded sand occur at Sections II(2) and VIII(2). At the former locality approximately 18 m of hard, structureless, normally graded, and horizontally laminated sand is interbedded with minor amounts of silt and clay. Large, slightly attenuated clay rip-up clasts occur near the base. In the middle and the top, amorphous pods and lenses of poorly sorted gravel with maximum dimensions of 5 m. Small scour and fill structures, and trough cross-beds occur in the

Plate 15. Massive sands. Photograph illustrates thick accumulation of massive and horizontally laminated sands with isolated lenses and pods of gravel in Unit 3 at Section II. Person to left at base of section.

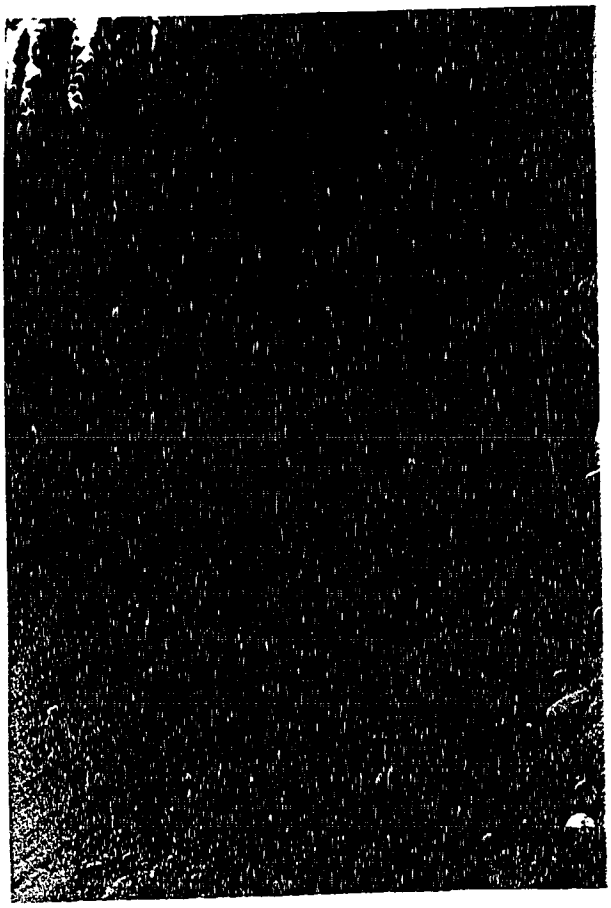

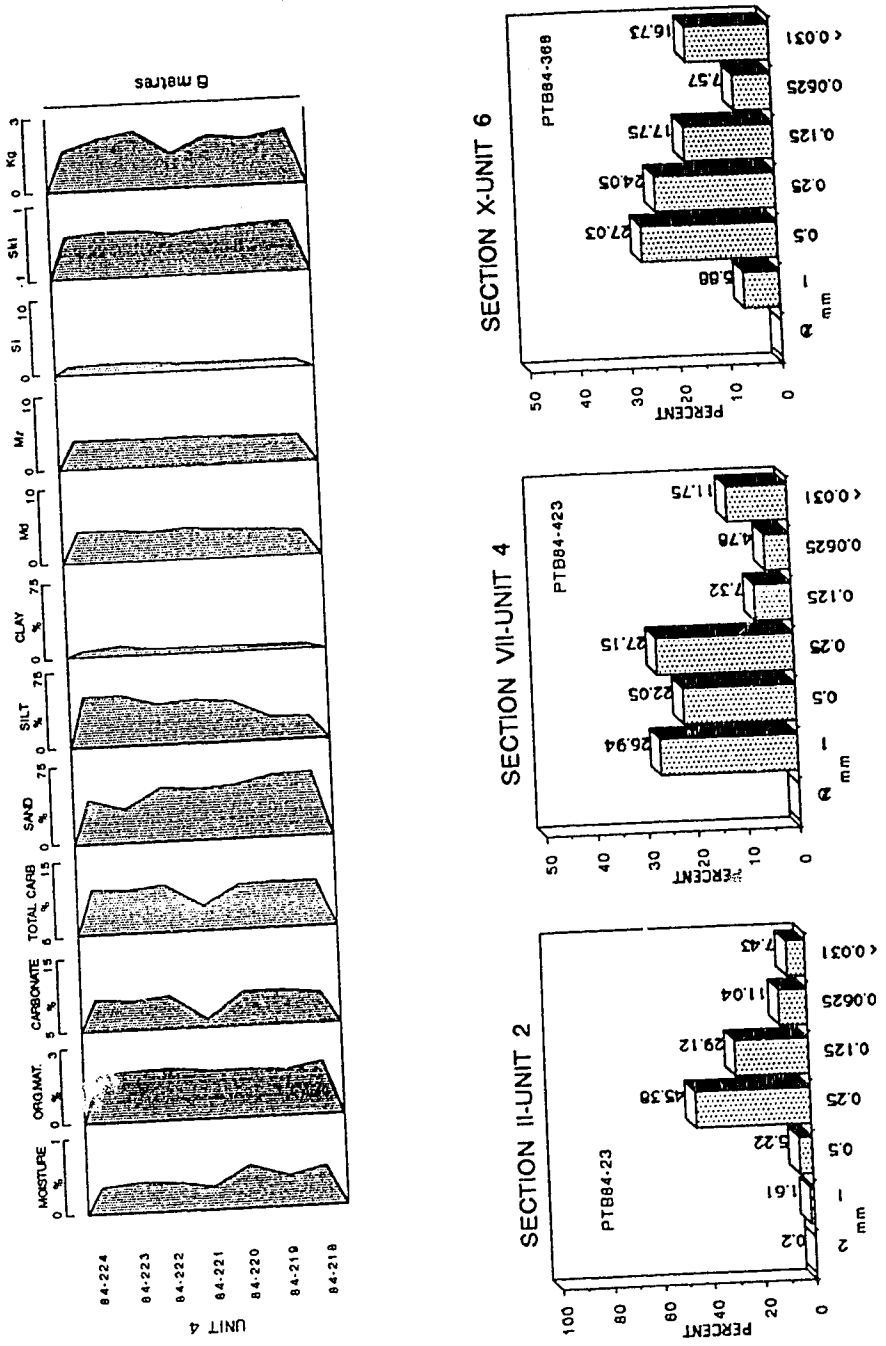

Figure 31. Top illustrates compositional variation with depth for Unit 4, West Air Section. Bottom histograms illustrate textural variation in massive sands from Sections II, VII, and X. See Figure 15 for caption detail.

upper part of the unit. Texturally, the matrix in the unit averages < 1% granules, 92% sand, and 7% silt/clay. The gravel pods contain rounded clasts from small pebble to cobble size. The basal contact is indeterminate, but oxidized gravels obliquely truncate the sand.

The oxidized, massive sands at Section VIII(2) are thinner (5 m), and do not contain the gravel pods evident at Section II. Occasional isolated clasts and small clusters of fine pebbles are interspersed along horizontal bedding planes in the matrix-supported unit. Some of these isolated clasts display penetrative deformation of underlying bedding planes. Bulk samples from this unit show the following textural ranges: 0-2% gravels, 75-94% sand, and 3-25% silt/clay. This primarily structureless sand unit also displays minor trough and planar cross-stratification.

At Section W.A., Unit 4 is a thick (10 m), hard, rhythmic accumulation of horizontally bedded silty sand which displays normal grading within each bed. Figure 31 illustrates the vertical compositional variation for seven samples. Beds range in thickness from 1-5 cm and have an average composition of 51% sand, 42% silt, and 7% clay. Interbed contacts are sharp and conformable and display minor oxidation streaks. The unit is fossiliferous, containing wood but no palynomorphs. ^{14}C dates from the top and base of Unit 4 are 23,280 ± 750 years B.P. (AECV-351C) and 37,190 ± 2870 years B.P. (AECV-353C), respectively.

The high silt content, chronologically controlled contacts and well stratified architecture of Unit 4 at W.A. prompted an attempt at retrieving paleomagnetic samples. Unfortunately, the graded beds displayed a blocky fracture patterning during sampling which limited sample retrieval to only two horizons in the upper part of the unit. The results of this limited analysis are given in an equal area projection in Figure 32. All eight samples for the two horizons indicate a tight cluster to the NW, with a normal magnetic alignment trend to 343.3° and plunge of 27.2°.

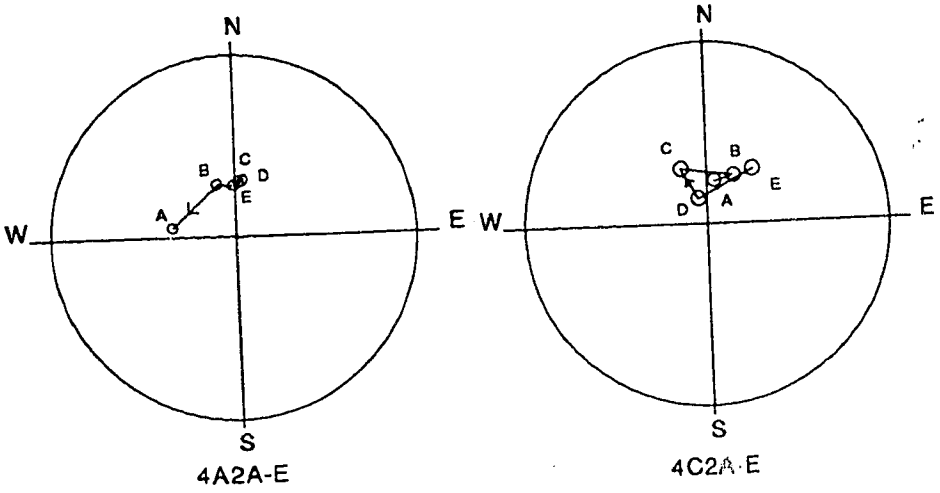

SECTION ONE-UNIT 3 SECTION TWO-UNIT 6

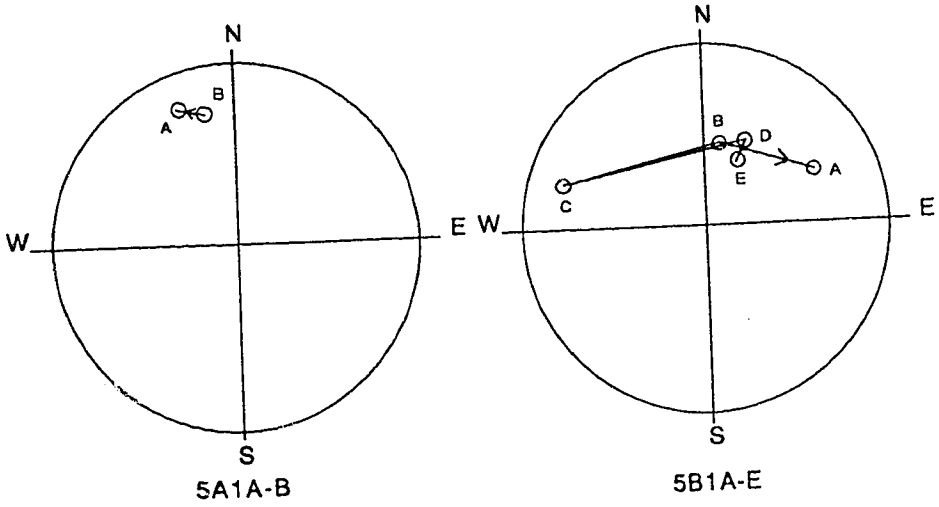

SECTION W.A.-UNIT 3 SECTION XII-UNIT 2

Figure 32. Equal area projections of NRM polarity fields for samples from four sections. Letters indicate horizons and arrow illustrates trend from base to top of unit. See text for further explanation.

Interpretation

Structureless and graded sands are frequently interbedded with horizontally laminated sands along the Finlay River. Blatt et al. (1980) concluded that massive sands are occasionally incorrectly identified. This is especially true where opaque minerals which define bedding planes are absent, where moisture content and poor accessibility minimize visual acuity, or where postdepositional modification masks the bedding planes.

Graded Sands

Isolated beds of sand which display grading reflect hydrodynamic histories comparable to graded gravels. These graded beds represent short lived bedload transfer of sediment during 'mass flow' events (cf. Harms et al. 1982). The gravity dominated beds result from accumulation at the base of existing subaqueous slopes (eg. barforms). Grading reflects normal sediment response to the reduced rate of flow discharge in fluvially dominated environments (cf. Miall 1977). Individual graded beds at WA(4) are interpreted to represent stacking of sediments formed by pulsating sediment gravity flows into a restricted channel marginal catchment basin.

Structureless Sands

Ungraded structureless sand beds can be products of mass movement. In this case, sand-dominated sediment gravity flows support grains by either grain dispersive pressure or turbulence (Lowe 1982). Fluidized and liquefied flows are not likely, given the absence of water escape structures in the sediments. Mixing during flow may be important in explaining the homogeneous texture of structureless sand beds. The two prominent examples of structureless sands at Sections II(2) and VIII(2) represent stacked sediment gravity flow deposits. The first locality also displays sporadically distributed cobble clusters and lenses within the unit.

Eyles et al. (1987) observed cobble clusters in thick structureless sand accumulations south of the study area. These authors provided alternative interpretations for the occurrence of such deposits: 1) the cobble clusters represent transverse sections through intermittently active debris flow chutes which deposited gravelly sediments over sand dominated basins; 2) cobble clusters reflect clasts which quickly settled through a grain-dominated flow on top of an existing sand bed or into a massive sand flow which was in the process of frictional freezing; or, 3) cobble clusters represent IRD (ice-rafted debris). The features present in Unit 3 at Section II are interpreted as products of either isolated gravelly chutes or IRD from which finer sediments were selectively winnowed following deposition.

At Section VIII, cobble clusters are absent, but a few isolated pebbles illustrating penetrative bedding structures are present. Both occurrences (II and VIII) represent accumulations of glacigenic sediments in a proglacial lake, whether by pelagic rain out, IRD, or debris flow accretion, or combination of these processes (cf. Eyles et al. 1985). The stratigraphic associations of the two localities are different. At Section II(2), massive sands overlie a massive diamicton interpreted to be a lodgment till, and show a lateral facies change into ice proximal gravels (up ice) interpreted to be supraglacial sediments formed during deglaciation. Calving of ice and frequent influx of sediment gravity flows into a deep proglacial lake during deglaciation are therefore indicated. At Section VIII(2), sands overlie ponded silts interpreted to be distal proglacial lakes sediments, and underlie gravels which are interpreted to be ice proximal. The paucity of IRD at Section VIII may indicate ice advancing into shallow water, rather than calving of ice into deep water during stagnating ice conditions. Similarly, the overall coarsening upward sequence indicates a proglacial lake formed during a glacial advance, rather than during a retreat.

ii) Horizontally Laminated Sands

Description

Isolated beds of horizontally laminated sands are rare, being present in only two sections [WA(2) and VII(2)] (Figure 12 and Plate 16). In addition to the association with structureless sands discussed above, horizontally stratified sands also occur with both planar and trough cross-stratified sands [IV(1) and VIII(2)] and with Type B (cf. Jopling and Walker 1968) ripple drift cross-laminated sands [IX(5 and 6)]. Horizontally laminated sands are one of the most commonly found types of sandy sediment (planar cross-stratified sands are equally common). Horizontally laminated and planar cross-stratified sand types occur together at Sections W(3 and 4), I(1), III(4), VII(4), VIII(3, 5 and 6), IX(1), X(3), XI(4), and XII(5).

This type of stratified sand occurs as beds of thin and horizontal sediment which display horizontal and straight or slightly wavy laminar contacts. All interlaminar contacts are conformable. Moisture content and sand grain mineralogy affect recognition of the laminae. Individual bed sets of horizontally stratified sand range in thickness from a single grain to 40 cm. Uninterrupted cosets consisting of interbedded horizontally laminated and structureless or planar cross-stratified sands are up to 2 m thick. Cosets consisting of horizontally laminated and trough cross-stratified sands are up to 1 m thick. Figure 33 illustrates the texture of horizontally laminated fine sands from Unit 5 at Section XII. At the base of Unit 6 at Section IX, horizontally laminated sand beds containing convoluted laminae with microfaults and flame structures are interbedded with stratified diamictons (subaqueous sediment gravity flow deposits), graded, and structureless sand. Individual laminations were not examined for evidence of normal or inverse grading.

A deposit of moderately well-sorted medium sand comprises the upper part of the oxidized gravels in Unit 6 at Section VIII (figure 33). Bed shape is defined by the underlying undulatory gravels and internal stratification is continuous and sheet-like

Plate 16. Horizontally laminated sands in Unit 6 of Section VIII. Person for scale above unit standing on boulder lag.

(Plate 16). The bimodal grain size distribution reflects the primary texture and coarser granules which demarcate the bedding plane boundaries between stacked beds. Disaggregated coal fragments and amber crystals occur along some bedding planes. The sand package is oxidized and conformably overlies disrupted gravel and sand.

Interpretation

Horizontally laminated sands can be produced under either lower or upper flow regimes. The precise mechanics of unidirectional, lower flow regime flat bed accumulation are not yet well understood, but appear to be the result of a combination of several factors including the near-bed flow structure and variations in packing and sorting (Harms et al. 1982). The mechanics of upper flow regime horizontal lamination deposition are clearer and involve burst [fining upward textures (FU)] and sweep [coarsening upward textures (CU)] processes (Cheel and Middleton 1986, 1987). The correct identification of flow regime can be difficult if based solely on the presence of flat beds, but in this study the fine texture of the sediments clearly indicates upper flow regime conditions.

Stability fields for bed phases in steady unidirectional flow indicate that lower flow regime flat beds are not physically possible with sediment smaller than approximately 0.5 mm (Middleton and Southard 1984). Grain size analysis of horizontally laminated sands from the Finlay River indicates all samples are finer than this critical size value indicating upper flow regime conditions.

Harms et al. (1963) observed horizontally laminated sands in association with trough and planar tabular cross-bedded sands in modern sands of the Red River in Louisiana. Although the two cross-bedded stratification types are clearly lower flow regime products, they interpreted the flat beds to be upper flow regime deposits. Indeed, Harms et al. (1982) suggested that the presence of trough cross-strata can be used to place associated flat beds in the upper flow regime. As discussed above,

horizontally laminated sands observed here are interbedded with cross-stratified , and massive sands. Harms and Fahnestock (1977) interpreted the transition from massive sands (upper part of upper flow regime) to horizontally stratified sands (lower part of upper flow regime) to cross-stratified sands (lower flow regime) relative to the Bouma sequence. The high frequency of horizontal stratification interbedded with associated trough and planar cross-stratified sediments implies fluctuating flow regimes, water depths and velocities. Such fluctuating conditions are known for proximal braided rivers (Rust 1978).

The convolute laminations shown in Plate 9 illustrate the effects of plastic deformation following rapid deposition of sediments (Blatt et al. 1980). Small microfaults in these convoluted beds (kink structures) indicate early diagenetic stresses (cf. Van Loon et al. 1985; Brodzikowski and Van Loon 1983) which can be generated during subaquatic sediment failure.

Oxidized sands deposited at the top of Unit 6 at Section VIII are interpreted to represent aeolian deposits overlying alluvial sands and oxidized ice proximal gravels. These medium sands are moderately well sorted but not as well sorted as most other aeolian accumulations. According to Ashley et al. (1985), aeolian deposits developed over ice contact outwash are generally not as well sorted as aeolian sediment developed over other types of deposits. Bedding planes are characteristically parallel, continuous and undulate slightly from concave to convex up as in other aeolian deposits. This stratification type may be explained by migrating wind ripples which create horizontally laminated sand sheets. Ashley et al. (1985) provide plates of cross sections through aeolian sediments in glacifluvial environments. Their plates (Figures 5-2, p. 221 and 5-4, p. 223) are similar in appearance to the sediments interpreted here as aeolian.

iii) Trough Cross-Stratified Sands

Description

A number of sections contain sand beds consisting of cross-bedding with tangential basal contacts (trough cross-stratification). Unit 9 at Section II is the only example of trough cross-stratified sands occurring in the absence of any other form of sand type. Here the thin beds are a minor component of a fining upwards gravel dominated deposit. Trough cross-stratified sands occur with planar cross-beds in Unit 6 at Section III and in several other complex associations in all other sections. In general, however, trough cross-stratified sands are extremely rare in terms of frequency of observation compared to planar cross-bedded sands.

Trough cross-beds examined in this study range in coset thickness from 0.3-2.0 m. Average coset thickness is approximately 90 cm. Individual trough cross-beds can range from a few centimetres to a metre in trough depth. Exposed angles of view are extremely variable and provide almost all possible orientation cuts through the troughs (cf. DeCelles et al. 1983). Subjective paleocurrent estimates based on these exposures indicate valley parallel or oblique flow from the NW. Sorting is generally good but ranges from well sorted to poorly sorted. Grain size is also highly variable with modal classes ranging from medium to coarse sand. Figure 33 contains a textural histogram from one trough cross-bedded deposit in Unit 5 at Section II. In general, trough cross-bed evidence along the Finlay River is similar to that from several exposures in Pleistocene sediments elsewhere in British Columbia.

Interpretation

Trough cross-stratified sands represent deposition under lower flow regime conditions (Harms and Fahnestock 1977) by migrating megaripples. Variation in size from small to large scale troughs are correlated infilling of different sized scours. The trough cross-bedding is genetically restricted to three dimensional dunes and not

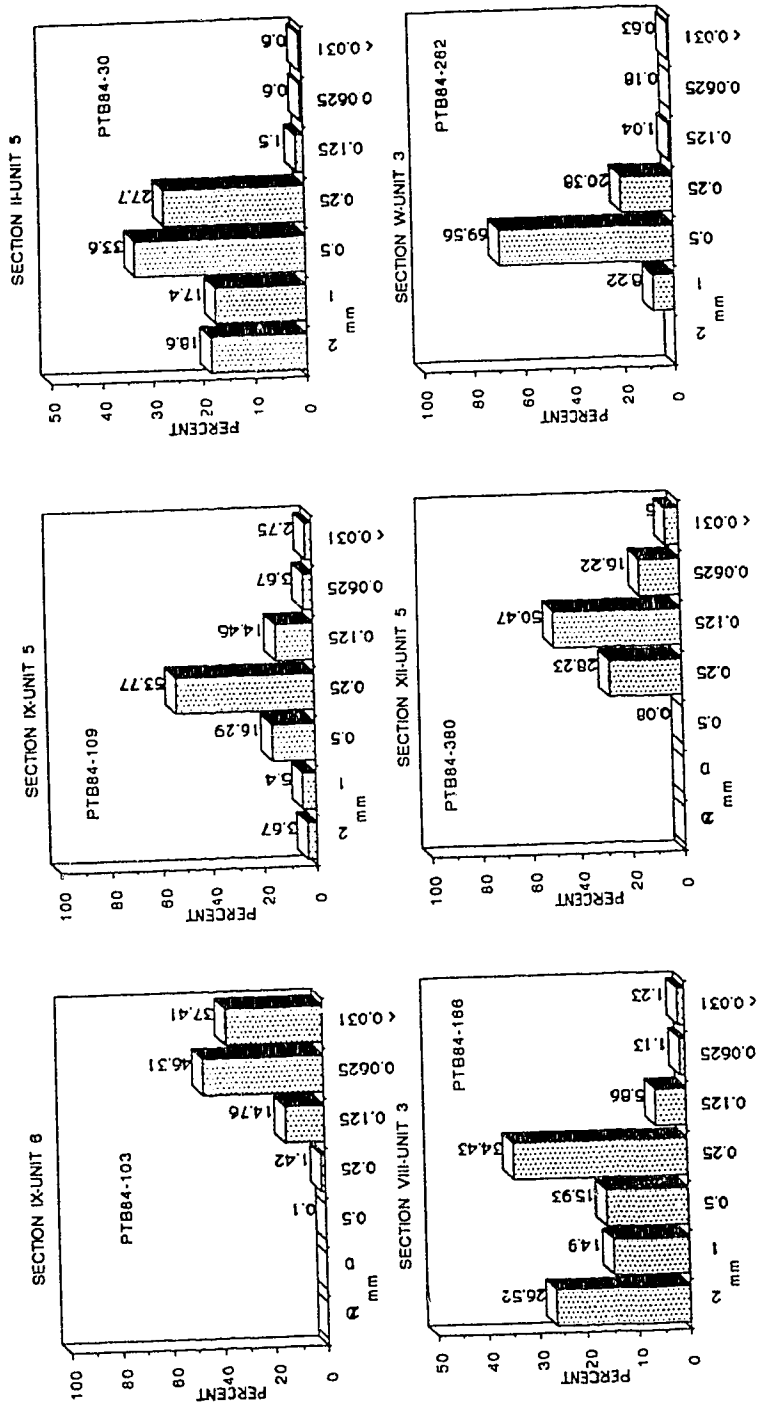

Figure 33. Textural histogram examples of aeolian sand (84-166), ripple drift laminated sand (84-103,109), trough cross-stratified (84-30), planar cross-stratified (84-262), and horizontally stratified sand (84-380). See text for key.

straight crested dunes (sand waves) in the terminology of Reineck and Singh (1980). Harms et al. (1982) note each trough set represents long erosional scours filled by curved laminae dipping downstream. Migration of dunes/megaripples (3-D large ripples) form the trough cross-stratification.

iv) Planar Cross-Stratified Sands

Description

Planar cross-stratified sand beds represent the most commonly occurring type of stratification for the sand grain size. Planar cross-stratified strata were identified on the basis of their cross sectional planar attitude and non-tangential bounding contacts. Associated bed types and their distribution have been itemized above. Isolated occurrences of planar cross-stratified sands also occur at Sections II(5 and 7), X(5), and W(1) (Figure 12).

Coset thickness of planar tabular cross-beds range from 0.2 - 4.0 m, with an average thickness of approximately 90 cm. Individual sets show considerable variation from a few centimetres to large inclined slopes over a metre in height. Interbed bed contacts are sharp and erosive, and vary from horizontal to inclined. Bed configuration depends on the extent of erosive truncation by overlying beds. Sorting ranges from poor to moderately well sorted. Particle size analysis shows modal concentrations from very fine sand to coarse sand, but medium to coarse sand size dominates. The planar cross-bedded strata encountered in this study were not evaluated critically for paleocurrent directions. Subjective evaluation suggests a normal down valley orientation for the planar cross-stratification.

More interesting is the observed distribution of planar cross-beds by lithostratigraphic unit. Most commonly, this sand stratification type is interbedded with gravels in large scale coarsening upward sequences. This is evident at the base of many lithostratigraphic units at sections such as W(4), III(6), VII(6), X(3), and

XI(4), or generally within the units as at sections II(5), and X(1). Planar cross-stratified sands are uncommonly interbedded with gravels in large scale upward fining sequences as evident in the following sections: W(3), III(6), VII(4), VIII(3), O.D.(3), and XII(5). Planar cross-bedded sands also occur in gravel dominated units where no obvious trend in texture is apparent [eg. I(1) and IV(1)].

Interpretation

Planar cross-stratified sands are interpreted to represent the downstream movement of sand waves in the middle lower flow regime (Harms and Fahnestock 1977). Laminations are inclined downstream to flow at angles of repose (25-35°) and represent lee side cascading of sand particles as small ripples migrate up the stoss side of the dune and avalanche down the lee face. Grain size characteristics are thought to be inherited by the migrating ripples upstream on the bar surfaces (cf. Harms and Fahnestock 1977).

Although sands comprise only a small part of the gravel dominated sediments in the Finlay River area, planar cross-bedding is evident in a number of units. Ashley et al. (1985) noted that the increasing frequency of planar cross-strata in braided stream deposits indicates an expected downstream response to waning flow conditions and unstable channel braiding. This reflects the higher occurrence of transverse and linguoid bars, as well as small scale bed forms in the distal deposits. According to Ashley et al. (1985), the preservation of deposits formed by overbank sedimentation is not possible in an unstable and aggrading braided channel situation, although Bridge (1985) considers this assumption to be fallacious. The presence of sandy planar cross-stratification within gravel deposits showing coarsening upward sequences and underlying tills represents a transition from distal to proximal depositional scenarios. Conversely, the presence of planar cross-bedded sand in gravel deposits showing fining

upward sequences and overlying tills indicates transitions from proximal to distal deposition.

v) Ripple Laminated Sands

Description

Only Type B sandy ripple drift cross-laminations (Jopling and Walker 1968) were commonly observed along the Finlay River [eg. Sections II(9), and IX(5 and 6)], although draped or sinusoidal laminated sands also occur (cf. Plate 17 for example of sandy silt drift cross-lamination). The latter may be mistakenly classified as deformed or crenulated horizontally laminated sands. The sporadic interbedded appearance of this stratification type precluded bedset measurements. In beds of Section IX(5 and 6), the ripple laminated sands show a median medium sand and very fine sand texture (cf. Figure 33). Grain size analysis indicates that significant proportions of silt are included with the various sand sized particles. This observation corresponds well to the higher frequency of occurrence of ripple drift cross-laminations in sandy silt dominated deposits noted above (eg. Section VIII). As with trough cross-stratified deposits, ripple drift deposits are a rare occurrence. Their distribution appears to be correlated to deposits interpreted earlier to be glacilacustrine.

Interpretation

Ripple drift cross-laminations observed in this study are interpreted to represent climbing ripple deposits associated with changing ratios of suspended/traction sediment during deposition. Type B laminae are intermediate forms of deposition between tractional (Type A) and suspension (drape laminated) dominated conditions (Ashley et al. 1985). Higher suspended loads favor the formation of Type B ripple drift laminations over Type A forms. Jopling and Walker (1968) noted that

Plate 17. Ripple-drift cross-lamination (in phase).

ripple drift cross-laminated deposits contain very little clay, and the median grain size is usually in the fine sand fraction. Grain size data in this study indicates ripple drift cross-lamination deposits are primarily in the fine sand fraction. Further the above authors observed ripple drift cross-lamination to be common in the bottomset and foreset parts of underflow generated sediments in glacial deltas. The high frequency of observation of Type B laminae at Sections IX and VIII is best explained in terms of proglacial glacilacustrine conditions within which fluctuating sediment load conditions are maintained by pulsating or sporadic density underflows.

F. FINES

All unconsolidated deposits containing appreciable amounts of clay and silt with or without minor percentages of sand and gravel are grouped into the fines category. Discussion centres on two primary sediment types: 1) silts; and, 2) clays.

i) Silts

Description

Silt occurs as a dominant particle size (> 50% by volume) in seven of the sections examined along the Finlay River: I(2), II(6), III(3), W.A.(3), VIII(1), IX(2), and XI(3) (Figure 12 and Plate 18). Minor but appreciable occurrences of silt interbeds are also evident at sections I(3) and X(6). Silt units with ripple drift cross-lamination [Type B (Jopling and Walker 1968) and draped lamination (Ashley et al. 1985)] sequences typify Sections I(2), III(3), and IX(2), and appear as interbedded deposits at Sections I(3), X(6), and W.A.(3). Interlaminar contacts are sharp, conformable and, in the case of Section I(2), contain organic smears along the contacts. Color ranges from pale olive (5Y 6/3) to black (10YR 2/1) and appears as bands. Minor oxidation is common. These silt sequences range in thickness from 1.5-3.0 m and average 2.0 m. Basal contacts of the deposits are conformable and sharp.

Plate 18. Resedimented silt deposit. Photograph illustrates subaqueous sediment gravity flow deposit of Unit 6 at Section II. Base of unit shows unloading structures. Scale to left is 15 cm.

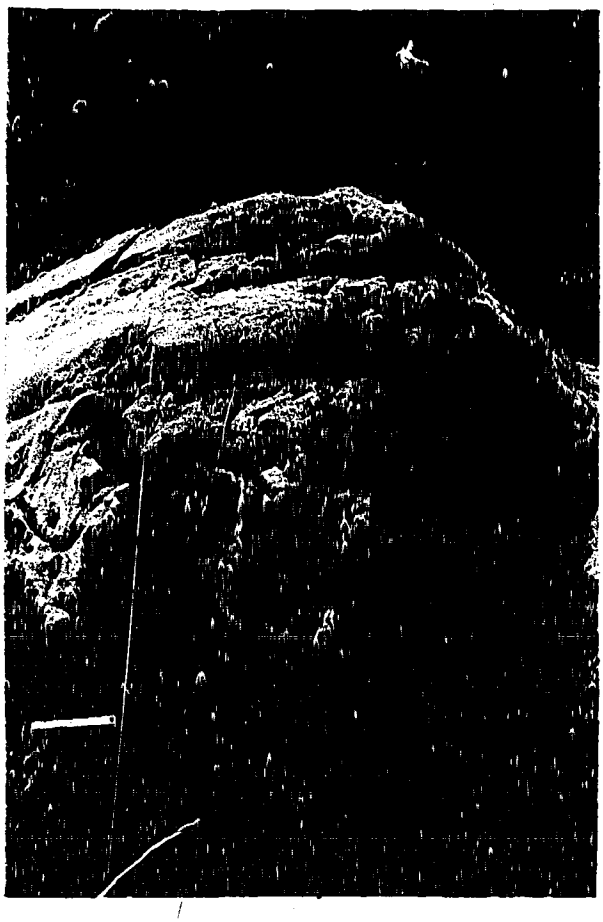

A vertical suite of samples from one unit (Section I-Unit 2) indicates only minor vertical fluctuations in the compositional parameters (Figure 34). Moisture content (0.32%), organic matter (1.28%), carbonate (8.94%) and total carbon (10.11%) content are fairly low (Table 6). Particle size changes indicate the greatest amount of variability with sand concentrations from 13-35%, silt from 50-67%, and clay from 15-23%. Sediments are poorly sorted (2.57Ø), strongly fine skewed (0.43Ø), and leptokurtic (1.30).

Values for samples from the other localities are in general agreement with the above example. For instance, a similar thin, sandy silt (draped laminated) interbed occurs near the base of Unit 3 at Section I. Texturally, this bed consists of 38% sand, 53% silt, and 9% clay. Moisture content (0.24%), organic matter (1.24%), carbonate (4.25%), and total carbon (5.44%) content values are all quite similar to the thicker accumulations. This deposit also displays very poor sorting (2.2Ø), and is leptokurtic (1.49), but is nearly symmetrical (0.0). A suite of paleomagnetic samples were obtained from this particular bed for NRM analysis (Figure 32). The equal area projection shows the changing mean vector trend and plunge of the magnetically oriented silt sized particles with depth (horizons A to E) (Figure 24). All samples display a normal polarity toward the NW with mean trend and plunge for the entire bed of 342.8° and 68.2°. The overall bed analysis indicates a fairly strong S1 eigenvalue (=0.944).

A contorted, silt-dominated bed (Unit 6) averaging 1.5 m in thickness occurs between two thick horizontally stratified gravel units at Section II. Inverse grading is evident in this disrupted deposit, as illustrated by compositional analysis (Figure 34). Stratification consists primarily of massive to deformed horizontally stratified laminae and beds. Texturally, the unit averages 34% sand, 51% silt, and 15% clay. Moisture content (0.35%), organic matter (1.48%), carbonate (6.68%), and total carbon (8.07%) values are all low. The unit is very poorly sorted (2.69Ø), fine

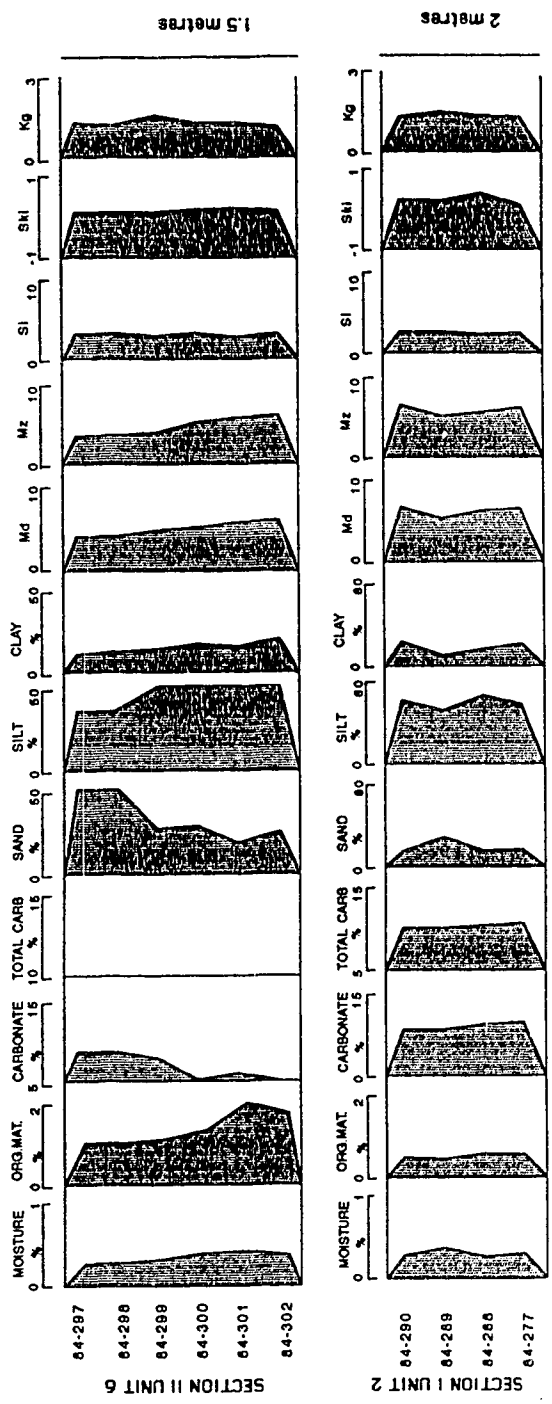

Figure 34. Compositional variation with depth for silt deposits for two units at Sections I and II.

Table 6. Summary of various compositional parameters for silt dominated deposits.

SECTION II-UNIT 6	MIN	MAX	MEAN	SD	N
SAND (%)	20	53	34	14.26	6
SILT (%)	37	64	51	11.54	6
CLAY (%)	10	22	15	4.22	6
MOISTURE (%)	0.24	0.49	0.35	0.11	6
ORGANIC MATTER (%)	1.05	2.16	1.48	0.46	6
CARBONATE (%)	4.76	8.98	6.68	1.95	6
TOTAL CARBON (%)	6.19	9.94	8.07	1.58	6
Md (Ø)	3.80	5.55	4.68	0.70	6
Mz (Ø)	3.93	5.78	4.86	0.80	6
Si (Ø)	2.31	2.91	2.69	0.22	6
Ski	0.15	0.24	0.19	0.03	6
Kg	1.04	1.77	1.30	0.25	6

SECTION I-UNIT 2	MIN	MAX	MEAN	SD	N
SAND (%)	13	35	21	9.81	4
SILT (%)	50	67	60	7.41	4
CLAY (%)	15	23	19	3.65	4
MOISTURE (%)	0.32	0.33	0.32	0.01	4
ORGANIC MATTER (%)	1.20	1.34	1.28	0.06	4
CARBONATE (%)	8.65	9.34	8.94	0.34	4
TOTAL CARBON (%)	9.74	10.55	10.11	0.39	4
Md (Ø)	4.85	5.65	5.26	0.36	4
Mz (Ø)	5.27	6.35	5.83	0.46	4
Si (Ø)	2.43	2.66	2.57	0.10	4
Ski	0.38	0.53	0.43	0.07	4
Kg	1.10	1.47	1.30	0.15	4

skewed (0.19), and leptokurtic (1.3). Two types of loading structures are present. The basal contact displays a high amplitude convoluted appearance, whereas the horizontally truncated upper half of the unit shows ball and pillow structures. A burrow and single gastropod shell were also found in the unit. Additionally, organic rich horizons were recognized in adjacent, undeformed exposures of this unit.

A suite of paleomagnetic samples were retrieved from Unit 6 at Section II in an area of minimal disturbance. The results of this analysis are illustrated in the equal area projection of the NRM fields in Figure 24. All samples are magnetically normal and are clustered to the north with a mean vector trend of 9.1° and plunge of 68.4°. Samples 4C2A-E indicate a clockwise progression of horizon vectors up section.

The silt-dominated sediments of Unit 1 at Section VIII are approximately 4 m thick, and consist of massive to horizontally laminated silts and sands. Sets are normally graded over a few centimetres and contain isolated stones (~1%) below which are penetrative structures which mirror the shape of the overlying clasts, and rounded clay rip-up clasts. Some pebbles show scour features filled with granular sediment around the clast margin. Type B ripple drift cross-lamination, an isolated stone, and pipe and dish structures are found near the base of the unit (Plate 19). The upper part of the unit displays flame and ball and pillow structures, with 'saucer-shaped' medium sands balled over graded silts and fine sands (Plate 20). The unit is conformably overlain by stratified sands.

The thickest silt accumulation along the Finlay River is the 10 m deposit characterizing Unit 3 at Section XI. This primarily horizontally stratified accumulation overlies a structureless diamicton along a sharp contact, and is in turn overlain by horizontally stratified gravels. Individual silt beds range from 2-10 cm in thickness and display normal grading. Interbed contacts are all sharp and conformable. Unloading and other deformation structures are not evident. Texturally, the unit consists of 2% sand, 79% silt, and 19% clay. With the exception of the

Plate 19. Photograph illustrates horizontal and ripple-drift cross-lamination in sandy silt deposit of Unit 1 at Section VIII. Pipe structures and isolated clast also evident in photograph. Trowel for scale.

Plate 20. Photograph illustrates unloading features at top of Unit 1 at Section VIII. Trowel for scale.

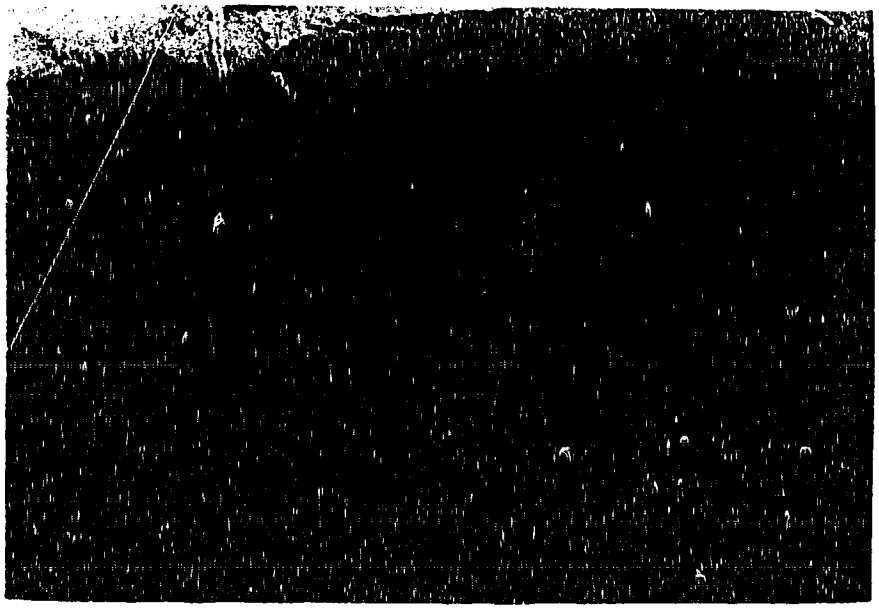

predominance of silt over clay, and large maximum thickness, this unit is essentially identical to the silty clay Unit 2 from Section XII.

Unit 3 at Section W.A. averages 3 m in thickness and possesses a sharp, curvilinear and unconformable basal contact overlying disrupted gravel and sand. The lateral margins of the bed contains horizontally continuous, fractured clay clasts, and occasional large clasts. Internally, sediments are massive, with crenulated, nonparallel bedding planes dipping in multidirections. This moderately well sorted deposit (Unit 3), intertongues with a convex (60 m wide) accumulation of dark, horizontally stratified silty sands (Unit 4). At present, the sediment is actively being reworked by wind action.

Interpretation

The relatively thin (2 m) draped and ripple cross-laminated silt deposits at Sections I(2 and 3), IX(2) and the clay-dominated unit 6 at Section X are interpreted to represent overbank fine sediments. Similar deposits have been identified by Miall (1985) and others. The silts overlie gravels and sands interpreted to represent aggrading braided channel sediments. Thus, the stratigraphic context supports an overbank sedimentation model. Ripple drift and draped laminae reflect deposition from fluids with high suspended sediment concentrations which experienced marked reduction in flow discharge (Ashley et al. 1985). Organic stains and streaks occurring as interbed contacts support a channel marginal environmental interpretation (cf. Miall 1977).

The deformed silts at Sections II(6) and VIII(1) represent sediment gravity flow deposits. The first occurrence at Section II is interpreted to represent a series of subaqueous liquefied flow sediments deposited over gravels. Deformation, in the form of load structures, is the result of reverse density gradients (Mills 1983). The basal deformation may represent loading in a mobile system as defined by Reineck and Singh

(1980). Diapiric trough structures develop along the contact parallel to flow during sediment movement. The upper loading structures reflect nonmobile deformation of sediments with different densities. Favorable conditions for the formation of pseudonodule load structures appear to be a rapid deposition of the fines, followed by a rapid deposition of coarser sands (Mills 1983) that shocks the saturated underlying sediments. Differential settling of sand into the saturated silts and concomitant upward migration of silt to accommodate the displacement results in the formation of the saucer shaped sand pillows (Reineck and Singh 1980).

The single trace fossil shaft observed in this deposit consists of a vertically tilted lined burrow (Plate 21). In the terminology of Ekdale et al. (1984), the feature represents an actively filled endogenic tube with a fecal pellet at its base. Paludal environments have received considerable attention in terms of modern analog studies for trace fossils, especially exogenic types (eg. Metz 1987). Insect remains are commonly encountered in cored Pleistocene glacilacustrine deposits (Hann and Karrow 1984). Proglacial lake sediments also contain burrow structures (Duck and McManus 1984). This burrow is interpreted to represent a feeding burrow (Fodinichnia) of an annelid, found in either fluvial or lacustrine environments (cf. Ekdale et al. 1984). The gastropod specimen is identified as Fossaria cf. modicella, a common pond snail. This ubiquitous species is found in perennial streams, lakes and ponds south of the tree line in North America (Clarke 1981). Fossaria sp. and other molluscs are commonly found in Quaternary ice proximal sediments in North America (Clayton 1961).

Several features point to subaqueous liquefied flows (laminar high density suspension deposits) and a current reworking origin for Unit 1 at Section VIII. The climbing ripples indicate current activity and tractional movement of migrating sediment. According to Reineck and Singh (1980), Type B climbing ripple laminations can be formed by any type of migrating ripple, as long as a continuous supply of sediment is available. The presence of dewatering pillars and some dish structures

Plate 21. Trace fossil with pellet in Unit 6 at Sectio II. Ruler for scale.

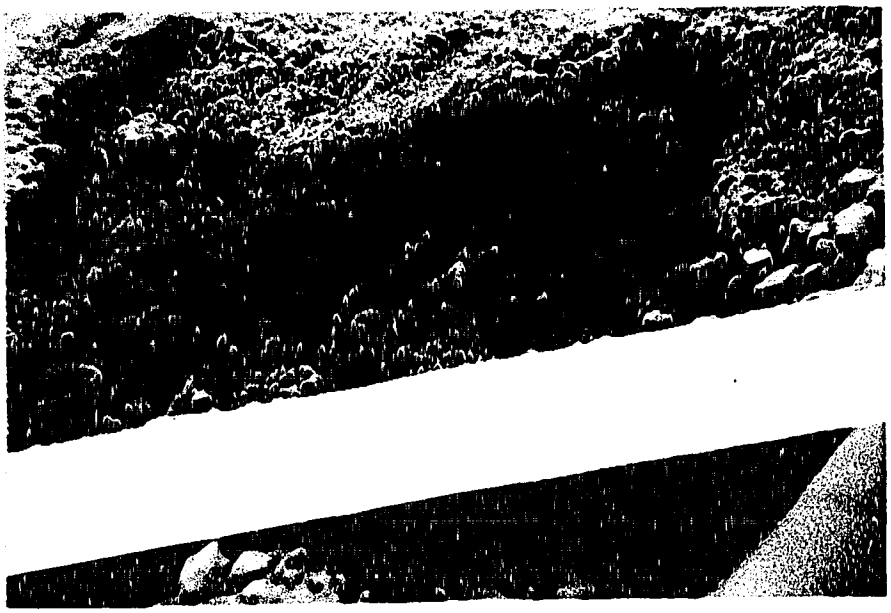

indicates deformation of water saturated sediment which is either liquefied or fluidized (Lowe 1982). Coarse silts and fine sands with normal grading typify liquefied flows (Lowe 1982). In Unit 1 pore water pressure attained equilibrium by restrictive water release along thin pipe structures. The uppermost deformation consists of flame structures generated by shear stresses during reverse density loading (Mills 1983). Minor sediment pulsation downstream accounts for the marked textural variation and also explains the loading and tilting of flames in a downstream direction. Deposition of Unit 1 may have occurred in a distal proglacial lacustrine environment. The isolated clasts in this matrix-dominated unit are interpreted as representing dropstones deposited from berg-ice [ice-rafted debris of Powell (1981)] or seasonal ice. Current activity continued to occur, as indicated by the current shadows (or current crescents) around clasts and subsequent infilling by granular particles (cf. Allen 1984). The proglacial lake may have been of considerable size, as none of the sediments present contain ice proximal features. Progressive coarsening of sediments over the silts further suggests advancing ice conditions rather than retreating ice conditions.

Silts and sands in Unit 3 at W.A. are difficult to interpret. Their position over sands and gravels, and the draped laminations near the base, suggest an interpretation of overbank sedimentation processes. Planar clayey silt rip-up structures along the unit margin, however, indicate fractured reactivation surfaces, and nonparallel stratification of 'massive' beds suggests local aeolian redeposition. Repeated wetting and drying of the surface and subsequent downthrow of the capped beds results in the faulted clayey silt skins in aeolian deposits (cf. Allen 1984). Pettijohn and Potter (1964, Plate 32A) illustrate a similar structural pattern in modern sand dunes. Boulders along the margin of the deposit possibly rolled in from the banks during sediment accretion.

ii) Clays

Description

Isolated laminae and pockets of clay, interstitial clay mixed with silt and sand, and clay skins over clasts occur throughout exposed sections of the Finlay River. Beds proportionately containing > 50% (by volume) particles 8-14 Ø in size range were classed as clays and prefixed by the next dominant grain size if required. Thick deposits of clay are present throughout the region in several forms, but relative to all other sediment types clays occur in lesser amounts.

Clay is found as the primary or dominant textural class in a number of well sorted deposits (Plate 22). At sections III (Unit 5), X (Unit 6), and XII (Unit 2), clay sediments dominate the lithostratigraphic units or major beds within these units (Figure 12). Deposits range in thickness from 1.75-4.00 m and average 2.9 m. Thicker deposits represent clay beds interbedded with beds of silt and sand. All of these clay deposits are laterally discontinuous. The sediments overlie fining upward sequences of gravel and sand (Section X-Unit 6), distorted gravels (Section III), or bedrock (Section XII). Basal contacts which were not indeterminate are sharp, and drape the underlying sediments (disconformities and paraconformities). At section III for example, clays drape a boulder lag for a distance of ~3 m along the basal contact of Unit 5.

Stratification varies from individual laminae 0.1 cm thick to graded beds 5.0 cm thick. Parallel stratification or draped lamination dominates the internal structure of finely laminated sediments, whereas massive and normally graded textures typify the thicker beds. Contacts are all conformable. Graded beds contain varying amounts of sand (11-40%) and silt/clay (60-89%) mixtures. At section X (Unit 6), alternating beds of sand, silt, and clay dominant strata are interbedded providing a lithostratigraphic unit average of 22% sand, 39% silt, and 39% clay. Graded beds at section XII(2), are rhythmic and texturally similar to each other, containing 47% silt

Plate 22. Graded clay dominated beds within Unit 6 at Section X. Exposed section is approximately 1.5 m in height.

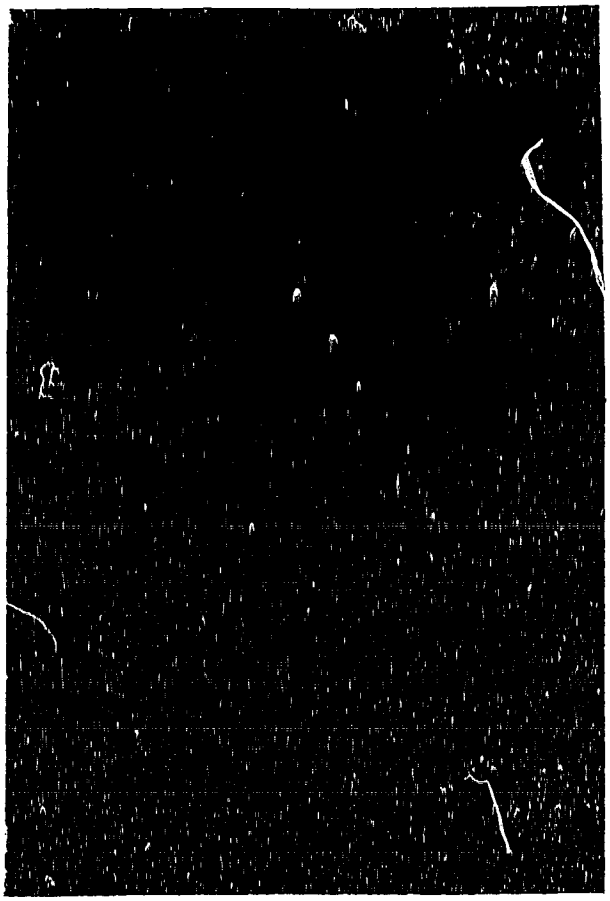

and 53% clay. Moisture content is low (0.3-1.8%) for all clay deposits. Organic matter varies from unit to unit. Horizons at Section X(6) contain 6.9-10.3% organic matter content, whereas section XII is generally low in organic matter (2.2%). An organic rich surface in Unit 6 at Section X was sampled for ^{14}C dating and provided a finite date of 29,880 ± 1680 years B.P. (AECV-349C).

Unit 2 at Section XII was subjected to paleomagnetic sampling and analysis. Figure 32 provides an equal area projection of the horizon mean vectors for the 20 samples. Except for a single aberrant value, the vectors are magnetically normal and clustered to the NE with a mean unit trend of 31.4° and plunge of 51.4°.

One package of clay dominated sediments 5 m in thickness at Section X (Unit 9) extends the breadth of the mappable exposure (750 m). Unit 9 consists of a compact and hard deposit of rhythmic silty clay beds and has a gradational basal contact over a thin subaqueous sediment gravity flow deposit (Unit 8). Beds vary in thickness from 1-20 cm, and display a weak normal gradation in texture. This gradation results in color banding, giving couplets of dark grey (5Y 4/1) clay and pale olive silts (5Y 6/3). The sediment within the beds is composed of an average of 1% sand, 25% silt, and 74% clay. Isolated small pebbles are randomly distributed through the unit and occasionally impart penetrative structures in the bedding planes. Draping of the clasts was not observed. Small rip-up clasts and flame structures are dispersed along the basal part of each bed. Interbed contacts are all conformable, convoluted to straight, and display some syndepositional deformation. Each depositional bed is internally structureless. Figure 35 displays the vertical compositional variability within the unit. The compositional characteristics are quite stable and remain the same through numerous beds. Unit averages indicate a low moisture content (0.65%), low organic matter content (2.79%), and low carbonate content (9.58%). The sediments are very poorly sorted (2.19Ø), fine skewed (0.16), and platykurtic (0.86).

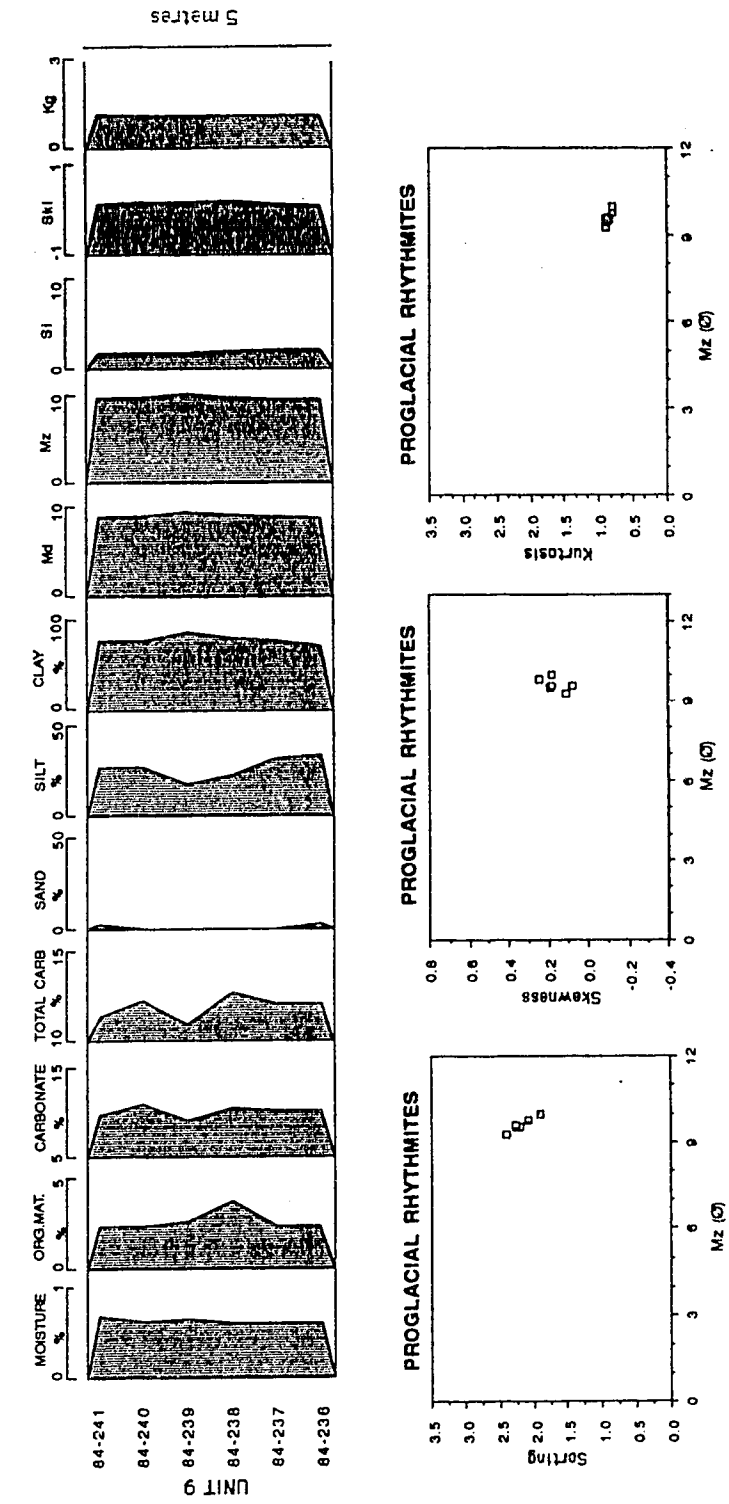

Figure 35. Top illustrates compositional variation in silty clay rhythmites of Unit 9 at Section X. Bottom bivariate graphs compare graphic statistics of same sediments as top. Point cluster distribution is similar to "diamictic varves" of Banerjee (1973b). See text.

Interpretation

The graded and draped laminated silty clay deposits observed at Sections III, X (2 and 6) and XII are interpreted to represent suspension rainout of sediments from stagnant or very slowly moving water (Ashley et al. 1985). The thickness and lateral extent of the deposits at sections III and XII suggest gradual release of sediment from suspension into depressions or small temporary ponds associated with the braided stream environment. A similar interpretation applies to the clay sediments in Units 2 and 6 at Section X, but at this section the clays also contribute to a fining upwards sequence.

Braided rivers, although laterally very active, also record overbank sedimentation onto floodplains and into abandoned channels (Bridge 1985). The thicker sediments at Section X may record sediment response to stream avulsion by channel infilling. Mud or dessication cracks were not observed, but their potential for preservation is generally low (cf. Miall 1977). According to Collinson and Thompson (1982), massive clays represent uninterrupted sedimentation or postdepositional biogenetic destruction of laminae. Evidence for biogenetic modification was not observed. Drifted plant material is commonly preserved in finer point bar sediments (Allen 1965) which may account for the organic rich streaks in Unit 6 of Section X.

The difficulty in distinguishing between paludal and overbank sediments is reduced in the slightly coarser sediments. Alluvium deposited through overbank sedimentation is seen as a primary depositional mechanism for most of the finely stratified silt and fine sand accumulations discussed below. In the following units interpreted to be overbank deposits, clay rich laminae are intercalated with the silts and sands : I(2), II(4), W.A.(3), IX(2), and XI(3).

The rhythmically bedded silty clay sediments of Unit 9 at Section X are interpreted to represent glacilacustrine rhythmites similar to those of Ashley et al. (1985). These episodic beds result from sedimentation of turbid density driven

underflows into a proglacial environment. Each couplet represents the uppermost Tc (suspension) and Td (traction-suspension) subdivisions of the Bouma sequence expected of distal low density turbidity currents (Lowe 1982). The loading structures and rip-up clasts observed are similar to those described by Banerjee (1973a) in glacilacustrine sediments which he termed diamictic varves. The interrelationship of various graphic parameters illustrated in the three bivariate graphs of Figure 35 occur in the same distributional range as that illustrated by Banerjee (1973b, p. 56) for glacilacustrine rhythmites. These distal turbidite sediments support the hypothesis that the local underlying diamicton (Unit 8) is also a subaqueous flow deposit, but of higher density.

IV. Stratigraphy

A. GENERAL STATEMENT

The stratigraphic objectives of this study emphasize the use of section specific lithostratigraphic units for research. The geological significance of these units required the identification and review of 15 sediment types which occur in varying frequencies within these numerous units. In Chapter 3, each sediment type was described in detail and representative occurrences within the various lithostratigraphic units were discussed. Genetic interpretations were also offered for each of the sediment types.

The purpose of this chapter is to present the composite Quaternary age stratigraphy of the northern Rocky Mountain Trench (RMT) based on correlation of the lithostratigraphic units described in Chapter 3. As noted by Tipper (1987), lithostratigraphic units are defined on lithological characteristics and are totally independent of time. Correlation, therefore, simply involves the recognition of lithologic equivalence and not necessarily time equivalence. Similar units are placed into broad sediment packages related to the sediment types and genetic interpretations. Stratigraphic position and geochronologic control, however, influence correlation (North American Commission on Stratigraphic Nomenclature 1983). The stratigraphy in the study area is, therefore, presented in a time-stratigraphic sequence from oldest to youngest. The process involved in correlation of equivalent lithostratigraphic units is provided within the discussion for each sediment package (see Figure 36 and Table 7).

The objectives of this study centre on the importance of past glaciations which, therefore, require an arbitrary but informal assignment of time equivalence to each glacial event. As such, the informal phrases lower till (within Lower Diamicton

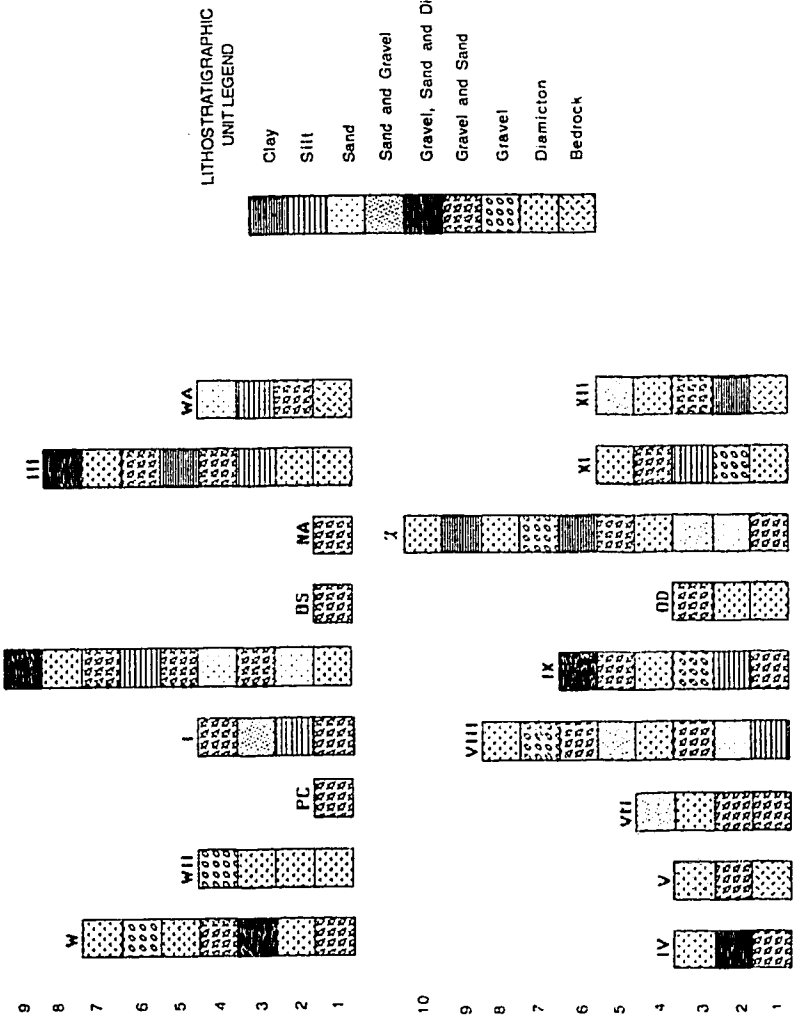

Figure 36. Schematic composite stratigraphic columns for 18 sections along the Finlay River. Lithostratigraphic unit numbers along left and textures as in legend. To locate lithostratigraphic unit follow scale across page to appropriate section. Section codes on top of columns are defined in Chapter 1, Figure 1. Not to scale.

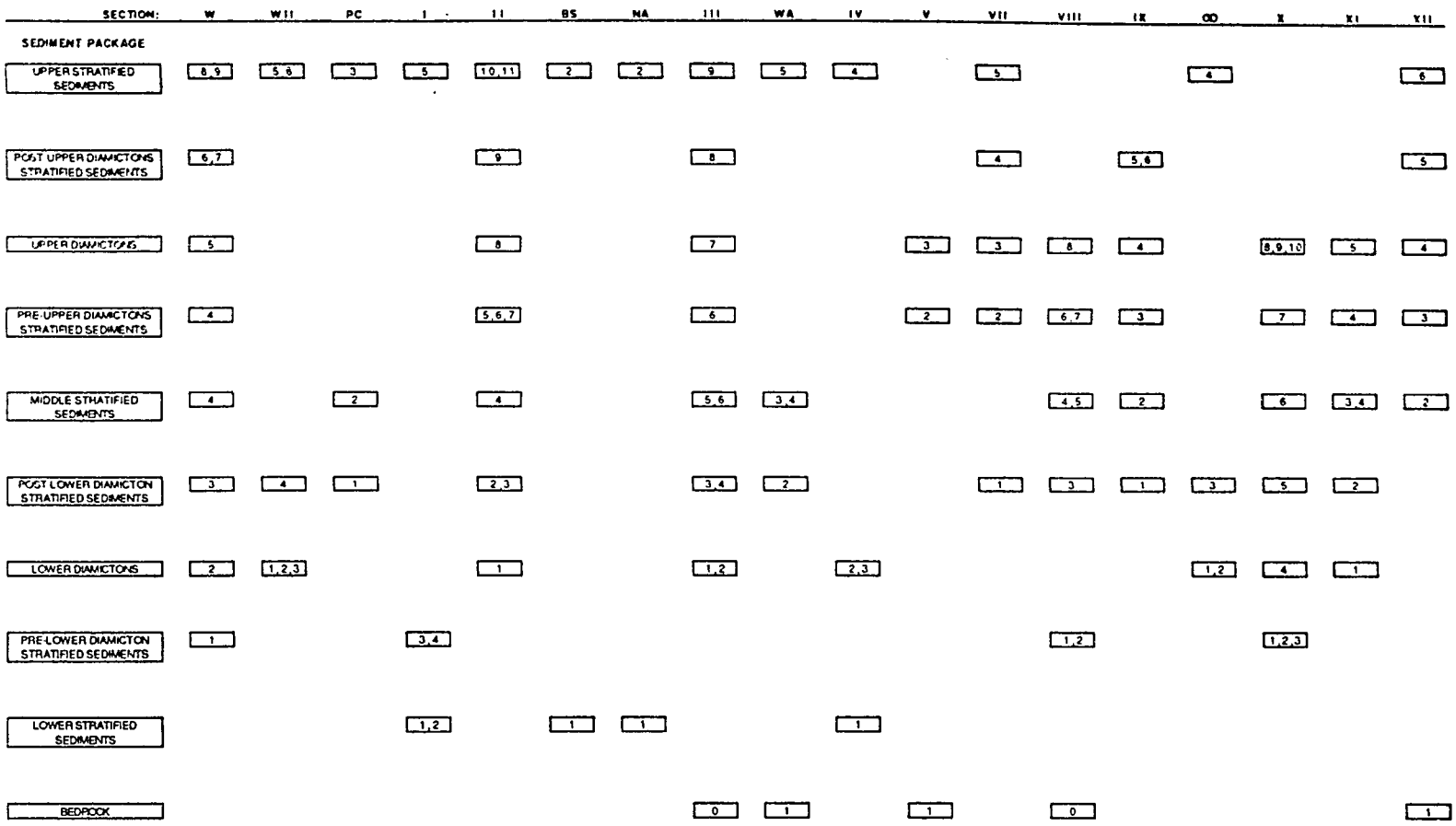

SECTION:	W	WII	PC	I	II	BS	MA	III	WA	IV	V	VII	VIII	IX	OO	X	XI	XII
SEDIMENT PACKAGE																		
UPPER STRATIFIED SEDIMENTS	8,9	5,8	3	5	10,11	2	2	9	5	4		5			4			6
POST UPPER DIAMICTONS STRATIFIED SEDIMENTS	6,7				9			8				4		5,6				5
UPPER DIAMICTONS	5				8			7			3	3	8	4		8,9,10	5	4
PRE-UPPER DIAMICTONS STRATIFIED SEDIMENTS	4				5,6,7			6			2	2	6,7	3		7	4	3
MIDDLE STRATIFIED SEDIMENTS	4		2		4			5,6	3,4				4,5	2		6	3,4	2
POST LOWER DIAMICTON STRATIFIED SEDIMENTS	3	4	1		2,3			3,4	2			1	3	1	3	5	2	
LOWER DIAMICTONS	2	1,2,3			1			1,2		2,3					1,2	4	1	
PRE-LOWER DIAMICTON STRATIFIED SEDIMENTS	1			3,4									1,2			1,2,3		
LOWER STRATIFIED SEDIMENTS				1,2		1	1			1								
BEDROCK								0	1		1		0					1

Table 7. Correlation of lithostratigraphic units in 18 sections along the Finlay River. Sediment packages listed to left in idealized stratigraphic column. Units within numbered boxes, section names along top defined in Figure 1.

sediment package) and upper till (within Upper Diamicton sediment package) are used to denote stratigraphically distinct deposits related to separate glaciations (Figure 37).

B. BEDROCK

The bedrock geology of the study area is illustrated in Figure 3 and itemized in Table 3 of Chapter 1 and will not be reviewed in detail here. Briefly, most of the RMT proper consists of Upper Cretaceous and Tertiary sandstone, conglomerate, shale, and coal. To the east, Paleozoic and Mesozoic faulted and folded sedimentary rocks occur within the Rocky Mountains. To the far west in the Omineca Mountains, low grade Paleozoic and Mesozoic metamorphic and igneous rocks are present.

Several of the exposed bluff sections encountered along the Finlay River display the variety of bedrock types which occur within the northern RMT. In certain cases, the bedrock was assigned a lithostratigraphic unit designation in conjunction with the unconsolidated sediments (Table 7). For instance, shale outcrops with coal inclusions were observed at the base of Sections VIII (Plate 2) and WA(1). Sandstone and conglomerate outcrops are more abundant and were observed in significant proportions all along the river valley. Bedrock outcrops at designated bluffs include Sections III, WA(1), V(1), and XII(1) (Plate 2).

A detailed examination of the bedrock outcrop at Section XII(1) was undertaken as a case example of the Sifton Formation (see section description in Appendix 16). Here, the 13 m of exposed rock consists of a poorly sorted cobble conglomerate with occasional silty sandstone interbeds. The conglomerates are massive to horizontally bedded, and contain well-rounded clasts consisting of ~2% boulders, ~30% cobbles, ~30% coarse pebbles , ~10% fine pebbles, and ~28% coarse sand matrix. The unit is moderately indurated and well oxidized. The diagnostic feature of this formation is the absence of igneous clasts. A pebble count at this locality indicates a high percentage of metamorphics (76%), some siliciclastics (18%), and even fewer carbonates (6%).

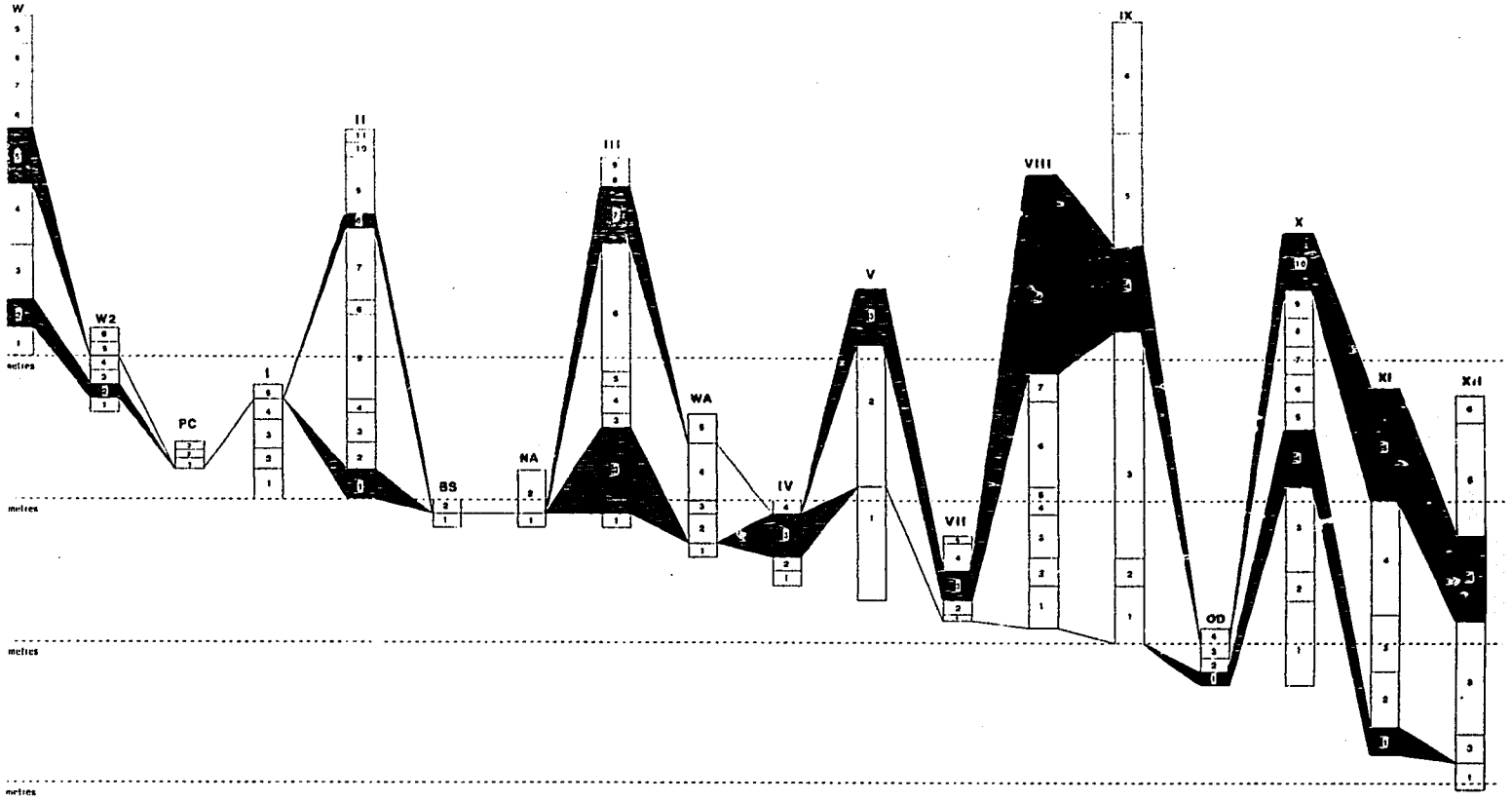

Figure 37. Stratigraphic correlation of two primary tills corresponding to major glaciations. All eighteen sections along the Finlay River illustrated. Section codes defined in Figure 1. Up-stream to left.

The lithological composition observed for the Sifton Formation is not unexpected. Rocks within the RMT are assumed to be predominantly products of regional low grade metamorphism (Gabrielse 1971). Hopkins et al. (1972), believed the Sifton Formation represents sediments deposited by a meandering river during the Late Early Oligocene (32-34 Ma). The palynomorph assemblage retrieved from a locality on the Parsnip River south of the study area by the above authors confirmed the age of this deposit. A correlative, slightly coarser facies, has been recorded by Hedley and Holland (1941) and Evenchick (1984), north of the Finlay River.

A prolonged period of active erosion along the RMT margins with coeval transportation and deposition of valley marginal siliciclastics and carbonates into the RMT itself during the early to mid-Tertiary is indicated. Subsequent fluvial reworking and deposition of the metamorphic, carbonate, and siliciclastic rock types during the mid-Tertiary resulted in the development of the Sifton Formation. Although a considerable amount of erosion, transportation, and deposition may have occurred following the deposition of the Sifton Formation and preceding the first glaciation (circa 32 Ma), very little evidence for this activity is preserved.

C. LOWER STRATIFIED SEDIMENTS

The lowermost stratified sediments in the northern RMT consist of various preglacial deposits. All preglacial sediments are identified on the basis of the following criteria: 1) absence of diagnostic igneous clasts; and, 2) stratigraphic position (eg. basal unit, directly overlying bedrock and/or underlying glacial sediments).

Of the 18 sections examined in this study, only four sections contained lithostratigraphic units which could be assigned to the Lower Stratified Sediments category (Figure 36 and Table 7). Pebble counts samples contain varying proportions of metamorphic and sedimentary clasts, but do not contain igneous clasts (Figure 38).

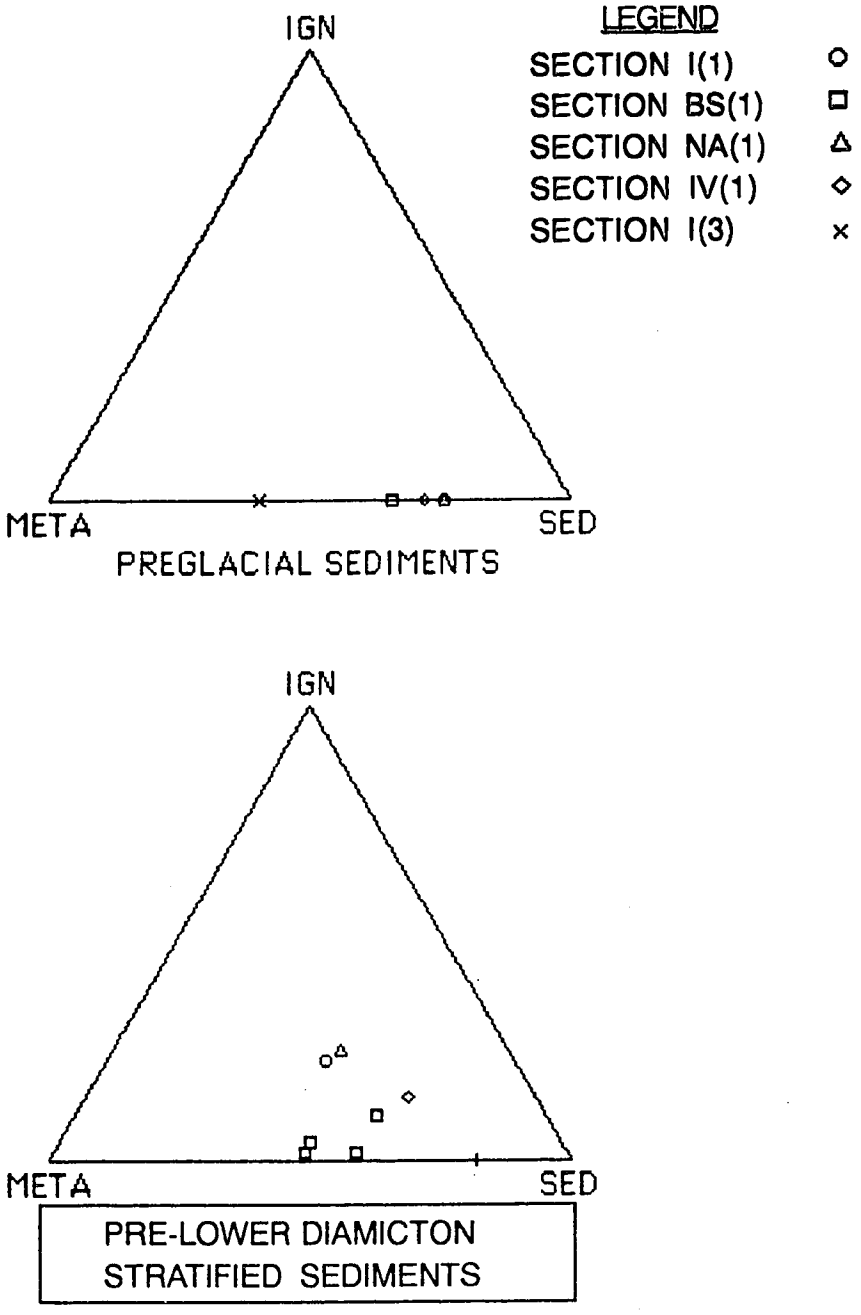

Figure 38. Lithological composition of various preglacial sediments (top) and stratified glacifluvial sediments (bottom) underlying Lower Diamicton Sediment package based on pebble counts from sections along the Finlay River.

These deposits consist of moderately to highly oxidized gravels with sand interbeds [I(1 and base of 3), BS(1), NA(1), and IV(1)] or massive, horizontal, and draped laminated organic silts [I(2)] overlying the oxidized gravels. Gravel sediment types observed in these lithostratigraphic units include stratified (horizontal and planar cross-stratified), and normally graded gravels. Sand sediment types consist of planar tabular and trough cross-stratified accumulations. Sediment types in the above package represent barforms and ripples found in a fluvial gravel-dominated braided stream environment (cf. Chapter 3). The horizontal and draped laminated organic silts correlated to this package were interpreted in Chapter 3 to represent channel marginal floodplain deposits (overbank fines) within the braided stream environment. Amino acid analysis of the organics in the silt unit indicates the carbonaceous sediment is derived from Tertiary coal strata (see Chapter 5). All of these sediments represent deposits of the fluvial activity which occurred from mid-Tertiary to earliest preglacial times.

D. PRE-LOWER DIAMICTON STRATIFIED SEDIMENTS

The onslaught of the earliest glaciation in the northern RMT is marked by the appearance of igneous clasts in sediments overlying oxidized preglacial deposits (Figure 36). Stratigraphic discussion centres on assemblages consisting of stratified sediments underlying till (i.e. till within the Lower Diamictons category).

During the early stages of glaciation stratified sediments were deposited in front of the advancing ice. These stratified sediments contained lithologies similar to those present in the ice mass (Table 7). In this study, the presence of igneous clasts in the pebble counts is believed to indicate glacier proximity. A ternary plot of clast lithologies for the lithostratigraphic units correlated to the Pre-Lower Diamicton Stratified Sediment package illustrates this phenomenon (Figure 38).

Two assemblages of stratified sediments are preserved in the forefront of the earliest glaciation: distal and proximal deposits. The first and older of the two sediment assemblages (distal) consists of interbedded sand and gravel and is evident at Sections W(1), I(3-top and 4-bottom), IV(2-bottom), and X(1, 2, and 3-bottom). In this first assemblage, sediment type is restricted to stratified gravels consisting of horizontal beds and planar cross-stratification, and planar cross-stratified sands (minor component of horizontal and trough cross-stratified sand). Pebble fabrics obtained from the stratified gravels can be summarized (Figure 39). The clast orientations show strong girdles and transverse to valley azimuthal trends (b-axis imbrication to the N). The above sediment types were interpreted in Chapter 3 to represent various parts of a braided river environment including longitudinal, transverse and diagonal barforms, lower flow regime ripples and megaripples, as well as upper flow regime flat beds. The entire suite of sediments are interpreted to represent the aggrading distal reaches of a braided river (paleoflow to the SSE) whose effective discharge was increasing as a result of an encroaching ice mass from the NNW.

The above interpretation is further supported by the stratigraphic transition upward into the second assemblage (proximal) of stratified sediments [Sections I(4-top), VIII(1 and 2), and X(3-top)]. At Sections I and X, this second assemblage consists of massive and inversely graded gravels, which were interpreted in Chapter 3 to represent modified grain flow deposits. Rapid frictional freezing of the highly concentrated coarse clast-supported flows is common in proximal deposits. These sediments are therefore considered to be deposited directly in front of the advancing ice. The representative lithostratigraphic units in Sections I and X differ from the underlying sediments in two ways: 1) they lack sand interbeds; and, 2) the clasts are generally coarser than in the underlying gravels.

Units 1 and 2 at Section VIII contains massive sands, horizontally laminated silts and sands, and ripple drift laminated sands, capped with flame, dish, and ball and pillow

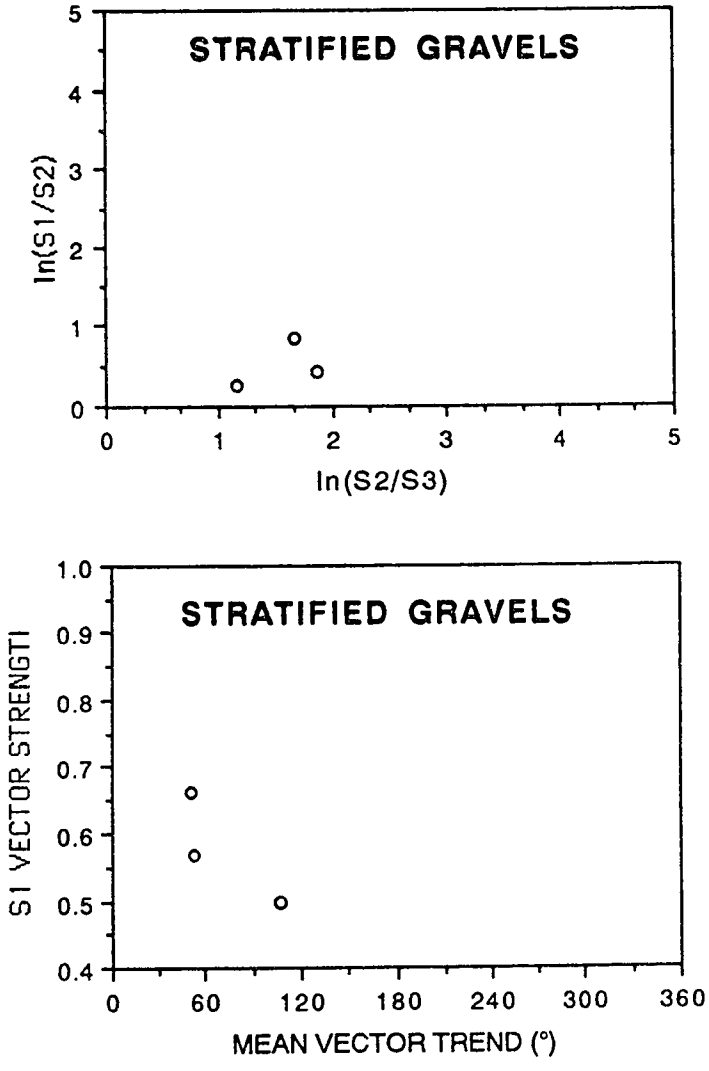

Figure 39. Top figure shows two-axis plot of normalized eigenvalues; bottom figure shows 3-D fabric trend vs. S1 strength for stratified gravels (n=3) in Pre-Lower Diamicton sediment package.

structures. These sediment types were interpreted to reflect subaqueous liquefied flow deposits (Chapter 3). The two units directly underlie an oxidized, distorted gravel accumulation interpreted to be an ice proximal accumulation (i.e. Unit 3). Units 1 and 2 (VIII) provide an isolated example of a coarsening upwards proglacial lake accumulation dominated by subaqueous sediment gravity flow activity. Both the modified grain flow deposits within the coarsening upward sequence (I and X) and the proglacial lake deposits under ice proximal gravels (VIII), indicate increasing proximity to the glacial ice source.

E. LOWER DIAMICTONS

Evidence for the earliest glaciation in the northern RMT consists of a variety of diamicton units (sediment gravity flow deposits and till) observed at eight sections [(W(2), WII(1 and 2), II(1), III(1 and 2), IV(2 and 3), OD(1), X(4), and XI(1)] (Table 7). Correlation between these sections is accomplished in several ways (see Figure 37). None of the sections examined along the Finlay River contains more than two diamictons interpreted to represent till. At five of the sections (W, II, III, X, and XI) where two tills are evident, the lower till is assumed to represent a single early glaciation. This assumption is confirmed at four (W, II, III, and X) of the five double till sections through the use of ^{14}C and amino acid racemization analysis of organics collected between the two tills. As a result, the lower tills in all of these sections are considered equivalent and, therefore, are placed in the Lower Diamicton sediment package (Figure 37).

Physical and stratigraphic attributes of the lower till units further support this correlation and the single early glaciation hypothesis. For instance, seven [all except III(2)] of the eight till units are thin (mean of 4.6 m) ranging in thickness from 2.5 to 10.0 m. Four of the eight tills correlated to the Lower Diamicton package were interpreted to represent basal meltout deposits (diamicton with clastic intrabeds) in

Chapter 3 (W, III, IV, and X). The remaining four tills (WII, II, OD, and XI) are also thin, but represent lodgment till (structureless diamicton).

Compositional characteristics for the correlated till deposits within the Lower Diamictons (excluding subtill sediment gravity flows) indicate both similarity and variability. The unit average compositional values for till from all eight sections arranged from up-stream to down-stream (left to right) do not illustrate increasing or decreasing down-stream trends, as most values change randomly down valley (Figure 40). Average values for the lower till samples (lodgment and basal meltout) are 0.35% moisture content, 1.33% organic matter content, 10.08% carbonate content, and 11.28% total carbon content. Additional compositional averages include: modal grain size (5.90Ø), mean grain size (6.03Ø), sorting (4.35Ø), skewness (0.05), and kurtosis (0.85).

Texturally, the 40 till samples average 36 ± 7.9% sand, 32 ± 6.7% silt, and 32 ± 6.3% clay. The percentage contribution of sand does show a minor decrease down valley. This sand percentage reduction is countered by increasing contributions of both silt and clay. The grain size observation may indicate the progressive effects of grinding, crushing, and abrasion by glacial ice as the valley glacier proceeded south along the RMT and continued to mine new bedrock sources in the valley. This change in grain size also indicates the greater contribution of carbonate bedrock and advance outwash sediments into the basal ice debris down valley.

The 18 pebble fabrics taken from sediments (17 till and 1 sediment gravity flow deposit) in the lithostratigraphic units identified as Lower Diamicton sediments can be illustrated collectively (Figures 41 and 42). The till fabrics indicate that both clustered and girdled distributions are present in the glacial sediments (Figure 41). Moreover, the plunge of clasts in the 17 till samples is evenly separated into up-valley (8 fabrics) and down-valley (9 fabrics) orientations, and the mean vector trend is approximately valley parallel. Most researchers believe that pebble fabrics in till are

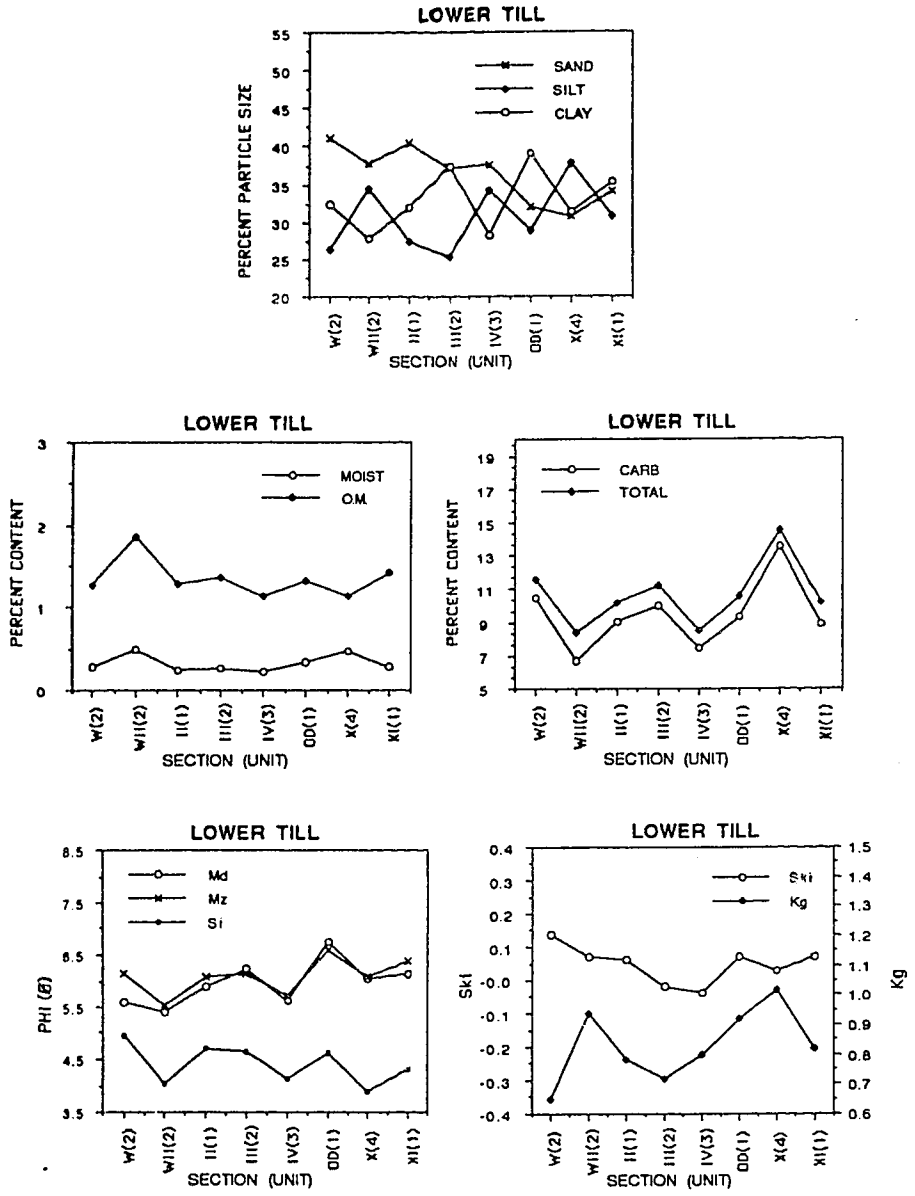

Figure 40. Bivariate graphs illustrating changing compositional values for various units at eight sections containing the lower till (in Lower Diamicton sediment package). Up-valley to left in each figure. Section codes defined in Figure 1.

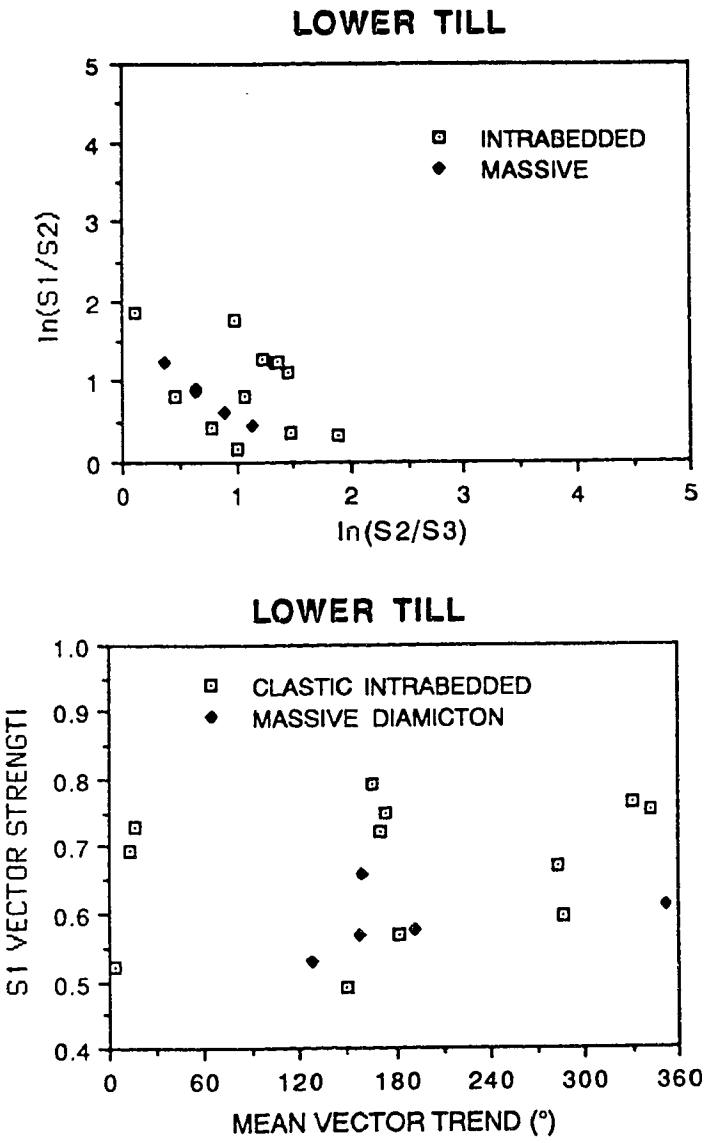

Figure 41. Top shows two-axis ratio plot of normalized eigenvalues; bottom shows 3-D pebble fabric vs. S1 trend strength for tills (n=17) in Lower Diamictons sediment package.

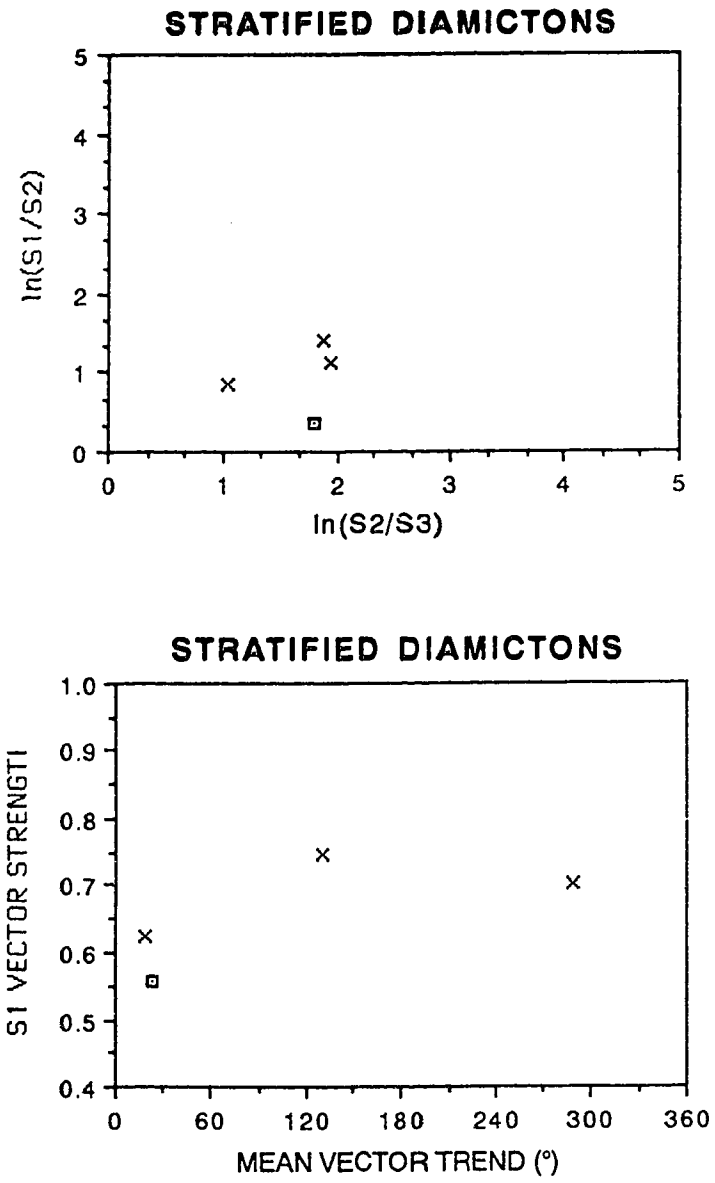

Figure 42. Top shows two-axis ratio plot of normalized eigenvalues; bottom shows 3-D pebble fabric vs. S1 strength for stratified diamictons (n=4) in Lower Diamictons (squares) and Post-Lower Diamictons (x) sediment packages.

primarily parallel to the original glacial flow (eg. Lawson 1979a, 1979b; Mills 1979a). The mean trend of the clasts in these fabrics indicates glacial flow was primarily parallel to the valley. The bidirectionally divided clast plunges do not aid in ascertaining the direction of flow. S1 values for meltout till (n=12) ranges from 0.492 to 0.793 (mean is 0.672), and for lodgment till (n=5) S1 ranges from 0.570 to 0.657 (mean is 0.588)

Fifteen pebble count samples from the eight sections were retrieved from the lower till and their lithological variability was quantified (Figure 43). The percentage contribution of igneous clasts out of the total is illustrated by section, again ordered from up-stream to down-stream (left to right). Igneous clasts are present, but the majority of the pebbles are sedimentary and metamorphic. As discussed in Chapter 1, igneous bedrock is limited in distribution to the west of the Finlay Ranges (Figure 3). The nearest source of this bedrock occurs 50 km west of Fort Ware in the upper reaches of the Finlay River. The bedrock information, paleoflow of the advance outwash to the SSE, and the valley parallel ice flow discussed above, suggests original glacial flow would have been to the SSE along the RMT.

Within the Lower Diamicton package, four of the eight tills [WII(2), III(2), X(4-top), and XI(1-top)] gradationally overlie stratified diamictons (banded diamictons) [WII(1), III(1), X(4-base), and XI(1-base)]. These subtill banded diamictons were interpreted in Chapter 3 to be the result of deposition of sediment gravity flows into depressions or cavities directly below the active ice mass. A single pebble fabric sample from this sediment type indicates a valley oblique azimuth trend towards 023.2°, plunge of 11.3°, and S1= 0.556 (Figure 42).

F. POST-LOWER DIAMICTON STRATIFIED SEDIMENTS

Following the glaciation of the Finlay River valley, a suite of sediments was deposited during deglaciation. Twelve sections (W, WII, PC, III, III, IV, VII, VIII, IX,

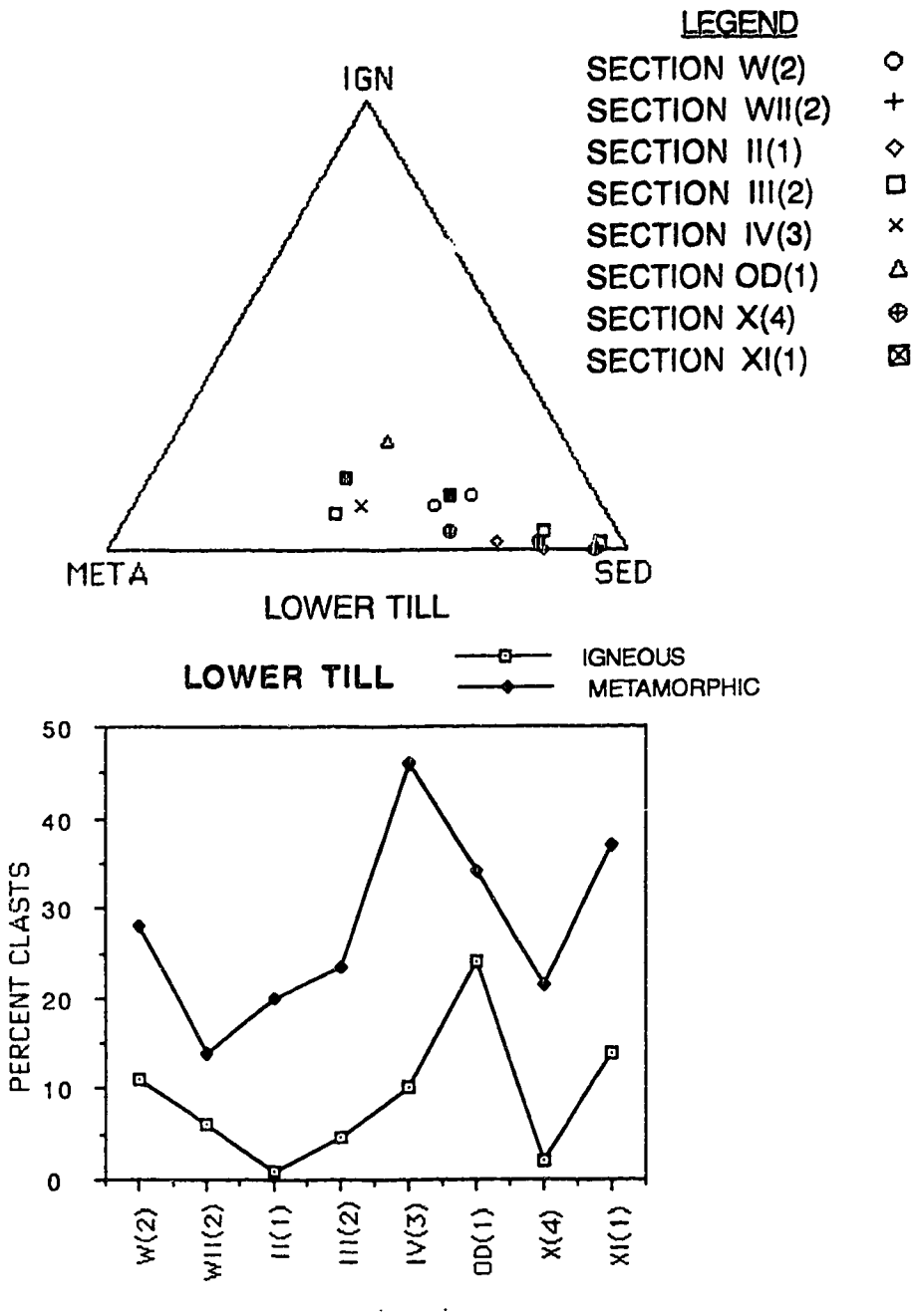

Figure 43. Top figure is ternary plot of lithologic composition in the lower till based on 15 samples from eight sections. Bottom figure shows downstream variation in the percentage of igneous and metamorphic clast composition based on unit averages at eight sections along the Finlay River. Section codes defined in Figure 1. Up-stream to left.

OD, X, and XI) contain lithostratigraphic units correlated to this sediment package (Figure 36 and Table 7). These sediments contain igneous clasts and are oxidized; the latter reflecting a period of prolonged exposure following the deglaciation of the area.

The following criteria were used to associate lithostratigraphic units with the Post-Lower Diamicton sediment package: 1) identification of the lower till directly below units at seven sections (W, WII, II, III, OD, X, and XI); 2) ^{14}C dates above the units at seven of the sections (W, II, III, WA, VIII, IX, and X); 3) identification of an upper till above the units at eight of the sections (W, II, III, VII, VIII, IX, X, and XI); and, 4) identification of fluvial sands and gravels above the units at ten of the sections (W, PC, II, III, WA, VIII, IX, X, XI, and XII).

At Sections W(3-base), WII(3), and OD(2), sediments consist of stratified diamicton gradationally overlying structureless diamicton. Fabric data (n=3) from the stratified diamictons in this sediment package are compared (Figure 42). Samples are girdled and trends show broad azimuthal directions. The S1 values for the 3 fabrics range from 0.631 to 0.760 (mean of 0.697). In Chapter 3 these stratified diamictons were interpreted to represent basal meltout till deposited over lodgment till (structureless diamicton).

Other sediment types include intercalated normally graded gravels, and poorly sorted massive sands [OD(3), and X(5)]. In Chapter 3, both sediment types were interpreted to represent modified grain flow deposits accreted during waning flow. In the above examples, the sediments display gradational basal contacts with till. These deposits are interpreted to represent ice proximal supraglacial debris accumulating during ice stagnation.

Other sediment types include structureless sands with massive gravel pods [II(2)] and large scale, planar cross-bedded gravels [XI(2)]. At Section II(2), a thick accumulation of horizontally stratified and massive sand with isolated cobble lenses was observed. Horizontally stratified sands represent upper flow regime sedimentation,

whereas the massive sands are products of subaqueous sediment gravity flows. Cobble lenses were interpreted to represent isolated dumps of ice-rafted debris. This accumulation was interpreted to reflect deglacial sedimentation in a proglacial lake (Chapter 3). A second, proglacial lake accumulation at Section XI(2) is indicated by the oxidized deltaic foreset beds overlying the lower till.

Intimately associated with the diamicton dominated ice proximal sediments are intertonguing beds of massive and horizontally laminated sands, and disrupted gravel sequences [W(3-top), WII(4), PC(1), II(3), III(4), WA(2), VII(1), VIII(3), IX(1), OD(3), X(5), and XI(2)]. Oxidation of the disrupted gravels and sands is pervasive in all sections. Deposition of the sand and gravel beds alternated with deposition of the diamictons described above. Pebble fabric data obtained from massive gravel beds correlated with this sediment package are illustrated (Figure 44). Clast orientation is random (trend) and strongly girdled. S1 eigenvalues for these modified grain flow accumulations (n=4) range from 0.474 to 0.658, and average 0.590. In chapter 3, the disrupted sediment type was interpreted to represent an ice contact outwash deposit. Prolonged exposure following deposition of the above sediments is indicated by the oxidized appearance of the sediments. The gravel and sand units described here also contribute to the overall fining upward sequence into finer grained sediments which overlie them.

G. MIDDLE STRATIFIED SEDIMENTS

Stratified sediments interpreted as fluvial rather than glacifluvial (preceding category) products, were assigned to the Middle Stratified sediment package (Figure 36). Deposits assigned to this sediment package are present at Sections W(4), PC(2), II(4), III(5 and 6-base), WA(3 and 4), VIII(4 and 5), IX(2), X(6), XI(3), and XII(2) (Table 7). The following criteria were used in designating lithostratigraphic units to this category: 1) stratigraphic position directly above the lower till (in Lower

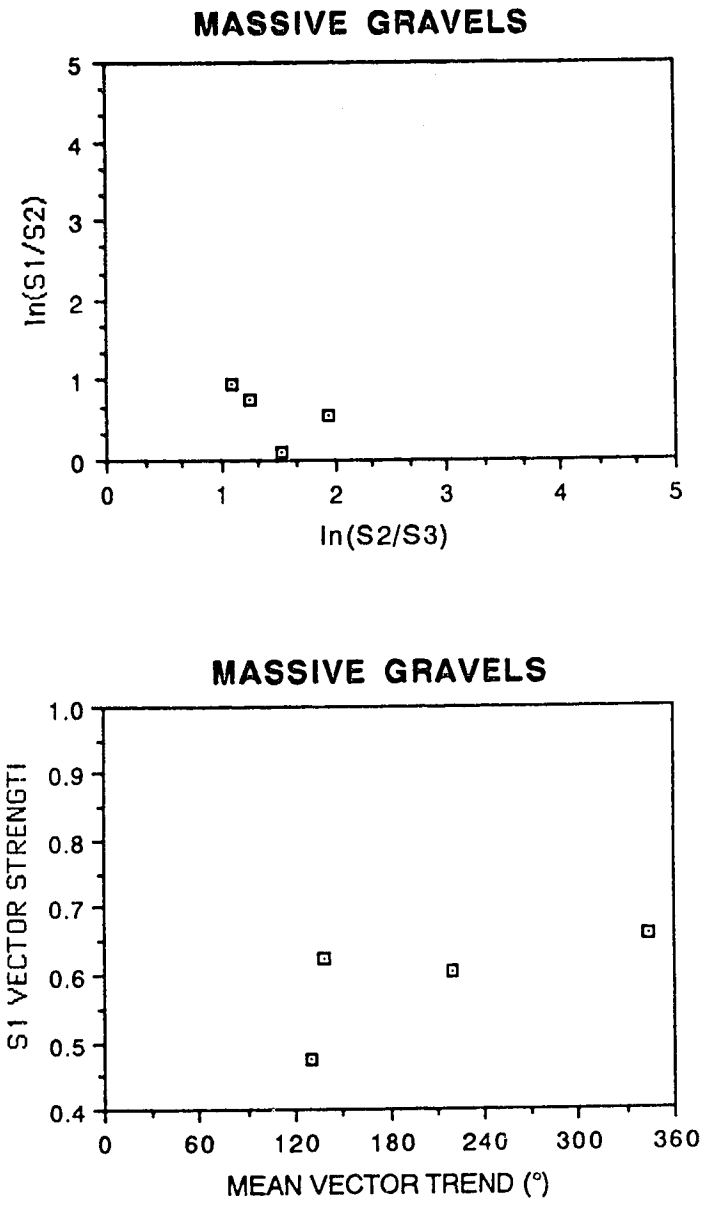

Figure 44. Top shows two-axis ratio plot of normalized eigenvalues; bottom shows 3-D pebble fabric vs. S1 strength for massive gravels (n=4) in Post-Lower Diamictons sediment package.

Diamictons) and/or supraglacial debris (in Post-Lower Diamictons) correlated to the first glaciation (W, PC, II, III, WA, VIII, IX, X, and XI); 2) stratigraphic position below advance outwash (Pre-Upper Diamictons) and/or the upper till (in Upper Diamictons) correlated to the second glaciation (W, II, III, VIII, IX, X, XI and XII); and, 3) geochronological control (W, II, III, WA, VIII, IX, and X). Finite ^{14}C wood dates at these sections range from 15,180 ± 100 years B.P. (TO-708) to 37,190 ± 2870 years B.P. (AECV-353C).

Two sediment associations characterize the fluvial deposits. Planar and trough cross-stratified sands interbedded with planar tabular and horizontally stratified fine gravels predominate. Representative units occur at Sections W(4), PC(2), III(6-base), and VIII(5). In the previous chapter, sediment types associated with these units were interpreted to represent distal braided river deposition. These thin units represent minor channel fills formed by accretion of down-stream migrating bars and ripples. Limited preservation of overbank fines and paludal deposits marginal to the braided channel deposits is further interpreted based on sediments at the following sections: II(4), WA(3), XI(3), and XII(2).

Two other deposits are also correlated to this sediment package based on multiple finite ^{14}C dates from within the respective units. The fabric from the transitional diamicton in Unit 4 at Section VIII is oriented towards azimuth 232.8°, and plunges 23.2° with the S1= 0.603. This sediment was interpreted to be a subaerial debris flow deposit deposited over an oxidized deglacial gravel package. The 10 m thick, rhythmic accumulation of normally graded sand in Unit 4 at Section WA was interpreted to represent stacking of sediment gravity flow deposits into a restricted, channel marginal, catchment basin (Chapter 3).

H. PRE-UPPER DIAMICTON STRATIFIED SEDIMENTS

The start of a second glaciation in the study area is marked by the presence of thick accumulations of stratified sediments. Representative deposits correlated to this package occur at ten sections [W(4), II(5,6 and 7), III(6), V(2), VII(2), VIII(6 and 7), IX(3), X(7), XI(4), and XII(3)] (Figure 36 and Table 7). Identification of lithostratigraphic units assigned to this sediment package is based on: 1) stratigraphic position directly below an upper till (in Upper Diamicton package) interpreted to represent a second glacial advance (all 10 sections); 2) stratigraphic position over oxidized sediments and fluvial sand and gravel (interglacial sediments in Middle Stratified Sediments package) indicating a prolonged period of subaerial exposure (all sections except V); and, 3) geochronological control based on amino acid and ^{14}C analysis (Sections W, II, III, VIII, IX, and X). Finite dates presented above denote the interglacial event, but reworked wood specimens can occur in this sediment package.

Most deposits consist of sedimentologically monotonous accumulations of interbedded sands and gravels. Sand beds are primarily planar and trough cross-stratified, whereas gravels show massive to crude horizontal bedding. In Chapter 3, these units were interpreted as products of deposition in a distal braided river. Several sections display coarsening upward sequences at the top of the sediment packages [II(5), VIII(7), and X(7)]. The units are dominated by coarse massive and inversely graded gravels. These two sediment types were considered to be products of modified grain flows and indicate increasing proximity to a glacier source (Chapter 3). The units reflect active sedimentation in a proximal braided river. Pebble fabrics obtained from 7 horizontally stratified gravel deposits are summarized in Figure 45. As evident in the illustrations, the gravel fabrics are strongly girdled and display valley transverse (a-axis) orientations, with b-axis plunges up-valley. Cross-bedding and fabric data indicate paleoflow to the SSE.

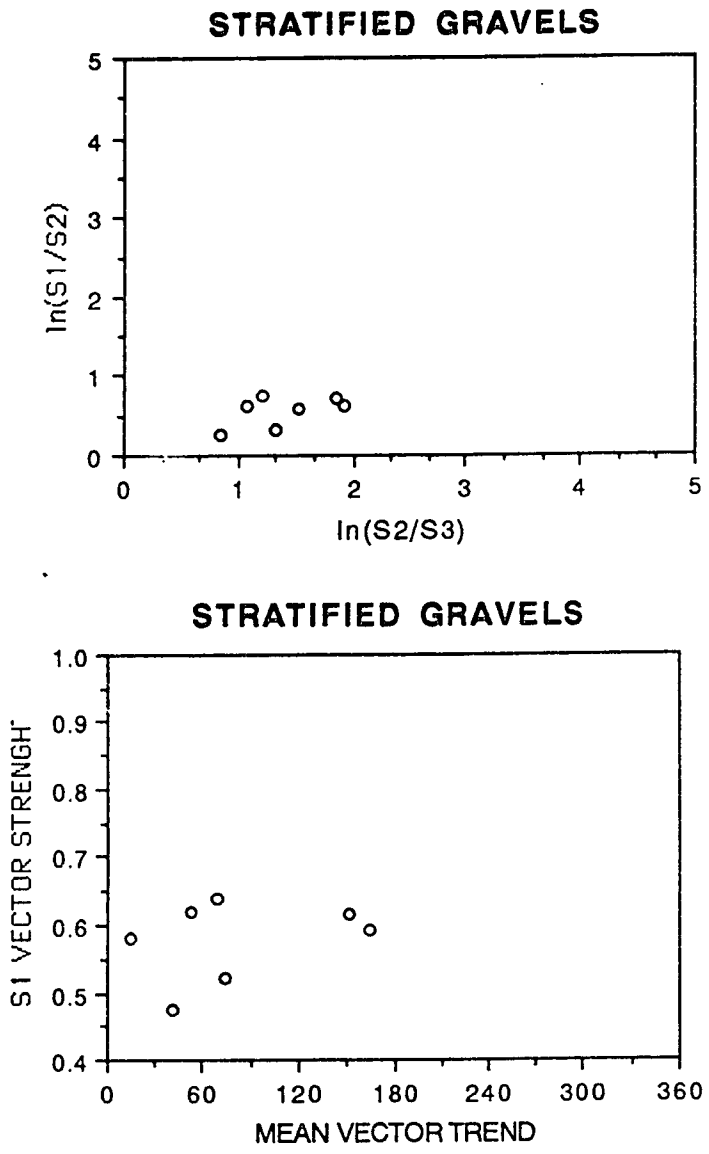

Figure 45. Top shows two-axis ratio plot of normalized eigenvalues; bottom shows 3-D pebble fabric trend vs. S1 strength for stratified gravels (n=7) in Pre-Upper Diamictons sediment package.

The most conspicuous aspect of these equivalent units is their great thickness, which attain a maximum height of 60.0 m and average 26.6 m. Normal fluvial sediment accumulation, even in a highly aggrading situation, rarely deposits such thick units (cf. Clague 1987). The presence of glacial ice in the northwestern corner of the study area could have provided the necessary isostatic depression required to alter the base level in the valley for thick sediment accretion. Rapid sedimentation of this advance outwash ensued and was terminated by the overriding glacial ice.

I. UPPER DIAMICTONS

As in the case of the first glaciation, evidence for the presence of a second glaciation is based on deposits of till and glacigenic sediment gravity flow deposits (Figure 37). Of the eighteen sections in the study area, ten contain sediments attributed to the last glaciation [W(5), II(8), III(7), V(3), VII(3), IX(4), X(8,9, and 10), XI(5), and XII(4)] (Table 7). All structureless sediments equated to this upper till were interpreted above as lodgment tills. The remaining deposits assigned to the Upper Diamictons sediment package are products of sediment gravity flow deposition or lodgment deformation.

Identification and correlation of the various lithostratigraphic units is based on the following criteria: 1) in the five double till sections, the upper till is associated with the second glacial advance (W, II, III, X, and XI); 2) absolute ^{14}C dates occur under (listed above) the upper till at five sections (W, II, III, VIII, and X) and above the till at three sections (IX, X, and XII); 3) all units (till and sediment gravity flows) overlie stratified sediments interpreted to be either advance outwash or nonglacial fluvial accumulations; and, 4) all upper till units display similar sedimentological and physical characteristics.

Compositional similarity and variability for tills associated with this glaciation are illustrated (Figure 46). Unit average compositional values are arranged from up-

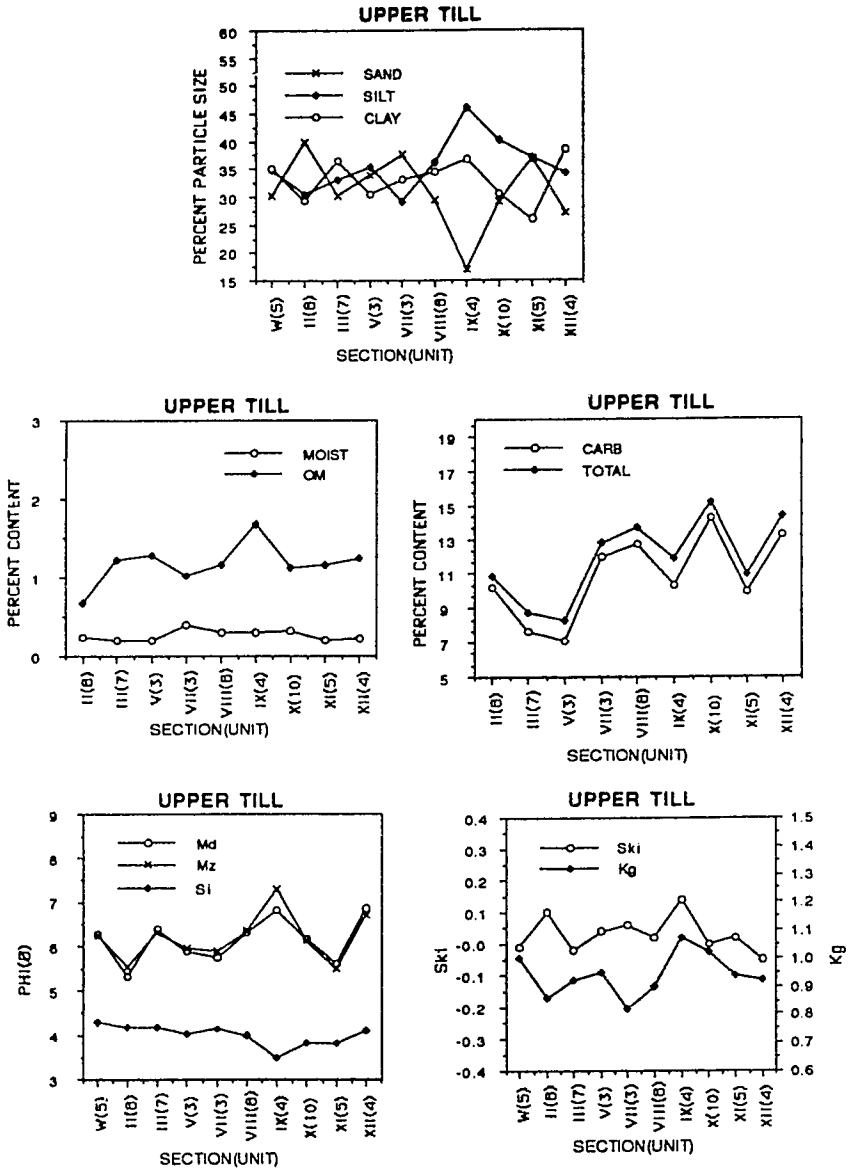

Figure 46. Bivariate graphs illustrating changing compositional values for various units at ten sections containing the upper till (in Upper Diamictons sediment package). Section codes defined in Figure 1. Up-stream to left.

stream to down-stream (left to right) for the ten sections. Average values for samples of the upper till are 0.26% moisture content, 1.16% organic matter content, 10.90% carbonate content, and 11.93% total carbon content. Total carbon and carbonate content show a general increase in percent content down-valley. These results are similar to the values defined for the lower till. Additional average compositional values include: modal grain size (6.15Ø), mean grain size (6.13Ø), sorting (4.06Ø), skewness (0.01), and kurtosis (0.93). Each of these graphic statistic determinations also indicate that site specific variability was an important factor during the process which was responsible for deposition of the upper till. Texturally, the upper till averages 32 ± 6.6% sand, 35 ± 4.6% silt, and 33 ± 6.9% clay. As with the lower till, a slight down-valley decrease in the percent of sand is evident.

A total of 19 pebble fabric samples were determined from units correlated to the Upper Diamictons sediment package (structureless and stratified diamictons). As discussed in Chapter 3, the structureless diamictons are considered to be lodgment tills [W(5), II(8), III(7), V(3), VII(3), VIII(8), IX(4), X(10), XI(5), and XII(4)]. S1 values for 16 samples of the upper till range from 0.476 to 0.904, and average 0.668. Figure 47 illustrates that upper till pebble fabrics are both girdled and clustered. Similarly, mean vector trend and plunge for these till deposits is primarily valley parallel, with most examples plunging up-valley (n=12), rather than down-valley (n=4). A valley parallel orientation, with up-valley clast dips, indicates glacial flow from the NNW (cf. Lawson 1979a; Mills 1979a). The above attributes indicate this upper till is markedly different from the various stratified diamictons interpreted to be products of sediment gravity flows (Figure 48).

The 3 fabrics obtained from stratified diamictons correlated to the Upper Diamicton sediment package are strongly girdled and display divergent mean trends (Figure 48). Unit 4 at Section IX is a transitional diamicton, whose 2 fabrics show S1 values of 0.555 and 0.561. In Chapter 3, this unit was interpreted to be a deformed

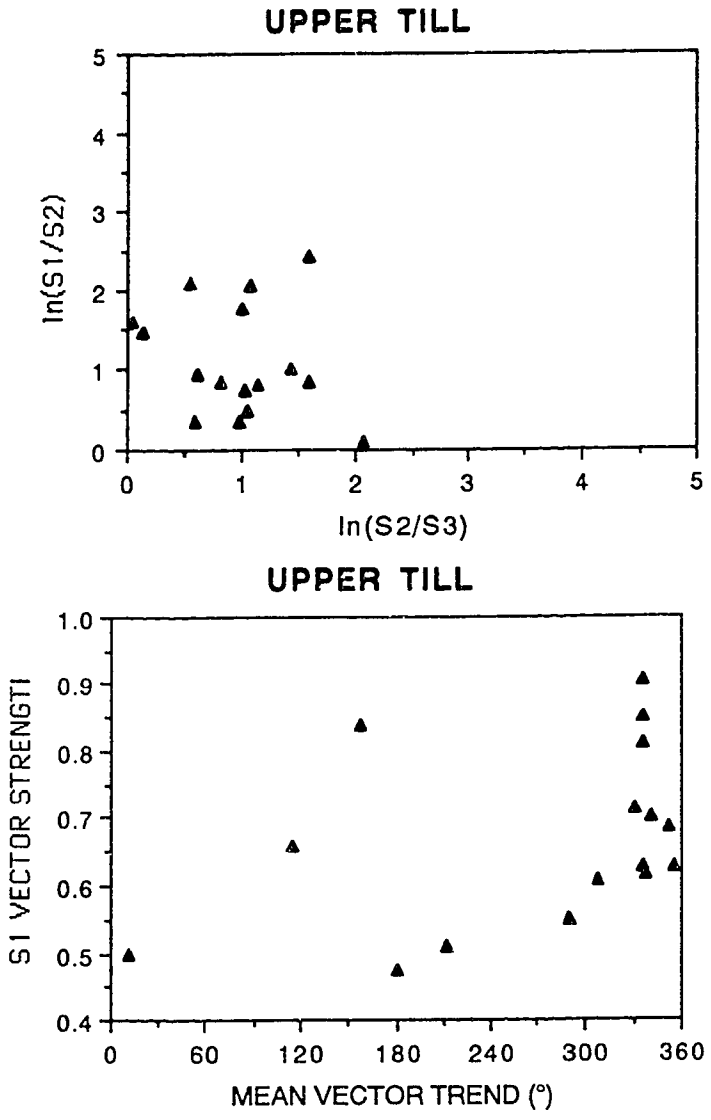

Figure 47. Top shows two-axis ratio plot of normalized eigenvalues; bottom shows 3-D pebble fabric trend vs. S1 strength for lodgment till (n=16) in Upper Diamictons sediment package.

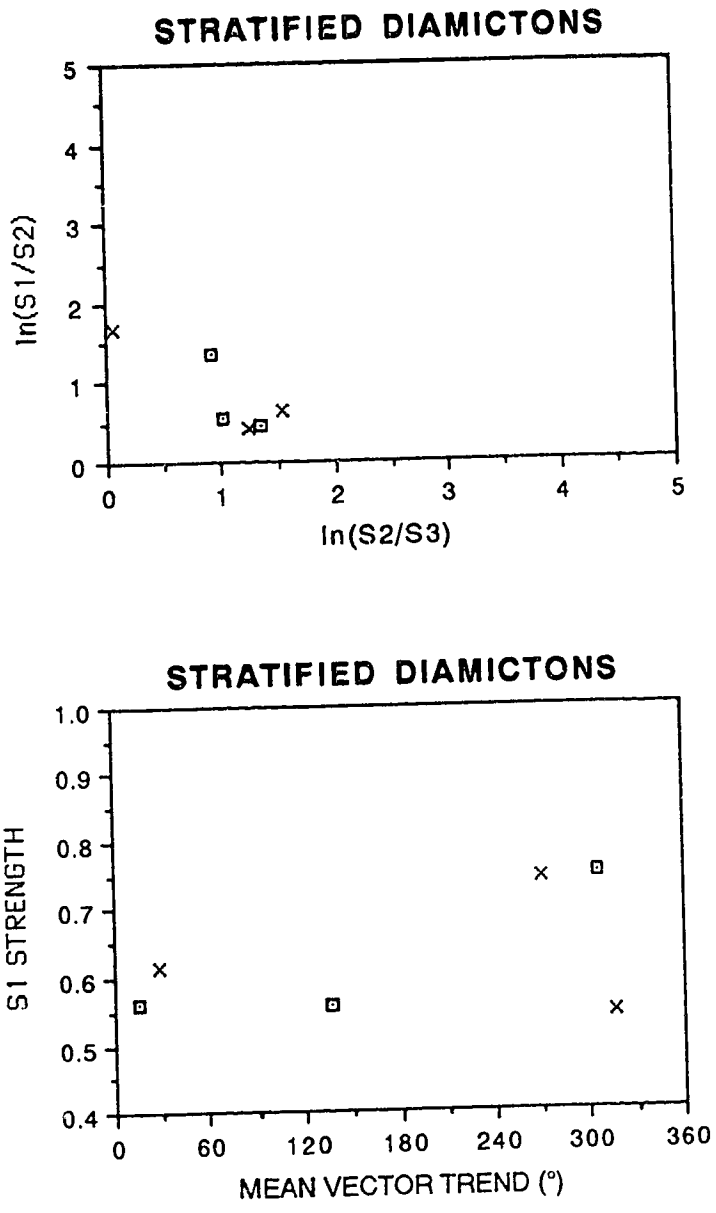

Figure 48. Top shows two-axis ratio plot of normalized eigenvalues; bottom shows 3-D pebble fabric trend vs. S1 strength for stratified diamictons (n=6) in Upper Diamictons (square) and Post-Upper Diamictons sediment packages.

lodgment till, possibly a product of an accelerated glacial ice advance (surge or ice stream). The second transitional diamicton [X(8)] has a valley oblique (azimuth 305°) and steep (plunge 8.6°) pebble fabric, and a S1 eigenvalue of 0.760. This diamicton was interpreted to represent a subaqueous sediment gravity flow deposit, formed by cohesive freezing. The gradational contact of this sediment gravity flow deposit with overlying proglacial silts and sands suggests deposition by a proglacial debris flow.

Lithological analysis of 14 pebble samples correlated to the upper till indicates a general dilution in the percentage of igneous clasts and an increase in the total percent of metamorphic clasts relative to the lower till. The scatter of points in the ternary plot of Figure 49 illustrates this relationship. The reduction in igneous clast percentage compared to that of the lower till indicates that the glaciation responsible for the upper till did not provide a renewed addition of igneous clasts into the pebble population. Therefore, ice did not originate from the same source as that identified for the lower till (i.e. > 50 km west of Ft. Ware). The valley glacier responsible for the upper till owes its origin to numerous cirques and tributary glaciers which fed into the main valley glacier. During this glacial event, pre-existing unconsolidated sediments were incorporated by the glacial ice. Reworking of sediments diluted the original concentration of igneous clasts and therefore reduced the percent of indicator clasts in the resultant till. A down-valley trend in lithologic composition is also shown in Figure 49. Lithologic variability appears random and probably denotes localized change in ice behavior.

J. POST-UPPER DIAMICTON STRATIFIED SEDIMENTS

Uppermost stratified sediments associated with the second deglaciation in the Finlay River valley resemble those deposits associated with the first deglaciation. Six sections [W(6 and 7), II(9), III(8), VII(4), IX(5 and 6), and XII(5)] contain

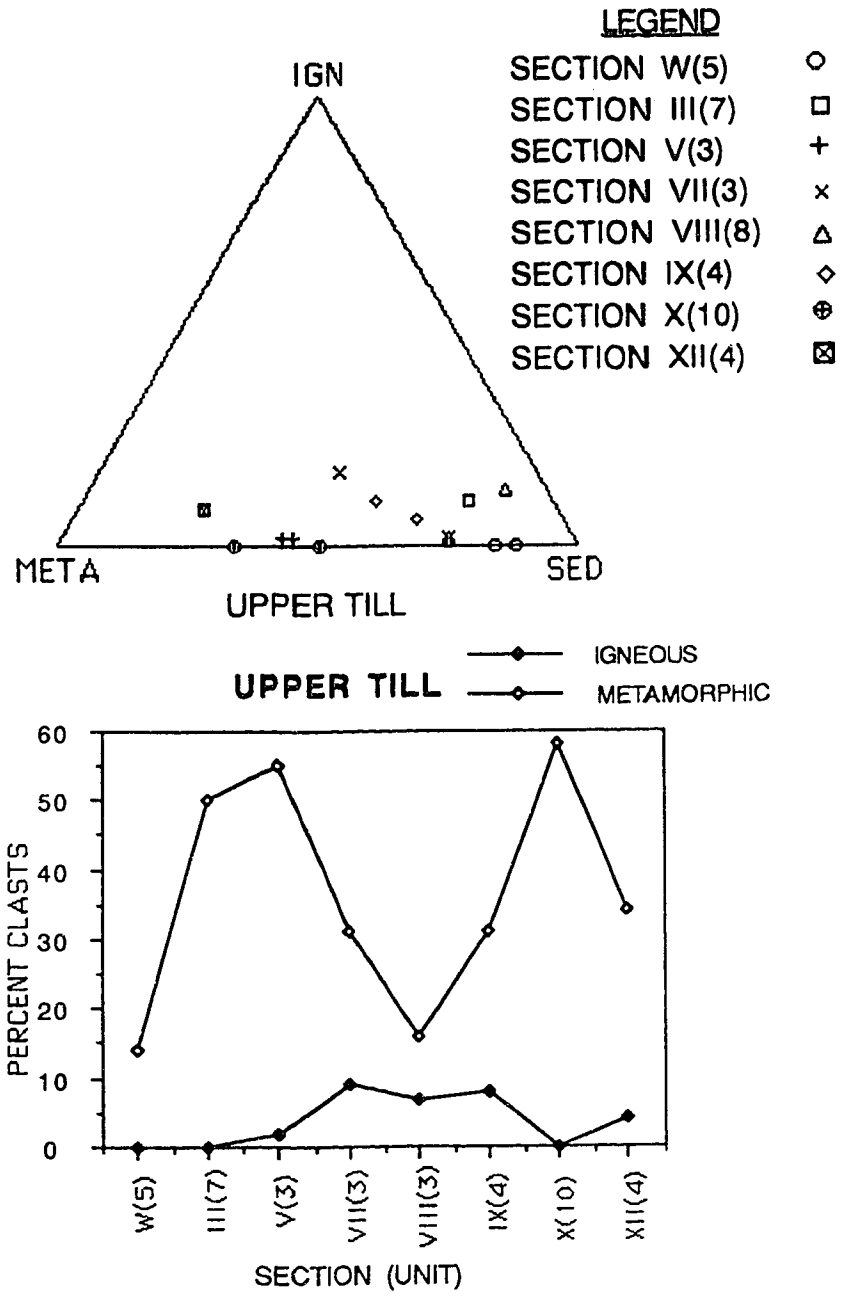

Figure 49. Top figure is ternary plot of lithologic composition in the upper till based on 14 samples from eight sections. Bottom figure shows down-stream variation in the percentage of igneous and metamorphic clast composition based on unit averages at eight sections along the Finlay River.

lithostratigraphic units which can be correlated to this sediment package (Figure 36 and Table 7). Identification and correlation of the units is based on: 1) stratigraphic position of the units over the upper till (all sections); 2) absolute ^{14}C dates (listed above) present below the units (Sections W, II, III, and IX); and, 3) stratigraphic position below terrace sands and gravels (all sections but IX).

At Sections VII(4) and XII(5) dominant sediment types include intercalated beds of normally graded gravels, and cross-stratified sands. The same sediment types are interbedded with isolated graded diamicton beds at W(6 and 7), II(9), and III(8). In Chapter 3, the high frequency of sand beds in association with stratified gravels at Sections VII and XII was interpreted to indicate distal braided river deposits and thus represent distal outwash accumulations following ice retreat from the area. Beds of graded diamictons show valley oblique (azimuths 025.5° and 317.1°) and steep (plunges 8.9° and 12.9°) pebble fabrics and S1 eigenvalues of 0.644 and 0.544 (Figure 48). These diamictons were interpreted to represent isolated glacigenic sediment gravity flow deposits. The fining upward sequences and intercalated glacigenic diamictons probably reflect proximal braided river glacifluvial deposits in an ice proximal environment.

At Section IX, intercalated beds of massive gravels, structureless sands, drift cross-laminated silts, and inversely graded stratified diamictons (Unit 6) are intimately associated with an up-valley gravelly foreset deposit (Unit 5). This sediment assemblage was interpreted to represent a prograding glacilacustrine deposit during deglaciation. As ice melted up-stream of this section, temporary blockage of the drainage down-stream created a proglacial lake environment which permitted development of large glacideltaic foreset beds (Unit 5) and alternating beds of subaqueously deposited sand, gravel, and diamicton (Unit 6).

K. UPPER STRATIFIED SEDIMENTS

The uppermost stratified sediment package which blankets most of the valley consists of well-sorted sand and gravel deposits [W(8 and 9), WII(5 and 6), PC(3), I(5), II(10 and 11), BS(2), NA(2), III(9), WA(5), IV(4), VII(5), OD(4), and XII(6)] (Figure 36 and Table 7). Lithostratigraphic units assigned to this sediment package: 1) overlie the upper till and/or deglacial stratified sediments; 2) contain ^{14}C dated organic remains indicating postglacial sediment accretion; and, 3) comprise the top nonglacial unit in all sections. The transition from deglacial sedimentation to postglacial and Holocene sedimentation and erosion is marked temporally by a series of absolute dates beginning at 10,100 ± 90 years B.P. (GSC-2036). Deposits correlated to this sediment package are evident along the entire course of exposures skirting the Finlay River and formed the basis of a study by Leslie (1988).

The youngest deposits which occur on the uppermost terraces are clearly exposed at all sections except Sections V, VIII, IX, X, and XI (Table 7). Sediment types present in these sections consist of well imbricated, and horizontally stratified fine pebble beds intercalated with ripple drift cross-laminated sands. These thin terrace sediments represent fluvial channel and overbank accumulations marking progressively lower stages of river incision into the underlying Pleistocene sediments. This pronounced incision (> 110 m) into the diamictons, gravels, sands and fines within the northern RMT is best explained in terms of ice disappearance from the area. As the second glacial ice mass melted back towards the NNW, isostatic rebound could have altered the base level considerably, such that accelerated erosion may have allowed the Finlay River to attain its present configuration within a few thousand years. Many sections are presently capped by brunisolic soils and cliff top dunes.

L. COMPOSITE STRATIGRAPHY

The sediment packages discussed above can be summarized in a composite stratigraphic column for the northern Rocky Mountain Trench (Figure 50). This figure lists the informal sediment package designations along the left side of the column. The figure also provides a brief interpretation of the dominant sedimentological processes which were assumed to have taken place during deposition of the lithostratigraphic units within each sediment package. This processual interpretation is based on the identification and intepretation of the 15 sediment types discussed in Chapter 3 and the distribution of these sediment types in the various lithostratigraphic units. The geochronological significance and inferred Quaternary history of the sediments examined in Finlay valley are reviewed in the following chapter.

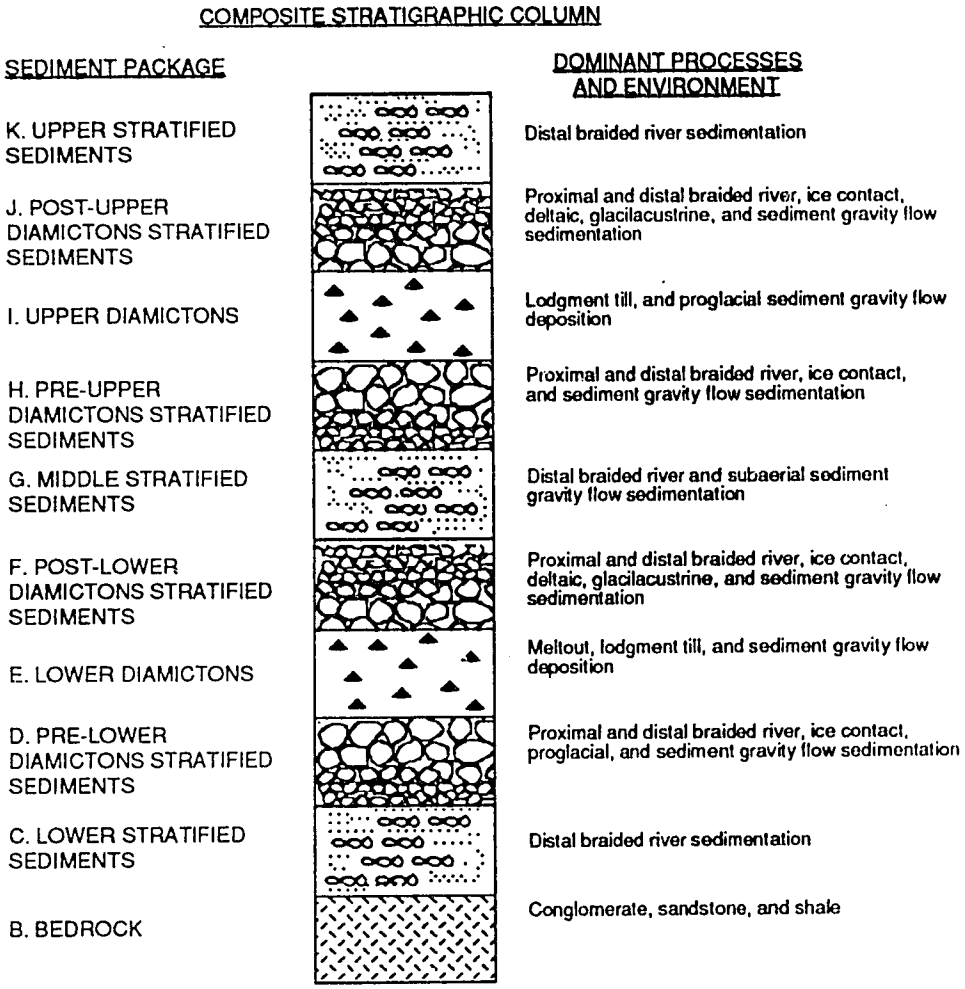

Figure 50. Schematic composite stratigraphic column for the Late Cenozoic geology of the northern Rocky Mountain Trench, British Columbia. Primary sediment packages to left of column, and dominant sedimentary processes to the right.

V. Geochronology and Geologic History

A. GENERAL STATEMENT

The geochronological interpretation of sediments preserved in the northern Rocky Mountain Trench (RMT) is based on the following premises: 1) deposits resulting from episodic or rare event sedimentation are more likely to be preserved than sediments deposited between episodic events; 2) stratigraphic completeness is generally poor, such that sedimentological evidence for Quaternary deposition is only rarely preserved; and, 3) the sedimentary packages defined in this study are time transgressive as a result of diachronous glacial and nonglacial events.

Following the work of Sadler (1981) and Dott (1983), several geologists have explored the concepts of stratigraphic completeness and episodic sedimentation (eg. Goodwin and Anderson 1985; McShea and Raup 1986; Anders et al. 1987). With the exception of the work of Clague (1986), these concepts have not been examined in a Quaternary context. The above studies indicate that the physical evidence for gradualistic sedimentation (GS) is rarely preserved, whereas the evidence for episodic sedimentation (ES) has a higher probability of preservation. Overprinting by repeated deposition and erosion results in a composite stratigraphic record, the preserved sediments of which represent very brief periods of activity or time. Most of the temporal span covered by geologic sections is, therefore, represented by a unknown number of stratigraphic breaks (SB) called unconformities.

The purpose of this chapter is to examine the evidence for geochronology in the northern RMT and to relate this evidence to the inferred Quaternary history. These objectives involve: 1) a discussion of the results of amino acid racemization and ^{14}C analysis; 2) the derivation of a chronologic paleomagnetic record based on the geochronology and stratigraphy; and, 3) a discussion of the nine sediment packages defined in Chapter 4 within the geochronologic record (inferred Quaternary history).

B. GEOCHRONOLOGY

The recognition and recovery of the organic remains permitted the establishment of geochronological control in the Finlay River valley region. Much of the organic material recovered consisted of small fragments of unidentifiable wood. As noted in Chapter 3, however, a few fragments of wood were identified as Picea sp. Several unidentifiable, peat-like fragments were brought back to the laboratory to confirm their composition as peat or coal. Samples considered suitable for detailed study were then submitted to amino acid and ^{14}C laboratories for analyses.

i) Amino Acid Racemization Analysis

The utility of amino acid racemization for geochronology or geothermometry commonly involves materials such as mollusc shell and bone (eg. Hicock and Rutter 1986). More rarely, wood remains are subjected to amino acid analysis. Rutter and Crawford (1984) reported on the analysis of over 75 samples of Pleistocene wood from Yukon and Alaska. They concluded that aspartic acid ratios for wood in this area ranged from 0.01-0.08 for Holocene, 0.14-0.24 for Mid- to Late Wisconsinan, and 0.24-0.36 for pre Mid-Wisconsinan specimens. Rutter and Vlahos (1988) concluded, in a study of wood kinetics using Picea sp., that taxonomic differentiation at the specific level is not required for amino acid studies.

All organic remains were first subjected to amino acid racemization analysis. Methods of analysis were reviewed in Chapter 2 and are detailed in Appendix 17. The results of this analysis are listed for 28 samples (Table 8). Based on the derived aspartic acid ratios following analysis, questionable materials were then interpreted as representing either Tertiary coal or detrital Pleistocene organics. As evident in the table, the adjusted D/L ratios of aspartic acid of Pleistocene organic materials recovered from the area range from 0.182 to 0.296. Coal fragments provided a D/L

Table 8. Aspartic acid ratios. List includes field number, corresponding laboratory number, aspartic acid D/L ratio, standard deviation, machine standard, adjusted aspartic acid ratio, section location, age, and sample material.

FIELD NO.	U. A. NO.	ASP	S.D.	STD.	ADJ.	SECTION	SAMPLE
PTB84-233	UA 1729	0.0000	0.0000	0.9808	0.0000	4	COAL
PTB84-179	UA 1726	0.0000	0.0000	0.9808	0.0000	8	COAL
PTB84-175	UA 1722	0.0000	0.0000	0.9248	0.0000	10	COAL
PTB84-174	UA 1721	0.1044	0.0166	0.9248	0.1129	10	COAL
PTB84-170	UA 1720a	0.2907	0.0120	0.9368	0.3103	10	40% WD
PTB84-170	UA 1720b	0.2763	0.0050	0.9368	0.2949	10	90% WD
PTB84-168	UA 1719	0.0000	0.0000	0.9248	0.0000	8	COAL
PTB84-149	UA 1718	0.0000	0.0000	0.9248	0.0000	3	COAL
PTB84-12	UA 1710	0.2570	0.0102	0.9248	0.2779	2	WOOD
PTB84-13	UA 1711	0.2777	0.0191	0.9808	0.2831	2	WOOD
PTB84-14	UA 1712	0.2698	0.0029	0.9248	0.2917	2	WOOD
PTB84-129	UA 1715	0.2824	0.0001	0.9248	0.3054	2	WOOD
PTB84-132	UA 1716	0.2030	0.0200	0.9924	0.2046	W	WOOD
PTB84-148	UA 1717	0.2285	0.0026	0.9928	0.2302	3	WOOD
PTB84-225	UA 1728	0.2150	0.0081	0.9248	0.2325	WA	WOOD
PTB84-336	UA 1733	0.2086	0.0043	0.9248	0.2256	WA	WOOD
PTB84-287	UA 1731	0.2654	0.0014	0.9248	0.2870	2	WOOD
PTB84-104[c]	UA 1713	0.0000	0.0000	0.9808	0.0000	9	MOSS
PTB84-356	UA 1735	0.1985	0.0000	0.9808	0.2024	9	WOOD
PTB84-345	UA 1734	0.2731	0.0250	0.9248	0.2953	8	WOOD
PTB84-183	UA 1727	0.2442	0.0122	0.9248	0.2641	8	WOOD
PTB84-178	UA 1725	0.2514	0.0262	0.9248	0.2718	8	WOOD
PTB84-177	UA 1724	0.2957	0.0043	0.9248	0.3197	8	WOOD
PTB84-176	UA 1723	0.2659	0.0068	0.9248	0.2875	8	WOOD
PTB84-296	UA 1732	0.0000	0.0000	0.9808	0.0000	1	COAL
PTB85-19	UA 2244	0.2793	0.0050	0.9368	0.2981	2	WOOD
PTB85-41	UA 2243	0.2388	0.0009	0.9924	0.2406	WA	WOOD
PTB85-8	UA 1820	0.1818	0.0005	0.8847	0.2055	W	WOOD
PTB85-7	UA 1819	0.2035	0.0028	0.9015	0.2257	W	WOOD

a- sample consists of mixed wood (40% by weight) and sediment
b- sample same as previous sample but partially cleaned so that wood represents 90% by weight
c-contaminated

ratio of 0.000. This latter value allowed the elimination of peat-like coal fragments from further analysis, except in the case of one fragment of coal (PTB84-174). The D/L ratio of 0.1044 for this coal sample indicated contamination with modern carbon. This mixed sample would, therefore, provide a test of the methodology of ^{14}C analysis used at the laboratory. The sample was, therefore, submitted to the Radiocarbon and Tritium Laboratory, Geochronology Section, Alberta Environment Centre in Vegreville for further analysis.

ii) ^{14}C Analysis

Radiocarbon analysis of organic materials provides the critical means of establishing age in Quaternary studies. Sixteen non-lignitized wood samples, one bulk organic sediment sample, and the single lignitized fragment (PTB84-174) were subjected to ^{14}C analysis following the initial amino acid racemization analysis. Most materials were sent to the provincial government Radiocarbon and Tritium Laboratory, Geochronology Section, Alberta Environment Centre in Vegreville, except for two small twig fragments which were sent to a commercial laboratory (Isotrace Laboratories) in Toronto for accelerator dating. The results of these analyses are provided in Table 9. The resultant dates presented are in ^{14}C years before present (B.P.) based on a 1950 datum. Finite Pleistocene dates range from 15,180 ± 100 years B.P. (TO-708) to 37,190 ± 2870 years B.P. (AECV-353C). This range corresponds to the late Mid- to Late Wisconsinan (cf. Fulton 1984). Five of the dates exceed the limit of counting resolution and appear as greater than estimates.

iii) Method Comparisons

The comparison of results derived from amino acid and ^{14}C analyses allows the validity of the both sets of results to be assessed. Bobrowsky et al. (1987a) showed how absolute ^{14}C dates correlated well with amino acid ratios for species specific

Table 9. Radiocarbon dates. List includes field sample number, section location, corresponding laboratory number, estimated age in radiocarbon years (before present relative to 1950 A.D.), and the delta carbon 13 correction for fractionation based on each run.

FIELD NO.	SECTION	LAB. NO.	C-14	Del C13
PTB84-174[a,d]	10	AECV-380C	33,490 ± 1780	-24.7
PTB84-170[d]	10	AECV-349C	29,880 ± 1680	N/A
PTB84-12[b,d]	2	AECV-376C		-30.5
PTB84-14[d]	2	AECV-348C	>40,000	N/A
PTB84-129[d]	2	AECV-379C	26,800 ±1450	-26.6
PTB84-132[c,d]	WARE	TO-709	18,750 ± 120	-25.0
PTB84-148[d]	3	TO-708	15,180 ± 100	-25.0
PTB84-336	WA	AECV-351C	23,280 ± 750	N/A
PTB84-104	9	AECV-377C	1,000 ± 90	-23.6
PTB84-356	9	AECV-352C	29,280 ± 1230	N/A
PTB84-345[d]	8	AECV-385C	>40,180	-23.9
PTB84-183[d]	8	AECV-383C	>40,400	-24.0
PTB84-178[d]	8	AECV-350C	36,510 ± 2570	N/A
PTB84-177[d]	8	AECV-382C	32,750 ± 3180	-24.0
PTB84-176[d]	8	AECV-381C	>40,330	N/A
PTB84-296[b]	1	AECV-384C		N/A
PTB85-19[d]	2	AECV-386C	>40,130	-28.2
PTB85-41	WA	AECV-353C	37,190 ± 2870	N/A
PTB85-8[c,d]	WARE	TO-709	18,750 ± 120	-25.0
PTB85-7[c,d]	WARE	TO-709	18,750 ± 120	-25.0

NOTES: Laboratories-AECV (Alberta Environmental Research Centre), TO (IsoTrace Laboratory)

a-probably coal contaminated

b-sample too small for conventional date

c-radiocarbon date based on combined sample of PTB85-7+8 and PTB84-132

d-subtill

N/A-not available

mollusc assemblages in postglacial marine deposits. A strong, positive correlation suggested that the independent values are probably unbiased. As a simple check of the two methods used here, a bivariate analysis of the paired data was generated. The relationship of the two data suites for the seven dated sections can be examined (Figure 51). Model I least squares regression was then applied to the data scatter for all points excluding the coal specimen. The generated best fit line is significant ($p < 0.01$) and displays a positive coefficient of correlation of 0.62. These results suggest that both sets of values are minimal unbiased estimators of age, and in the absence of finite ^{14}C dates, aspartic acid ratios are suitable for relative dating and correlation.

For the wood samples in this study, the aspartic acid ratios ranged from 0.18 to 0.30 and ^{14}C years ranged from c. 15,000 to 37,000 years B.P.. Late Wisconsinan wood collected in the state of Washington displayed a similar correspondence between the two types of analytical results (Hicock and Rutter 1986). In the latter study, the aspartic acid ratio ranged from 0.18 to 0.28 and ^{14}C years ranged from 22,000 to 28,000. Minor discrepancies in calculable D/L ratios are expected given different depositional histories for the two areas, but as a first-order approximation, the results of this study are in good agreement with expected Pleistocene wood values.

C. GEOCHRONOLOGICAL IMPLICATIONS

The finite dates obtained in this study provide time estimates for periods of nonglacial activity. Although subsequent reworking of wood specimens may have occurred in the past and thus contributed to inaccurate depositional ages for the units from which the specimens are derived, the antiquity of the specimens remains unchanged. Finite dates (and their standard deviations) from this and other studies from Finlay valley were plotted on a graph in chronological order (Figure 52). As illustrated in Figure 52, the dates can be divided into two groups. The oldest group of dates range from c. 15,000 to 40,000 years B.P. This period of ice-free conditions

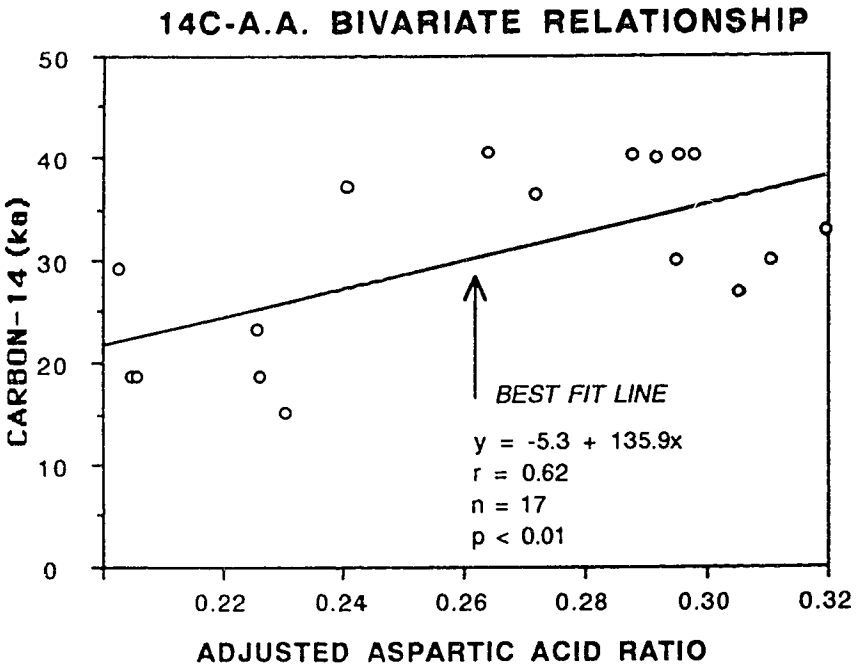

Figure 51. Bivariate graph comparing radiocarbon years to amino acid D/L ratios for 17 samples from Finlay valley, B.C..

corresponds to the Mid-Wisconsinan and in British Columbia is referred to as the Olympia nonglacial interval (Clague 1981). Fifteen of the dates listed in Table 9 are subtill dates, and six of these dates are finite. The till under which these dates occur represents sediment deposited during the last major Cordilleran glaciation in the RMT. This glaciation corresponds to the Late Wisconsinan and in British Columbia is referred to as the Fraser Glaciation (Clague 1981).

Till underlying the Olympia nonglacial sediments cannot be confidently assigned to a particular glacial event. In western Canada, till exceeding the limits of ^{14}C resolution is often assumed to represent the product of glaciation during the Early Wisconsinan (oxygen isotope stage 4) (eg. Bobrowsky et al. 1987b; Fulton 1984a, 1984b). Early glaciations can, however, date back to oxygen isotope stages 6, 8 or older, especially in the absence of supportive dates. The assumption of Early Wisconsinan correlation is unfounded and a cautious approach requires the penultimate glaciation in this region to be regarded as pre-Late Wisconsinan.

The second group of dates correspond to the postglacial and Holocene. Postglacial dates in the region begin as early as 10,400 ± 170 years B.P. (GSC-1654) and continue to the present (only the 4 oldest postglacial dates are shown in Figure 52). Relying on the postglacial date of 10,400 ± 170 years B.P. and the youngest subtill date of 15,180 ± 100 years B.P. (see Tables 3 and 9), the most recent glaciation in the area is interpreted to have lasted less than 5,000 years. This short lived event contrasts with the prevalent belief of a lengthy Late Wisconsinan Cordilleran glaciation in northeastern B.C. (eg. Mathews 1978). Clague (1981) concluded that the Fraser Glaciation in British Columbia began about 20,000 to 25,000 years ago, with Cordilleran ice attaining its maximum size approximately 15,000 years ago. The time of deglaciation varied across the province, but is assumed to have started about 13,000 years ago (Clague 1981). In contrast to this scenario, geochronological data in this

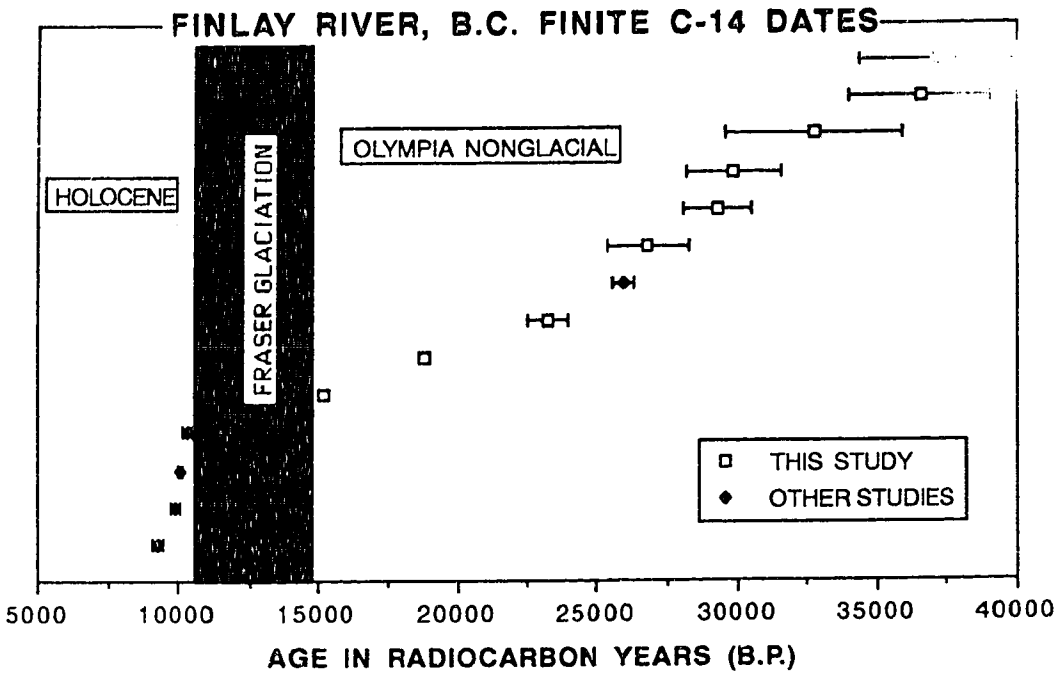

Figure 52. Finite 14C dates from the Finlay valley relative to the Olympia Nonglacial interval, Fraser Glaciation, and Holocene. Dates used in 'other studies' listed discussed in Chapter 1.

study indicates that the Late Wisconsinan glaciation in northeastern British Columbia began after this maximum period (15 ka) and ended at the start of the Holocene.

D. PALEOMAGNETIC HISTORY

Geochronological control and stratigraphic position of the lithostratigraphic units permit the paleomagnetic samples from the northern RMT to be arranged chronologically. The eight stations sampled for paleomagnetic data are listed in Appendix 15 and are summarized in Table 10. Mean trend and plunge, and the three normalized eigenvalues are given for each station in this table. The youngest five localities can be assigned a minimum age of deposition based on associated ^{14}C dates, whereas the remaining three stations are placed into their proper relative chronostratigraphic position according to the composite stratigraphy outlined in Chapter 4.

The declination and inclination magnetograms for the late Pleistocene in the northern Rocky Mountain Trench can be examined (Figure 53). The minor fluctuations of the mean trend and plunge through time primarily illustrate secular variation of the magnetic field. Other factors such as major stratigraphic breaks and measurement error contribute to the observed oscillations. Clearly, however, the mean trend fluctuates on either side of the present day geomagnetic pole (cf. Hedlin and Evans 1987). The mean plunge shows greater variability, which may be a product of post-depositional changes in the bedding plane from an original horizontal aspect.

Trend and plunge values are commonly smoothed using a running mean of the absolute values (eg. Hedlin and Evans 1987). In this study, a three-horizon moving average was calculated for the samples to smooth the paleomagnetic record. Figure 54 shows the smoothed declination and inclination magnetograms for northern RMT. Approximate age of deposition is also given in the centre of the diagram.

Table 10. Three dimensional stereographic natural remanent magnetic data listing mean trend, plunge, eigenvalues, and correlated age for averaged samples from the northern Rocky Mountain Trench, British Columbia.

SAMPLE	TREND	PLUNGE	S1	S2	S3	AGE
4C2A-E	9.1	68.4	0.957	0.036	0.007	15 ka
5A1A-B	343.3	27.2	0.990	0.011	0.000	23 ka
4C1A-E	30.3	64.2	0.766	0.026	0.008	27 ka
4D4A-E	322.5	65.1	0.945	0.043	0.011	33 ka
4D4F-J	2.1	65.9	0.988	0.061	0.004	33 ka
5B1A-E	31.4	51.4	0.739	0.257	0.004	> 44 ka
4B1A-E	5.1	20.2	0.955	0.027	0.018	> 44 ka
4A2A-E	342.8	68.2	0.944	0.055	0.001	> 44 ka

LEGEND

4C2A-E = Section Two, Unit Six, Station One YOUNGEST

5A1A-B = Section West Air, Unit Three, Station One

4C1A-E = Section Two, Unit Four, Station One

4D4A-E = Section Eight, Unit Four, Station One

(4D4F-J = Section Eight, Unit Four, Station Two)

5B1A-E = Section Twelve, Unit Two, Station One

4B1A-E = Section Ware Two, Unit One, Station One

4A2A-E = Section One, Unit Three, Station One OLDEST

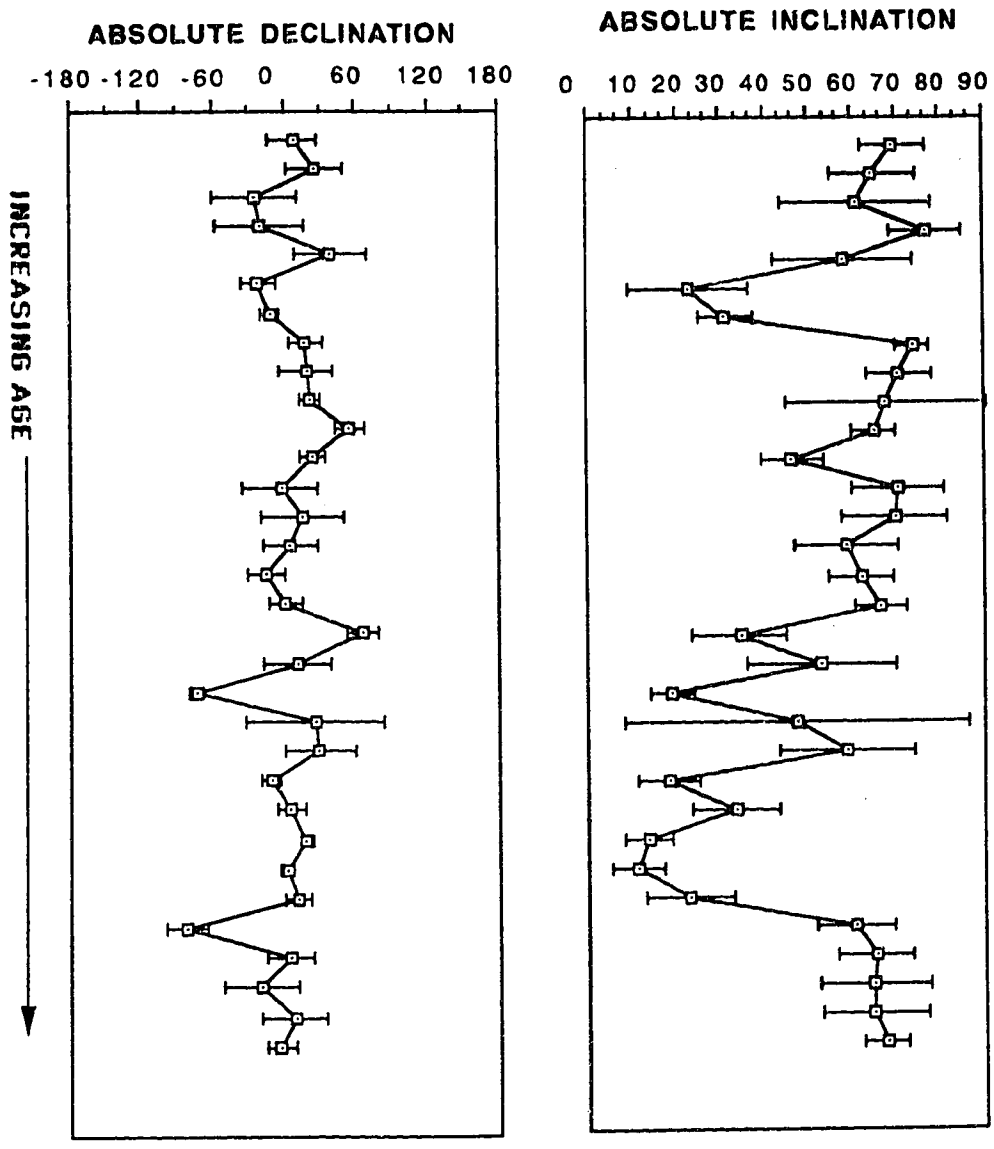

Figure 53. Declination and inclination magnetograms for six sections listed in preceding table. Error bars represent Fisherian alpha 95. No vertical scale. Vertical order is chronologic but relative.

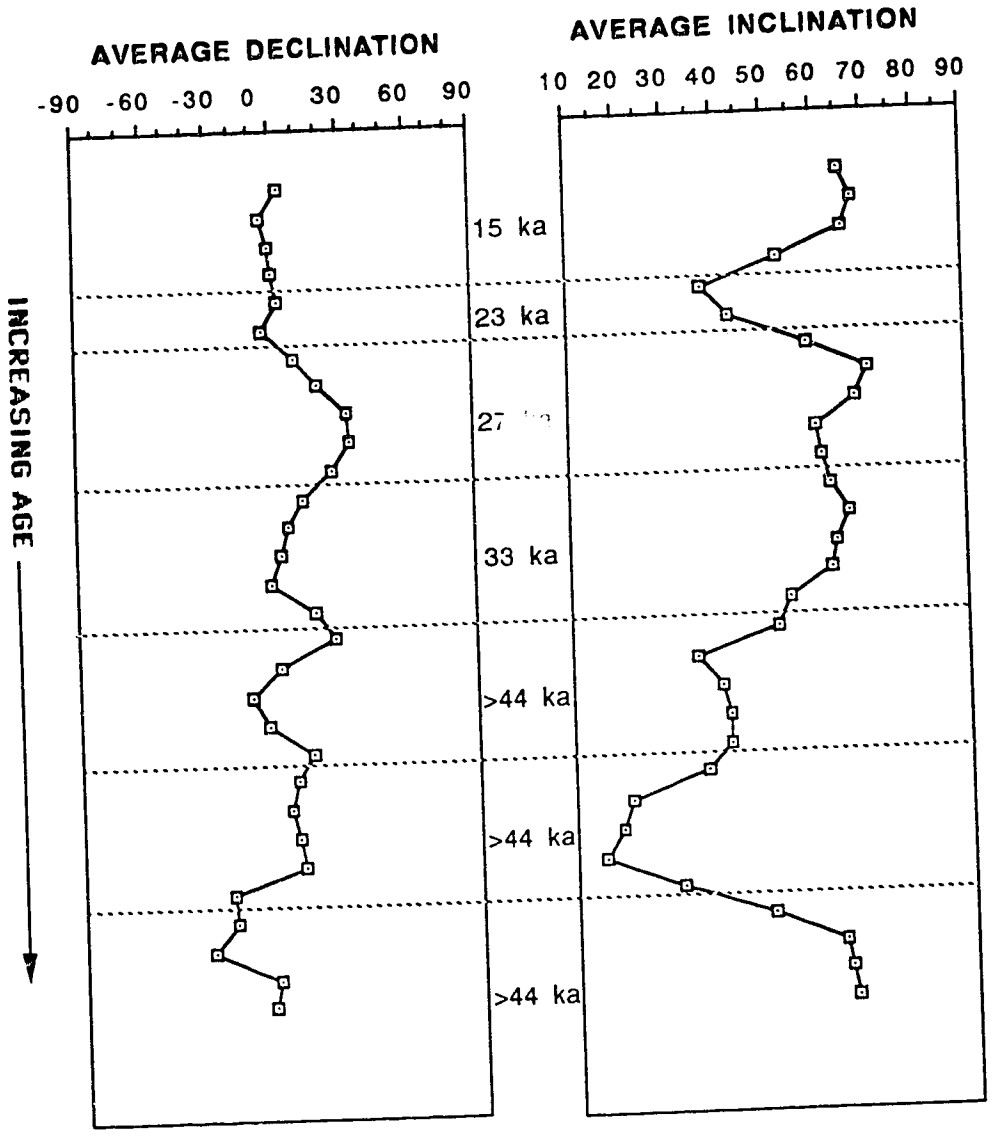

Figure 54. Smoothed declination and inclination magnetograms using a three-horizon moving vector average. Raw data in Appendix 15. Sections and ages in preceding table. No vertical scale.

The data are relevant insofar as normal polarity typifies the magnetic signature. Absent in this study is evidence for the Blake Event, which is thought to date to 100,000 years B.P. and which has been recorded further north in the Yukon Territory (Hedlin and Evans 1987). The absence of magnetic reversals in this study is unfortunate, as it would have provided a key method of correlating and dating several of the early deposits. Nonetheless, a normal polarity signature indicates that none of the nonglacial sediments sampled correlate to the late Sangamonian during which time the Blake Event should appear.

E. QUATERNARY HISTORY

The succession of Quaternary sediments in Finlay valley represents the products of two glaciations, and three nonglacial periods. Dominant sedimentological processes, varied considerably from one period of erosion and deposition to another. The chronostratigraphic interpretation which follows details the large scale processes responsible for the sedimentary record observed within the northern RMT. This interpretation is accomplished by integrating the geochronologic data presented above with the nine sediment packages presented in Chapter 4. Section abbreviations defined in Chapter 1.

i) Preglacial (GS)

During the preglacial period the ancestral Finlay River flowed to the southeast along the RMT. Interpretation of deposits preserved at four sections suggests the sediments to be products of a distal braided river (Figure 55-A). At this time, the migrating river channel eroded bedrock exposed in the RMT and deposited the coarser materials as longitudinal, transverse, and diagonal bars [I(1), BS(1), NA(1), and IV(1)]. During flood or high water events, sediment moving by in suspension was often deposited as overbank fines on the floodplain or in small ponds marginal to the main

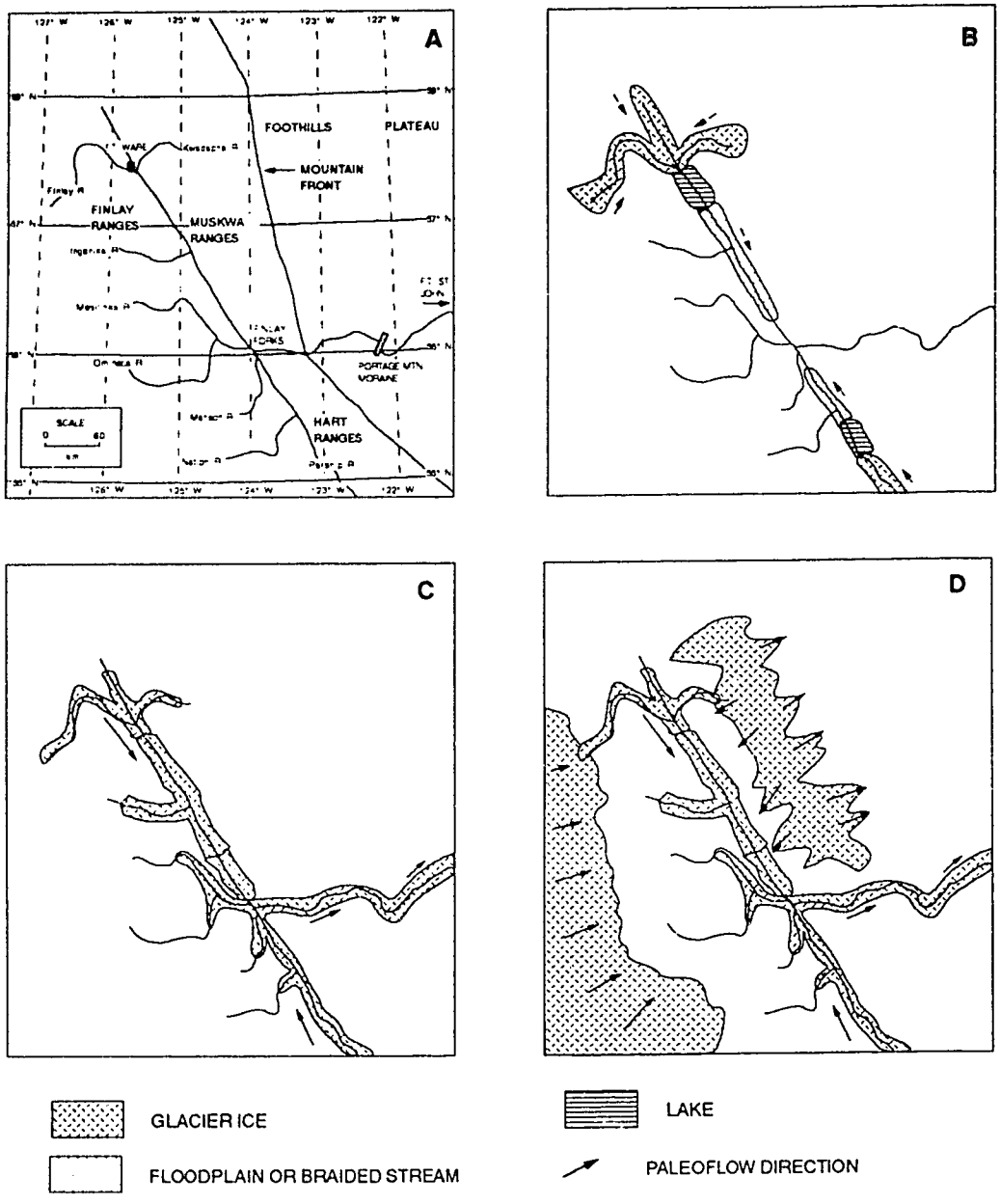

Figure 55. Paleogeographic reconstructions for the northern RMT. A) Preglacial valley, and B-D) Penultimate Glaciation Advance Phase. See text.

channel [1(2)]. Throughout the preglacial period, this fluvial activity resulted in very little sediment accretion and, therefore, minimal input into the sedimentary record (~2.1% of the total unconsolidated sediment).

ii) Penultimate Advance Phase (ES)

At the beginning of the penultimate glaciation, an increase in sediment supply occurred and consequently contributed to the accumulation of advance outwash sediments (~7.0% of the total sediment). Whereas the preceding fluvial deposits are commonly oxidized as a result of prolonged subaerial exposure, the unoxidized and manganese stained glacifluvial sediments indicate continuous and rapid accretion in response to an advancing ice front (Figure 55-B). Glacifluvial sediments deposited at this time show a coarsening-upward sequence reflecting the transition from distal to proximal braided river deposits [W(1), I(3), IV(2), and X(1 and 2)]. Locally deposited inversely graded gravels indicate ice proximal sediment accretion [I(4), and X(3)], whereas coarsening-upward glacilacustrine sediments indicate proglacial lake deposits [VIII(1 and 2)].

iii) Penultimate Glaciation (ES)

The major centre of ice accumulation in British Columbia during Pleistocene glaciations was the Coast Mountains area. Moisture supply from the Pacific Ocean and prevailing westerlies fueled this mountainous area with sufficient precipitation for the development of incipient ice (see Chapter 1). As the ice centre expanded during the penultimate glaciation, several outlet glaciers extended eastward from the ice cap margin. One of these outlet glaciers probably originated in the headwaters of the Finlay River, near Thutade Lake. Igneous bedrock in the area was incorporated into the advancing ice mass and was subsequently transported down-valley (towards the SSE) during the advance (Figure 55-C). At some locations, lodgment till was deposited by

the advancing glacier [WII(2), II(1), O.D.(1), and XI(1)]. During this event, isolated subglacial cavities were infilled with remobilized glacial debris, resulting in deposition of the banded diamicton sediments [WII(1), III(1), IX(4-base), X(4-base), and XI(1-base)]. Continued climatic deterioration and ice cap expansion resulted in the development of an ice sheet which expanded eastward across the southward flowing valley glacier in the RMT (Figure 55-D). Geomorphological evidence including drumlinoid features and grooves west of the Finlay Ranges indicates ice flow to the east (Mathews 1980). Some of these surficial features may relate to this penultimate glaciation. The expanding ice sheet then coalesced with local Rocky Mountain ice, continued to expand eastward and deposited indicator igneous clasts as far east as the Alaska highway (Figure 56-A). Roughly 6.7% of the total unconsolidated sediment correlates to this glaciation.

The above interpretation explains the presence of indicator clasts east of the foothills and the random down-valley fluctuation of igneous clast concentration (Figure 43). The departure of this dispersal curve from the normal negative logarithmic curve shape documented by Clarke (1987) requires explanation. Lateral influx (from the west) of exotic clasts into the main valley glacier (flowing SSE) by an expanding ice sheet would increase the concentration of igneous clasts at select locations along the valley and thus explain the atypical dispersal curve (cf. Figure 43).

iv) Penultimate Retreat Phase (ES)

As climatic conditions improved and the ice sheet disappeared, the ablating valley glacier deposited basal meltout till [W(2), III(2), IV(3), and X(4)] and lodgment till [WII(3) and OD(2)] over stratified sediments. The presence of ice proximal sediments [W(3), WII(4), PC(1), II(3), III(3 and 4), WA(2), VII(1), VIII(3), IX(1), OD(3), and X(5)] indicates <u>in situ</u> ice disintegration occurred at this time (Figure 56-B). The proglacial lakes observed in section are explained by down-stream blockage of

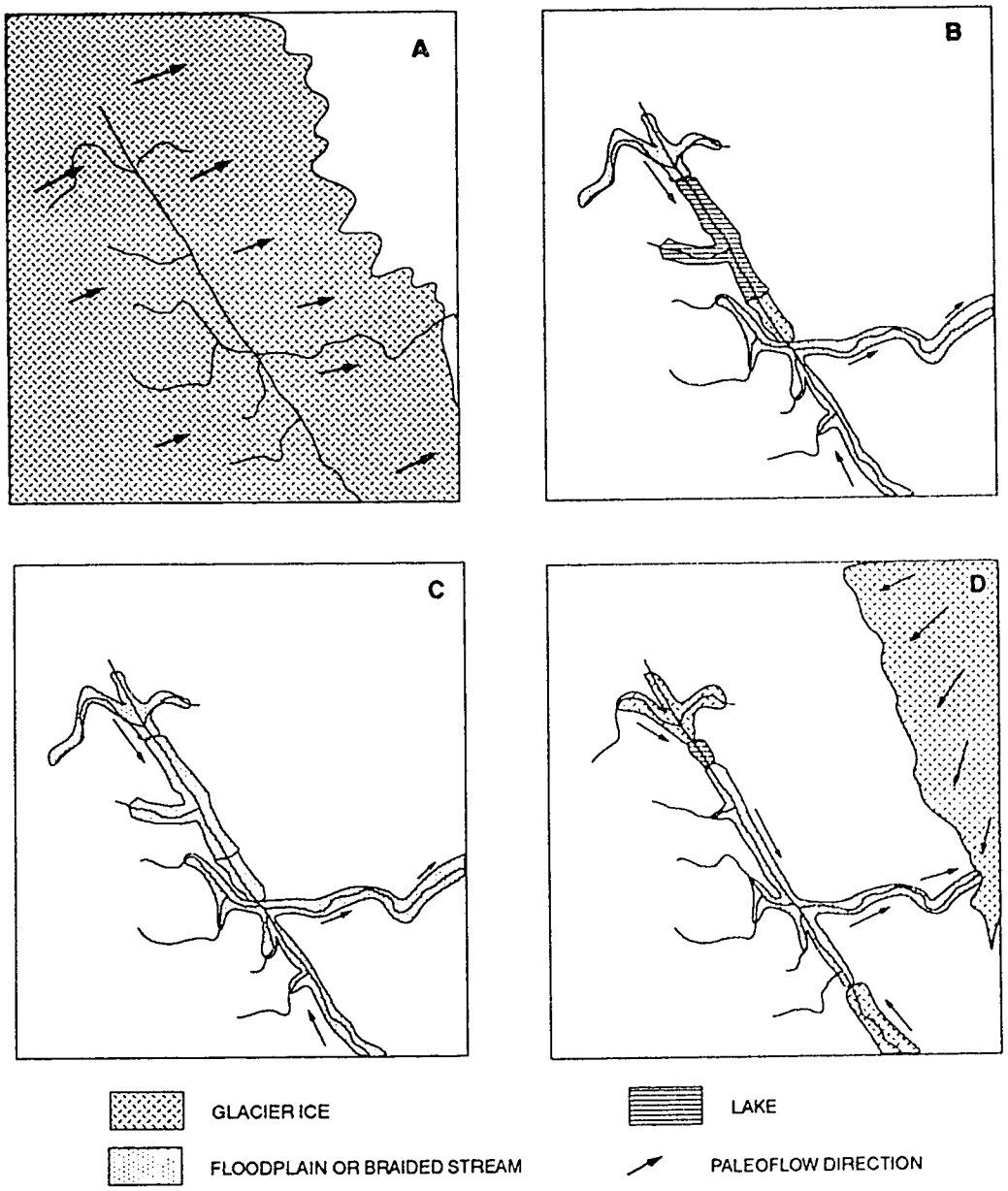

Figure 56. Paleogeographic reconstructions for the northern RMT. A) Penultimate Glaciation, B) Penultimate Retreat Phase, C) Olympia Nonglacial Interval, and D) Late Wisconsinan Advance Phase. See text.

drainage by large stagnant ice blocks [eg. II(2) and XI(2)]. Approximately 11.2% of the unconsolidated sediment in the valley correlates to this event.

v) Olympia Nonglacial (GS)

Continued climatic amelioration and the start of a nonglacial interval occurred sometime before 44,000 years B.P. (GSC-837). This nonglacial interval could have coincided with part or all of oxygen isotope stages 3, 5e, or earlier events (cf. Fulton 1984). Pollen and macrofossil evidence from the study area indicates the nonglacial environment consisted of spruce-dominated forests, with minor amounts of fir and alder (a typical boreal forest assemblage).

Sedimentary deposits from this period indicate that fluvial activity dominated the geologic environment (Figure 56-C). Most sediment reflects distal braided river channel deposition [W(4), PC(2), III(6), VIII(5), and XI(4)], or fluvial overbank sedimentation [II(4), III(5), WA(3), IX(2), X(6), XI(3), and XII(2)]. Minor aeolian sedimentation [VIII(3)] and sediment gravity flow deposition [WA(4) and VIII(4)] also occurred. Compared to the total sedimentary package, very little evidence of this lengthy period is preserved (~8.6%).

vi) Late Wisconsinan Advance Phase (ES)

The start of the last glaciation in the RMT is inferred based on the presence of thick deposits of advance outwash [w(4), II(5, 6, and 7), III(6), V(2), (VII(2), VIII(6), IX(3), X(7), XI(4), and XII(3)]. A build-up of ice to the north of the study area would have provided adequate isostatic depression to change the base level for rapid glacifluvial sedimentation. These horizontally stratified gravel accumulations indicate distal braided river sediment accretion (Figure 56-D). As the Late Wisconsinan ice approached from the NNW, coarsening-upward sequences [eg. V(2) and VIII(7)] and local proglacial lake deposits [X(8 and 9)] were deposited at a number

of locations. Although temporally brief, much of the unconsolidated sediment observed in the northern RMT was deposited during this event (~26.1%). Comparable volumes of episodically deposited advance outwash has been observed south of the study region (Clague 1987).

vii) Late Wisconsinan Glaciation (ES)

As the Late Wisconsinan valley glacier traveled through the study area, lodgment till was deposited along Finlay valley [W(5), II8), III(7), V(3), VII(3), VIII(8), IX(4), X(10), IX(5), and XII(4)]. Drumlins and grooves observed in the valley correlate to this final glaciation (Leslie 1988). This southward moving glacier joined with ice moving north along Parsnip River (cf. Tipper 1971a, 1971b), and the combined glacier ice was subsequently deflected eastward down the preglacial Peace valley (Figure 57-A). This Late Wisconsinan Cordilleran glaciation is interpreted to have reached its maximum extent in the vicinity of the kame moraine near Portage Mountain (Figure 57-A). Approximately 18.8% of the unconsolidated sediment observed along Finlay valley correlates to the 5,000 year period of Late Wisconsinan glaciation.

viii) Late Wisconsinan Glaciation Retreat Phase (ES and GS)

As the Late Wisconsinan ended, rapid ice retreat took place. Deglaciation of the Laurentide glacier near Fort St. John began approximately 13.5 ka (Rutter 1984), whereas deglaciation of coastal B.C. west of the RMT began about 13 ka (Clague 1985). As such, deglaciation of the Cordilleran valley glacier near Hudson Hope probably began by at least 12 ka, so that by 10.1 ka the middle reaches of the Omineca valley were ice-free. Blockage of the regional drainage south of Deserter's Canyon resulted in the progradation of a large glacideltaic complex near McGraw Creek [IX(5 and 6)] (Figure 57-B). For the most part, deglacial sedimentation was localized and restricted to thin

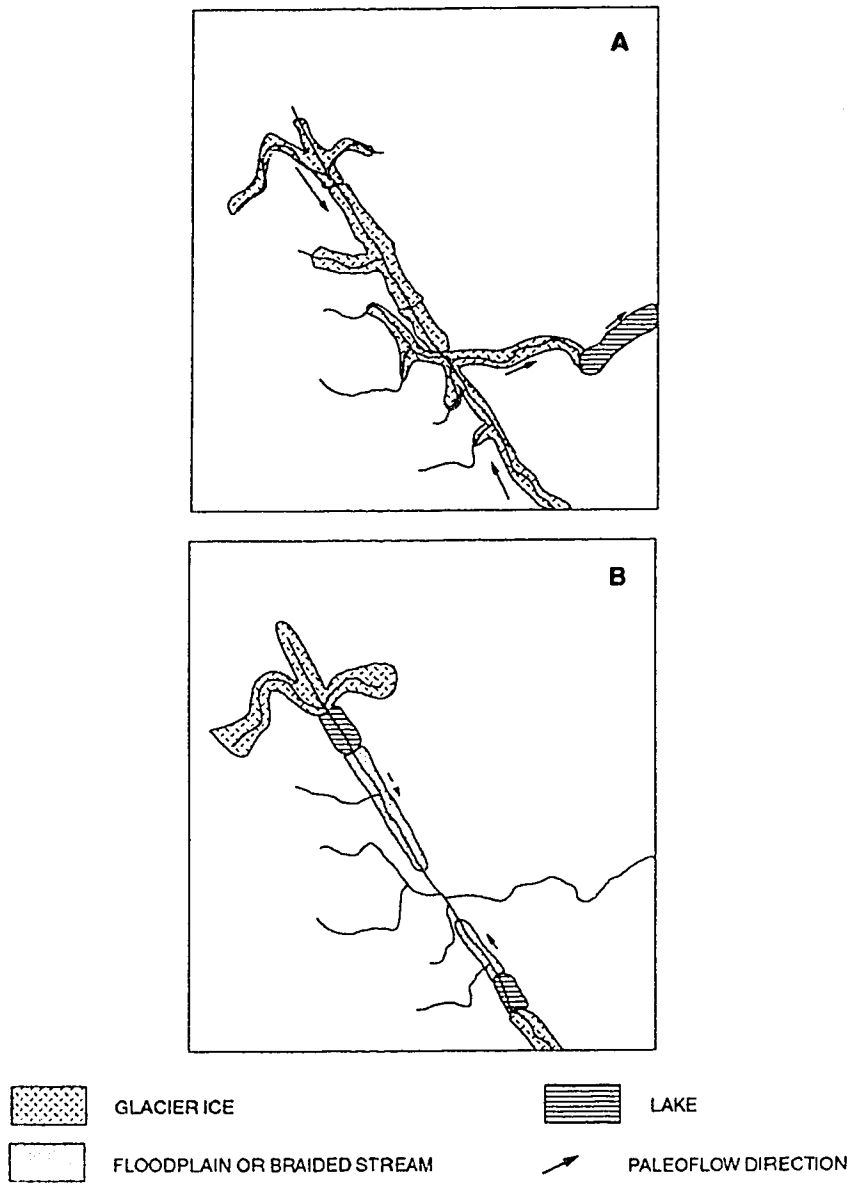

Figure 57. Paleogeographic reconstructions for the northern RMT. A) Late Wisconsinan Glaciation, and B) Late Wisconsinan Retreat Phase

ice marginal outwash deposits [W(6 and 7), II(9), III(8), VII(4), and XII(5)]. Isostatic rebound, coupled with significant meltwater provided the catalyst for terracing and deep incision through over 100 m of Quaternary drift. Meltwater channels and eskers related to this period are evident in the valley (Leslie 1988).

Erosion of the Quaternary sediments filling the RMT is also assumed to have been an "episodic event" (~15.9% of total sediment). This event may have been as short as one thousand years, after which the present day river base level was reached. In the Peace River District of Alberta, interpretation of ^{14}C dates suggested that postglacial river incision required less than a few thousand years (Bobrowsky et al. 1988).

ix) Holocene (GS)

Throughout the Holocene, erosion and sedimentation has been minimal (~3.6% of total sediment). Distal braided river deposition, with minor overbank sedimentation, and localized aeolian sediment reworking characterizes the predominant sediment activity during the last 10 ka (Leslie 1988). The Finlay River is presently described as a meandering-braided river, which drains much of the Muskwa and Finlay Ranges of the northern Cordillera into the Peace River (see Chapter 1).

VI. CONCLUSIONS

The major purpose of this study was to determine the origin, timing, duration, and extent of glacial advances in the northern Rocky Mountain Trench (RMT) (Chapter 1). Detailed field and laboratory analysis centred on the examination of evidence obtained from 18 cliff-sections exposed along the Finlay River of northeastern British Columbia (Chapter 2). Unconsolidated deposits present in the valley were classified according to 15 major sediment types within four broad textural groups: diamicton, gravel, sand, and fines (silt and clay). Only objective criteria were used in defining the various sediment types. Genetic origins were then interpreted for each sediment type (Chapter 3). The classification of observed sediment into the 15 sediment types and the genetic interpretation which followed each type proved critical in the determination of a regional composite stratigraphic history (Chapter 4). Integration of the geochronologic evidence obtained from the study area with the regional stratigraphy permitted the interpretation of an inferred Quaternary geologic history (Chapter 5).

The philosophical premise of this study assumes that deposits associated with rare or episodic events are preferentially preserved in the sedimentological record, whereas long term geological events are rarely preserved. In this study, gradualistic sedimentation is represented by the following sediment packages: Lower Stratified Sediments, Middle Stratified Sediments, and Upper Stratified Sediments. These nonglacial accumulations are represented by only 14.3% of the summed vertical height for the 18 sections, but may represent most of the 32 Ma years which transpired since the emplacement of the RMT. Rare or episodic events are represented by the remaining glacigenic sediment packages and include all sedimentation during a glaciation or immediately preceding/following the glaciation. Rare event sediments constitute 85.7% of the exposed sediment, but probably required ~10-30 ka years to deposit.

All geological observations in northeastern B.C. prior to this study, have been explained in terms of a presumed lengthy Late Wisconsinan event. In the Peace District, Mathews (1973) concluded that the presence of slates, schists, and volcanics within 8 km west of Fort St. John indicated Cordilleran glacier ice advanced into the area. East of this point, red granites and gneisses predominate indicating a Laurentide glacier provenance from the northeast. From this junction northward along the Alaska highway, Mathews (1954, 1955, 1972, 1973, 1978, 1980) envisioned a coalescence of the two ice sheets (Cordilleran and Laurentide) to have occurred during the Late Wisconsinan.

The above conclusions influenced Rutter (1968, 1976, 1977) in his interpretation of the Quaternary geologic history of the upper Peace River valley (now occupied by Williston Lake). At the time, Rutter suggested that a number of the diamictons evident in section were till. Thus, he concluded that a pre-Late Wisconsinan Cordilleran glaciation had affected much of the area, and that subsequently three Late Wisconsinan events also occurred in the northern RMT. The sediment type analysis provided in this study, however, suggests that many of these diamictons are not till, but rather products of sediment gravity flow deposition. Double till exposures and geochronologic control further modify this original interpretation. As such, Rutter's original four glacial events are now considered to be representative of only two glaciations (Bobrowsky 1987).

The presence of western provenance erratics in both the surface counts and in the diamictons of the Peace River District, as well as at higher elevations in the northern Rocky Mountains, is indisputable evidence of extensive Cordilleran ice movement from the far west. At some time in the past, eastward moving ice crossed the RMT, mixed with local Rocky Mountain ice, and then expanded eastward onto the plateau region of B.C. bringing with it a suite of indicator clasts. This event has always been assumed to

correspond to the Late Wisconsinan, but definitive evidence confirming this speculation is lacking (Bobrowsky 1984).

All evidence presented in this study indicates that the dispersal of erratics in northeastern B.C. is a product of the Cordilleran penultimate glaciation (Figure 58). Research in northwestern Alberta indicates Laurentide ice did not reach the Peace River District during the penultimate glaciation (Liverman in preparation). As such, an ice-free area existed in northeastern B.C. during the Cordilleran penultimate glaciation. Following this first glaciation and a lengthy nonglacial interval, a second glaciation (the Late Wisconsinan) began some 25,000 years ago, probably in the Coast Mountain Ranges of British Columbia. Approximately 10,000 years later, Cordilleran glacial ice moved to the southeast along Finlay valley. This second glaciation reached its maximum extent in the area of the Portage Mountain moraine sometime after 15 ka. Active ice retreat then occurred so that by ca. 10.5 ka the RMT was ice-free as far north as the Omineca valley. Late Wisconsinan Cordilleran ice, therefore, traveled 350 km to the SSE and E, and then retreated another 200 km in less than 5,000 years. Evidence in the vicinity of Fort St. John indicates that the Laurentide glacier reached its maximum extent east of Portage Mountain after 25 ka, with deglaciation occurring between 13.5 and 11.4 ka (Rutter 1984). From the above discussion, it is evident that the during the Late Wisconsinan, the Cordilleran and Laurentide Ice Sheets behaved independently and did not coalesce in northeastern British Columbia. Similar asynchronous ice sheet behavior is interpreted to have occurred throughout the Quaternary in southwestern Alberta (Rutter 1984). An ice-free corridor is, therefore, assumed to have existed throughout the Quaternary in northeastern British Columbia (Bobrowsky 1988). Separate investigation is required directly north of Finlay valley and along the foothills of northeastern British Columbia to add credence to this study.

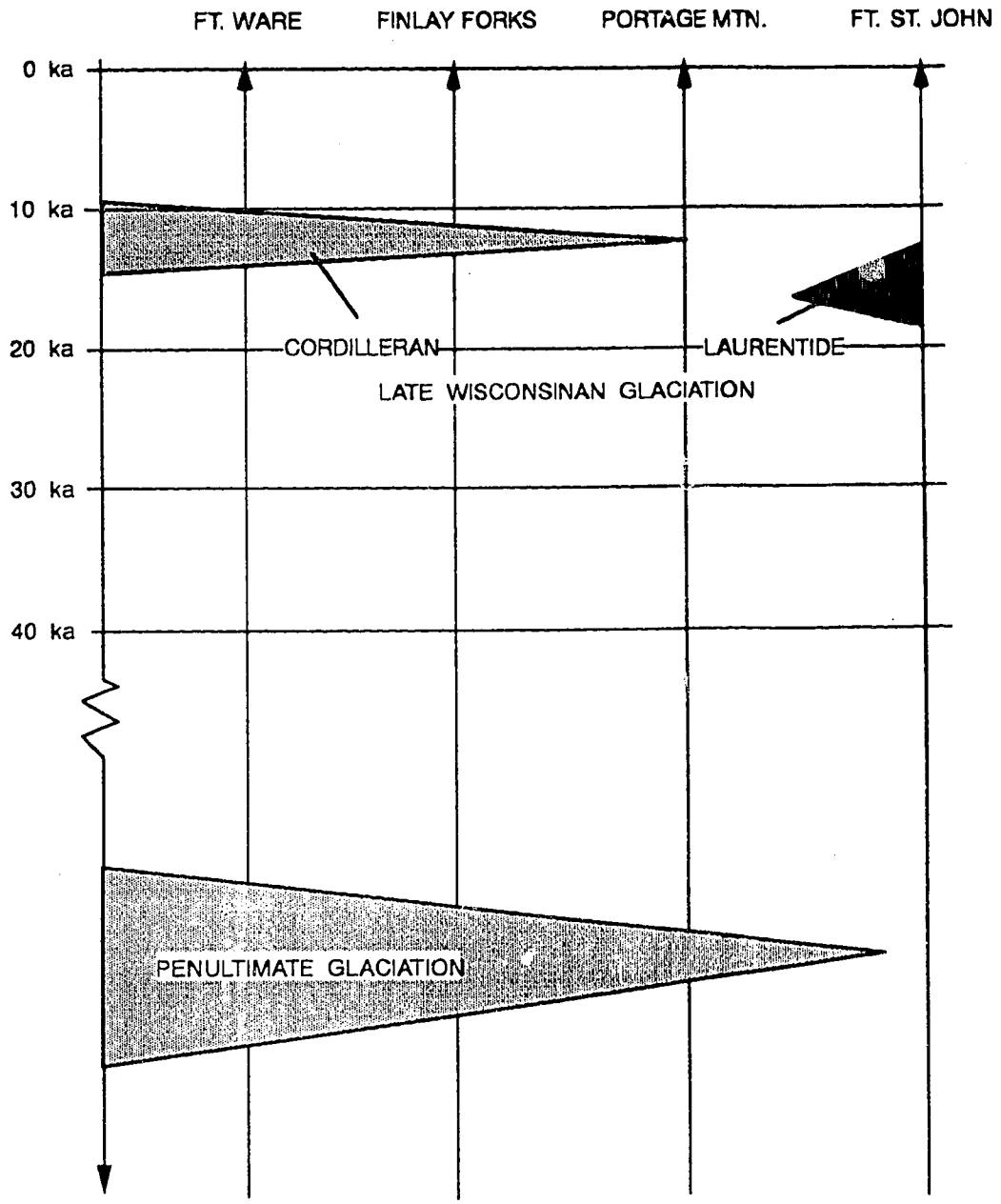

Figure 58. Time-distance diagram illustrating the relationship between Cordilleran and Laurentide glaciations in northeastern British Columbia. Note the absence of a Laurentide penultimate glaciation, the extensive Cordilleran penultimate glaciation, and the nonsynchronous Late Wisconsinan glaciations in the "ice-free-corridor".

BIBLIOGRAPHY

Allen, J.R.L. 1965. A review of the origin and characteristics of recent alluvial sediments. Sedimentology, **5**: 89-191.

Allen, J.R.L. 1984. Sedimentary Structures, Their Character and Physical Basis. Developments in Sedimentology 30. Elsevier, New York.

Alley, R.B., Blakenship, D.D., Bentley, C.R., and Rooney, S.T. 1986. Deformation of till beneath ice stream B, West Antarctica. Nature, **322**: 57-59.

Anders, M. H., Krueger, S. W., and Sadler, P. M. 1987. A new look at sedimentation rates and the completeness of the stratigraphic record. Journal of Geology, **95**: 1-14.

Anderson, T.W., and Stephens, M.A. 1972. Tests for randomness of directions against equatorial and bimodal alternatives. Biometrika, **59**: 613-621.

Armstrong, J.E. 1946. Geology and mineral deposits of northern British Columbia west of the Rocky Mountains. Geological Survey of Canada, Bulletin 5, 46 p.

Armstrong, J.E., and Tipper, H.W. 1948. Glaciation in north central British Columbia. American Journal of Science, **246**: 283-310.

Ashley, G.M., Shaw, J., and Smith, N.D. (Editors) 1985. Glacial Sedimentary Environments. Society of Economic Paleontologists and Mineralogists, Short Course No. 16, Tulsa, Oklahoma.

ASTM 1964. Procedure for Testing Soils. American Society for Testing Materials, Philadelphia.

Banerjee, I. 1973a. Part A: Sedimentology of Pleistocene Glacial Varves in Ontario, Canada. Geological Survey of Canada, Bulletin 226, pp. 1-44.

Banerjee, I. 1973b. Part B: Nature of the Grain-Size Distribution of some Pleistocene Glacial Varves of Ontario, Canada. Geological Survey of Canada, Bulletin 226, pp. 45-60.

Barrett, P. 1980. The shape of rock particles: a critical review. Sedimentology, **27**: 291-303.

Beach, H.H., and Spivak, J. 1943. The origin of Peace River Canyon, British Columbia. American Journal of Science, **241**: 366-376.

Blakenship, D.D., Bentley, C.R., Rooney, S.T., and Alley, R.B. 1986. Seismic measurements reveal a saturated porous layer beneath an active Antarctic ice stream. Nature, **322**: 54-57.

Blatt, H., Middleton, G., and Murray, R. 1980. Origin of Sedimentary Rocks. Prentice-Hall, Inc., Englewood Cliffs, New Jersey.

Bobrowsky, P.T. 1984. Quaternary geologic history of the north central Rocky Mountain Trench, British Columbia. *In* Proceedings of the 1st Northern Workshop. *Edited by* A.S.A. Mohsen and W.C. MacKay. Boreal Institute for Northern Studies, Edmonton.

Bobrowsky, P.T. 1987. Quaternary Stratigraphy of the Northern Canadian Cordillera Based on New Evidence from the Finlay River of Northeastern British Columbia. XIIth INQUA Congress, Program with Abstracts, p. 132.

Bobrowsky, P.T. 1988. Ice Free Conditions in the Northern Canadian Cordillera at 18 ka and Timing of the Late Wisconsinan. American Quaternary Association, Program and Abstracts of the Tenth Biennial Meeting, p. 108.

Bobrowsky, P.T., Lamothe, M., and Shilts, W.W. 1987a. Late Quaternary glaciation and deglaciation in the Baie des Chaleurs area, northern New Brunswick. Geological Association of Canada-Mineralogical Association of Canada, Program with Abstracts, **12**, p. 26.

Bobrowsky, P.T., Levson, V., Liverman, D.G.E., and Rutter, N.W. 1987b. Quaternary Geology of Northwestern Alberta and Northeastern British Columbia, Excursion Guide Book A-24, Xilth International Union for Quaternary Research Congress. National Research Council of Canada, Ottawa, 67 p.

Bobrowsky, P.T., Damkjar, E.R., and Gibson, T.H. 1988 A geological and archaeological study of HcQh-6, Peace River, Alberta (Permit 88-5). Report on file with the Archaeological Survey of Alberta, Alberta Culture and Multiculturalism, 79 p.

Boothroyd, J.C., and Ashley, G.M. 1975. Processes, Bar Morphology, and Sedimentary Structures on Braided Outwash Fans, Northeastern Gulf of Alaska. *In* Glaciofluvial and Glaciolacustrine Sedimentation. *Edited by* A.V. Jopling and B.C. McDonald. S.E.P.M., Special Publication No. 23, Tulsa, Oklahoma, pp. 193-222.

Bostock, H.S. 1970. Physiographic regions of Canada. Geological Survey of Canada, Map1254A.

Boulton, G.S. 1968. Flow tills and related deposits on some Vestspitsbergen glaciers. Journal of Glaciology, **7**: 391-412.

Boulton, G.S. 1970a. On the deposition of subglacial and melt-out tills at the margins of certain Svalbard glaciers. Journal of Glaciology, **9**: 231-245.

Boulton, G.S. 1970b. On the origin and transport of englacial debris in Svalbard Glaciers. Journal of Glaciology, **9**: 213-229.

Boulton, G.S. 1972. Modern Arctic glaciers as depositional models for former ice sheets. Journal of the Geological Society, London, **128**: 361-393.

Boulton, G.S. 1976. The development of geotechnical properties in glacial till. *In* Glacial Till. *Edited by* R.F. Legget. Royal Society of Canada, Ottawa, pp. 292-303.

Boulton, G.S. 1978. Boulder shapes and grain-size distributions of debris as indicators of transport paths through a glacier and till genesis. Sedimentology, **25**: 773-799.

Boulton, G.S., and Eyles, N. 1979. Sedimentation by valley glaciers; a model and genetic classification. *In* Moraines and Varves-Origin/Genesis/Classification. *Edited by* Ch. Schlüchter. Balkema, Rotterdam, pp. 11-23.

Bowes, G.E. (Editor) 1963. Peace River Chronicles. Prescott Publishing, Vancouver.

Bridge, J. S. 1985. Paleochannel patterns inferred from alluvial deposits: a critical evaluation. Journal of Sedimentary Petrology, **55**: 579-589.

Bridgland, D.R. (Editor) 1986. Clast Lithological Analysis. Quaternary Research Association, Cambridge, United Kingdom, 207 p.

Brodzikowski, K., and van Loon, A.J. 1983. Sedimentology and deformational history of unconsolidated Quaternary sediments of the Jaroszow Zone (Sudetic Foreland). Geologia Sudetica, **18**: 123-195.

Broster, B.E. 1986. Till variability and compositional stratification: examples from the Port Huron lobe. Canadian Journal of Earth Sciences, **23**, pp. 1823-1841.

Broster, B.E., and Hicock, S.R. 1985. Multiple flow and support mechanisms and the development of inverse grading in a subaquatic glacigenic debris flow. Sedimentology, **32**: 645-657.

Cas, R. A. F., and Landis, C. A. 1987. A debris-flow deposit with multiple plug-flow channels and associated side accretion deposits. Sedimentology, **34**: 901-910.

Catto, N.R. 1988. Geology 482 Field Manual. University of Alberta, Edmonton.

Cheel, R.J., and Middleton, G.V. 1986. Horizontal laminae formed under upper flow regime plane bed conditions. Journal of Geology, **94**: 489-504.

Cheel, R.J., and Middleton, G.V. 1987. Horizontal laminae formed under upper flow regime plane bed conditions: a reply. Journal of Geology, **95**: 282.

Cheel, R.J., and Rust, B.R. 1982. Coarse-grained facies of glaciomarine deposits near Ottawa, Canada. *In* Research in Glacial, Glacio-Fluvial and Glacio-Lacustrine

Systems. *Edited by* R. Davidson-Arnott, W. Nickling and B.D. Fahey. Geo-Books, Norwich, England, pp. 279-295.

Cheeney, R.F. 1983. Statistical Methods in Geology. George Allen and Unwin, London.

Church, M., and Gilbert, M. 1975. Proglacial fluvial and lacustrine environments. *In* Glaciofluvial and Glaciolacustrine Sedimentation. *Edited by* A.V. Jopling and B.C. McDonald. S.E.P.M., Special Publication No. 23, Tulsa, Oklahoma, pp. 22-100.

Churcher, C.S., and M. Wilson 1979. Quaternary mammals from the eastern Peace River District, Alberta. Journal of Paleontology, **53**: 71-76.

Clague, J.J. 1974. The St. Eugene Formation and the Development of the Southern Rocky Mountain Trench. Canadian Journal of Earth Sciences, **11**: 916-938.

Clague, J.J. 1980. Late Quaternary Geology and Geochronology of British Columbia. Geological Survey of Canada, Paper 80-13, pp. 1-28.

Clague, J. J. 1981. Late Quaternary Geology and Geochronology of British Columbia, Part 2: Summary and Discussion of Radiocarbon-Dated Quaternary History. Geological Survey of Canada, Paper 80-35, pp. 1-41.

Clague, J. J. 1985. Deglaciation of the Prince Rupert--Kitimat area, British Columbia. Canadian Journal of Earth Sciences, **22**: 256-265.

Clague, J. J. 1986. The Quaternary stratigraphic record of British Columbia -- evidence for episodic sedimentation and erosion controlled by glaciation. Canadian Journal of Earth Sciences, **23**: 885-894.

Clague, J. J. 1987. Quaternary stratigraphy and history, Williams Lake, British Columbia. Canadian Journal of Earth Sciences, **24**, pp. 147-158.

Clapperton, C.M. 1975. The debris content of surging glaciers in Svalbard and Iceland. Journal of Glaciology, **14**: 395-406.

Clark, P. U. 1987. Subglacial sediment dispersal and till composition. Journal of Geology, **95**: 527-541.

Clarke, A.H. 1981. The Freshwater Molluscs of Canada. National Museum of Natural Sciences, National Museums of Canada, Ottawa.

Clayton, L. 1961. Late Wisconsin Mollusca from ice-contact deposits in Logan County, North Dakota. North Dakota Academy of Science, Proceedings, **15**: 11-18.

Clayton, L., Teller, J. T., and Attig, J. W. 1985. Surging of the southwestern part of the Laurentide Ice Sheet. Boreas, **14**: 235-241.

Collinson, J.D., and Thompson, D.B. 1982. Sedimentary Structures. George Allen and Unwin, London.

Compton, R.R. 1962. Manual of Field Geology. John Wiley and Sons, Inc., New York.

Dardis, G.F. 1985. Till facies associations in drumlins and some implications for their mode of formation. Geografiska Annaler, **67A**: 13-22.

Dawson, G.M. 1878. On the superficial geology of British Columbia. Quarterly Journal Geological Society of London, **34**: 89-128.

Dawson, G.M. 1888. Recent observations on the glaciation of British Columbia and adjacent regions. American Geologist, **3**: 249-253.

Dawson, G.M. 1890. On the glaciation of the northern part of the Cordillera, with an attempt to correlate the events of the Glacial Period in the Cordillera and Great Plains. American Geologist, **6**: 153-162.

Dean, W.E., Jr. 1974. Determination of carbonate and organic matter in calcareous sediments and sedimentary rocks by loss on ignition: comparison with other methods. Journal of Sedimentary Petrology, **44**: 242-248.

DeCelles, P.G., Langford, R.P., and Schwartz, R.K. 1983. Two new methods of paleocurrent determination from trough cross-stratification. Journal of Sedimentary Petrology, **53**: 629-642.

Dolmage, V. 1928. Finlay River District, British Columbia. Geological Survey of Canada, Summary Report, 1927, Part A, pp. 19A-41A.

Dolmage, V., and Campbell, D.D. 1963. The geology of the Portage Mountain Damsite, Peace River, B.C. The Canadian Mining and Metallurgical Bulletin, **56**: 711-723.

Domack, E. W., and Lawson, D.E. 1985. Pebble fabric in an ice-rafted diamicton. Journal of Geology, **93**: 577-591.

Dott, R.H., Jr. 1973. Paleocurrent analysis of trough cross stratification. Journal of Sedimentary Petrology, **43**, pp. 779-783.

Dott, R.H. Jr. 1983. Episodic sedimentation - how normal is average? How rare is rare? Does it matter? Journal of Sedimentology, **53**: 5-23.

Dowdeswell, J. A., Hambrey, M. J., and Wu, R. 1985. A comparison of clast fabric and shape in Late Precambrian and modern glacigenic sediments. Journal of Sedimentary Petrology, **55**: 691-704.

Dowdeswell, J. A., and Sharp, M. J. 1986. Characterization of pebble fabrics in modern terrestrial glacigenic sediments. Sedimentology, **33**: 699-710.

Drake, L.D. 1974. Till fabric control by clast shape. Geological Society of America, Bulletin, **85**: 247-250.

Dreimanis, A. 1962. Quantitative gasometric determination of calcite and dolomite by using Chittick apparatus. Journal of Sedimentary Petrology, **32**: 520-529.

Dreimanis, A. 1976. Tills: their origin and properties. *In* Glacial Till. *Edited by* R.F. Legget. Royal Society of Canada, Ottawa, pp. 11-49.

Dreimanis, A. 1983. Penecontemporaneous partial disaggregation and/or resedimentation during the formation and deposition of subglacial till. Acta Geològica Hispànica, **18**: 153-160.

Dreimanis, A. 1984. Discussion: Lithofacies types and vertical profile models; an alternative approach to the description and environmental interpretation of glacial diamict and diamictite sequences. Sedimentology, **31**: 885-886.

Dreimanis, A., and Lundqvist, J. 1984. What should be called Till? Striae, **20**: 5-10.

Drozdowski, E. 1985. On the effects of bedrock protruberances upon the depositional and relief-forming processes in different marginal environments of Spitsbergen glaciers. Palaeogeography, Palaeoclimatology, Palaeoecology, **51**: 397-413.

Duck, R. W., and McManus, J. 1984. Traces produced by chironomid larvae in sediments of an ice-contact proglacial lake. Boreas, **13**: 89-93.

Dumanski, J. (Editor) 1978. Manual for describing soils in the field, Revised. Canada Soil Survey Committee, Ottawa.

Ekdale, A.A., Bromley, R.G., and Pemberton, S.G. 1984. Ichnology: Trace fossils in sedimentology and stratigraphy. Society of Economic Paleontologists and Mineralogists, Short Course No. 15, Oklahoma.

Elliot, T. 1978. Deltas. *In* Sedimentary Environments and Facies. *Edited by* H.G. Reading. Elsevier, New York, pp. 97-142.

Environment Canada 1984. Canadian Climatic Normals, 1951-1980, Volumes 1-8. Canadian Government Publishing, Ottawa.

Eschner, T.R., and Kircher, J.E. 1984. Interpretation of grain-size distributions from measured sediment data, Platte River, Nebraska. Sedimentology, **31**: 569-573.

Evenchick, C.A. 1984. Structure and stratigraphy in the hanging wall of Sifton Fault, Sifton Ranges, northern British Columbia. In Current Research, Part A, Geological Survey of Canada. Paper 84-1A, pp. 105-108.

Evenson, E.B., Dreimanis, A., and Newsome, J.W. 1977. Subaquatic flow tills: a new interpretation for the genesis of some laminated till deposits. Boreas, **6**: 115-133.

Eyles, C.H., and Eyles, N. 1983. Sedimentation in a large lake: A reinterpretation of the late Pleistocene stratigraphy at Scarborough Bluffs, Ontario, Canada. Geology, **11**: 146-152.

Eyles, C.H., Eyles, N., and Miall, A.D. 1985. Models of glaciomarine sedimentation and their application to the interpretation of ancient glacial sequences. Palaeogeography, Palaeoclimatology, Palaeoecology, **51**: 15-84.

Eyles, N. 1979. Facies of supraglacial sedimentation on Icelandic and Alpine temperate glaciers. Canadian Journal of Earth Sciences, **16**: 1341-1361.

Eyles, N. 1987. Late Pleistocene debris-flow deposits in large glacial lakes in British Columbia and Alaska. Sedimentary Geology, **53**, pp. 33-71.

Eyles, N., Clark, B. M., and Clague, J. J. 1987. Coarse-grained sediment gravity flow facies in a large supraglacial lake. Canadian Journal of Earth Sciences, **34**: 193-216.

Eyles, N., Eyles, C.H., and Miall, A.D. 1983. Lithofacies types and vertical profile models; an alternative approach to the description and environmental interpretation of glacial diamict and diamictite sequences. Sedimentology, **30**: 393-410.

Fenton, M., and Dreimanis, A. 1976. Methods of stratigraphic correlation of till in central and western Canada. *In* Glacial Till. *Edited by* R.F. Legget. Royal Society of Canada, Ottawa, pp. 67-82.

Fielding, C.R. 1984. Upper delta plain lacustrine and fluviolacustrine facies from the Westphalian of the Durham coalfield, NE England. Sedimentology, **31**: 547-567.

Fielding, C.R. 1987. Lower delta plain interdistributary deposits--An example from the Westphalian of the Lancashire Coalfield, northwest England. Geological Journal, **22**: 151-162.

Fisher, R.V. 1971. Features of coarse-grained, high-concentration fluids and their deposits. Journal of Sedimentary Petrolology, **41**: 916-927.

Fladmark, K. 1983. Times and Places: Environmental Correlates of Mid-to-Late Wisconsinan Human Population Expansion in North America. *In* Early Man in the New World. *Edited by* Richard Shutler, Jr. Sage Publications, London, pp. 13-41.

Fladmark, K., Driver, J.C., and Alexander, D. 1988 The Paleoindian Component at Charlie Lake Cave (HbRf-39), British Columbia. American Antiquity, **53**: 371-384.

Flint, R.F., Sanders, J.E., and Rodgers, J. 1960a. Symmictite: a name for nonsorted terrigenous sedimentary rocks that contain a wide range of particle sizes. Geological Society of America, Bulletin, 71: 507-510.

Flint, R.F., Sanders, J.E., and Rodgers, J. 1960b. Diamictite, a substitute name for symmictite. Geological Society of America, Bulletin, **71**, pp. 1809-1810.

Folk, R.L. 1974. Petrology of Sedimentary Rocks. Hemphill Publishing Co., Austin, Texas.

Fulton, R.J. 1971. Radiocarbon geochronology of southern British Columbia. Geological Survey of Canada, Paper 71-37, 28 p.

Fulton, R.J. (Editor) 1984a. Quaternary Stratigraphy of Canada- A Canadian Contribution to IGCP Project 24. Geological Survey of Canada, Paper 84-10, Ottawa.

Fulton, R.J. 1984b. Quaternary glaciation, Canadian Cordillera. *In* Quaternary Stratigraphy of Canada- A Canadian Contribution to IGCP Project 24. *Edited by* R.J. Fulton. Geological Survey of Canada, Paper 84-10, Ottawa, pp. 39-47.

Fritz, W. J., and Harrison, S. 1985. Transported trees from the 1982 Mount St. Helens sediment flows: their use as paleocurrent indicators. Sedimentary Geology, **42**: 49-64.

Gabrielse, H. 1971. Operation Finlay, north-central British Columbia. In Report of Activities, Part A, Geological Survey of Canada. Paper 71-1A, pp. 23-26.

Gabrielse, H., Dodds, C.J., Mansy, J.L. (1971-75), and Eisbacher, G.H. (1969-71) n.d. Geology of Toodoggone River (94E) and Ware West Half (94F). Open File Report 483, Geological Survey of Canada, Ottawa.

Gabrielse, H., Dodds, C.J., and Mansy, J.L. 1977. Operation Finlay, British Columbia. Current Research, Report of Activities, Part A, Paper 77-1A, pp. 243-246.

Giardino, J.R., and Vitek, J.D. 1985. A statistical interpretation of the fabric of a rock glacier. Arctic and Alpine Research, **17**: 165-177.

Gibbard, P. 1980. The origin of stratified Catfish Creek Till by basal melting. Boreas, **9**: 71-85.

Gillberg, G. 1977. Redeposition: a process in till formation. Geologiska Föreningens i Stockholm Förhandlingar, **99**: 246-253.

Glen, J.W., Donner, J.J., and West, R.G. 1957. On the mechanism by which stones in till become oriented. American Journal of Science, **255**: 194-205.

Goodwin, C.I., and Sinclair, A.J. 1982. Average lead isotope growth curves for shale-hosted zinc-lead deposits, Canadian Cordillera. Economic Geology, **77**: 675-690.

Goodwin, P.W., and Anderson, E. J. 1985. Punctuated aggradational cycles: a general hypothesis of episodic stratigraphic accumulation. Journal of Geology, **93**: 515-533.

Gorsline, D.S. 1984. A review of fine-grained sediment origins, characteristics, transport and deposition. *In* Fine Grained Sediments: Deep-Water Processes and

Facies. *Edited by* D.A.V. Stow and D.J.W. Piper. Blackwell Publications, Oxford, pp. 17-34.

Gravenor, C. P. 1986. Magnetic and pebble fabrics in subaquatic debris-flow deposits. Journal of Geology, **94**: 683-698.

Greguss, P. 1955. Identification of living gymnosperms on the basis of xylotomy. Akademiai Kiado, Budapest.

Gross, D.L., and Moran, S.R. 1981. Grain-size and mineralogical gradations within tills of the Allegheny Plateau. *In* Till: a symposium. *Edited by* R.P. Goldthwait. Ohio State University Press, Columbus, pp. 251-274.

Gustavson, T.C., Ashley, G.M., and Boothroyd, J.C. 1975. Depositional Sequences in Glaciolacustrine Deltas. *In* Glaciofluvial and Glaciolacustrine Sedimentation. *Edited by* A.V. Jopling and B.C. McDonald. S.E.P.M., Special Publication No. 23, Tulsa, Oklahoma, pp. 264-280.

Haldorsen, S. 1982. The genesis of tills from Åstadalen, southeastern Norway. Norsk Geologisk Tidsskrift, **62**, pp. 17-38.

Haldorsen, S., and Shaw, J. 1982. The problem of recognizing melt-out till. Boreas, **11**: 261-277.

Hann, B.J., and Karrow, P.F. 1984. Pleistocene paleoecology of the Don and Scarborough Formations, Toronto, Canada, based on cladoceran microfossils at the Don Valley Brickyard. Boreas, **13**: 377-399.

Hampton, M.A. 1972. The role of subaqeous debris flow in generating turbidity currents. Journal of Sedimentary Petrology, **42**: 775-793.

Hampton, M.A. 1975. Competence of fine-grained debris flows. Journal of Sedimentary Petrology, **45**: 834-844.

Harington, C.R. 1978. Quaternary vertebrate faunas of Canada and Alaska and their suggested chronological sequence. Syllogeus, **15**: 1-105.

Harington, C.R., Tipper, H.W., and Mott, R.J. 1974. Mammoth from Babine Lake, British Columbia. Canadian Journal of Earth Sciences, **11**: 285-303.

Harland, W.B., Herod, K.N., and Krinsley, D.H. 1966. The definition and identification of tills and tillites. Earth-Science Reviews, **2**: 225-256.

Harms, J.C., and Fahnestock, R.K. 1977. Stratification, bed forms, and flow phenomena (with an example from the Rio Grande). *In* Sedimentary Processes: Hydraulic Interpretation of Primary Sedimentary Structures. *Compiled by* G.V.Middleton. SEPM, Reprint Series No. 3, Tulsa, pp. 95-127.

Harms, J.C., MacKenzie, D.B., and McCubbin, D.G. 1963. Stratification in modern sands of the Red River, Louisiana. Journal of Geology, **71**: 566-580.

Harms, J.C., Southard, J.B., and Walker, R.G. 1982. Structures and Sequences in Clastic Rocks. S.E.P.M., Short Course No. 9, Tulsa, Oklahoma.

Harrison, P.W. 1957. A clay-till fabric: its character and origin. Journal of Geology, **65**: 275-308.

Hedley, M.S., and Holland, S.S. 1941. Reconnaissance in the area of Turnagain and Upper Kechika Rivers, northern British Columbia. Department of Mines, B.C., Bulletin 12, 52 p.

Hedlin, M.A.H., and Evans, M.E. 1987. A palaeomagnetic study of some Pleistocene sediments in northern Canada and its bearing on the secular variation of the geomagnetic field. Geophysical Journal of the Royal Astronomical Society, **90**: 693-703.

Hein, F.J. 1984. Deep-sea and fluvial braided channel conglomerates: a comparison of two case studies. *In* Sedimentology of Gravels and Conglomerates. *Edited by* E.H. Koster and R.J. Steel. Canadian Society of Petroleum Geologists, Memoir 10, Calgary, pp. 33-49.

Hein, F.J., and Walker, R.G. 1977. Bar evolution and development of stratification in the gravelly, braided, Kicking Horse River, British Columbia. Canadian Journal of Earth Sciences, **14**: 562-570.

Hicock, S.R., and Rutter, N. W. 1986. Pleistocene aminostratigraphy of the Georgia Depression, southwest British Columbia. Canadian Journal of Earth Sciences, **23**: 383-392.

Hollard, S.S. 1976. Landforms of British Columbia, A Physiographic Outline. British Columbia Department of Mines and Petroleum Resources, Victoria.

Hopkins, W.S., Jr., Rutter, N.W., and Rouse, G.E. 1972. Geology, Paleoecology, and Palynology of some Oligocene Rocks in the Rocky Mountain Trench of British Columbia. Canadian Journal of Earth Sciences, **9**: 460-470.

Hudleston, P.J. 1980. The progressive development of inhomogeneous shear and crystallographic fabric in glacial ice. Journal of Structural Geology, **2**:189-196.

Humphrey, N., Raymond, C., and Harrison, W. 1986. Discharges of turbid water during mini-surges of Variegated Glacier, Alaska, U.S.A. Journal of Glaciology, **32**: 195-207.

Iken, A., and Bindschadler, RR. A. 1986. Combined measurements of subglacial wa... pressure and surface velocity of Findelelgletscher, Switzerland: conclusions about drainage system and sliding mechanism. Journal of Glaciology, **32**: 101-119.

Irish, E.J.W. 1969. Halfway River Map-Area, British Columbia (94 B). Geological Survey of Canada, Paper 69-11, 154 p.

Jackson, E.V. 1976. Generalized Geological Map of the Canadian Cordillera, Map A. B.C. Department of Mines and Petroleum Resources, Victoria.

Johansen, D.A. 1940. Plant Micro-Technique. McGraw Hill, New York.

Johnson, A.M., and Rodine, J.R. 1984. Debris Flow. *In* Slope Instability. *Edited by* D. Brunsden and D.B. Prior. John Wiley and Sons, pp. 257-361.

Johnson, T.C., Halfman, J.D., Busch, W.H., and Flood, R.D. 1984. Effects of bottom currents and fish on sedimentation in a deep-water, lacustrine environment. Geological Society of America Bulletin, **95**: 1425-1436.

Johnston, W.A. 1926. The Pleistocene of Cariboo and Cassiar Districts, British Columbia, Canada. Royal Society of Canada, Transactions, Section IV, pp. 137-147.

Jones, R.K., and Annas, R. 1981. Vegetation. *In* The Soil Landscapes of British Columbia. *Edited by* K.W.G. Valentine, P.N. Sprout, T.W. Baker and L.M. Lavkulich. B.C. Ministry of the Environment, Victoria, pp. 35-45.

Jopling, A.V., and Walker, R.G. 1968. Morphology and origin of ripple-drift cross-lamination, with examples from the Pleistocene of Massachusetts. Journal of Sedimentary Petrology, **38**: 971-984.

Karrow, P.F. 1976. The texture, mineralogy, and petrography of North American tills. *In* Glacial Till. *Edited by* R.F. Legget. Royal Society of Canada, Ottawa, pp. 83-98.

Kemmis, T.J., and Hallberg, G.R. 1984. Discussion: Lithofacies types and vertical profile models; an alternative approach to the description and environmental interpretation of glacial diamict and diamictite sequences. Sedimentology, **31**: 886-890.

Kemmis, T.J., Hallberg, G.R., and Lutenegger, A.J. 1981. Depositional Environments of Glacial Sediments and Landforms of the Des Moines Lobe, Iowa. Iowa Geological Survey, Iowa.

Kennedy, S. K., and Ehrlich, R. 1985. Origin of shape changes of sand and silt in a high-gradient stream system. Journal of Sedimentary Petrology, **55**: 57-64.

Kerr, F.A. 1934. Glaciation in northern British Columbia. Royal Society of Canada, Transactions, Section IV, pp. 17-31.

Klassen, R.W. 1978. A unique stratigraphic record of late Tertiary-Quaternary events in southeastern Yukon. Canadian Journal of Earth Sciences, **15**: 1884-1886.

Klassen, R.W. 1987. The Tertiary-Pleistocene stratigraphy of the Liard Plain, southeastern Yukon Territory. Geological Survey of Canada, Paper 86-17, pp. 1-16.

Krajina, V.J. 1965. Biogeoclimatic zones and biogeocoenoses of British Columbia. Ecology of Western North America, **1**: 1-17.

Krüger, J. 1979. Structures and textures in till indicating subglacial deposition. Boreas, **8**, pp. 323-340.

Krüger, J. 1984. Clasts with stoss-lee form in lodgement tills: a discussion. Journal of Glaciology, **30**: 241-243.

Kurtz, D.D., and Anderson, J.B. 1979. Recognition and sedimentologic description of recent debris flow deposits from the Ross and Weddell Seas, Antarctica. Journal of Sedimentary Petrology, **49**: 1159-1170.

Landim, P.M.B., and Frakes, L.A. 1968. Distinction between tills and other diamictons based on textural characteristics. Journal of Sedimentary Petrology, **38**: 1213-1223.

Lavkulich, L.M., and Valentine, K.W.G. 1981. The Canadian System of Soil and Soil Climate Classification. *In* The Soil Landscapes of British Columbia. *Edited by* K.W.G. Valentine, P.N. Sprout, T.E. Baker and L.M. Lavkulich. B.C. Ministry of the Environment, Victoria, pp. 59-65.

Lawson, D.E. 1979a. A comparison of the pebble orientations in ice and deposits of the Matanuska Glacier, Alaska. Journal of Geology, **87**: 629-645.

Lawson, D.E. 1979b. A sedimentological analysis of the western terminus region of the Matanuska Glacier, Alaska: U.S. Army Cold Regions Research and Engineering Laboratory Report 79-9, 122 p.

Lawson, D.E. 1982. Mobilization, movement and deposition of active subaerial sediment flows, Matanuska Glacier, Alaska. Journal of Geology, **90**: 279-300.

Leech, G.B. 1966. The Rocky Mountain Trench. Geological Survey of Canada. Paper 66-14, pp. 307-329.

Levson, V.M. 1986. Quaternary sedimentation and stratigraphy of montane glacial deposits in parts of Jasper National Park, Canada. Unpublished M.Sc. thesis, Department of Geology, Edmonton, Alberta.

Lindsay, J.F. 1968. The development of clast fabric in mudflows. Journal of Sedimentary Petrology, **38**: 1242-1253.

Lindsay, J.F. 1970. Clast fabric of till and its development. Journal of Sedimentary Petrology, **40**: 629-641.

Lineback, J.A. 1971. Pebble orientation and ice movement in south-central Illinois. *In* Till: a Symposium. *Edited by* R.P. Goldthwait. Ohio State University, Columbus, pp. 328-334.

Liverman, D.G.E. in preparation. Quaternary geology of the Grande Prairie map sheet, west-central Alberta. Ph.D. thesis, Department of Geology, University of Alberta, Edmonton, Alberta.

Lowdon, J.A., Robertson, I.M., and Blake, W., Jr. 1971. Geological Survey of Canada Radiocarbon Dates XI. Geological Survey of Canada, Paper 71-7, 70 p.

Leslie, L. 1988. Late Glacial Geology of the Finlay River Valley, British Columbia. Unpublished M.Sc. Thesis, Department of Geology, University of Alberta, Edmonton. Alberta.

Lowe, D.R. 1976. Subaqueous liquified and fluidized sediment flows and their deposits. Sedimentology, **23**: 285-308.

Lowe, D.R. 1979. Sediment gravity flows: their classification and some problems of application to natural flows and deposits. *In* Geology of Continental Slopes. *Edited by* J.L. Doyle and O.H. Pilkey. Society of Economic Paleontologists and Mineralogists, 27, Tulsa, pp. 75-82.

Lowe, D.R. 1982. Sediment gravity flows: II. Depositional models with special reference to the deposits of high-density turbidity currents. Journal of Sedimentary Petrology, **52**: 279-297.

Macdonald, D.I.M., and Jefferson, T.H. 1985. Orientation studies of waterlogged wood: a paleocurrent indicator. Journal of Sedimentary Petrology, **55**: 235-239.

Macqueen, R.W., and Thompson, R.I. 1978. Carbonate-hosted lead-zinc concentrations in northeastern British Columbia with emphasis on the Robb Lake deposit. Canadian Journal of Earth Sciences, **15**: 1737-1762.

Major, J. J., and Voight, B. 1986. Sedimentology and clast orientations of the 18 May 1980 southwest-flank lahars, Mount St. Helens, Washington. Journal of Sedimentary Petrology, **56**, pp. 691-705.

Malde, H.E. 1983. Panoramic Photographs. American Scientist, **71**: 132-140.

Mansy, J.L., and Gabrielse, H. 1978. Stratigraphy, terminology and correlation of Upper Proterozoic rocks in Omineca and Cassiar Mountains, north-central British Columbia. Geological Survey of Canada, Paper 77-19, pp. 1-17.

Marcussen, I. 1975. Distinguishing between lodgement till and flow till in Weichselian deposits. Boreas, **4**: 113-123.

Mark, D.M. 1973. Analysis of axial orientation data, including till fabrics. Geological Society of America, Bulletin, **84**: 1369-1374.

Mark, D.M. 1974. On the interpretation of till fabrics. Geology, **2**: 101-104.

Mathews, W.H. 1954. Quaternary stratigraphy and geomorphology of the Fort St. John area, northeastern British Columbia. Geological Society of America Bulletin, **65**: 1345.

Mathews, W.H. 1955. Late Pleistocene Divide of the Cordilleran Ice Sheet. Geological Society of America, Bulletin, **66**, pp. 1657.

Mathews, W.H. 1972. Quaternary Geology, Charlie Lake, British Columbia. In Report of Activities, Part A, Geological Survey of Canada. Paper 72-1A, pp. 169-170.

Mathews, W.H. 1973. Quaternary geology, Charlie Lake, British Columbia. In Report of Activities, Part A, Geological Survey of Canada. Paper 73-1A, pp. 210-211.

Mathews, W.H. 1978. Quaternary Stratigraphy and Geomorphology of Charlie Lake (94A) map-area, British Columbia. Geological Survey of Canada, Paper 76-20.

Mathews, W.H. 1980. Retreat of the Last Ice Sheets in Northeastern British Columbia and Adjacent Alberta. Geological Survey of Canada, Bulletin 331.

Mathews, W.H., and Rouse, G.E. 1963. Late Tertiary Volcanic rocks and Plant-Bearing Deposits in British Columbia. Geological Society of America, Bulletin, **74**: 55-60.

May, R.W., and Dreimanis, A. 1976. Compositional variability in tills. *In* Glacial Till. *Edited by* R.F. Legget. Royal Society of Canada, Ottawa, pp. 99-120.

May, R.W., Dreimanis, A., and Stankowski, W. 1980. Quantitative evaluation of clast fabrics within the Catfish Creek Till, Bradtville, Ontario. Canadian Journal of Earth Science, **17**: 1064-1074.

McCabe, A. M. 1986. Glaciomarine facies deposited by retreating tidewater glaciers: an example from the Late Pleistocene of Northern Ireland. Journal of Sedimentary Petrology, **56**: 880-894.

McCabe, A. M., and Dardis, G. F., and Hanvey, P. M. 1987. Sedimentation at the margins of a late Pleistocene ice-lobe terminating in shallow marine environments, Dundalk Bay, eastern Ireland. Sedimentology, **34**: 473-493.

McConnell, R.G. 1896. Report of an exploration of the Finlay and Omenica Rivers. Geological Survey of Canada, Annual Report, N.S., 7, 40 p.

McDonald, B.C., and Shilts, W.W. 1975. Interpretation of Faults in Glaciofluvial Sediments. *In* Glaciofluvial and glaciolacustrine sedimentation. *Edited by* A.V. Jopling and B.C. McDonald. S.E.P.M., Special Publication No. 23, Tulsa, Oklahoma, pp. 123-131.

McElhinny, M.W. 1973. Palaeomagnetism and plate tectonics. Cambridge University Press, Cambridge.

McKeague, J.A. (Editor) 1978. Manual on soil sampling and methods of analysis, 2nd edition. Canadian Society of Soil Science, Ottawa.

McMeeking, R. M., and Johnson, R. E. 1986. On the mechanics of surging glaciers. Journal of Glaciology, **32**: 120-132.

McPherson, J.G., Shanmugam, G., and Moiola, R.J. 1987. Fan-deltas and braid deltas: Varieties of coarse-grained deltas. Geological Society of America, Bulletin, **99**: 331-340.

McPherson, J.G., Shanmugam, G., and Moiola, R.J. 1988. Fan-deltas and braid deltas: Varieties of coarse-grained deltas: reply. Geological Society of America, Bulletin, **100**: 1309-1310.

McShea, D. W., and Raup, D. M. 1986. Completeness of the geological record. Journal of Geology, **94**: 569-574.

Metz, R. 1987. Insect traces from nonmarine ephemeral puddles. Boreas, **16**: 189-195.

Middleton, G.V., and Southard, J.B. 1984. Mechanics of Sediment Movement. S.E.P.M., Short Course No. 3, Tulsa, Oklahoma.

Miall, A.D. 1977. A review of the braided-river depositional environment. Earth Science Reviews, **13**: 1-62.

Miall, A.D. 1985. Architectural-Element Analysis: A New Method of Facies Analysis Applied to Fluvial Deposits. Earth-Science Review, **22**: 261-308.

Mills, H.H. 1977a. Basal till fabrics of modern alpine glaciers. Geological Society of America, Bulletin, **88**: 824-828.

Mills, H.H. 1977b. Textural characteristics of drift from some representative Cordilleran glaciers. Geological Society of America, Bulletin, **88**: 1135-1143.

Mills, H. H. 1984. Clast oreintation in Mount St. Helens debris-flow deposits, North Fork Toutle River, Washington. Journal of Sedimentary Petrology, **54**: 626-634.

Mills, P.C. 1983. Genesis and diagnostic value of soft-sediment deformation structures - a review. Sedimentary Geology, **35**: 83-104.

Monger, J.W.H., Souther, J.G., and Gabrielse, H. 1972. Evolution of the Canadian Cordillera: a plate-tectonic model. American Journal of Science, **272**: 577-602.

Morrow, D.W., Krouse, H.R., Ghent, E.D., Taylor, G.C., and Dawson, K.R. 1978. A hypothesis concerning the origin of barite in Devonian carbonate rocks of northeastern British Columbia. Canadian Journal of Earth Sciences,**15**: 1391-1406.

Munsell Soil Color Charts 1975. Munsell Color. Kollmorgen Corporation, Maryland.

Nardin, T.R., Hein, F.J., Gorsline, D.S., and Edwards, B.D. 1979. A review of mass movement processes, sediment and acoustic characteristics, and contrasts in slope and base-of-slope systems versus canyon-fan-basin systems. SEPM Special Publication, 27, pp. 61-73.

Nickling, W.G. 1983. Grain-size characteristics of sediment transported during dust storms. Journal of Sedimentary Petrology, **53**: 1011-1024.

Nielsen, P.E. 1982. Till fabric reoriented by subglacial shear. Geologiska Föreningens i Stockholm Förhandlingar, **103**: 383-387.

North American Commission on Stratigraphic Nomenclature 1983. North American Stratigraphic Code. American Association of Petroleum Geologists, Bulletin, **67**: 841-875.

Perttunen, M., and Hirvas, H. 1982. An attempt to use the roundness of quartz grains for till stratigraphy. Geological Society of Finland, Bulletin, **54**: 25-33.

Pettijohn, W.A., and Lemke, R.W. 1971. Unarmored till balls in unusual abundance near Minot, North Dakota. *In* Till a Symposium. *Edited by* R.P. Goldthwait. Ohio State University, pp. 383-394.

Pierson, T.C. 1981. Dominant particle support mechanisms in debris flows at Mt Thomas, New Zealand, and implications for flow mobility. Sedimentology, **28**: 49-60.

Postma, G. 1986. Classification for sediment gravity-flow deposits based on flow conditions during sedimentation. Geology, **14**: 291-294.

Powell, R.D. 1981. A model for sedimentation by tidewater glaciers. Annals of Glaciology, **2**: 129-134.

Powell, R.D. 1984. Glacimarine processes and inductive lithofacies modelling of ice shelf and tidewater glacier sediments based on Quaternary examples. Marine Geology, **57**: 1-52.

Powers, M. 1953. A new roundness scale for sedimentary particles. Journal of Sedimentary Petrology, **23**: 117-119.

Rampton, V.N. 1987. Late Wisconsin deglaciation and Holocene river evolution near Fort Nelson, northeastern British Columbia. Canadian Journal of Earth Sciences, **24**: 188-191.

Ramsden, J., and Westgate, J.A. 1971. Evidence for reorientation of a till fabric in the Edmonton area, Alberta. *In* Till a Symposium. *Edited by* R.P. Goldthwait. Ohio State University Press, pp. 335-344.

Rappol, M. 1984. Till in southeast Drente and the origin of the Hondsrug Complex, The Netherlands. Eiszeitalter u. Gegenwart, **34**: 7-27.

Rappol, M. 1985. Clast-fabric strength in tills and debris flows compared for different environments. Geologie en Mijnbouw, **64**: 327-332.

Reading, H.G. 1978. Facies. *In* Sedimentary Environments and Facies. *Edited by* R.G. Reading. Elsevier, New York, pp. 4-14.

Reimchen, T.H.F., and Rutter, N.W. 1972. Quaternary Geology, Dawson Creek, British Columbia (93 P). In Report of Activities, Part A, Geological Survey of Canada. pp. 176-177.

Reineck, H.E., and Singh, I.B. 1980. Depositional Sedimentary Environments. Springer-Verlag, New York.

Rich, E.E. (Editor) 1955. A Journal of A Voyage From Rocky Mountain Portage in Peace River To the Sources on Finlays Branch and North West Ward in Summer 1824, by Samuel Black. The Hudson's Bay Record Society, London.

Rouse, G.E., and Mathews, W.H. 1979. Tertiary geology and palynology of the Quesnel area, British Columbia. Bulletin of Canadian Petroleum Geology, **27**: 418-445.

Rowe, J.S. 1977. Forest Regions of Canada. Minister of Supply and Services, Ottawa.

Royse, C.F., Jr. 1968. Recognition of fluvial environments by particle-size characteristics. Journal of Sedimentary Petrology, **38**: 1171-1178.

Rust, B.R. 1972. Pebble orientation in fluvial sediments. Journal of Sedimentary Petrology, **42**: 384-388.

Rust, B.R. 1978. Depositional models for braided alluvium. *In* Fluvial Sedimentology. *Edited by* A.D. Miall. Canadian Society of Petroleum Geologists, Memoir 5, Calgary, pp. 605-625.

Rutter, N.W. 1968. Surficial geology of the Peace River Dam and reservoir area, British Columbia. Current Research, Part A, Report of Activities, Geological Survey of Canada, Paper 68-1A, pp. 182-183.

Rutter, N.W. 1976. Multiple glaciation in the Canadian Rocky Mountains with special emphasis on northeastern British Columbia. *In* Quaternary Stratigraphy of North America. *Edited by* W.C. Mahaney. Dowden, Hutchinson and Ross, Stroudsburg, Pennsylvania, pp. 409-440.

Rutter, N.W. 1977. Multiple Glaciation in the area of Williston Lake, British Columbia. Geological Survey of Canada, Bulletin 273, 31 p.

Rutter, N.W. 1981. Relationship between Late Pleistocene Laurentide and Cordilleran glaciations, Canada. *In* Quaternary Glaciations in the Northern Hemisphere. *Edited by* V. Sibrava and F.W. Shotton. Geological Survey, IGCP Project 73/1/24, Report No. 6, Prague, pp. 205-218.

Rutter, N.W. 1984. Pleistocene history of the western Canadian ice-free corridor. *In* Quaternary Stratigraphy of Canada- A Canadian Contribution to IGCP Project 24. *Edited by* R.J. Fulton. Geological Survey of Canada, Paper 84-10, Ottawa, pp. 49-56.

Rutter, N.W., and Crawford, R.J. 1984. Utilizing wood in amino acid dating. *In* Quaternary Dating Methods. *Edited by* W.C. Mahaney. Elsevier Science Publishers, Amsterdam, pp. 195-209.

Rutter, N.W., Geist, V., and Shackleton, D.M. 1972. A Bighorn Sheep skull 9280 years old from British Columbia. Journal of Mammalogy, **53**: 641-644.

Rutter, N.W., and Taylor, G.C. 1968. Bedrock geology along Ingenika and Finlay Rivers, Peace River Reservoir area, British Columbia. Geological Survey of Canada, Paper 68-10, 9 p.

Rutter, N.W., and Vlahos, C.K. 1988. Amino acid racemization kinetics in wood; Applications to geochronology and geothermometry. Geological Society of America, Special Paper 227. (in press)

Sadler, P.M. 1981. Sediment accumulation rates and the completeness of stratigraphic sections. Journal of Geology, **89**: 569-584.

Selwyn, A.R.C. 1877. Report on exploration in British Columbia in 1875. In Report of Progress for 1875-76, Geological Survey of Canada. pp. 28-86.

Shultz, A.W. 1984. Subaerial debris-flow deposition in the Upper Paleozoic Cutler Formation, western Colorado. Journal of Sedimentary Petrology, **54**: 759-772.

Shaw, J. 1975. Sedimentay Successions in Pleistocene Ice-Marginal Lakes. *In* Glaciofluvial and Glaciolacustrine Sedimentation. *Edited by* A.V. Jopling and B.C. McDonald. S.E.P.M., Special Publication No. 23, Tulsa, Oklahoma, pp. 281-303.

Shaw, J. 1979. Genesis of the Sveg tills and Rogen moraines of central Sweden: a model of basal melt-out. Boreas, **8**: 409-426.

Shaw, J. 1982. Melt-out till in the Edmonton area, Alberta, Canada. Canadian Journal of Earth Sciences, **19**: 1548-1569.

Shaw, J. 1987. Glacial sedimentary processes and enviromental reconstruction based on lithofacies. Sedimentology, **34**: 103-116.

Shepard, F. 1954. Nomenclature based on sand-silt-clay ratios. Journal of Sedimentary Petrology, **24**: 151-158.

Shilts, W.W. 1981. Surficial Geology of the Lac Mégantic Area, Québec. Geological Survey of Canada, Memoir 397, 102 p.

Singer, M.J., and Janitsky, P. (Editors) 1986. Field and Laboratory Procedures Used in a Soil Chronosequence Study. United States Geological Survey, Denver, Colorado.

Slaymaker, O., and McPherson, H.J. 1977. An overview of geomorphic processes in the Canadian Cordillera. Zeitschrift fur Geomorphologie, **21**: 169-186.

Slingerland, R.L., and Williams, E.G. 1979. Paleocurrent analysis in light of trough cross-stratification geometry. Journal of Geology, **87**: 724-732.

Spurling, B.E. (Editor) 1980. The Site C heritage resource inventory and assessment: Final Report. British Columbia Power and Hydro Power Authority, Department of Archaeology, Simon Fraser University, Burnaby, British Columbia.

Steiger, J.R., and Holowaychuk, N. 1971. Particle-size and carbonate analysis of glacial till and lacustrine deposits in western Ohio. *In* Till a Symposium. *Edited by* R.P. Goldthwait. Ohio State University Press, pp. 275-289.

Szabo, J.P., and Angle, M.P. 1983. The influence of local bedrock: an important consideration in the interpretation of textural and mineralogic analyses of till. Journal of Sedimentary Petrology, **53**: 981-989.

Tarling, D.H. 1971. Principles and Applications of Palaeomagnetism. Chapman and Hall, London.

Thomas, G.S.P. 1984. A late Devensian glaciolacustrine fan-delta at Rhosesmor, Clwyd, North Wales. Geological Journal, **19**, pp. 125-141.

Tipper, H.W. 1971a. Glacial geomorphology and Pleistocene history of central British Columbia. Geological Survey of Canada, Bulletin 196, 89 p.

Tipper, H.W. 1971b. Multiple Glaciation in central British Columbia. Canadian Journal of Earth Sciences, **8**: 743-752.

Tipper, H.W., Campbell, R.B., Taylor, G.C., and Stott, D.F. 1979. Map 1424A Parsnip River British Columbia Sheet 93. Geological Survey of Canada, Ottawa.

Tipper, H.W., Woodsworth, G.J., and Gabrielse, H. 1981. Tectonic Assemblage Map of the Canadian Cordillera and Adjacent Parts. Geological Survey of Canada, Map 150EA, Ottawa.

Tipper, J. C. 1987. On the directional nature of stratigraphic correlation. Geological Magazine, **124**: 149-155.

Tyrrell, J.B. 1919. Was there a "Cordilleran glacier" in British Columbia? Journal of Geology, **27**: 55-60.

Valentine, K.W.G., Fladmark, K.R., and Spurling, B.E. 1980. The description, chronology and correlation of buried soils and cultural layers in a terrace section, Peace River Valley, British Columbia. Canadian Journal of Soil Science, **60**: 185-197.

Van Loon, A.J. 1983. The stress systems in mudflows during deposition, as revealed by the fabric of some Carboniferous pebbly mudstones in Spain. Geologie en Mijnbouw, **62**: 493-498.

Van Loon, A.J., Brodzikowski, K., and Gotowala, R. 1985. Kink structures in unconsolidated fine-grained sediments. Sedimentary Geology, **41**: 283-300.

Visher, G. S. 1969. Grain size distributions and depositional processes. Journal of Sedimentary Petrology, **39**: 1074-1106.

Visser, J.N.J. 1983. The problems of recognizing ancient subaqueous debris flow deposits in glacial sequences. Transactions, Geological Society of South Africa, **86**: 127-135.

Visser, J.N.J., Hall, K.J., and Loock, J.C. 1986. The application of stone counts in the glacigene Permo-Carboniferous Dwyka Formation, South Africa. Sedimentary Geology, **46**: 197-212.

Vivian, R., and Bocquet, G. 1973. Subglacial cavitation phenomena under the Glacier d'Argentière, Mont Blanc, France. Journal of Glaciology, **12**: 439-451.

von Brunn, V., and Gravenor, C.P. 1983. A model for Late Dwyka Glaciomarine sedimentation in the eastern Karoo Basin. Geological Society of South Africa, Transactions, **86**: 199-209.

Vørren, T.O. 1977. Grain-size distribution and grain-size parameters of different till types on Hardangervidda, south Norway. Boreas, **6**: 219-227.

Walker, R.G. 1975. Generalized facies models for resedimented conglomerates of turbidite association. Geological Society of America, Bulletin, **86**: 737-748.

Walker, R.G. 1984. General Introduction: Facies, Facies Sequences and Facies Models. *In* Facies Models. *Edited by* R.G. Walker. Geological Association of Canada, Geoscience Canada, Reprint Series **1**, pp. 1-9.

Wentworth, C.K. 1936. An analysis of the shapes of glacial cobbles. Journal of Sedimentary Petrology, **6**: 85-96.

White, J.M., and Mathewes, R.W. 1982. Holocene vegetation and climatic change in the Peace River district, Canada. Canadian Journal of Earth Sciences, **19**, pp. 555-570.

White, J. M., and Mathewes, R. W. 1986. Postglacial vegetation and climatic change in the Upper Peace River district, Alberta. Canadian Journal of Botany, **64**: 2305-2318.

Williams, G. P. 1966. Particle roundness and surface texture effects on fall velocity. Journal of Sedimentary Petrology, **36**: 255-259.

Woodcock, N.H. 1977. Specification of fabric shapes using an eigenvalue method. Geological Society of America, Bulletin, **88**: 1231-1236.

Woodcock, N.H., and Naylor, M.A. 1983. Randomness testing in three-dimensional orientation data. Journal of Structural Geology, **5**: 539-548.

Young, G.K., and Alley, N.F. 1981. The northern and central Plateaus and Mountains. *In* The Soil Landscapes of British Columbia. *Edited by* K.W.G. Valentine, P.N. Sprout, T.E. Baker and L.M. Lavkulich. B.C. Ministry of the Environment, Victoria, pp. 149-160.

Young, J.A.T. 1969. Variations in till macrofabric over very short distances. Geological Society of America, Bulletin, **80**: 2343-2352.

Zingg, T. 1935. Beitrage zur Schatteranalyse. Schweizerische Mineralogische und Petrographische Mitteilungen, **15**: 39-140.

Appendix 1. Summarized pebble lithology data for samples from the northern Rocky Mountain Trench. Each sample provides frequency of igneous, metamorphic and sedimentary clasts. Sedimentary clasts also summarized according to carbonate and scilicic lastic proportions.

SAMPLE NO.	IGN	META	SED	CARBON	CLASTICS	TOTAL
PTB84-5	1	20	29	8	21	50
PTB84-7	0	15	10	3	7	25
PTB84-8	1	12	12	8	4	25
PTB84-27	7	48	45	0	45	100
PTB84-29	30	36	34	0	34	100
PTB84-34	5	42	53	0	53	100
PTB84-35	3	35	62	0	62	100
PTB84-39	0	22	9	3	6	31
PTB84-42	10	32	58	0	58	100
PTB84-48	4	26	20	6	14	50
PTB84-56	1	2	47	22	25	50
PTB84-57	2	7	41	23	18	50
PTB84-59	6	13	31	12	19	50
PTB84-60	5	8	37	17	20	50
PTB84-68	5	11	34	16	18	50
PTB84-69	9	20	14	0	14	43
PTB84-71	0	12	38	14	24	50
PTB84-73	7	10	33	15	18	50
PTB84-75	0	17	33	11	22	50
PTB84-79	7	11	32	12	20	50
PTB84-84	17	13	20	8	12	50
PTB84-85	1	18	31	21	10	50
PTB84-87	9	17	24	16	8	50
PTB84-90	0	12	38	22	16	50
PTB84-94	4	15	31	18	13	50
PTB84-97	14	12	24	9	15	50
PTB84-99	0	17	33	18	15	50
PTB84-102	7	15	28	14	14	50
PTB84-105	3	14	33	19	14	50
PTB84-108	7	13	30	22	8	50
PTB84-111	0	18	32	20	12	50
PTB84-120	9	17	24	9	15	50
PTB84-122	5	17	28	19	9	50
PTB84-125	0	12	38	27	11	50
PTB84-128	10	14	26	15	11	50
PTB84-131	7	11	32	18	14	50
PTB84-134	16	15	19	7	12	50
PTB84-135	6	14	30	19	11	50
PTB84-142	18	20	12	7	5	50
PTB84-147	5	16	29	24	5	50
PTB84-150	6	12	32	21	11	50
PTB84-159	4	30	16	11	5	50
PTB84-162	6	17	27	15	12	50
PTB84-164	5	18	27	21	6	50
PTB84-167	11	13	26	18	8	50

SAMPLE NO.	IGN	META	SED	CARBON	CLASTICS	TOTAL
PTB84-171	1	8	41	37	4	50
PTB84-173	7	12	31	16	15	50
PTB84-181	5	16	29	20	9	50
PTB84-185	9	10	31	24	7	50
PTB84-193	1	12	37	33	4	50
PTB84-194	6	4	40	35	5	50
PTB84-202	2	24	24	5	19	50
PTB84-215	4	11	35	22	13	50
PTB84-228	20	11	19	11	8	50
PTB84-230	12	16	22	12	10	50
PTB84-232	0	14	36	30	6	50
PTB84-242	0	6	44	32	12	50
PTB84-244	12	12	26	14	12	50
PTB84-261	11	18	21	8	13	50
PTB84-263	8	23	19	12	7	50
PTB84-286	1	12	37	33	4	50
PTB84-312	0	8	42	34	8	50
PTB84-355	0	3	47	43	4	50
PTB84-358	0	8	42	33	9	50
PTB84-359	2	16	32	29	3	50
PTB84-360	0	3	47	43	4	50
PTB84-361	8	12	30	25	5	50
PTB84-365	8	6	36	31	5	50
PTB84-367	0	9	41	37	4	50
PTB84-369	0	13	37	33	4	50
PTB84-372	0	13	37	34	3	50
PTB84-373	1	12	37	33	4	50
PTB84-374	8	19	23	14	9	50
PTB84-376	0	38	12	3	9	50
PTB84-378	4	12	34	24	10	50
PTB84-384	8	14	28	14	14	50
PTB84-387	13	9	28	15	13	50
PTB84-388	6	14	30	25	5	50
PTB84-420	7	25	18	10	8	50
PTB84-422	13	20	17	9	8	50
PTB84-424	5	26	19	11	8	50
PTB85-1	6	24	20	4	16	50
PTB85-3	8	25	17	6	11	50
PTB85-5	3	31	16	5	11	50
PTB85-12	7	32	11	2	9	50
PTB85-15	1	25	24	9	15	50
PTB85-21	1	27	22	12	10	50
PTB85-23	1	28	21	8	13	50
PTB85-40	5	23	22	10	12	50
PTB85-48	12	17	21	9	12	50
PTB85-59	0	33	17	11	6	50
PTB85-60	0	25	25	18	7	50
PTB85-61	4	34	12	5	7	50
PTB85-80	8	23	19	7	12	50

REPLICATE NO.	IGN	META	SED	CARBON	CLASTICS	TOTAL
PTB84-27	0	9	41	30	11	50
PTB84-29	7	16	27	13	14	50
PTB84-34	0	9	41	27	14	50
PTB84-35	1	7	42	30	12	50
PTB84-42	5	14	31	18	13	50
PTB84-48	2	9	28	16	12	39
PTB84-56	1	5	44	23	21	50
PTB84-57	3	22	25	13	12	50
PTB84-59	8	21	21	12	9	50
PTB84-60	8	15	27	17	10	50
PTB84-68	3	23	24	17	7	50
PTB84-71	0	9	41	25	16	50
PTB84-73	5	19	26	16	10	50
PTB84-75	0	31	19	8	11	50
PTB84-79	4	24	22	11	11	50
PTB84-84	20	21	9	6	3	50
PTB84-378	14	4	32	19	13	50
PTB84-384	14	17	19	11	8	50

Appendix 2. Class specific percentages of all phi values for textural analyses data for bulk samples from the northern Rocky Mountain Trench, B.C.

SAMPLE	0	1	2	3	4	5	6	7	8	9	10	>10
PTB84-4	2	3	8	11	14	27	17	6	3	3	3	3
PTB84-9	23	18	13	6	1	0	0	0	0	0	0	39
PTB84-51	9	8	7	9	2	3	7	8	5	9	11	22
PTB84-52	7	8	8	8	5	10	5	10	5	5	3	26
PTB84-53	10	9	8	8	3	5	5	7	7	7	7	24
PTB84-54	11	10	7	10	4	3	5	7	5	9	6	23
PTB84-55	12	10	6	8	2	6	5	9	5	8	9	20
PTB84-61	6	5	5	9	3	5	9	9	6	10	10	23
PTB84-62	5	3	5	10	4	6	9	9	5	11	10	23
PTB84-63	5	5	6	9	3	7	7	8	7	9	10	24
PTB84-64	4	4	6	9	9	9	7	10	5	6	4	27
PTB84-65	5	5	5	9	5	6	5	10	6	10	9	25
PTB84-112	2	3	3	3	0	3	11	16	13	7	6	33
PTB84-113	3	2	3	3	0	0	8	15	15	9	8	34
PTB84-114	0	1	0	1	10	18	25	14	6	3	3	19
PTB84-115	2	4	2	5	1	5	11	13	10	11	9	27
PTB84-116	2	1	2	3	0	3	12	17	13	10	6	31
PTB84-136	7	7	6	6	1	2	8	11	9	8	9	26
PTB84-137	4	3	4	3	1	0	3	14	13	11	10	34
PTB84-138	6	4	4	5	1	3	10	14	9	7	4	33
PTB84-139	7	7	7	5	2	0	6	12	10	10	3	31
PTB84-140	6	1	5	4	2	6	8	8	15	8	1	36
PTB84-151	8	9	8	8	1	2	5	12	7	7	6	27
PTB84-152	10	10	8	8	7	6	6	11	3	4	2	25
PTB84-153	10	10	9	8	6	7	6	9	5	3	1	26
PTB84-154	9	10	10	11	4	4	7	10	4	4	1	26
PTB84-155	10	10	10	10	6	4	8	8	6	2	1	25
PTB84-156	7	9	9	9	3	6	6	10	7	3	2	29
PTB84-169	7	8	8	8	4	5	10	11	7	6	6	20
PTB84-186	11	14	10	9	10	9	7	9	5	6	3	7
PTB84-187	1	4	4	5	9	19	24	15	8	3	3	5
PTB84-188	4	4	5	4	15	12	26	18	7	1	1	3
PTB84-189	1	5	6	7	13	16	21	14	7	2	3	5
PTB84-190	0	4	2	6	16	23	17	11	7	4	3	7
PTB84-191	0	1	3	2	4	8	14	15	16	7	10	20
PTB84-192	0	2	2	2	12	20	15	11	11	8	5	12
PTB84-201	0	0	1	7	39	27	12	6	2	1	1	4
PTB84-203	4	3	6	7	6	10	10	10	10	10	7	17
PTB84-204	4	4	7	8	7	9	8	10	10	7	8	18
PTB84-205	4	3	7	9	8	11	11	9	8	7	7	16
PTB84-206	3	5	7	8	9	10	9	10	9	6	7	17
PTB84-207	4	3	5	5	7	7	10	10	10	8	7	24
PTB84-208	3	4	4	6	5	6	11	10	12	8	8	23
PTB84-209	3	4	8	8	7	8	9	8	9	7	9	20
PTB84-210	5	5	8	7	7	8	10	7	10	8	7	18
PTB84-211	4	6	7	8	8	7	9	9	8	8	8	18
PTB84-212	5	6	7	7	8	9	7	9	6	8	6	22
PTB84-218	0	1	1	17	48	17	2	5	3	1	1	4

SAMPLE	0	1	2	3	4	5	6	7	8	9	10	>10
PTB84-219	0	1	1	11	51	22	5	2	2	1	1	3
PTB84-220	0	1	1	11	38	33	4	5	0	2	1	4
PTB84-221	0	0	1	7	38	26	14	5	2	2	0	5
PTB84-222	0	1	0	17	36	29	6	2	3	0	1	5
PTB84-223	0	1	1	7	25	36	13	4	3	1	2	7
PTB84-224	0	1	1	11	27	37	11	4	3	0	1	4
PTB84-236	0	0	0	1	1	2	3	9	19	15	14	36
PTB84-237	0	0	0	0	0	0	1	9	17	20	14	39
PTB84-238	0	0	0	0	0	0	0	3	18	22	15	42
PTB84-239	0	0	0	0	0	0	1	1	12	21	20	45
PTB84-240	0	0	0	0	0	0	1	9	19	17	16	38
PTB84-241	0	0	0	0	2	1	2	6	18	17	15	39
PTB84-264	10	7	10	9	7	6	9	9	7	5	4	17
PTB84-265	8	10	10	11	9	9	8	8	6	15	3	3
PTB84-266	5	3	5	4	4	6	11	11	13	9	9	20
PTB84-267	5	6	6	7	6	7	11	11	10	8	7	16
PTB84-268	10	11	11	8	7	9	6	8	7	5	4	14
PTB84-269	0	3	3	3	7	5	8	6	13	14	8	30
PTB84-270	0	1	0	1	6	7	8	12	16	12	10	27
PTB84-271	0	1	1	1	1	4	5	12	17	18	10	30
PTB84-272	0	1	1	1	2	6	8	14	12	15	9	31
PTB84-273	0	1	1	1	2	6	4	17	16	12	11	29
PTB84-274	0	0	0	0	0	0	0	12	20	18	11	39
PTB84-275	0	1	1	1	3	0	10	14	15	13	9	33
PTB84-276	0	0	0	3	2	9	18	10	23	16	13	6
PTB84-277	0	2	4	5	8	20	21	11	8	6	5	10
PTB84-278	0	0	1	1	14	32	17	11	7	3	2	12
PTB84-279	0	0	3	8	24	18	18	10	4	5	1	9
PTB84-280	0	2	3	3	5	18	25	12	9	6	4	13
PTB84-281	0	0	0	3	26	35	18	6	4	1	3	4
PTB84-282	0	0	1	11	41	28	8	3	3	2	1	2
PTB84-283	0	0	0	3	43	32	8	5	2	2	1	4
PTB84-284	0	1	3	11	19	25	17	10	5	2	2	5
PTB84-285	9	9	6	12	7	5	5	9	8	5	3	22
PTB84-297	3	7	11	14	18	17	12	5	3	2	3	5
PTB84-298	3	9	11	13	15	15	13	6	3	4	2	6
PTB84-299	1	3	7	9	5	31	21	8	1	5	1	8
PTB84-300	1	3	8	8	11	21	16	9	6	7	3	7
PTB84-301	0	2	2	7	9	12	28	15	9	7	3	6
PTB84-302	1	2	1	9	12	16	15	10	12	8	5	9
PTB84-303	8	6	9	8	5	5	5	9	7	7	4	27
PTB84-304	8	7	8	9	8	8	6	6	7	8	2	23
PTB84-305	6	7	7	8	5	2	9	9	8	6	6	27
PTB84-306	2	2	3	4	5	9	7	9	8	9	8	34
PTB84-307	1	2	4	4	1	2	11	11	12	10	4	38
PTB84-308	2	2	4	2	2	19	9	10	10	10	8	22
PTB84-309	1	2	1	3	8	12	8	10	9	10	9	27
PTB84-310	3	4	4	3	3	4	4	7	8	13	13	34
PTB84-311	7	8	8	10	5	5	3	12	8	7	3	24
PTB84-313	0	1	1	14	36	24	10	3	1	1	2	7
PTB84-314	3	3	3	3	8	12	18	10	8	8	4	20
PTB84-315	4	4	4	4	10	14	14	11	7	7	5	16

SAMPLE	0	1	2	3	4	5	6	7	8	9	10	>10
PTB84-316	6	4	4	7	5	8	14	12	10	8	4	18
PTB84-317	2	2	2	7	15	21	16	8	6	4	3	14
PTB84-318	3	4	6	8	9	10	12	9	9	6	16	8
PTB84-319	6	8	8	12	14	12	10	6	5	3	4	12
PTB84-320	5	6	5	9	13	13	11	10	8	3	3	14
PTB84-321	5	7	7	9	12	11	14	8	5	5	3	14
PTB84-324	11	11	7	8	6	7	8	10	6	4	5	17
PTB84-325	11	7	6	8	4	6	8	10	8	4	7	21
PTB84-326	13	11	8	5	4	5	10	9	8	8	4	15
PTB84-327	10	10	6	7	2	4	7	10	9	7	5	23
PTB84-328	11	9	6	8	1	5	6	13	8	6	7	20
PTB84-329	11	9	7	6	2	2	8	12	9	8	6	20
PTB84-330	4	8	10	8	5	6	9	11	11	9	6	13
PTB84-331	11	12	10	6	6	5	7	10	7	8	2	16
PTB84-333	11	12	9	8	7	8	11	10	8	4	3	9
PTB84-334	7	9	10	14	15	10	9	8	3	3	1	11
PTB84-335	8	11	11	11	9	5	10	7	9	5	2	12
PTB84-337	0	0	0	1	2	8	11	14	12	14	12	26
PTB84-338	0	1	2	3	4	3	39	21	10	5	3	9
PTB84-339	0	2	4	4	3	14	29	20	11	4	3	6
PTB84-340	0	2	2	3	3	10	30	23	12	4	3	8
PTB84-341	0	2	1	1	5	11	25	26	13	5	3	8
PTB84-342	0	2	2	2	3	12	29	24	13	4	1	8
PTB84-343	0	3	3	4	3	9	28	24	14	3	3	6
PTB84-344	0	2	3	4	3	12	32	23	11	3	2	5
PTB84-346	0	0	0	6	30	33	15	5	3	2	1	5
PTB84-347	0	0	0	2	15	41	21	7	5	2	2	5
PTB84-348	0	0	0	0	1	1	2	10	20	21	14	31
PTB84-349	0	2	2	1	1	2	7	15	15	16	12	27
PTB84-350	0	1	1	1	1	1	3	10	21	18	14	29
PTB84-351	11	8	10	11	6	9	10	10	3	4	4	14
PTB84-352	6	9	11	12	10	8	6	8	7	5	4	14
PTB84-353	5	9	8	9	11	9	9	8	7	5	5	15
PTB84-354	6	4	3	4	2	8	13	13	11	7	5	24
PTB84-357	0	2	3	4	6	28	28	16	4	3	1	5
PTB84-362	7	6	8	7	2	4	7	11	8	7	8	25
PTB84-363	9	8	7	8	2	2	7	11	8	8	6	24
PTB84-370	0	2	2	2	3	7	13	13	15	8	9	26
PTB84-375	2	6	12	20	16	13	8	9	5	2	1	6
PTB84-379	4	4	5	6	4	6	6	10	8	9	7	31
PTB84-381	0	0	0	0	0	1	10	18	18	15	12	26
PTB84-382	4	6	8	9	6	7	7	7	7	8	6	25
PTB84-389	8	8	8	10	8	9	5	10	7	6	2	19
PTB84-390	0	0	0	0	2	15	26	30	11	5	3	8
PTB84-391	0	0	0	0	3	8	31	22	14	6	5	11
PTB84-394	12	11	8	4	2	3	8	8	11	6	7	20
PTB84-395	5	7	7	6	5	5	7	12	10	9	4	23
PTB84-396	13	9	7	7	8	7	8	7	9	8	6	11
PTB84-397	7	10	9	4	5	8	8	10	10	8	6	15
PTB84-398	10	9	6	5	5	9	8	9	10	7	7	15
PTB84-399	12	15	13	10	6	5	5	7	6	4	2	15
PTB84-400	2	3	1	7	13	10	15	13	12	7	6	11

SAMPLE	0	1	2	3	4	5	6	7	8	9	10	>10
PTB84-401	6	3	5	6	9	10	8	8	11	8	8	18
PTB84-402	3	4	3	10	12	12	11	10	8	8	5	14
PTB84-403	5	6	6	6	7	8	9	9	9	10	7	18
PTB84-404	7	6	7	6	10	9	7	9	9	7	4	19
PTB84-405	6	5	6	5	5	8	8	12	10	9	6	20
PTB84-406	3	3	5	8	6	9	13	14	12	11	4	12
PTB84-407	9	4	6	5	5	5	10	12	12	10	8	14
PTB84-408	5	4	5	2	1	0	7	14	13	12	8	29
PTB84-409	5	3	3	3	4	5	14	14	15	7	8	19
PTB84-410	7	8	7	6	4	5	7	10	10	8	6	22
PTB84-411	13	14	15	12	4	5	4	6	5	5	3	14
PTB84-412	5	6	7	6	5	6	6	10	12	9	6	22
PTB84-413	6	6	11	9	6	4	7	10	6	10	6	19
PTB84-414	5	6	5	12	4	5	5	10	9	8	5	26
PTB84-415	4	4	5	7	3	4	7	10	9	10	9	28
PTB84-416	4	6	8	6	7	7	6	10	7	9	7	23
PTB84-417	5	11	19	10	8	7	6	8	8	6	3	9
PTB84-418	5	6	9	10	8	9	7	9	10	5	7	15
PTB85-1	13	13	20	7	20	18	2	0	0	0	1	6
PTB85-4	7	7	8	1	16	15	14	11	8	3	2	8
PTB85-9	4	3	2	3	3	4	7	13	10	13	10	28
PTB85-10	4	2	4	1	8	7	6	10	10	11	8	29
PTB85-13	0	0	5	11	15	33	18	5	1	4	1	7
PTB85-16	12	12	17	2	14	4	6	7	8	3	3	12
PTB85-17	9	7	9	7	7	6	9	6	10	8	5	17
PTB85-18	5	7	11	10	8	10	6	9	5	8	5	16
PTB85-20	5	5	7	9	10	14	9	6	10	5	6	14
PTB85-22	6	6	6	4	15	11	5	7	10	7	5	18
PTB85-24	4	3	5	1	13	7	8	10	11	9	9	20
PTB85-25	4	4	5	6	5	7	9	9	12	9	8	22
PTB85-26	5	5	5	6	5	4	8	11	11	10	7	23
PTB85-27	6	5	5	5	4	6	8	10	11	10	7	23
PTB85-28	9	7	6	1	11	5	8	10	9	8	6	20
PTB85-29	7	7	9	14	10	9	10	8	8	4	3	11
PTB85-30	6	7	8	10	9	6	12	8	10	5	6	13
PTB85-31	6	5	5	7	9	8	9	12	8	6	7	18
PTB85-32	7	6	6	7	12	13	7	6	9	8	5	14
PTB85-33	8	7	8	10	10	9	9	9	9	5	2	14
PTB85-34	5	7	12	5	16	7	8	9	8	6	5	12
PTB85-35	7	8	8	5	11	4	9	12	8	7	4	17
PTB85-36	8	6	8	7	7	8	12	9	10	5	3	17
PTB85-37	7	5	6	7	8	5	14	11	7	8	6	16
PTB85-38	5	5	9	1	15	5	9	10	6	10	5	20
PTB85-42	5	6	7	1	11	5	7	10	10	8	8	22
PTB85-43	5	6	8	6	10	6	9	7	8	9	5	21
PTB85-44	6	6	7	6	8	5	7	7	13	5	7	23
PTB85-47	7	6	7	3	9	3	6	12	8	7	7	25
PTB85-49	9	11	11	12	7	5	7	9	6	4	3	16
PTB85-50	7	6	7	3	13	8	9	10	7	6	6	18
PTB85-53	6	4	4	5	6	7	8	10	10	10	7	23
PTB85-54	3	4	4	5	8	8	8	10	11	8	8	23
PTB85-56	7	4	5	3	3	3	12	12	10	10	7	24

SAMPLE	0	1	2	3	4	5	6	7	8	9	10	>10
PTB85-57	9	6	5	5	5	4	9	7	12	8	8	22
PTB85-63	4	5	7	6	3	3	8	10	10	12	8	24
PTB85-64	4	4	5	6	4	5	8	13	10	10	6	25
PTB85-65	6	5	5	2	12	10	5	7	10	10	8	20
PTB85-66	4	4	5	3	9	9	10	8	11	9	6	22
PTB85-67	5	5	5	7	7	7	7	9	9	13	8	18
PTB85-68	5	4	6	6	6	9	7	10	11	9	7	20
PTB85-69	5	5	5	7	9	5	7	11	10	9	7	20
PTB85-70	5	4	4	6	9	10	6	8	10	9	6	23
PTB85-71	6	6	8	8	7	8	6	8	9	9	5	20
PTB85-72	5	6	7	5	10	12	4	9	10	9	5	18
PTB85-73	6	5	8	4	8	7	7	8	11	11	8	17
PTB85-74	5	6	7	5	8	10	10	12	13	7	4	13
PTB85-75	5	8	12	10	6	8	9	10	10	6	4	12
PTB85-76	5	6	10	4	12	11	10	11	9	6	4	12
PTB85-77	5	6	11	4	14	8	10	12	8	7	5	10
PTB85-78	7	8	14	1	17	10	8	8	10	5	4	8
PTB85-79	3	4	6	6	8	6	6	11	10	9	7	24
PTB84-245	11	5	6	6	8	9	9	8	8	8	5	17
PTB84-246	10	2	5	7	8	10	10	10	9	8	6	15
PTB84-247	6	3	5	6	9	7	10	10	9	9	7	19
PTB84-248	9	2	6	6	7	9	9	10	8	8	8	18
PTB84-249	6	3	4	6	7	7	9	9	9	8	8	24
PTB84-250	6	3	4	5	6	7	9	8	8	9	8	27
PTB84-251	9	2	4	6	8	7	8	8	9	9	6	24
PTB84-252	11	4	7	6	8	9	9	9	8	7	6	16
PTB84-253	10	2	5	5	6	8	6	8	8	7	7	28
PTB84-254	8	3	5	6	7	9	8	10	8	8	8	20
PTB84-255	9	4	5	7	8	9	9	9	10	7	7	16
PTB84-256	10	6	6	6	8	8	8	8	8	8	7	17
PTB84-257	7	3	5	7	9	10	11	10	10	8	7	13
PTB84-258	7	3	5	7	9	9	11	11	9	9	6	14
PTB84-259	6	3	6	7	7	10	1	10	10	18	7	15
PTB84-260	7	4	6	7	9	10	10	11	9	9	6	12

Appendix 3. Cumulative histograms for bulk samples analyzed by hydrometer from northeastern British Columbia. Raw data presented in Appendix 2.

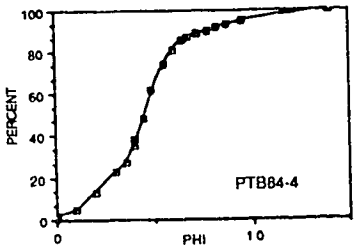
PERCENT
PTB84-4
PHI

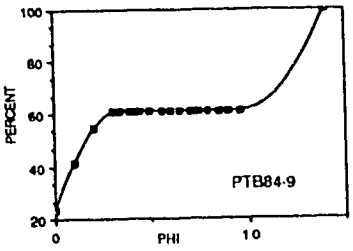
PERCENT
PTB84-9
PHI

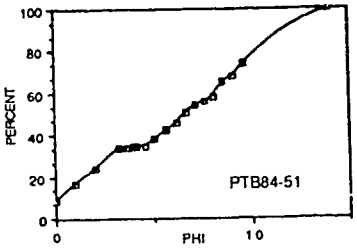
PERCENT
PTB84-51
PHI

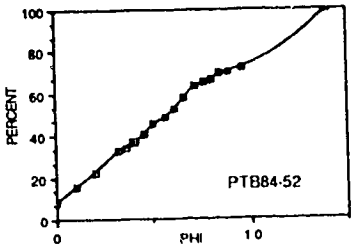
PERCENT
PTB84-52
PHI

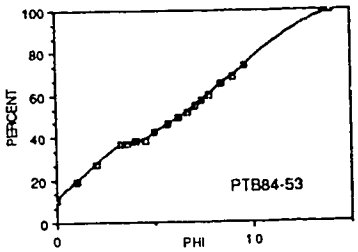
PERCENT
PTB84-53
PHI

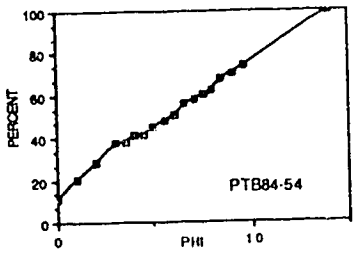
PERCENT
PTB84-54
PHI

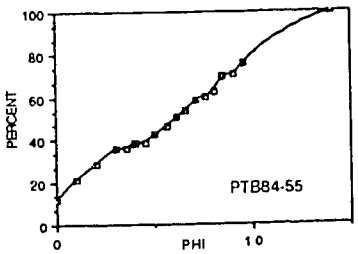
PERCENT
PTB84-55
PHI

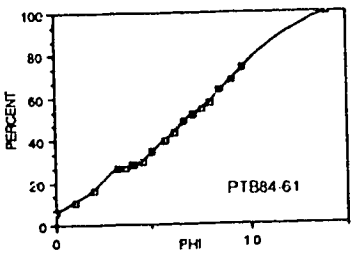
PERCENT
PTB84-61
PHI

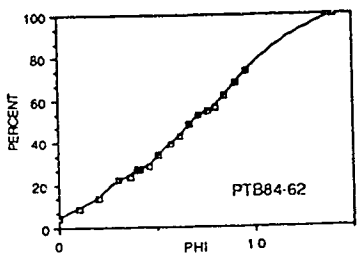
PERCENT
PTB84-62
PHI

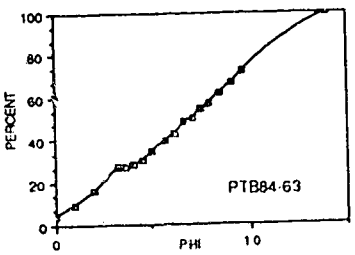
PERCENT
PTB84-63
PHI

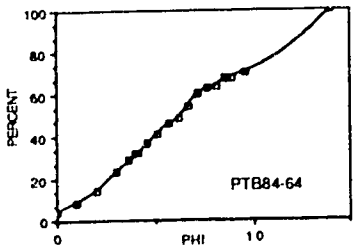
PERCENT
PHI
PTB84-64

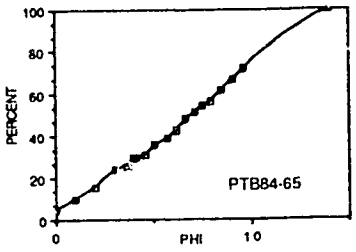
PERCENT
PHI
PTB84-65

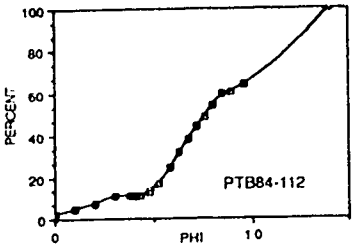
PERCENT
PHI
PTB84-112

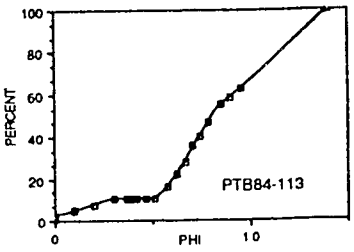
PERCENT
PHI
PTB84-113

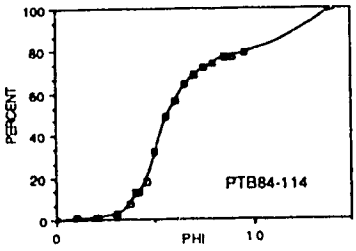
PERCENT
PHI
PTB84-114

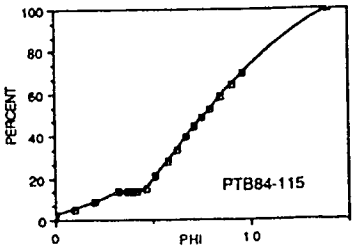
PERCENT
PHI
PTB84-115

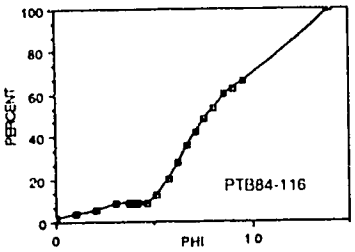
PERCENT
PHI
PTB84-116

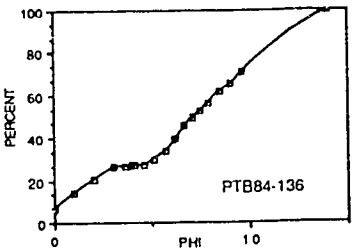
PERCENT
PHI
PTB84-136

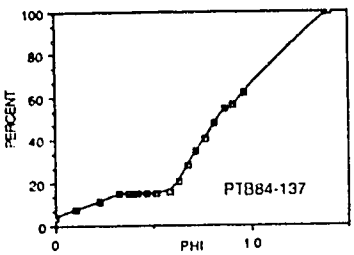
PERCENT
PHI
PTB84-137

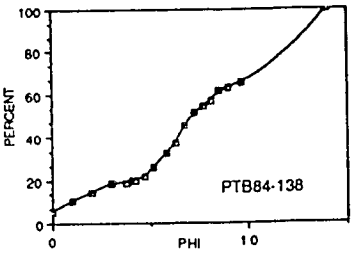
PERCENT
PHI
PTB84-138

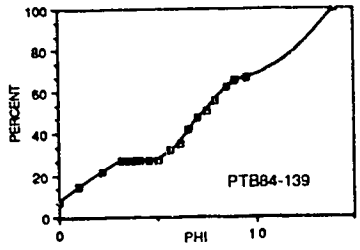
PERCENT
PHI
PTB84-139

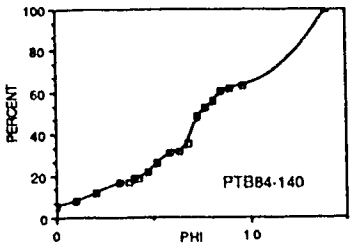
PERCENT
PHI
PTB84-140

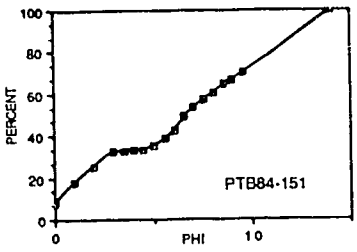
PERCENT
PHI
PTB84-151

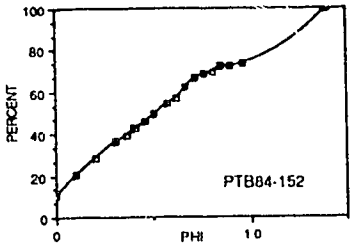
PERCENT
PHI
PTB84-152

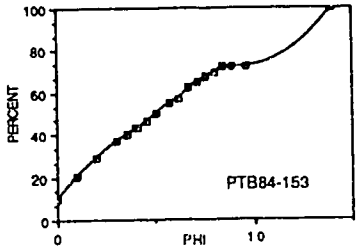
PERCENT
PHI
PTB84-153

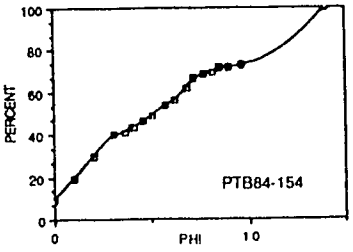
PERCENT
PHI
PTB84-154

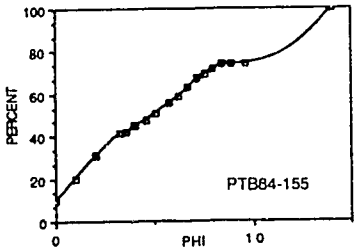
PERCENT
PHI
PTB84-155

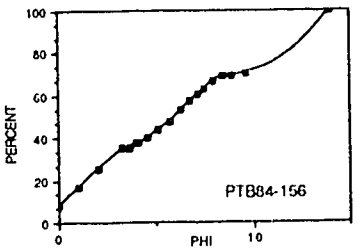
PERCENT
PHI
PTB84-156

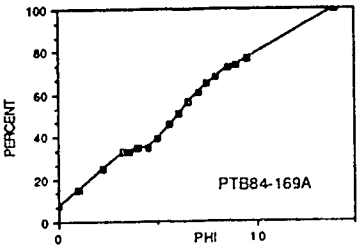
PERCENT
PHI
PTB84-169A

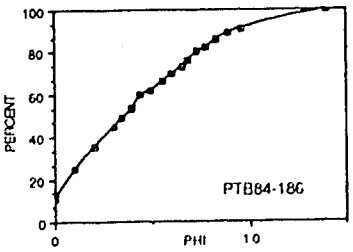
PERCENT
PHI
PTB84-186

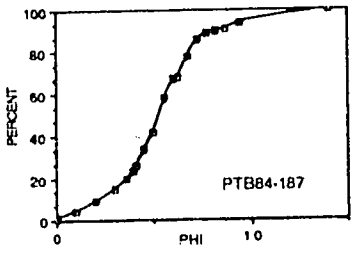
PERCENT
PHI
PTB84-187

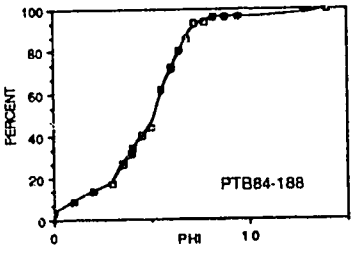
PERCENT
PHI
PTB84-188

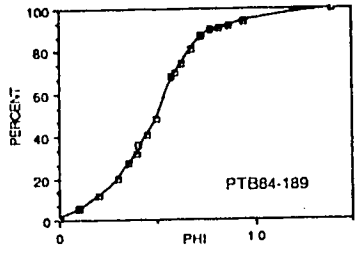
PERCENT
PHI
PTB84-189

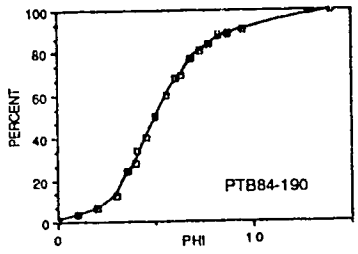
PERCENT
PHI
PTB84-190

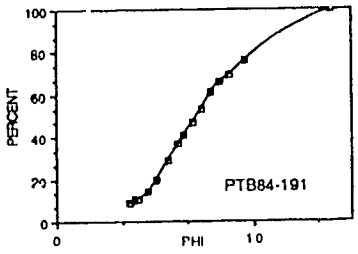
PERCENT
PHI
PTB84-191

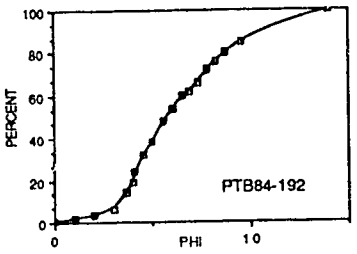
PERCENT
PHI
PTB84-192

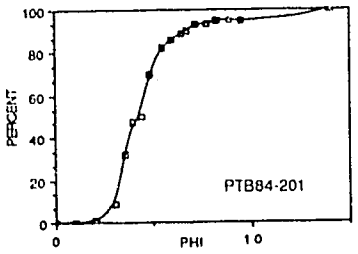
PERCENT
PHI
PTB84-201

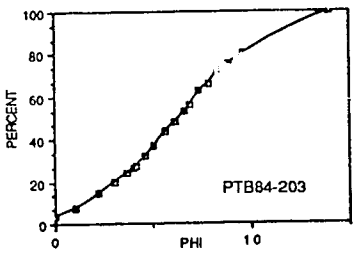
PERCENT
PHI
PTB84-203

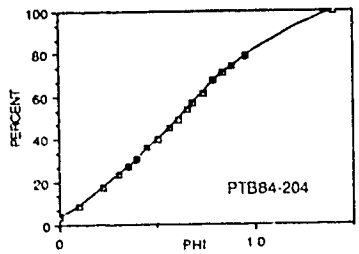
PERCENT
PHI
PTB84-204

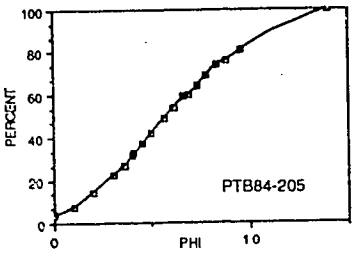
PERCENT
PHI
PTB84-205

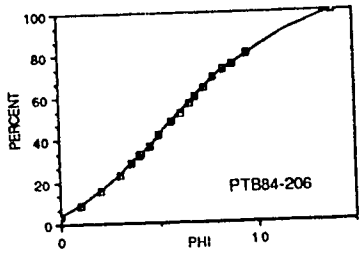
PERCENT
100
80
60
40
20
0
PTB84-206
0
PHI
10

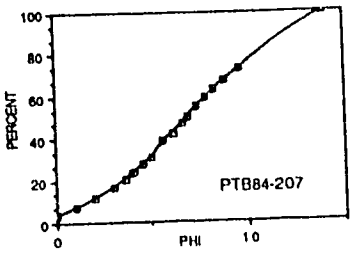
PERCENT
100
80
60
40
20
0
PTB84-207
0
PHI
10

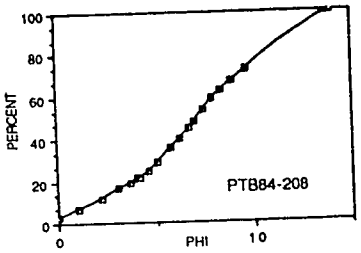
PERCENT
100
80
60
40
20
0
PTB84-208
0
PHI
10

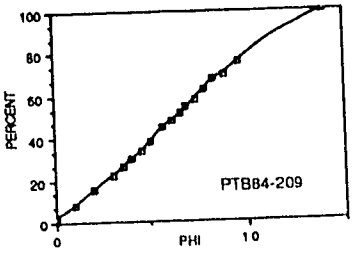
PERCENT
100
80
60
40
20
0
PTB84-209
0
PHI
10

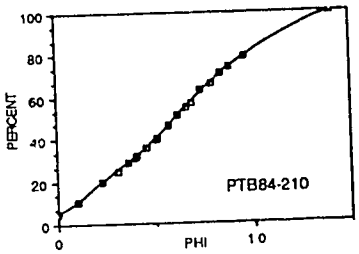
PERCENT
100
80
60
40
20
0
PTB84-210
0
PHI
10

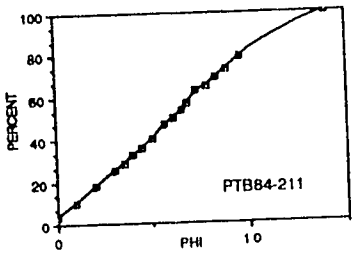
PERCENT
100
80
60
40
20
0
PTB84-211
0
PHI
10

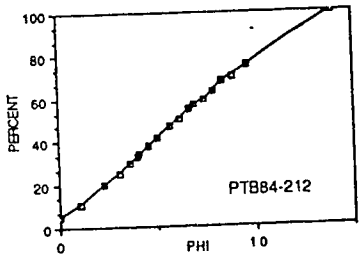
PERCENT
100
80
60
40
20
0
PTB84-212
0
PHI
10

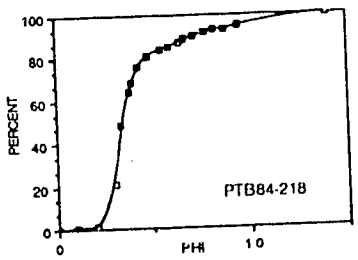
PERCENT
100
80
60
40
20
0
PTB84-218
0
PHI
10

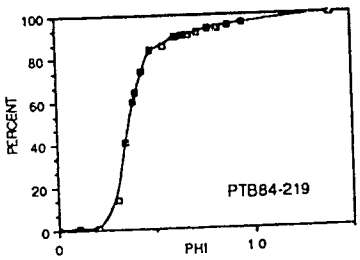
PERCENT
100
80
60
40
20
0
PTB84-219
0
PHI
10

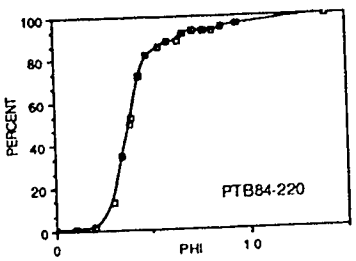
PERCENT
100
80
60
40
20
0
PTB84-220
0
PHI
10

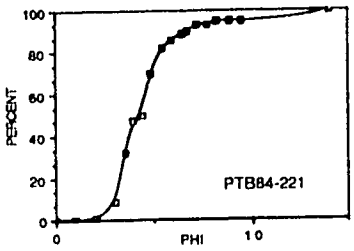
PERCENT
PHI
PTB84-221

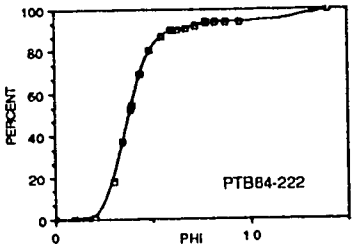
PERCENT
PHI
PTB84-222

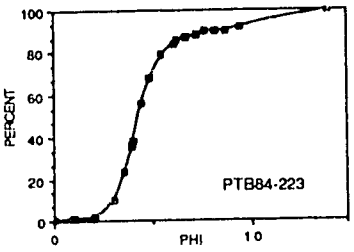
PERCENT
PHI
PTB84-223

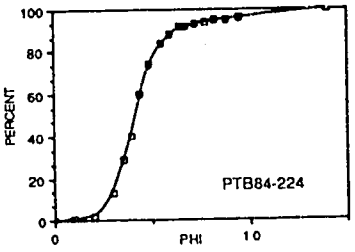
PERCENT
PHI
PTB84-224

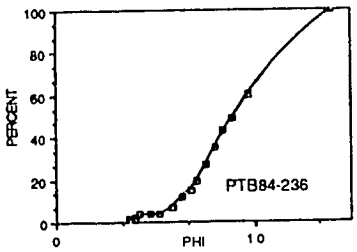
PERCENT
PHI
PTB84-236

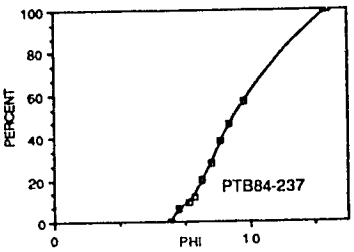
PERCENT
PHI
PTB84-237

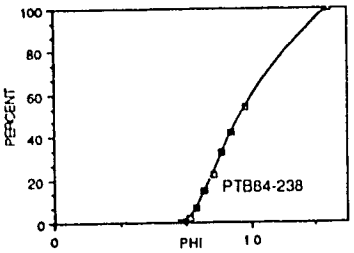
PERCENT
PHI
PTB84-238

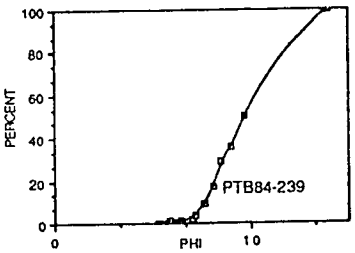
PERCENT
PHI
PTB84-239

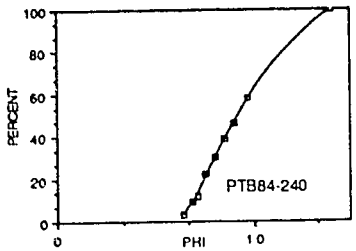
PERCENT
PHI
PTB84-240

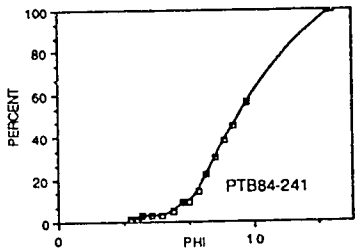
PERCENT
PHI
PTB84-241

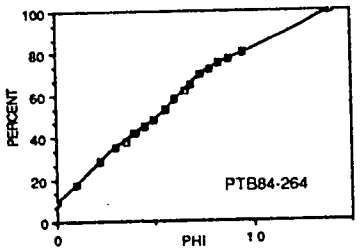
PERCENT
PHI
PTB84-264

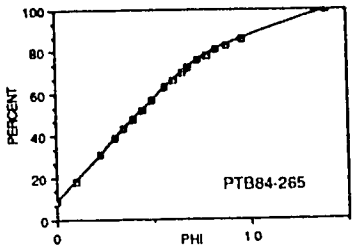
PERCENT
PHI
PTB84-265

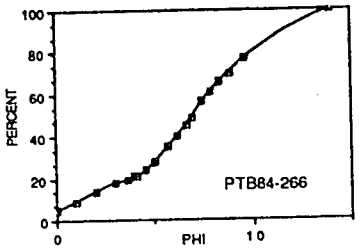
PERCENT
PHI
PTB84-266

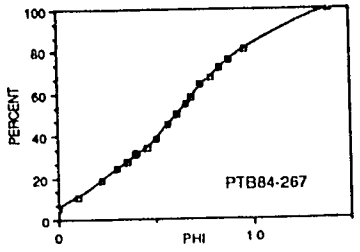
PERCENT
PHI
PTB84-267

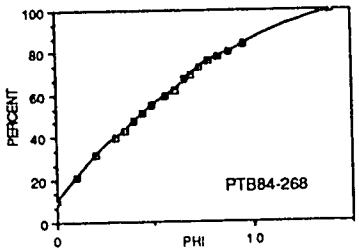
PERCENT
PHI
PTB84-268

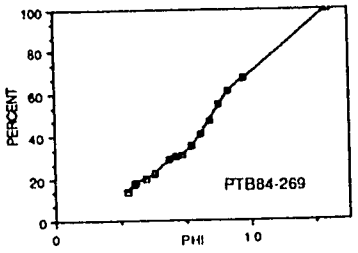
PERCENT
PHI
PTB84-269

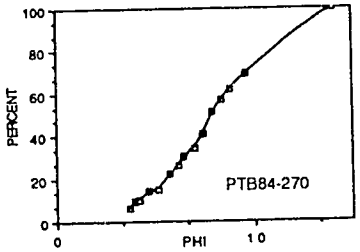
PERCENT
PHI
PTB84-270

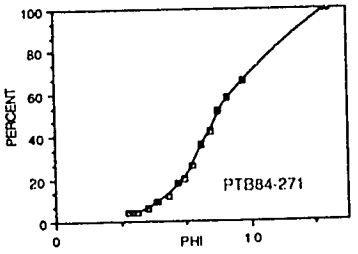
PERCENT
PHI
PTB84-271

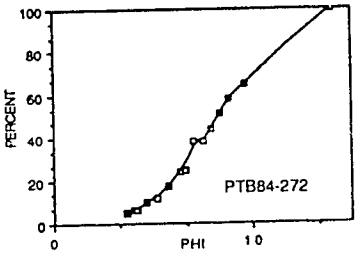
PERCENT
PHI
PTB84-272

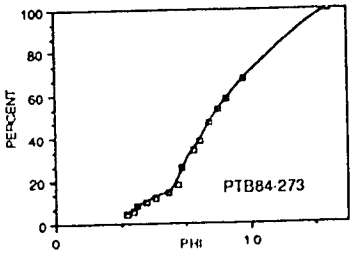
PERCENT
PHI
PTB84-273

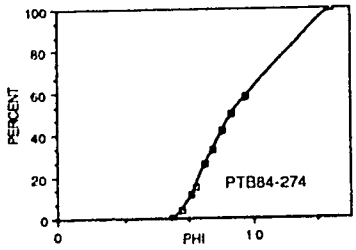
PERCENT
PHI
PTB84-274

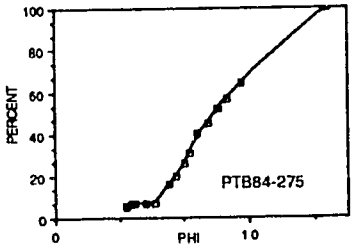
PERCENT
PHI
PTB84-275

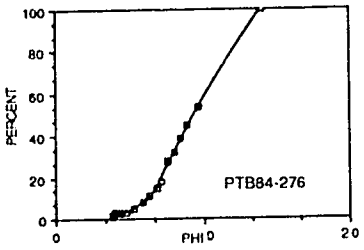
PERCENT
PHI
PTB84-276

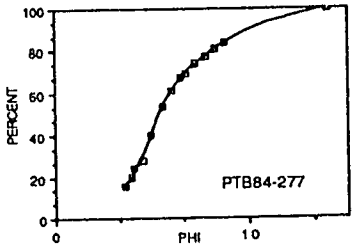
PERCENT
PHI
PTB84-277

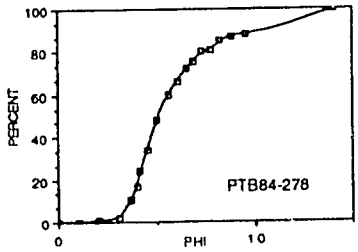
PERCENT
PHI
PTB84-278

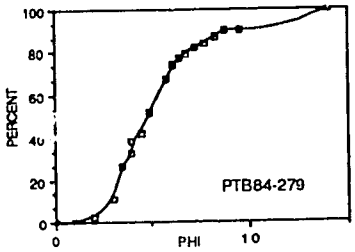
PERCENT
PHI
PTB84-279

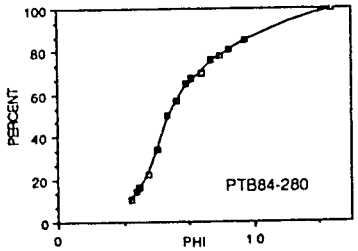
PERCENT
PHI
PTB84-280

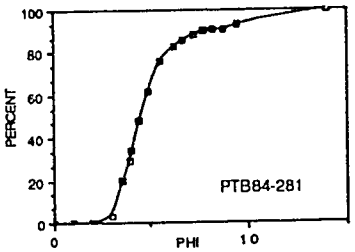
PERCENT
PHI
PTB84-281

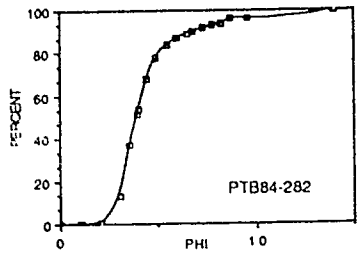
PERCENT
PHI
PTB84-282

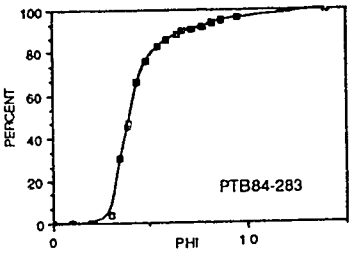
PERCENT
PHI
PTB84-283

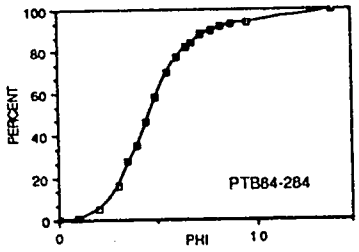
PERCENT
100
80
60
40
20
0
0
PHI
10
PTB84-284

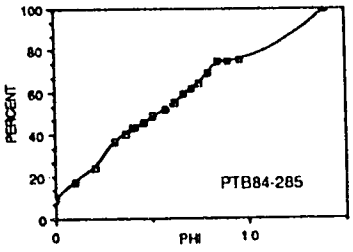
PERCENT
100
80
60
40
20
0
0
PHI
10
PTB84-285

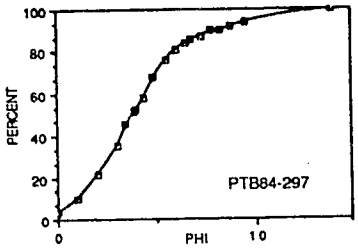
PERCENT
100
80
60
40
20
0
0
PHI
10
PTB84-297

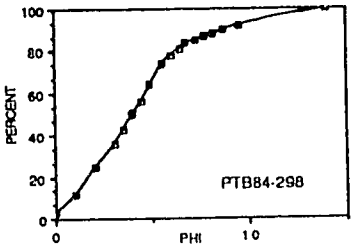
PERCENT
100
80
60
40
20
0
0
PHI
10
PTB84-298

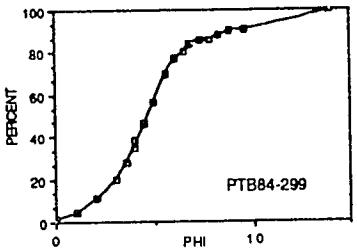
PERCENT
100
80
60
40
20
0
0
PHI
10
PTB84-299

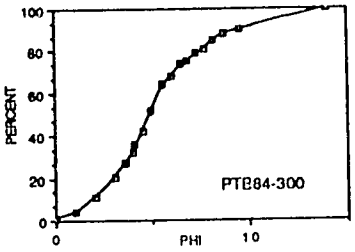
PERCENT
100
80
60
40
20
0
0
PHI
10
PTB84-300

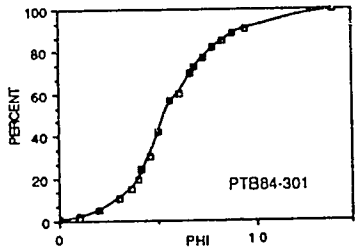
PERCENT
100
80
60
40
20
0
0
PHI
10
PTB84-301

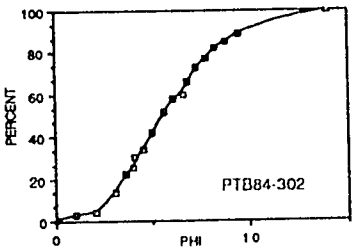
PERCENT
100
80
60
40
20
0
0
PHI
10
PTB84-302

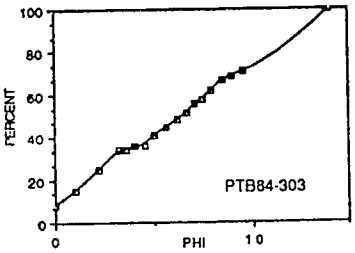
PERCENT
100
80
60
40
20
0
0
PHI
10
PTB84-303

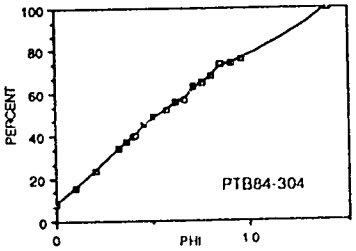
PERCENT
100
80
60
40
20
0
0
PHI
10
PTB84-304

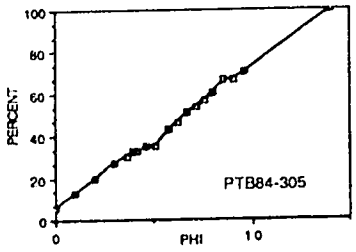
PERCENT
100
80
60
40
20
0
PTB84-305
0
PHI
10

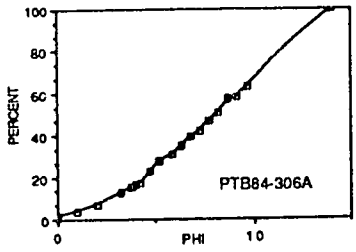
PERCENT
100
80
60
40
20
0
PTB84-306A
0
PHI
10

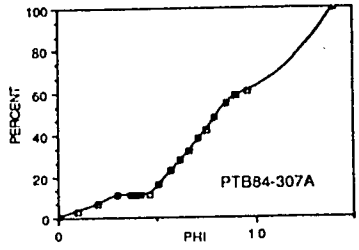
PERCENT
100
80
60
40
20
0
PTB84-307A
0
PHI
10

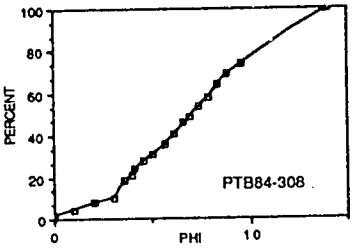
PERCENT
100
80
60
40
20
0
PTB84-308
0
PHI
10

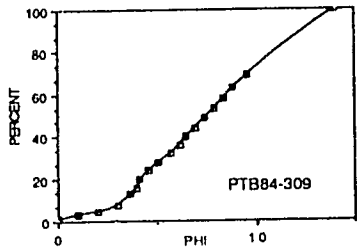
PERCENT
100
80
60
40
20
0
PTB84-309
0
PHI
10

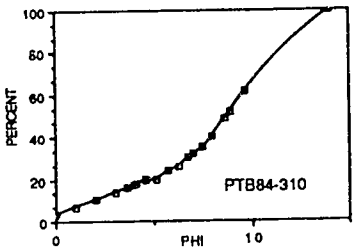
PERCENT
100
80
60
40
20
0
PTB84-310
0
PHI
10

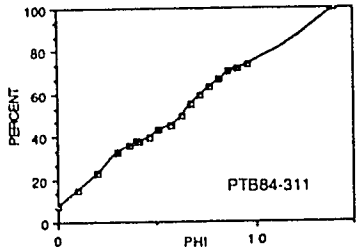
PERCENT
100
80
60
40
20
0
PTB84-311
0
PHI
10

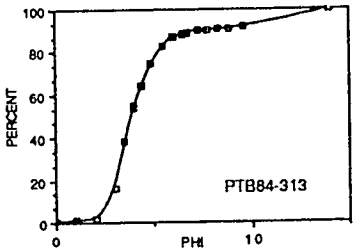
PERCENT
100
80
60
40
20
0
PTB84-313
0
PHI
10

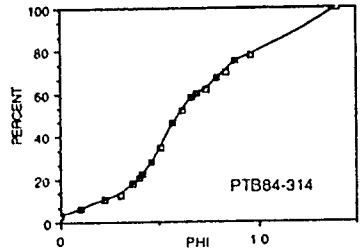
PERCENT
100
80
60
40
20
0
PTB84-314
0
PHI
10

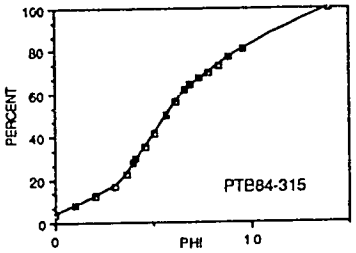
PERCENT
100
80
60
40
20
0
PTB84-315
0
PHI
10

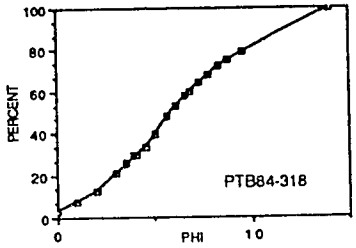
PERCENT
100
80
60
40
20
0
0
PHI
10
PTB84-318

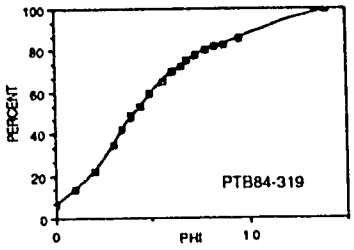
PERCENT
100
80
60
40
20
0
0
PHI
10
PTB84-319

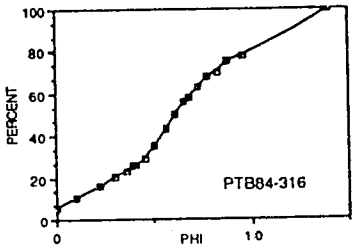
PERCENT
100
80
60
40
20
0
0
PHI
10
PTB84-316

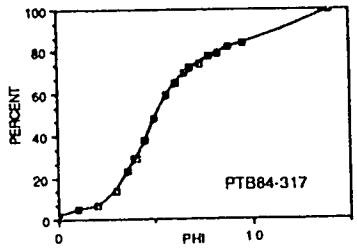
PERCENT
100
80
60
40
20
0
0
PHI
10
PTB84-317

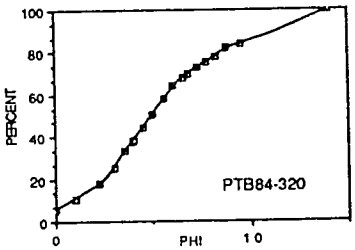
PERCENT
100
80
60
40
20
0
0
PHI
10
PTB84-320

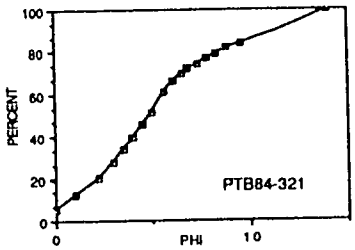
PERCENT
100
80
60
40
20
0
0
PHI
10
PTB84-321

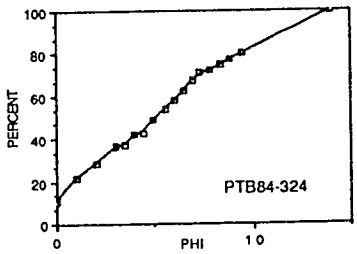
PERCENT
100
80
60
40
20
0
0
PHI
10
PTB84-324

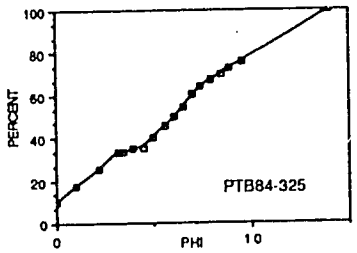
PERCENT
100
80
60
40
20
0
0
PHI
10
PTB84-325

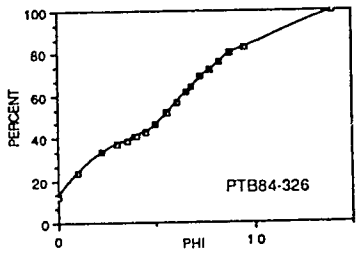
PERCENT
100
80
60
40
20
0
0
PHI
10
PTB84-326

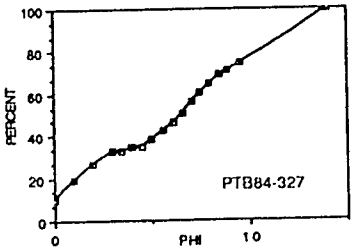
PERCENT
100
80
60
40
20
0
0
PHI
10
PTB84-327

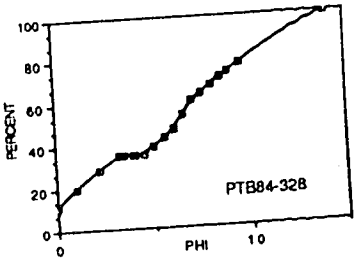
PERCENT
PHI
PTB84-328

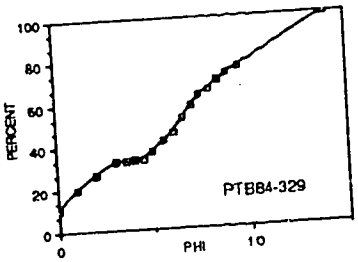
PERCENT
PHI
PTB84-329

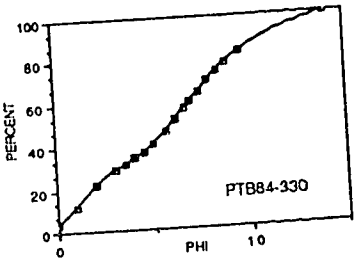
PERCENT
PHI
PTB84-330

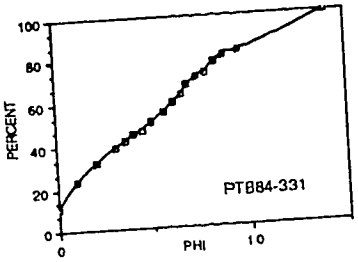
PERCENT
PHI
PTB84-331

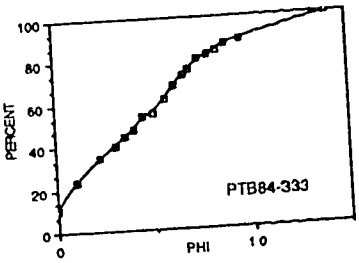
PERCENT
PHI
PTB84-333

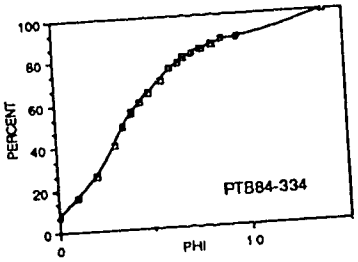
PERCENT
PHI
PTB84-334

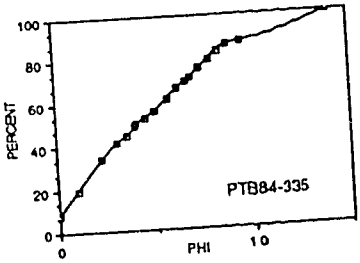
PERCENT
PHI
PTB84-335

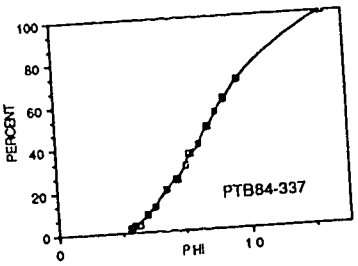
PERCENT
PHI
PTB84-337

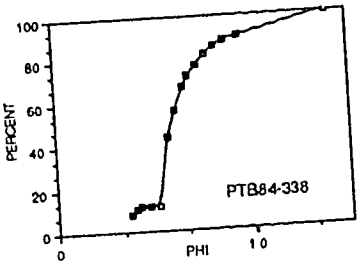
PERCENT
PHI
PTB84-338

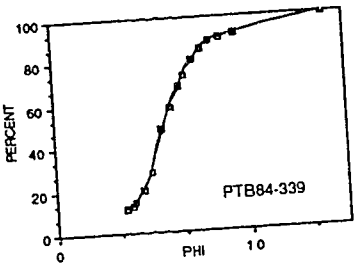
PERCENT
PHI
PTB84-339

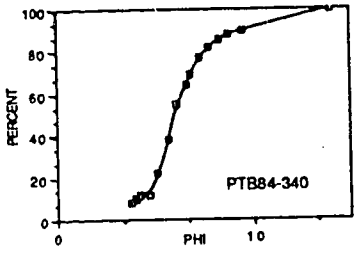
PERCENT
PHI
PTB84-340

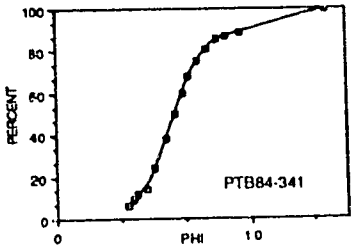
PERCENT
PHI
PTB84-341

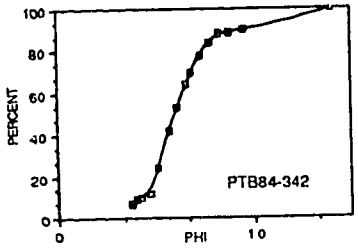
PERCENT
PHI
PTB84-342

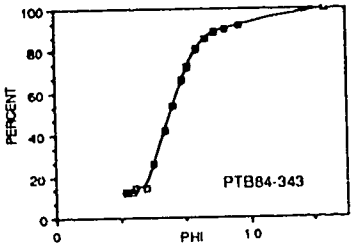
PERCENT
PHI
PTB84-343

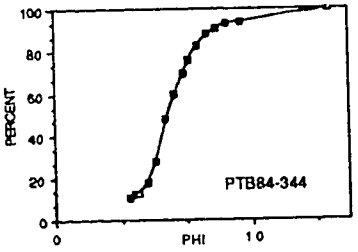
PERCENT
PHI
PTB84-344

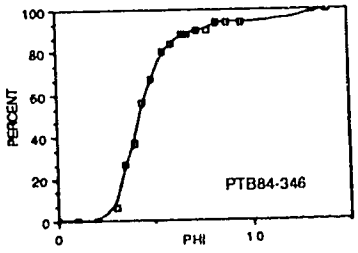
PERCENT
PHI
PTB84-346

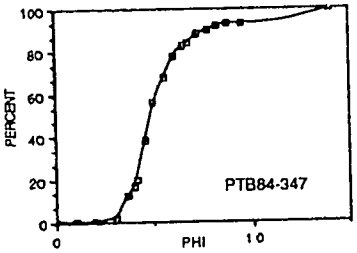
PERCENT
PHI
PTB84-347

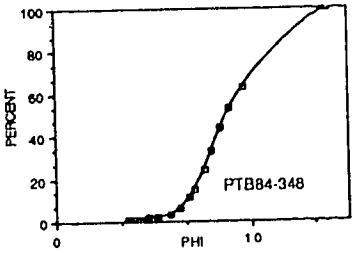
PERCENT
PHI
PTB84-348

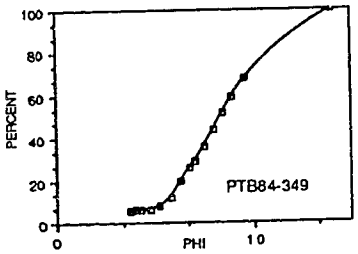
PERCENT
PHI
PTB84-349

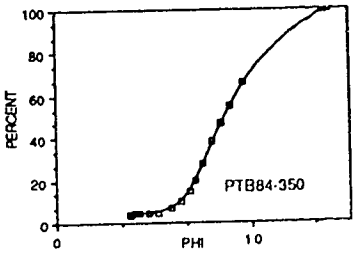
PERCENT
PHI
PTB84-350

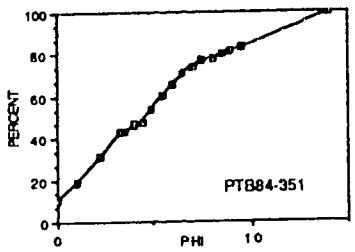
PERCENT
100
80
60
40
20
0
PTB84-351
0
PHI
10

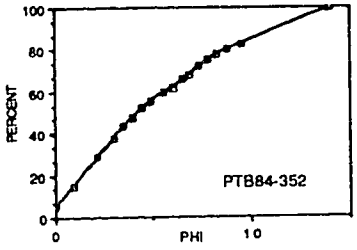
PERCENT
100
80
60
40
20
0
PTB84-352
0
PHI
10

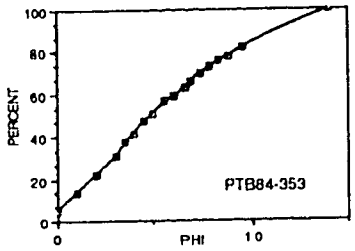
PERCENT
100
80
60
40
20
0
PTB84-353
0
PHI
10

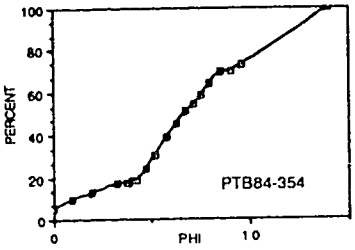
PERCENT
100
80
60
40
20
0
PTB84-354
0
PHI
10

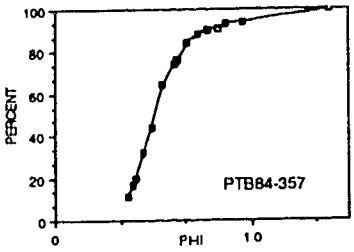
PERCENT
100
80
60
40
20
0
PTB84-357
0
PHI
10

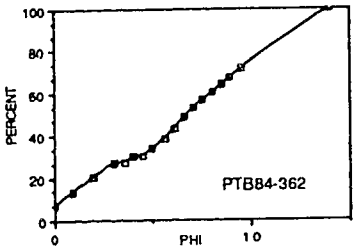
PERCENT
100
80
60
40
20
0
PTB84-362
0
PHI
10

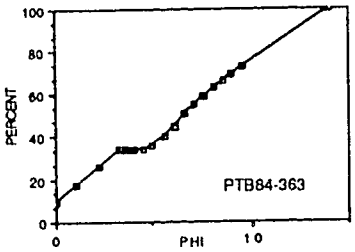
PERCENT
100
80
60
40
20
0
PTB84-363
0
PHI
10

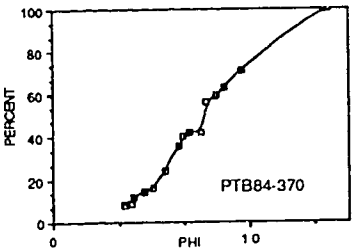
PERCENT
100
80
60
40
20
0
PTB84-370
0
PHI
10

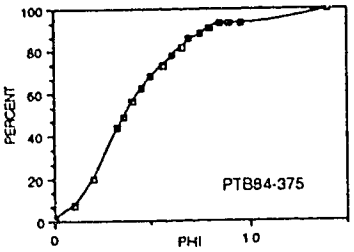
PERCENT
100
80
60
40
20
0
PTB84-375
0
PHI
10

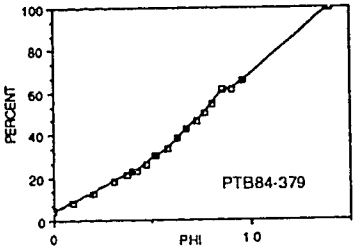
PERCENT
100
80
60
40
20
0
PTB84-379
0
PHI
10

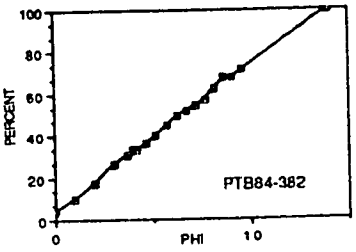
PERCENT
PHI
PTB84-382

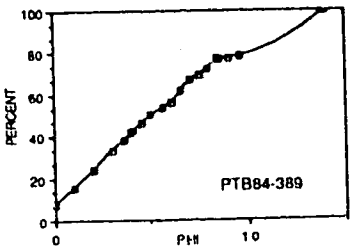
PERCENT
PHI
PTB84-389

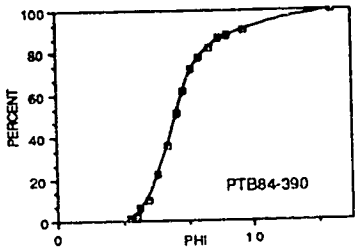
PERCENT
PHI
PTB84-390

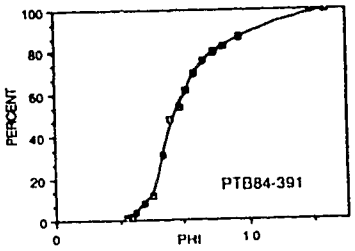
PERCENT
PHI
PTB84-391

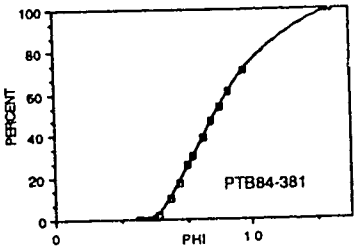
PERCENT
PHI
PTB84-381

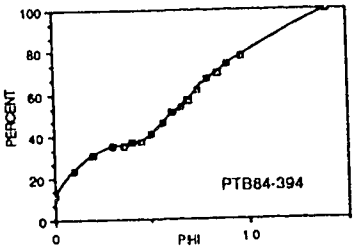
PERCENT
PHI
PTB84-394

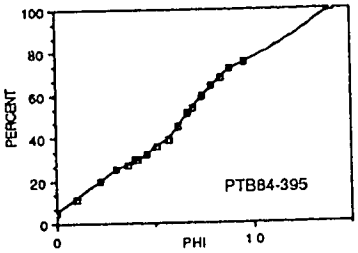
PERCENT
PHI
PTB84-395

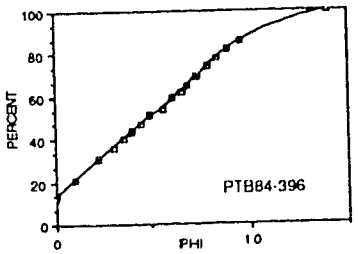
PERCENT
PHI
PTB84-396

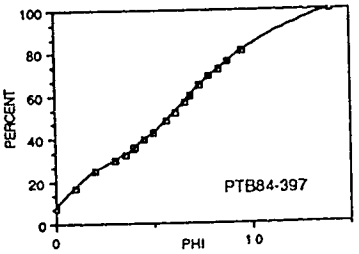
PERCENT
PHI
PTB84-397

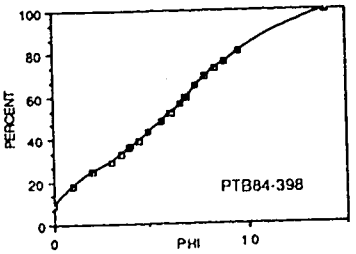
PERCENT
PHI
PTB84-398

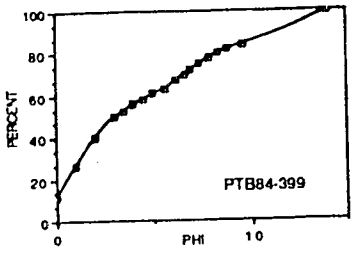
PERCENT
100
80
60
40
20
0
PTB84-399
0
PHI
10

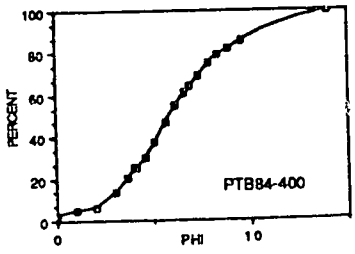
PERCENT
100
80
60
40
20
0
PTB84-400
0
PHI
10

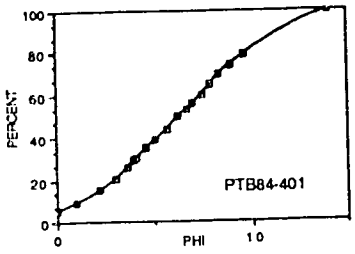
PERCENT
100
80
60
40
20
0
PTB84-401
0
PHI
10

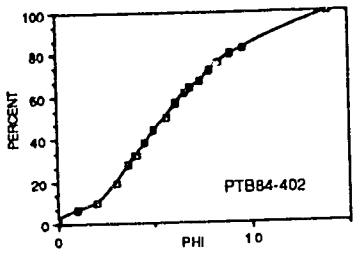
PERCENT
100
80
60
40
20
0
PTB84-402
0
PHI
10

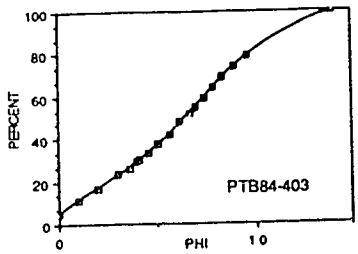
PERCENT
100
80
60
40
20
0
PTB84-403
0
PHI
10

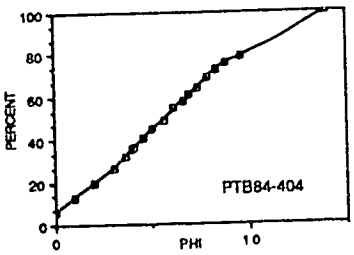
PERCENT
100
80
60
40
20
0
PTB84-404
0
PHI
10

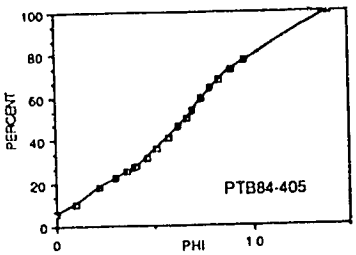
PERCENT
100
80
60
40
20
0
PTB84-405
0
PHI
10

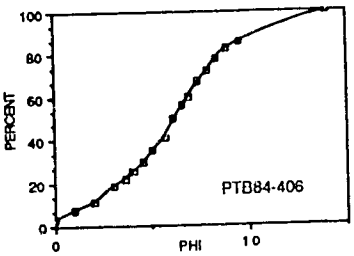
PERCENT
100
80
60
40
20
0
PTB84-406
0
PHI
10

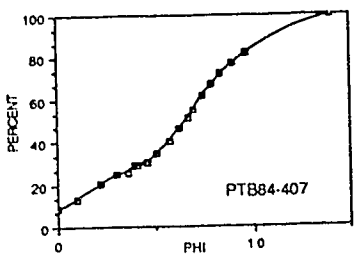
PERCENT
100
80
60
40
20
0
PTB84-407
0
PHI
10

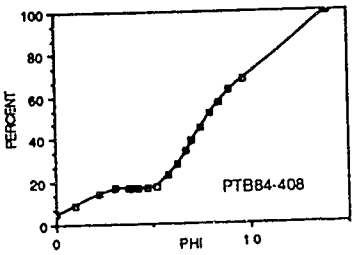
PERCENT
100
80
60
40
20
0
PTB84-408
0
PHI
10

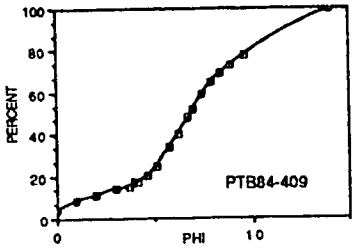
PERCENT
100
80
60
40
20
0
PTB84-409
0
PHI
10

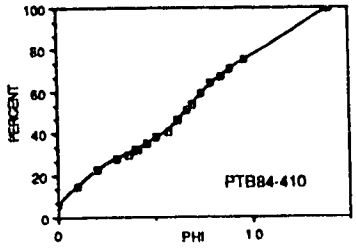
PERCENT
100
80
60
40
20
0
PTB84-410
0
PHI
10

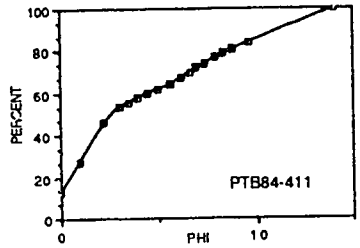
PERCENT
100
80
60
40
20
0
PTB84-411
0
PHI
10

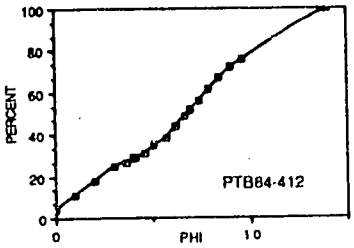
PERCENT
100
80
60
40
20
0
PTB84-412
0
PHI
10

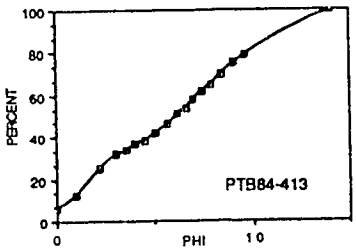
PERCENT
100
80
60
40
20
0
PTB84-413
0
PHI
10

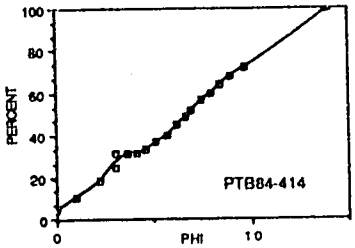
PERCENT
100
80
60
40
20
0
PTB84-414
0
PHI
10

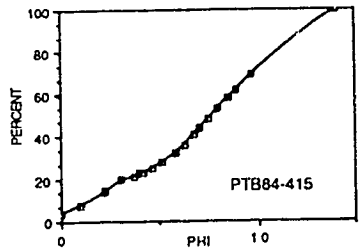
PERCENT
100
80
60
40
20
0
PTB84-415
0
PHI
10

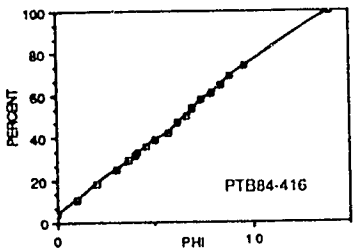
PERCENT
100
80
60
40
20
0
PTB84-416
0
PHI
10

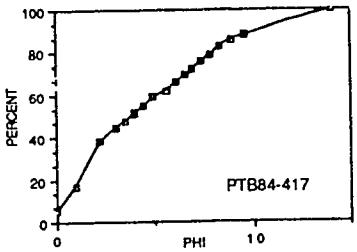
PERCENT
100
80
60
40
20
0
PTB84-417
0
PHI
10

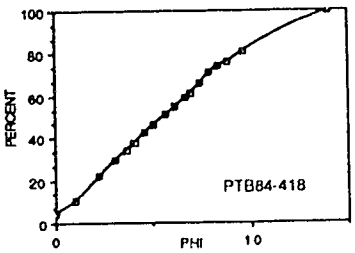
PERCENT
100
80
60
40
20
0
PTB84-418
0
PHI
10

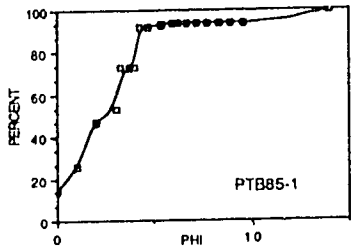
PERCENT
PHI
PTB85-1

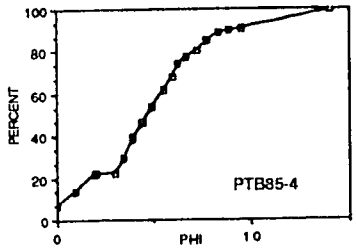
PERCENT
PHI
PTB85-4

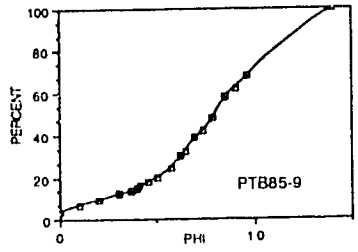
PERCENT
PHI
PTB85-9

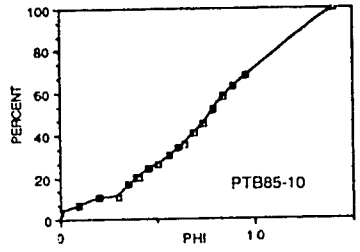
PERCENT
PHI
PTB85-10

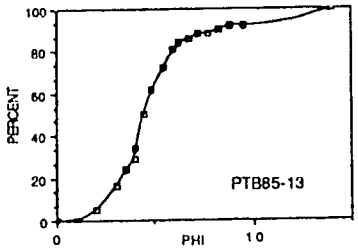
PERCENT
PHI
PTB85-13

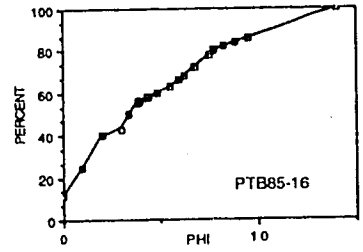
PERCENT
PHI
PTB85-16

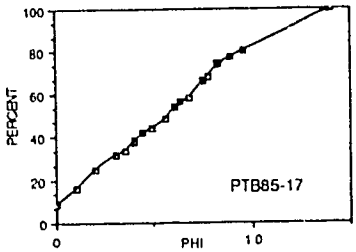
PERCENT
PHI
PTB85-17

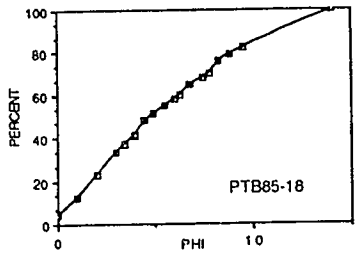
PERCENT
PHI
PTB85-18

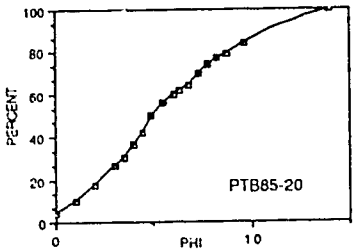
PERCENT
PHI
PTB85-20

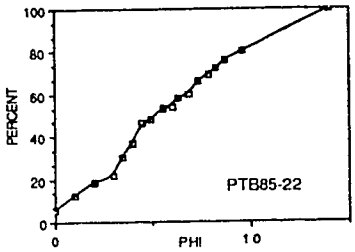
PERCENT
PHI
PTB85-22

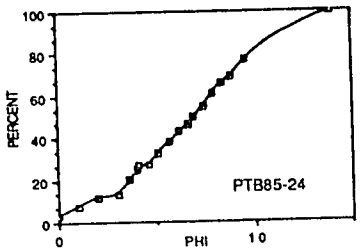
PERCENT
100
80
60
40
20
0
PTB85-24
0
PHI
10

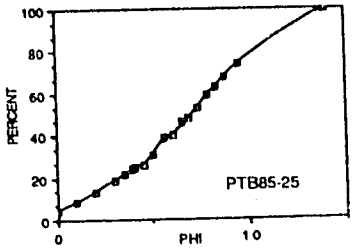
PERCENT
100
80
60
40
20
0
PTB85-25
0
PHI
10

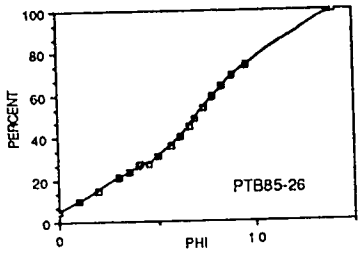
PERCENT
100
80
60
40
20
0
PTB85-26
0
PHI
10

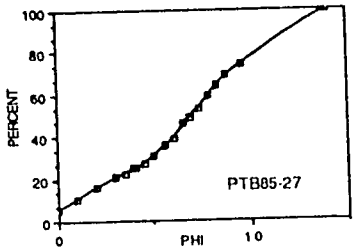
PERCENT
100
80
60
40
20
0
PTB85-27
0
PHI
10

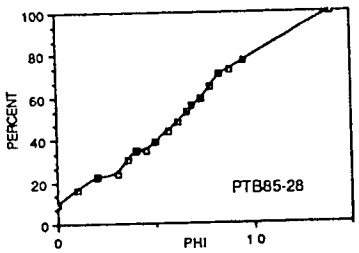
PERCENT
100
80
60
40
20
0
PTB85-28
0
PHI
10

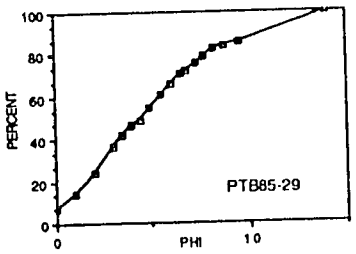
PERCENT
100
80
60
40
20
0
PTB85-29
0
PHI
10

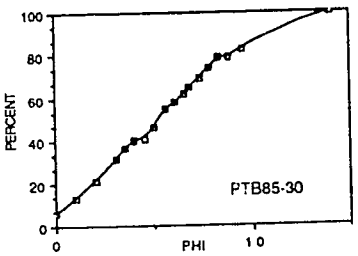
PERCENT
100
80
60
40
20
0
PTB85-30
0
PHI
10

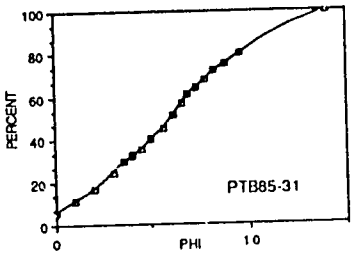
PERCENT
100
80
60
40
20
0
PTB85-31
0
PHI
10

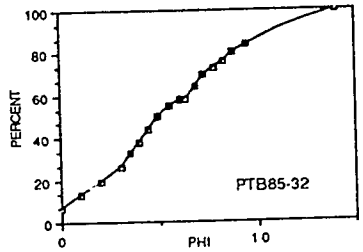
PERCENT
100
80
60
40
20
0
PTB85-32
0
PHI
10

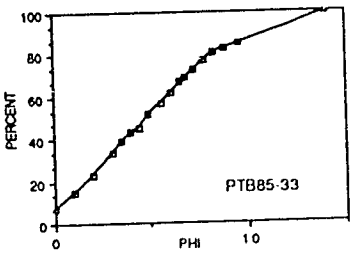
PERCENT
100
80
60
40
20
0
PTB85-33
0
PHI
10

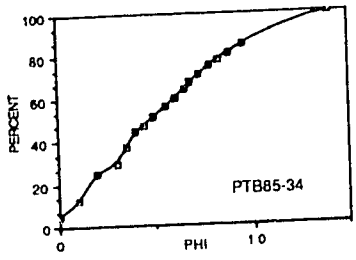
PERCENT
100
80
60
40
20
0
0
PHI
10
PTB85-34

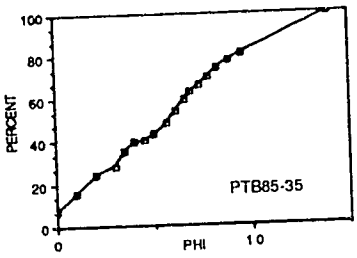
PERCENT
100
80
60
40
20
0
0
PHI
10
PTB85-35

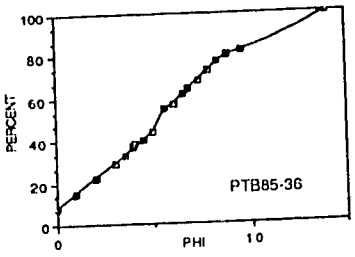
PERCENT
100
80
60
40
20
0
0
PHI
10
PTB85-36

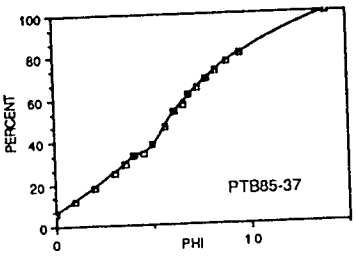
PERCENT
100
80
60
40
20
0
0
PHI
10
PTB85-37

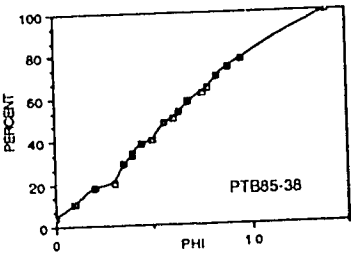
PERCENT
100
80
60
40
20
0
0
PHI
10
PTB85-38

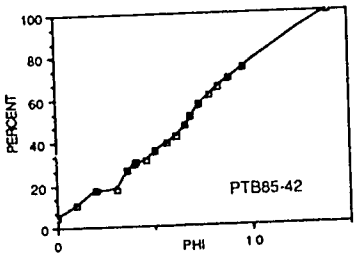
PERCENT
100
80
60
40
20
0
0
PHI
10
PTB85-42

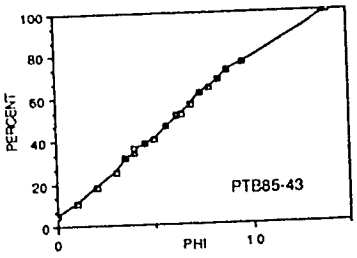
PERCENT
100
80
60
40
20
0
0
PHI
10
PTB85-43

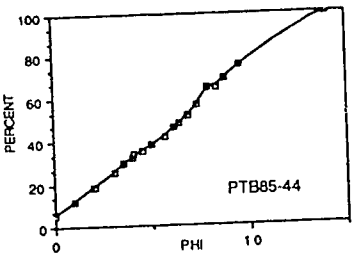
PERCENT
100
80
60
40
20
0
0
PHI
10
PTB85-44

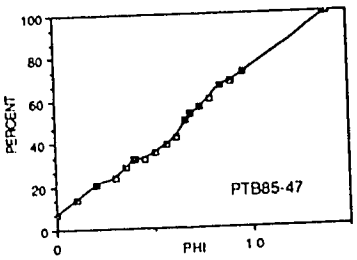
PERCENT
100
80
60
40
20
0
0
PHI
10
PTB85-47

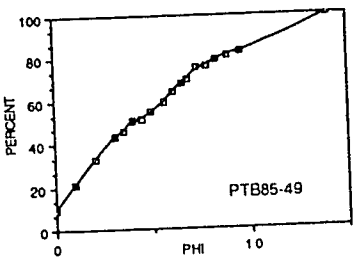
PERCENT
100
80
60
40
20
0
0
PHI
10
PTB85-49

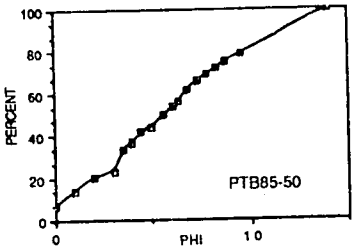
PERCENT
100
80
60
40
20
0
PTB85-50
0
PHI
10

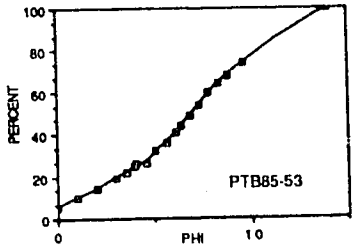
PERCENT
100
80
60
40
20
0
PTB85-53
0
PHI
10

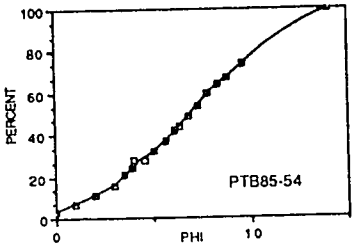
PERCENT
100
80
60
40
20
0
PTB85-54
0
PHI
10

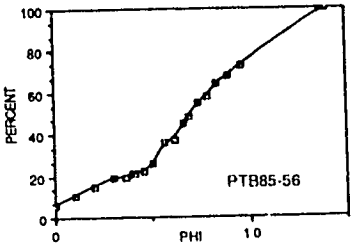
PERCENT
100
80
60
40
20
0
PTB85-56
0
PHI
10

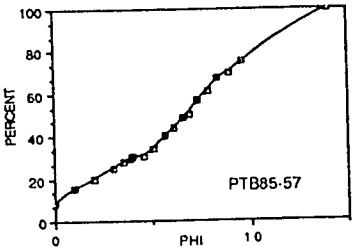
PERCENT
100
80
60
40
20
0
PTB85-57
0
PHI
10

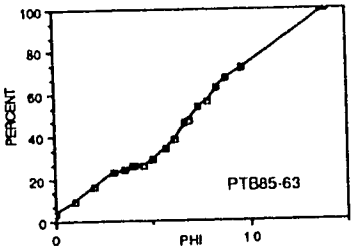
PERCENT
100
80
60
40
20
0
PTB85-63
0
PHI
10

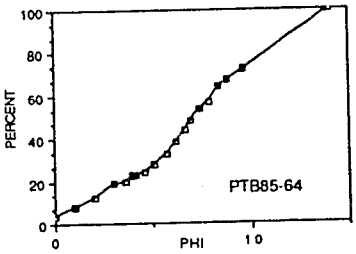
PERCENT
100
80
60
40
20
0
PTB85-64
0
PHI
10

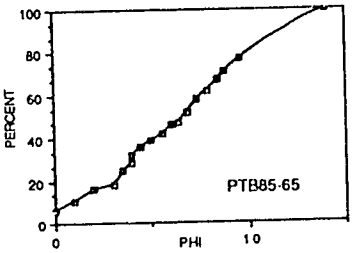
PERCENT
100
80
60
40
20
0
PTB85-65
0
PHI
10

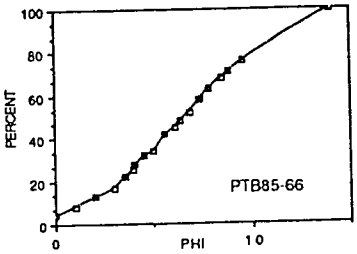
PERCENT
100
80
60
40
20
0
PTB85-66
0
PHI
10

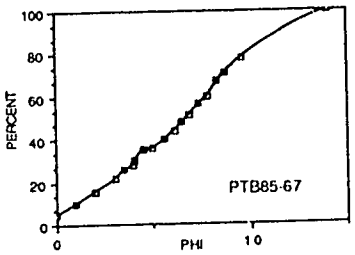
PERCENT
100
80
60
40
20
0
PTB85-67
0
PHI
10

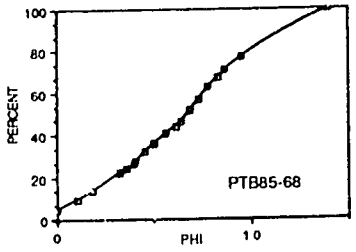
PERCENT
100
80
60
40
20
0
PTB85-68
0
PHI
10

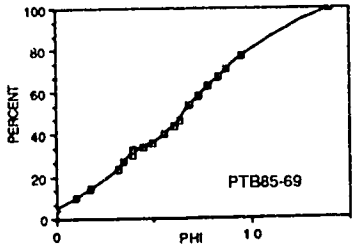
PERCENT
100
80
60
40
20
0
PTB85-69
0
PHI
10

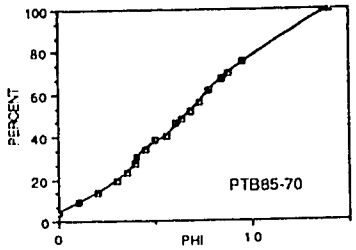
PERCENT
100
80
60
40
20
0
PTB85-70
0
PHI
10

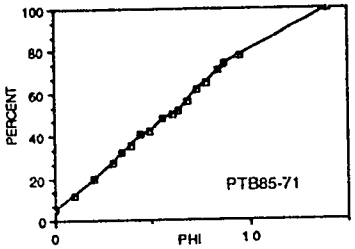
PERCENT
100
80
60
40
20
0
PTB85-71
0
PHI
10

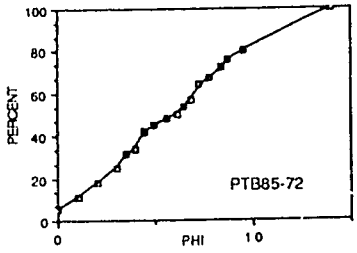
PERCENT
100
80
60
40
20
0
PTB85-72
0
PHI
10

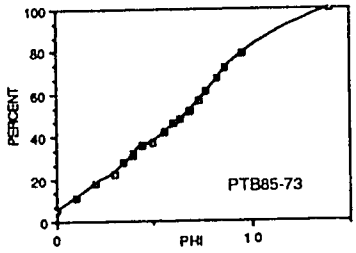
PERCENT
100
80
60
40
20
0
PTB85-73
0
PHI
10

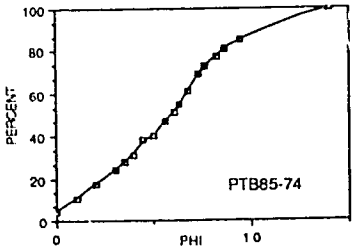
PERCENT
100
80
60
40
20
0
PTB85-74
0
PHI
10

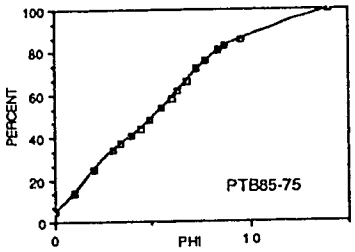
PERCENT
100
80
60
40
20
0
PTB85-75
0
PHI
10

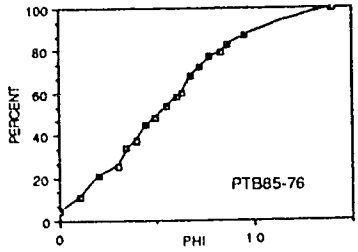
PERCENT
100
80
60
40
20
0
PTB85-76
0
PHI
10

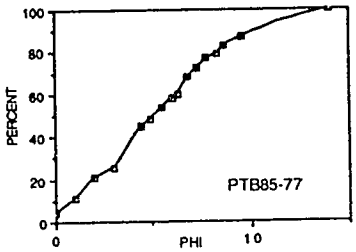
PERCENT
100
80
60
40
20
0
PTB85-77
0
PHI
10

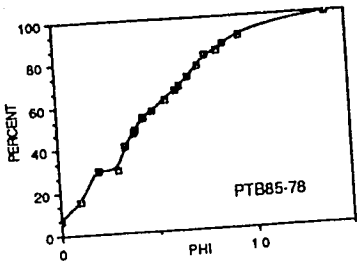
PERCENT
100
80
60
40
20
0
0
PHI
10
PTB85-78

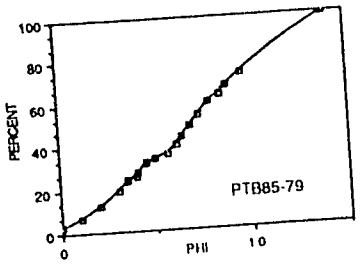
PERCENT
100
80
60
40
20
0
0
PHI
10
PTB85-79

Appendix 4. Percentage of sand silt and clay for bulk diamicton samples for samples from the northern Rocky Mountain Trench.

SAMPLE NO.	SAND	SILT	CLAY	TOTAL
PTB84-4	38	53	9	100
PTB84-9	61	0	39	100
PTB84-51	35	23	42	100
PTB84-52	36	30	34	100
PTB84-53	38	24	38	100
PTB84-54	42	20	38	100
PTB84-55	38	25	37	100
PTB84-61	28	29	43	100
PTB84-62	27	29	44	100
PTB84-63	28	29	43	100
PTB84-64	32	31	37	100
PTB84-65	29	27	44	100
PTB84-112	11	43	46	100
PTB84-113	11	38	51	100
PTB84-114	12	63	25	100
PTB84-115	14	39	47	100
PTB84-116	8	45	47	100
PTB84-136	27	30	43	100
PTB84-137	15	30	55	100
PTB84-138	20	36	44	100
PTB84-139	28	28	44	100
PTB84-140	18	37	45	100
PTB84-151	34	26	40	100
PTB84-152	43	26	31	100
PTB84-153	43	27	30	100
PTB84-154	44	25	31	100
PTB84-155	46	26	28	100
PTB84-156	37	29	34	100
PTB84-169	35	33	32	100
PTB84-186	54	30	16	100
PTB84-187	23	66	11	100
PTB84-188	32	63	5	100
PTB84-189	32	58	10	100
PTB84-190	28	58	14	100
PTB84-191	10	53	37	100
PTB84-192	18	57	25	100
PTB84-201	47	47	6	100
PTB84-203	26	40	34	100
PTB84-204	30	37	33	100
PTB84-205	31	39	30	100
PTB84-206	32	38	30	100
PTB84-207	24	37	39	100
PTB84-208	22	39	39	100
PTB84-209	30	34	36	100
PTB84-210	32	35	33	100
PTB84-211	33	33	34	100
PTB84-212	33	31	36	100
PTB84-219	64	31	5	100

PTB84-220	51	42	7	100
PTB84-221	46	47	7	100
PTB84-222	54	40	6	100
PTB84-223	34	56	10	100
PTB84-224	40	55	5	100
PTB84-236	2	33	65	100
PTB84-237	0	27	73	100
PTB84-238	0	21	79	100
PTB84-239	0	14	86	100
PTB84-240	0	29	71	100
PTB84-241	2	27	71	100
PTB84-264	43	31	26	100
PTB84-265	48	31	21	100
PTB84-266	21	41	38	100
PTB84-267	30	39	31	100
PTB84-268	47	30	23	100
PTB84-269	16	32	52	100
PTB84-270	8	43	49	100
PTB84-271	4	38	58	100
PTB84-272	5	40	55	100
PTB84-273	5	43	52	100
PTB84-274	0	32	68	100
PTB84-275	6	39	55	100
PTB84-276	5	60	35	100
PTB84-277	19	60	21	100
PTB84-278	16	67	17	100
PTB84-279	35	50	15	100
PTB84-280	13	64	23	100
PTB84-281	29	63	8	100
PTB84-282	53	32	15	100
PTB84-283	46	47	7	100
PTB84-284	34	57	9	100
PTB84-285	43	27	30	100
PTB84-297	53	37	10	100
PTB84-298	51	37	12	100
PTB84-299	25	61	14	100
PTB84-300	31	52	17	100
PTB84-301	20	64	16	100
PTB84-302	25	53	22	100
PTB84-303	36	26	38	100
PTB84-304	40	27	33	100
PTB84-305	33	28	39	100
PTB84-306	16	33	51	100
PTB84-307	12	36	52	100
PTB84-308	12	48	40	100
PTB84-309	15	39	46	100
PTB84-310	17	23	60	100
PTB84-311	38	28	34	100
PTB84-313	52	38	10	100
PTB84-314	20	48	32	100
PTB84-315	26	46	28	100
PTB84-316	26	44	30	100
PTB84-317	28	51	21	100
PTB84-318	30	40	30	100

PTB84-319	48	33	19	100
PTB84-320	38	42	20	100
PTB84-321	40	38	22	100
PTB84-324	43	31	26	100
PTB84-325	36	32	32	100
PTB84-326	41	32	27	100
PTB84-327	35	30	35	100
PTB84-328	35	32	33	100
PTB84-329	35	31	34	100
PTB84-330	35	37	28	100
PTB84-331	45	29	26	100
PTB84-333	47	37	16	100
PTB84-334	55	30	15	100
PTB84-335	50	31	19	100
PTB84-337	3	45	52	100
PTB84-338	10	73	17	100
PTB84-339	13	74	13	100
PTB84-340	10	75	15	100
PTB84-341	9	75	16	100
PTB84-342	9	78	13	100
PTB84-343	13	75	12	100
PTB84-344	12	78	10	100
PTB84-346	36	56	8	100
PTB84-347	17	74	9	100
PTB84-348	1	33	66	100
PTB84-349	6	39	55	100
PTB84-350	4	35	61	100
PTB84-351	46	32	22	100
PTB84-352	48	29	23	100
PTB84-353	42	33	25	100
PTB84-354	19	45	36	100
PTB84-357	15	76	9	100
PTB84-362	30	30	40	100
PTB84-363	34	28	38	100
PTB84-370	9	48	43	100
PTB84-375	56	35	9	100
PTB84-379	23	30	47	100
PTB84-381	0	47	53	100
PTB84-382	33	28	39	100
PTB84-389	42	31	27	100
PTB84-390	2	82	16	100
PTB84-391	3	75	22	100
PTB84-394	37	30	33	100
PTB84-395	30	34	36	100
PTB84-396	44	31	25	100
PTB84-397	35	36	29	100
PTB84-398	35	36	29	100
PTB84-399	56	23	21	100
PTB84-400	26	50	24	100
PTB84-401	29	37	34	100
PTB84-402	32	41	27	100
PTB84-403	30	35	35	100
PTB84-404	36	34	30	100
PTB84-405	27	38	35	100

PTB84-406	25	48	27	100
PTB84-407	29	39	32	100
PTB84-408	17	34	49	100
PTB84-409	18	48	34	100
PTB84-410	32	32	36	100
PTB84-411	58	20	22	100
PTB84-412	29	34	37	100
PTB84-413	38	27	35	100
PTB84-414	32	29	39	100
PTB84-415	23	30	47	100
PTB84-416	31	30	39	100
PTB84-417	53	29	18	100
PTB84-418	38	35	27	100
PTB85-1	73	20	7	100
PTB85-4	39	48	13	100
PTB85-9	15	34	51	100
PTB85-10	19	33	48	100
PTB85-13	31	57	12	100
PTB85-16	57	25	18	100
PTB85-17	39	31	30	100
PTB85-18	41	30	29	100
PTB85-20	36	39	25	100
PTB85-22	37	33	30	100
PTB85-24	26	36	38	100
PTB85-25	24	37	39	100
PTB85-26	26	34	40	100
PTB85-27	25	35	40	100
PTB85-28	34	32	34	100
PTB85-29	47	35	18	100
PTB85-30	40	36	24	100
PTB85-31	32	37	31	100
PTB85-32	38	35	27	100
PTB85-33	43	36	21	100
PTB85-34	45	32	23	100
PTB85-35	39	33	28	100
PTB85-36	36	39	25	100
PTB85-37	33	37	30	100
PTB85-38	35	30	35	100
PTB85-42	30	32	38	100
PTB85-43	35	30	35	100
PTB85-44	33	32	35	100
PTB85-47	32	29	39	100
PTB85-49	50	27	23	100
PTB85-50	36	34	30	100
PTB85-53	25	35	40	100
PTB85-54	24	37	39	100
PTB85-56	22	37	41	100
PTB85-57	30	32	38	100
PTB85-63	25	31	44	100
PTB85-64	23	36	41	100
PTB85-65	30	32	38	100
PTB85-66	25	38	37	100
PTB85-67	29	32	39	100
PTB85-68	27	37	36	100

PTB85-69	31	33	36	100
PTB85-70	28	34	38	100
PTB85-71	35	31	34	100
PTB85-72	33	35	32	100
PTB85-73	31	33	36	100
PTB85-74	31	45	24	100
PTB85-75	41	37	22	100
PTB85-76	37	41	22	100
PTB85-77	40	38	22	100
PTB85-78	47	36	17	100
PTB85-79	27	33	40	100
PTB84-245	36	34	30	100
PTB84-246	32	39	29	100
PTB84-247	29	36	35	100
PTB84-248	30	36	34	100
PTB84-249	26	34	40	100
PTB84-250	24	32	44	100
PTB84-251	29	32	39	100
PTB84-252	36	35	29	100
PTB84-253	28	30	42	100
PTB84-254	29	35	36	100
PTB84-255	33	37	30	100
PTB84-256	36	32	32	100
PTB84-257	31	41	28	100
PTB84-258	31	40	29	100
PTB84-259	29	31	40	100
PTB84-260	33	40	27	100

Apppendix 5. Numerical values used in calculation of graphic statistics for all samples analyzed for textural analysis from northeastern British Columbia.

SAMPLE NO.	5Ø	16Ø	25Ø	50Ø	75Ø	84Ø	95Ø
PTB84-4	1.00	2.35	3.30	4.55	5.55	6.20	9.20
PTB84-9	-1.00	-0.40	0.15	1.65	12.20	12.90	13.15
PTB84-51	-0.50	1.05	2.20	6.65	9.65	10.70	12.60
PTB84-52	-0.50	1.10	2.35	5.90	10.20	11.85	13.30
PTB84-53	-0.70	0.60	1.75	6.35	9.75	10.90	12.80
PTB84-54	-0.70	0.45	1.60	6.15	9.75	11.20	13.05
PTB84-55	-0.80	0.45	1.60	6.25	9.50	10.55	12.55
PTB84-61	-0.20	2.05	3.05	7.00	9.75	10.90	12.80
PTB84-62	0.05	2.35	3.80	6.90	9.75	10.90	12.80
PTB84-63	0.05	2.05	3.00	7.15	9.85	11.00	12.85
PTB84-64	0.15	2.25	3.25	6.40	10.70	12.05	13.40
PTB84-65	0.10	2.05	3.60	7.10	10.00	11.20	13.10
PTB84-112	1.00	5.25	5.95	7.75	11.25	12.30	13.50
PTB84-113	1.00	5.75	6.45	8.05	11.05	12.10	13.40
PTB84-114	3.45	4.45	4.80	5.65	8.05	11.00	13.15
PTB84-115	0.70	4.75	5.50	7.70	10.20	11.35	13.10
PTB84-116	1.65	5.45	6.05	7.80	10.90	12.05	13.40
PTB84-136	-0.30	1.30	2.90	7.25	10.15	11.30	13.10
PTB84-137	0.25	4.80	6.50	8.35	10.95	11.95	13.25
PTB84-138	-0.20	2.35	5.15	7.20	11.35	12.45	13.55
PTB84-139	-0.30	1.25	2.90	7.45	11.40	12.45	13.55
PTB84-140	-0.10	3.05	6.15	7.40	11.80	12.70	13.65
PTB84-151	-0.35	0.85	2.00	6.70	10.45	11.75	13.35
PTB84-152	-0.60	0.55	1.65	5.25	10.30	12.05	13.40
PTB84-153	-0.60	0.65	1.55	5.05	10.65	12.25	13.50
PTB84-154	-0.60	0.70	1.65	5.35	10.55	12.05	13.45
PTB84-155	-0.60	0.65	1.50	5.05	10.15	12.15	13.50
PTB84-156	-0.40	0.95	2.05	6.05	10.95	12.30	13.55
PTB84-169	-0.40	1.10	2.25	6.10	9.25	10.85	12.90
PTB84-186	-0.50	0.35	1.05	3.55	6.65	8.00	10.85
PTB84-187	1.05	3.25	4.10	5.30	6.65	7.10	9.85
PTB84-188	0.10	2.75	3.45	5.20	6.20	6.65	7.95
PTB84-189	0.95	2.65	3.40	5.10	6.40	7.05	10.30
PTB84-190	1.35	3.15	3.65	4.95	6.65	7.70	10.90
PTB84-191	3.10	4.85	5.55	7.25	9.45	10.55	12.55
PTB84-192	2.70	3.80	4.15	5.75	8.10	9.20	11.60
PTB84-201	2.60	3.20	3.40	4.40	5.05	5.60	8.10
PTB84-203	0.15	2.45	3.85	6.35	8.90	10.35	12.65
PTB84-204	0.15	2.05	3.20	6.25	9.00	10.35	12.65
PTB84-205	0.35	2.20	3.45	5.75	8.75	10.10	12.50
PTB84-206	0.25	2.05	3.25	5.90	8.80	10.15	12.35
PTB84-207	0.25	2.85	4.25	6.95	9.80	11.05	12.85
PTB84-208	0.45	2.80	4.65	7.10	9.85	11.05	12.85
PTB84-209	0.35	2.05	3.35	6.45	9.45	10.70	12.70
PTB84-210	0.00	1.75	3.05	6.10	9.10	10.60	12.90
PTB84-211	0.15	1.75	3.05	6.20	9.15	10.35	12.55
PTB84-212	-0.10	1.70	3.05	6.15	9.65	10.95	12.90

PTB84-218	2.35	2.85	3.10	3.45	4.15	5.05	8.40
PTB84-219	2.50	3.05	3.20	3.65	4.30	4.65	7.50
PTB84-220	2.45	3.10	3.30	3.90	4.45	4.95	8.60
PTB84-221	2.65	3.20	3.40	4.45	5.05	5.70	8.10
PTB84-222	2.40	2.90	3.20	3.90	4.60	5.20	11.50
PTB84-223	2.45	3.30	3.70	4.25	5.20	6.05	10.55
PTB84-224	2.45	3.10	3.40	4.20	4.85	5.45	8.10
PTB84-236	5.55	6.90	7.45	9.05	10.95	11.90	13.15
PTB84-237	6.25	7.35	7.90	9.25	11.20	12.10	13.35
PTB84-238	7.10	7.70	8.20	9.45	11.40	12.20	13.45
PTB84-239	7.30	8.10	8.40	9.75	11.40	12.15	13.25
PTB84-240	6.55	7.30	7.80	9.25	11.10	12.00	13.30
PTB84-241	5.90	7.30	7.80	9.35	11.10	11.95	13.15
PTB84-264	-0.60	0.85	1.90	5.20	8.10	10.10	12.60
PTB84-265	-0.30	0.75	1.70	4.25	7.20	9.00	12.15
PTB84-266	0.05	2.70	4.80	7.10	9.45	10.65	12.65
PTB84-267	-0.15	1.80	3.25	6.15	8.70	10.05	12.50
PTB84-268	-0.50	0.55	1.35	4.35	7.55	9.40	12.10
PTB84-269	3.20	3.90	5.50	8.15	10.75	11.90	13.45
PTB84-270	3.50	5.30	6.20	7.90	10.35	11.50	13.15
PTB84-271	4.40	6.15	6.95	8.30	10.55	11.65	13.05
PTB84-272	3.70	5.75	6.60	8.30	10.75	11.75	13.15
PTB84-273	3.90	6.10	6.55	8.20	10.45	11.45	12.95
PTB84-274	6.45	7.20	7.60	9.05	11.40	12.30	13.50
PTB84-275	3.70	6.00	6.80	8.35	11.00	12.10	13.50
PTB84-276	3.90	5.20	5.55	7.05	8.60	9.20	10.05
PTB84-277	3.00	3.75	4.20	5.45	7.40	8.75	11.60
PTB84-278	3.30	3.95	4.15	5.10	6.95	8.10	12.50
PTB84-279	2.45	3.20	3.45	4.85	6.25	7.75	12.50
PTB84-280	3.00	4.20	4.75	5.65	7.70	9.20	12.10
PTB84-281	3.10	3.45	3.85	4.55	5.35	6.20	9.60
PTB84-282	2.50	3.10	3.25	3.90	4.60	5.25	7.75
PTB84-283	3.05	3.25	3.40	4.05	4.75	5.55	8.25
PTB84-284	1.95	3.05	3.45	4.70	5.85	6.70	10.00
PTB84-285	-0.55	0.75	2.10	5.50	9.15	11.65	13.30
PTB84-297	0.25	1.55	2.30	3.80	5.45	6.45	10.20
PTB84-298	0.15	1.35	2.05	3.95	5.55	6.70	10.50
PTB84-299	1.15	2.65	3.40	4.65	5.80	6.70	11.50
PTB84-300	1.10	2.55	3.35	4.85	6.60	8.00	11.00
PTB84-301	2.05	3.75	4.15	5.30	6.95	7.85	10.50
PTB84-302	2.10	3.20	4.00	5.55	7.60	8.60	11.20
PTB84-303	-0.50	1.10	2.30	6.40	10.45	11.95	13.40
PTB84-304	-0.50	1.05	2.30	5.55	9.45	11.30	13.25
PTB84-305	-0.20	1.55	2.75	6.70	10.35	11.60	13.20
PTB84-306	1.40	3.85	4.95	8.15	10.85	11.85	13.15
PTB84-307	1.50	5.10	6.00	8.15	11.95	12.75	13.65
PTB84-308	1.10	3.40	4.15	7.00	9.70	11.10	13.00
PTB84-309	2.00	3.95	4.75	7.55	10.30	11.45	13.10
PTB84-310	0.25	3.60	6.00	8.70	10.75	11.70	13.05
PTB84-311	-0.40	1.05	2.25	6.25	9.65	11.35	13.05
PTB84-313	2.35	3.00	3.25	3.90	4.95	5.65	11.50
PTB84-314	0.40	3.40	4.45	6.05	8.90	10.95	13.15
PTB84-315	0.25	2.85	3.85	5.65	8.50	9.95	12.35
PTB84-316	-0.15	2.20	3.90	6.15	8.70	10.75	12.95

PTB84-317	1.05	3.15	3.75	4.10	7.30	9.15	12.50
PTB84-318	0.40	2.45	3.55	5.85	8.85	10.50	12.75
PTB84-319	-0.15	1.35	2.35	4.25	6.85	9.05	12.25
PTB84-320	-0.10	2.00	2.95	4.95	7.85	9.65	12.80
PTB84-321	-0.15	1.55	2.75	4.85	7.45	9.45	12.65
PTB84-324	-0.55	0.45	1.55	5.15	8.55	10.35	12.80
PTB84-325	-0.60	0.85	2.20	6.10	9.15	10.90	12.85
PTB84-326	-0.65	0.30	1.20	5.45	8.20	9.85	12.65
PTB84-327	-0.60	0.60	1.85	6.55	9.60	11.15	13.05
PTB84-328	-0.65	0.55	1.75	6.30	9.15	10.65	12.70
PTB84-329	-0.50	0.50	1.75	6.40	9.15	10.85	12.80
PTB84-330	0.20	1.40	2.40	5.95	8.35	9.55	11.90
PTB84-331	-0.50	0.35	1.15	5.00	8.10	9.60	12.85
PTB84-333	-0.50	0.35	1.20	4.25	6.85	8.15	11.70
PTB84-334	-0.40	0.95	1.95	3.55	6.05	7.65	12.05
PTB84-335	-0.30	0.70	1.50	4.10	7.35	8.35	12.50
PTB84-337	4.40	5.45	6.35	8.10	10.10	11.15	12.85
PTB84-338	3.30	5.25	5.40	5.90	7.15	8.05	11.85
PTB84-339	2.00	4.30	4.95	5.75	6.90	7.70	10.50
PTB84-340	3.00	4.90	5.25	6.00	7.15	7.90	11.30
PTB84-341	3.60	4.75	5.15	6.10	7.20	7.90	11.15
PTB84-342	3.20	4.75	5.10	6.00	7.00	7.60	11.30
PTB84-343	2.00	4.70	5.10	6.10	7.00	7.55	10.40
PTB84-344	2.30	4.55	5.00	5.70	6.75	7.35	10.20
PTB84-346	2.75	3.25	3.55	4.30	5.25	5.95	10.80
PTB84-347	3.20	3.90	4.20	4.70	5.80	6.65	11.50
PTB84-348	6.20	7.15	7.65	8.70	10.65	11.60	13.05
PTB84-349	3.50	6.00	6.65	8.30	10.30	11.30	13.00
PTB84-350	5.20	6.85	7.35	8.65	10.35	11.30	12.85
PTB84-351	-0.60	0.60	1.65	4.65	7.05	9.60	12.70
PTB84-352	-0.10	1.05	1.95	4.25	7.85	9.65	12.55
PTB84-353	-0.05	1.25	2.35	4.90	8.00	9.70	12.30
PTB84-354	-0.15	2.90	4.80	6.65	9.95	11.45	13.20
PTB84-357	3.00	4.05	4.30	5.20	6.30	6.85	10.20
PTB84-362	-0.30	1.40	2.75	6.85	10.05	11.35	13.10
PTB84-363	-0.50	0.85	2.15	6.55	9.90	11.30	13.05
PTB84-370	3.00	5.10	5.70	7.70	10.15	11.30	13.00
PTB84-375	0.55	1.70	2.30	3.65	5.80	6.75	11.50
PTB84-379	0.05	2.55	4.50	7.70	10.80	11.85	13.25
PTB84-381	5.45	6.30	6.75	8.20	10.15	11.15	13.05
PTB84-382	0.15	1.85	2.85	6.30	10.05	11.35	13.05
PTB84-389	-0.30	1.05	2.25	5.05	8.35	11.15	13.15
PTB84-390	4.20	4.95	5.30	6.20	7.15	8.05	11.40
PTB84-391	4.30	5.30	5.55	6.30	7.75	8.95	11.85
PTB84-394	-0.50	0.35	1.25	6.20	9.30	10.90	13.10
PTB84-395	-0.15	1.70	3.00	6.65	9.65	11.55	13.30
PTB84-396	-0.80	0.35	1.50	4.80	7.90	9.00	11.60
PTB84-397	0.30	0.85	2.05	5.85	8.60	9.90	12.10
PTB84-398	-0.60	0.70	2.05	5.80	8.35	9.75	12.05
PTB84-399	-0.40	0.25	0.95	3.05	7.35	9.40	12.70
PTB84-400	1.10	3.25	4.10	5.85	7.85	9.20	11.70
PTB84-401	-0.05	2.40	3.55	6.25	9.10	10.50	12.75
PTB84-402	0.45	2.70	3.45	5.75	8.30	9.80	12.55
PTB84-403	0.05	1.95	3.45	6.45	9.05	10.35	12.60

PTB84-404	-0.20	1.50	2.85	5.30	8.60	10.70	12.95
PTB84-405	-0.20	1.85	3.65	6.70	9.25	10.80	12.90
PTB84-406	0.40	2.65	4.00	6.20	8.15	9.05	12.05
PTB84-407	-0.80	1.55	3.60	6.55	8.65	9.70	11.90
PTB84-408	0.00	2.80	6.05	7.85	10.55	11.80	13.20
PTB84-409	0.15	3.80	5.20	6.90	9.20	10.65	12.90
PTB84-410	-0.20	1.10	2.50	6.65	9.70	11.25	13.20
PTB84-411	-0.80	0.25	0.90	2.65	7.50	9.55	12.40
PTB84-412	0.05	1.65	3.05	6.75	9.45	10.90	12.90
PTB84-413	-0.30	1.35	2.20	6.10	9.05	10.40	12.70
PTB84-414	-0.05	1.85	2.75	6.80	10.20	11.60	13.25
PTB84-415	0.35	2.55	4.65	7.75	10.35	11.45	13.05
PTB84-416	0.10	1.70	3.05	6.65	9.65	11.05	12.85
PTB84-417	-0.10	0.95	1.55	3.80	7.05	8.30	11.45
PTB84-418	0.15	1.70	2.55	5.55	8.30	9.95	12.15
PTB85-1	-0.70	0.20	0.95	2.65	4.05	4.10	11.80
PTB85-4	-0.30	1.25	3.25	4.70	6.45	7.65	11.70
PTB85-9	0.30	4.20	5.85	8.05	10.45	11.55	13.15
PTB85-10	0.40	3.60	5.05	7.80	10.55	11.80	13.30
PTB85-13	2.00	3.00	3.15	4.45	5.65	6.25	12.10
PTB85-16	-0.50	0.30	1.05	3.45	7.20	8.75	12.30
PTB85-17	-0.60	1.00	2.00	5.75	8.35	10.20	12.65
PTB85-18	0.05	1.35	2.30	4.90	8.25	9.95	12.70
PTB85-20	0.00	1.80	2.90	5.00	8.00	9.65	12.20
PTB85-22	-0.10	1.60	3.25	5.30	8.80	10.60	13.05
PTB85-24	0.35	3.25	4.00	7.00	9.45	10.55	12.75
PTB85-25	0.05	2.45	4.15	7.15	9.75	11.00	13.00
PTB85-26	0.05	2.20	3.85	7.05	9.95	11.35	13.25
PTB85-27	-0.20	2.10	4.15	7.05	9.85	11.20	13.10
PTB85-28	-0.50	0.95	3.15	6.35	9.20	10.85	13.00
PTB85-29	-0.40	1.15	2.10	4.55	7.15	8.25	12.10
PTB85-30	-0.20	1.40	2.40	5.25	7.85	9.55	12.05
PTB85-31	-0.05	2.00	3.20	6.15	8.95	10.30	12.15
PTB85-32	-0.30	1.45	2.90	5.00	8.30	9.65	12.55
PTB85-33	-0.40	1.15	2.25	4.85	7.65	9.40	12.75
PTB85-34	0.00	1.30	2.05	4.85	7.75	9.20	12.00
PTB85-35	-0.30	1.05	2.30	5.85	8.45	10.25	12.90
PTB85-36	-0.35	1.25	2.55	5.35	8.10	10.40	13.15
PTB85-37	-0.20	1.65	3.05	5.95	8.65	10.25	12.70
PTB85-38	0.15	1.75	3.30	6.10	9.05	10.65	12.85
PTB85-42	0.00	1.75	3.50	6.85	9.75	11.05	12.95
PTB85-43	-0.05	1.65	3.00	6.00	9.20	10.95	12.95
PTB85-44	-0.05	1.65	3.05	6.85	9.65	11.05	13.05
PTB85-47	-0.25	1.40	3.25	6.75	10.25	11.65	13.35
PTB85-49	-0.30	0.65	1.45	4.05	7.50	9.95	12.95
PTB85-50	-0.20	1.35	3.15	5.70	8.90	10.70	13.00
PTB85-53	-0.15	2.45	4.00	7.05	9.80	11.15	13.05
PTB85-54	0.45	3.05	4.00	7.05	9.80	11.00	13.00
PTB85-56	-0.20	2.30	5.05	7.05	9.95	11.25	13.10
PTB85-57	-0.40	1.15	3.05	6.95	9.65	10.95	12.95
PTB85-63	0.15	1.95	3.95	7.20	10.05	11.40	13.10
PTB85-64	0.15	2.50	4.65	7.05	10.00	11.35	13.05
PTB85-65	-0.20	2.15	3.60	6.85	9.45	10.75	12.95
PTB85-66	0.15	3.00	4.00	6.75	9.50	11.05	13.05

PTB85-67	0.00	2.15	3.45	6.85	9.25	10.55	12.80
PTB85-68	0.00	2.20	3.80	6.75	9.35	10.80	12.85
PTB85-69	-0.05	2.05	3.35	6.65	9.35	10.65	12.70
PTB85-70	0.05	2.55	3.85	6.75	9.70	11.15	13.15
PTB85-71	-0.05	1.55	2.75	6.25	9.00	10.75	12.90
PTB85-72	-0.05	1.65	3.05	6.15	8.65	10.30	12.65
PTB85-73	-0.10	1.65	3.25	6.70	8.95	10.15	12.30
PTB85-74	0.05	1.75	3.20	5.95	7.90	9.05	12.00
PTB85-75	-0.05	1.25	2.05	5.25	7.75	9.00	12.25
PTB85-76	0.05	1.45	3.00	5.20	7.65	8.90	12.00
PTB85-77	0.05	1.45	2.95	5.20	7.55	8.80	11.75
PTB85-78	-0.20	1.05	1.65	4.20	7.15	8.30	10.95
PTB85-79	0.50	2.55	3.80	7.05	9.95	11.20	13.05
PTB84-245	-1.44	1.00	2.46	5.56	8.25	10.13	13.15
PTB84-246	-0.89	1.76	3.10	5.78	8.50	9.75	12.26
PTB84-247	-0.38	2.34	3.69	6.44	9.19	10.46	13.00
PTB84-248	-0.95	1.89	3.30	6.19	9.10	10.43	13.16
PTB84-249	-0.41	2.53	3.99	6.94	9.80	11.15	13.75
PTB84-250	-0.32	2.67	4.15	7.24	10.16	11.63	14.42
PTB84-251	-0.88	2.12	3.60	6.70	9.76	10.63	14.02
PTB84-252	-1.83	1.08	2.52	5.53	8.55	9.99	12.85
PTB84-253	-1.47	1.85	3.54	7.00	10.48	12.09	15.29
PTB84-254	-0.79	2.05	3.46	6.38	9.32	10.68	13.45
PTB84-255	-1.13	1.64	3.00	5.83	8.71	10.01	12.68
PTB84-256	-1.93	1.03	2.59	5.73	8.89	10.33	13.30
PTB84-257	-0.32	2.10	3.31	5.83	8.31	9.51	11.92
PTB84-258	-0.39	2.80	3.31	5.90	8.45	9.65	12.10
PTB84-259	-0.24	2.24	3.49	6.05	8.60	9.80	12.20
PTB84-260	-0.60	1.89	3.12	5.68	8.21	9.36	11.68

Appendix 6. Summarized graphic statistics of particle size analysis data for bulk samples from the northern Rocky Mountain Trench. Data presented is median phi (Md), mean phi (Mz), inclusive graphic standard deviation (Si), inclusive graphic skewness (Ski), and kurtosis (Kg).

SAMPLE	Md	Mz	Si	SKi	KG
PTB84-4	4.55	4.37	2.20	0.00	1.49
PTB84-9	1.65	4.72	5.47	0.66	0.48
PTB84-51	6.65	6.13	4.40	-0.13	0.72
PTB84-52	5.90	6.28	4.78	0.09	0.72
PTB84-53	6.35	5.95	4.62	-0.08	0.69
PTB84-54	6.15	5.93	4.77	-0.03	0.69
PTB84-55	6.25	5.75	4.55	-0.10	0.69
PTB84-61	7.00	6.65	4.18	-0.11	0.80
PTB84-62	6.90	6.72	4.07	-0.07	0.88
PTB84-63	7.15	6.73	4.18	-0.12	0.77
PTB84-64	6.40	6.90	4.46	0.10	0.73
PTB84-65	7.10	6.78	4.26	-0.09	0.83
PTB84-112	7.75	8.43	3.66	0.11	0.97
PTB84-113	8.05	8.63	3.47	0.07	1.10
PTB84-114	5.65	7.03	3.11	0.59	1.22
PTB84-115	7.70	7.93	3.53	-0.01	1.08
PTB84-116	7.80	8.43	3.43	0.12	0.99
PTB84-136	7.25	6.62	4.53	-0.16	0.76
PTB84-137	8.35	8.37	3.76	-0.12	1.20
PTB84-138	7.20	7.33	4.61	-0.02	0.91
PTB84-139	7.45	7.05	4.90	-0.11	0.67
PTB84-140	7.40	7.72	4.50	0.00	1.00
PTB84-151	6.70	6.43	4.80	-0.05	0.66
PTB84-152	5.25	5.95	5.00	0.17	0.66
PTB84-153	5.05	5.98	5.04	0.22	0.64
PTB84-154	5.35	6.03	4.97	0.17	0.65
PTB84-155	5.05	5.95	5.01	0.22	0.67
PTB84-156	6.05	6.43	4.95	0.09	0.64
PTB84-169	6.10	6.02	4.45	0.00	0.78
PTB84-186	3.55	3.97	3.63	0.22	0.83
PTB84-187	5.30	5.22	2.30	-0.02	1.41
PTB84-188	5.20	4.87	2.16	-0.28	1.17
PTB84-189	5.10	4.93	2.52	0.00	1.28
PTB84-190	4.95	5.27	2.58	0.23	1.30
PTB84-191	7.25	7.55	2.86	0.14	0.99
PTB84-192	5.75	6.25	2.70	0.30	0.92
PTB84-201	4.40	4.40	1.43	0.17	1.37
PTB84-203	6.35	6.38	3.87	0.01	1.01
PTB84-204	6.25	6.22	3.97	0.01	0.88
PTB84-205	5.75	6.02	3.82	0.11	0.94
PTB84-206	5.90	6.03	3.86	0.06	0.89
PTB84-207	6.95	6.95	3.96	-0.03	0.93
PTB84-208	7.10	6.98	3.94	-0.06	0.98
PTB84-209	6.45	6.40	4.03	0.00	0.83
PTB84-210	6.10	6.15	4.17	0.04	0.87
PTB84-211	6.20	6.10	4.03	-0.01	0.83
PTB84-212	6.15	6.27	4.28	0.04	0.81

PTB84-218	3.45	3.78	1.47	0.55	2.36
PTB84-219	3.65	3.78	1.16	0.40	1.86
PTB84-220	3.90	3.98	1.39	0.33	2.19
PTB84-221	4.45	4.45	1.45	0.17	1.35
PTB84-222	3.90	4.00	1.95	0.40	2.66
PTB84-223	4.25	4.53	1.91	0.43	2.21
PTB84-224	4.20	4.25	1.44	0.22	1.60
PTB84-236	9.05	9.28	2.40	0.11	0.89
PTB84-237	9.25	9.57	2.26	0.18	0.88
PTB84-238	9.45	9.78	2.09	0.24	0.81
PTB84-239	9.75	10.00	1.91	0.18	0.81
PTB84-240	9.25	9.52	2.20	0.19	0.84
PTB84-241	9.35	9.53	2.26	0.08	0.90
PTB84-264	5.20	5.38	4.31	0.09	0.87
PTB84-265	4.25	4.67	3.95	0.21	0.93
PTB84-266	7.10	6.82	3.90	-0.11	1.11
PTB84-267	6.15	6.00	3.98	-0.03	0.95
PTB84-268	4.35	4.77	4.12	0.19	0.83
PTB84-269	8.15	7.98	3.55	-0.01	0.80
PTB84-270	7.90	8.23	3.01	0.12	0.95
PTB84-271	8.30	8.70	2.69	0.16	0.98
PTB84-272	8.30	8.60	2.93	0.09	0.93
PTB84-273	8.20	8.58	2.71	0.13	0.95
PTB84-274	9.05	9.52	2.34	0.27	0.76
PTB84-275	8.35	8.82	3.01	0.14	0.96
PTB84-276	7.05	7.15	1.93	0.03	0.83
PTB84-277	5.45	5.98	2.55	0.38	1.10
PTB84-278	5.10	5.72	2.43	0.53	1.35
PTB84-279	4.85	5.27	2.66	0.40	1.47
PTB84-280	5.65	6.35	2.63	0.42	1.26
PTB84-281	4.55	4.73	1.67	0.38	1.78
PTB84-282	3.90	4.08	1.33	0.36	1.59
PTB84-283	4.05	4.28	1.36	0.46	1.58
PTB84-284	4.70	4.82	2.13	0.21	1.37
PTB84-285	5.50	5.97	4.82	0.13	0.81
PTB84-297	3.80	3.93	2.73	0.18	1.29
PTB84-298	3.95	4.00	2.91	0.15	1.21
PTB84-299	4.65	4.67	2.58	0.17	1.77
PTB84-300	4.85	5.13	2.86	0.20	1.25
PTB84-301	5.30	5.63	2.31	0.24	1.24
PTB84-302	5.55	5.78	2.73	0.19	1.04
PTB84-303	6.40	6.48	4.82	0.02	0.70
PTB84-304	5.55	5.97	4.65	0.12	0.79
PTB84-305	6.70	6.62	4.54	-0.03	0.72
PTB84-306	8.15	7.95	3.78	-0.11	0.82
PTB84-307	8.15	8.67	3.75	0.05	0.84
PTB84-308	7.00	7.17	3.73	0.04	0.88
PTB84-309	7.55	7.65	3.56	0.02	0.82
PTB84-310	8.70	8.00	3.96	-0.29	1.10
PTB84-311	6.25	6.22	4.61	0.00	0.74
PTB84-313	3.90	4.18	2.05	0.49	2.21
PTB84-314	6.05	6.80	3.82	0.21	1.17
PTB84-315	5.65	6.15	3.61	0.16	1.07
PTB84-316	6.15	6.37	4.12	0.06	1.12

PTB84-317	4.10	5.47	3.23	0.58	1.32
PTB84-318	5.85	6.27	3.88	0.14	0.95
PTB84-319	4.25	4.88	3.80	0.27	1.13
PTB84-320	4.95	5.53	3.87	0.22	1.08
PTB84-321	4.85	5.28	3.91	0.19	1.12
PTB84-324	5.15	5.32	4.50	0.10	0.78
PTB84-325	6.10	5.95	4.55	-0.02	0.79
PTB84-326	5.45	5.20	4.40	0.00	0.78
PTB84-327	6.55	6.10	4.71	-0.09	0.72
PTB84-328	6.30	5.83	4.55	-0.09	0.74
PTB84-329	6.40	5.92	4.60	-0.09	0.74
PTB84-330	5.95	5.63	3.81	-0.05	0.81
PTB84-331	5.00	4.98	4.34	0.09	0.79
PTB84-333	4.25	4.25	3.80	0.11	0.88
PTB84-334	3.55	4.05	3.56	0.29	1.24
PTB84-335	4.10	4.38	3.85	0.21	0.90
PTB84-337	8.10	8.23	2.71	0.10	0.92
PTB84-338	5.90	6.40	2.00	0.46	2.00
PTB84-339	5.75	5.92	2.14	0.13	1.79
PTB84-340	6.00	6.27	2.01	0.27	1.79
PTB84-341	6.10	6.25	1.93	0.24	1.51
PTB84-342	6.00	6.12	1.94	0.22	1.75
PTB84-343	6.10	6.12	1.99	0.02	1.81
PTB84-344	5.70	5.87	1.90	0.16	1.85
PTB84-346	4.30	4.50	1.89	0.42	1.94
PTB84-347	4.70	5.08	1.95	0.53	2.13
PTB84-348	8.70	9.15	2.15	0.29	0.94
PTB84-349	8.30	8.53	2.76	0.06	1.07
PTB84-350	8.65	8.93	2.27	0.14	1.05
PTB84-351	4.65	4.95	4.27	0.16	1.01
PTB84-352	4.25	4.98	4.07	0.28	0.88
PTB84-353	4.90	5.28	3.98	0.17	0.90
PTB84-354	6.65	7.00	4.16	0.05	1.06
PTB84-357	5.20	5.37	1.79	0.28	1.48
PTB84-362	6.85	6.53	4.52	-0.08	0.75
PTB84-363	6.55	6.23	4.67	-0.07	0.72
PTB84-370	7.70	8.03	3.07	0.11	0.92
PTB84-375	3.65	4.03	2.92	0.33	1.28
PTB84-379	7.70	7.37	4.33	-0.13	0.86
PTB84-381	8.20	8.55	2.36	0.25	0.92
PTB84-382	6.30	6.50	4.33	0.05	0.73
PTB84-389	5.05	5.75	4.56	0.21	0.90
PTB84-390	6.20	6.40	1.87	0.32	1.60
PTB84-391	6.30	6.85	2.06	0.46	1.41
PTB84-394	6.20	5.82	4.70	-0.05	0.69
PTB84-395	6.65	6.63	4.50	-0.01	0.83
PTB84-396	4.80	4.72	4.04	0.03	0.79
PTB84-397	5.85	5.53	4.05	-0.02	0.74
PTB84-398	5.80	5.42	4.18	-0.07	0.82
PTB84-399	3.05	4.23	4.27	0.43	0.84
PTB84-400	5.85	6.10	3.09	0.11	1.16
PTB84-401	6.25	6.38	3.96	0.03	0.95
PTB84-402	5.75	6.08	3.61	0.13	1.02
PTB84-403	6.45	6.25	4.00	-0.05	0.92

PTB84-404	5.80	6.00	4.29	0.08	0.94
PTB84-405	6.70	6.45	4.22	-0.07	0.96
PTB84-406	6.20	5.97	3.37	-0.05	1.15
PTB84-407	6.55	5.93	3.96	-0.19	1.03
PTB84-408	7.85	7.48	4.25	-0.16	1.20
PTB84-409	6.90	7.12	3.64	0.02	1.31
PTB84-410	6.65	6.33	4.57	-0.06	0.76
PTB84-411	2.65	4.15	4.33	0.48	0.82
PTB84-412	6.75	6.43	4.26	-0.07	0.82
PTB84-413	6.10	5.95	4.23	-0.02	0.78
PTB84-414	6.80	6.75	4.45	-0.02	0.73
PTB84-415	7.75	7.25	4.15	-0.17	0.91
PTB84-416	6.65	6.47	4.27	-0.04	0.79
PTB84-417	3.80	4.35	3.59	0.27	0.86
PTB84-418	5.55	5.73	3.88	0.08	0.86
PTB85-1	2.65	2.32	2.87	0.10	1.65
PTB85-4	4.70	4.53	3.42	0.04	1.54
PTB85-9	8.05	7.93	3.78	-0.13	1.14
PTB85-10	7.80	7.73	4.00	-0.09	0.96
PTB85-13	4.45	4.57	2.34	0.31	1.66
PTB85-16	3.45	4.17	4.05	0.32	0.85
PTB85-17	5.75	5.55	4.31	0.00	0.86
PTB85-18	4.90	5.40	4.07	0.20	0.87
PTB85-20	5.00	5.48	3.81	0.18	0.98
PTB85-22	5.30	5.83	4.24	0.18	0.97
PTB85-24	7.00	6.93	3.70	-0.05	0.93
PTB85-25	7.15	6.87	4.10	-0.10	0.95
PTB85-26	7.05	6.87	4.29	-0.06	0.89
PTB85-27	7.05	6.78	4.29	-0.09	0.96
PTB85-28	6.35	6.05	4.52	-0.05	0.91
PTB85-29	4.55	4.65	3.67	0.13	1.01
PTB85-30	5.25	5.40	3.89	0.08	0.92
PTB85-31	6.15	6.15	3.92	-0.01	0.87
PTB85-32	5.00	5.37	4.00	0.15	0.98
PTB85-33	4.85	5.13	4.05	0.15	1.00
PTB85-34	4.85	5.12	3.79	0.15	0.86
PTB85-35	5.85	5.72	4.30	0.01	0.88
PTB85-36	5.35	5.67	4.33	0.13	1.00
PTB85-37	5.95	5.95	4.10	0.02	0.94
PTB85-38	6.10	6.17	4.15	0.04	0.91
PTB85-42	6.85	6.55	4.29	-0.08	0.85
PTB85-43	6.00	6.20	4.29	0.07	0.86
PTB85-44	6.85	6.52	4.33	-0.08	0.81
PTB85-47	6.75	6.60	4.62	-0.04	0.80
PTB85-49	4.05	4.88	4.33	0.31	0.90
PTB85-50	5.70	5.92	4.34	0.09	0.94
PTB85-53	7.05	6.88	4.18	-0.07	0.93
PTB85-54	7.05	7.03	3.89	-0.03	0.89
PTB85-56	7.05	6.87	4.25	-0.08	1.11
PTB85-57	6.95	6.35	4.47	-0.14	0.83
PTB85-63	7.20	6.85	4.32	-0.10	0.87
PTB85-64	7.05	6.97	4.17	-0.05	0.99
PTB85-65	6.85	6.58	4.14	-0.08	0.92
PTB85-66	6.75	6.93	3.97	0.02	0.96

PTB85-67	6.85	6.52	4.04	-0.09	0.90
PTB85-68	6.75	6.58	4.10	-0.05	0.95
PTB85-69	6.65	6.45	4.08	-0.06	0.87
PTB85-70	6.75	6.82	4.13	0.00	0.92
PTB85-71	6.25	6.18	4.26	0.00	0.85
PTB85-72	6.15	6.03	4.09	-0.01	0.93
PTB85-73	6.70	6.17	4.00	-0.14	0.89
PTB85-74	5.95	5.58	3.64	-0.07	1.04
PTB85-75	5.25	5.17	3.80	0.05	0.88
PTB85-76	5.20	5.18	3.67	0.07	1.05
PTB85-77	5.20	5.15	3.61	0.05	1.04
PTB85-78	4.20	4.52	3.50	0.17	0.83
PTB85-79	7.05	6.93	4.06	-0.04	0.84
PTB84-245	5.56	5.56	4.49	0.02	1.03
PTB84-246	5.78	5.76	3.99	-0.01	1.00
PTB84-247	6.44	6.41	4.06	-0.01	1.00
PTB84-248	6.19	6.17	4.27	-0.01	1.00
PTB84-249	6.94	6.87	4.30	-0.03	1.00
PTB84-250	7.24	7.18	4.47	-0.02	1.01
PTB84-251	6.70	6.48	4.39	-0.05	0.99
PTB84-252	5.53	5.53	4.45	0.00	1.00
PTB84-253	7.00	6.98	5.10	-0.01	0.99
PTB84-254	6.38	6.37	4.32	-0.01	1.00
PTB84-255	5.83	5.83	4.18	0.00	0.99
PTB84-256	5.73	5.70	4.63	-0.01	0.99
PTB84-257	5.83	5.81	3.71	-0.01	1.00
PTB84-258	5.90	6.12	3.60	0.04	1.00
PTB84-259	6.05	6.03	3.77	-0.01	1.00
PTB84-260	5.68	5.64	3.73	-0.02	0.99

Appendix 7. Graphic statistic measures, equations and terminological classifications used for bulk samples from northeastern B.C., adapted from Folk (1974).

The descriptive statistics generated include measures of central tendency, a measure of uniformity (sorting of the sediment), a measure of skewness (degree of asymmetry) and a measure of peakedness (kurtosis). Calculated measures and the equations employed follow:

Median (Md) = (Ø50)

Mean (Mz) = (Ø16+Ø50+Ø84)/3

Inclusive Graphic Standard Deviation (Si) = (Ø84-Ø16)/4 + (Ø95-Ø5)/6.6

Inclusive Graphic Skewness (Ski) = $\frac{(Ø16+Ø84-2Ø50)}{2(Ø84-Ø16)} + \frac{(Ø5+Ø95-2Ø50)}{2(Ø95-Ø5)}$

Kurtosis (Kg) = (Ø95-Ø5)/ 2.44(Ø75-Ø25)

For the measures of central tendency the values are presented in phi units. The mean is much preferred over the median estimate, although both are presented for comparison. Inclusive graphic standard deviation, also in phi units, provides a numerical estimate of sediment sorting (includes 90% of the curve) usually ranging from 0 to > 4.0. Terminological classification of these values is as follows:

< 0.35 Ø very well sorted	1.00-2.00Ø poorly sorted
0.35-0.50Ø well sorted	2.00-4.00Ø very poorly sorted
0.50-0.71Ø moderately well sorted	> 4.00Ø extremely poorly sorted
0.71-1.00Ø moderately sorted	

Inclusive graphic skewness, is a unitless measure covering 90% of the grain size distribution. The distance of the tails from the median are determined by this measure with values ranging between -1.0 and 1.0. Terminological classification of these values is as follows:

+1.00 to +0.30	strongly fine-skewed
+0.30 to +0.10	fine-skewed
+0.10 to -0.10	near-symmetrical
-0.10 to -0.30	coarse skewed
-0.30 to -1.00	strongly coarse skewed

The final statistic, kurtosis, is another unitless measure which describes the ratio of tail sorting to modal sorting in the lognormal frequency distribution. Values range from 0 to > 3.00 for which the following terminological classification can be used:

< 0.67	very platykurtic
0.67-0.90	platykurtic
0.90-1.11	mesokurtic
1.11-1.50	leptokurtic
1.50-3.00	very leptokurtic
>3.00	extremely leptokurtic

Appendix 8. Percentage of gravel, very coarse sand, coarse sand, medium sand, fine sand, very fine sand, and silt/clay for sieved bulk samples from the northern Rocky Mountain Trench.

SAMPLE NO.	-1.0Ø	0.0Ø	1.0Ø	2.0Ø	3.0Ø	4.0Ø	> 5.0Ø	TOTAL
PTB84-2	0.45	0.68	0.45	0.68	5.68	21.59	70.45	100
PTB84-3	1.60	2.70	2.10	44.90	32.90	9.30	6.50	100
PTB84-6	0.10	0.10	0.10	2.41	34.81	33.80	28.67	100
PTB84-10	0.30	0.10	0.81	8.27	30.75	34.78	25.00	100
PTB84-11	6.23	7.86	8.46	34.27	15.58	9.94	17.66	100
PTB84-15	23.70	19.80	21.60	18.20	5.00	4.50	7.20	100
PTB84-16	13.01	16.82	20.42	18.22	7.11	7.11	17.32	100
PTB84-17	1.40	2.69	8.67	35.09	18.15	11.76	22.23	100
PTB84-18	34.45	21.92	13.15	13.46	6.52	4.08	6.42	100
PTB84-19	26.10	15.42	18.29	28.26	8.32	1.44	2.16	100
PTB84-20	0.10	0.20	0.20	0.10	0.50	28.01	70.88	100
PTB84-21	26.67	24.41	18.36	21.23	4.51	1.64	3.18	100
PTB84-22	2.74	2.43	3.75	44.42	21.10	13.39	12.17	100
PTB84-23	0.20	1.61	5.22	45.38	29.12	11.04	7.43	100
PTB84-24	16.57	0.81	1.12	1.52	4.67	26.52	48.78	100
PTB84-25	32.48	26.35	12.05	12.46	5.01	3.58	8.07	100
PTB84-28	0.40	0.20	0.20	0.71	6.76	36.73	54.99	100
PTB84-30	18.60	17.40	33.60	27.70	1.50	0.60	0.60	100
PTB84-31	21.79	17.87	25.20	29.72	2.91	1.31	1.20	100
PTB84-32	10.76	5.01	2.75	4.38	3.88	11.64	61.58	100
PTB84-33	33.74	19.34	12.08	18.93	7.15	3.73	5.04	100
PTB84-36	14.34	25.13	22.08	22.08	7.02	4.58	4.78	100
PTB84-37	9.18	11.43	14.90	23.57	21.12	13.98	5.82	100
PTB84-40	30.87	34.92	14.88	8.91	2.94	2.43	5.06	100
PTB84-41	35.99	23.72	16.46	13.29	3.58	2.76	4.19	100
PTB84-43	0.20	0.31	0.31	19.90	44.08	25.61	9.59	100
PTB84-45	1.16	1.45	3.48	26.81	19.86	16.81	30.43	100
PTB84-46	15.38	27.23	26.52	16.09	4.05	2.83	7.89	100
PTB84-49	19.79	30.77	22.05	11.69	3.90	5.13	6.67	100
PTB84-58	19.46	24.97	29.14	23.62	1.87	0.10	0.83	100
PTB84-66	0.10	0.10	0.10	0.10	1.83	31.07	66.70	100
PTB84-67	23.25	18.21	13.79	21.91	8.54	5.56	8.74	100
PTB84-70	22.82	20.47	26.41	21.80	2.66	2.35	3.48	100
PTB84-72	37.00	30.78	19.98	8.66	1.02	1.02	1.53	100
PTB84-74	57.20	36.71	5.07	0.10	0.10	0.10	0.71	100
PTB84-76	0.20	0.20	0.10	19.80	52.18	20.41	7.11	100
PTB84-78	46.84	25.66	15.27	7.74	2.14	0.92	1.43	100
PTB84-80	0.61	0.31	1.12	22.55	23.16	27.04	25.20	100
PTB84-82	0.91	0.30	0.51	1.42	1.02	2.84	92.99	100
PTB84-83	29.33	30.78	21.87	13.68	2.28	0.83	1.24	100
PTB84-86	34.79	26.65	20.35	16.17	0.92	0.41	0.71	100
PTB84-88	9.46	12.27	7.07	6.44	3.85	12.16	48.75	100
PTB84-89	12.26	22.68	29.93	25.33	4.39	2.35	3.06	100
PTB84-91	17.02	35.58	28.64	10.50	2.34	1.63	4.28	100
PTB84-92	0.10	0.10	0.70	7.61	8.21	23.12	60.16	100
PTB84-93	29.16	13.04	20.53	27.31	5.03	2.16	2.77	100
PTB84-95	21.82	28.85	20.68	12.41	4.76	4.76	6.72	100

PTB84-96	18.76	24.46	27.01	26.40	2.34	0.41	0.61	100
PTB84-98	28.13	27.40	24.06	16.67	1.67	0.63	1.46	100
PTB84-100	13.56	24.46	18.45	13.97	7.03	8.15	14.37	100
PTB84-101	5.69	13.21	34.45	37.91	5.18	1.42	2.13	100
PTB84-103	0.00	0.00	0.10	1.42	14.76	46.31	37.41	100
PTB84-107	36.35	37.47	18.13	6.72	0.71	0.31	0.31	100
PTB84-109	3.67	5.40	16.29	53.77	14.46	3.67	2.75	100
PTB84-110	21.22	28.12	21.93	20.00	3.96	1.83	2.94	100
PTB84-118	21.68	23.21	15.54	9.10	2.86	3.78	23.82	100
PTB84-119	27.10	20.74	21.97	21.25	3.18	1.23	4.52	100
PTB84-121	3.47	0.20	0.82	0.82	2.04	15.09	77.57	100
PTB84-124	25.94	21.57	13.33	16.79	9.66	7.02	5.70	100
PTB84-126	0.10	0.41	0.31	4.27	8.65	26.04	60.22	100
PTB84-127	34.39	27.21	17.56	10.27	2.77	2.26	5.54	100
PTB84-130	28.60	23.08	26.15	20.33	1.23	0.10	0.51	100
PTB84-133	23.73	28.50	39.05	8.22	0.20	0.10	0.20	100
PTB84-141	21.35	18.69	24.21	24.31	6.64	1.84	2.96	100
PTB84-143	0.20	0.20	0.50	2.01	9.97	32.02	55.09	100
PTB84-144	37.15	19.55	10.34	9.31	5.02	6.04	12.59	100
PTB84-157	50.55	1.72	2.83	8.98	10.60	8.58	16.75	100
PTB84-158	35.76	24.69	10.86	10.35	6.15	4.20	7.99	100
PTB84-160	0.00	0.10	0.20	3.71	21.56	49.05	25.38	100
PTB84-161	2.46	7.68	25.41	51.43	7.27	2.46	3.28	100
PTB84-163	36.67	26.35	17.98	11.85	5.82	0.82	0.51	100
PTB84-165	0.51	0.10	0.51	22.79	48.93	21.26	5.90	100
PTB84-166	26.52	14.90	15.93	34.43	5.86	1.13	1.23	100
PTB84-172	22.06	19.51	17.67	13.48	3.06	2.45	21.76	100
PTB84-180	47.58	29.80	14.95	5.05	0.61	0.40	1.62	100
PTB84-182	21.84	3.06	4.80	8.06	7.14	11.12	43.98	100
PTB84-184	33.37	33.77	26.63	5.13	0.30	0.30	0.50	100
PTB84-214	6.27	10.89	45.63	32.58	2.26	0.92	1.44	100
PTB84-227	37.89	23.82	16.53	16.94	3.29	0.62	0.92	100
PTB84-229	32.29	27.65	18.97	14.13	3.13	1.61	2.22	100
PTB84-231	32.76	33.06	16.84	8.52	2.03	2.54	4.26	100
PTB84-234	18.09	23.33	18.50	14.90	6.68	7.09	11.41	100
PTB84-235	0.00	17.16	13.39	43.13	17.49	5.48	3.36	100
PTB84-243	0.00	35.60	24.66	25.06	6.06	3.31	5.31	100
PTB84-262	0.00	8.22	69.56	20.38	1.04	0.18	0.63	100
PTB84-322	0.00	2.83	28.45	46.72	17.95	1.77	2.29	100
PTB84-323	0.03	21.34	39.55	19.53	11.09	2.70	5.76	100
PTB84-332	0.06	28.54	15.50	27.14	14.57	6.17	8.03	100
PTB84-364	0.02	29.84	22.84	24.38	6.76	5.42	10.75	100
PTB84-366	6.14	4.84	10.32	51.17	17.77	5.73	4.03	100
PTB84-368	0.00	6.88	27.03	24.05	17.75	7.57	16.73	100
PTB84-371	0.00	18.25	40.75	24.51	9.35	2.00	5.14	100
PTB84-377	0.00	5.16	18.29	63.36	10.79	0.90	1.50	100
PTB84-380	0.00	0.00	0.08	28.23	50.47	16.22	5.00	100
PTB84-383	0.05	14.98	50.23	28.00	5.36	0.61	0.78	100
PTB84-386	0.00	14.34	59.41	23.44	2.22	0.14	0.44	100
PTB84-392	0.00	5.19	8.63	42.94	22.98	12.16	8.10	100
PTB84-393	0.00	0.14	0.17	0.17	0.69	9.57	89.26	100
PTB84-419	0.00	17.26	33.38	15.76	17.18	6.28	10.15	100
PTB84-421	1.24	0.19	0.59	38.68	38.66	12.01	8.64	100
PTB84-423	0.00	26.94	22.05	27.15	7.32	4.78	11.75	100

PTB85-2	34.49	22.17	20.87	7.06	8.25	1.79	5.37	100
PTB85-6	38.10	30.00	24.40	3.20	2.70	0.80	0.80	100
PTB85-11	30.51	10.40	10.00	32.73	0.81	11.92	3.64	100
PTB85-14	61.07	6.14	1.91	0.80	4.63	6.24	19.22	100
PTB85-39	29.09	12.04	12.44	32.10	1.20	10.13	3.01	100
PTB85-46	5.90	2.90	3.80	20.30	1.10	49.10	16.90	100

Appendix 9. Textural histograms for all unconsolidated nondiamicton samples from the Finlay River detailed in Appendix 8.

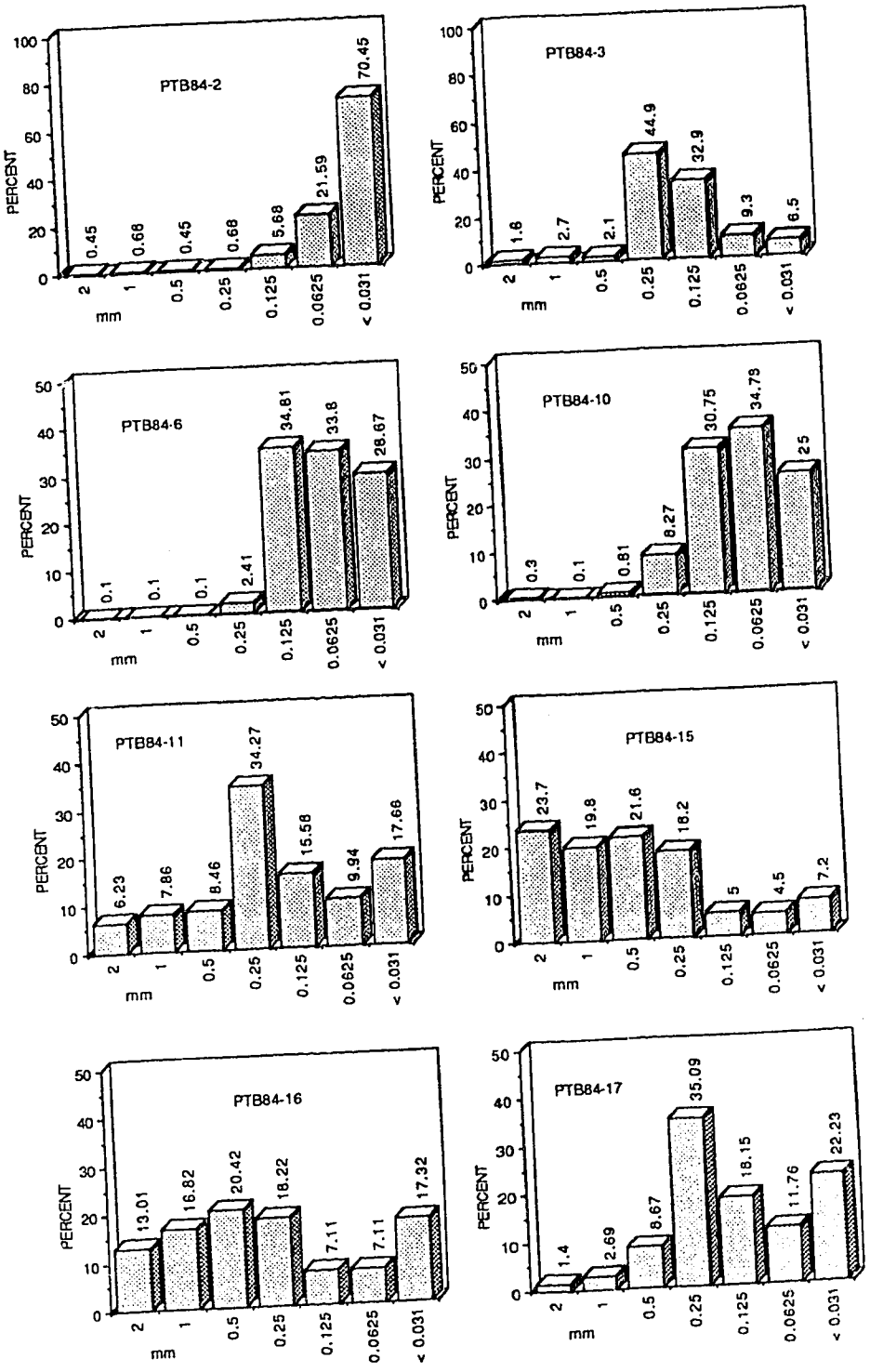
PTB84-2
PERCENT
0.45
0.68
0.45
0.68
5.68
21.59
70.45
2
1
0.5
0.25
0.125
0.0625
< 0.031
mm
PTB84-3
1.6
2.7
2.1
44.9
32.9
9.3
6.5
PTB84-6
0.1
0.1
0.1
2.41
34.81
33.8
28.67
PTB84-10
0.3
0.1
0.81
8.27
30.75
34.78
25
PTB84-11
6.23
7.86
8.46
34.27
15.58
9.94
17.66
PTB84-15
23.7
19.8
21.6
18.2
5
4.5
7.2
PTB84-16
13.01
16.82
20.42
18.22
7.11
7.11
17.32
PTB84-17
1.4
2.69
8.67
35.09
18.15
11.76
22.23

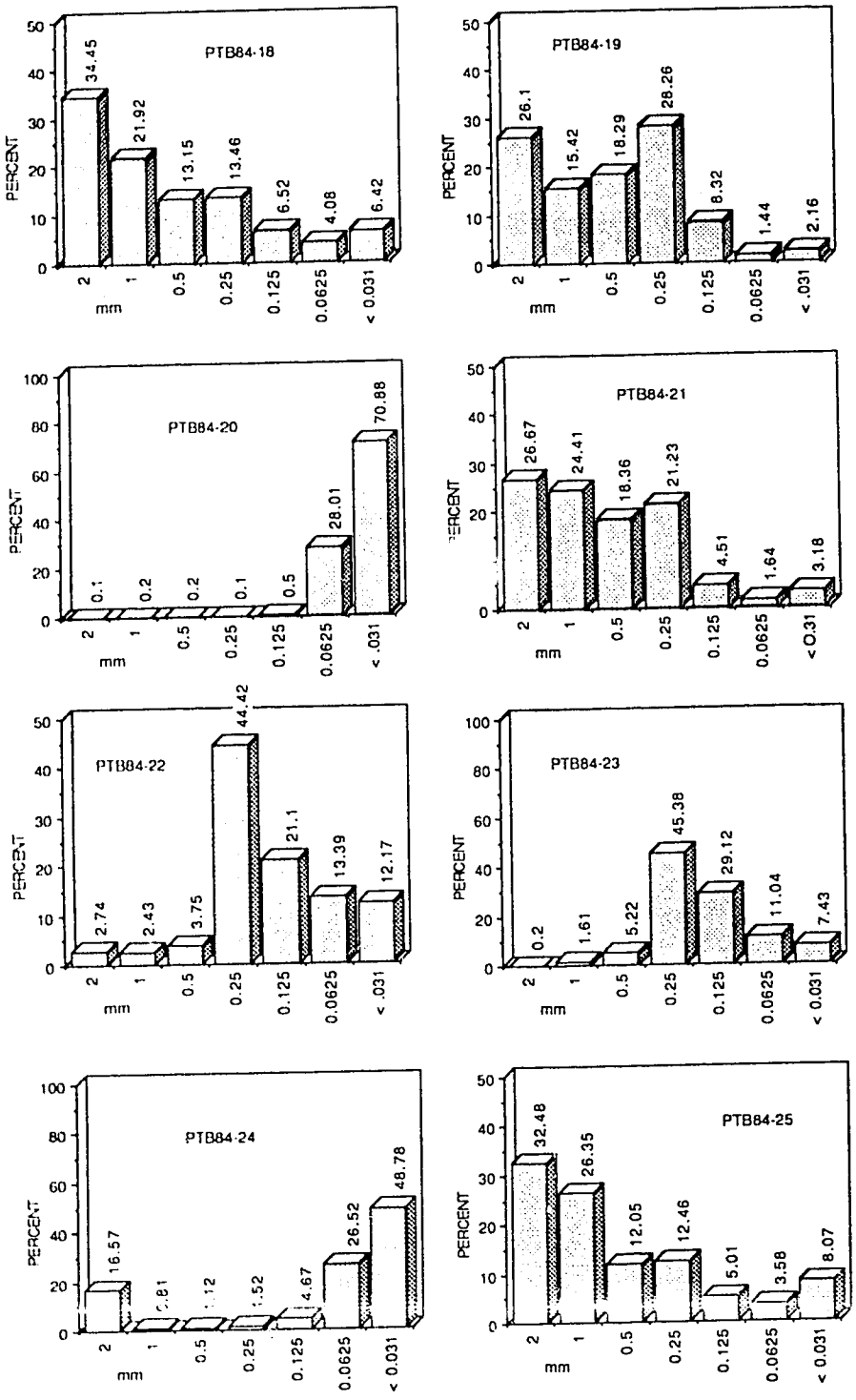
PTB84-18
PERCENT
34.45
21.92
13.15
13.46
6.52
4.08
6.42
2
1
0.5
0.25
0.125
0.0625
< 0.031
mm
PTB84-19
26.1
15.42
18.29
28.26
8.32
1.44
2.16
< .031
PTB84-20
0.1
0.2
0.2
0.1
0.5
28.01
70.88
< .031
PTB84-21
26.67
24.41
18.36
21.23
4.51
1.64
3.18
< 0.31
PTB84-22
2.74
2.43
3.75
44.42
21.1
13.39
12.17
< .031
PTB84-23
0.2
1.61
5.22
45.38
29.12
11.04
7.43
< 0.031
PTB84-24
16.57
26.52
48.78
< 0.031
PTB84-25
32.48
26.35
12.05
12.46
5.01
3.58
8.07
< 0.031

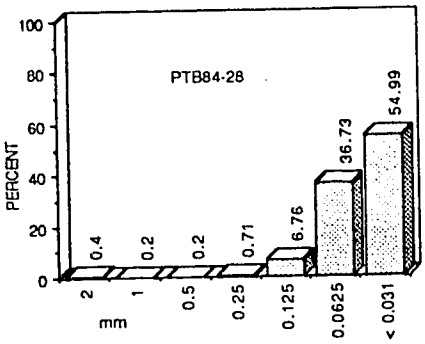
PTB84-28
PERCENT
0.4
0.2
0.2
0.71
6.76
36.73
54.99
2
1
0.5
0.25
0.125
0.0625
< 0.031
mm

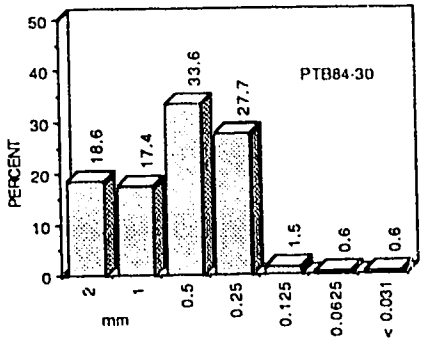
PTB84-30
PERCENT
18.6
17.4
33.6
27.7
1.5
0.6
0.6
2
1
0.5
0.25
0.125
0.0625
< 0.031
mm

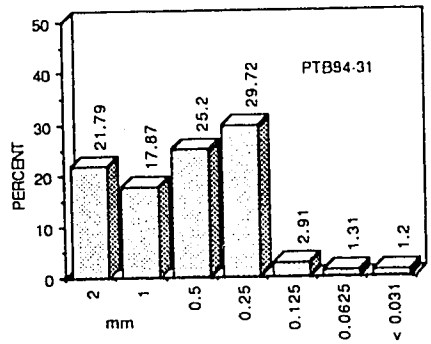
PTB84-31
PERCENT
21.79
17.87
25.2
29.72
2.91
1.31
1.2
2
1
0.5
0.25
0.125
0.0625
< 0.031
mm

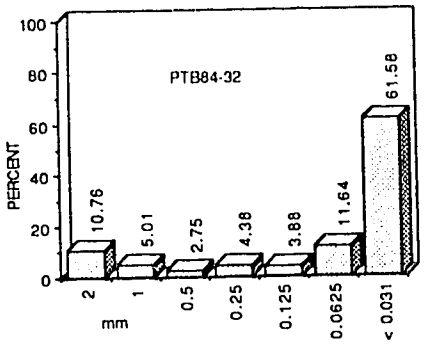
PTB84-32
PERCENT
10.76
5.01
2.75
4.38
3.88
11.64
61.58
2
1
0.5
0.25
0.125
0.0625
< 0.031
mm

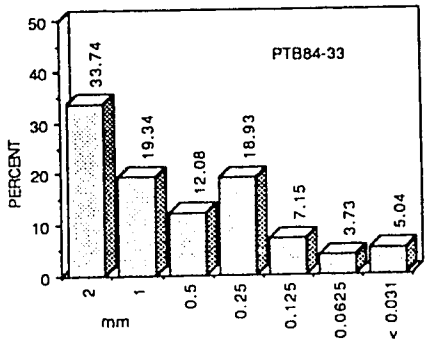
PTB84-33
PERCENT
33.74
19.34
12.08
18.93
7.15
3.73
5.04
2
1
0.5
0.25
0.125
0.0625
< 0.031
mm

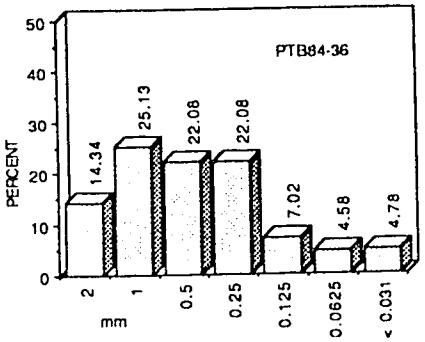
PTB84-36
PERCENT
14.34
25.13
22.08
22.08
7.02
4.58
4.78
2
1
0.5
0.25
0.125
0.0625
< 0.031
mm

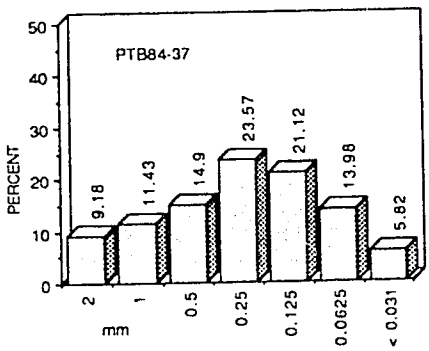
PTB84-37
PERCENT
9.18
11.43
14.9
23.57
21.12
13.98
5.82
2
1
0.5
0.25
0.125
0.0625
< 0.031
mm

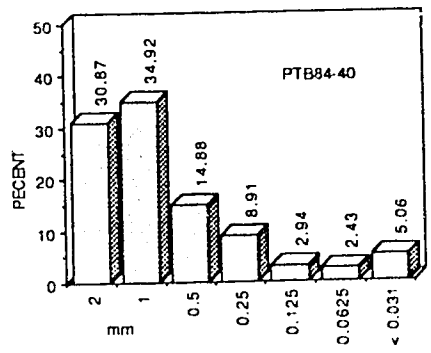
PTB84-40
PECENT
30.87
34.92
14.88
8.91
2.94
2.43
5.06
2
1
0.5
0.25
0.125
0.0625
< 0.031
mm

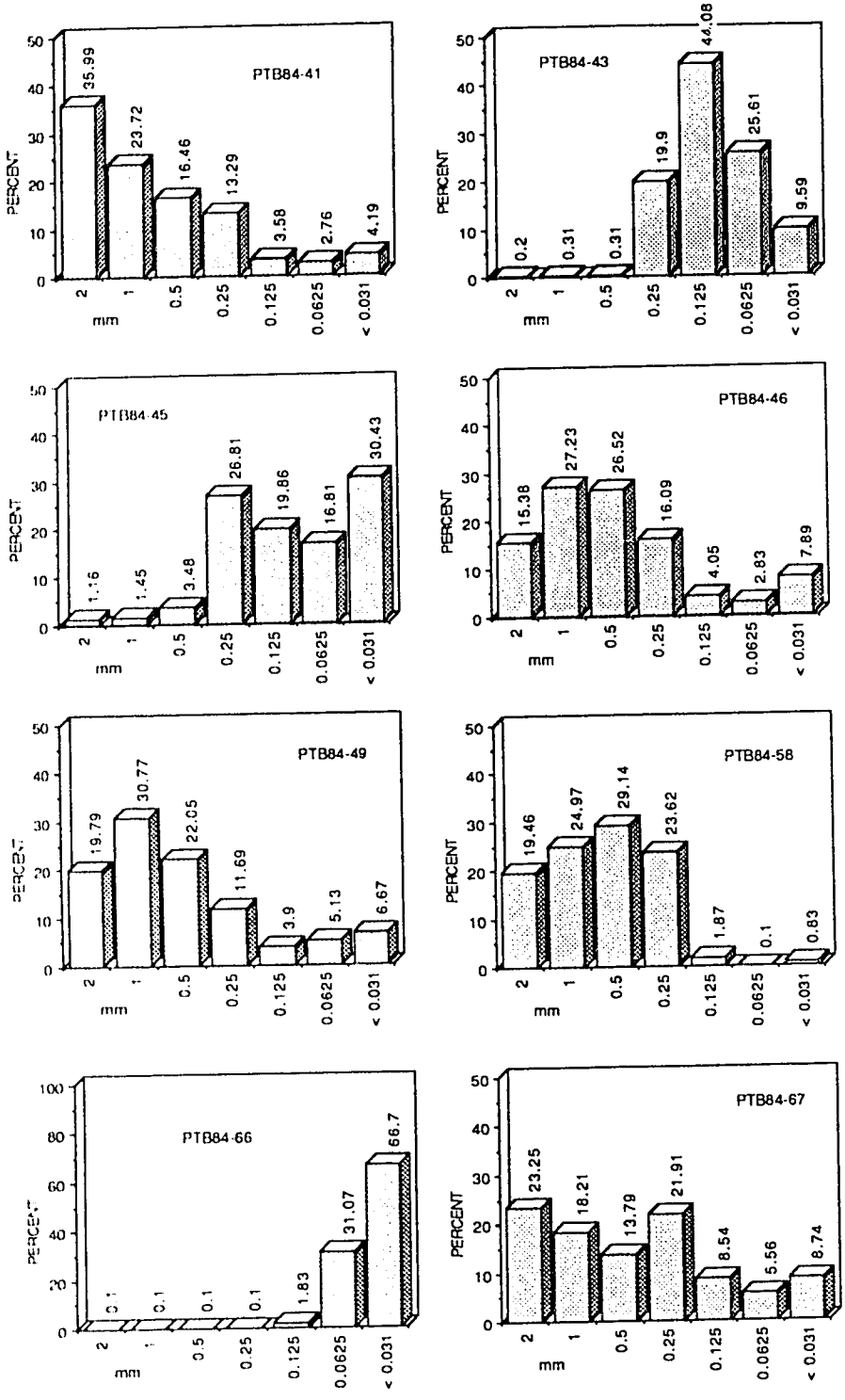
PTB84-41
PERCENT
35.99
23.72
16.46
13.29
3.58
2.76
4.19
mm
2
1
0.5
0.25
0.125
0.0625
< 0.031
PTB84-43
0.2
0.31
0.31
19.9
44.08
25.61
9.59
PTB84-45
1.16
1.45
3.48
26.81
19.86
16.81
30.43
PTB84-46
15.38
27.23
26.52
16.09
4.05
2.83
7.89
PTB84-49
19.79
30.77
22.05
11.69
3.9
5.13
6.67
PTB84-58
19.46
24.97
29.14
23.62
1.87
0.1
0.83
PTB84-66
0.1
0.1
0.1
0.1
1.83
31.07
66.7
PTB84-67
23.25
18.21
13.79
21.91
8.54
5.56
8.74

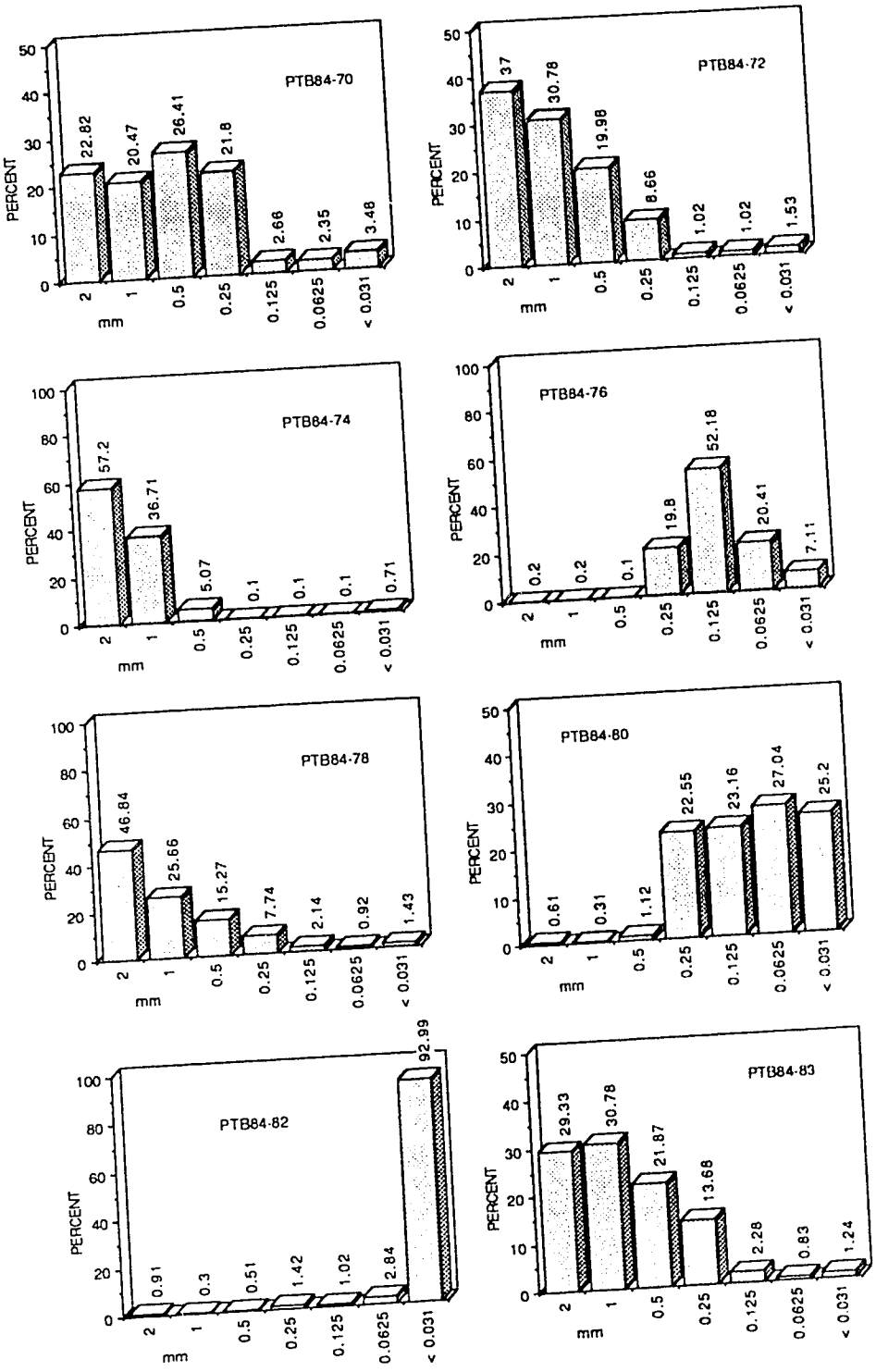
PTB84-70
PERCENT
22.82
20.47
26.41
21.8
2.66
2.35
3.48
2
1
0.5
0.25
0.125
0.0625
< 0.031
mm
PTB84-72
37
30.78
19.98
8.66
1.02
1.02
1.53
PTB84-74
57.2
36.71
5.07
0.1
0.1
0.1
0.71
PTB84-76
0.2
0.2
0.1
19.8
52.18
20.41
7.11
PTB84-78
46.84
25.66
15.27
7.74
2.14
0.92
1.43
PTB84-80
0.61
0.31
1.12
22.55
23.16
27.04
25.2
PTB84-82
0.91
0.3
0.51
1.42
1.02
2.84
92.99
PTB84-83
29.33
30.78
21.87
13.68
2.28
0.83
1.24

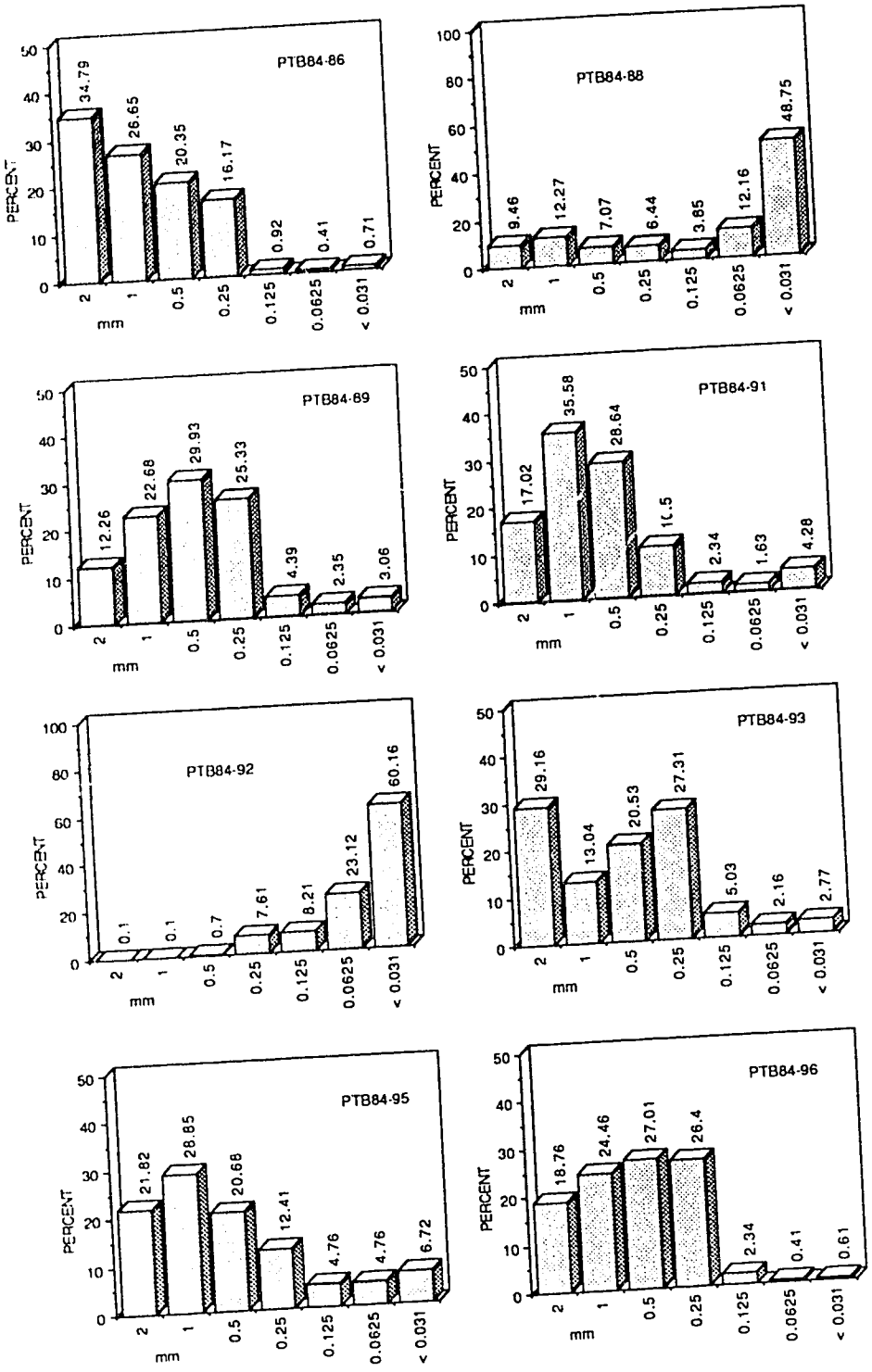
PTB84-86
PERCENT
34.79
26.65
20.35
16.17
0.92
0.41
0.71
2
1
0.5
0.25
0.125
0.0625
< 0.031
mm
PTB84-88
9.46
12.27
7.07
6.44
3.85
12.16
48.75
PTB84-89
12.26
22.68
29.93
25.33
4.39
2.35
3.06
PTB84-91
17.02
35.58
28.64
1.63
4.28
PTB84-92
0.1
0.1
0.7
7.61
8.21
23.12
60.16
PTB84-93
29.16
13.04
20.53
27.31
5.03
2.16
2.77
PTB84-95
21.82
28.85
20.68
12.41
4.76
6.72
PTB84-96
18.76
24.46
27.01
26.4
2.34
0.41
0.61

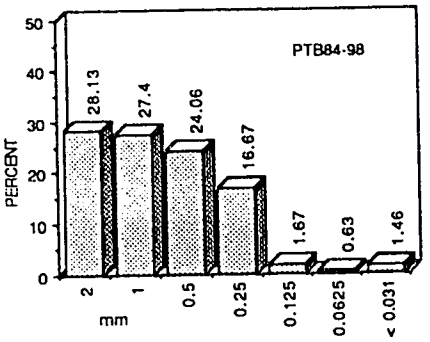
PTB84-98
PERCENT
28.13
27.4
24.06
16.67
1.67
0.63
1.46
2
1
0.5
0.25
0.125
0.0625
< 0.031
mm

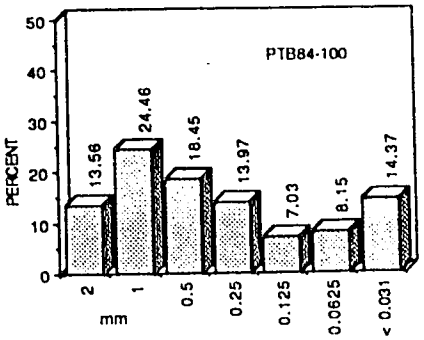
PTB84-100
PERCENT
13.58
24.46
18.45
13.97
7.03
8.15
14.37
2
1
0.5
0.25
0.125
0.0625
< 0.031
mm

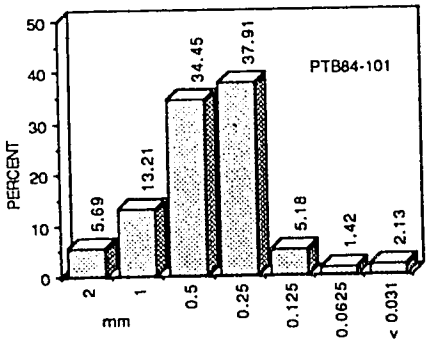
PTB84-101
PERCENT
5.69
13.21
34.45
37.91
5.18
1.42
2.13
2
1
0.5
0.25
0.125
0.0625
< 0.031
mm

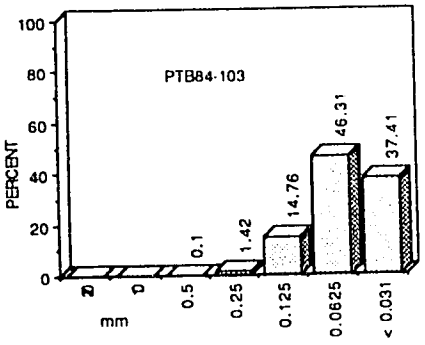
PTB84-103
PERCENT
0.1
1.42
14.76
46.31
37.41
0.5
0.25
0.125
0.0625
< 0.031
mm

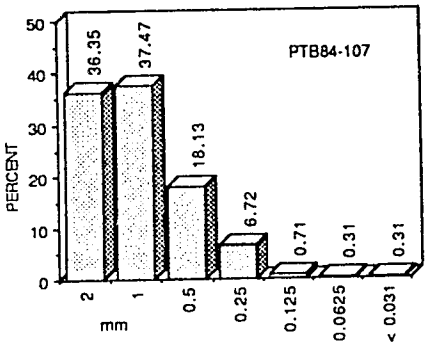
PTB84-107
PERCENT
36.35
37.47
18.13
6.72
0.71
0.31
0.31
2
1
0.5
0.25
0.125
0.0625
< 0.031
mm

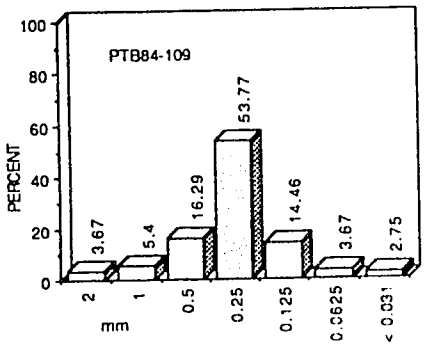
PTB84-109
PERCENT
3.67
5.4
16.29
53.77
14.46
3.67
2.75
2
1
0.5
0.25
0.125
0.0625
mm

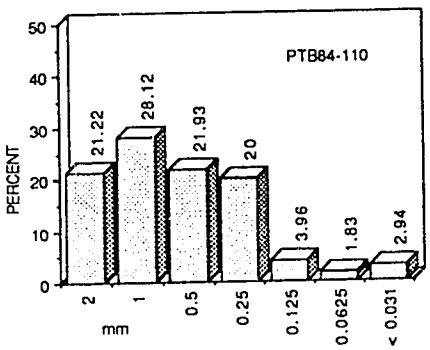
PTB84-110
PERCENT
21.22
28.12
21.93
20
3.96
1.83
2.94
2
1
0.5
0.25
0.125
0.0625
< 0.031
mm

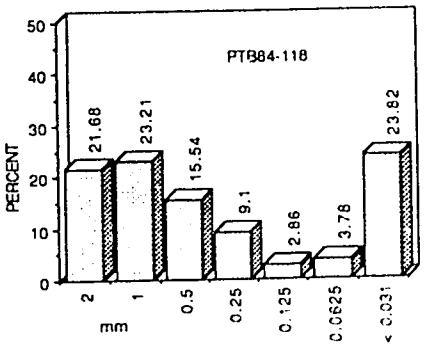
PTB84-118
PERCENT
21.68
23.21
15.54
9.1
2.86
3.78
23.82
2
1
0.5
0.25
0.125
0.0625
mm

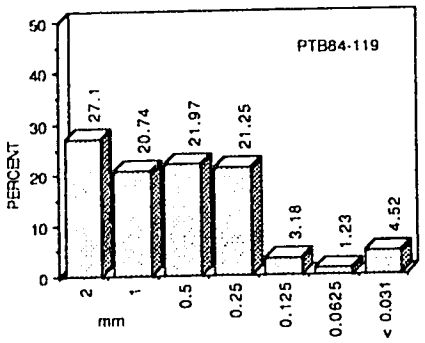
PTB84-119
PERCENT
27.1
20.74
21.97
21.25
3.18
1.23
4.52
2
1
0.5
0.25
0.125
0.0625
< 0.031
mm

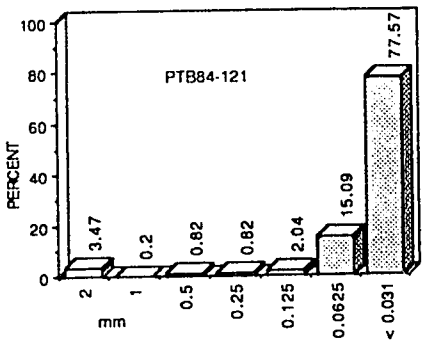
PTB84-121
PERCENT
3.47
0.2
0.82
0.82
2.04
15.09
77.57
2
1
0.5
0.25
0.125
0.0625
< 0.031
mm

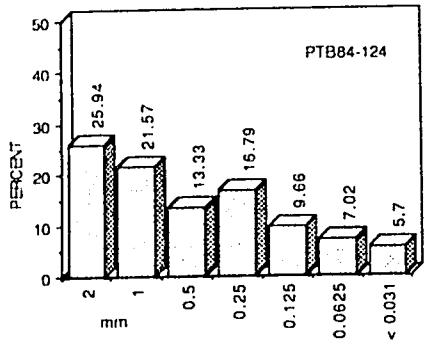
PTB84-124
PERCENT
25.94
21.57
13.33
16.79
9.66
7.02
5.7
2
1
0.5
0.25
0.125
0.0625
< 0.031
mm

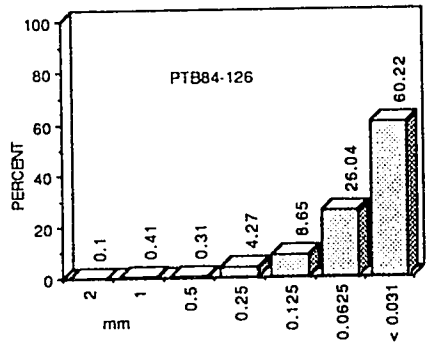
PTB84-126
PERCENT
0.1
0.41
0.31
4.27
8.65
26.04
60.22
2
1
0.5
0.25
0.125
0.0625
< 0.031
mm

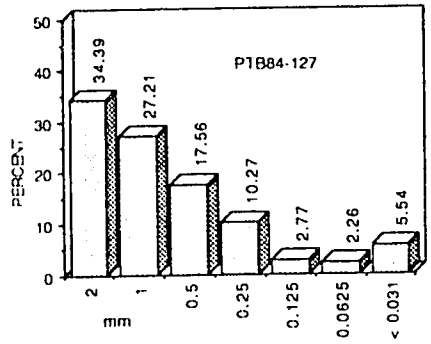
PTB84-127
PERCENT
34.39
27.21
17.56
10.27
2.77
2.26
5.54
2
1
0.5
0.25
0.125
0.0625
< 0.031
mm

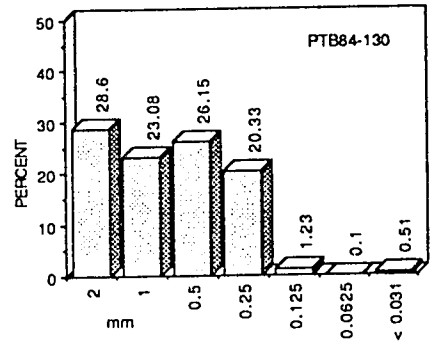
PTB84-130
PERCENT
28.6
23.08
26.15
20.33
1.23
0.1
0.51
2
1
0.5
0.25
0.125
0.0625
< 0.031
mm

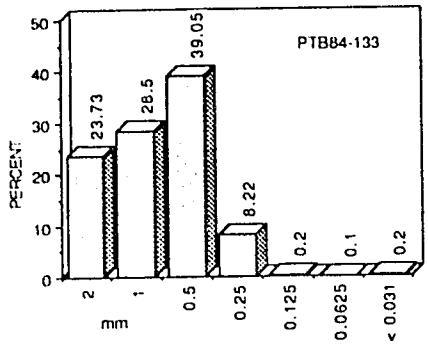
PTB84-133
PERCENT
23.73
28.5
39.05
8.22
0.2
0.1
0.2
2
1
0.5
0.25
0.125
0.0625
< 0.031
mm

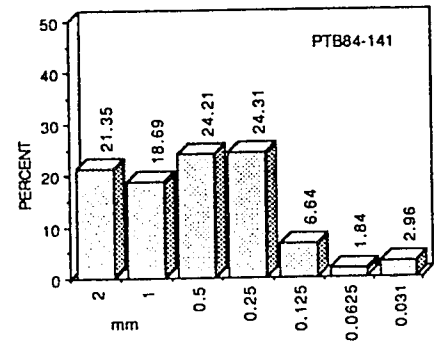
PTB84-141
PERCENT
21.35
18.69
24.21
24.31
6.64
1.84
2.96
2
1
0.5
0.25
0.125
0.0625
0.031
mm

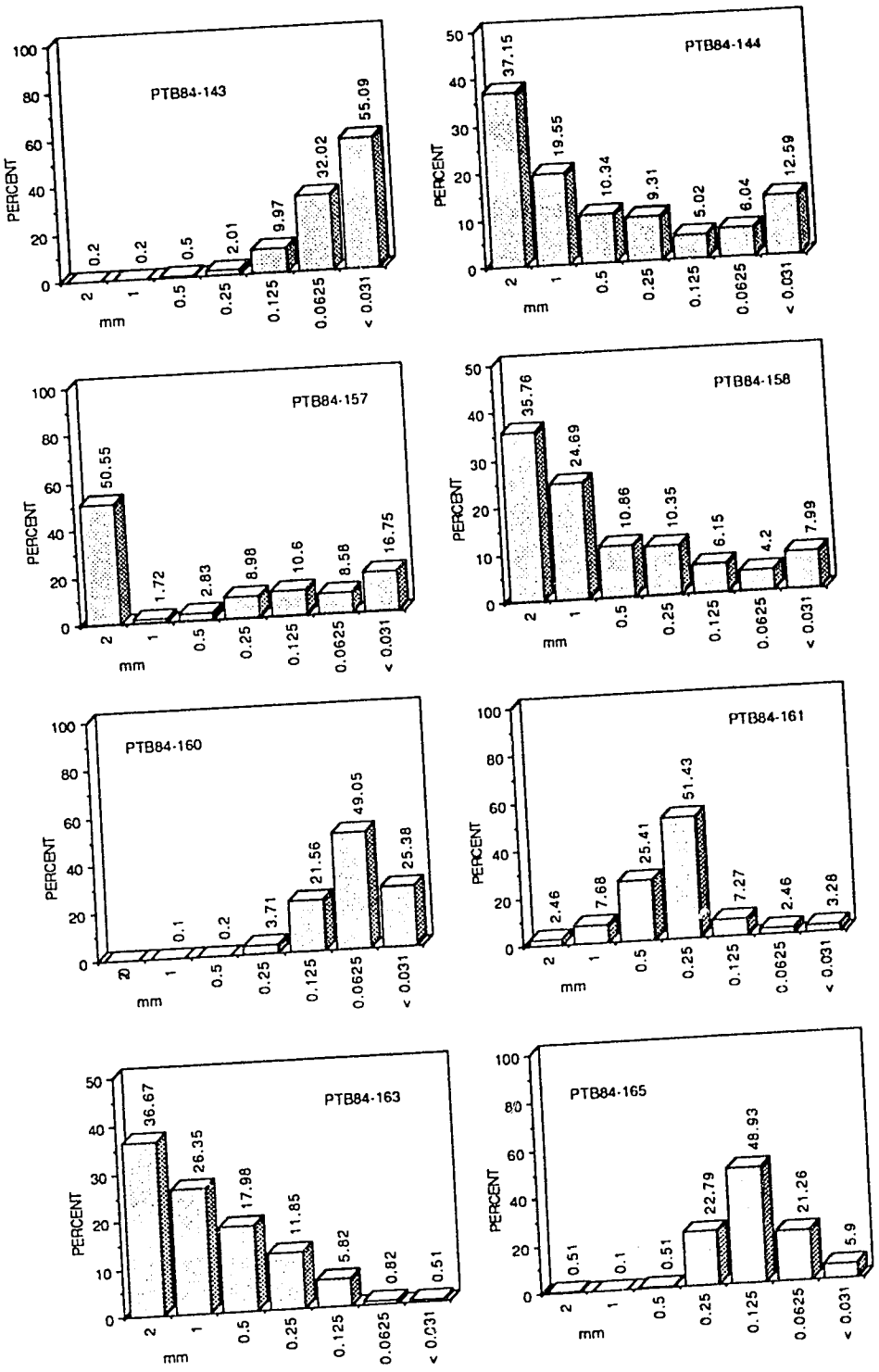
PTB84-143
PERCENT
mm
2
1
0.5
0.25
0.125
0.0625
< 0.031
0.2
0.2
0.5
2.01
9.97
32.02
55.09
PTB84-144
37.15
19.55
10.34
9.31
5.02
6.04
12.59
PTB84-157
50.55
1.72
2.83
8.98
10.6
8.58
16.75
PTB84-158
35.76
24.69
10.86
10.35
6.15
4.2
7.99
PTB84-160
0.1
0.2
3.71
21.56
49.05
25.38
PTB84-161
2.46
7.68
25.41
51.43
7.27
2.46
3.28
PTB84-163
36.67
26.35
17.98
11.85
5.82
0.82
0.51
PTB84-165
0.51
0.1
0.51
22.79
48.93
21.26
5.9

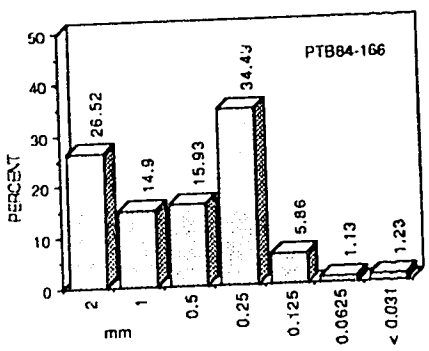
PTB84-166
PERCENT
26.52
14.9
15.93
34.43
5.86
1.13
1.23
2
1
0.5
0.25
0.125
0.0625
< 0.031
mm

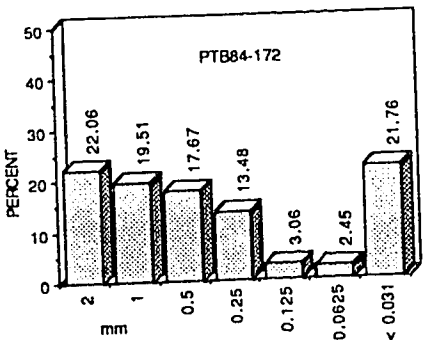
PTB84-172
PERCENT
22.06
19.51
17.67
13.48
3.06
2.45
21.76
2
1
0.5
0.25
0.125
0.0625
< 0.031
mm

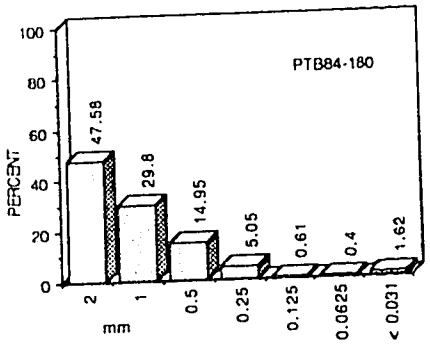
PTB84-180
PERCENT
47.58
29.8
14.95
5.05
0.61
0.4
1.62
2
1
0.5
0.25
0.125
0.0625
< 0.031
mm

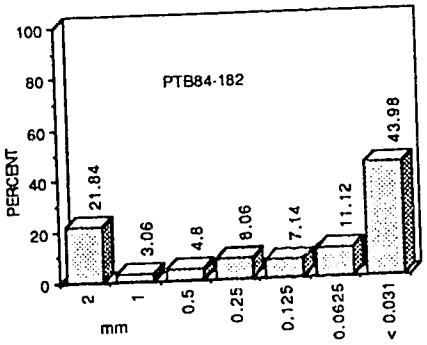
PTB84-182
PERCENT
21.84
3.06
4.8
8.06
7.14
11.12
43.98
2
1
0.5
0.25
0.125
0.0625
< 0.031
mm

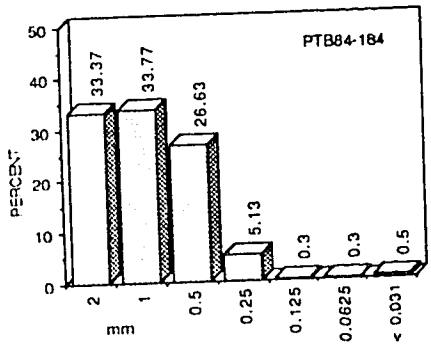
PTB84-184
PERCENT
33.37
33.77
26.63
5.13
0.3
0.3
0.5
2
1
0.5
0.25
0.125
0.0625
< 0.031
mm

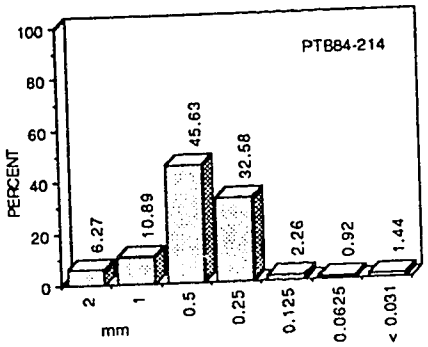
PTB84-214
PERCENT
6.27
10.89
45.63
32.58
2.26
0.92
1.44
2
1
0.5
0.25
0.125
0.0625
< 0.031
mm

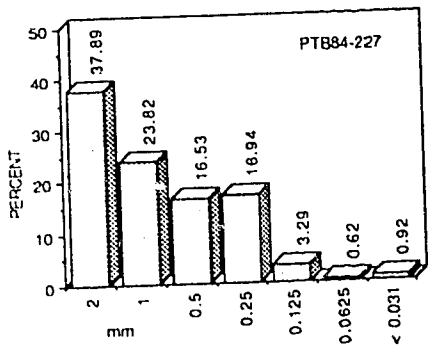
PTB84-227
PERCENT
37.89
23.82
16.53
18.94
3.29
0.62
0.92
2
1
0.5
0.25
0.125
0.0625
< 0.031
mm

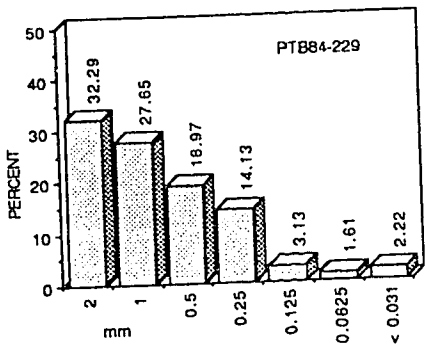
PTB84-229
PERCENT
32.29
27.65
18.97
14.13
3.13
1.61
2.22
2
1
0.5
0.25
0.125
0.0625
< 0.031
mm

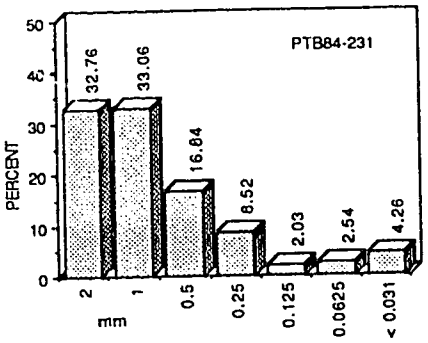
PTB84-231
PERCENT
32.76
33.06
16.64
8.52
2.03
2.54
4.26
2
1
0.5
0.25
0.125
0.0625
< 0.031
mm

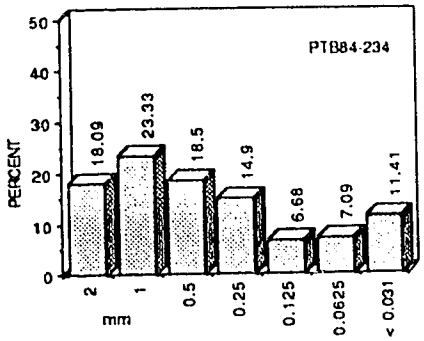
PTB84-234
PERCENT
18.09
23.33
18.5
14.9
6.68
7.09
11.41
2
1
0.5
0.25
0.125
0.0625
< 0.031
mm

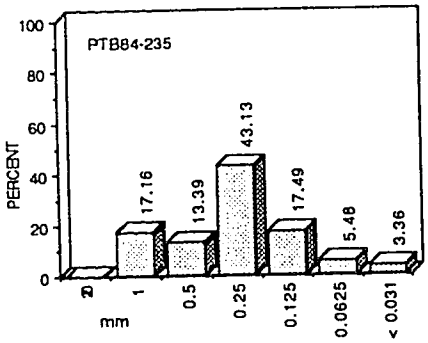
PTB84-235
PERCENT
17.16
13.39
43.13
17.49
5.48
3.36
2
1
0.5
0.25
0.125
0.0625
< 0.031
mm

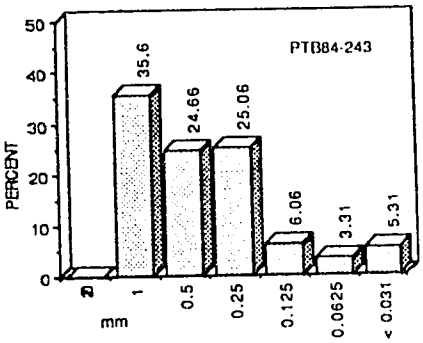
PTB84-243
PERCENT
35.6
24.66
25.06
6.06
3.31
5.31
2
1
0.5
0.25
0.125
0.0625
< 0.031
mm

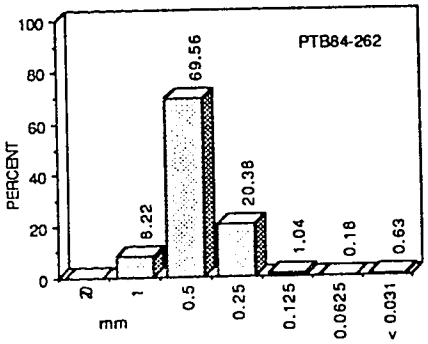
PTB84-262
PERCENT
8.22
69.56
20.38
1.04
0.18
0.63
2
1
0.5
0.25
0.125
0.0625
< 0.031
mm

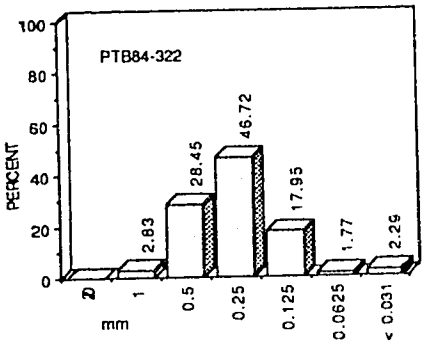
PTB84-322
PERCENT
2.83
28.45
46.72
17.95
1.77
2.29
2
1
0.5
0.25
0.125
0.0625
< 0.031
mm

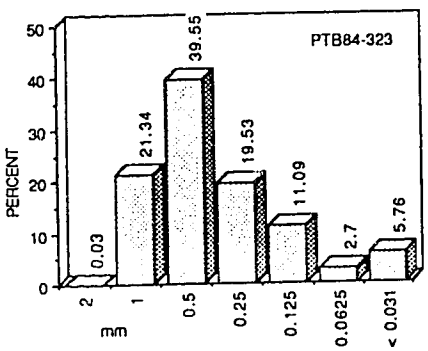
PTB84-323
PERCENT
0.03
21.34
39.55
19.53
11.09
2.7
5.76
2
1
0.5
0.25
0.125
0.0625
< 0.031
mm

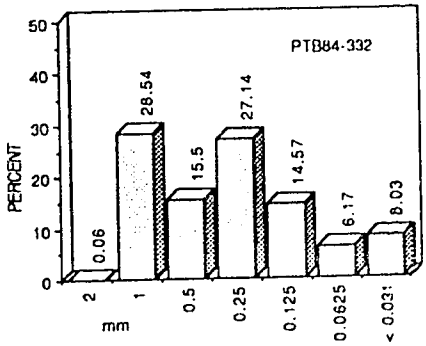
PTB84-332
PERCENT
0.06
28.54
15.5
27.14
14.57
6.17
8.03
2
1
0.5
0.25
0.125
0.0625
< 0.031
mm

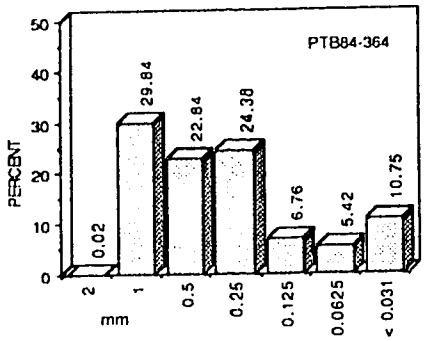
PTB84-364
PERCENT
mm
2
1
0.5
0.25
0.125
0.0625
< 0.031
0.02
29.84
22.84
24.38
6.76
5.42
10.75

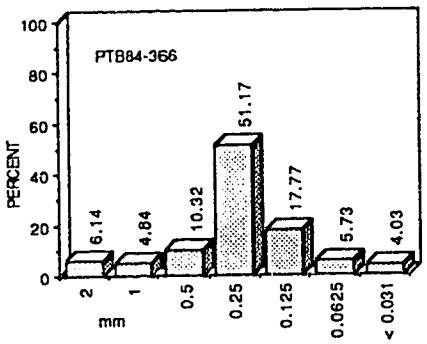
PTB84-366
PERCENT
mm
2
1
0.5
0.25
0.125
0.0625
< 0.031
6.14
4.84
10.32
51.17
17.77
5.73
4.03

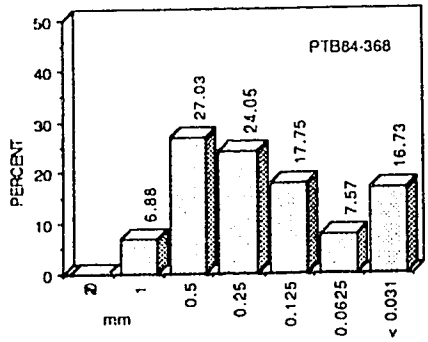
PTB84-368
PERCENT
mm
2
1
0.5
0.25
0.125
0.0625
< 0.031
6.88
27.03
24.05
17.75
7.57
16.73

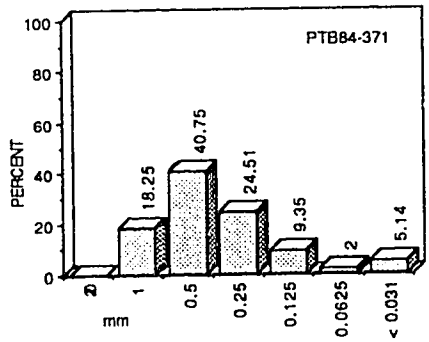
PTB84-371
PERCENT
mm
2
1
0.5
0.25
0.125
0.0625
< 0.031
18.25
40.75
24.51
9.35
2
5.14

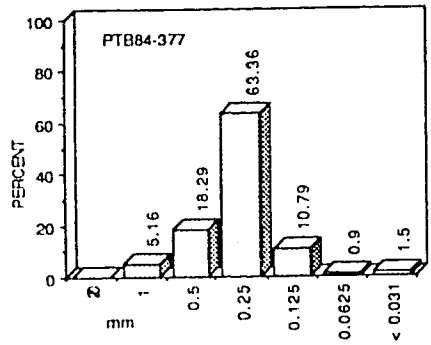
PTB84-377
PERCENT
mm
2
1
0.5
0.25
0.125
0.0625
< 0.031
5.16
18.29
63.36
10.79
0.9
1.5

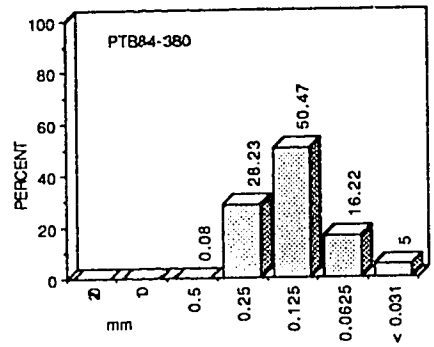
PTB84-380
PERCENT
mm
2
1
0.5
0.25
0.125
0.0625
< 0.031
0.08
28.23
50.47
16.22
5

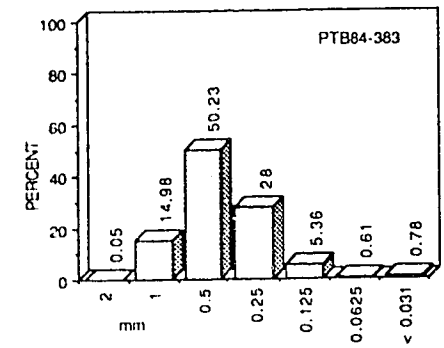
PTB84-383
PERCENT
mm
2
1
0.5
0.25
0.125
0.0625
< 0.031
0.05
14.98
50.23
28
5.36
0.61
0.78

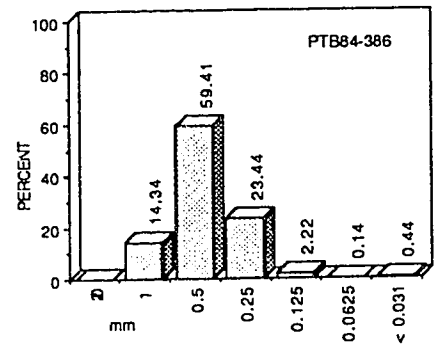
PTB84-386
PERCENT
mm
2
1
0.5
0.25
0.125
0.0625
< 0.031
14.34
59.41
23.44
2.22
0.14
0.44

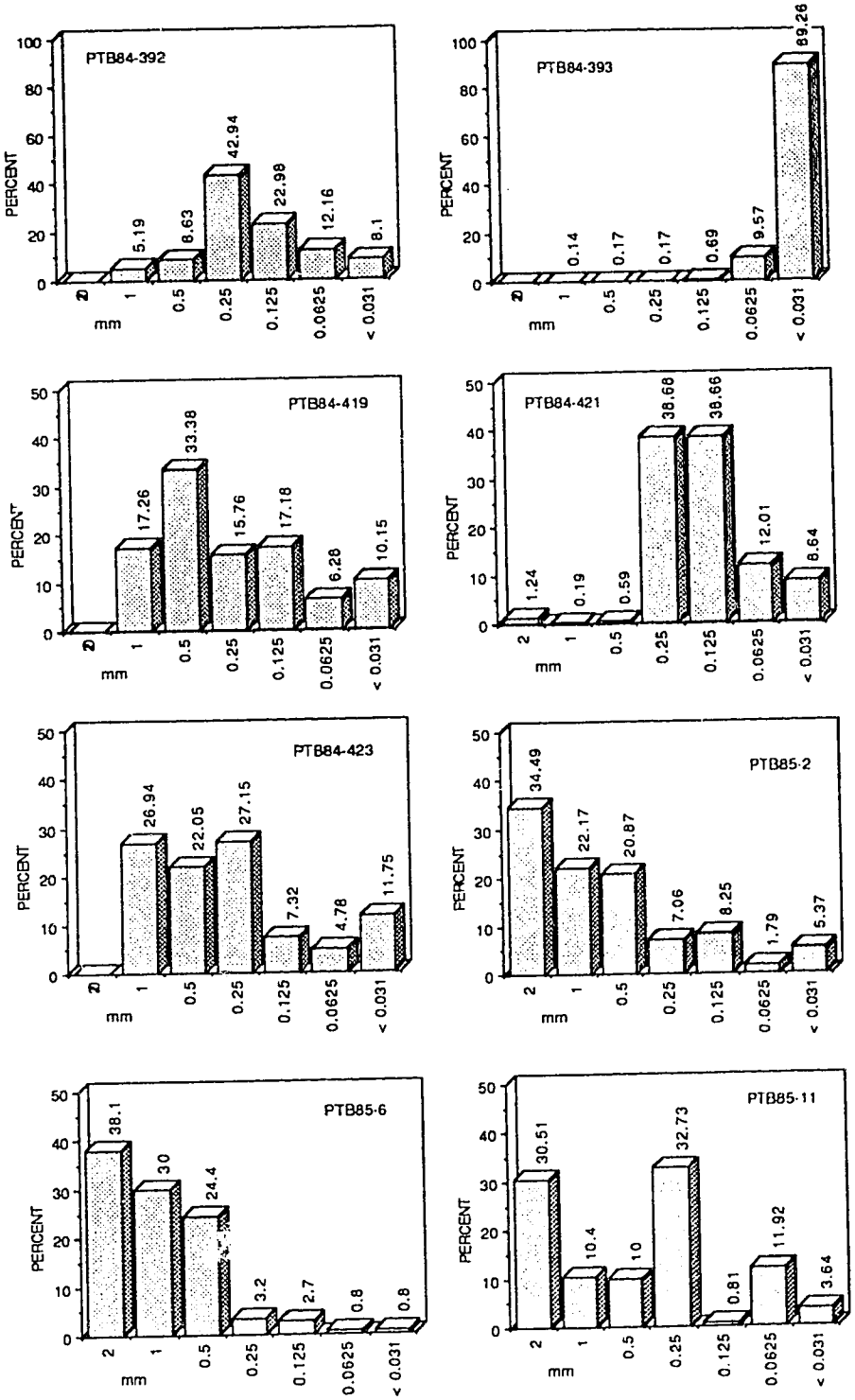
PTB84-392
PERCENT
mm
5.19
8.63
42.94
22.98
12.16
8.1
PTB84-393
0.14
0.17
0.17
0.69
9.57
89.26
PTB84-419
17.26
33.38
15.76
17.18
6.28
10.15
PTB84-421
1.24
0.19
0.59
38.68
38.66
12.01
8.64
PTB84-423
26.94
22.05
27.15
7.32
4.78
11.75
PTB85-2
34.49
22.17
20.87
7.06
8.25
1.79
5.37
PTB85-6
38.1
30
24.4
3.2
2.7
0.8
0.8
PTB85-11
30.51
10.4
10
32.73
0.81
11.92
3.64
2
1
0.5
0.25
0.125
0.0625
< 0.031

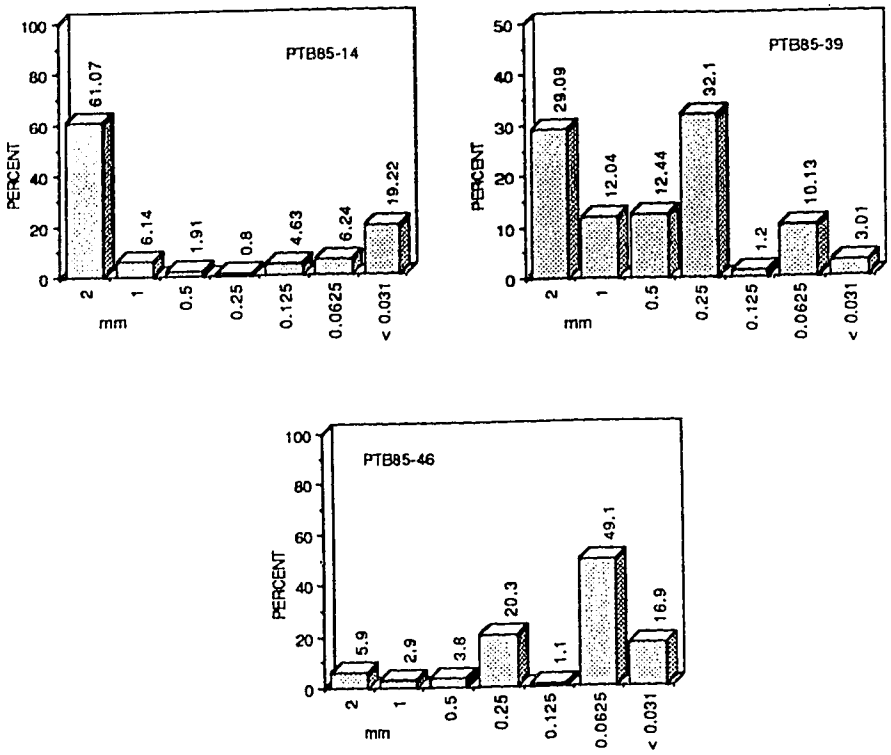
PTB85-14
PERCENT
100
80
60
40
20
0
61.07
6.14
1.91
0.8
4.63
6.24
19.22
2
1
0.5
0.25
0.125
0.0625
< 0.031
mm
PTB85-39
PERCENT
50
40
30
20
10
0
29.09
12.04
12.44
32.1
1.2
10.13
3.01
2
1
0.5
0.25
0.125
0.0625
< 0.031
mm
PTB85-46
PERCENT
100
80
60
40
20
0
5.9
2.9
3.8
20.3
1.1
49.1
16.9
2
1
0.5
0.25
0.125
0.0625
< 0.031
mm

Appendix 10. Muffle furnace determined percentage moisture, organic matter, carbonate and total carbon for bulk diamicton samples from the northern Rocky Mountain Trench.

SAMPLE NO.	% MOISTURE	% ORG M.	% CARONBATE	% TOTAL CARBON
PTB84-4	0.236	1.235	4.251	5.434
PTB85-51	0.213	1.444	7.591	8.925
PTB84-52	0.221	1.519	8.208	9.603
PTB84-55	0.198	1.625	8.525	10.012
PTB84-61	0.261	1.278	7.796	8.974
PTB84-62	0.203	1.204	7.704	8.815
PTB84-63	0.200	1.198	7.549	8.657
PTB84-64	0.196	1.183	7.492	8.586
PTB84-65	0.193	1.230	7.720	8.855
PTB84-112	0.322	2.288	7.548	9.663
PTB84-113	0.484	1.969	22.827	24.347
PTB84-114	0.188	1.467	4.799	6.196
PTB84-115	0.245	1.822	6.320	8.026
PTB84-116	0.354	1.821	10.065	11.703
PTB84-136	0.329	2.057	7.323	9.230
PTB84-137	0.310	2.558	6.086	8.488
PTB84-138	0.319	2.527	5.567	7.953
PTB84-139	0.263	2.288	5.178	7.347
PTB84-140	0.591	2.318	7.164	9.316
PTB84-151	0.262	1.366	10.597	11.818
PTB84-152	0.255	1.452	10.769	12.064
PTB84-153	0.285	1.275	10.783	11.921
PTB84-154	0.242	1.230	10.285	11.389
PTB84-155	0.277	1.184	10.396	11.457
PTB84-156	0.348	1.194	9.881	10.957
PTB84-169	1.859	10.319	13.337	22.279
PTB84-186	0.470	1.591	2.527	4.078
PTB84-187	1.512	9.652	3.894	13.170
PTB84-188	1.948	11.938	2.346	14.004
PTB84-189	0.722	4.406	2.984	7.259
PTB84-190	0.729	4.245	3.388	7.489
PTB84-191	0.847	3.375	5.398	8.591
PTB84-192	1.201	2.296	5.566	7.734
PTB84-203	0.456	1.383	14.815	15.994
PTB84-204	0.285	0.906	9.949	10.766
PTB84-205	0.252	0.980	12.288	13.147
PTB84-206	0.278	1.048	11.985	12.908
PTB84-207	0.326	1.269	12.677	13.786
PTB84-208	0.330	1.355	13.030	14.208
PTB84-209	0.226	1.044	14.112	15.009
PTB84-210	0.229	1.163	13.156	14.165
PTB84-211	0.263	1.060	12.758	13.682
PTB84-212	0.325	1.326	11.844	13.013
PTB84-218	0.506	2.317	9.199	11.303
PTB84-219	0.427	1.808	9.595	11.229
PTB84-220	0.546	1.890	9.396	11.109
PTB84-221	0.289	1.893	5.857	7.639
PTB84-222	0.374	2.001	9.617	11.426

PTB84-223	0.385	1.995	8.789	10.609
PTB84-224	0.355	1.744	9.416	10.996
PTB84-234	0.277	1.007	15.159	16.013
PTB84-236	0.593	2.514	9.810	12.077
PTB84-237	0.591	2.595	9.724	12.067
PTB84-238	0.601	3.971	10.004	13.578
PTB84-239	0.710	2.751	8.425	10.943
PTB84-240	0.669	2.516	10.331	12.587
PTB84-241	0.725	2.422	9.176	11.375
PTB84-264	0.381	1.772	6.764	8.417
PTB84-265	0.325	1.606	6.664	8.163
PTB84-266	0.603	2.286	7.254	9.374
PTB84-267	0.756	1.973	5.943	7.798
PTB84-268	0.363	1.671	6.821	8.378
PTB84-269	0.511	2.854	5.241	7.946
PTB84-270	0.545	2.841	5.398	8.086
PTB84-271	0.545	1.982	5.743	7.611
PTB84-272	0.596	2.110	5.889	7.875
PTB84-273	0.558	2.184	4.942	7.018
PTB84-274	0.485	2.245	5.662	7.779
PTB84-275	0.451	1.977	6.137	7.992
PTB84-276	0.426	2.864	5.164	7.880
PTB84-277	0.323	1.332	9.344	10.551
PTB84-278	0.317	1.335	9.108	10.321
PTB84-279	0.331	1.203	8.645	9.744
PTB84-280	0.317	1.256	8.662	9.809
PTB84-281	0.192	0.963	8.000	8.886
PTB84-282	0.225	1.008	7.648	8.579
PTB84-283	0.236	0.971	6.873	7.777
PTB84-284	0.213	0.972	7.107	8.009
PTB84-285	0.214	1.226	9.230	10.343
PTB84-297	0.235	1.048	8.750	9.707
PTB84-298	0.247	1.050	8.981	9.936
PTB84-299	0.297	1.234	7.417	8.559
PTB84-300	0.361	1.496	4.764	6.189
PTB84-301	0.494	2.161	5.373	7.417
PTB84-302	0.468	1.893	4.793	6.596
PTB84-304	0.439	1.221	11.298	12.380
PTB84-305	0.227	1.025	14.170	15.050
PTB84-306	0.260	1.611	11.016	12.450
PTB84-307	0.261	1.474	11.326	12.633
PTB84-308	0.268	1.505	10.758	12.101
PTB84-309	0.310	1.698	11.128	12.637
PTB84-310	0.382	1.784	12.613	14.172
PTB84-311	0.266	1.382	8.812	10.072
PTB84-313	0.204	0.998	9.896	10.796
PTB84-314	0.310	1.482	11.576	12.886
PTB84-315	0.260	1.294	12.124	13.262
PTB84-316	0.289	1.027	9.214	10.147
PTB84-317	0.318	0.848	8.788	9.562
PTB84-318	0.278	1.074	10.288	11.251
PTB84-319	0.285	0.900	9.015	9.834
PTB84-320	0.234	0.929	8.294	9.146
PTB84-321	0.221	1.029	12.167	13.071

PTB84-324	0.251	0.882	10.469	11.258
PTB84-325	0.159	0.971	6.311	7.221
PTB84-326	0.213	0.881	9.926	10.720
PTB84-327	0.315	0.928	10.151	10.985
PTB84-328	0.221	0.945	9.809	10.661
PTB84-329	0.214	0.971	9.664	10.541
PTB84-330	0.219	0.899	9.196	10.013
PTB84-331	0.242	0.896	8.701	9.519
PTB84-333	0.196	0.865	8.967	9.754
PTB84-334	0.170	0.743	7.750	8.436
PTB84-335	0.196	0.810	8.966	9.704
PTB84-337	0.860	4.223	5.803	9.781
PTB84-338	0.754	4.774	3.604	8.207
PTB84-339	0.796	5.448	3.144	8.421
PTB84-340	1.471	5.669	3.630	9.094
PTB84-341	0.808	5.726	4.583	10.047
PTB84-342	0.840	5.412	4.783	9.936
PTB84-343	0.863	5.754	3.431	8.987
PTB84-344	1.060	5.981	4.098	9.834
PTB84-346	0.324	1.741	7.794	9.399
PTB84-347	0.373	1.800	7.074	8.747
PTB84-348	1.093	2.697	3.914	6.506
PTB84-349	0.827	2.550	5.057	7.478
PTB84-350	0.804	2.648	4.973	7.489
PTB84-351	0.173	0.792	9.039	9.759
PTB84-352	0.221	0.967	10.757	11.620
PTB84-353	0.286	1.578	6.221	7.701
PTB84-354	0.216	1.428	6.963	8.292
PTB84-357	0.346	1.878	9.784	11.479
PTB84-362	0.266	1.156	12.810	13.818
PTB84-363	0.277	1.184	11.564	12.612
PTB84-370	1.440	6.683	14.736	20.434
PTB84-375	0.306	1.871	1.597	3.438
PTB84-379	0.264	1.363	12.855	14.043
PTB84-381	0.325	2.194	11.219	13.167
PTB84-382	0.273	1.294	9.833	11.000
PTB84-389	0.258	1.132	7.905	8.948
PTB84-390	0.317	1.384	9.368	10.622
PTB84-391	0.353	1.640	9.549	11.032
PTB84-394	0.362	1.131	12.070	13.065
PTB84-395	0.430	1.055	11.793	12.723
PTB84-396	0.310	0.945	12.283	13.112
PTB84-397	0.368	1.207	12.537	13.593
PTB84-398	0.481	1.267	12.064	13.178
PTB84-399	0.307	1.060	11.043	11.986
PTB84-400	0.352	1.060	11.063	12.006
PTB84-401	0.335	0.968	13.733	14.568
PTB84-402	0.274	1.139	12.325	13.323
PTB84-403	0.323	1.159	13.734	14.734
PTB84-404	0.266	1.060	22.781	23.599
PTB84-405	0.306	1.280	14.322	15.419
PTB84-406	0.285	0.774	13.008	13.681
PTB84-407	0.446	1.424	12.990	14.229
PTB84-408	1.841	1.443	10.720	12.008

PTB84-409	0.516	1.337	10.798	11.990
PTB84-410	0.523	1.292	11.837	12.976
PTB84-411	0.267	0.871	9.632	10.419
PTB84-412	0.296	1.208	12.999	14.051
PTB84-413	0.279	1.074	11.958	12.903
PTB84-414	0.352	1.042	13.189	14.094
PTB84-415	0.751	1.232	12.386	13.465
PTB84-416	0.323	0.867	13.646	14.394
PTB84-417	0.370	0.891	10.672	11.468
PTB84-418	0.443	1.000	10.771	11.662
PTB85-1	0.171	0.661	10.042	10.637
PTB85-4	0.251	0.650	-2.970	-2.301
PTB85-9	0.693	1.579	8.258	9.707
PTB85-10	0.523	1.378	8.014	9.282
PTB85-13	0.306	0.749	7.422	8.115
PTB85-16	0.244	0.645	10.050	10.631
PTB85-17	0.226	0.729	11.322	11.969
PTB85-18	0.235	0.612	9.086	9.642
PTB84-20	0.191	1.149	5.609	6.694
PTB85-22	0.226	1.244	4.799	5.984
PTB84-24	0.190	1.331	9.266	10.473
PTB85-25	0.188	1.398	9.723	10.986
PTB85-26	0.197	1.417	9.144	10.432
PTB85-27	0.218	1.742	9.218	10.800
PTB85-28	0.298	1.543	7.989	9.409
PTB85-29	0.125	1.019	5.374	6.339
PTB85-30	0.156	1.120	5.681	6.738
PTB85-31	0.194	1.164	6.461	7.550
PTB85-32	0.190	1.173	6.259	7.359
PTB85-33	0.167	1.045	5.302	6.292
PTB85-34	0.158	1.090	6.585	7.603
PTB85-35	0.155	1.121	7.622	8.658
PTB85-36	0.167	1.118	6.984	8.024
PTB85-37	0.483	1.161	7.495	8.569
PTB85-38	0.182	1.214	8.460	9.571
PTB85-42	0.353	2.755	5.919	8.512
PTB85-43	0.338	2.045	5.656	7.585
PTB85-44	0.300	2.554	4.939	7.367
PTB85-47	0.343	1.332	9.345	10.552
PTB85-49	0.224	1.046	10.643	11.577
PTB85-50	0.284	1.375	9.385	10.631
PTB85-53	0.249	1.284	14.036	15.140
PTB85-54	0.391	1.071	13.627	14.552
PTB85-56	0.281	1.218	14.161	15.207
PTB85-57	0.277	1.247	14.504	15.570
PTB85-63	0.235	1.288	13.077	14.196
PTB85-64	0.227	1.211	12.964	14.017
PTB85-65	0.237	1.184	13.424	14.449
PTB85-66	0.200	1.140	14.430	15.406
PTB85-67	0.216	1.348	12.865	14.039
PTB85-68	0.219	1.301	13.194	14.323
PTB85-69	0.207	1.301	12.612	13.748
PTB85-70	0.235	1.267	13.497	14.592
PTB85-71	0.178	1.122	12.741	13.720

PTB85-72	0.175	1.155	12.330	13.343
PTB85-73	0.201	1.284	12.172	13.299
PTB85-74	0.176	1.156	11.606	12.628
PTB85-75	0.170	0.772	11.567	12.250
PTB85-76	0.217	1.232	6.179	7.335
PTB85-77	0.257	1.340	6.953	8.200
PTB85-78	0.215	1.194	5.758	6.884
PTB85-79	0.304	1.850	8.961	10.644
PTB84-245	0.500	14.070		
PTB84-246	1.000	13.636		
PTB84-246	0.500	12.563		
PTB84-248	2.500	13.846		
PTB84-249	2.985	12.308		
PTB84-250	1.000	13.131		
PTB84-251	1.500	13.198		
PTB84-252	0.500	14.070		
PTB84-253	1.000	12.626		
PTB84-254	1.493	11.616		
PTB84-255	0.000	11.500		
PTB84-256	1.500	15.736		
PTB84-257	0.000	12.438		
PTB84-258	0.000	11.881		
PTB84-259	0.495	11.443		
PTB84-260	0.495	11.443		

Appendix 11. Raw trend and plunge data for pebble fabric samples from the Finlay River.

84-39	84-39B	84-48	84-56	84-56B	84-57	84-57B	84-60	84-105	84-122
90 2	202 18	357 9	200 14	355 12	18 12	346 22	4 25	347 2	165 10
286 4	184 16	201 2	213 0	163 10	338 14	168 0	188 8	337 4	68 26
168 22	228 32	165 20	209 4	347 7	173 9	308 23	71 30	259 25	228 1
292 4	250 4	167 24	169 3	355 14	155 24	122 35	353 9	10 49	328 14
163 12	142 24	138 18	21 11	90 9	10 27	341 18	159 3	190 37	150 6
155 19	136 30	184 13	182 16	334 2	163 48	197 7	340 23	90 56	123 40
95 2	266 42	129 10	66 32	150 4	180 11	178 14	2 2	357 54	60 21
186 22	220 14	172 3	192 13	38 10	166 25	186 0	360 2	340 6	207 34
59 8	112 18	285 6	13 13	7 8	28 28	173 49	356 43	26 17	249 4
163 13	275 4	178 1	14 18	12 9	360 12	200 67	340 14	192 4	243 13
126 16	106 22	252 12	205 8	28 10	179 44	198 19	19 50	42 15	146 7
138 12	294 24	177 2	32 8	188 22	168 28	167 14	124 10	15 29	179 12
168 13	169 0	360 2	26 10	5 1	141 46	353 16	29 14	40 23	46 6
142 28	179 33	241 6	17 11	41 18	142 15	152 3	346 52	57 33	313 1
153 14	123 23	148 46	350 7	47 33	39 6	357 3	216 31	224 28	313 14
307 12	186 6	133 14	9 21	26 50	203 8	174 8	353 3	125 14	282 2
348 16	106 10	197 6	10 2	194 1	154 47	196 13	334 87	357 28	293 19
174 30	146 16	168 10	22 31	7 14	48 18	145 13	51 53	320 13	113 14
175 16	292 48	175 15	329 20	351 4	205 17	12 60	68 37	19 15	146 14
240 1	22 17	145 4	58 18	26 18	168 37	195 4	236 38	232 7	252 12
298 24	210 32	330 2	81 2	98 14	184 22	170 44	247 22	33 6	239 11
198 2	133 22	170 4	10 16	193 8	344 22	178 0	22 15	358 24	263 1
174 16	136 12	162 12	170 17	20 16	350 23	352 7	16 1	45 7	140 28
150 4	8 12	341 3	172 0	52 20	151 3	347 13	199 14	91 28	300 10
342 1	108 18	162 4	217 4	195 4	172 3	3 14	328 4	15 10	212 21
160 00	64 5	220 0	204 20	48 5	354 13	147 32	341 10	130 0	150 1
113 17	117 5	170 2	264 2	126 30	103 8	140 27	21 18	243 45	130 7
341 3	22 22	170 30	87 2	128 10	229 8	181 11	339 31	64 14	19 23
289 2	99 6	178 9	354 5	250 6	346 30	171 11	359 8	223 20	327 24
108 16	171 20	33 3	104 22	126 16	155 33	164 7	334 7	116 12	160 7
162 17	207 8	132 8	202 2	18 4	197 11	167 25	57 16	62 14	10 4
118 13	124 7	178 10	5 4	43 14	171 21	323 15	202 11	339 12	118 9
6 75	180 12	161 20	180 0	27 6	146 3	151 7	208 15	102 26	168 4
194 15	64 10	228 12	8 10	4 20	150 41	150 10	318 10	92 32	356 7
108 0	196 23	14 22	42 2	359 14	329 14	354 4	109 3	18 16	138 4
28 53	135 1	348 23	194 1	122 24	181 6	157 10	68 2	11 6	301 7
193 1	279 25	122 4	4 30	24 19	353 6	221 41	5 57	14 6	225 49
102 29	177 14	174 11	195 12	107 31	7 15	144 12	147 2	348 10	6 8
232 2	242 17	159 40	22 25	174 34	336 10	151 0	293 8	4 12	356 62
134 27	183 8	206 22	86 2	340 2	7 27	164 11	150 10	358 9	303 12
119 13	241 4	154 15	3 9	138 3	213 46	342 20	163 3	326 9	330 16
121 6	103 10	195 2	22 7	20 12	328 45	143 30	354 12	89 8	79 0
318 39	132 12	38 16	10 19	172 6	160 3	179 4	152 4	132 0	83 6
134 10	250 16	178 2	121 10	236 4	149 22	357 5	42 48	360 6	18 10
80 14	187 8	39 10	99 50	43 10	345 1	182 58	34 36	6 24	154 5
77 5	258 16	13 14	343 23	28 29	353 10	153 10	140 1	338 10	91 4
141 26	261 17	25 13	65 10	32 0	338 31	148 0	29 30	37 8	147 15
82 9	16 54	345 36	12 27	3 2	342 5	175 3	331 18	106 33	145 9
63 8	79 14	170 15	68 32	17 33	134 18	167 5	316 6	263 42	220 48
327 15	163 40	164 10	342 12	20 13	354 24	120 19	340 8	261 9	100 8

84-135	84-135B	84-147	84-150	84-171	84-193	84-194	84-202	84-213	84-242
185 38	120 80	70 7	268 10	268 85	322 16	333 14	213 18	76 9	171 11
97 9	200 19	249 15	140 20	140 1	151 21	335 10	299 28	55 10	291 7
31 52	181 2	302 28	253 27	353 17	60 8	332 17	32 11	338 10	334 12
18 5	171 0	109 6	288 34	299 8	117 30	316 8	175 48	91 37	167 14
62 32	114 2	291 55	82 28	52 31	331 14	330 8	250 19	332 4	159 12
56 18	298 38	82 6	168 13	348 12	352 5	352 9	143 0	323 38	315 13
89 12	288 2	84 23	97 28	348 19	1 26	335 7	198 38	336 19	352 6
72 28	280 36	329 8	319 32	60 3	323 7	339 1	212 23	5 28	97 34
62 34	354 6	117 2	101 0	82 22	327 7	351 18	254 28	4 4	338 10
12 3	94 23	112 9	286 14	81 40	180 0	329 4	26 4	199 36	347 26
198 29	194 4	110 11	280 36	212 11	323 18	356 19	266 57	356 17	10 18
28 12	160 9	68 3	279 11	15 15	318 11	338 6	248 48	211 0	348 26
138 23	9 17	280 1	273 12	153 22	322 6	322 18	217 25	209 18	352 22
340 23	122 22	263 9	247 10	353 23	350 10	7 8	43 2	250 10	351 15
195 10	330 44	280 19	202 46	188 26	330 10	351 4	39 13	56 14	343 6
10 12	348 13	123 16	70 12	267 82	40 19	336 5	73 15	257 0	355 3
5 36	226 43	245 5	174 27	359 17	348 8	344 13	314 14	317 4	184 0
32 2	16 14	115 1	203 23	328 22	168 13	331 18	208 48	318 7	150 16
38 9	350 9	122 2	131 0	183 11	344 10	330 2	191 25	316 9	336 15
203 16	298 59	255 20	297 18	208 15	330 13	329 15	218 75	340 6	152 6
23 9	27 19	134 2	84 15	169 5	2 52	324 22	43 23	241 16	144 1
175 0	140 6	305 28	107 26	206 51	23 30	129 2	34 28	234 4	348 6
176 9	18 48	159 36	298 34	288 8	334 28	324 14	42 17	120 4	161 29
22 11	200 0	121 2	295 27	358 26	353 14	310 22	233 4	278 2	164 11
23 22	211 2	252 38	184 26	94 9	337 17	314 7	233 30	13 70	103 26
130 18	170 1	105 29	355 3	360 23	123 10	318 13	28 0	298 71	189 6
153 15	342 2	214 34	312 24	172 28	307 11	340 19	256 60	246 28	349 6
134 5	46 3	240 2	305 19	13 15	337 16	4 13	297 67	274 36	318 13
188 10	295 10	87 4	130 20	355 19	322 11	138 1	92 16	239 38	152 4
211 23	161 3	76 20	52 58	164 14	351 12	329 18	269 57	296 37	338 1
4 36	40 40	124 40	291 16	143 13	348 6	332 19	74 0	82 16	197 41
23 20	139 19	187 52	48 84	354 28	318 11	6 20	178 46	303 13	158 13
24 9	330 20	278 24	78 2	238 47	336 5	360 2	213 8	320 4	127 18
47 4	316 20	149 5	303 48	173 48	158 4	332 12	248 23	300 63	343 22
5 31	31 22	117 32	316 11	338 27	339 13	84 10	283 33	286 34	189 16
8 30	189 10	154 21	115 10	208 25	331 5	351 6	242 10	273 10	354 3
17 32	344 4	291 20	247 6	183 16	346 3	322 13	8 33	328 12	345 31
101 48	355 23	298 11	91 4	245 12	325 11	171 8	288 27	283 8	150 2
43 60	107 50	286 21	318 15	191 6	321 3	346 17	238 40	281 28	133 6
16 40	1 4	203 8	239 10	51 9	300 11	342 16	98 23	353 3	158 9
81 26	264 8	198 8	136 33	205 22	338 17	128 4	224 45	139 27	140 21
169 34	15 31	273 10	296 18	274 12	340 8	348 11	229 50	289 22	333 1
143 24	61 15	293 34	275 8	151 23	159 10	1 4	209 2	209 25	338 3
143 22	317 17	152 22	88 40	182 25	333 9	348 1	64 18	243 4	153 12
174 16	160 6	290 3	64 29	160 14	333 17	332 10	263 36	303 19	327 5
200 38	185 11	78 0	66 63	108 25	334 6	330 18	263 47	258 9	320 12
195 15	176 3	94 8	151 9	96 34	348 31	344 14	213 15	261 10	340 9
21 50	157 18	23 2	263 8	51 5	325 12	342 18	241 61	284 4	150 10
174 10	343 12	302 19	334 34	201 9	11 3	318 4	64 24	350 33	349 1
32 35	233 21	293 29	69 32	202 30	337 9	326 19	360 67	294 22	129 21
-99 0	-99 0	-99 0	-99 0	-99 0	-99 0	-99 0	-99 0	-99 0	-99 0

84-311	84-354	84-358	84-359	84-360	84-361	84-373	84-374	84-388	85-20
217 58	37 10	313 5	330 15	80 47	285 6	226 5	223 14	45 6	28 13
360 42	53 9	4 9	316 19	174 15	344 9	256 5	157 1	5 12	115 5
322 23	28 8	315 13	1 12	47 50	272 34	247 11	151 24	164 10	257 13
173 20	274 43	293 13	20 26	150 51	57 19	67 8	137 2	34 5	276 12
143 0	278 48	338 10	15 14	19 6	180 2	77 0	132 8	46 3	322 8
163 0	251 22	27 32	139 11	127 22	283 19	264 13	240 21	97 22	263 25
349 9	360 19	350 11	274 10	149 4	38 12	323 10	328 24	172 8	305 18
319 16	349 20	313 8	99 7	152 18	99 2	97 1	308 3	28 40	272 25
168 2	211 9	140 27	66 1	45 25	349 26	243 16	91 9	150 5	74 20
149 35	75 3	6 8	186 36	21 4	307 14	82 6	33 14	138 33	331 0
23 21	14 1	172 9	118 33	127 57	126 1	117 29	219 26	129 25	135 10
14 4	303 8	167 7	115 4	124 29	331 17	223 20	99 10	333 3	5 14
360 25	96 0	345 12	175 33	190 24	312 3	322 34	311 4	68 4	3 0
37 3	316 20	309 14	163 6	360 32	304 20	234 13	101 0	17 10	186 10
164 20	9 28	350 9	68 20	298 67	118 2	133 7	35 23	42 35	113 10
349 3	254 57	317 8	36 12	357 18	156 9	18 12	229 13	170 51	235 12
311 1	132 17	201 5	96 12	56 64	247 29	339 10	271 2	348 12	113 3
16 9	359 3	153 8	106 7	153 14	282 22	28 22	236 3	53 14	135 15
341 7	4 1	143 4	18 8	26 18	294 9	8 22	324 32	69 6	90 21
3 3	32 15	336 6	160 13	302 63	325 6	32 23	60 6	146 0	269 5
174 20	312 15	306 18	57 1	35 53	312 4	172 25	111 13	296 10	100 13
39 36	345 8	11 4	89 36	162 26	286 10	4 15	93 6	101 48	327 10
172 4	42 24	199 20	187 14	6 4	326 9	310 24	67 18	293 11	324 9
333 2	51 16	190 7	2 5	166 11	282 26	303 4	130 22	173 00	283 2
162 37	63 25	344 33	358 8	138 16	110 2	302 10	100 6	13 23	58 36
17 29	1 16	315 22	21 10	143 5	279 10	251 11	108 28	133 18	301 5
182 23	349 13	348 2	1 10	44 14	150 22	58 26	296 18	36 16	101 2
1 25	11 7	317 2	16 6	337 25	105 6	336 10	321 2	299 20	290 74
142 24	34 2	312 4	184 19	212 7	307 15	340 2	113 13	68 19	320 26
126 6	358 36	340 16	37 11	132 22	265 20	48 13	109 8	78 15	70 9
149 30	359 53	179 2	184 6	11 5	90 21	44 13	326 7	36 22	55 59
126 9	71 22	338 26	24 25	74 12	315 28	217 6	130 5	167 4	310 6
113 38	49 26	314 14	128 11	6 34	350 2	244 10	290 9	24 24	299 11
336 40	33 1	6 4	93 26	346 27	134 5	38 7	58 24	348 6	210 6
324 24	300 8	326 14	155 14	26 4	265 48	149 14	129 2	148 11	110 12
174 13	320 11	343 18	107 20	194 30	314 24	131 3	243 8	49 6	116 21
306 24	325 18	333 24	86 75	142 2	302 13	67 13	155 18	349 6	136 22
144 25	36 13	123 36	113 21	79 39	313 2	37 0	319 12	217 6	339 24
223 26	266 14	354 21	110 12	236 16	305 8	230 16	315 5	105 36	26 15
105 0	38 12	336 11	161 6	24 18	157 41	169 0	140 18	63 11	307 31
225 22	353 31	323 10	112 33	168 4	304 2	100 12	95 15	77 13	167 21
219 18	55 5	311 10	182 4	266 47	251 23	339 8	316 11	56 11	307 8
141 10	54 2	301 18	130 13	173 33	121 3	334 16	101 2	347 6	174 4
88 32	347 5	149 4	68 10	53 4	132 5	313 3	271 8	29 6	92 25
328 9	38 21	323 14	310 7	75 9	133 10	332 21	324 24	345 1	339 2
106 31	63 0	298 21	268 4	192 14	323 2	354 14	82 4	39 16	143 9
120 22	43 4	168 4	252 9	94 24	311 6	312 19	76 8	56 4	318 36
312 12	6 5	6 24	71 10	98 17	316 17	351 12	354 18	53 18	182 20
332 1	60 9	4 10	41 10	194 13	317 21	170 0	333 4	17 30	342 15
343 36	17 15	339 23	105 8	29 35	334 18	173 21	153 9	318 5	162 22
-99 0	-99 0	-99 0	-99 0	-99 0	-99 0	-99 0	-99 0	-99 0	-99 0

85-22	85-47	85-49	85-50	85-58	85-60	85-61	85-81	85-82	85-83
78 2	179 14	267 11	215 17	247 9	5 9	31 4	337 26	261 12	280 3
97 39	34 11	281 20	311 7	219 23	2 1	172 29	328 5	210 1	98 11
123 0	159 16	265 15	311 10	221 22	204 4	127 8	320 16	352 19	73 24
38 4	166 0	262 7	115 12	30 1	227 14	289 32	332 9	35 5	212 7
314 19	314 8	222 25	131 8	297 21	332 28	26 38	26 12	100 2	58 5
150 6	285 0	286 34	139 14	331 18	314 54	147 4	258 10	229 6	109 19
145 17	72 20	338 9	324 5	7 44	343 10	309 2	56 9	36 21	214 6
328 14	332 11	280 9	109 11	49 1	308 4	356 5	96 14	356 10	304 26
332 21	174 44	297 18	307 3	336 11	327 19	145 19	205 4	316 8	101 3
355 8	59 31	282 10	304 12	359 52	5 40	141 18	288 22	117 8	110 14
297 7	321 10	117 40	126 13	342 26	116 8	72 15	160 40	48 0	138 15
86 28	2 6	119 1	54 5	271 89	339 9	124 5	328 29	302 0	130 2
48 43	180 24	44 2	67 16	357 2	324 6	190 11	199 12	219 24	85 19
24 21	171 62	281 10	111 1	329 12	306 4	339 2	327 29	287 21	312 9
216 19	270 41	264 14	135 4	328 50	336 6	116 16	145 8	74 13	162 22
164 22	299 4	299 21	322 3	265 86	357 6	329 4	32 40	314 0	117 15
283 7	309 9	310 3	145 5	319 15	162 12	172 12	330 17	334 28	212 2
243 54	140 22	31 12	138 2	233 55	230 6	341 10	177 11	105 1	247 5
224 36	81 9	289 22	158 8	229 26	337 4	115 4	28 29	41 10	256 5
238 16	221 50	305 16	314 1	208 28	251 18	321 26	321 6	303 5	229 5
209 28	359 5	212 23	69 21	17 19	152 16	120 39	97 12	246 1	98 18
206 11	151 5	118 0	317 8	67 19	175 15	219 9	38 13	154 6	43 10
57 34	141 37	298 27	134 4	202 7	313 13	172 6	28 23	338 11	226 2
254 33	346 21	285 11	135 2	177 19	252 19	160 9	332 20	260 12	110 24
281 62	327 2	274 25	334 6	271 31	203 8	339 21	321 10	254 12	29 10
154 16	197 15	96 3	95 4	307 46	2 2	36 24	182 13	17 6	53 16
56 6	167 6	287 38	129 8	192 26	327 15	12 3	328 10	19 3	35 9
180 22	312 7	308 8	110 5	241 27	28 0	311 50	138 18	65 6	78 19
314 50	59 51	296 30	150 21	282 20	174 6	46 39	325 23	67 10	123 0
22 6	346 2	297 6	294 1	184 3	332 6	120 4	271 32	228 13	97 39
26 41	112 9	292 10	117 19	157 26	337 7	359 14	70 65	80 8	80 30
268 69	154 4	304 5	317 18	187 19	349 5	53 6	293 8	56 6	1 27
91 49	172 5	276 21	161 1	232 16	142 6	191 24	286 28	213 0	299 12
98 20	199 7	356 35	322 7	257 35	319 16	336 45	359 9	257 17	355 24
155 23	80 3	283 22	217 19	353 4	332 7	136 19	355 13	49 22	203 6
3 29	112 23	133 0	129 6	219 16	152 14	118 13	288 2	254 9	41 21
203 58	150 38	127 7	141 8	225 23	11 22	108 38	268 7	308 6	34 15
312 25	78 4	269 11	104 4	244 19	7 3	360 16	310 0	349 15	116 1
243 24	355 16	143 19	121 10	272 56	360 9	45 5	247 1	191 19	78 12
165 33	204 18	247 48	242 22	170 25	347 7	319 22	223 19	49 14	106 15
138 0	21 31	122 0	74 1	284 34	134 15	86 8	272 1	355 4	244 8
193 18	157 20	205 38	220 16	188 12	359 8	132 6	111 5	42 5	60 21
164 18	252 9	317 3	80 18	257 39	333 17	332 22	286 5	11 65	42 3
203 12	51 4	53 9	247 28	232 2	342 7	347 3	275 10	257 11	244 3
189 8	117 29	323 32	296 1	152 3	337 16	326 9	267 51	63 42	84 16
205 27	139 39	309 41	6 4	71 31	284 6	337 1	64 19	76 16	1 8
358 3	219 47	46 12	147 2	246 21	325 26	336 10	113 16	330 24	219 6
227 26	331 7	220 15	312 6	29 13	335 16	32 18	191 19	224 7	226 1
324 15	335 7	208 17	312 1	320 67	355 25	135 19	31 25	354 14	220 0
322 13	49 4	282 12	134 5	157 26	15 38	31 8	144 00	170 2	43 2
-99 0	-99 0	-99 0	-99 0	-99 0	-99 0	-99 0	-99 0	-99 0	-99 0

85-84	85-85	85-86	85-87	85-88	85-89	85-90	85-91	85-92	85-93
318 38	210 22	311 6	298 16	228 9	65 6	80 20	228 10	204 19	123 9
208 65	227 0	337 19	338 26	43 2	315 14	154 20	43 5	232 23	106 0
321 29	271 6	124 48	188 24	28 65	334 12	199 14	91 2	156 15	163 21
40 17	187 22	330 29	108 3	36 60	31 2	41 26	59 12	149 3	173 7
35 12	227 34	38 30	78 9	35 51	343 18	124 35	31 10	258 9	313 11
37 7	115 19	103 9	37 21	19 19	127 12	9 3	100 5	196 7	225 10
359 32	201 14	358 8	229 37	109 59	277 1	127 25	70 3	127 20	163 12
331 6	344 19	321 9	36 31	277 1	189 24	28 80	61 19	204 16	113 7
309 5	210 18	332 20	227 55	89 1	352 4	294 49	60 20	191 18	56 5
31 4	240 16	160 2	51 36	355 13	220 17	87 44	300 15	235 21	162 15
212 1	269 30	347 20	220 31	290 17	20 10	140 19	328 29	158 27	148 19
254 2	314 5	1 17	320 15	295 4	87 42	47 1	301 9	213 8	149 15
337 9	43 3	125 35	227 17	34 24	137 2	56 9	26 21	221 10	293 9
237 5	343 22	137 3	188 21	46 8	357 1	107 17	253 0	151 32	42 39
350 24	149 9	159 2	187 5	75 6	186 1	332 16	72 15	192 32	186 7
229 10	120 24	100 12	176 15	7 46	62 1	1 34	253 27	298 17	143 40
182 16	167 5	314 6	298 9	28 15	262 26	59 34	1 6	230 36	123 47
232 34	334 51	3 35	119 8	357 10	355 1	185 23	16 5	304 15	130 22
276 5	34 9	170 8	288 6	39 6	252 0	47 31	23 5	216 17	113 18
351 10	117 7	314 3	308 19	217 8	272 10	137 13	13 13	238 8	131 14
180 12	30 1	339 25	49 16	47 23	2 14	57 24	4 23	357 11	114 2
275 3	185 16	328 22	247 31	53 6	119 14	173 38	23 14	344 2	103 9
239 10	224 21	346 15	189 19	206 14	245 2	25 33	26 14	211 3	224 10
152 14	162 21	147 4	337 31	30 8	89 13	193 24	285 30	204 3	187 10
175 16	196 8	358 2	63 29	260 4	330 49	40 23	286 11	302 21	145 11
348 15	330 4	349 16	83 18	34 9	311 55	220 14	42 14	267 8	222 16
53 12	292 9	337 11	308 46	88 18	284 39	181 45	122 11	341 2	113 12
226 15	344 3	352 2	177 21	40 30	270 37	190 41	59 29	172 42	257 30
241 17	346 2	321 16	127 31	51 2	2 9	194 17	232 7	225 11	102 26
95 40	285 7	156 6	69 44	110 18	122 10	214 2	215 3	229 19	128 9
8 24	136 5	311 2	297 29	249 6	162 5	229 17	31 7	238 5	189 14
325 34	195 27	357 17	58 20	73 14	137 12	38 0	44 5	241 18	123 4
200 12	189 20	162 30	67 8	264 8	83 18	187 30	255 4	90 4	120 24
5 17	360 8	125 3	57 40	64 9	72 46	154 15	303 39	220 41	182 9
359 26	113 23	165 20	7 28	270 11	140 15	126 30	4 12	150 6	70 11
17 42	307 11	308 11	43 35	5 14	96 5	170 14	341 6	131 2	220 24
351 29	162 9	316 15	359 14	156 10	253 1	236 4	47 36	260 11	157 8
66 64	111 3	341 50	218 9	263 18	240 14	188 29	208 6	41 7	202 15
229 4	338 15	72 21	69 11	6 9	234 3	186 36	48 23	273 10	153 14
280 1	324 3	357 6	163 13	80 24	123 30	166 36	87 36	340 8	181 25
271 10	157 28	7 4	109 8	226 2	329 13	203 25	21 16	68 15	134 2
263 16	255 9	350 36	63 22	84 0	191 8	192 20	32 2	222 2	200 1
180 9	179 2	339 10	337 19	251 8	245 2	23 10	99 9	213 33	145 10
172 11	131 2	307 10	48 32	195 11	98 1	175 41	89 17	231 23	168 15
347 18	316 26	306 11	119 22	85 9	319 17	208 22	241 16	213 15	186 11
216 9	156 14	309 6	38 42	95 7	109 8	128 25	245 5	267 11	151 5
48 20	199 8	335 5	41 41	328 8	248 15	246 24	171 8	226 12	222 5
8 11	324 5	138 6	343 11	12 23	38 44	181 34	77 1	280 8	194 6
188 5	320 41	129 9	347 8	355 14	137 61	263 45	48 5	11 4	228 16
344 6	211 5	68 21	242 14	323 14	120 11	202 13	84 4	372 8	164 44
-99 0	-99 0	-99 0	-99 0	-99 0	-99 0	-99 0	-99 0	-99 0	-99 0

85-94	85-95	84-L1	84-L2	84-L3	84-L4	84-L5	84-L6	84-L7	84-286
301 27	218 19	313 3	114 0	21 38	334 9	356 6	186 49	287 5	117 27
128 4	73 5	184 11	271 30	15 14	353 13	317 4	181 26	88 20	315 7
303 19	139 15	270 24	258 32	4 29	7 14	176 10	12 5	178 36	75 1
312 14	68 13	108 13	98 28	338 12	142 16	339 16	344 20	260 21	198 24
166 9	89 18	8 19	271 17	342 5	312 44	340 4	265 5	72 12	332 6
173 6	300 28	316 2	72 29	230 34	18 3	174 36	238 28	283 22	95 5
108 5	86 16	178 15	67 12	311 22	352 14	78 24	355 24	20 20	254 25
124 47	191 0	150 36	59 10	212 5	98 26	129 26	167 21	233 11	126 26
201 23	107 30	138 15	16 6	245 16	188 16	342 27	348 14	232 6	35 24
190 22	122 22	170 24	265 15	132 4	14 62	312 25	55 13	50 0	2 15
293 5	56 2	350 29	267 21	350 4	185 8	338 20	6 40	338 66	104 3
288 20	33 15	346 26	251 36	347 3	225 9	357 17	298 36	335 33	281 7
175 14	201 15	160 4	283 9	49 24	144 9	156 4	340 18	199 13	39 38
330 30	197 0	357 20	250 44	297 6	338 19	130 33	4 12	304 50	150 31
350 17	217 3	164 1	112 1	340 24	353 22	242 12	134 12	258 21	161 9
168 15	321 25	140 24	286 17	108 0	352 17	322 16	338 21	193 14	228 21
196 21	122 22	331 27	244 24	335 6	316 22	337 8	155 16	179 2	158 31
290 36	305 19	318 26	245 19	224 45	334 54	344 22	310 10	293 11	339 19
343 15	31 25	350 16	288 28	340 2	330 40	360 4	306 14	252 20	69 17
161 2	12 14	318 20	6 38	198 16	147 24	355 40	213 16	125 4	250 8
9 6	37 8	326 10	284 33	240 8	189 22	97 54	39 26	29 11	98 10
346 28	58 12	118 38	123 22	8 18	348 15	83 36	25 18	9 6	298 20
357 18	80 4	125 2	288 49	232 4	172 19	310 4	337 26	314 6	281 16
155 3	304 2	306 8	152 26	248 16	138 14	329 42	319 4	343 6	100 32
190 2	129 1	356 5	248 8	290 14	46 4	350 34	349 18	6 19	331 3
176 4	84 23	322 14	79 8	333 1	328 32	14 21	139 3	24 29	14 7
354 1	86 9	274 19	260 21	349 14	302 16	5 13	306 39	232 31	119 15
167 11	99 2	298 24	269 35	348 8	360 4	320 30	280 5	321 12	52 15
170 5	92 19	109 20	303 29	330 20	147 3	325 4	332 18	64 5	271 19
205 12	196 24	176 2	288 16	29 20	332 21	360 5	206 3	302 13	333 12
360 35	242 14	174 8	261 36	360 19	301 6	124 49	172 16	150 12	343 24
48 39	97 7	146 13	273 13	198 1	354 41	17 19	354 4	226 14	156 9
16 14	100 9	310 34	240 14	336 22	34 12	125 9	165 37	240 8	250 26
286 14	137 23	236 32	148 39	328 20	332 30	114 53	331 24	38 3	229 1
6 5	331 16	316 30	260 18	313 12	352 20	344 29	280 20	149 19	143 9
289 18	60 35	356 10	281 6	324 20	132 30	191 32	34 18	263 7	173 12
4 26	7 15	346 26	101 23	36 28	323 0	22 9	127 4	129 50	152 33
94 3	86 17	150 7	87 1	10 25	321 10	344 3	203 24	107 11	124 6
309 12	326 44	342 10	62 7	306 18	149 1	148 52	143 22	251 27	202 28
208 0	85 24	114 21	320 36	160 16	327 18	72 44	238 26	309 28	312 8
300 35	253 25	318 34	259 42	340 8	356 14	148 32	182 32	229 21	263 9
175 15	284 30	348 43	89 27	18 1	345 9	131 50	167 24	223 11	187 33
260 10	222 1	351 56	268 12	360 4	319 12	88 26	162 16	231 5	247 7
346 9	213 26	324 22	284 8	4 2	164 21	170 15	9 32	11 22	153 7
232 25	200 26	336 9	285 39	337 13	340 56	319 16	56 20	199 20	156 10
336 25	119 5	17 36	270 29	188 8	164 48	143 3	186 20	26 18	52 2
146 11	169 45	307 40	278 10	344 30	136 3	168 33	188 7	344 14	360 67
330 11	10 27	165 23	260 4	342 2	145 44	276 3	129 33	256 8	108 3
354 30	355 7	154 39	274 3	352 16	182 10	44 59	156 2	289 7	4 17
28 12	5 6	130 4	237 40	38 26	45 4	331 34	316 34	104 41	301 5
-99 0	-99 0	-99 0	-99 0	-99 0	-99 0	-99 0	-99 0	-99 0	-99 0

Appendix 12. Three dimensional Schmidt stereo projections of pebble fabric data from the Finlay River of northeastern British Columbia. Raw data listed in Appendix 11.

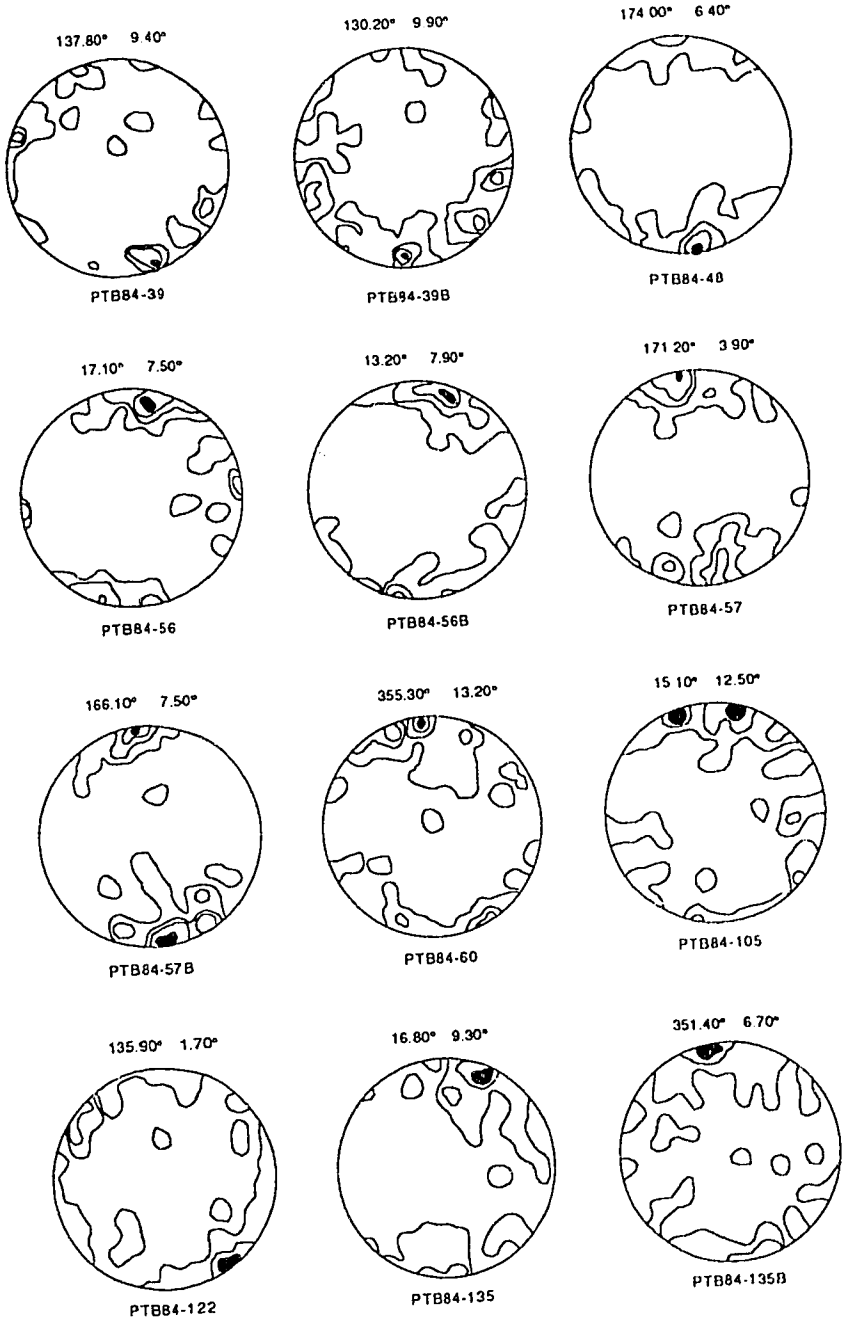
137.80° 9.40°
PTB84-39
130.20° 9.90°
PTB84-39B
174.00° 6.40°
PTB84-48
17.10° 7.50°
PTB84-56
13.20° 7.90°
PTB84-56B
171.20° 3.90°
PTB84-57
166.10° 7.50°
PTB84-57B
355.30° 13.20°
PTB84-60
15.10° 12.50°
PTB84-105
135.90° 1.70°
PTB84-122
16.80° 9.30°
PTB84-135
351.40° 6.70°
PTB84-135B

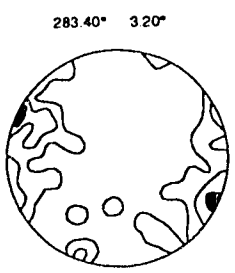

PTB84-147

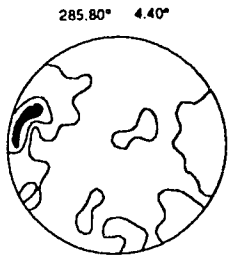

PTB84-150

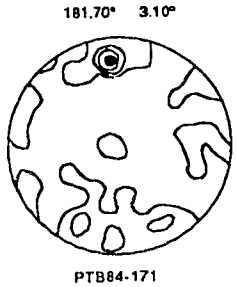

PTB84-171

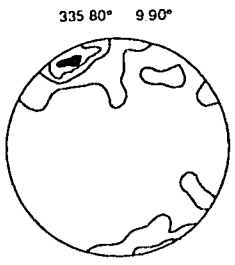

PTB84-193

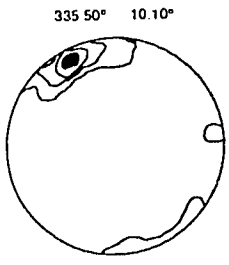

PTB84-194

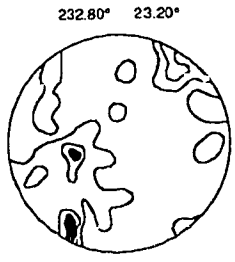

PTB[illegible]4-202

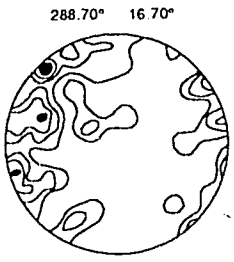

PTB84-213

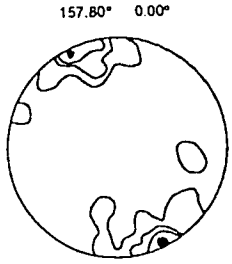

PTB84-242

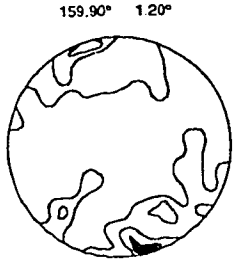

PTB84-311

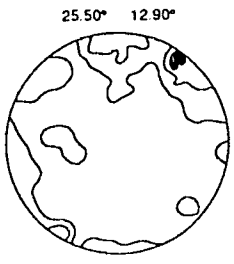

PTB84-354

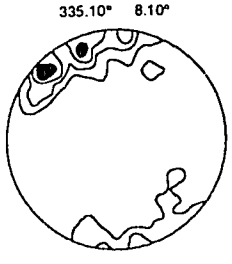

PTB84-358

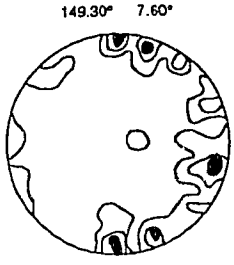

PTB84-359

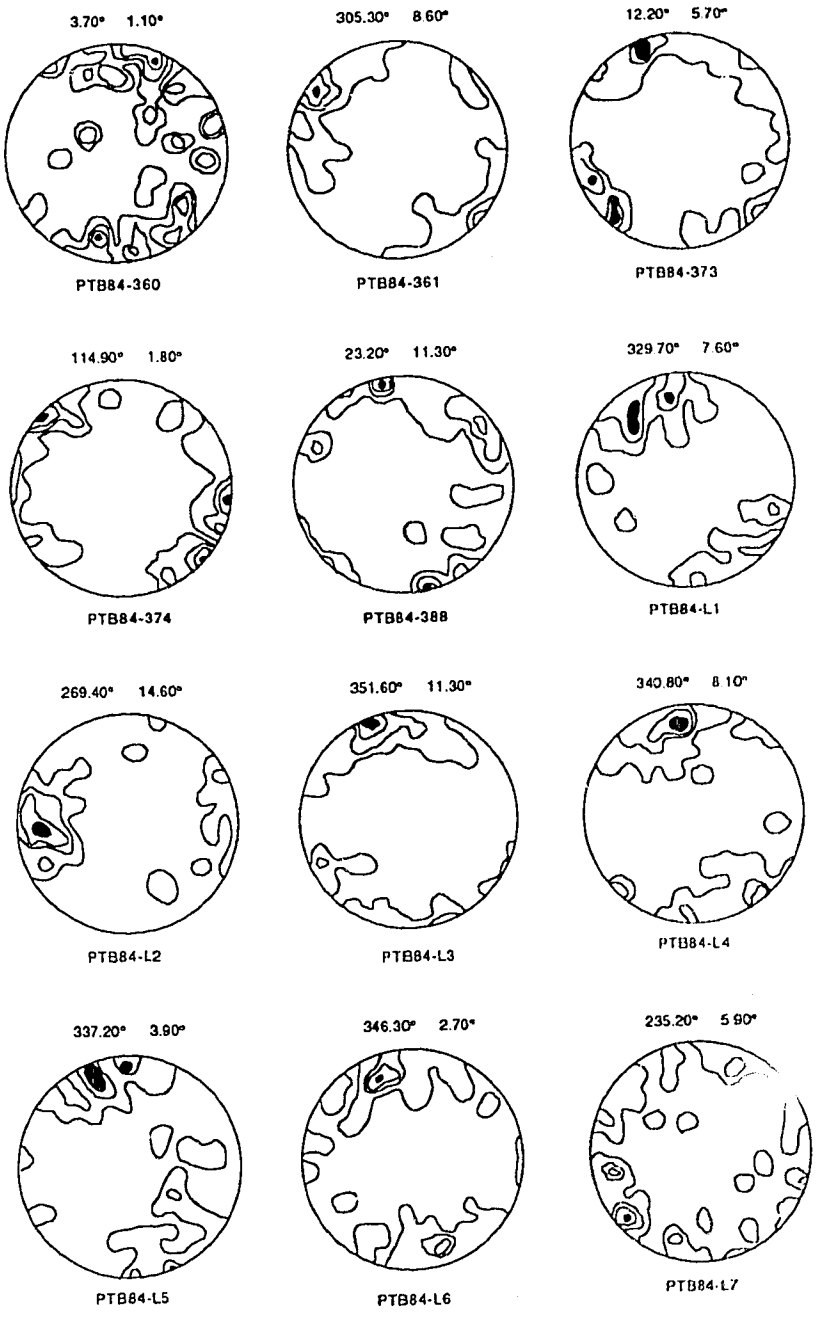
3.70° 1.10°
PTB84-360
305.30° 8.60°
PTB84-361
12.20° 5.70°
PTB84-373
114.90° 1.80°
PTB84-374
23.20° 11.30°
PTB84-388
329.70° 7.60°
PTB84-L1
269.40° 14.60°
PTB84-L2
351.60° 11.30°
PTB84-L3
340.80° 8.10°
PTB84-L4
337.20° 3.90°
PTB84-L5
346.30° 2.70°
PTB84-L6
235.20° 5.90°
PTB84-L7

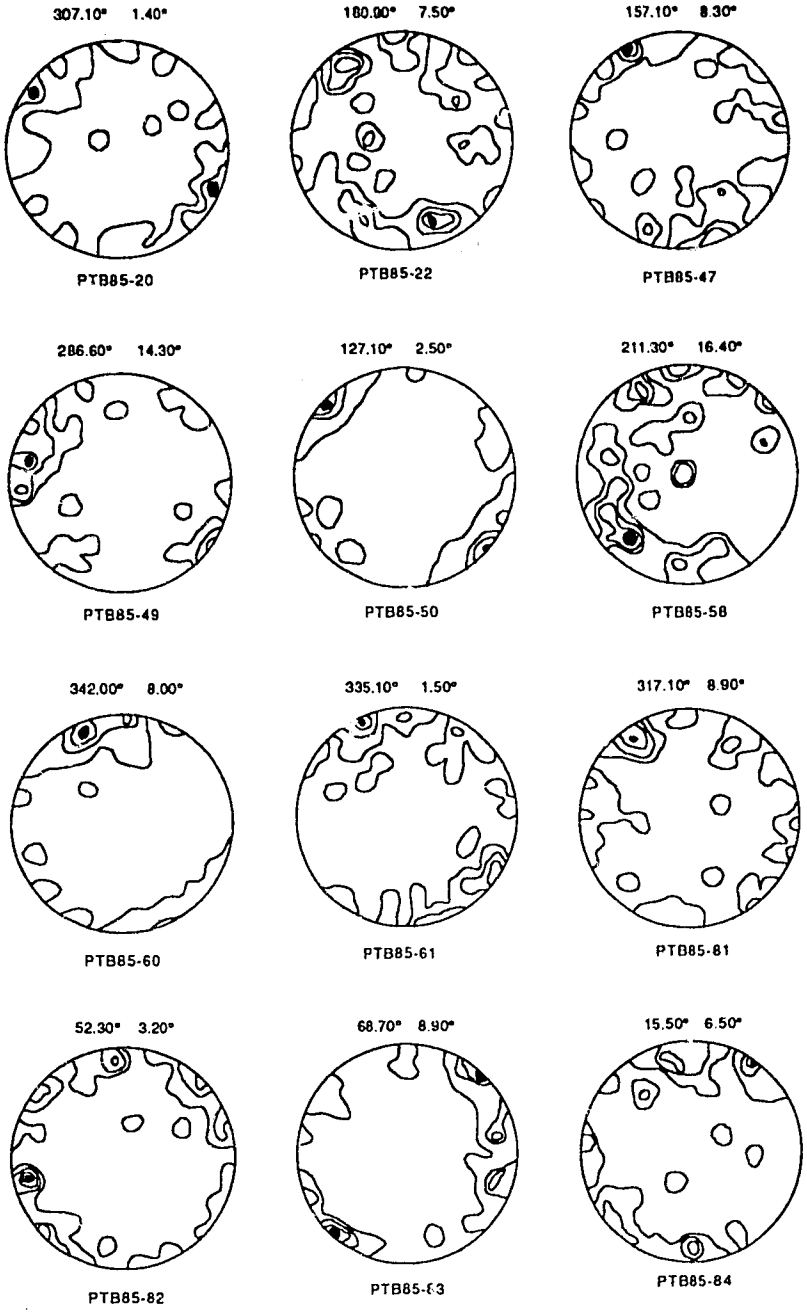
307.10° 1.40°
PTB85-20
180.00° 7.50°
PTB85-22
157.10° 8.30°
PTB85-47
286.60° 14.30°
PTB85-49
127.10° 2.50°
PTB85-50
211.30° 16.40°
PTB85-58
342.00° 8.00°
PTB85-60
335.10° 1.50°
PTB85-61
317.10° 8.90°
PTB85-81
52.30° 3.20°
PTB85-82
68.70° 8.90°
PTB85-83
15.50° 6.50°
PTB85-84

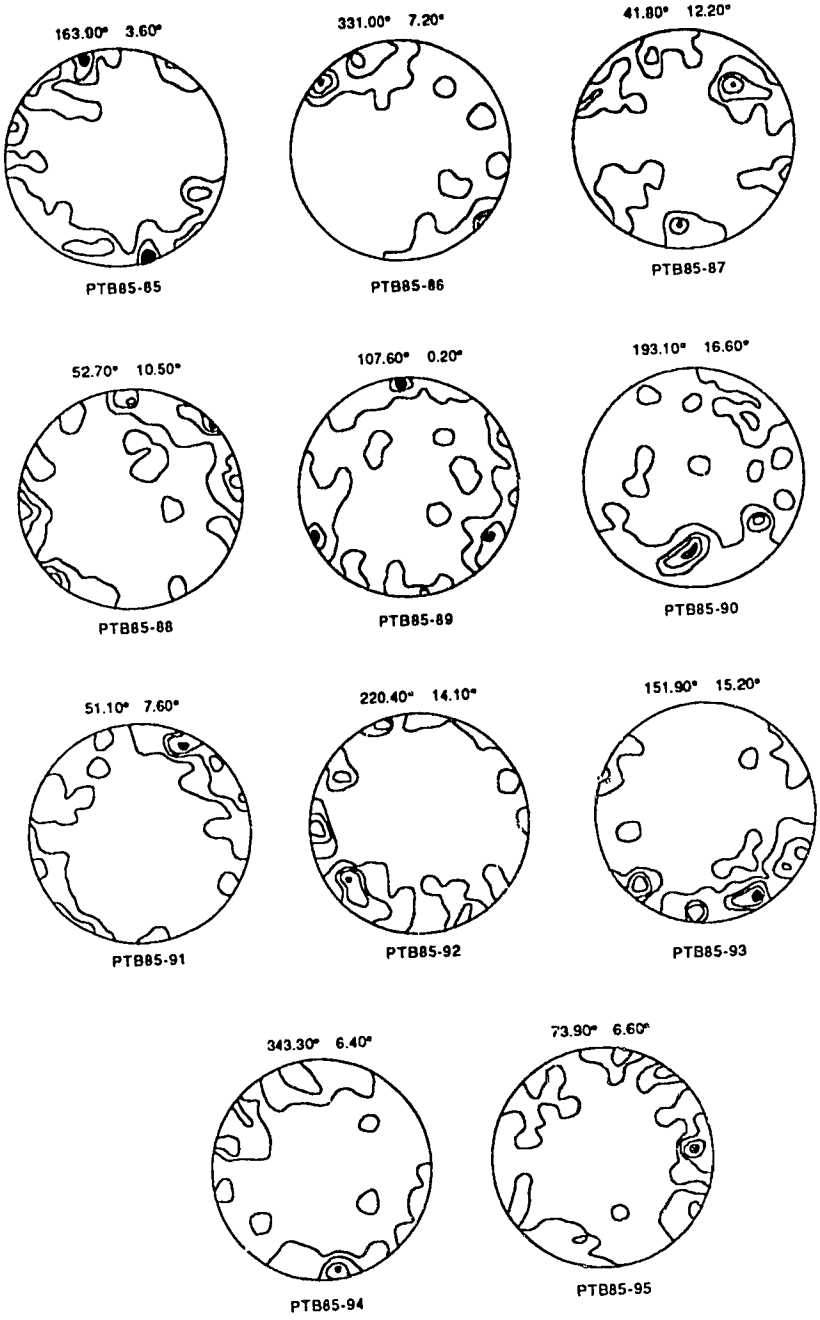
163.00° 3.60°
PTB85-85
331.00° 7.20°
PTB85-86
41.80° 12.20°
PTB85-87
52.70° 10.50°
PTB85-88
107.60° 0.20°
PTB85-89
193.10° 16.60°
PTB85-90
51.10° 7.60°
PTB85-91
220.40° 14.10°
PTB85-92
151.90° 15.20°
PTB85-93
343.30° 6.40°
PTB85-94
73.90° 6.60°
PTB85-95

Appendix 13. Three dimensional pebble fabric data listing mean trend, plunge, eigenvectors and eigenvalues for all samples from the northern Rocky Mountain Trench, British Columbia.

SAMPLE	TREND	PLUNGE	VECTOR 1	VECTOR 2	VECTOR 3	S1	S2	S3
84-39	137.80	9.40	31.163	14.678	4.159	0.623	0.294	0.083
84-39B	130.20	9.90	23.703	21.640	4.657	0.474	0.433	0.093
84-48	174.00	6.40	37.506	9.688	2.806	0.750	0.194	0.056
84-56	17.10	7.50	36.448	10.579	2.972	0.729	0.212	0.059
84-56B	13.20	7.90	34.795	12.959	2.247	0.696	0.259	0.045
84-57	171.20	3.90	36.132	8.174	5.695	0.723	0.163	0.114
84-57B	166.10	7.50	39.642	6.003	4.354	0.793	0.120	0.087
84-60	355.30	13.20	31.421	12.052	6.527	0.628	0.241	0.131
84-105	15.10	12.50	28.063	16.140	5.796	0.561	0.323	0.116
84-122	135.90	1.70	27.726	17.715	4.559	0.555	0.354	0.091
84-135	16.80	9.30	31.528	13.712	4.760	0.631	0.274	0.095
84-135B	351.40	6.70	30.499	12.656	6.845	0.610	0.253	0.137
84-147	283.40	3.20	33.550	11.400	5.050	0.671	0.228	0.101
84-150	285.80	4.40	29.905	10.921	9.174	0.598	0.218	0.183
84-171	181.70	3.10	28.382	13.083	8.535	0.568	0.262	0.171
84-193	335.80	9.90	42.621	5.510	1.869	0.852	0.110	0.037
84-194	335.50	10.10	45.212	3.985	0.802	0.904	0.080	0.016
84-202	232.80	23.20	30.128	12.025	7.846	0.603	0.241	0.157
84-213	288.70	16.70	27.434	16.711	5.855	0.549	0.334	0.117
84-242	157.80	0.00	41.898	5.133	2.969	0.838	0.103	0.059
84-286	127.40	3.00	26.400	18.273	5.327	0.528	0.365	0.107
84-311	159.90	1.20	32.848	10.463	6.689	0.657	0.209	0.134
84-354	25.50	12.90	30.708	15.938	3.354	0.614	0.319	0.067
84-358	335.10	8.10	40.574	6.887	2.538	0.811	0.138	0.051
84-359	149.30	7.60	24.622	21.933	3.444	0.492	0.439	0.069
84-360	3.70	1.10	26.141	16.477	7.382	0.523	0.330	0.148
84-361	305.30	8.60	38.011	8.698	3.291	0.760	0.174	0.066
84-373	12.20	5.70	24.930	22.253	2.817	0.499	0.445	0.056
84-374	114.90	1.80	32.854	14.269	2.877	0.657	0.285	0.058
84-388	23.20	11.30	27.821	19.164	3.015	0.556	0.383	0.060
84-L1	329.70	7.60	35.749	7.313	6.938	0.715	0.146	0.139
84-L2	269.40	14.60	37.320	6.506	6.174	0.746	0.130	0.123
84-L3	351.60	11.30	34.387	12.600	3.014	0.688	0.252	0.060
84-L4	340.80	8.10	35.082	7.939	6.979	0.702	0.159	0.140
84-L5	337.20	3.90	30.821	13.334	5.845	0.616	0.267	0.117
84-L6	346.30	2.70	30.902	12.581	6.518	0.618	0.252	0.130
84-L7	235.20	5.90	25.364	18.978	5.659	0.507	0.380	0.113
85-20	307.10	1.40	30.330	14.443	5.227	0.607	0.289	0.105
85-22	180.90	7.50	23.811	16.835	9.354	0.476	0.337	0.187
85-47	157.10	8.30	28.503	15.149	6.348	0.570	0.303	0.127
85-49	286.60	14.30	35.230	11.060	3.711	0.705	0.221	0.074
85-50	127.50	2.50	37.691	10.630	1.679	0.754	0.213	0.034
85-58	211.30	16.40	25.478	17.796	6.727	0.510	0.356	0.135
85-60	342.00	8.00	37.685	9.523	2.792	0.754	0.190	0.056
85-61	335.10	1.50	31.401	14.060	4.539	0.628	0.281	0.091
85-81	317.10	8.90	27.189	17.756	5.055	0.544	0.355	0.101

85-82	52.30	3.20	28.484	18.627	2.889	0.570	0.373	0.058
85-83	68.70	8.90	32.009	15.535	2.456	0.640	0.311	0.049
85-84	15.50	6.50	29.082	15.581	5.337	0.582	0.312	0.107
85-85	163.90	3.60	29.697	16.698	3.606	0.594	0.334	0.072
85-86	331.00	7.20	38.236	8.835	2.929	0.765	0.177	0.059
85-87	41.80	12.20	23.684	18.419	7.897	0.474	0.368	0.158
85-88	52.70	10.50	31.017	14.601	4.382	0.620	0.292	0.088
85-89	107.60	0.20	24.861	19.179	5.960	0.497	0.384	0.119
85-90	193.10	16.60	28.766	15.115	6.118	0.575	0.302	0.122
85-91	51.10	7.60	33.034	14.252	2.714	0.661	0.285	0.054
85-92	220.40	14.10	30.204	17.311	2.485	0.604	0.346	0.050
85-93	151.90	15.20	30.848	16.702	2.450	0.617	0.334	0.049
85-94	343.30	6.40	32.884	12.814	4.302	0.658	0.256	0.086
85-95	73.90	6.60	26.168	18.785	5.046	0.523	0.376	0.101

Appendix 14. Pebble fabric samples and significance values for derived eigenvalues from the northern Rocky Mountain Trench. Critical alpha values for S1 are 0.484 at 0.01%, 0.471 at 0.025% and 0.460 at 0.05%; for S3 values are 0.198 at 0.01%, 0.207 at 0.025% and 0.216 at 0.05% (after Anderson and Stephens 1972). Critical value for S1/S3 ratio is 2.35 at alpha level of 0.01% (after Woodcock and Naylor 1983). All values for sample size of n=50.

SAMPLE	S1 SIG	S3 SIG	S1/S3 SIG	SAMPLE	S1 SIG	S3 SIG	S1/S3 SIG
84-39	p < 0.01	p < 0.01	p < 0.01	84-L1	p < 0.01	p < 0.01	p < 0.01
84-39B	p < 0.025	p < 0.01	p < 0.01	84-L2	p < 0.01	p < 0.01	p < 0.01
84-48	p < 0.01	p < 0.01	p < 0.01	84-L3	p < 0.01	p < 0.01	p < 0.01
84-56	p < 0.01	p < 0.01	p < 0.01	84-L4	p < 0.01	p < 0.01	p < 0.01
84-56B	p < 0.01	p < 0.01	p < 0.01	84-L5	p < 0.01	p < 0.01	p < 0.01
84-57	p < 0.01	p < 0.01	p < 0.01	84-L6	p < 0.01	p < 0.01	p < 0.01
84-57B	p < 0.01	p < 0.01	p < 0.01	84-L7	p < 0.01	p < 0.01	p < 0.01
84-60	p < 0.01	p < 0.01	p < 0.01	85-20	p < 0.01	p < 0.01	p < 0.01
84-105	p < 0.01	p < 0.01	p < 0.01	85-22	p < 0.025	p < 0.01	p < 0.01
84-122	p < 0.01	p < 0.01	p < 0.01	85-47	p < 0.01	p < 0.01	p < 0.01
84-135	p < 0.01	p < 0.01	p < 0.01	85-49	p < 0.01	p < 0.01	p < 0.01
84-135B	p < 0.01	p < 0.01	p < 0.01	85-50	p < 0.01	p < 0.01	p < 0.01
84-147	p < 0.01	p < 0.01	p < 0.01	85-58	p < 0.01	p < 0.01	p < 0.01
84-150	p < 0.01	p < 0.01	p < 0.01	85-60	p < 0.01	p < 0.01	p < 0.01
84-171	p < 0.01	p < 0.01	p < 0.01	85-61	p < 0.01	p < 0.01	p < 0.01
84-193	p < 0.01	p < 0.01	p < 0.01	85-81	p < 0.01	p < 0.01	p < 0.01
84-194	p < 0.01	p < 0.01	p < 0.01	85-82	p < 0.01	p < 0.01	p < 0.01
84-202	p < 0.01	p < 0.01	p < 0.01	85-83	p < 0.01	p < 0.01	p < 0.01
84-213	p < 0.01	p < 0.01	p < 0.01	85-84	p < 0.01	p < 0.01	p < 0.01
84-242	p < 0.01	p < 0.01	p < 0.01	85-85	p < 0.01	p < 0.01	p < 0.01
84-286	p < 0.01	p < 0.01	p < 0.01	85-86	p < 0.01	p < 0.01	p < 0.01
84-311	p < 0.01	p < 0.01	p < 0.01	85-87	p < 0.025	p < 0.01	p < 0.01
84-354	p < 0.01	p < 0.01	p < 0.01	85-88	p < 0.01	p < 0.01	p < 0.01
84-358	p < 0.01	p < 0.01	p < 0.01	85-89	p < 0.01	p < 0.01	p < 0.01
84-359	p < 0.01	p < 0.01	p < 0.01	85-90	p < 0.01	p < 0.01	p < 0.01
84-360	p < 0.01	p < 0.01	p < 0.01	85-91	p < 0.01	p < 0.01	p < 0.01
84-361	p < 0.01	p < 0.01	p < 0.01	85-92	p < 0.01	p < 0.01	p < 0.01
84-373	p < 0.01	p < 0.01	p < 0.01	85-93	p < 0.01	p < 0.01	p < 0.01
84-374	p < 0.01	p < 0.01	p < 0.01	85-94	p < 0.01	p < 0.01	p < 0.01
84-388	p < 0.01	p < 0.01	p < 0.01	85-95	p < 0.01	p < 0.01	p < 0.01

Appendix 15. Natural remanent magnetic data for all horizons and units sampled in the northern Rocky Mountain Trench. Each sample represents the average analytical results from four separate samples within a single horizon. Data presented consist of sample identification, average declination, average inclination, R value, k value, Fisher's 0.05 level of significance for both declination and inclination.

SAMPLE	DECLINATION	INCLINATION	R	k	DEC .05	INC .05
4A2A	278.3	60.5	3.9541	65.38	17.70	8.71
4A2B	3.8	65.1	3.9571	69.90	19.96	8.42
4A2C	340.6	65.0	3.9028	30.87	30.14	12.76
4A2D	8.0	64.9	3.9145	35.11	28.12	11.94
4A2E	356.4	67.5	3.9855	206.57	12.78	4.88
4B1A	348.6	18.0	3.9699	99.57	7.40	7.04
4B1B	4.8	33.6	3.9416	51.40	11.81	9.84
4B1C	18.1	13.7	3.9831	177.03	5.43	5.27
4B1D	1.8	11.3	3.9801	150.49	5.83	5.72
4B1E	11.6	23.1	3.9403	50.22	10.82	9.95
4C1E	18.0	73.9	3.9905	314.55	14.29	3.95
4C1D	18.7	70.6	3.9671	91.27	22.20	7.36
4C1C	21.9	67.8	3.9554	67.33	8.58	22.74
4C1B	55.5	65.2	3.9844	191.76	12.07	5.06
4C1A	24.7	46.6	3.9684	94.84	10.50	7.22
4C2A	8.2	69.6	3.9679	93.41	20.87	7.27
4C2B	26.4	65.0	3.9414	51.23	23.28	9.85
4C2C	335.8	61.3	3.8277	17.41	35.73	17.15
4C2D	340.8	77.1	3.9567	69.32	37.74	8.45
4C2E	39.7	58.3	3.8497	19.96	30.36	15.97
4D4F	356.8	70.8	3.9327	44.55	32.11	10.58
4D4G	15.7	69.8	3.9107	33.60	35.42	12.21
4D4H	4.9	58.8	3.9157	35.59	22.88	11.86
4D4I	344.7	62.1	3.9664	89.34	15.90	7.44
4D4J	0.8	66.7	3.9786	140.40	14.97	5.92
5B1A	64.9	34.5	3.9276	41.44	13.31	10.97
5B1B	10.4	52.8	3.8313	17.78	28.03	16.96
5B1C	287.3	19.1	3.9846	194.83	5.32	5.02
5B1D	26.0	47.6	3.2408	3.95	58.04	39.12
5B1E	29.2	58.7	3.8598	21.40	29.69	15.41
4D4A	322.0	65.5	3.9025	30.77	30.80	12.78
4D4B	343.4	54.7	3.6500	8.57	43.30	25.03
4D4C	307.7	58.5	3.8997	29.91	24.83	12.96
4D4D	275.8	64.9	3.8765	24.30	34.02	14.43
4D4E	1.8	67.9	3.7141	10.49	59.70	22.43
5A1A	339.0	23.0	3.8933	28.11	14.54	13.38
5A1B	348.2	31.4	3.9756	122.75	7.43	6.34

Appendix 16. Location coordinates of all exposures disc ssed in text. Section name underlined, and coded section abbreviation in bold and brackets. Section drawing, ternary plots of pebble lithologies, ternary plots and histograms of textural analyses, compositional curves and composite stratigraphic columns for each described section follow location coordinates.

Ware Section (W): NTS 94 F/5-Ware Sheet, 57° 22' 24" N and 125° 33' 36" W, UTM 10VCU 460 618, top at 820 m elevation. Bluff on west side of Finlay River faces northeast, seven km southeast of Fort Ware, approximately 2000 horizontal m and 72 vertical m of cliff exposure. (Water level at 750m)

Ware Two Section (W2): NTS 94 F/5-Ware Sheet, 57° 22' 18" N and 125° 31' 54" W, UTM 10VCU 478 614, top at 750 m elevation. Bank cut on east side of Finlay River faces southwest, eight km southeast of Fort Ware, approximately 450 horizontal m and 8 vertical m of cliff exposure. (Water level at 742m)

Paul Creek Section (PC): NTS 94 F/6-Paul River Sheet, 57° 18' 36" N and 125° 27' 06" W, UTM 10VCU 524 544, top at 740 m elevation. Bank cut on east side of Finlay River and south side of Paul Creek faces northwest, 16.5 km southeast of Fort Ware, approximately 200 horizontal m and 10 vertical m of cutbank exposure. (Water level at 730m)

Section One (I): NTS 94 F/6-Paul River Sheet, 57° 17' 35" N and 125° 27' 45" W, UTM 10VCU 516 525, top at 746 m elevation. Bluff on west side of Finlay River faces north,17.5 km southeast of Fort Ware and 2.5 km northwest of Finbow airstrip, approximately 750 horizontal m and 21 vertical m of cliff exposure. (Water level at 725m)

Section Two (II): NTS 94 F/6-Paul River Sheet, 57° 18' 06" N and 125° 26' 36" W, UTM 10VCU 527 535, top at 788 m elevation. Bluff on east side of Finlay River faces west-southwest, three km north of the Finbow airstrip, approximately 1800 horizontal m and 63 vertical m of cliff exposure. (Water level at 725m)

Bad Smell Secion (BS): NTS 94 F/6-Paul River Sheet, 57° 17' 00" N and 125° 27' 15" W, UTM 10VCU 522 512, top at 726 m elevation. Bluff on west side of Finlay River faces southeast, 3/4 km north of the Finbow airstrip, approximately 50 horizontal m and 6 vertical m of cliff exposure. (Water level at 720 m)

Section Three (III): NTS 94 F/6-Paul River Sheet, 57° 16' 42" N and 125° 28' 30" W, UTM 10VCU 507 509, top at 786 m elevation. Bluff on west side of Finlay River faces southeast, one km northwest of Finbow airstrip, approximately 2000 horizontal m and 66 vertical m of cliff exposure. (Water level at 720m)

North Air Section (NA): NTS 94 F/6-Paul River Sheet, 57° 16' 42" N and 125° 27' 24" W, UTM 10VCU 519 508, top at 740 m elevation. Bank cut on east side Finlay River faces north, one half kilometre northwest of Finbow airstrip, approximately 200 horizontal m and 20 vertical m of riverbank exposure. (Water level at 720m)

West Air Section (WA): NTS 94 F/6-Paul River Sheet, 57° 16' 02" N and 125° 27' 50" W, UTM 10VCU 514 497, top at 740 m elevation. Bank exposure on east side of Finlay River faces west-southwest, one half kilometre west of Finbow

airstrip, approximately 200 horizontal m and 25 vertical m of riverbank exposure. (Water level at 715m)

Section Four (IV): NTS 94 F/6-Paul River Sheet, 57° 15' 42" N and 125° 26' 15" W, UTM 10VCU 530 489, top at 723 m elevation. Bluff on west side of Finlay River faces north, one kilometre southeast of the Finbow airstrip, approximately 400 horizontal m and 13 vertical m of cliff exposure. (Water level at 710m)

Section Five (V): NTS 94 F/6-Paul River Sheet, 57° 15' 12" N and 125° 24' 10" W, UTM 10VCU 551 478, top at 760 m elevation. Cliff on east side of Finlay River faces northwest, three km southeast of Finbow airstrip, approximately 750 horizontal m and 53 vertical m of cliff exposure. (Water level at 707m)

Opposite Bank Section (OB): NTS 94 F/3-Truncate Creek Sheet, 57° 14' 40" N and 125° 25' 15" W, UTM 10VCU 534 470, top at 755 m elevation. Cliff on west side of Finlay River faces east, two and a half kilometres south of Finbow airstrip, approximately 200 horizontal m and 49 vertical m of exposure. (Water level at 706m)

Section Seven (VII): NTS 94 F/3-Truncate Creek Sheet, 57° 11' 20" N and 125° 19' 20" W, UTM 10VCU 597 404, top at 720 m elevation. Bluff on east side of Finlay River faces west, 11.5 km southeast of Finbow airstrip, 750 horizontal m and 16 vertical m of cutbank exposure. (Water level at 704m)

Section Eight (VIII): NTS 94 F/3-Truncate Creek Sheet, 57° 10' 30" N and 125° 20' 20" W, UTM 10VCU 587 389, top at 781 m elevation. Bluff on west side of Finlay River faces northeast, four km southeast of the mouth of Russel Creek and 13 km southeast of the Finbow airstrip, approximately 750 horizontal m and 78 vertical m of cliff exposure. (Water level at 703m)

Section Nine (IX): NTS 94 F/3-Truncate Creek Sheet, 57° 11' 00" N and 125° 17' 30" W, 10VCU 615 398, top at 811 m elevation. Bluff on east side of Finlay River faces southwest, one kilometre north of the mouth of McGraw Creek and 14 km southeast of the Finbow airstrip, approximately 1300 horizontal m and 111 vertical m of cliff exposure. (Water level at 700m)

Odie Section (OD): NTS 94 F/3-Truncate Creek Sheet, 57° 09' 06" N and 125° 15' 10" W, UTM 10VCU 637 362, top at 702 m elevation. Bluff on west side of Finlay River faces northeast, one kilometre downstream of the mouth of Del Creek and 18 km southeast of the Finbow airstrip, approximately 200 horizontal m and nine vertical m of cutbank exposure. (Water level at 693m)

Section Ten (X): NTS 94 F/3-Truncate Creek Sheet, 57° 08' 50' N and 125° 15' 06" W, UTM 10VCU 647 355, top at 770 m elevation. Bluff on east side of Finlay River faces west, one and a half km downstream of the mouth of Del Creek and 19 km southeast of the Finbow airstrip, approximately 1100 horizontal m and 78 vertical m of cliff exposure. (Water level at 692m)

Section Eleven (XI): NTS 94 F/3-Truncate Creek Sheet, 57° 02' 40" N and 125° 09' 55" W, UTM 10VCU 687 242, top at 745 m elevation. Bluff on west side of Finlay River faces northeast, three km northwest of mouth of Akie River, 600 horizontal m and 65 vertical m of cliff exposure. (Water level at 680m)

Section Twelve (XII): NTS 94 C/14-Ed Bird Creek Sheet, 56° 58' 10" N and 125° 04' 45" W, UTM 10VCU 735 158, top at 745 m elevation. Bluff on west side of Finlay River faces north, three km southwest of Pesika Creek, 1300 horizontal m and 72 vertical m of cliff exposure. (Water level at 673m)

SYMBOL LEGEND FOR APPENDIX FIGURES

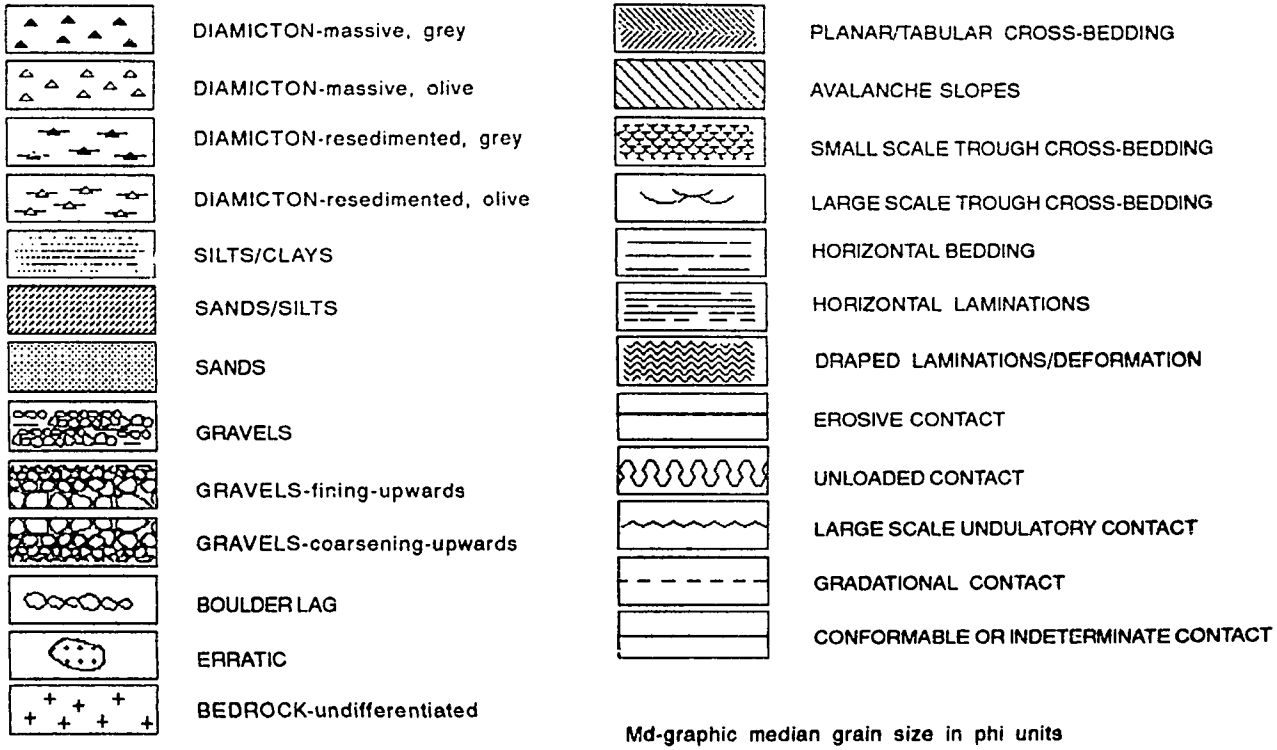

MOISTURE-moisture content in percent
ORG MAT.-organic matter content in percent
CARBONATE-carbonate content in percent
TOTAL CARB-total carbon in percent

Md-graphic median grain size in phi units
Mz-graphic mean grain size in phi units
Si-inclusive graphic standard deviation in phi units
Ski-inclusive graphic skewness
Kg-graphic kurtosis

Legend for symbols and notation used in all appendix figures.

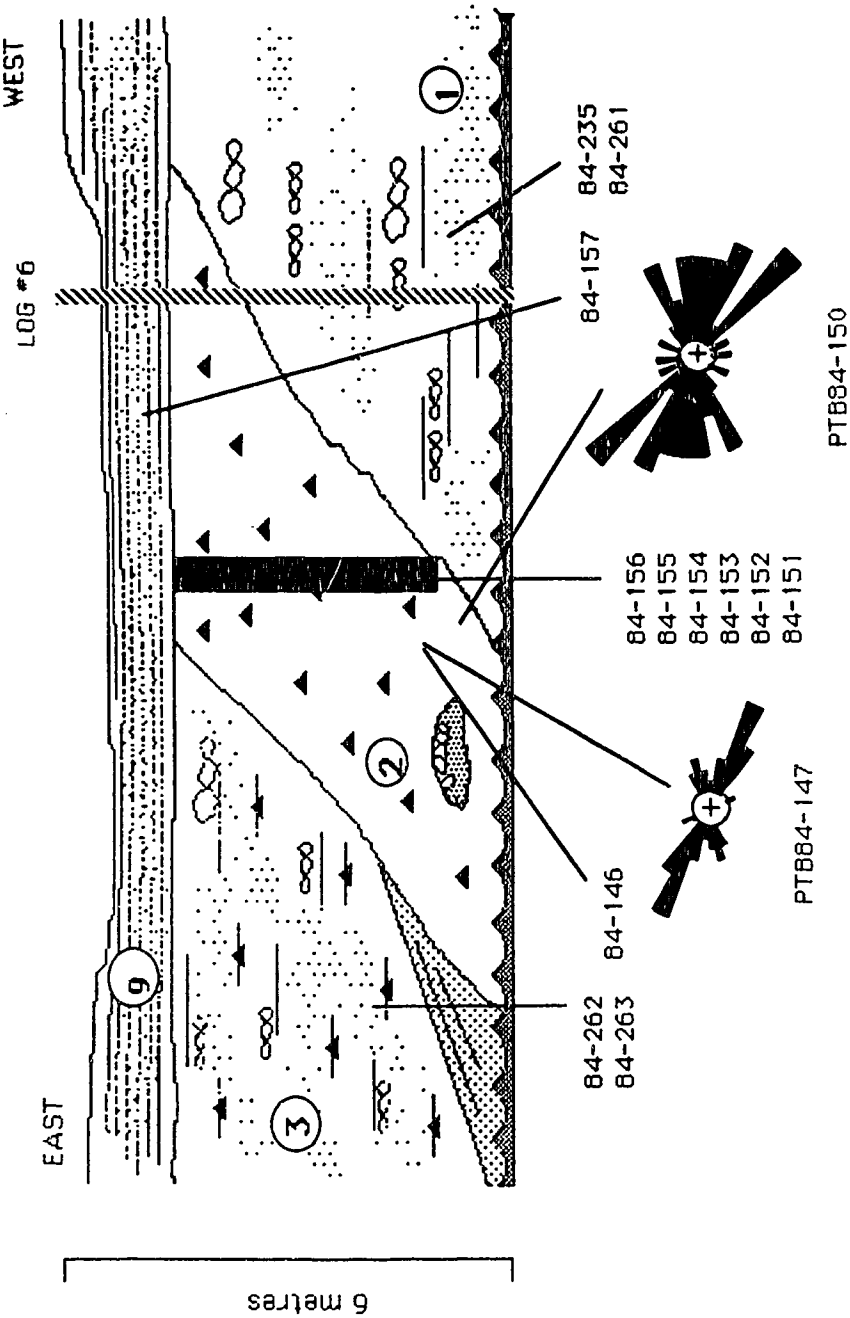

Section drawing of primary face of basal portion of Section Ware, far southeast end of bluff.

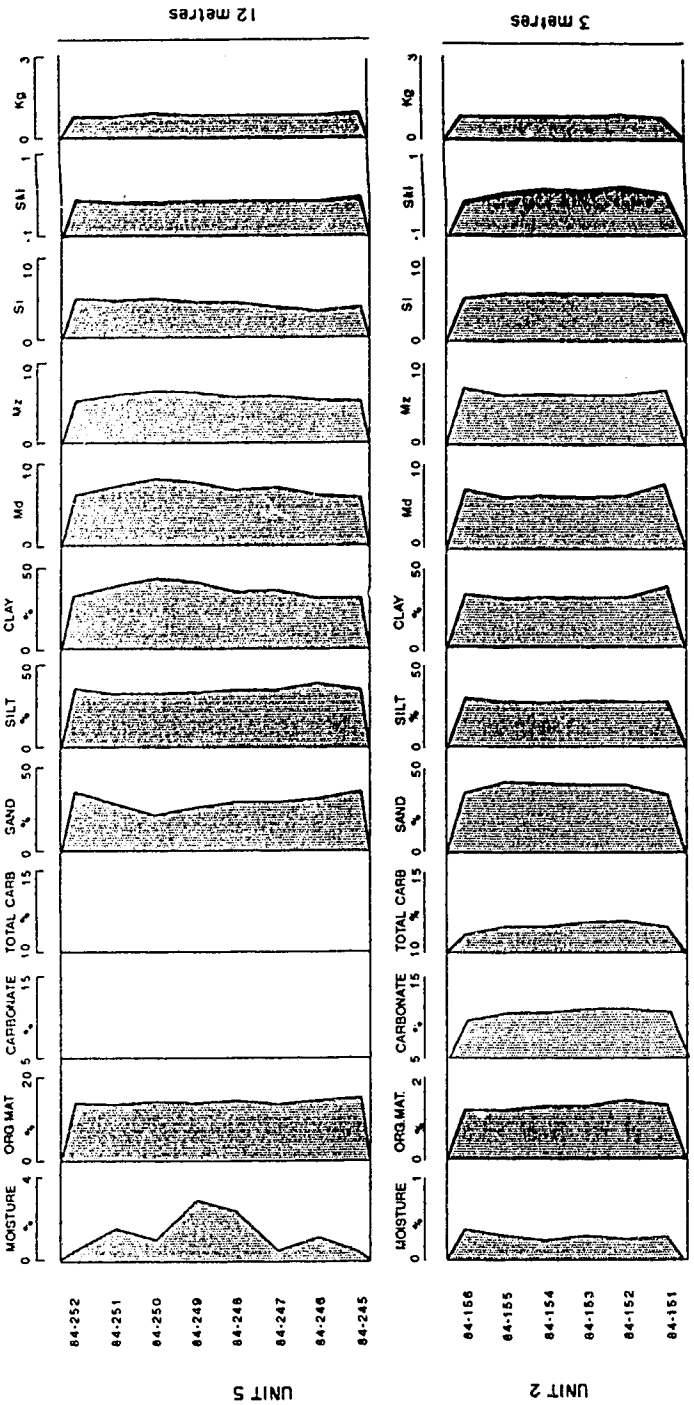

Compositional variation with depth for Units 2 and 5, Ware Section.

SECTION WARE

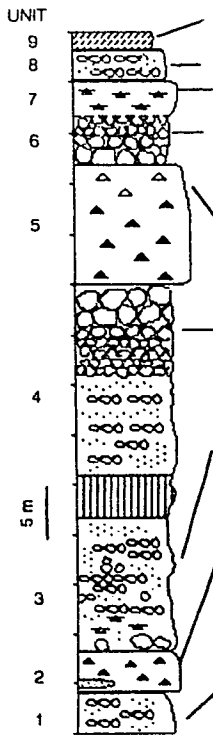

SAND- primarily matrix-supported; 0-4m thick; horizontal to cross laminated; fine gravel (50%), sand (33%), silt/clay (17%); moderate sorting; basal contact straight conformable to unconformable erosive; 84-157; 2.5Y 4/2 (dark greyish brown)

GRAVEL-fluvial; variable thickness; horizontally bedded; interstratified cross-bedded sands; basal contact erosive, curvilinear

DIAMICTON-matrix-supported; 0-1.5m thick; limited laterally to 150m; finely laminated near top to massive near bottom; cobbles (2%), pebbles (15%), matrix (~80%) consists of sand (39%), silt (48%), clay (13%); porous; very leptokurtic; near symmetrical; very poorly sorted; basal contact undulatory, sharp to gradational; 85-4,5; 5Y 6/3 (pale olive)

GRAVEL-primarily pebble clast-supported; massive; fining-upwards sequence; thickness 0-5m; clasts rounded; no imbrication; cobble to sand; matrix is fine gravel (35%), sand (60%), silt/clay (5%); upper contact erosive, conformable to gradational, basal contact gradational to straight conformable; 85-2,3; 2.5Y 6/6 (olive yellow)

DIAMICTON-matrix-supported; massive; +12.5 m thick; not stony (~10%); stone free zone 1.5 m thick in centre of unit; pebbles (10%), striated; pebble fabric near top to 335°, S1=0.811 and near base to 157°, S1=0.836; matrix is sand (30%), silt (35%), clay (35%); mesokurtic; near symmetrical; extremely poorly sorted; groundwater diagenesis near top; upper contact conformable to gradational; lower contact indeterminate; 84-242,245,246,247,248,249,250,251,252,358; 2.5Y 6/4 (light yellowish brown) at top to 5Y 2.5/1 (black) at bottom

GRAVEL AND SAND- primarily pebble clast-supported; thickness +20 m; well cemented; cobbles (15%), pebbles (30%), sand (30%); porosity high (25%); poorly sorted; clasts rounded; massive to horizontally bedded; moderate imbrication; fabric to NW; sand beds intercalated with gravels show sharp, straight, basal contacts and undulatory erosive upper contacts, both horizontal laminations and planar cross laminations; unit shows coarsening-upwards sequence; minimum age 18,750±120 ybp; upper and lower contacts indeterminate; 84-130,131,132,243,244,85-1,6,7,8; 2.5Y 4/2 (dark greysich brown) to 10YR 4/4 (dark yellowish brown)

GRAVEL, SAND AND INTERBEDDED DIAMICTON- primarily pebble clast-supported; +15m thick; coarse sand wedges intercalated with diamictons (matrix- and clast-supported) near base; cobbles (15%), coarse pebbles (20%), fine pebbles (25%), sand (40%); clasts rounded to well-rounded; fining-upwards sequence; massive to horizontally bedded; sands cross-bedded; clay rip ups in horizontally laminated sand beds; upper contact sharp, conformable to indeterminate; lower contact gradational to unconformable and sharp; 84-133,134,262,263; 10YR 4/3 (dark brown)

DIAMICTON- matrix-supported, primarily massive, compact; thickness 0-5 m; bi-convex sand and gravel lenses near base; deformed silty clay wisps and oxidized laminations near basal contact; stony (30%); clasts subrounded, mainly pebbles (40%), and some cobbles (5%); striated; pebble fabrics towards 284°, S1=0.598, 0.671; matrix is sand (41%), silt (26%), clay (33%); very platykurtic; finely skewed; extremely poorly sorted; upper contact gradational to unconformably erosive; basal contact gradational to sharp and conformable; 84-146,147,150,151,152,153,154,155,156; 2.5Y3/0 (very dark grey) to 5Y 4/2 (olive grey)

GRAVEL AND SAND- primarily clast-supported, coarse clast unit; thickness 0-3 m; horizontally bedded; sand interbeds 0.1-1 m thick, planar cross-stratified with small pebble clasts; cobbles (0-35%), coarse pebbles (20-30%), fine pebbles (10-55%), matrix (15-20%); matrix is sand (96%), silt/clay (4%); clasts rounded to well-rounded; moderate imbrication; basal contact indeterminate, upper contact gradational to sharp and conformable; 10YR 3/3 (dark brown); 84-235, 261

Composite stratigraphic column of Section Ware; lithostratigraphic units along left and unit descriptions along right.

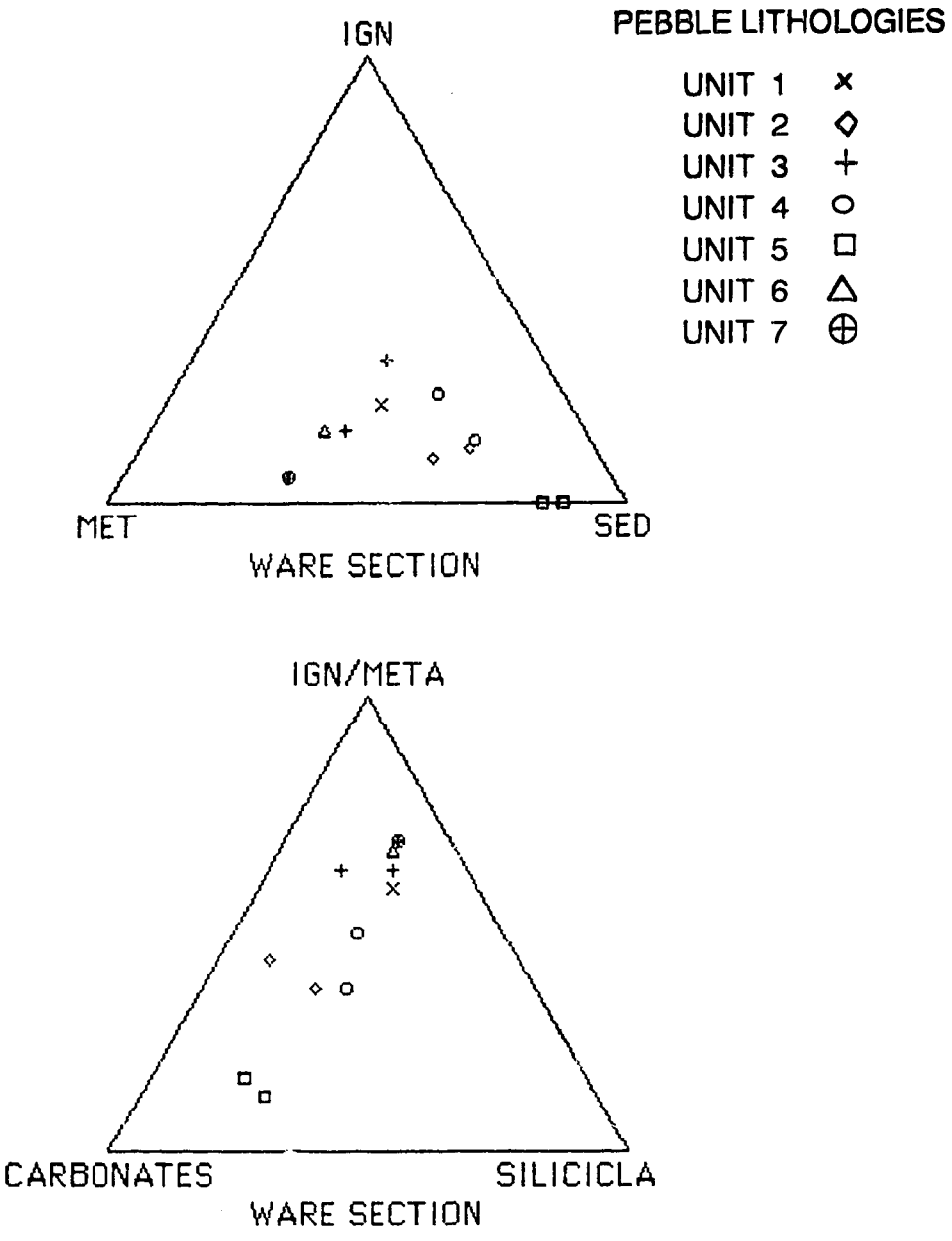

Ternary diagrams comparing pebble lithologies for seven units at the Ware Section.

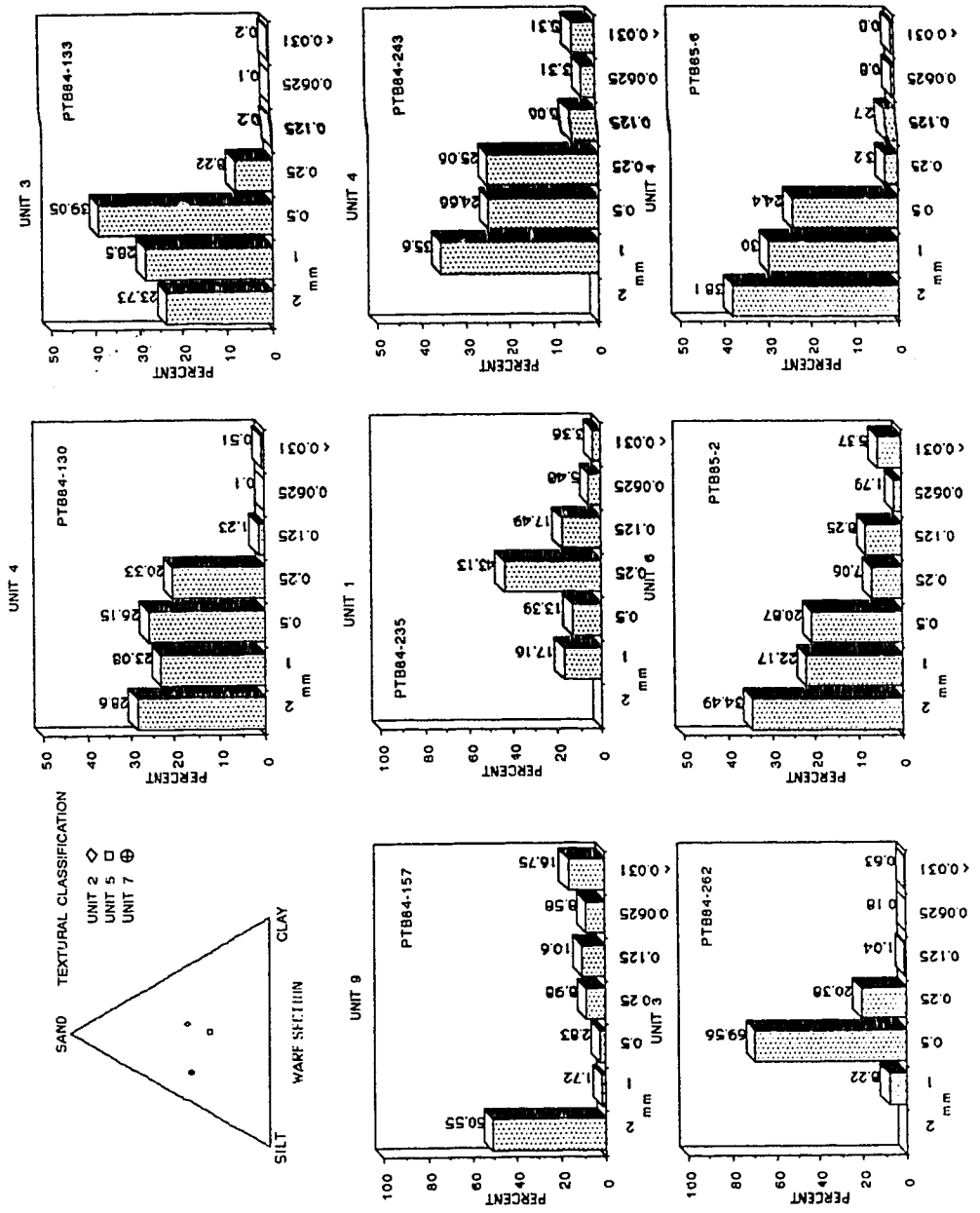

Textural diagrams from samples from various units at the Ware Section. Ternary diagram illustrates variation in diamictons; histograms illustrate variation in nondiamicton samples. See text for further explanation and key to sample numbers.

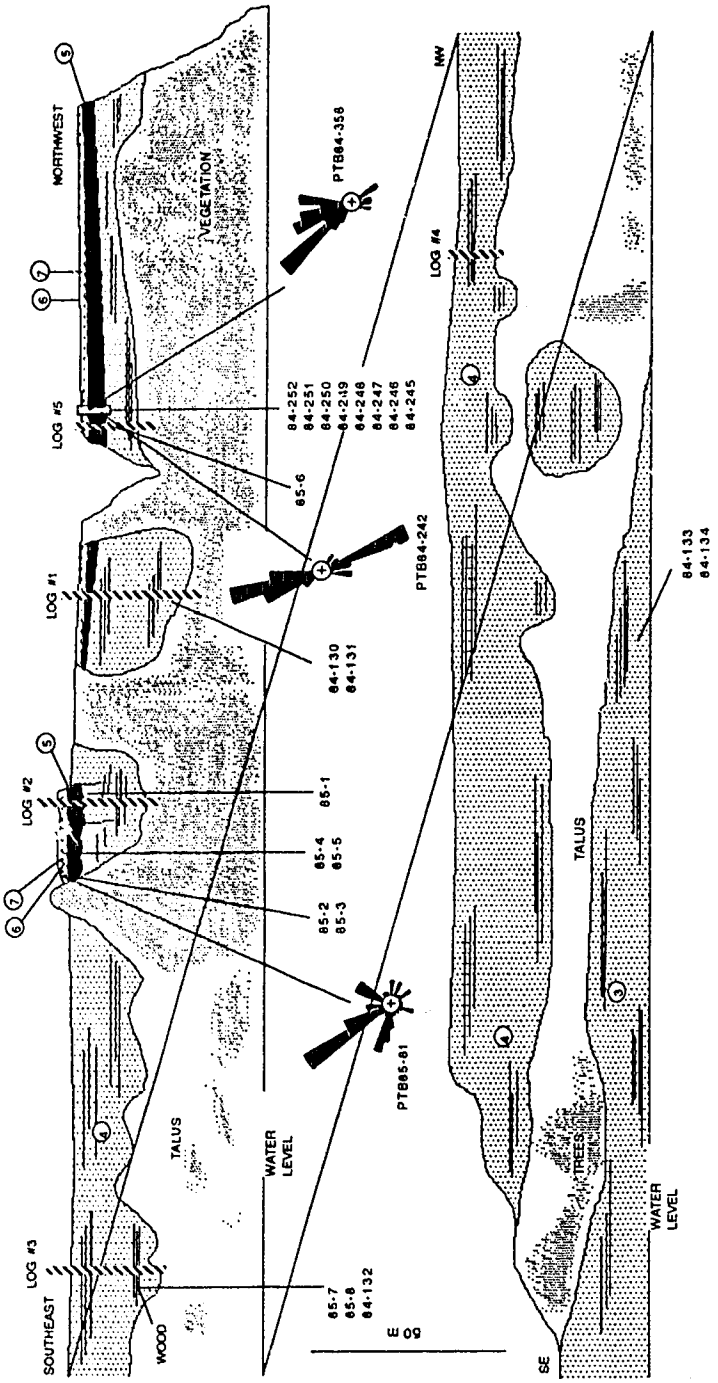

Section drawing of primary face of Section Ware showing relation of major diamictons, sands and gravels to covered portions. See text for explanation.

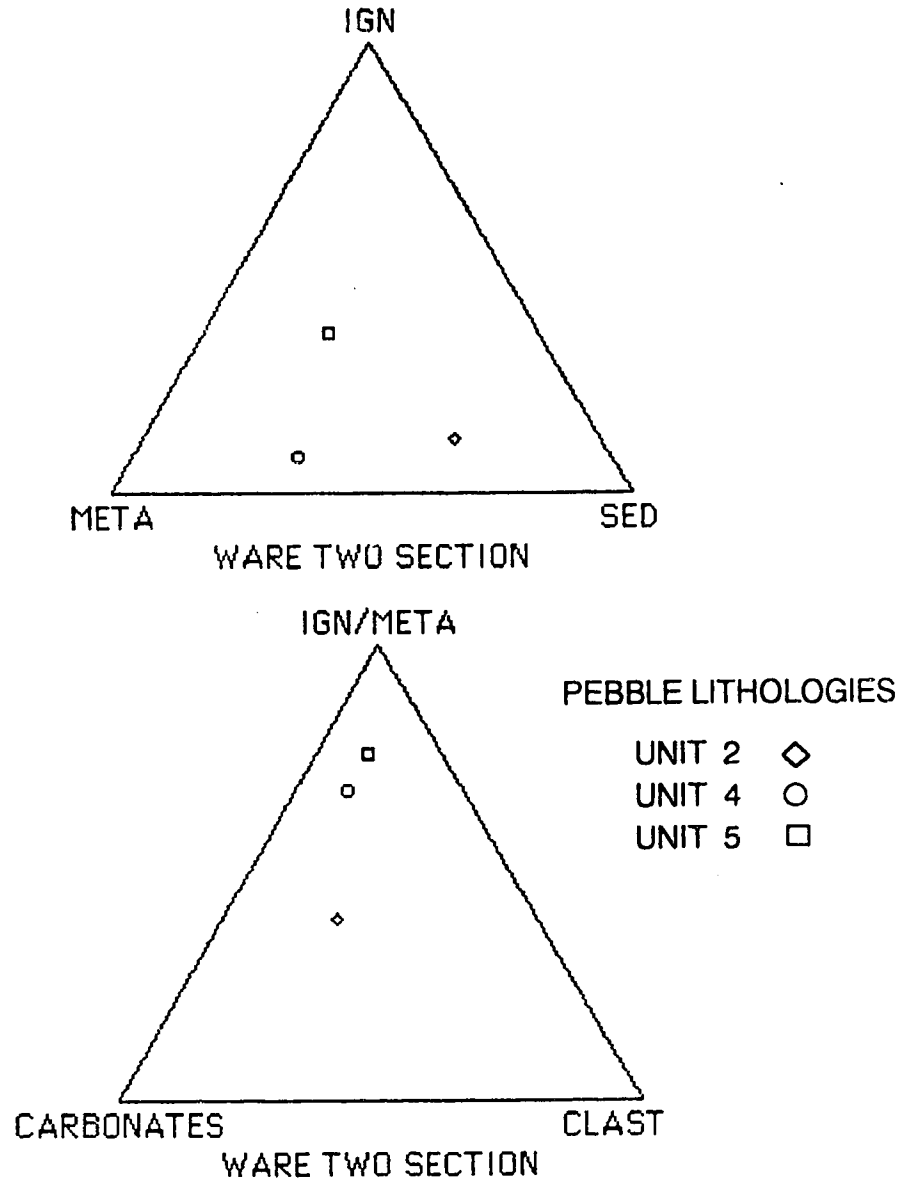

Ternary diagrams comparing pebble lithologies for three lithostratigraphic units at the Ware Two Section.

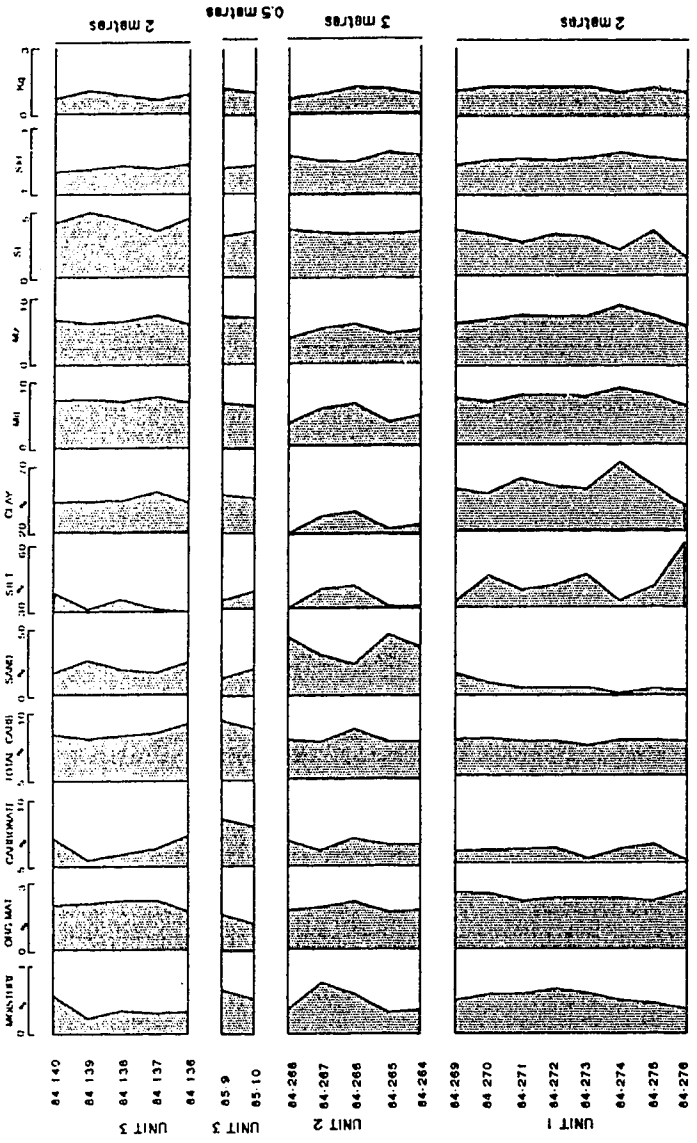

Compositional variation with depth for Units 1, 2, and 3, Ware Two Section.

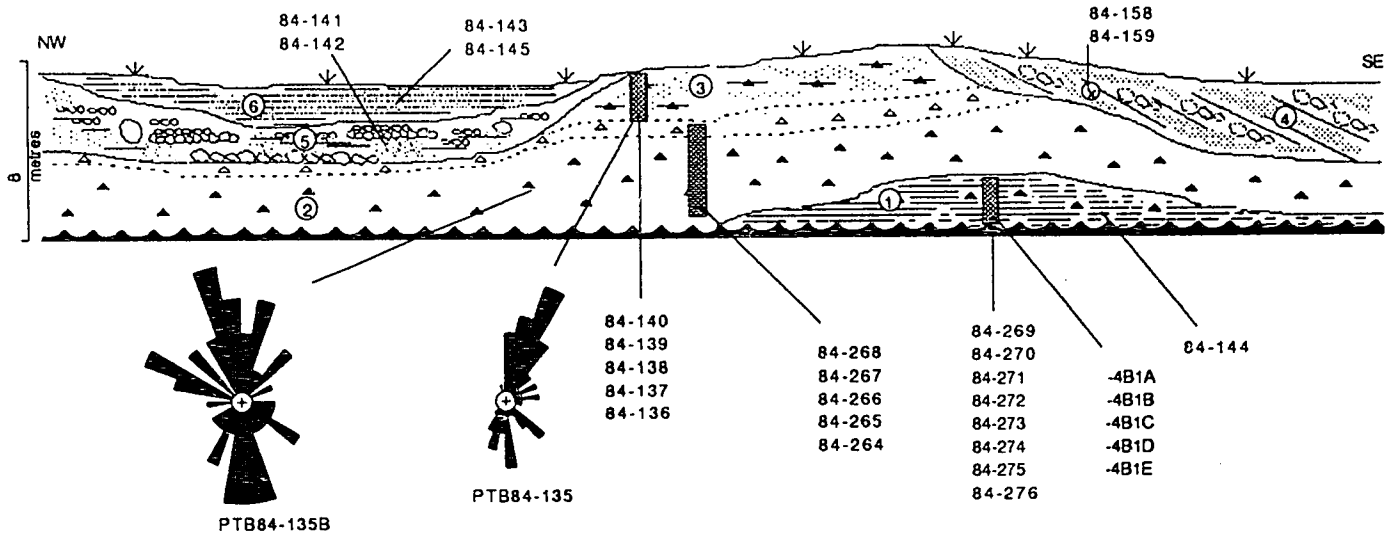

Section drawing of entire face of Ware Two Section showing various lithostratigraphic units, samples, sample locations, and pebble fabrics.

SECTION WARE TWO

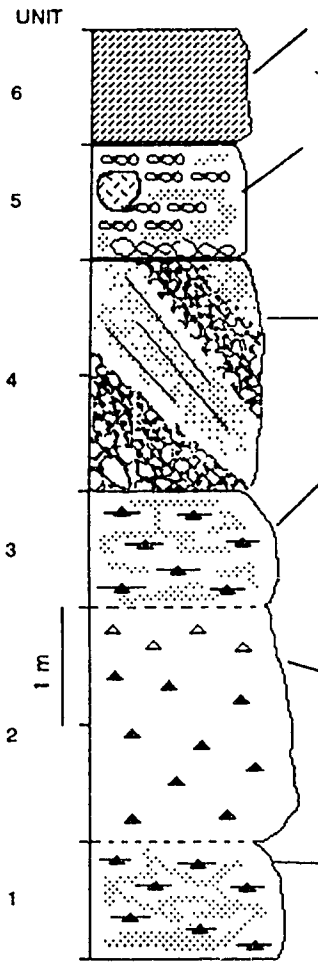

SAND-matrix-supported unit ranges in thickness from 0-1.5 m; horizontally laminated bands of sand beds 5 cm thick and silt clay laminae 1 cm thick; gravel (0.20%), sand (44.70%), silts/clays (55.10%); clasts rounded; moderate sorting, unimodal texture; basal contact sharp; 84-143,145; 5Y 7/3 (pale yellow);

GRAVEL-clast-supported unit ranges in thickness from 0-1.5 m; horizontally bedded with minor sand interbeds; coarse pebbles (40%), fine pebbles (20%), matrix (40%); clasts rounded, imbricated; matrix is gravel (21.3%), sand (75.5%), silt/clay (3%); sorting moderate; unimodal texture; boulder lag at base; basal contact sharp, erosive; erratics; 84-141,142; 10YR 4/2 (dark greyish brown)

GRAVEL-clast-supported unit ranges in thickness from 0-2 m; steeply bedded, alternating sand and gravel beds (30 cm thick), dipping (<45°) to SE; floating cobbles and boulders; matrix is gravel (36%), sand (56%), silt/clay (8%); coarsely skewed, leptokurtic; basal contact is conformable and erosive; 84-158,159; 10YR 6/3 (pale brown);

DIAMICTON-matrix-supported, deformed, flow structures; ranges in thickness from 0-3 m; silty clay beds with intraclasts interbedded with silty sand beds; sand wisps; low stone content (10%); matrix is sand (17%), silt (33%), clay (49%); platykurtic, coarsely skewed; very poorly sorted; 85-9,10, 84-136,137,138,139,140; basal contact undulatory and gradational; banded 2.5Y 8/4 (pale yellow) to 2.5Y 3/0 (very dark grey)

DIAMICTON-matrix-supported, massive, hard; ranges in thickness from 0->3 m; extremely poorly sorted; symmetric skewness; mesokurtic; moderate stone content, subrounded to subangular, striated; matrix is sand (38%), silt (34%), clay (28%); basal contact is undulatory and gradational; 84-135, 264, 265, 266, 267, 268; 2.5Y 8/4 (pale yellow) at top to 5Y 3/1 (very dark grey) at bottom

DIAMICTON-matrix-supported, minor deformation, horizontally bedded, hard; unit ranges in thickness from 0->2m; dropstones, flow structures; low stone content, rounded; matirx is sand (6%), silt (41%), clay (53%); mesokurtic; finely skewed; very poorly sorted; 84-144, 269, 270, 271, 272, 273, 274, 275, 276; banded 5Y 4/1(dark grey) to 5Y 6/2 (light olive grey); basal contact indeterminate

Composite stratigraphic column of the Ware Two section; lithostratigraphic units along left, and unit descriptions along right.

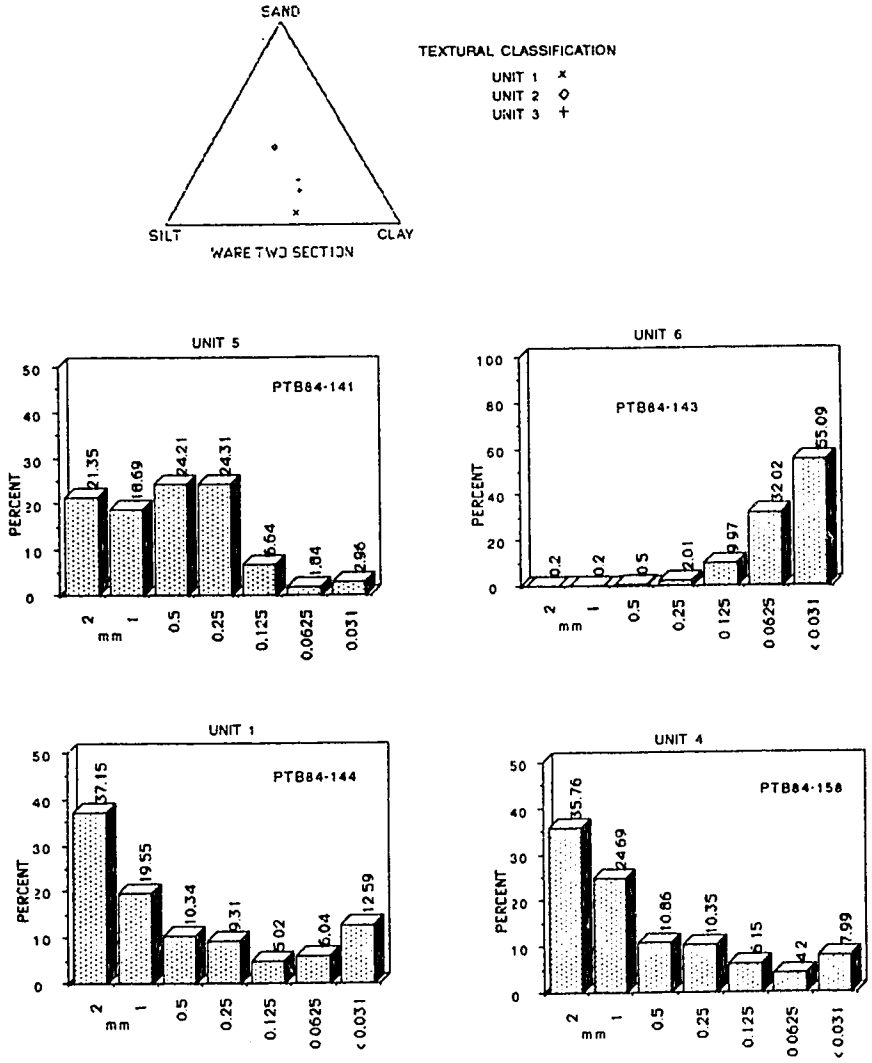

Textural diagrams for samples from various units at the Ware Two Section. Ternary diagram illustrates variation in diamictons; histograms illustrate variation in nondiamicton samples. See text for further explanation and key to sample numbers.

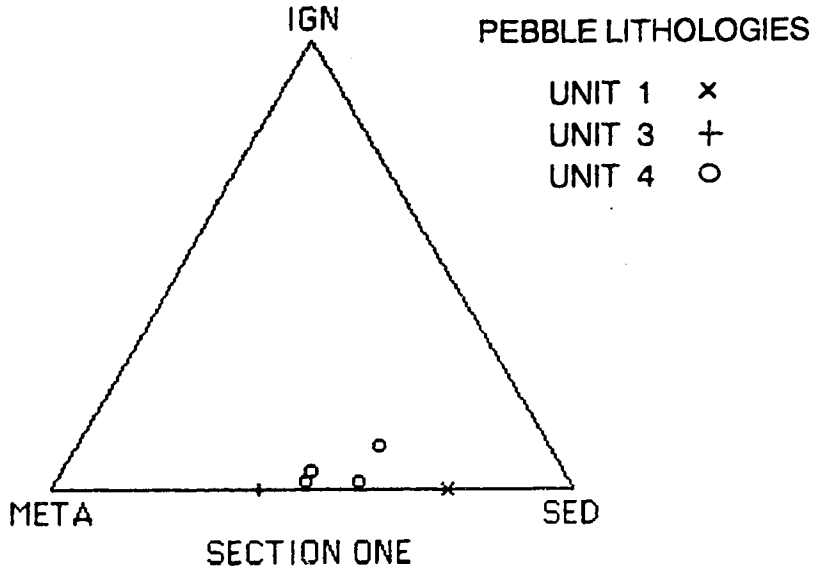

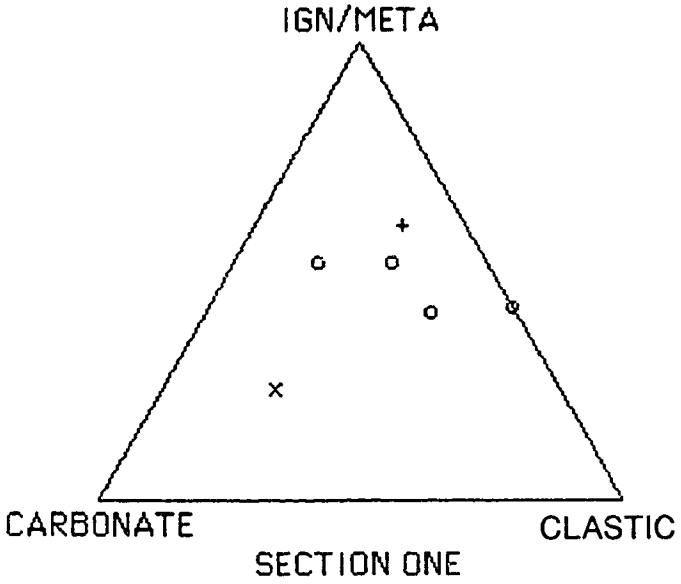

Ternary diagrams comparing pebble lithologies for three units at Section One.

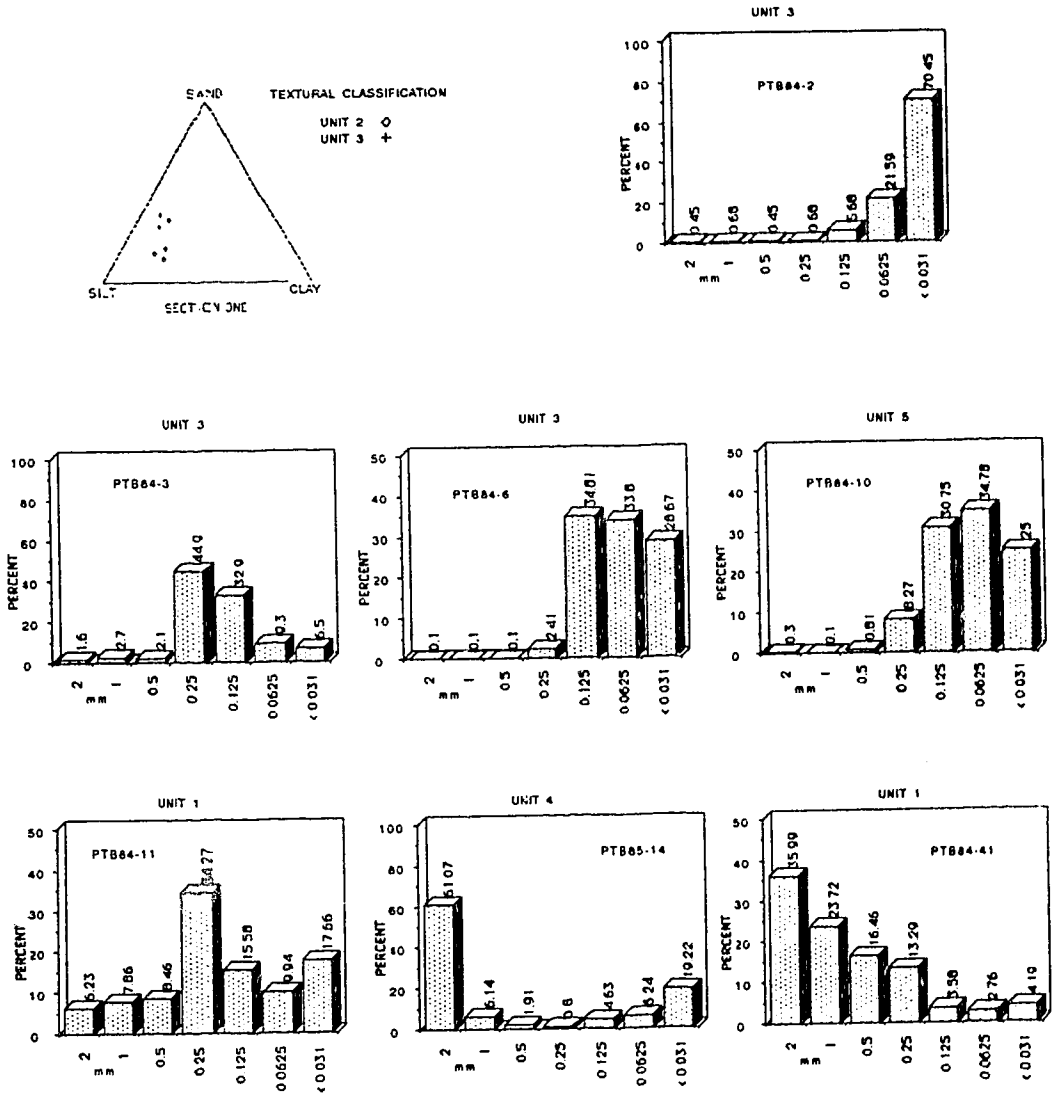

Textural diagrams for samples from various units at Section One. Ternary diagram illustrates variation in diamictons; histograms illustrate variation in nondiamicton samples. See text for further explanation and key to sample numbers.

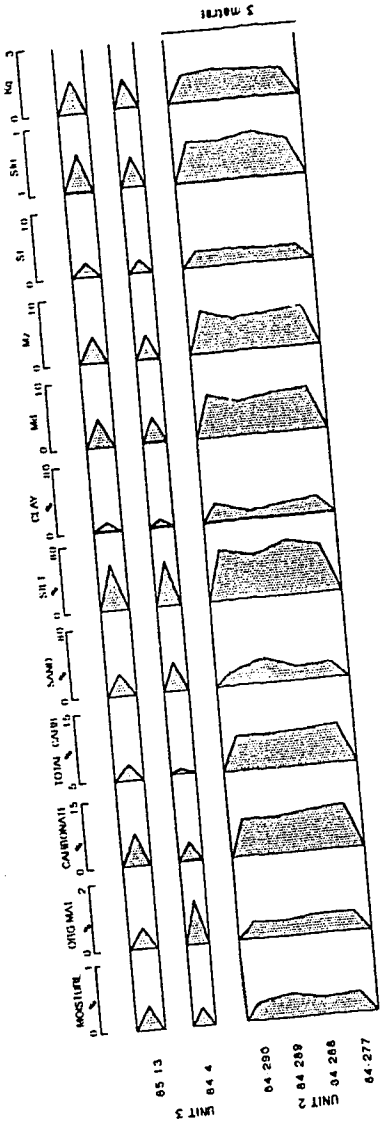

Compositional variation with depth for Units 2 and 3, Section One.

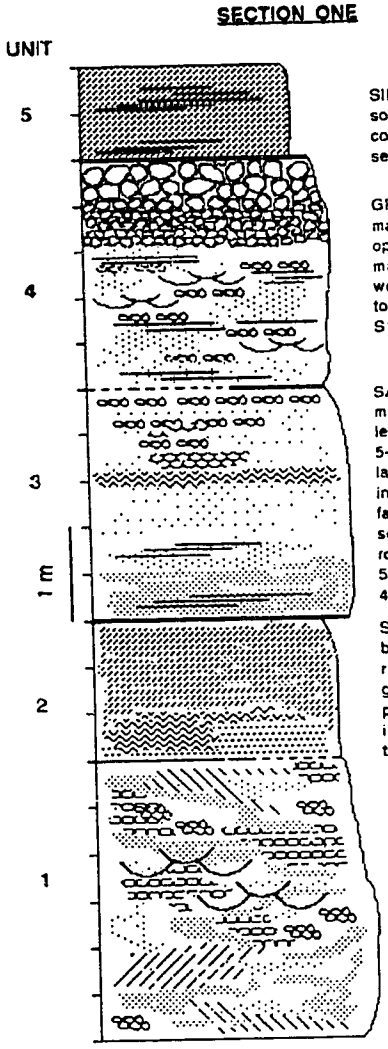

SILT AND SAND-matrix-supported; 0-2 m thick, homogeneous; well sorted; horizontal and ripple laminated very fine sands, unimodal, lower contact abrupt and drapes underlying gravels; soil developed on sediment; 84-11,41; 10 YR 4/2 (dark greyish brown)

GRAVEL AND SAND-primarily cobble-supported unit, 0-7 m thick, massive to large scale trough cross beds; coarsening-upwards sequence, open work gravels and horizontally bedded pebbles intercalated with matrix filled cobbles; matrix is granules with minor silt and clay; clasts well-rounded; poor imbrication; poor sorting; lower contact gradational to sharp and unconformable; pebble fabric to 51.1° (plunge of 7.6°), S1=0.661; 84-5,8,14,42, 85-15, 91; 10 YR 6/3 (pale brown)

SAND AND GRAVEL-primarily sand matrix-supported; 0-11 m thick; massive and horizontally laminated sand beds with 10 cm thick pebble lenses (convexo-concave) near base; horizontally bedded pebbles within 5-10 cm thick sand and silt interbed lenses (plano-convex) and cross laminated sand near top; ice wedge pseudomorphs; diagnostic sandy silt interbed, 30 cm thick and drape laminated through entire unit; pebble fabric to 52.3° (plunge of 3.2°), S1= 0.570; coarsening-upwards sequence; good imbrication; moderately well sorted; clasts primarily rounded; lower contact sharp, undulatory and unconformable; 7.5 YR 5/2 (brown); 84-1, 2, 3, 4, 6, 7, 9; 85-13, 82; 4A2A,4A2B,4A2C,4A2D,4A2E

SILT-matrix-supported; 0-3 m thick; occasional wood smears along bedding planes; basal portion of unit consists of horizontal and ripplelaminated silts; banded in color; very deformed; lower contact gradational to sharp and conformable; moderately well sorted; upper portionis massive, black, organic silts; basal contact is erosive to indeterminate; 2.5Y 5/2 (greyish brown) to 5Y 5/3 (olive) for bottom to black at top; 84-277,278,279,280,296 (wood)

GRAVELS AND SANDS-primarily coarse pebble supported, 0-11 m thick; poor horizontal bedding to massive; large scale (>1m) low angle planar and trough cross beds; no boulders, cobbles (30%), pebbles and granules (50%), matrix (20%); matrix is bimodal silts and medium sands; horizontal and cross laminated sand interbeds intercalated with gravels; mainly very coarse sand lenses of variable shape, poor imbrication; clasts subrounded to well rounded; moderately sorted; very oxidized; upper contact indistinct to sharp, erosive, 84-11, 41,125; 10 YR 5/4 (yellowish brown)

Composite stratigraphic column of Section One; lithostratigraphic units along left and unit descriptions along right.

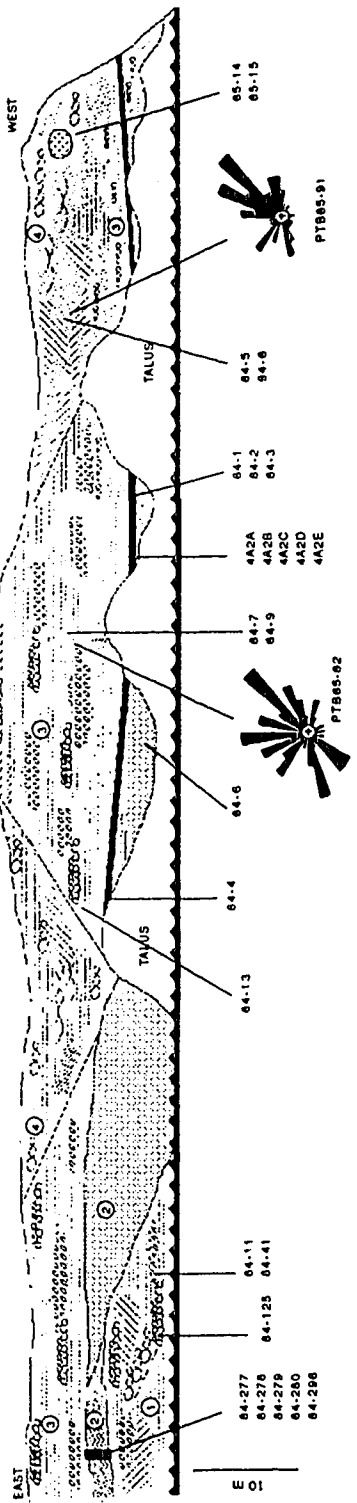

Section drawing of the primary face of Section One showing various lithostratigraphic units, samples, and sample locations.

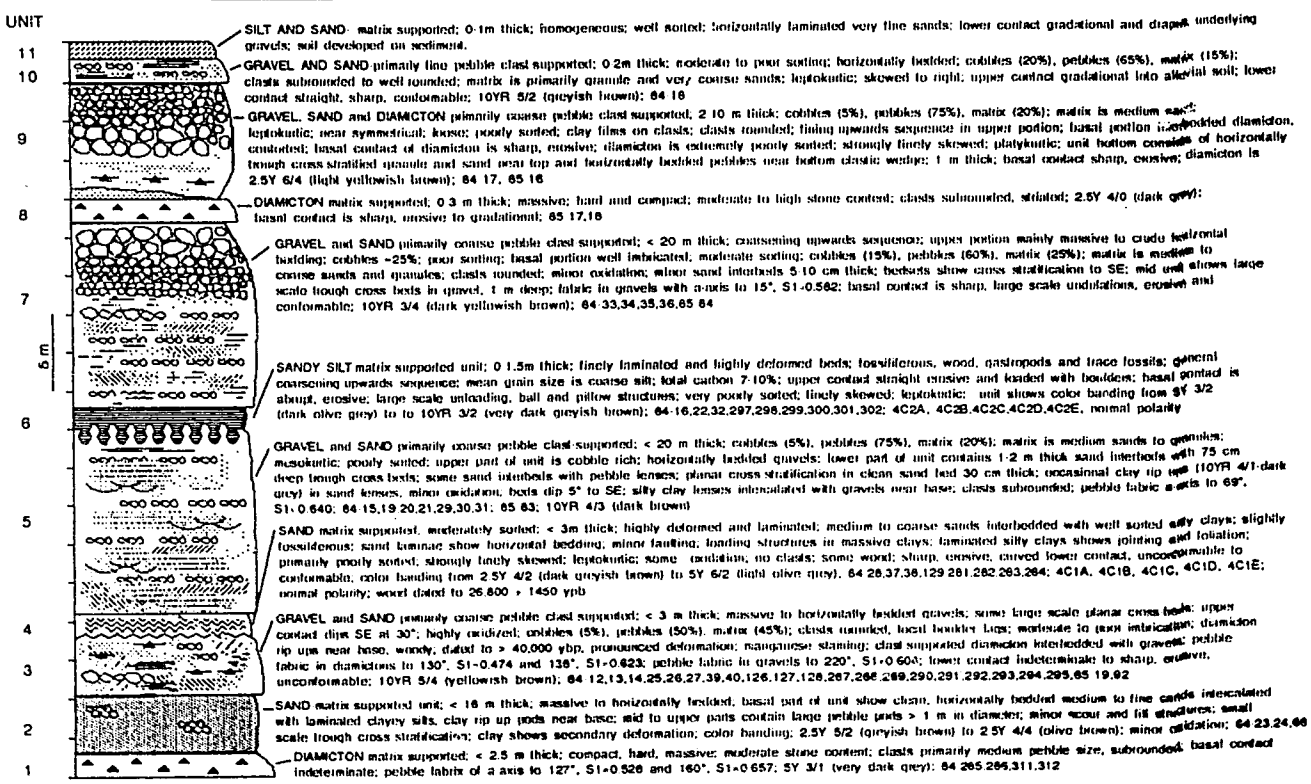

Composite stratigraphic column of Section Two; lithostratigraphic units along left and unit descriptions along right.

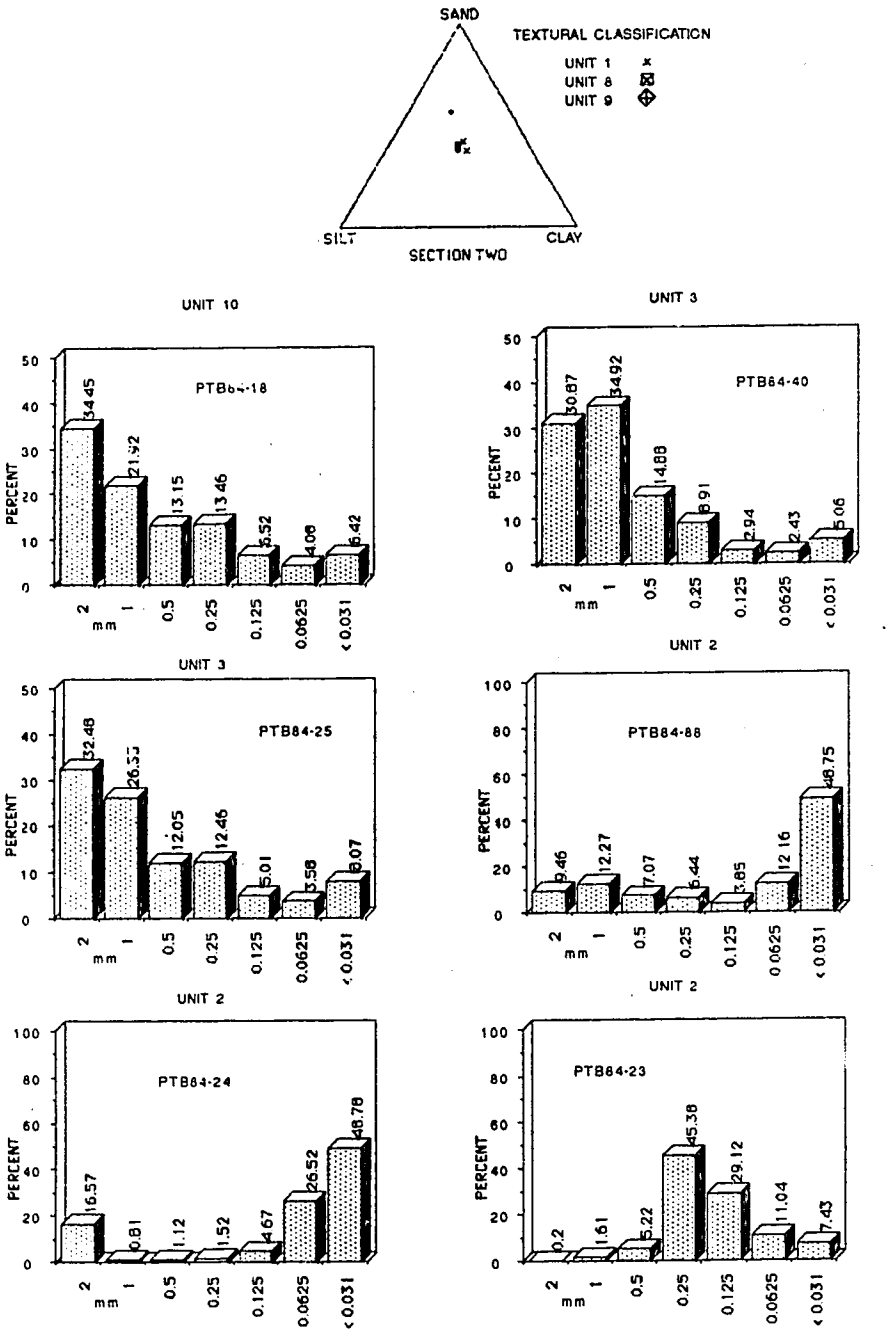

Textural diagrams for samples from various units at Section Two. Ternary diagram illustrates variation in diamictons; histograms illustrate variation in nondiamicton samples. See text for further explanation and key to sample numbers.

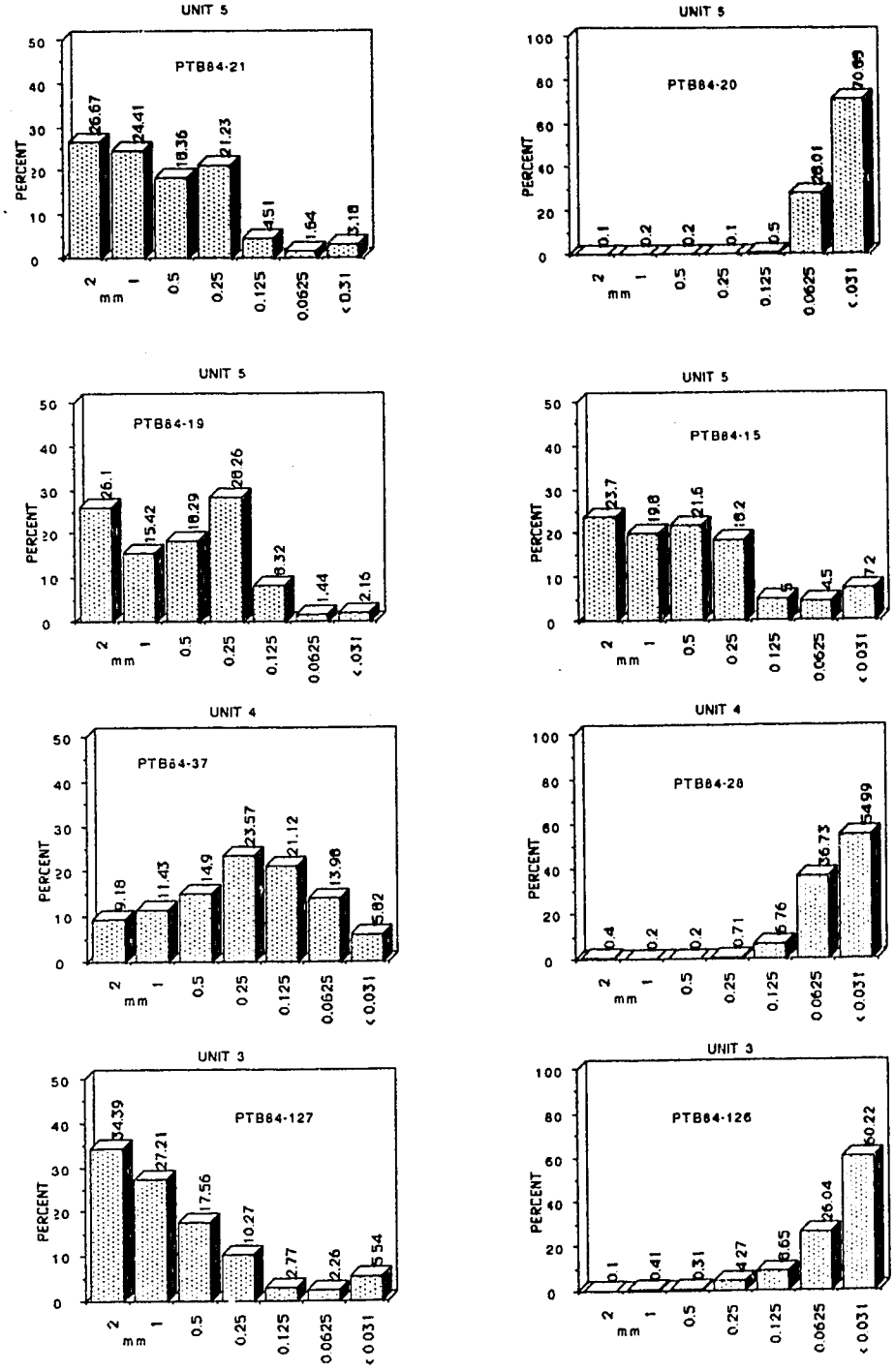

Textural diagrams for samples from various units at Section Two. Continued.

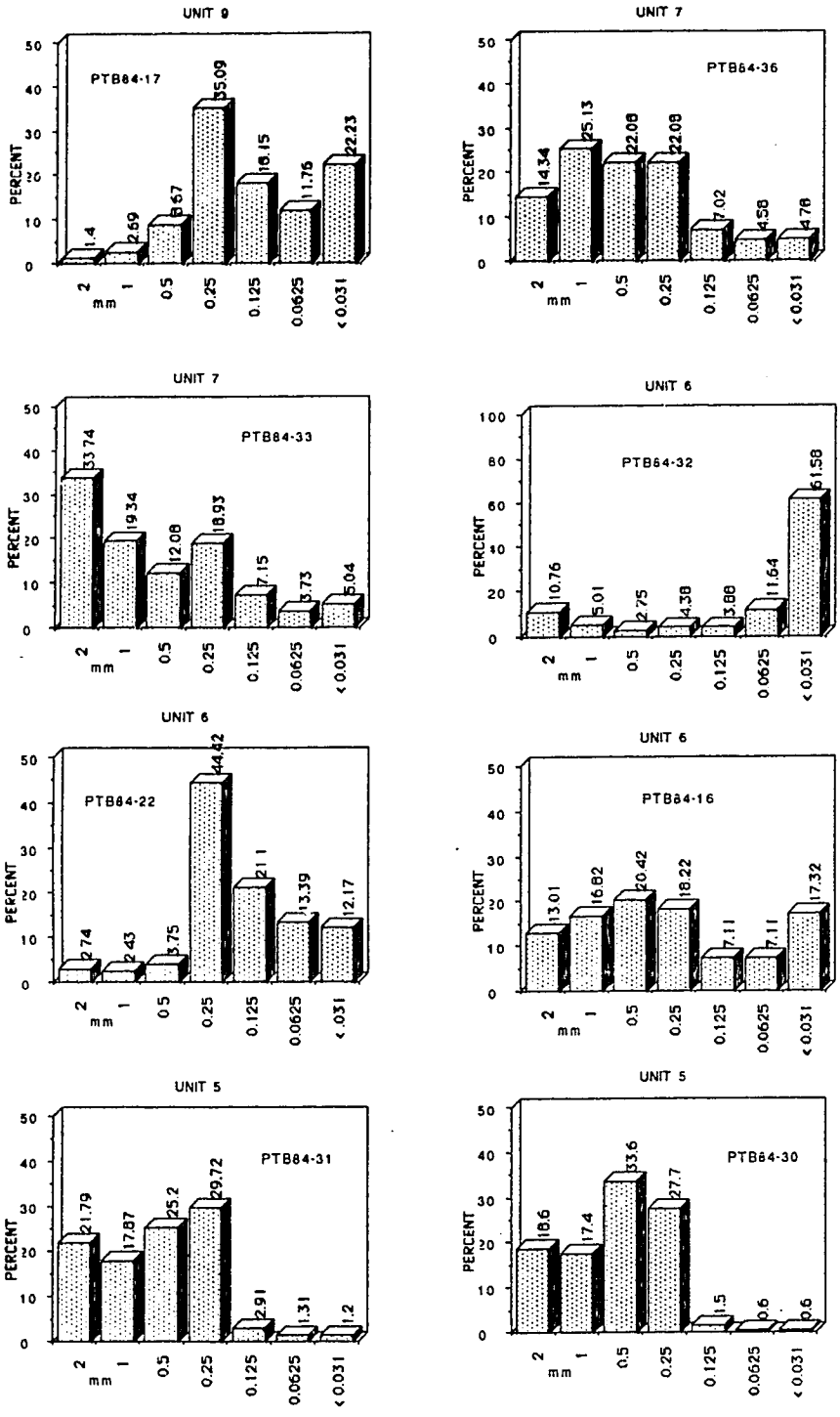

Textural diagrams for samples from various units at Section Two. Continued.

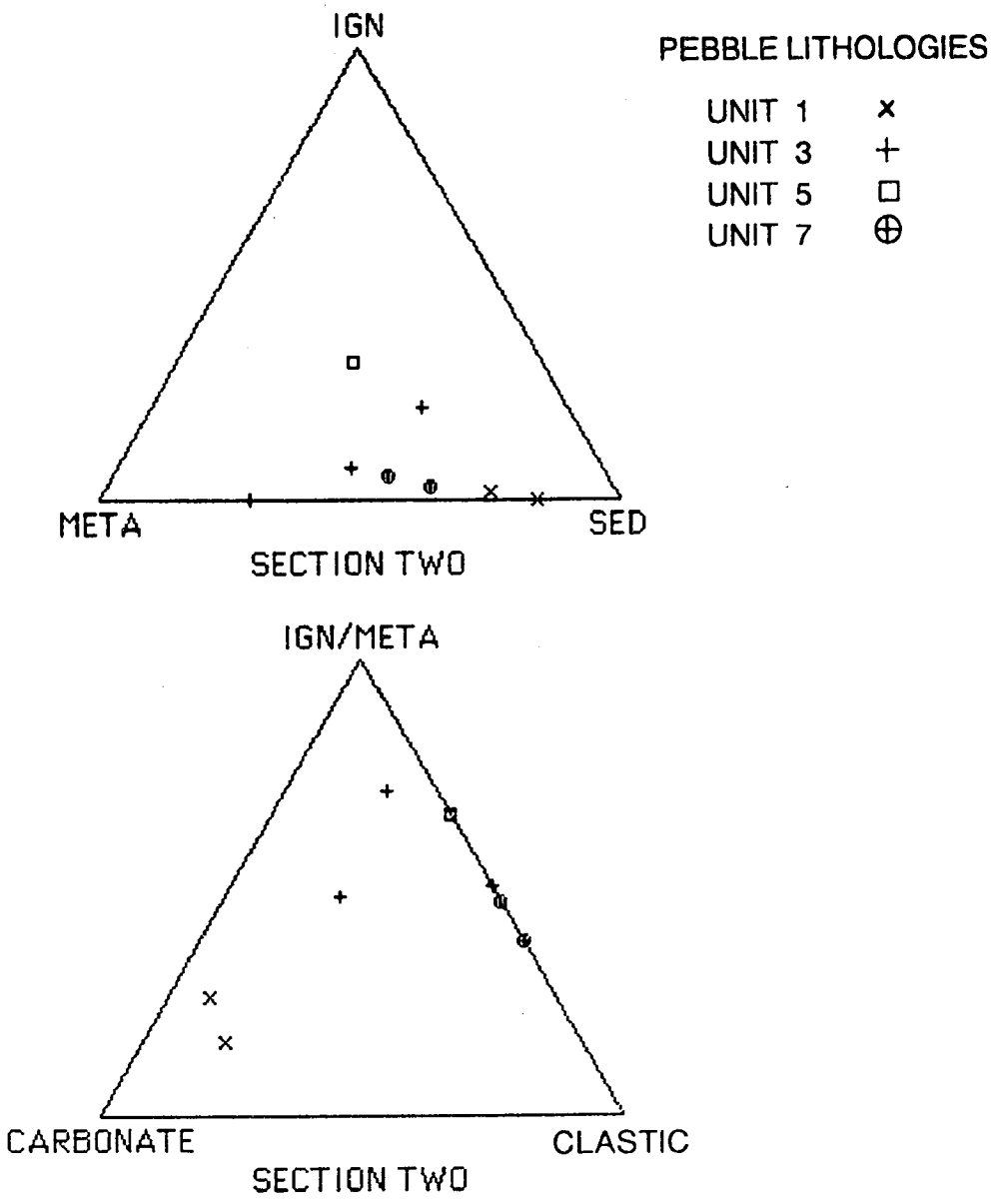

Ternary diagrams comparing pebble lithologies for four units at Section Two.

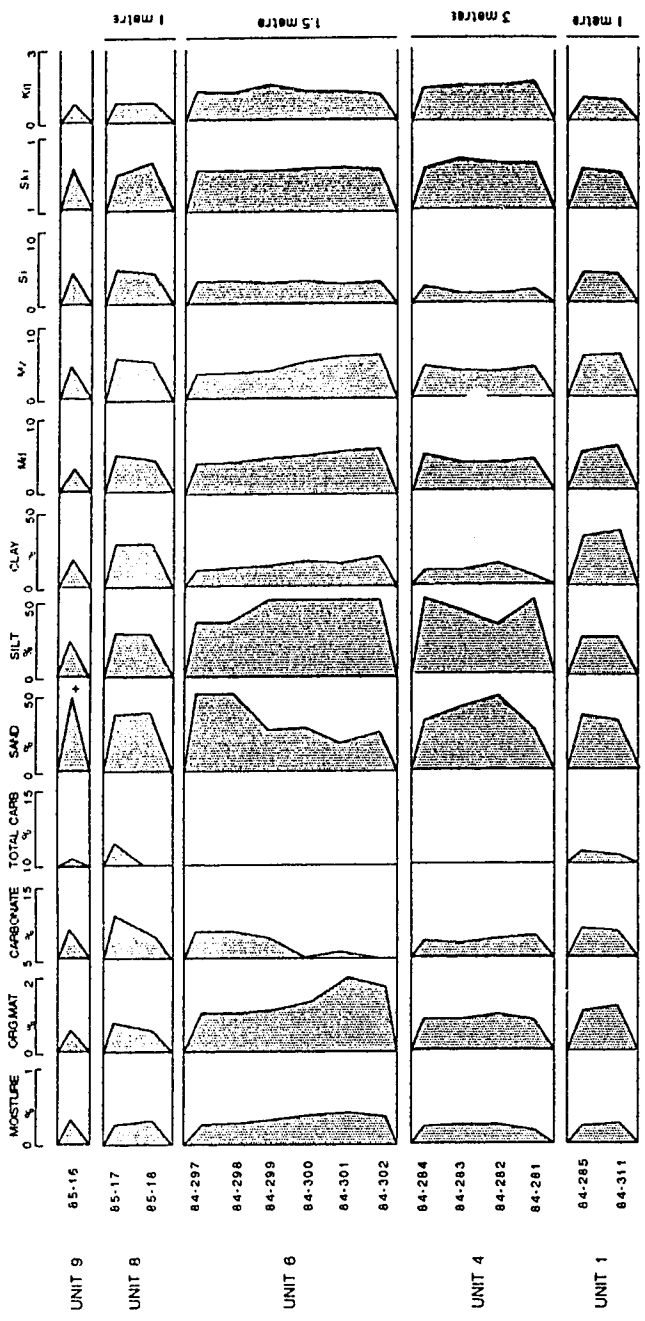

Compositional variation with depth for Units 1, 4, 6, 9 and 10, Section Two.

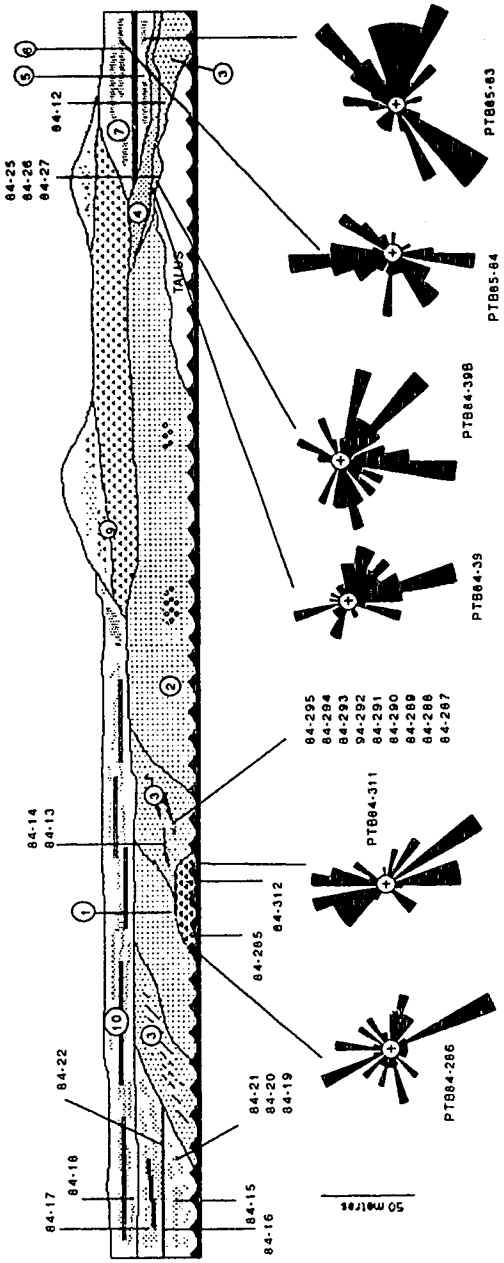

Section drawing of primary face of Section Two, northern half, showing relation of major diamictons, sands and gravels to covered portions. Lithostratigraphic units labeled with circled numbers. Sample locations also illustrated.

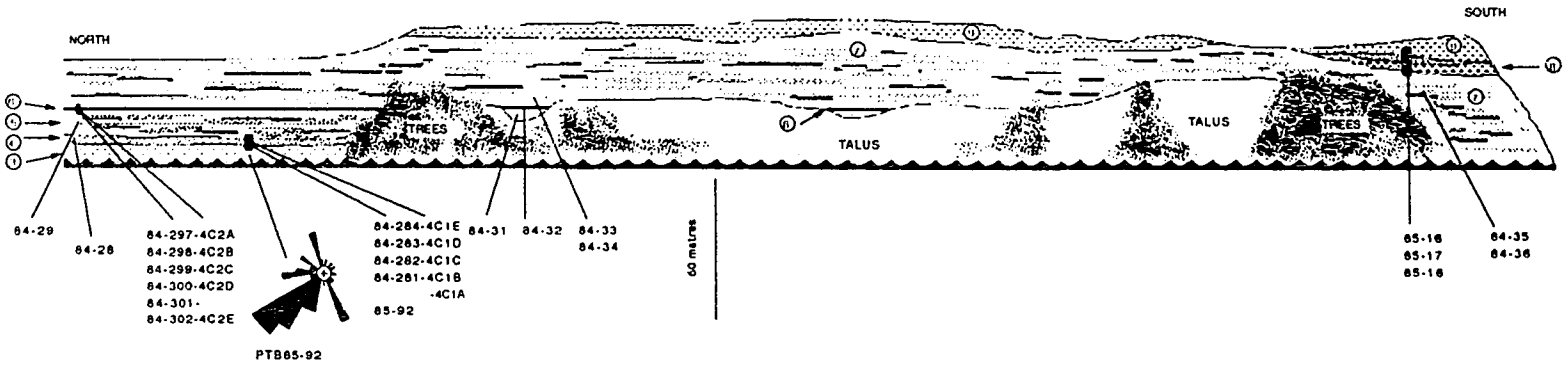

Section drawing of primary face of Section Two, southern half, showing relation of major diamictons, sands, and gravels with covered portions. Lithostratigraphic units labeled witH circled numbers. Samples and sample locations also illustrated. See text for explanation.

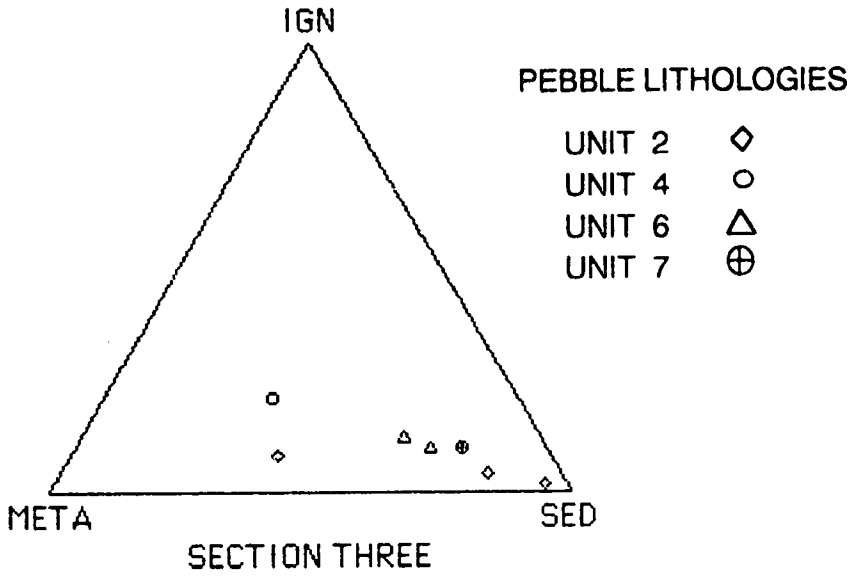

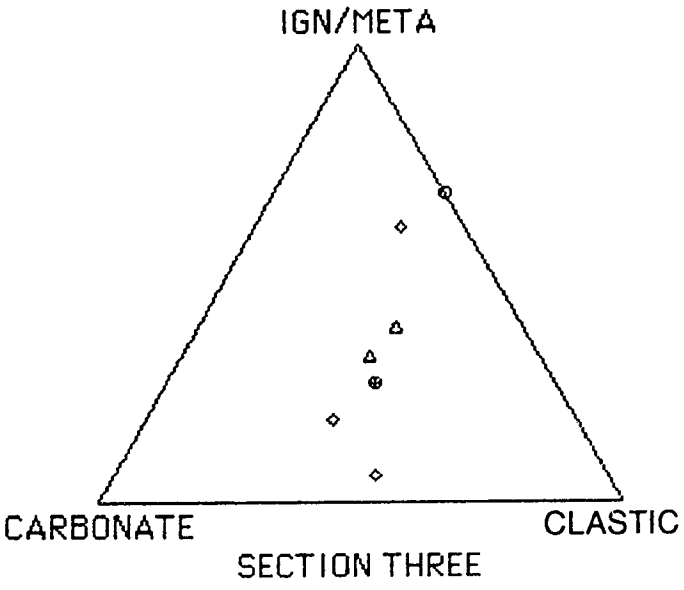

Ternary diagram comparing pebble lithologies for four units at Section Three.

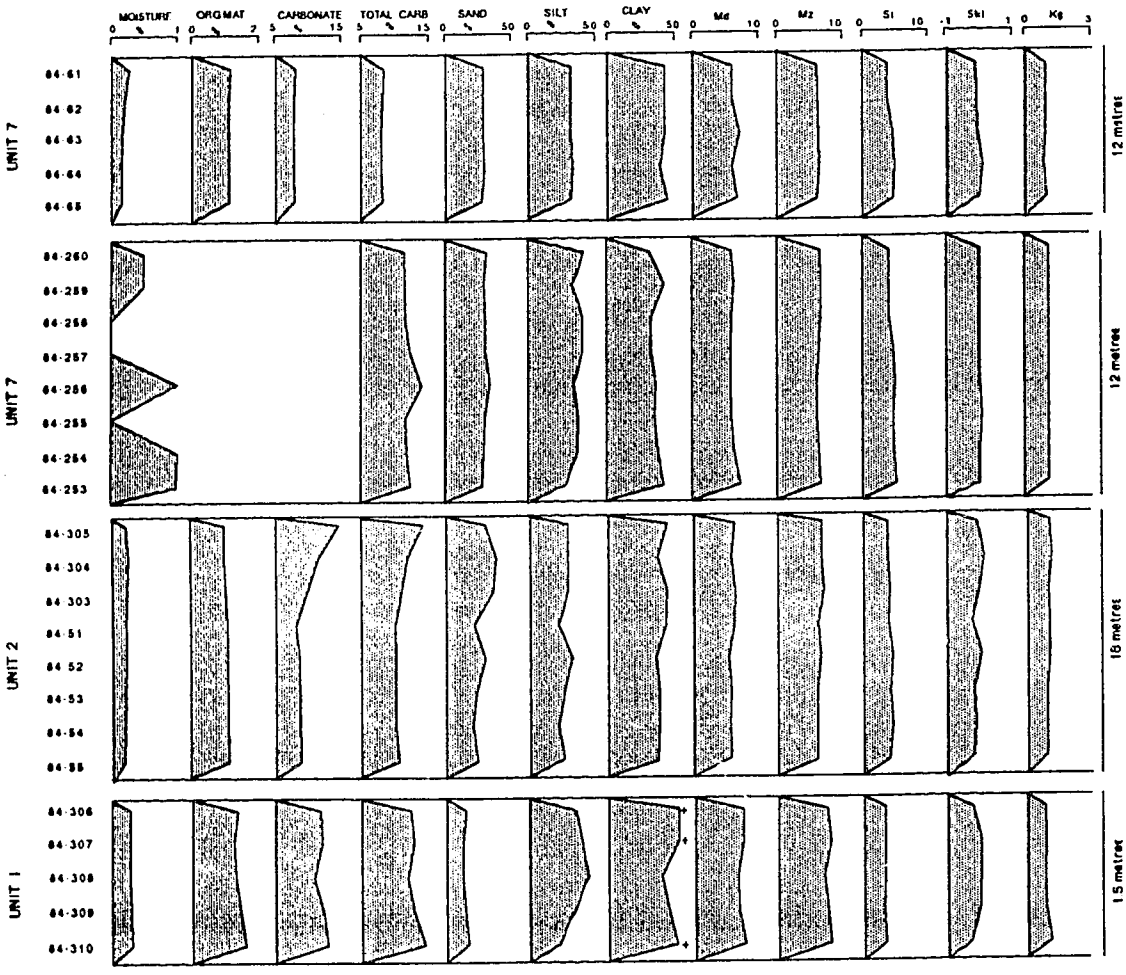

Compositional variation with depth for Units 1, 2, and 7, Section Three.

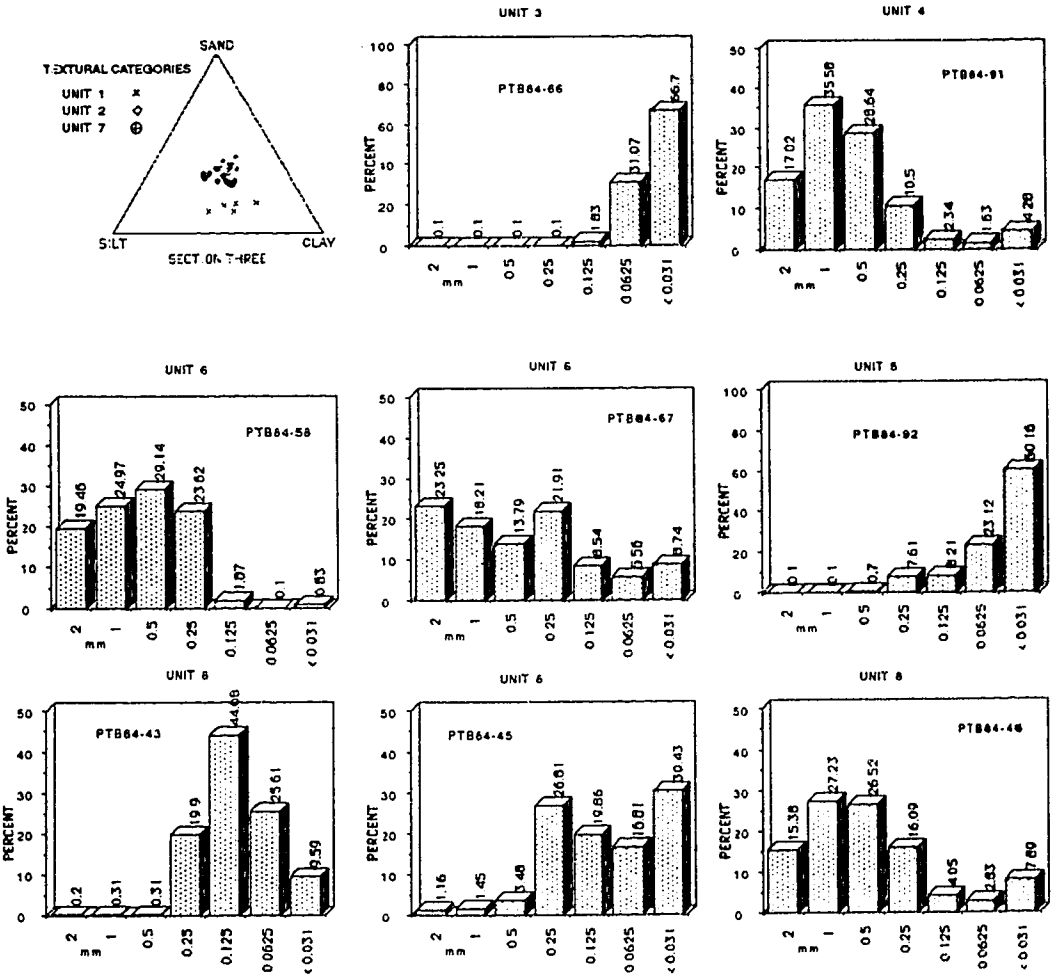

Textural diagrams for samples from various units at Section Three. Ternary diagram illustrates variation in diamictons; histograms illustrate variation in nondiamciton samples. See text for further explanation and key to samples.

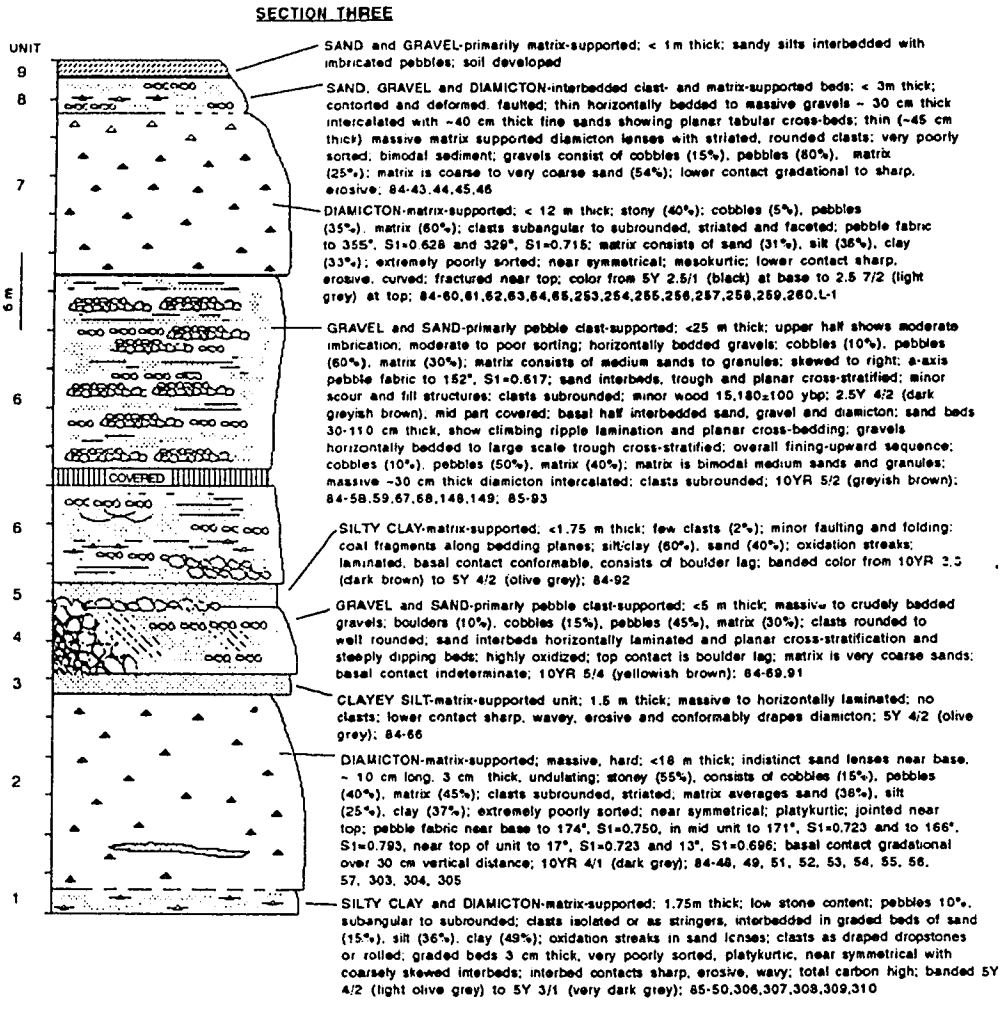

Composite stratigraphic column of Section Three, lithostratigraphic units along left and unit descriptions along right.

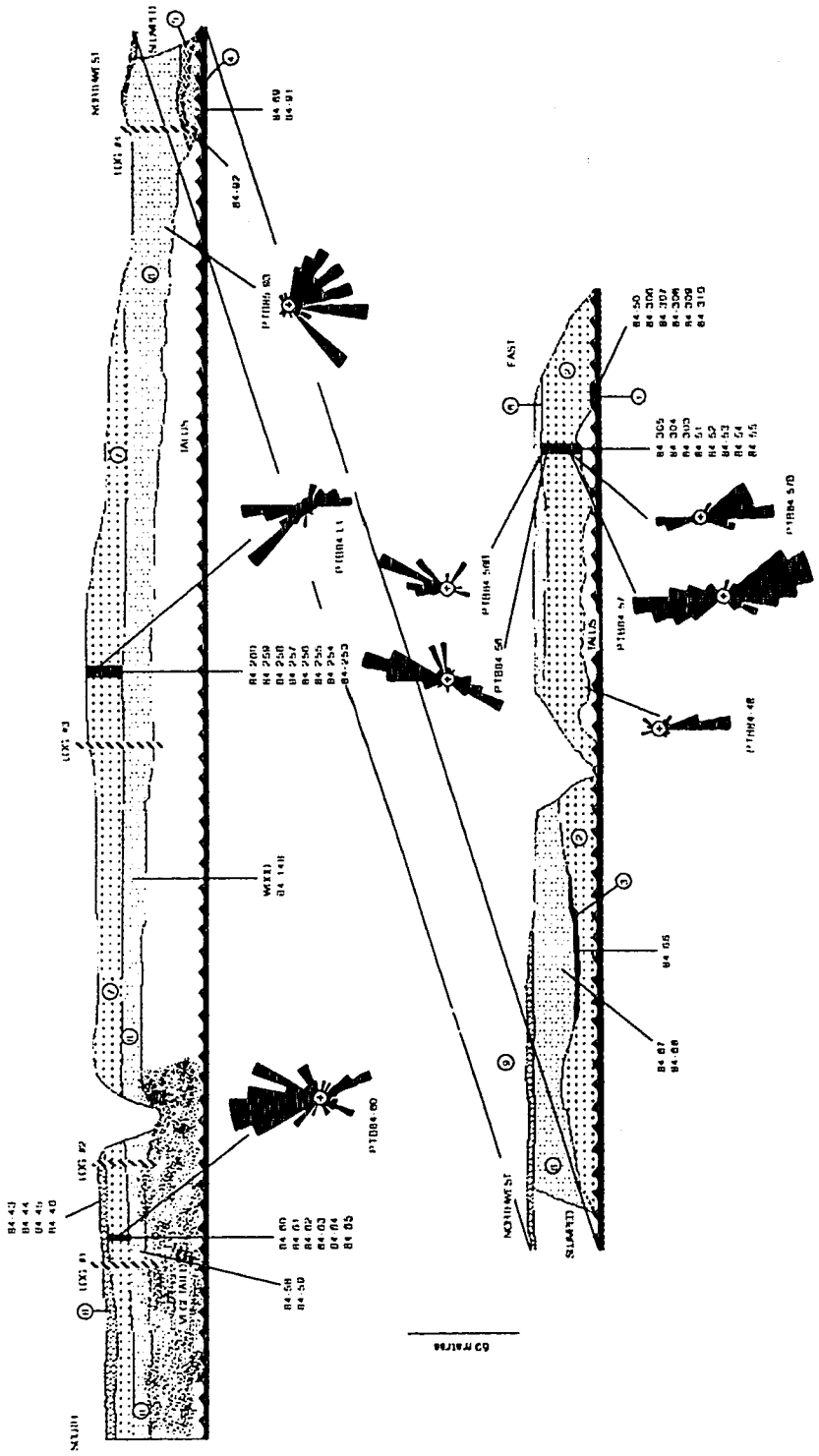

Section drawing of primary bluff face at Section Three illustrating lithostratigraphic units, samples, and sample locations. See text for further explanation.

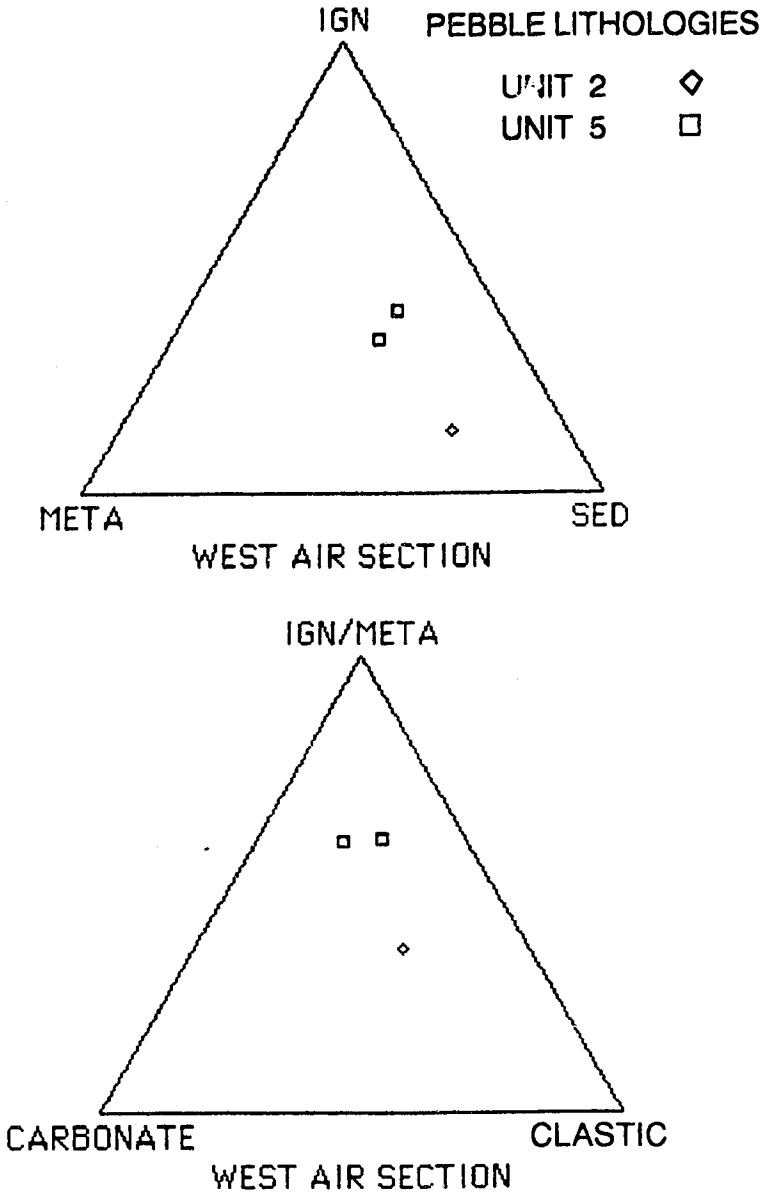

Ternary diagrams comparing pebble lithologies for two units at West Air Section.

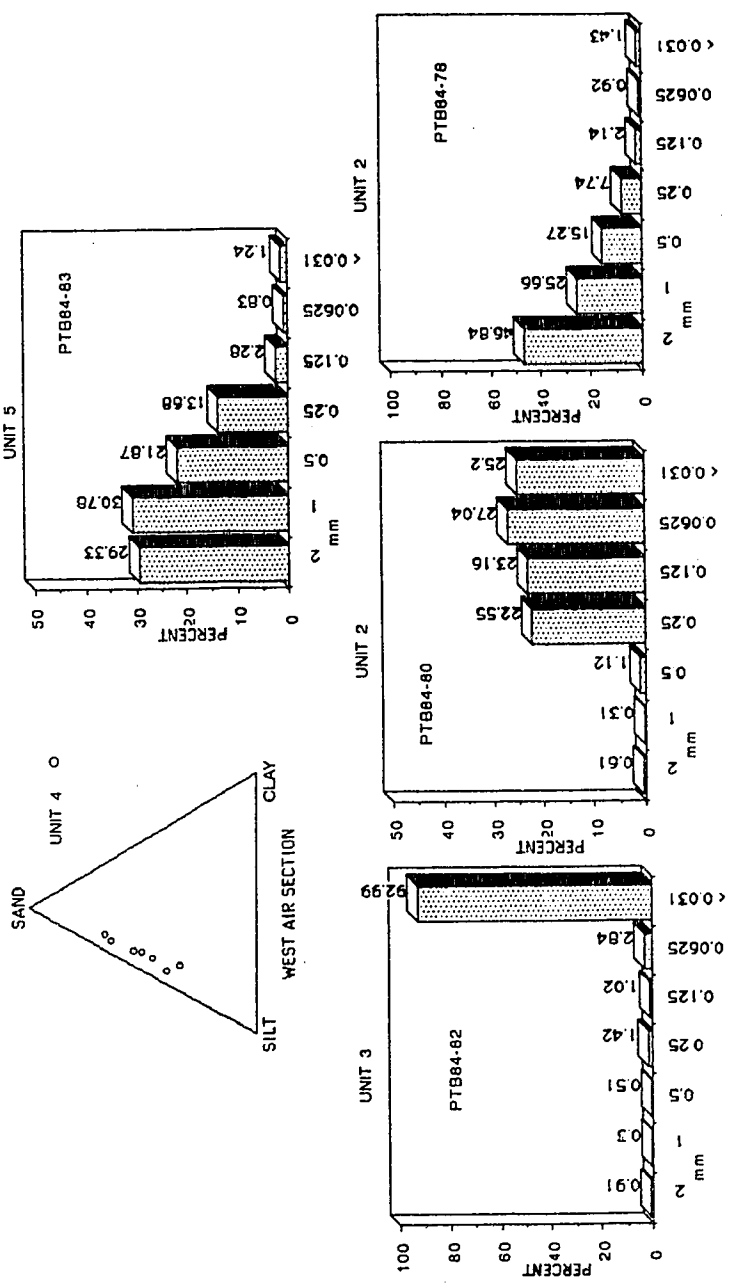

Textural diagrams from various units at West Air Section. Ternary diagram illustrates variation in matrix supported diamictons, histograms illustrate variation for other samples. See text for explanation and keyto samples.

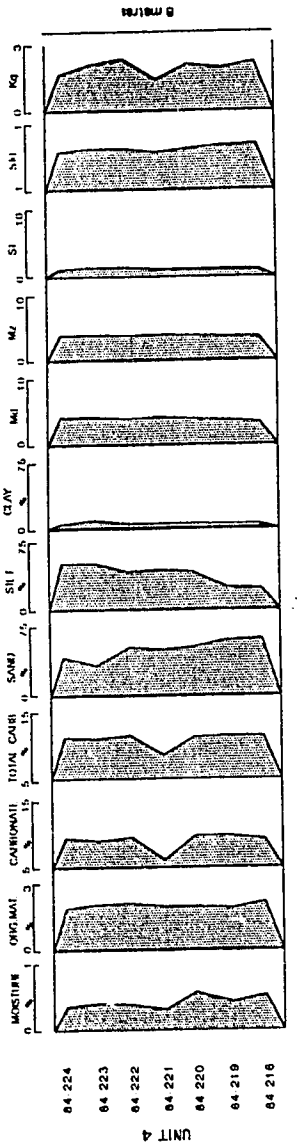

Compositional variation with depth for unit 4, West Air Section.

WEST AIR SECTION

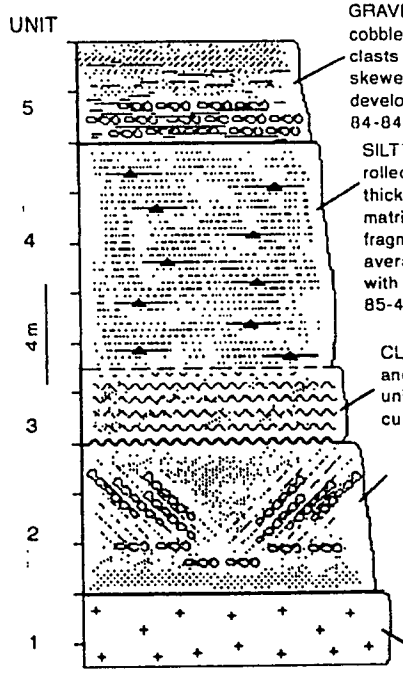

GRAVEL and SAND-primarily pebble clast-supported; 4 m thick; horizontally bedded gravels; cobbles (5%), c. pebbles (35%), f. pebbles (25%), matrix (35%); moderate to well imbricated; clasts rounded to well-rounded; matrix medium sand to granule (95%); loose; moderately sorted; skewed to right; leptokurtic; top part is silty sands, horizontally laminated, 1 m thick; soil developed on sands; basal contact straight, sharp, erosive, conformable; 10YR 6/3 (pale brown); 84-84,227,228

SILTY SAND-matrix-supported; 0-10 m thick; graded beds of sandy or silty diamicton, with rare rolled pebble or cobble stones; massive to horizontally laminated within graded beds; beds 1-5 cm thick; contacts erosive, conformable; oxidation and hardpan surfaces intercalated with loose matrix; matrix averages sand (51%), silt (42%), clay (7%); fossiliferous; wood and coal fragments; wood dates 37,190 ± 2870 ybp near base, 23,280 ± 750 ybp near top; magnetic average is 343° declination, 27° inclination, S1=0.990; gradational basal contact, intertonguing with oxidized gravels; 10YR 2/1 (black); 84-218, 219, 220, 221, 222, 223, 224, 225, 336, 85-41; 5A1A,5A1B

CLAYEY SILT-matrix-supported; 0-3 m thick; very slightly deformed; horizontally laminated and crenulated; faulted; interspersed diamicton rip up clasts and minor boulders (10%) along unit margin; moderately well sorted; very leptokurtic; skewed to left; basal contact sharp, curvilinear, erosive, unconformable; 2.5Y 6/4 (light yellowish brown); 84-82

GRAVEL and SAND-primarily pebble clast-supported; 0-7 m thick; gravels horizontally bedded, dipping >20° to N and S, deformed; cobbles (5%), pebbles (60%), matrix (30%); matrix is granules (47%), and very c. sands (26%); clasts rounded, no striations, moderately sorted; leptokurtic; skewed to right; sand interbeds, ~40 cm thick; sharp basal contacts; horizontally laminated; faulted; poorly sorted; mesokurtic; medium sand to silt; unit highly oxidized; basal contact sharp, erosive, curvilinear, unconformable; coal inclusions;10YR 5/8 (yellowish brown) to 2.5Y6/4 (yellowish brown); 84-78,79,80

BEDROCK-shaley meta-siltstone, green, friable with coal inclusions near base, grades up into beige meta-sandstone near top, basal contact indeterminate; 0 to +5 m thick; 84-226

Composite stratigraphic column of West Air Section, lithostratigraphic units along left and unit descriptions along right.

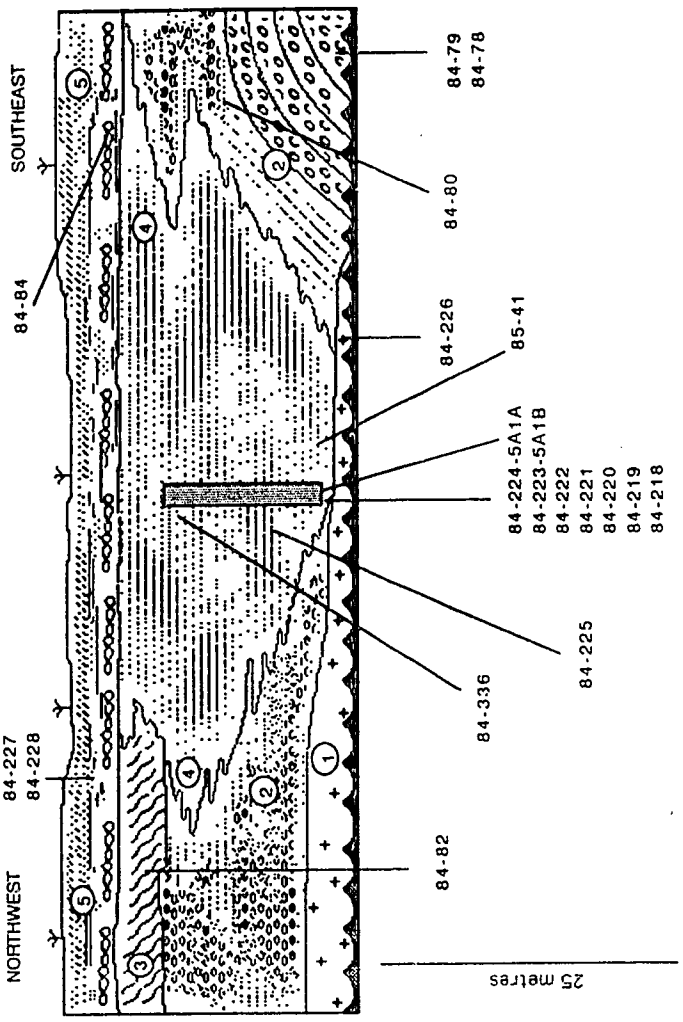

Section drawing of primary face of West Air Section illustrating relationship between lithostratigraphic units, samples, and sample locations. See text for further explanation.

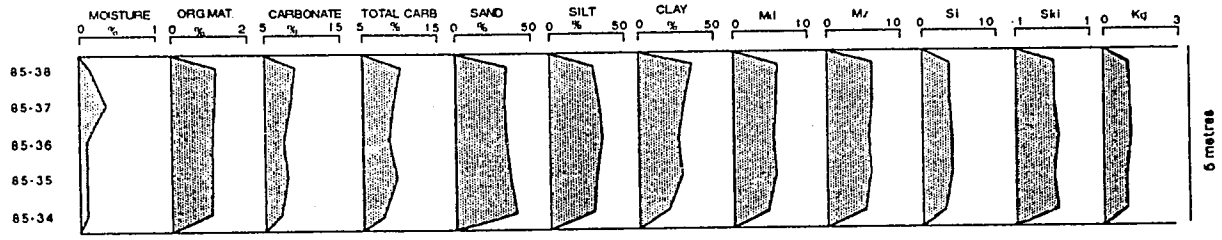

Compositional variation with depth for Unit 3, Section Four.

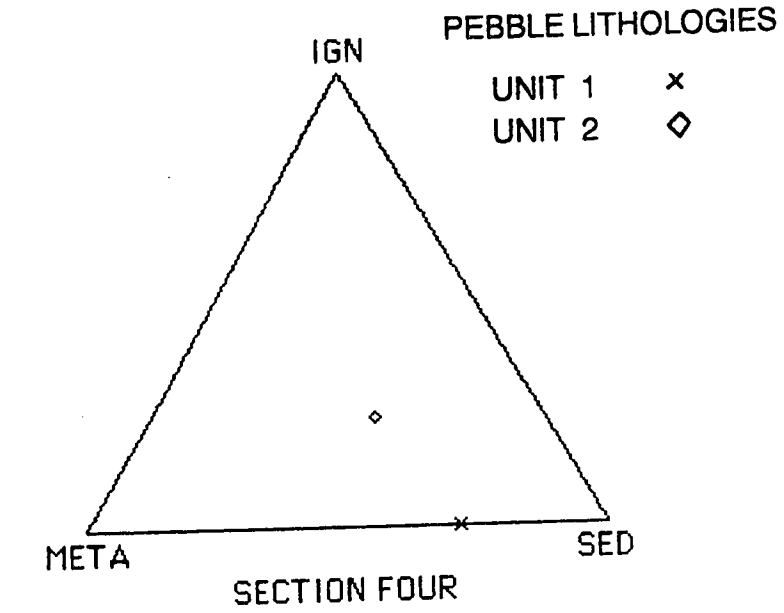

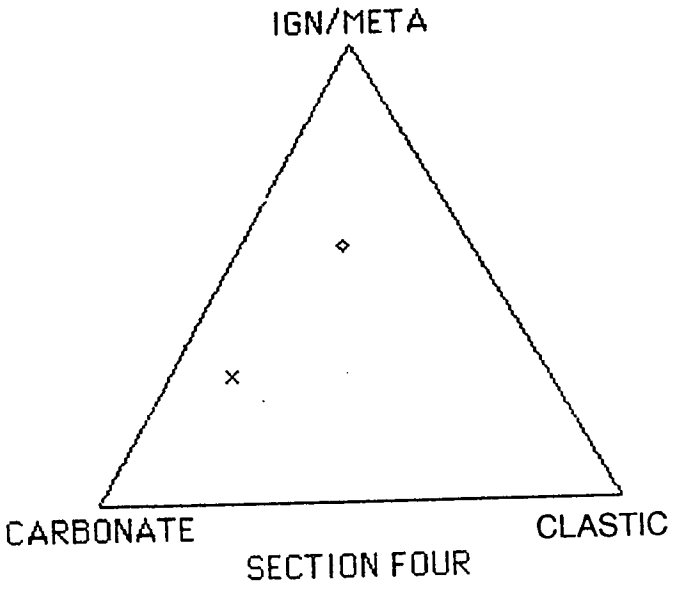

Ternary diagrams comparing pebble lithologies for two units at Section Four.

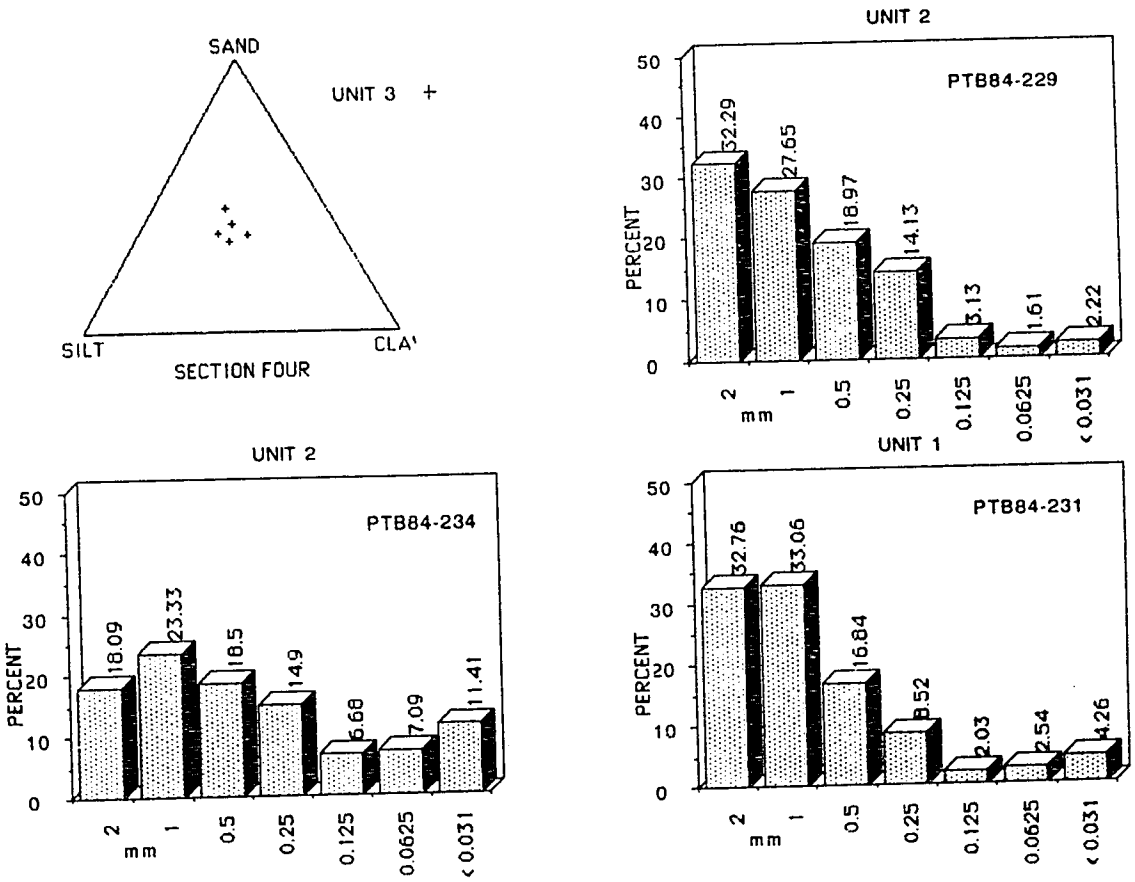

Textural diagrams from various units at Section Four. Ternary diagram illustrates variation in matrix-supported diamicton; histograms illustrate variation in other samples. See text for explanation and key to samples.

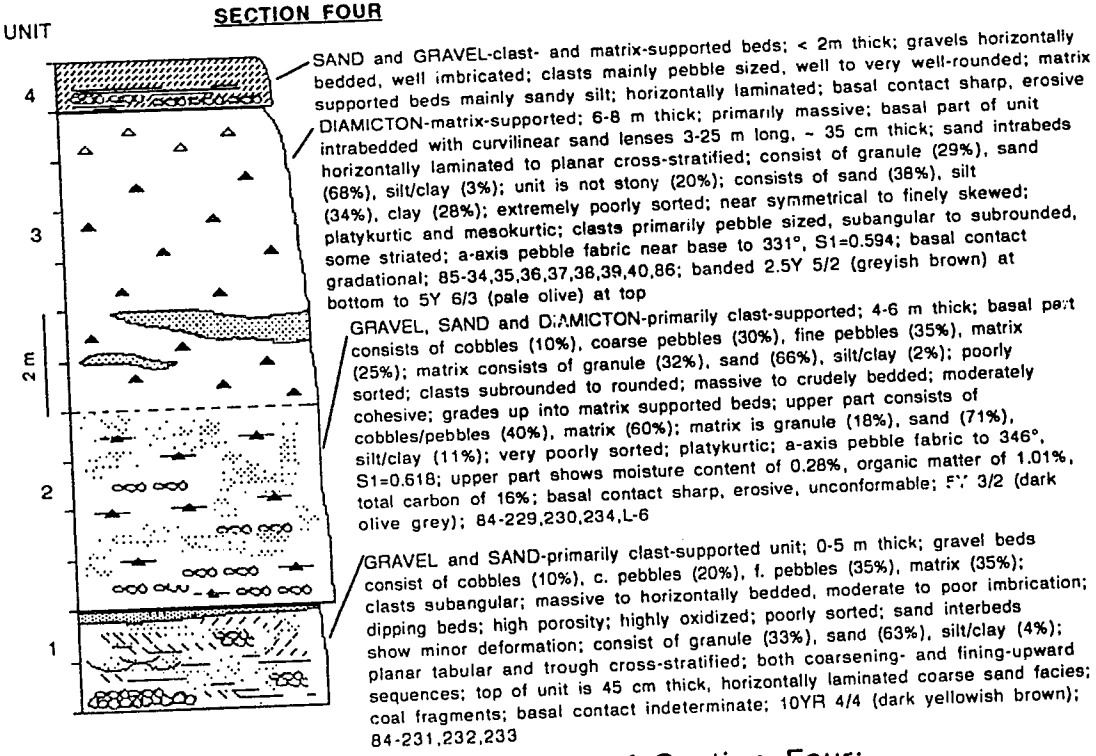

Composite stratigraphic column of Section Four; lithostratigraphic units along left, and unit descriptions along right.

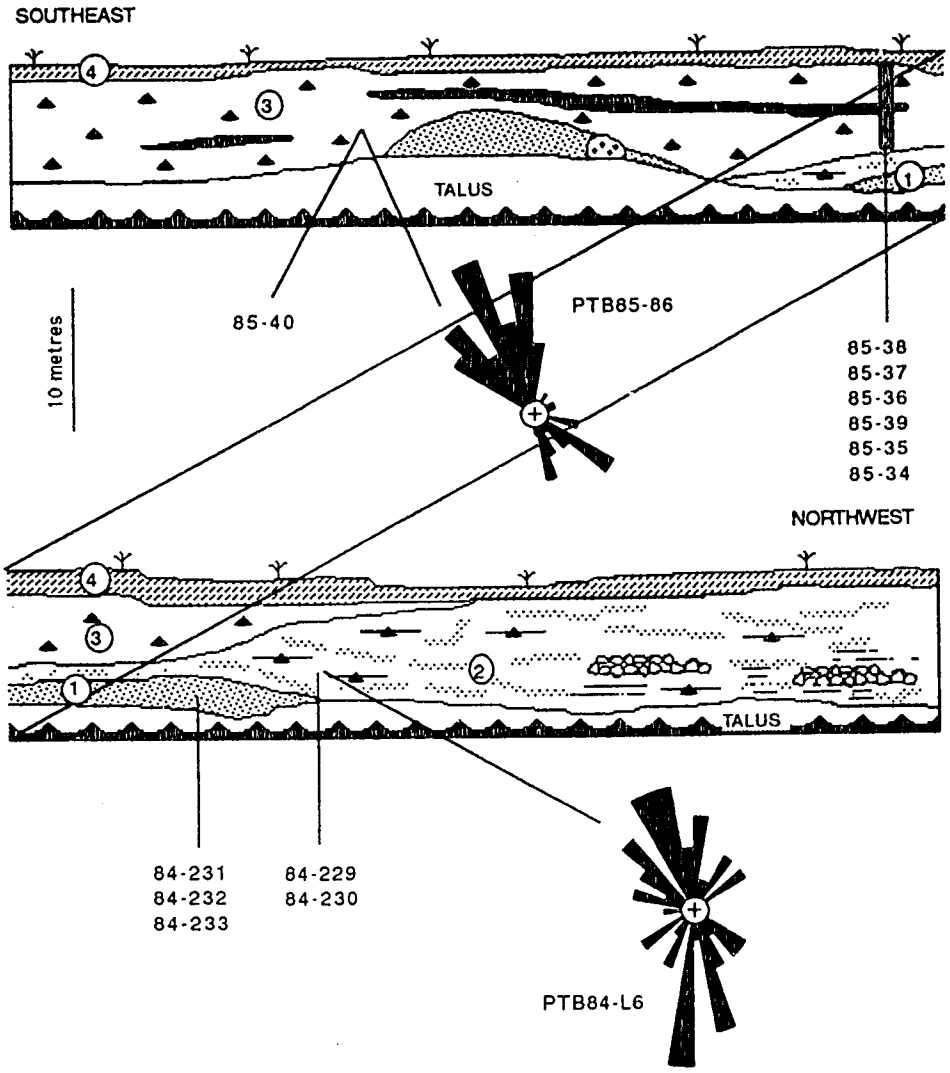

Section drawing of Section Four primary face illustrating relationship between lithostratigraphic units, samples and sample locations. See text for further explanation.

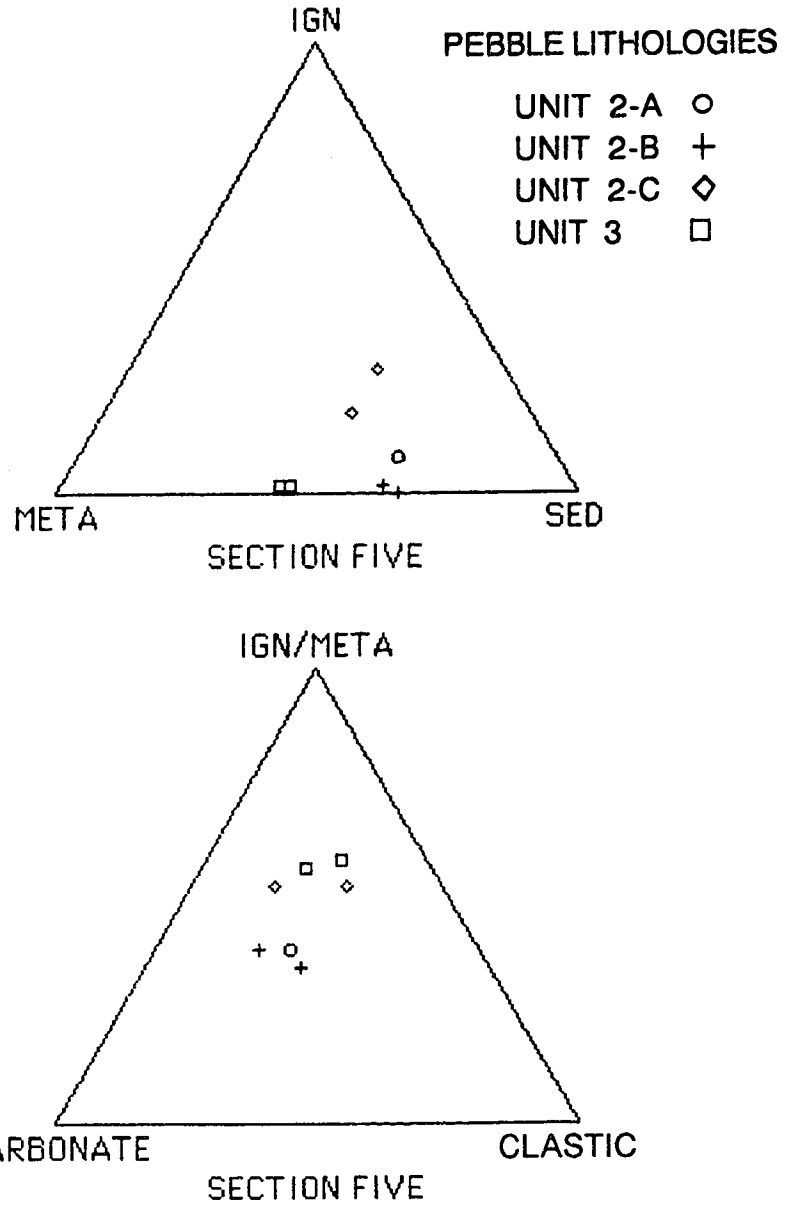

Ternary diagrams comparing pebble lithologies for two units (including three subunits) at Section Five.

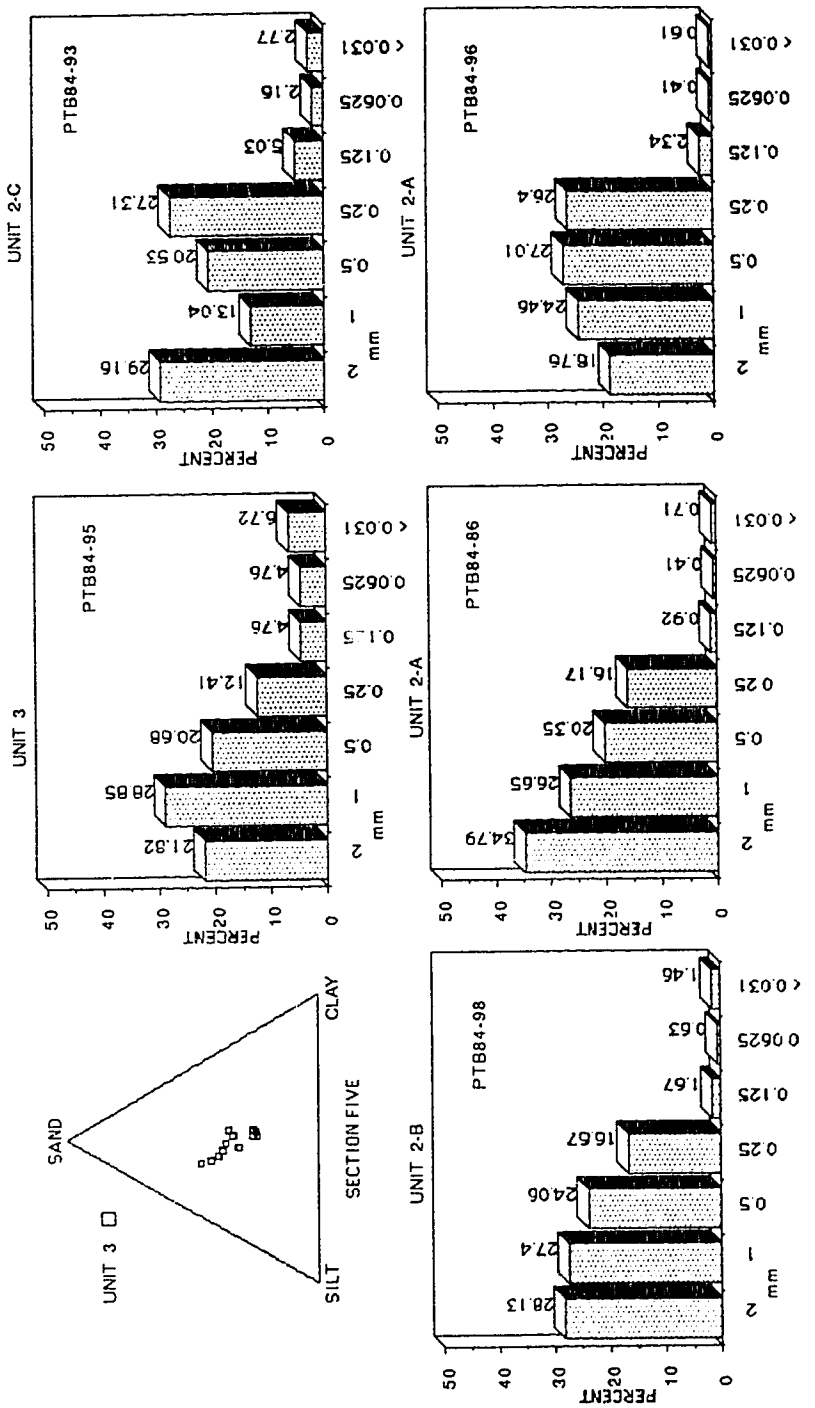

Textural diagrams for various units at Section Five. Diamicton and nondiamicton samples. See text for explanation and key to samples.

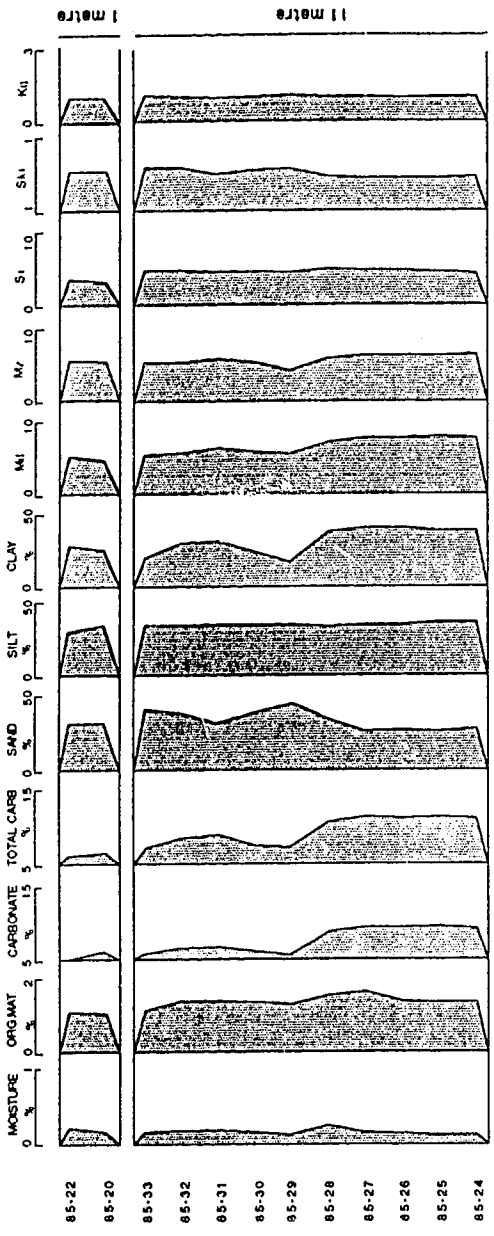

Compositional variation with depth for Unit 3, Section Five.

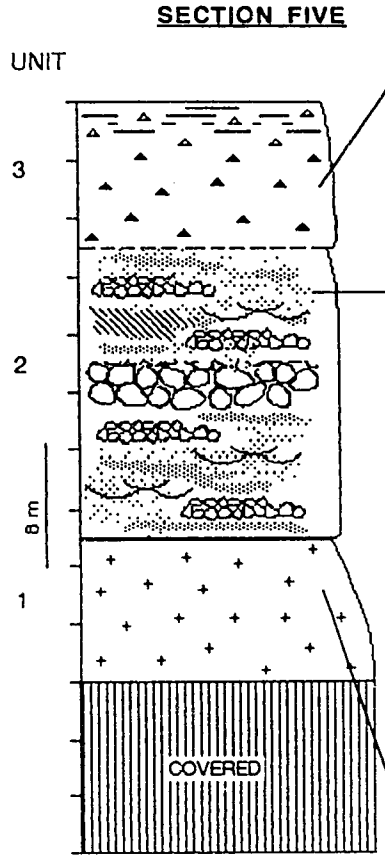

DIAMICTON-matrix-supported; 0-12 m thick; massive at base to foliated near top, parting structures in upper 2 m; stony (35%); cobbles (15%), pebbles (20%), matrix (65%); matrix averages sand (33%), silt (35%), clay (32%); unit tends to coarsen-upwards; very poorly sorted; near symmetrical to finely skewed; mesokurtic; clasts subangular to subrounded; soil developed on top; a-axis pebble fabric to 346°, S1=0.616 near base, to 307°, S1=0.607 just below foliation and to 181°, S1=0.476 in foliated zone at top; basal contact gradational to indistinct; 84-L5,20,21,22,23,24,25,26,27,28,29,30,31,32,33,95; 10YR 4/1 (dark grey) to 2.5Y 6/6 (olive grey)

GRAVEL and SAND-clast- and matrix-supported beds; < 40 m thick; upper third of unit: primarily pebble clast-supported beds 0.35-1.0 m thick; cobbles (10%), c. pebbles (25%), f. pebbles (40%), matrix (25%); matrix is med. sands (27%) and granules (24%); planar and trough cross-stratified; occasionally massive to horizontally bedded; imbrication moderate to good; moderately to poorly sorted; matrix-supported beds 20 cm thick; med. to f. sands (70%); c. sands (20%); some beds with f. pebble stringers (10%); well-sorted; massive to planar and trough cross-stratified; 2.5Y 3/2 (v. dark greyish brown); 84-94,93; middle third of unit: primarily cobble clast-supported beds, 1.5-3 m thick; cobbles (30%), c. pebbles (30%), f. pebbles (20%), matrix (20%); matrix is c. sand to granule (80%); poorly sorted; skewed to right; poor imbrication; clasts subrounded to well-rounded; massive; matrix-supported beds, 30 cm thick; med. to f. sands (80%), c. sands (20%); no clasts; massive; well sorted; 10YR 4/2 (dark greyish brown); 84-85, 98,99; lower third of unit: primarily fine pebble clast-supported, 1-3 m thick; cobbles (15%), c. pebbles (25%), f. pebbles (35%), matrix (25%); moderately to poorly sorted; clast subrounded to well rounded; loose; minor oxidation, massive to trough cross-stratified; moderate imbrication; matrix is med. to v.c. sand; matrix-supported facies, 25 cm thick; med. sand (80%), c. sand (20%); no clasts; well sorted; planar cross-stratified; lower third a-axis pebble fabric to 164°, S1= 0.594; 2.5Y 3/2 (v. dark greyish brown); 84-86,87,96,97; 85-85; basal contact of unit sharp, erosive to indeterminate

BEDROCK-moderately well indurated pebble conglomerate interbedded with poorly indurated sandstone, 0-40 m thick; basal contact indeterminate, mostly covered

Composite stratigraphic column of Section Five, lithostratigraphic units along left and unit descriptions along right.

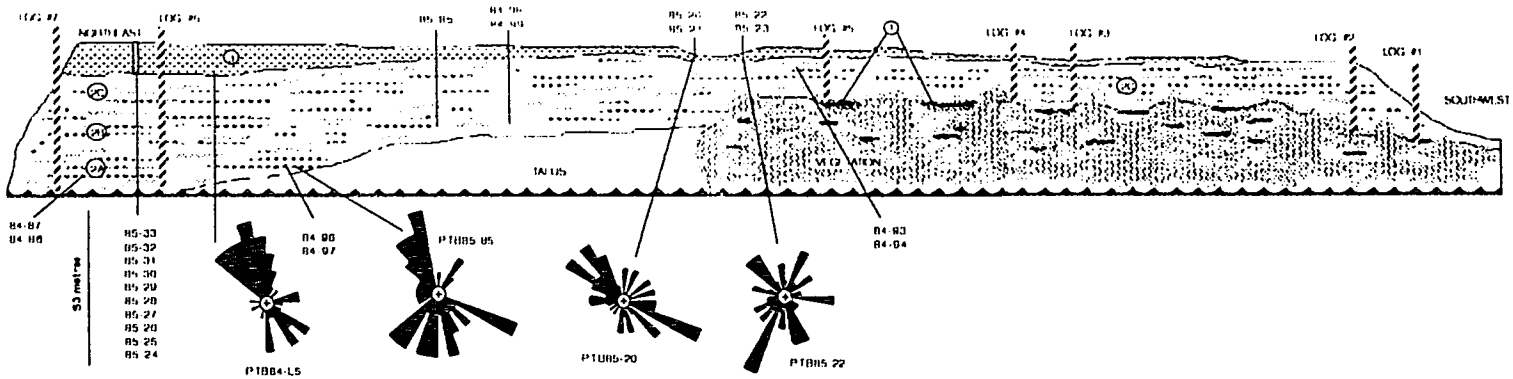

Section drawing of primary face of Section Five illustrating relationship between lithostratigraphic units, samples and sample locations. Seetext for further explanation.

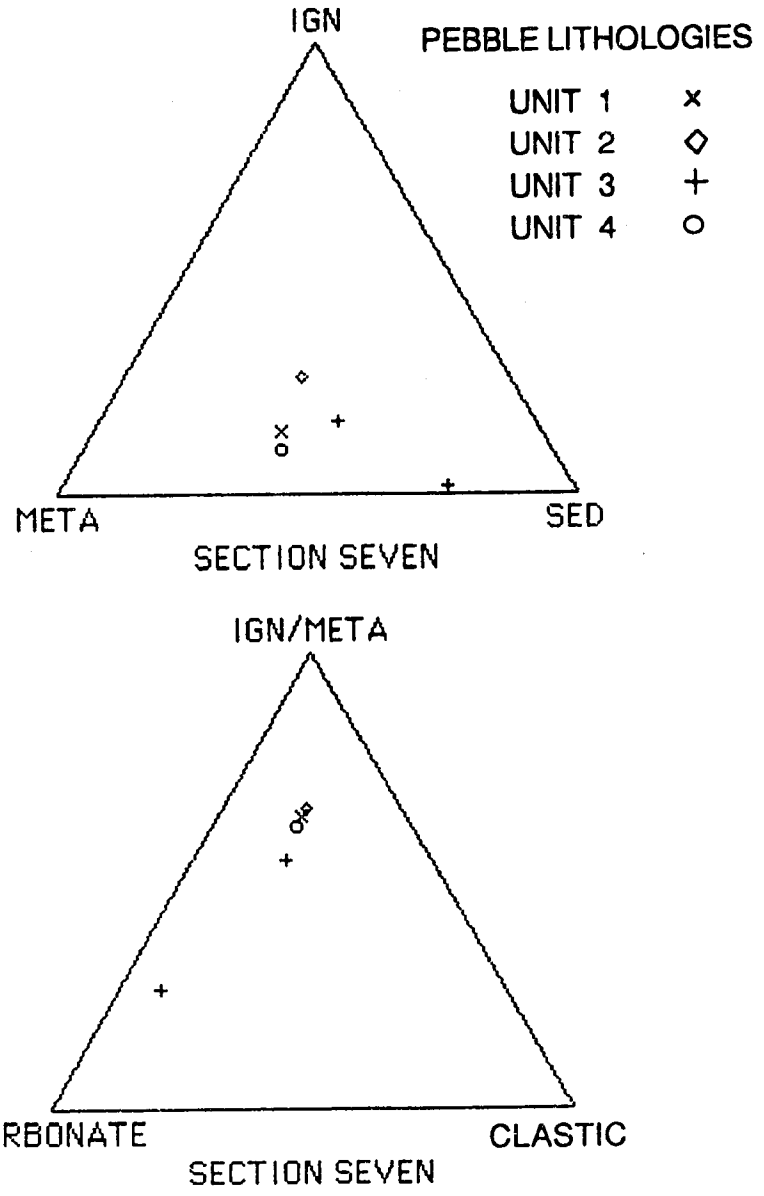

Ternary diagrams comparing pebble lithologies for four units at Section Seven.

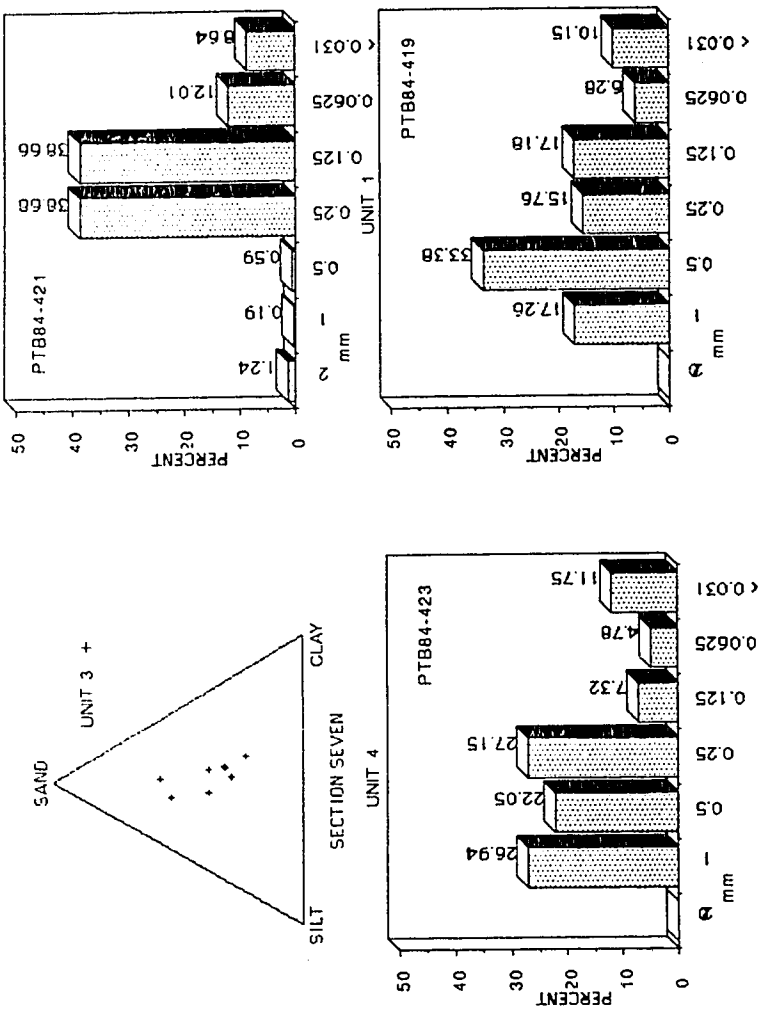

Textural diagrams for various units at Section Seven. Diamicton samples given in ternary plot, nondiamicton samples given in histograms. See text for explanation and key to samples.

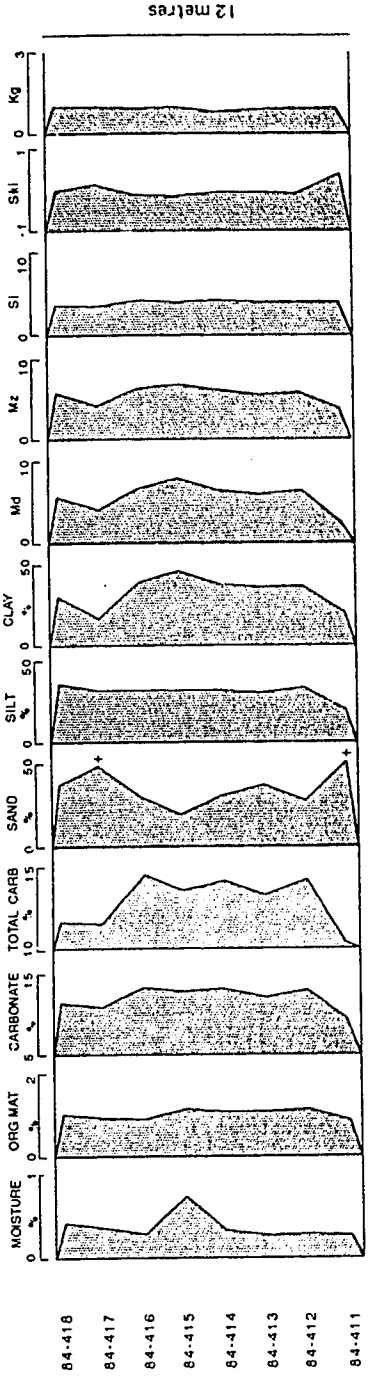

Compositional variation with depth for Unit 3, Section Seven.

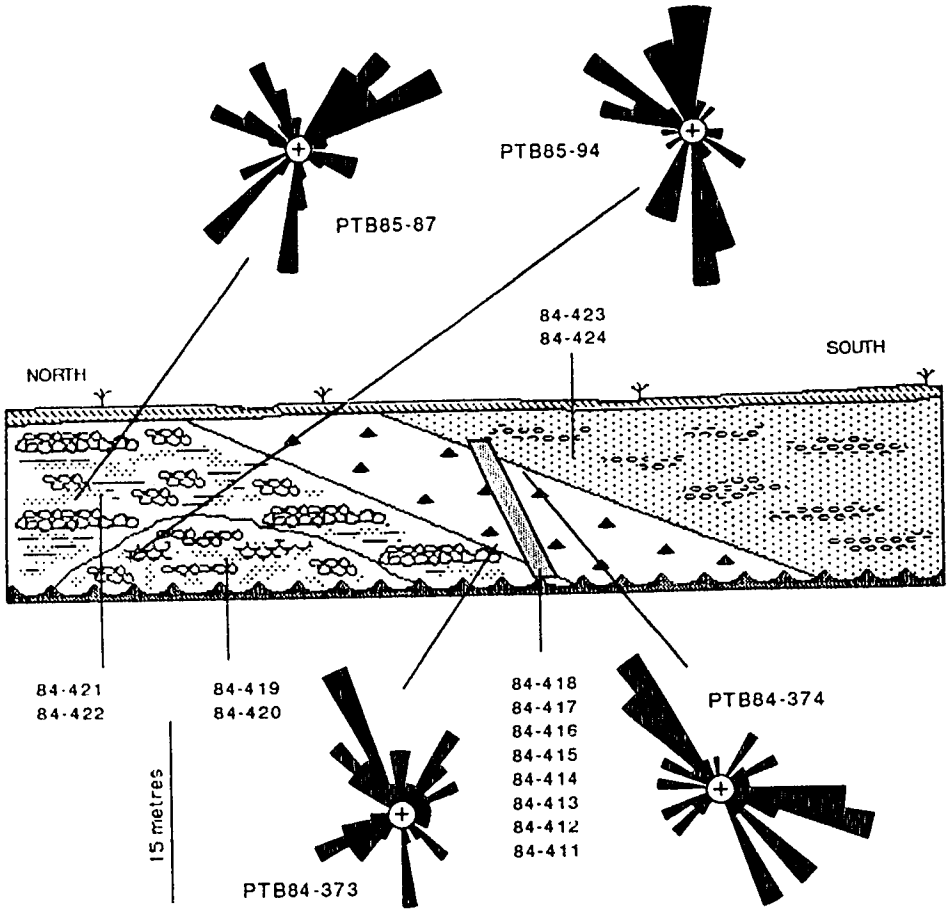

Section drawing of primary face at Section Seven, illustrating relationship between lithostratigraphic units, samples and sample locations. See text of further explanation.

SECTION SEVEN

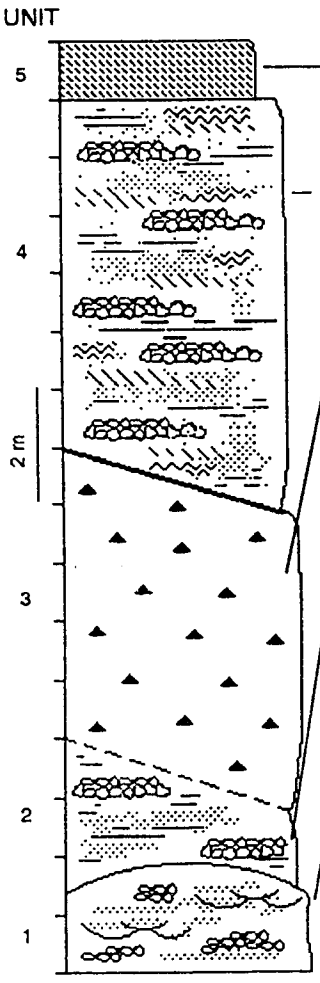

SILTS-matrix-supported; < 1m thick; massive; soil developed; basal contact indistinct to conformable

SAND and GRAVEL-primarily sand matrix-supported; <16m thick; sand beds horizontally to planar cross-stratified; undulating bed contacts; consists of med to c. sands (76%); finely skewed; platykurtic; poorly sorted; minor folding and faulting; moderately imbricated; pebble gravel interbeds; horizontally bedded and deformed; clasts rounded; basal contact sharp, erosive, inclined and unconformable; 10YR 4/3 (dark brown); 84-423,424

DIAMICTON-matrix-supported; 12 m thick; massive; not stony (20%); clasts subrounded; striated, pebble sized; matrix averages sand (38%), silt (30%), clay (32%); extremely poorly sorted; strongly fine skewed to coarse skewed; platykurtic; a-axis pebble fabric near base to 12°,S1=0.499, near top to 115°,S1=0.657; basal contact gradational, inclined; 5Y3/1 (dark grey); 84-373, 374, 411, 412, 413, 414, 415, 416, 417, 418

GRAVEL and SAND-primarily f. pebble clast-supported; 7m thick; horizontally bedded to massive; cobbles (10%), c. pebbles (25%), f. pebbles (30%), matrix (35%); sand interbeds (10%), ~20 cm thick; very well sorted; horizontally laminated; med. sand (34%), f. sand (34%); moderate imbrication; clasts rounded; minor oxidation; basal contact sharp, erosive, curved and conformable; 10YR 3/2 (v. dark grey); a-axis pebble fabric to 42°, S1= 0.474; 84-421,422; 85-87

GRAVEL and SAND-primarily f. pebble clast-supported; 6m thick no cobbles, c. pebbles (10%), f. pebbles (40%), sand (45%), silt/clay (5%); massive to horizontally bedded; some imbrication; minor trough cross-stratification; intercalated open-work gravels; minor cementation and oxidation; minor sand interbeds; massive; unit poorly sorted; matrix skewed to right; basal contact indeterminate; a-axis pebble fabric to 343°, S1= 0.658; 84-419,420, 85-94

Composite stratigraphic column of Section Seven; lithostratigraphic units along left, and unit descriptions along right.

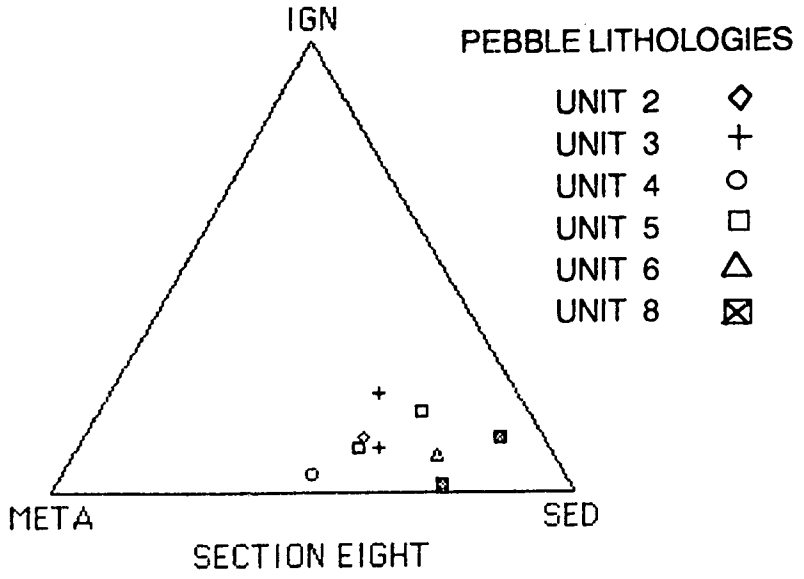

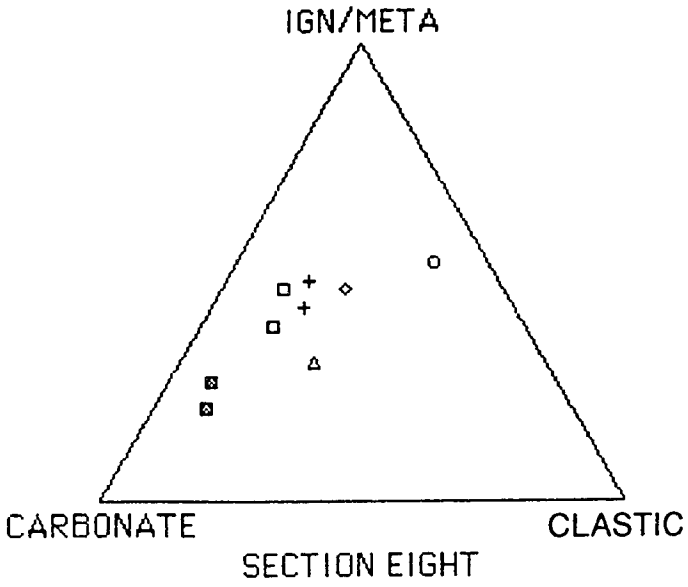

Ternary diagrams comparing pebble lithologies for six units at Section Eight.

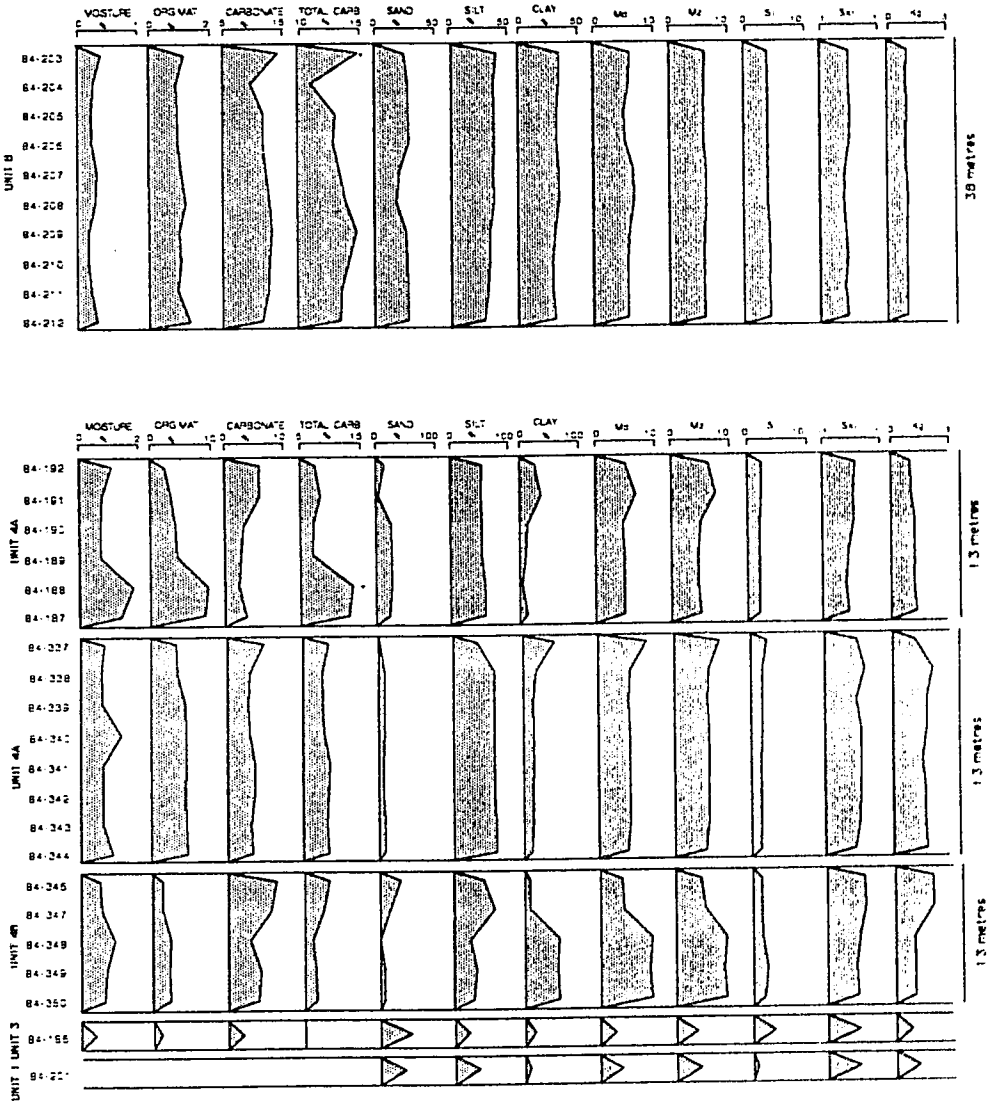

Compositional variation with depth for Units 1, 3, 4 and 8, Section Eight. Units 4A, 4B, and 4C denotes three sample locations of the same unit.

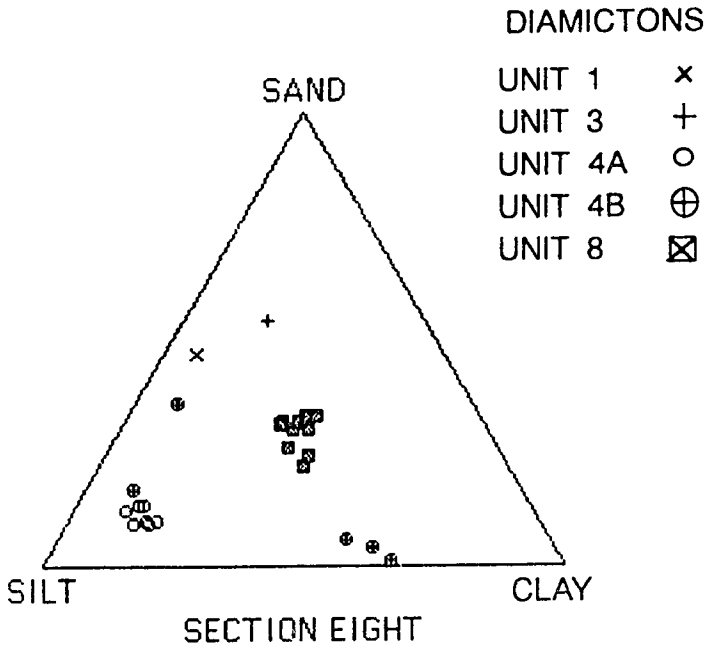

Ternary diagram showing textural variation for both diamictons and nondiamictons from four units (including two sample locations-4A and 4B) at Section Eight.

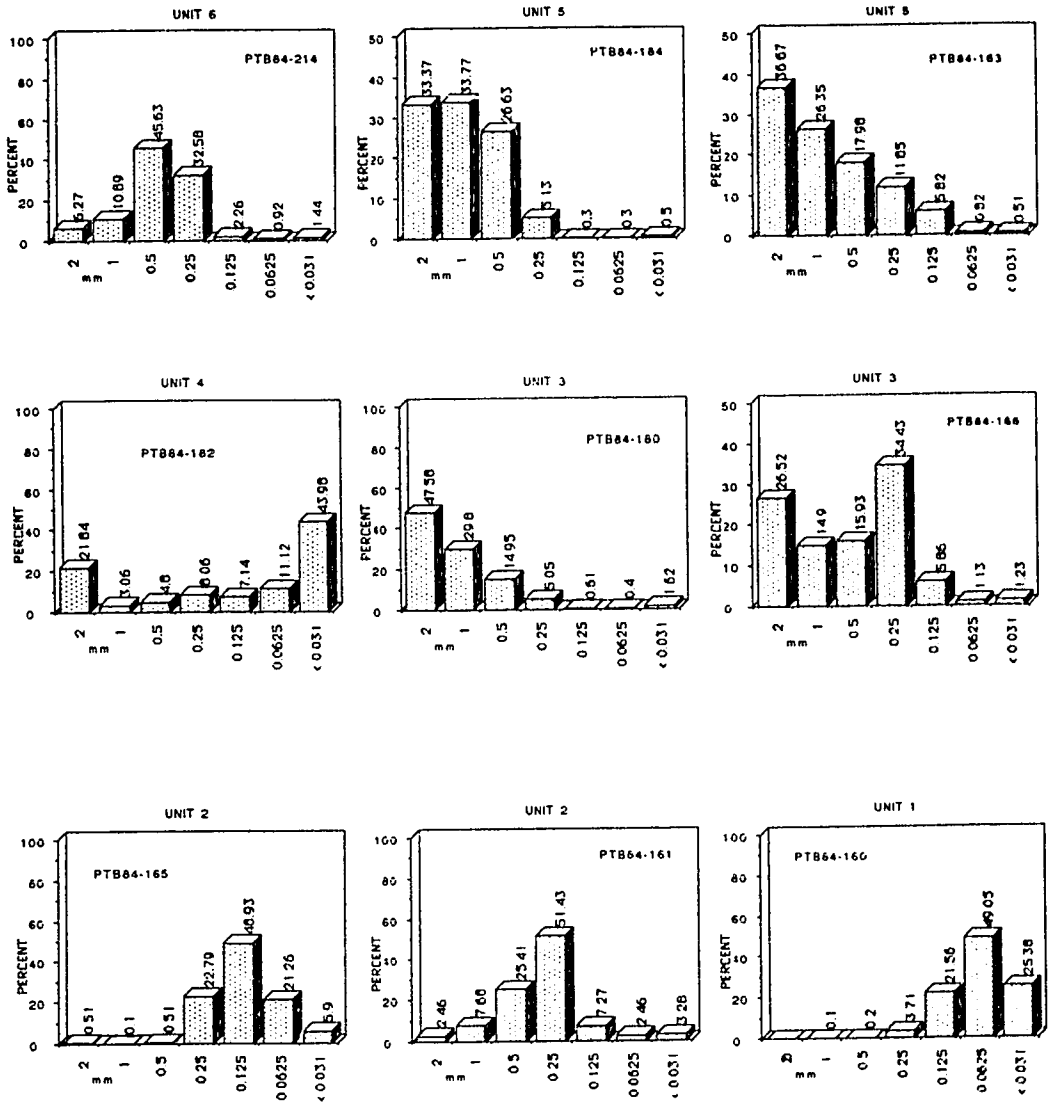

Textural histograms for nondiamicton samples for various units at Section Eight. See text for explanation and key to samples.

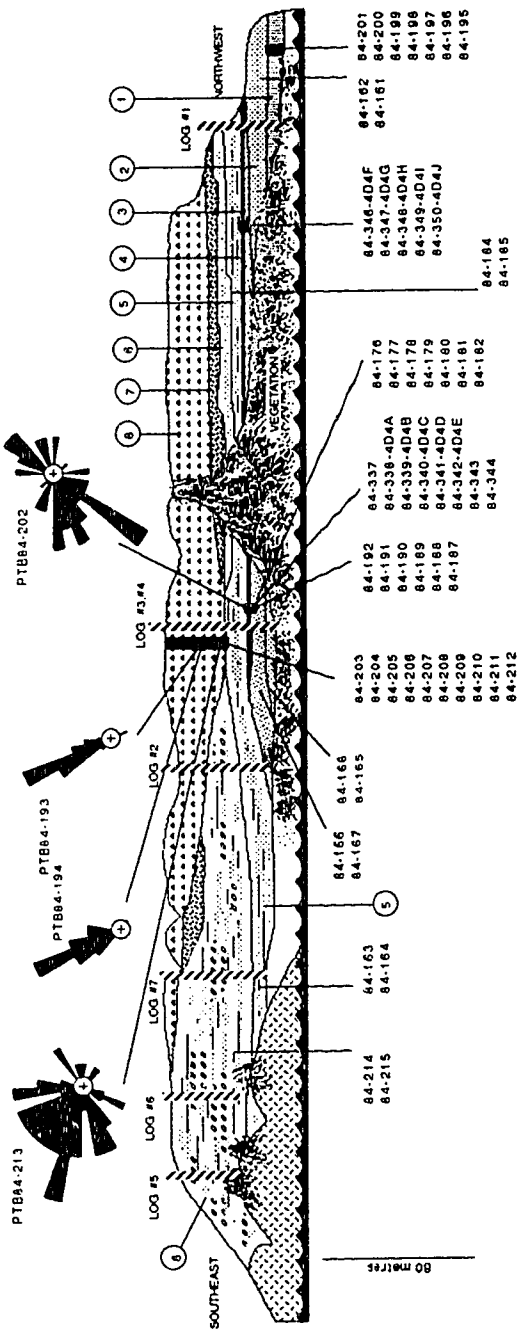

Section drawing of entire face of Section Eight showing various lithostratigraphic units, samples, sample locations, and pebble fabrics.

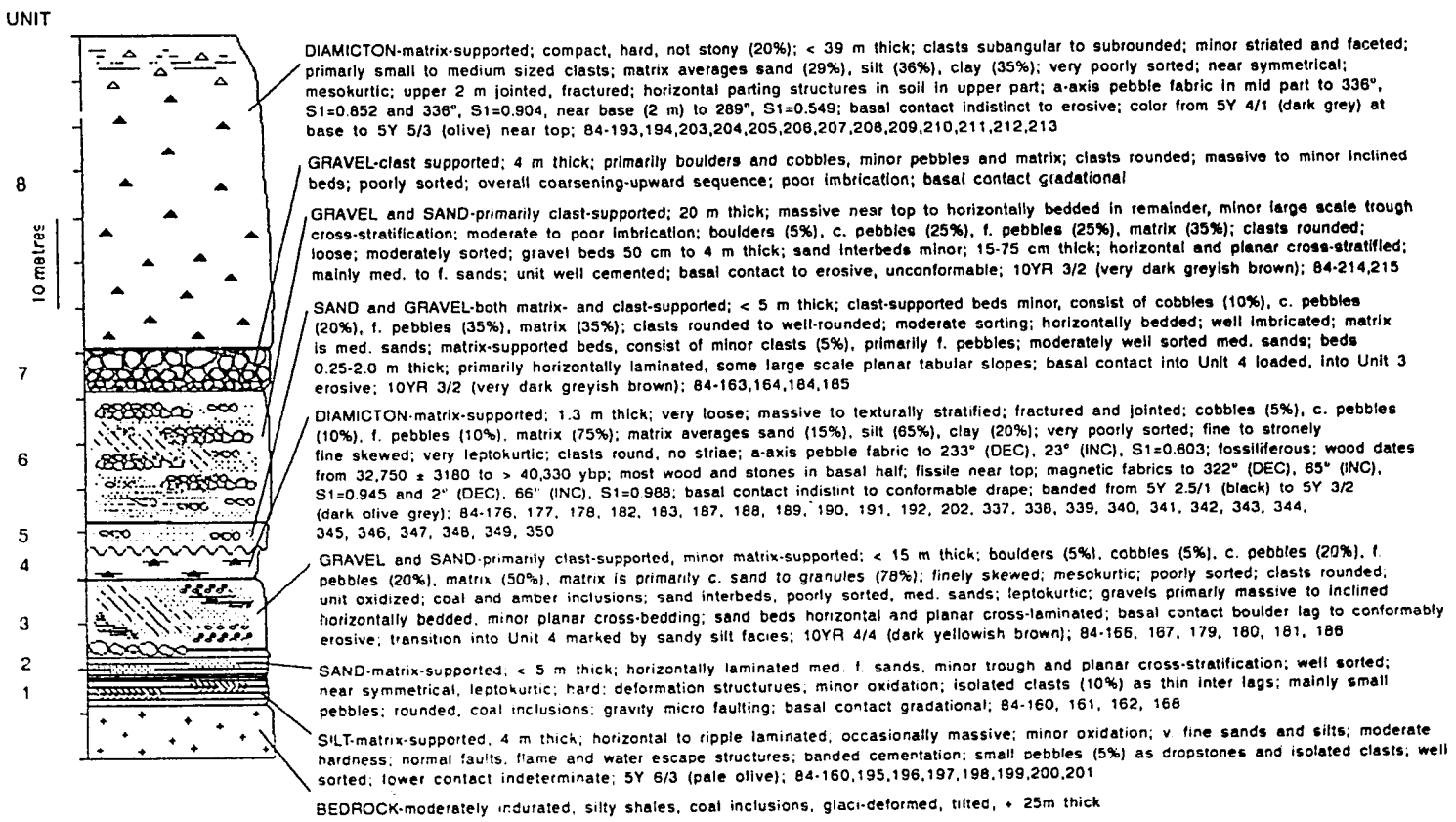

Composite stratigraphic column of Section Eight; lithostratigraphic units along left, and unit descriptions along right.

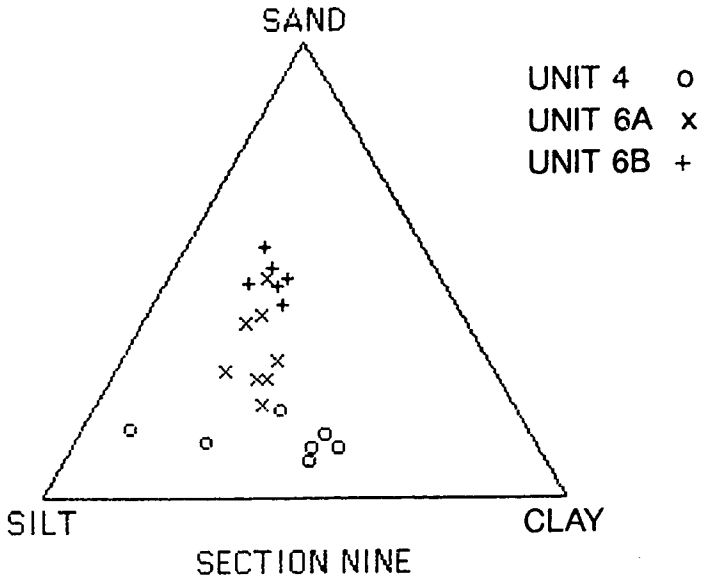

Ternary diagram illustrating textural variation in various diamictons from Section Nine.

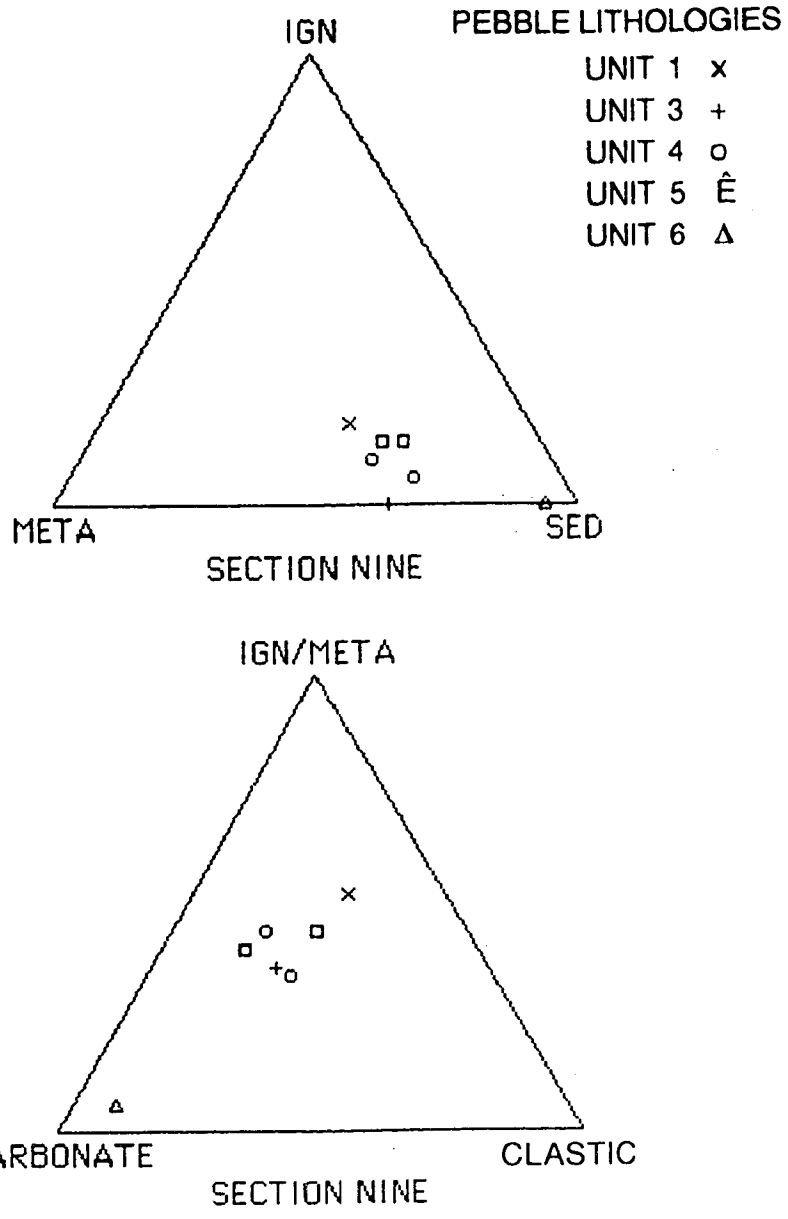

Ternary diagrams comparing pebble lithologies for four units at Section Nine.

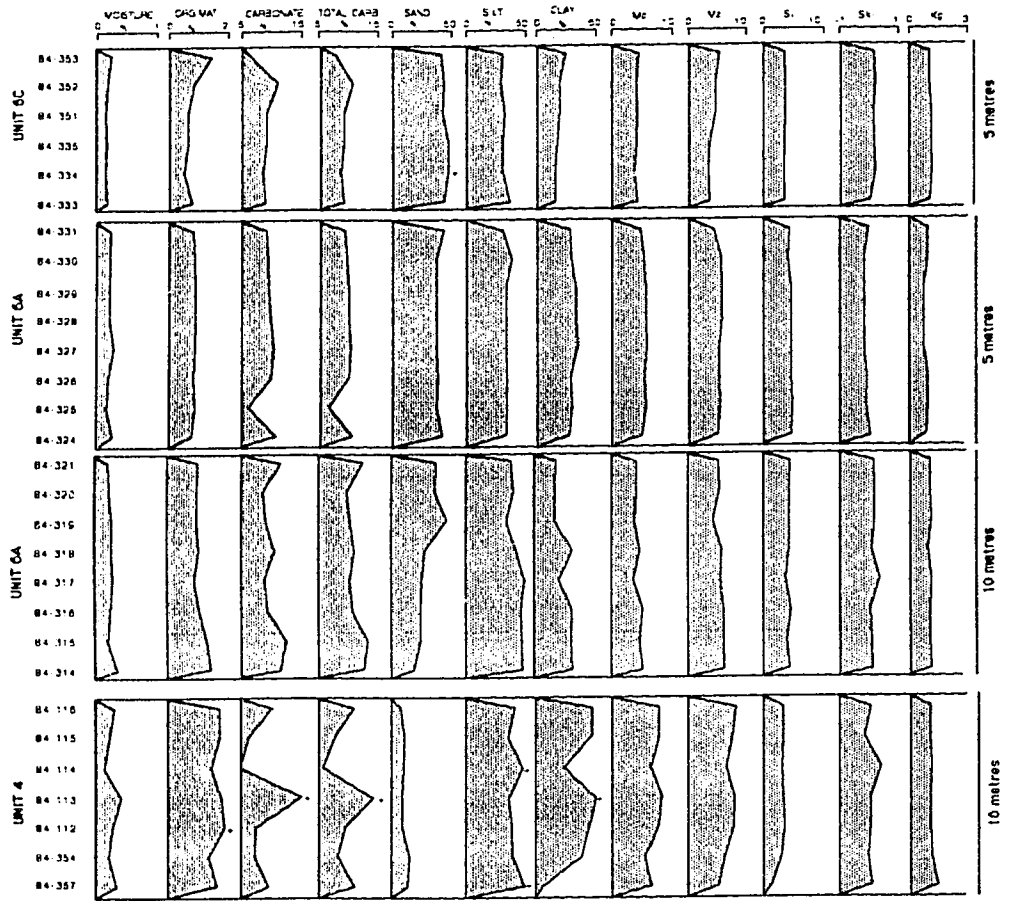

Compositional variation with depth for Units 4 and 6 (including subunits), Section Nine. Unit 6 subsamples samples arranged stratigraphically.

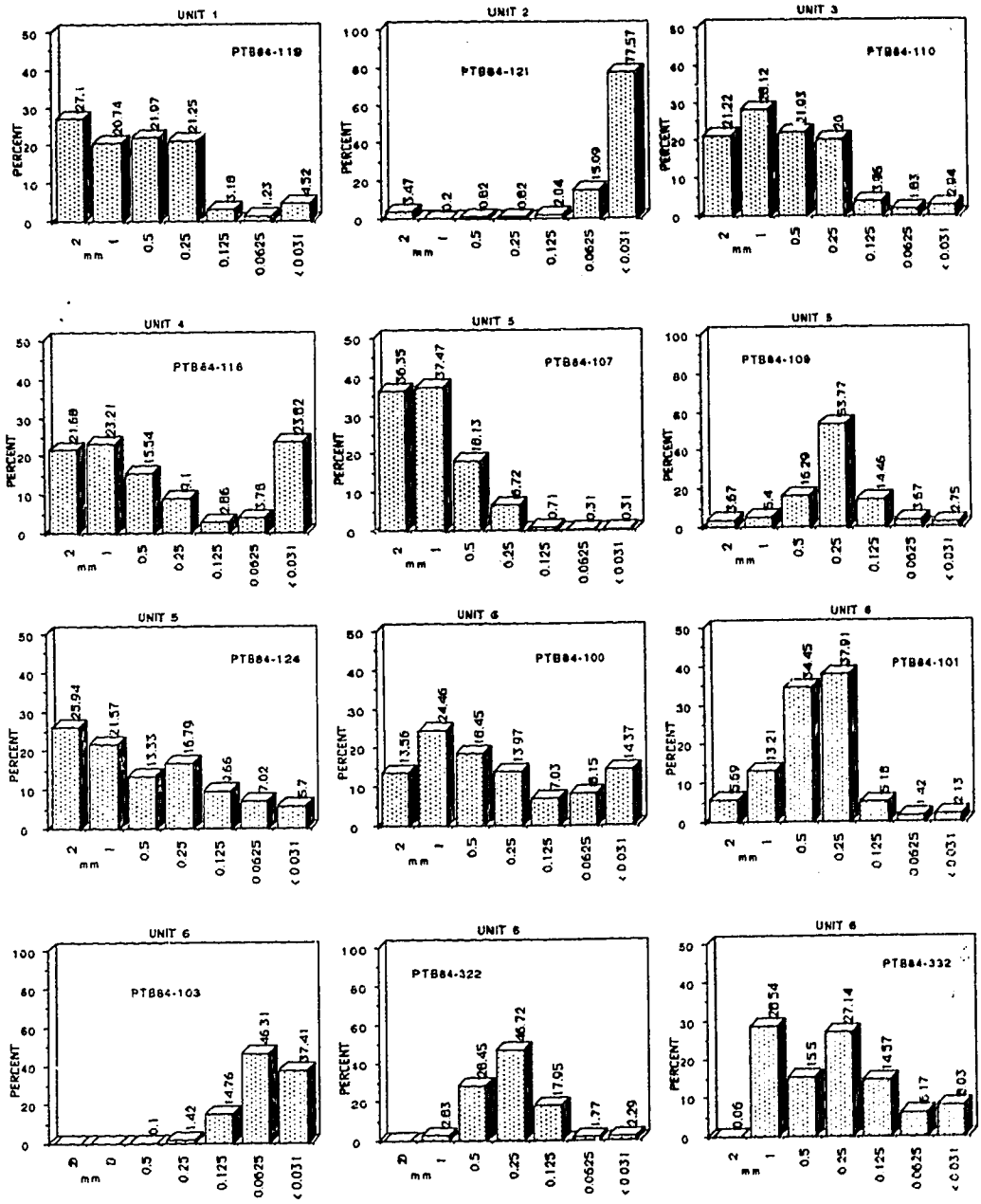

Textural diagrams for samples from various units at Section Nine. See text for further explanation and key to samples.

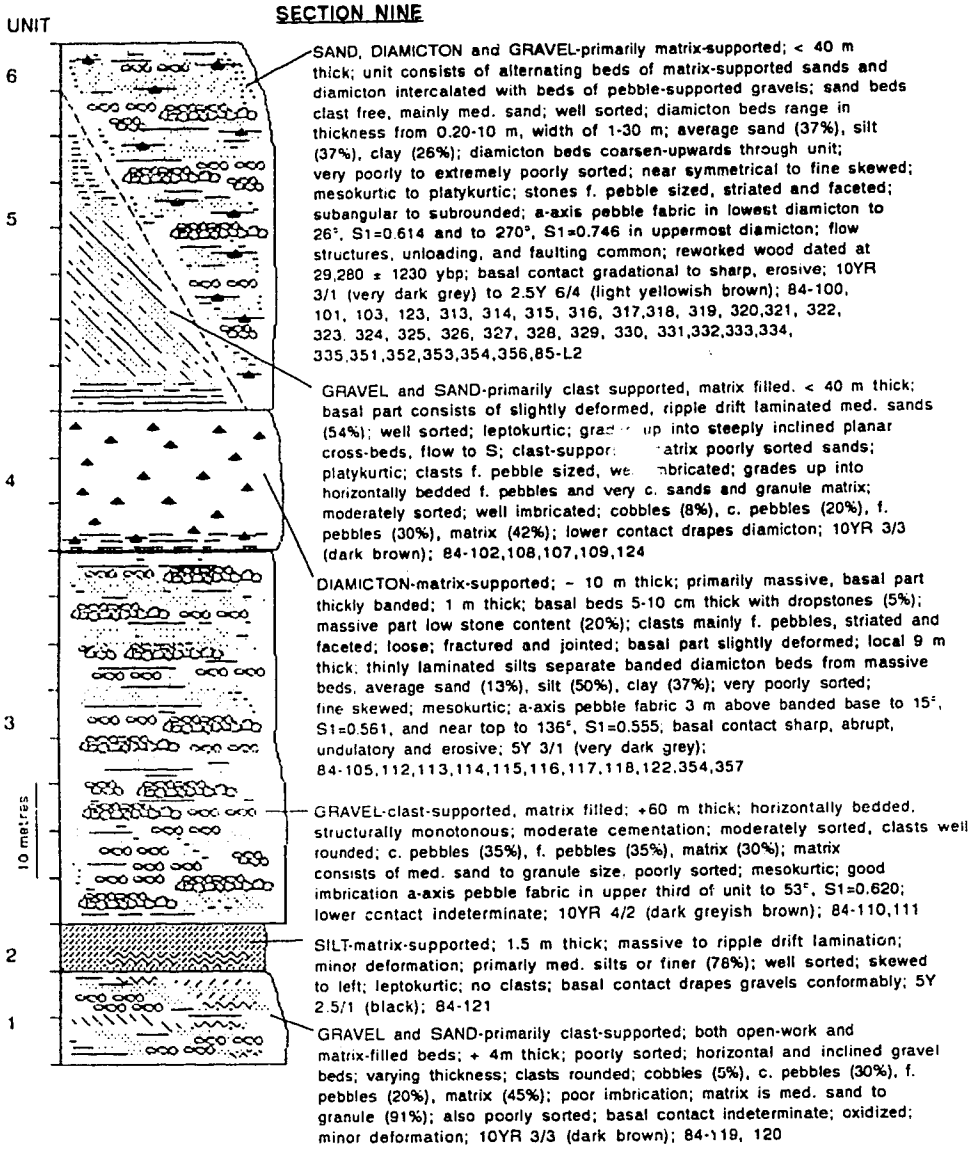

Composite stratigraphic column of Section Nine; lithostratigraphic units along left, and unit descriptions along right.

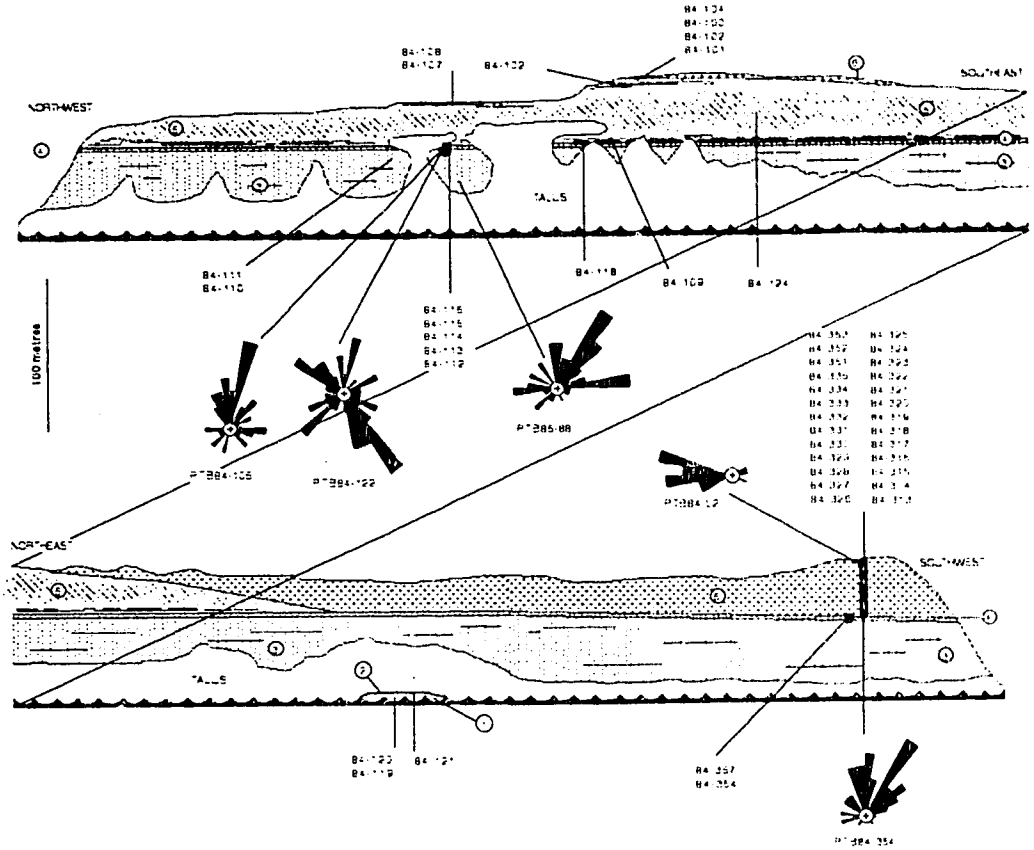

Section drawing of entire face of Section Nine. Illustration shows relationship between lithostratigraphic units, sample locations, and pebble fabrics.

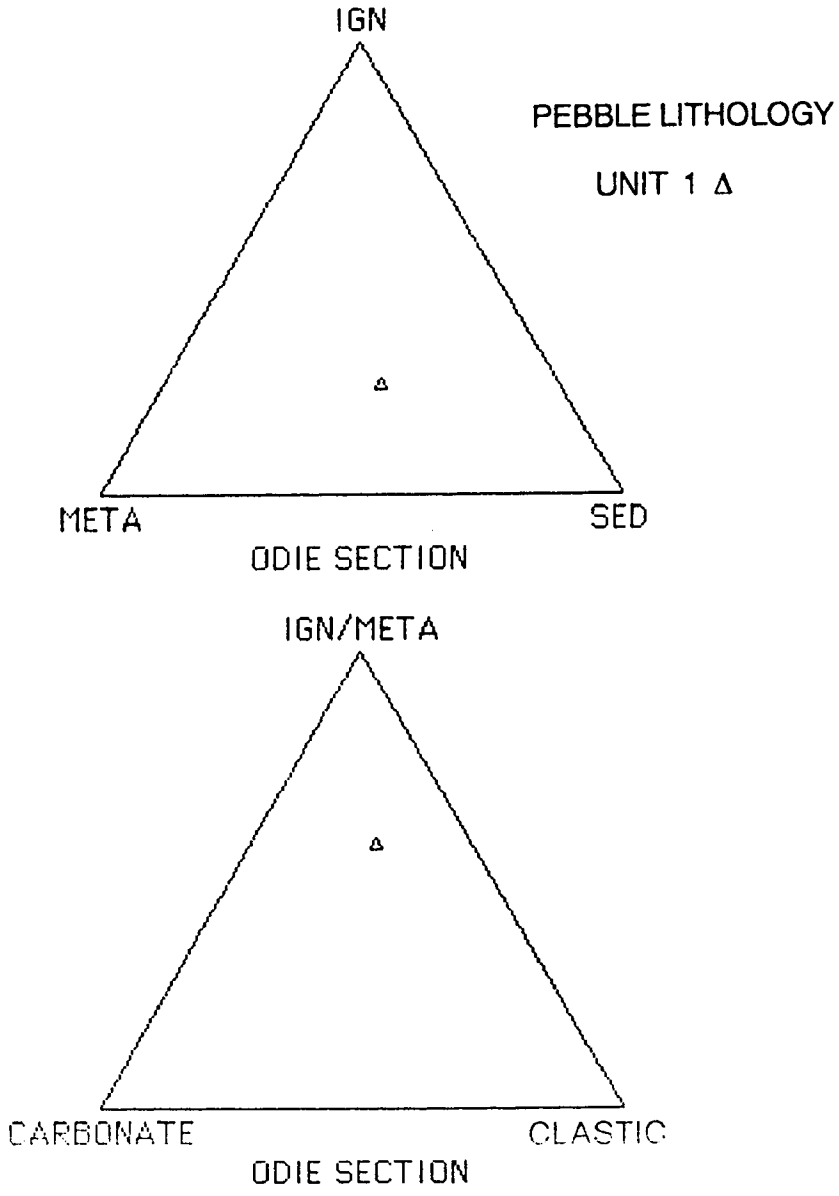

Pebble lithology for Unit 1 at the Odie Section.

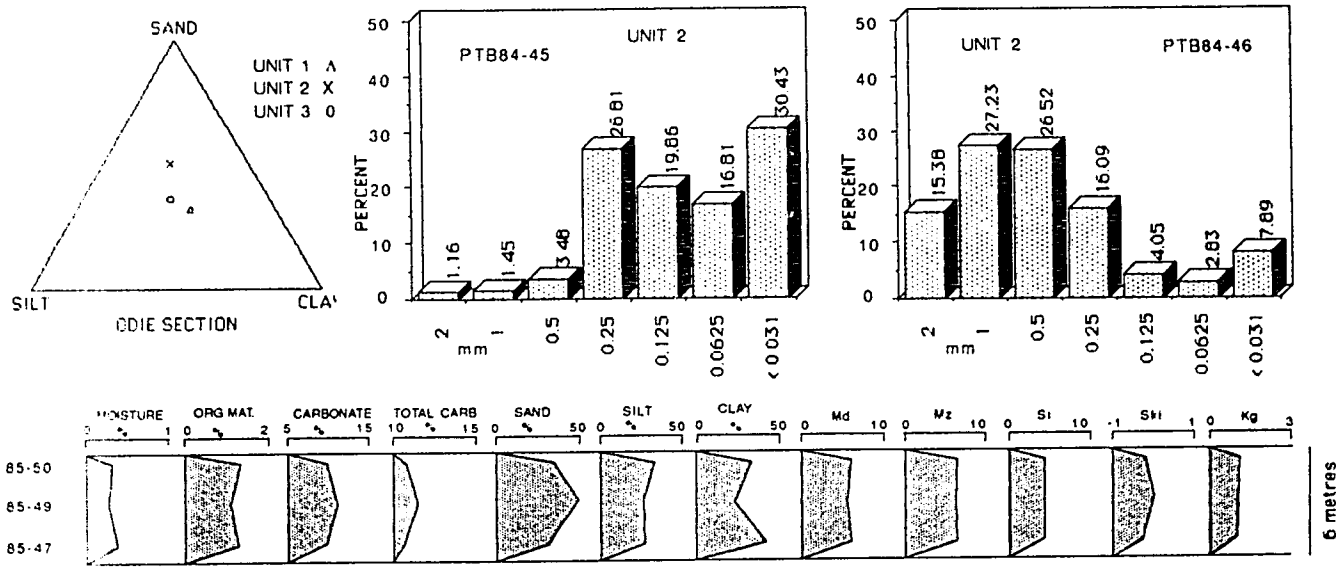

Textural and compositional variation for various samples from Section Odie. See text for explanation and key to samples.

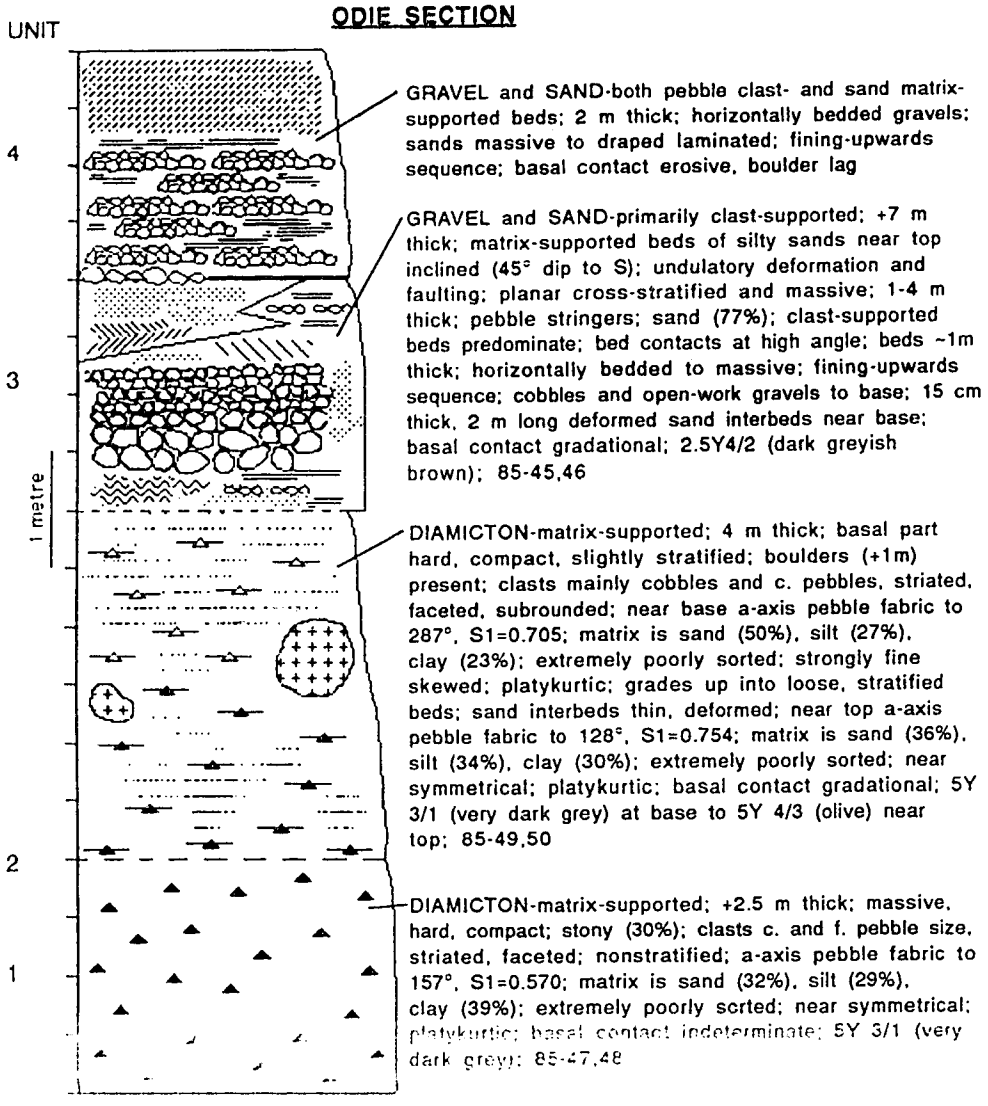

Composite stratigraphic column of the ODIE Section. Lithostratigraphic units along left and unit descriptions along right.

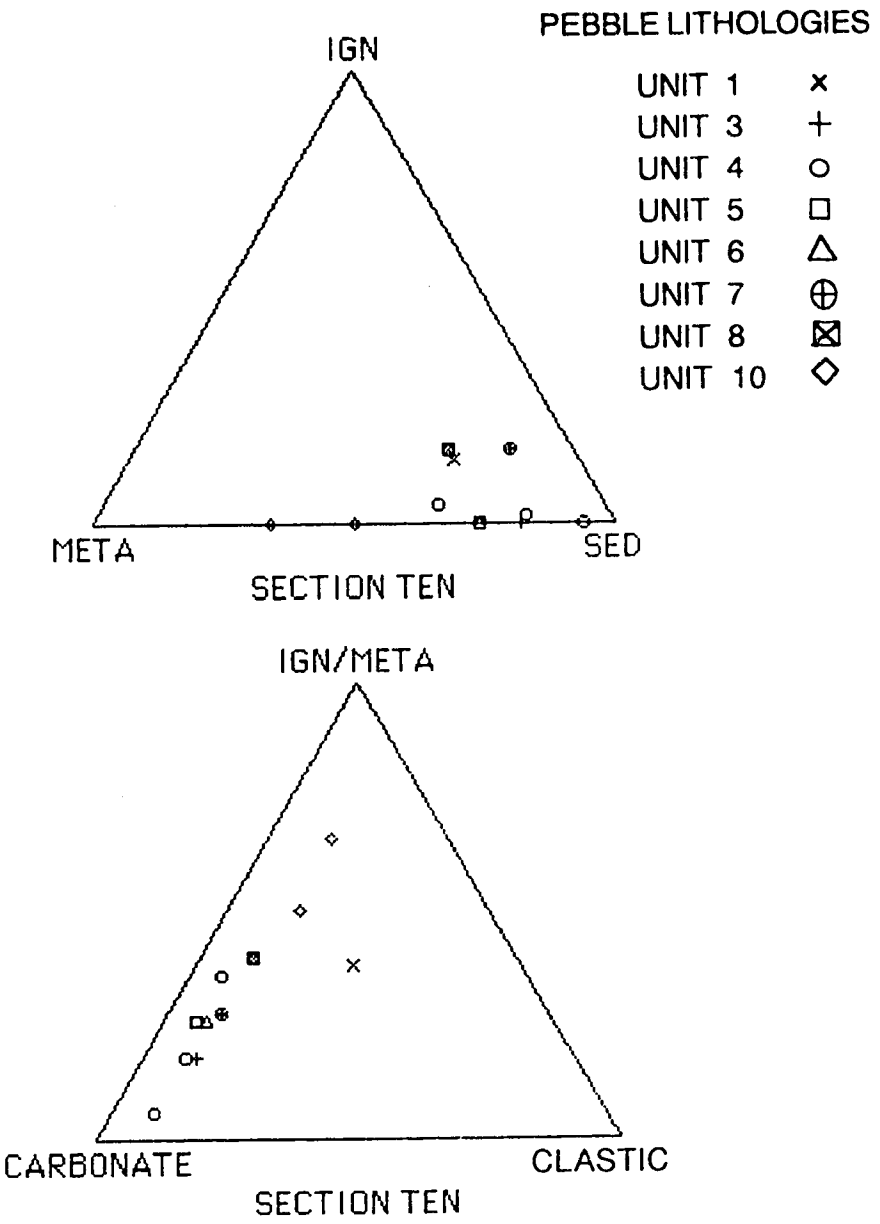

Ternary diagrams comparing pebble lithologies for eight lithostratigraphic units at Section Ten.

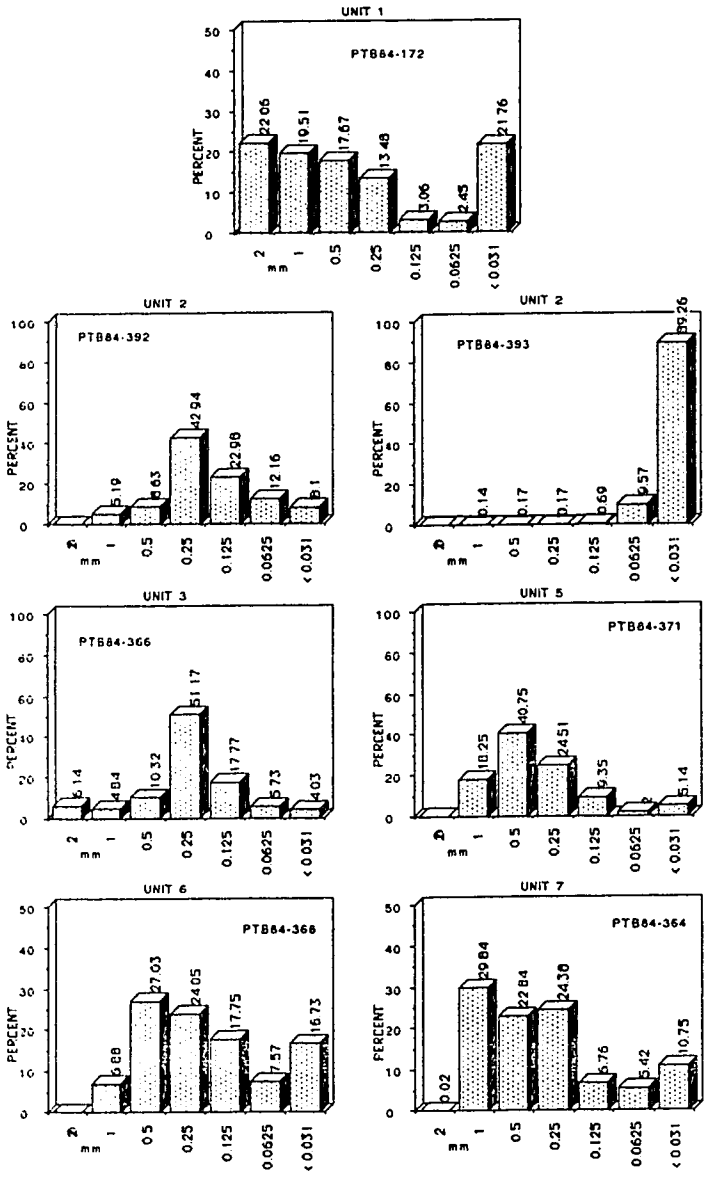

Textural histograms from various units at Section Ten. Diagrams illustrate variation in nondiamicton samples. See text for explanation and key to samples.

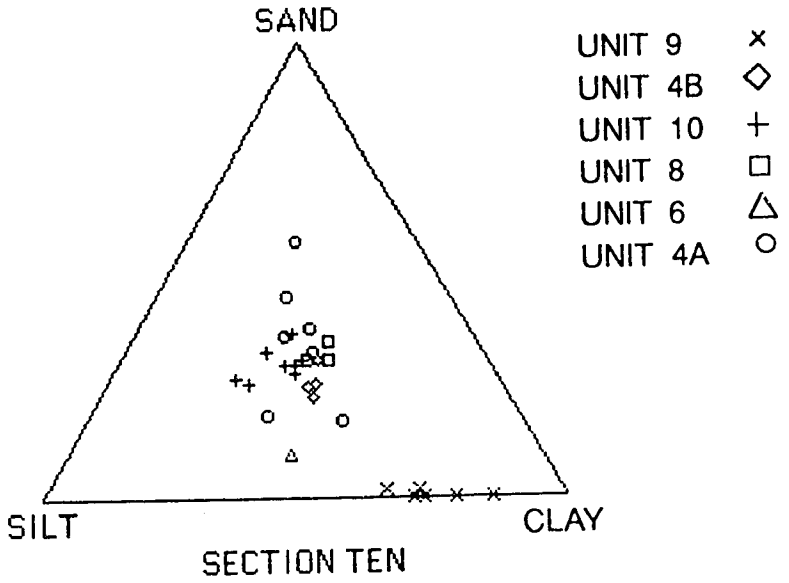

Ternary diagram comparing textural variation in diamicton samples from six units (including two sample locations for Unit 4) at Section Ten.

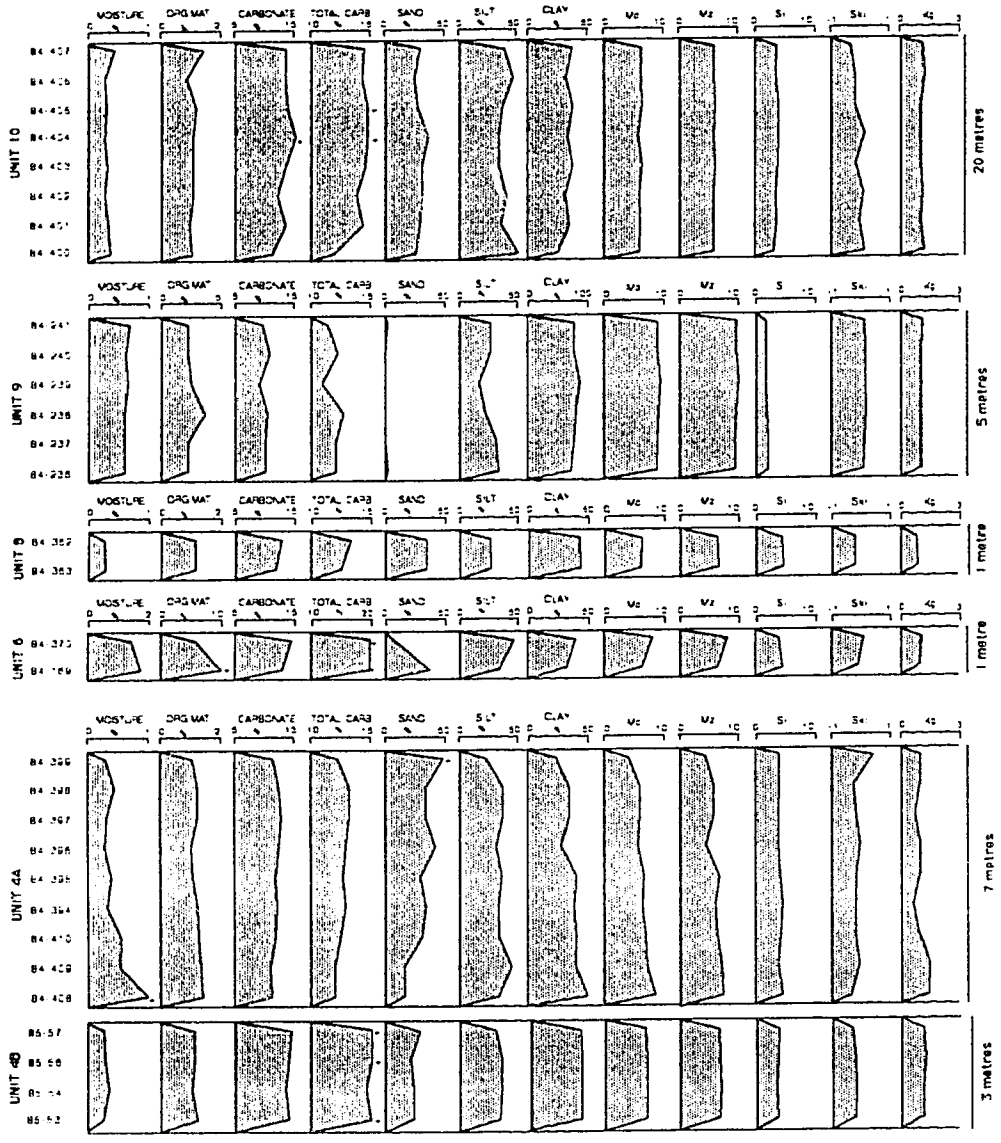

Compositional variation with depth for Units 4, 6, 8, 9, and10, Section Ten. Note changing scales.

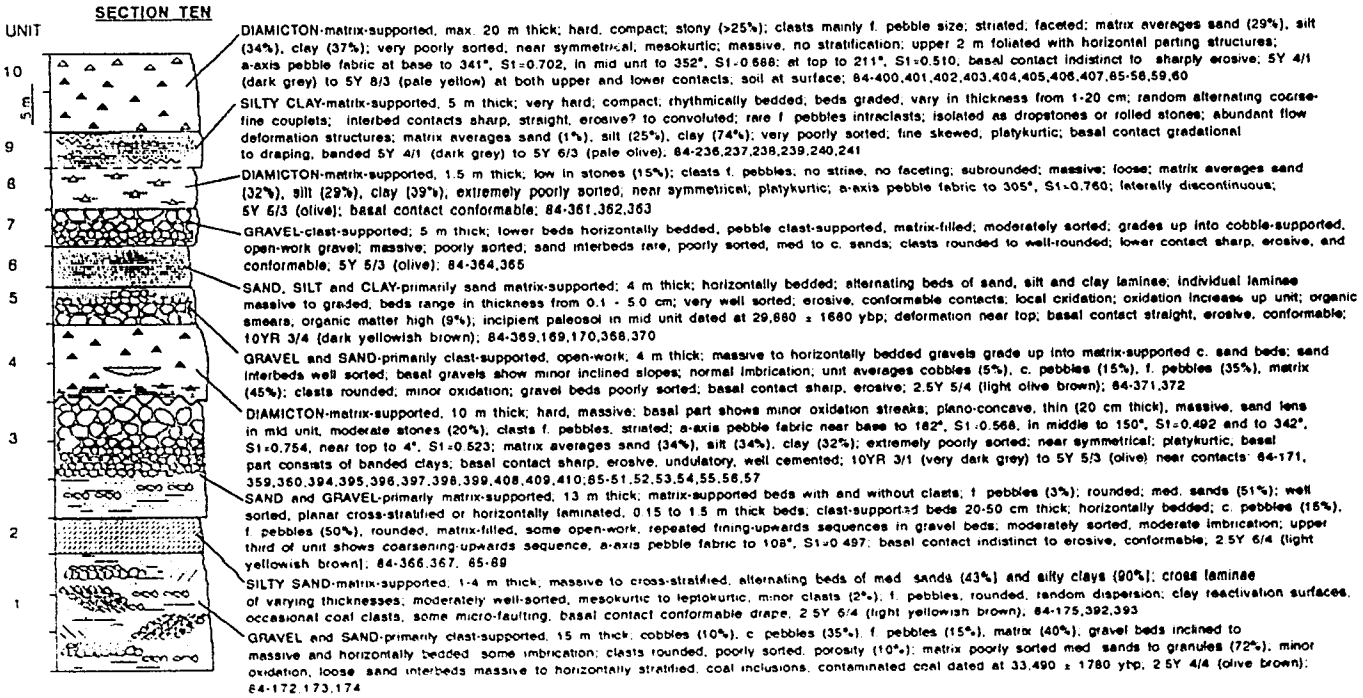

Composite stratigraphic column of Section Ten, lithostratigraphic units along left and unit descriptions along right.

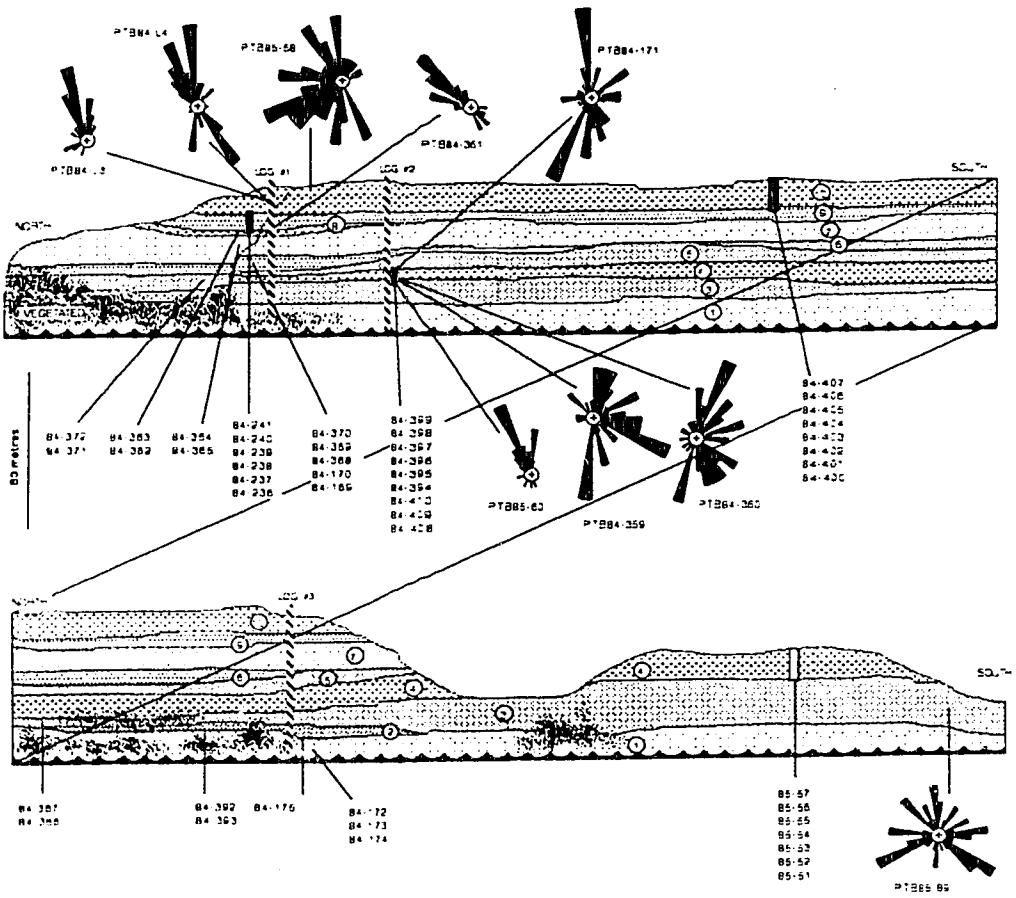

Section drawing of primary face of Section Ten. Lithostratigraphic units, sample locations and pebble fabrics illustrated.

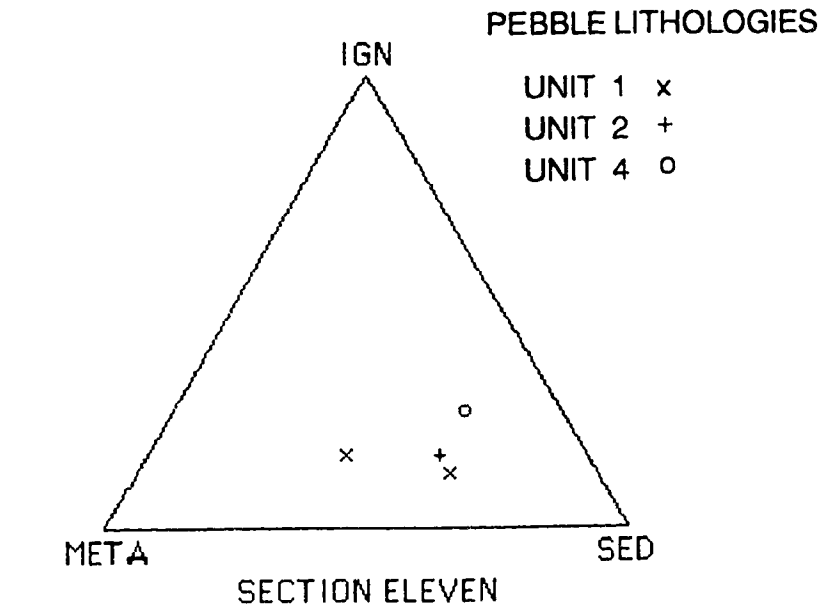

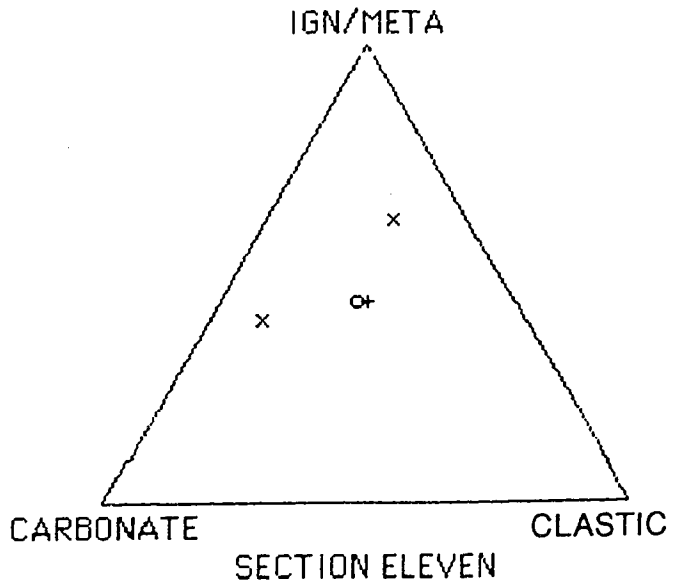

Ternary diagrams comparing pebble lithologies for three units at Section Eleven.

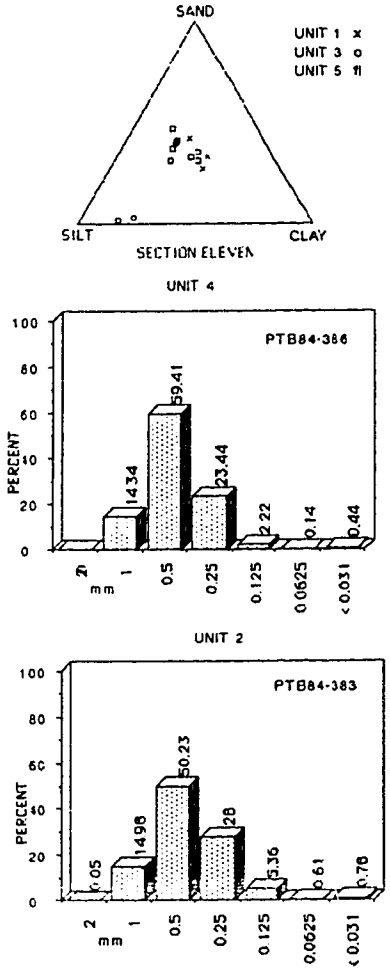

Textural diagrams for various units at Section Eleven; both diamicton and nondiamicton samples. See text for explanation and key to samples.

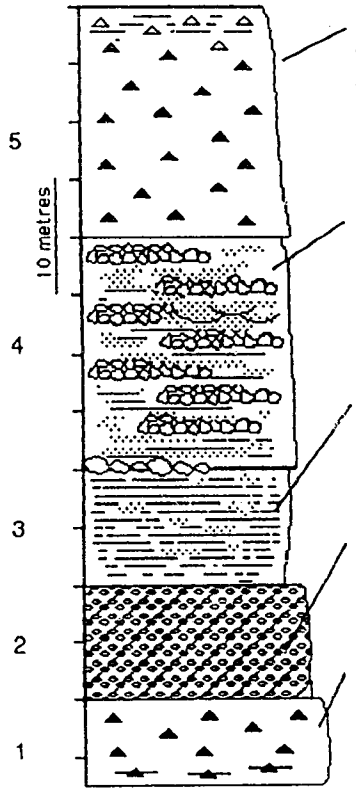

DIAMICTON-matrix-supported; 25 m thick; massive to slightly foliated in top 2 m; moderate stoniness(25%); clasts primarly small pebble sized, minor striae, subangular to subrounded; matrix averages sand (37%), silt (37%), clay (26%); very poorly sorted; near symmetrical; mesokurtic; large plano-concave gravel lens, 3 m thick, 11 m long near top of unit; basal contact indeterminate, color from 5Y 3/1 (very dark grey) to 2.5Y 4/4 (olive brown) at top; 85-71,72,73,74,75,76,77,78

GRAVEL and SAND-primarily clast-supported; 25 m thick; horizontally bedded gravels, minor large scale trough cross-beds; moderate to good imbrication; moderate to poorly sorted; minor oxidation; cobbles (5%), c. pebbles (20%), f. pebbles (35%), matrix (40%); sand interbeds mainly c. sand (60%); leptokurtic; well sorted; horizontal to planar tabular cross-stratification; basal contact boulder lag to sharp, erosive; 10YR 5/2 (greyish brown); 84-386,387

SILT-matrix-supported; 10 m thick; horizontally bedded; graded beds 1-3 cm thick; minor isolated clasts (5%), small pebble sized; matrix averages sand (2%), silt (79%), clay (19%); strongly fine skewed; poorly sorted; very leptokurtic; basal contact indeterminate; 5Y 2.5/2 (black); 84-390,391

GRAVEL-clast-supported; 9 m thick; steeply inclined planar cross-bed slopes; moderately to poorly sorted; oxidized; boulders (2%), cobbles (10%), c. pebbles (30%), f. pebbles (30%), matrix (28%); clasts rounded; matrix consists of c. sands (50%); matrix poorly sorted; loose; basal contact erosive and unconformable; 84-383,384,385

DIAMICTON-matrix-supported; + 3 m thick; upper half massive, low stone content (20%); basal 1 m thickly banded, few clasts (5%); all clasts small pebble sized; subangular; minor striated; matrix averages sand (34%), silt (31%), clay (35%); extremely poorly sorted; fine skewed; platykurtic; graded beds at base 3-10 cm thick; sharp interbed contacts, conformable, erosional; a-axis pebble fabric 1.5 m above base to 23°, S1=0.556 and 193°, S1=0.575; color 5Y 3/1 (very dark grey); 84-382, 388, 389; 85-79, 80, 90

Composite stratigraphic column of Section Eleven, lithostratigraphic units along left, and unit descriptions along right.

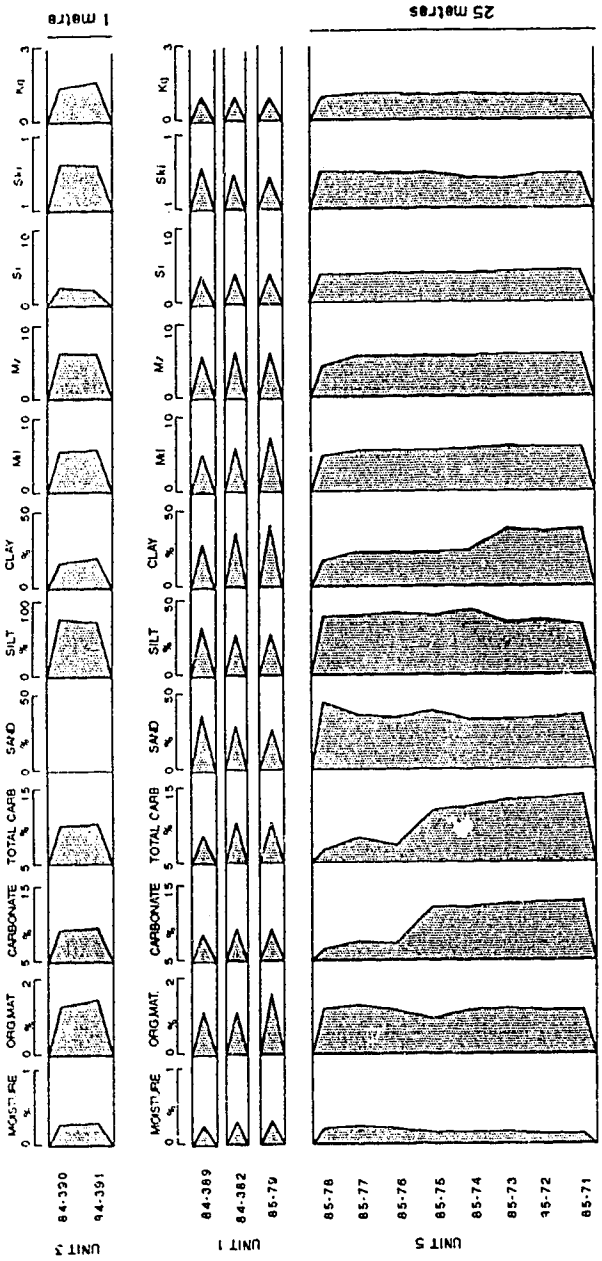

Compositional variation with depth for Units 1, 3, and 5, Section Eleven.

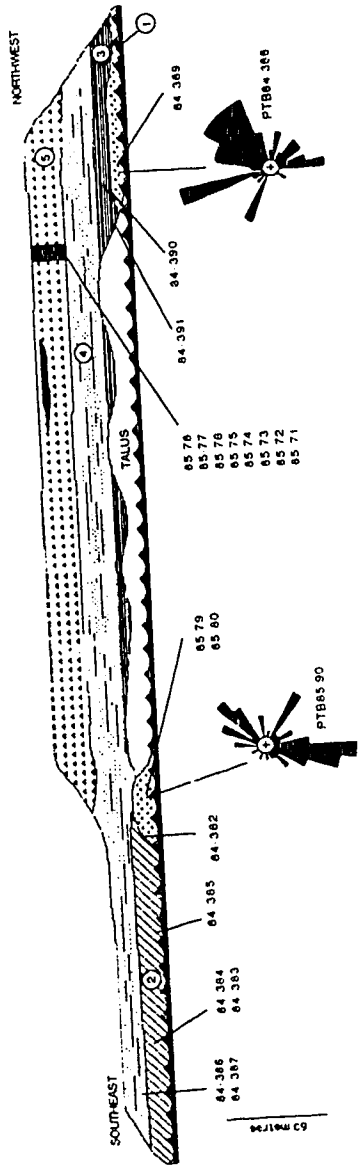

Section drawing of primary bluff face of Section Eleven. Lithostratigraphic units, sample locations and pebbles fabrics illustrated.

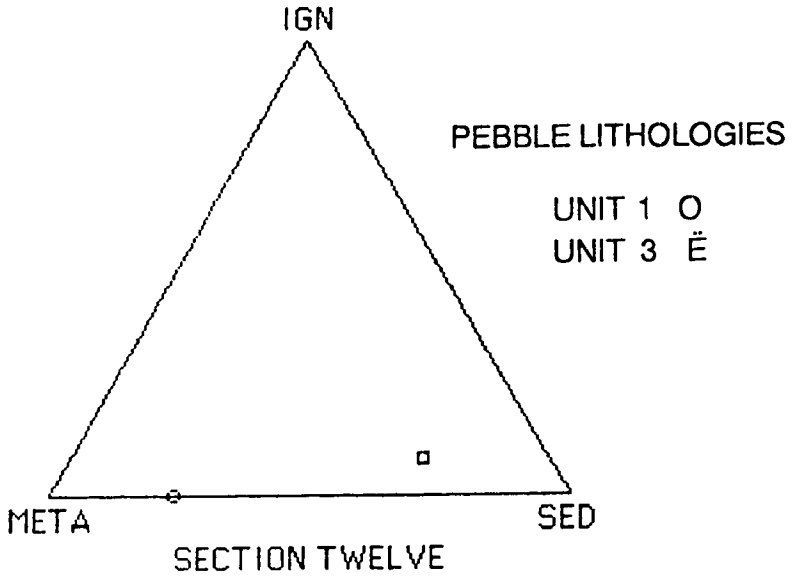

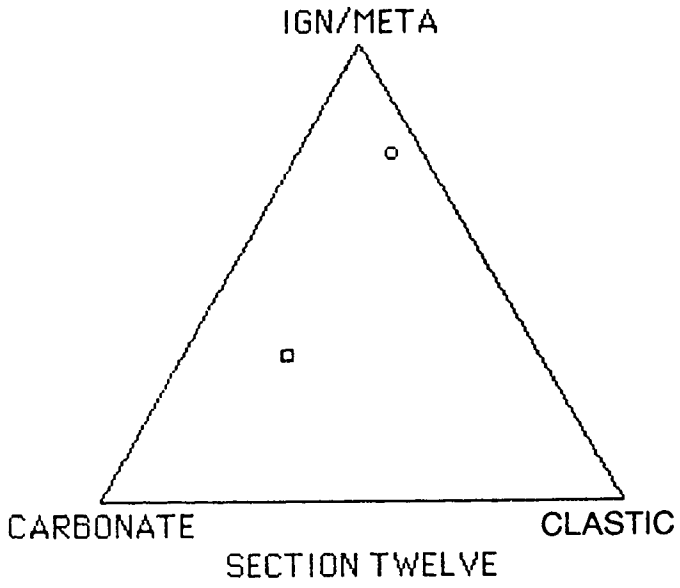

Ternary diagrams comparing pebble lithologies for two units at Section Twelve.

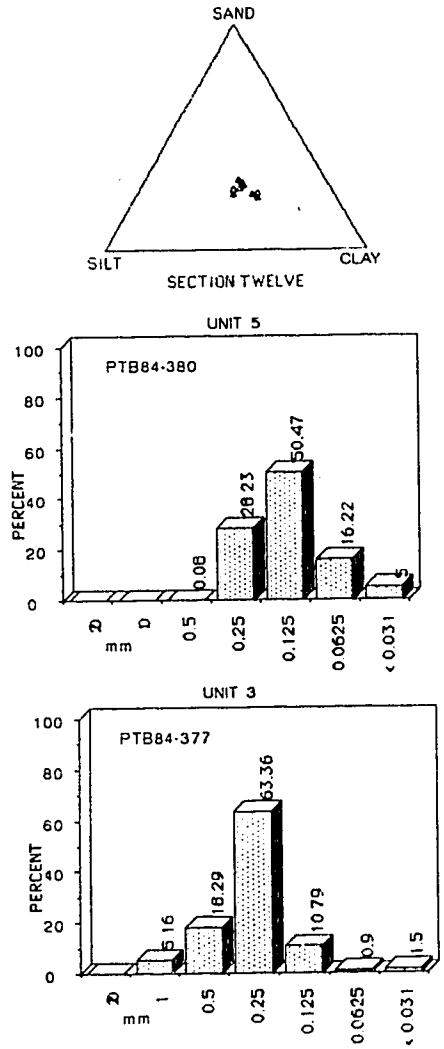

Textural diagrams illustrating variation in both nondiamicton and diamicton samples from Section Twelve. See text for explanation and key to samples.

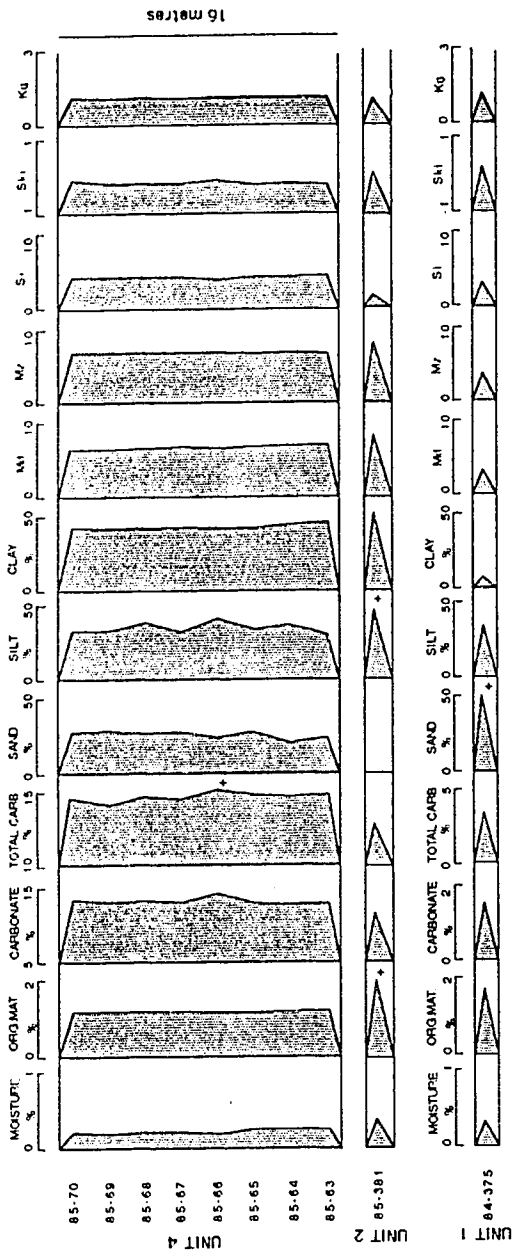

Compositional variation with depth for Units 1, 2, and 4, Section Twelve. Note changing scales.

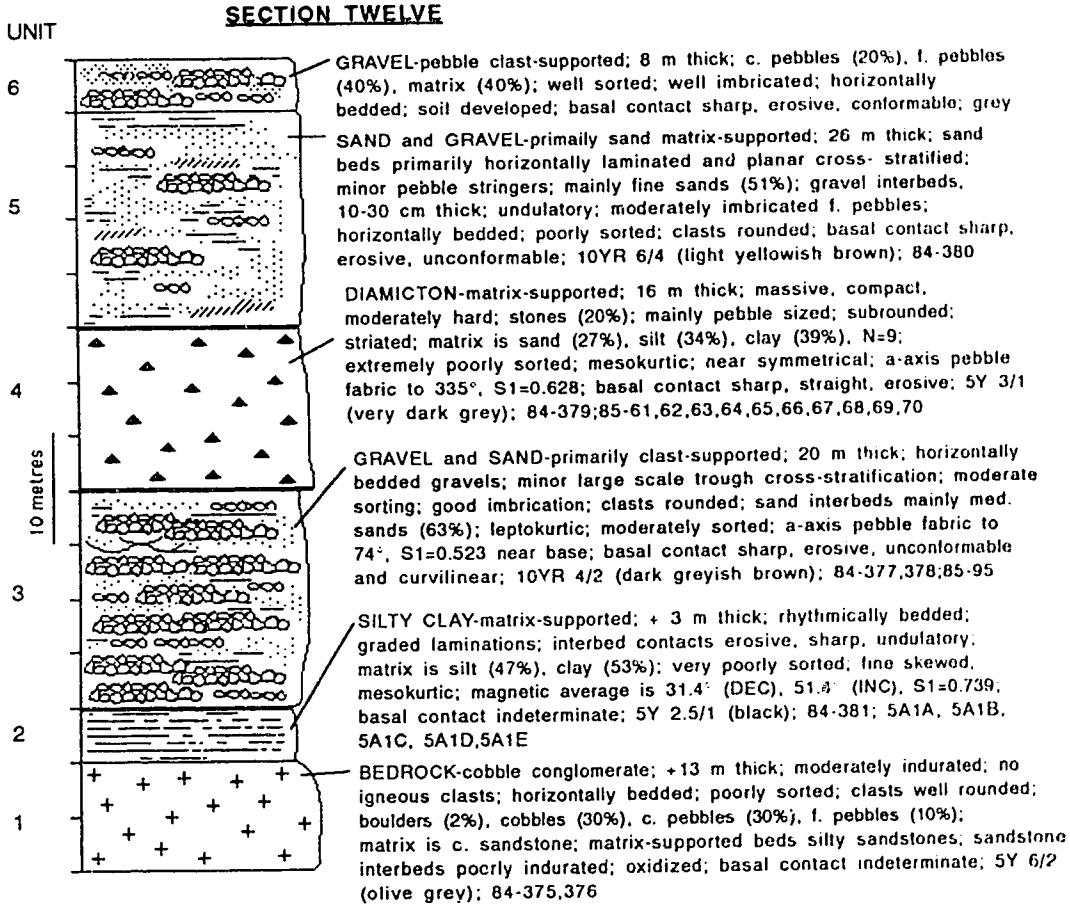

Composite stratigraphic column of Section Twelve; lithostratigraphic units along left, and unit descriptions along right.

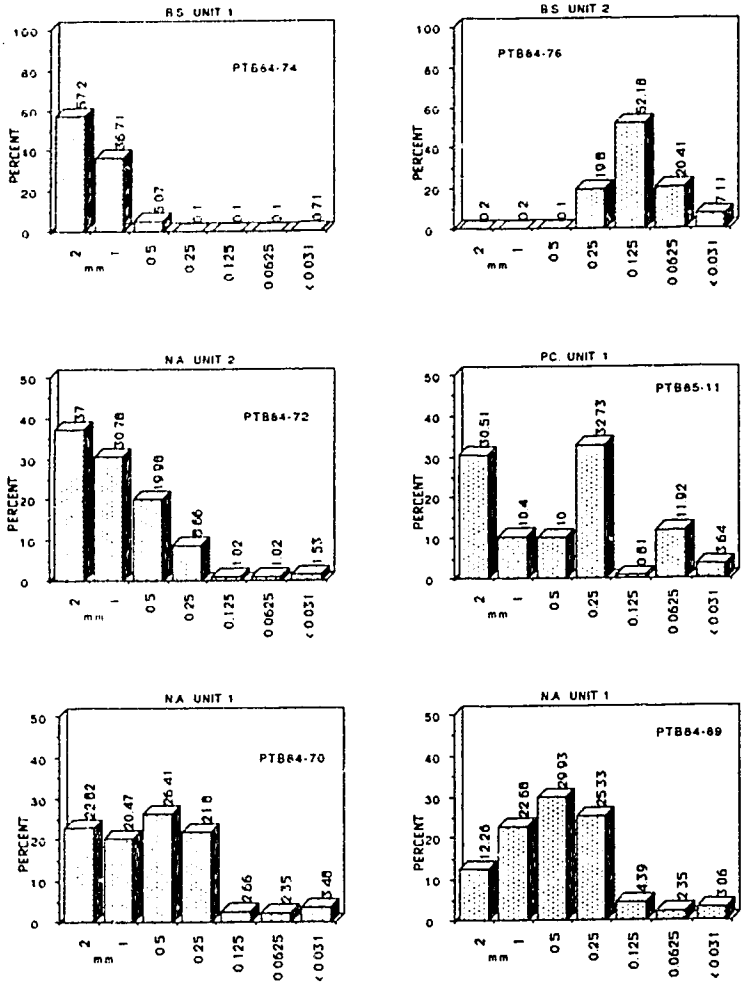

Textural histograms for several units from three sections (PC, NA, and BS). See text for explanation and key to section and sample numbers.

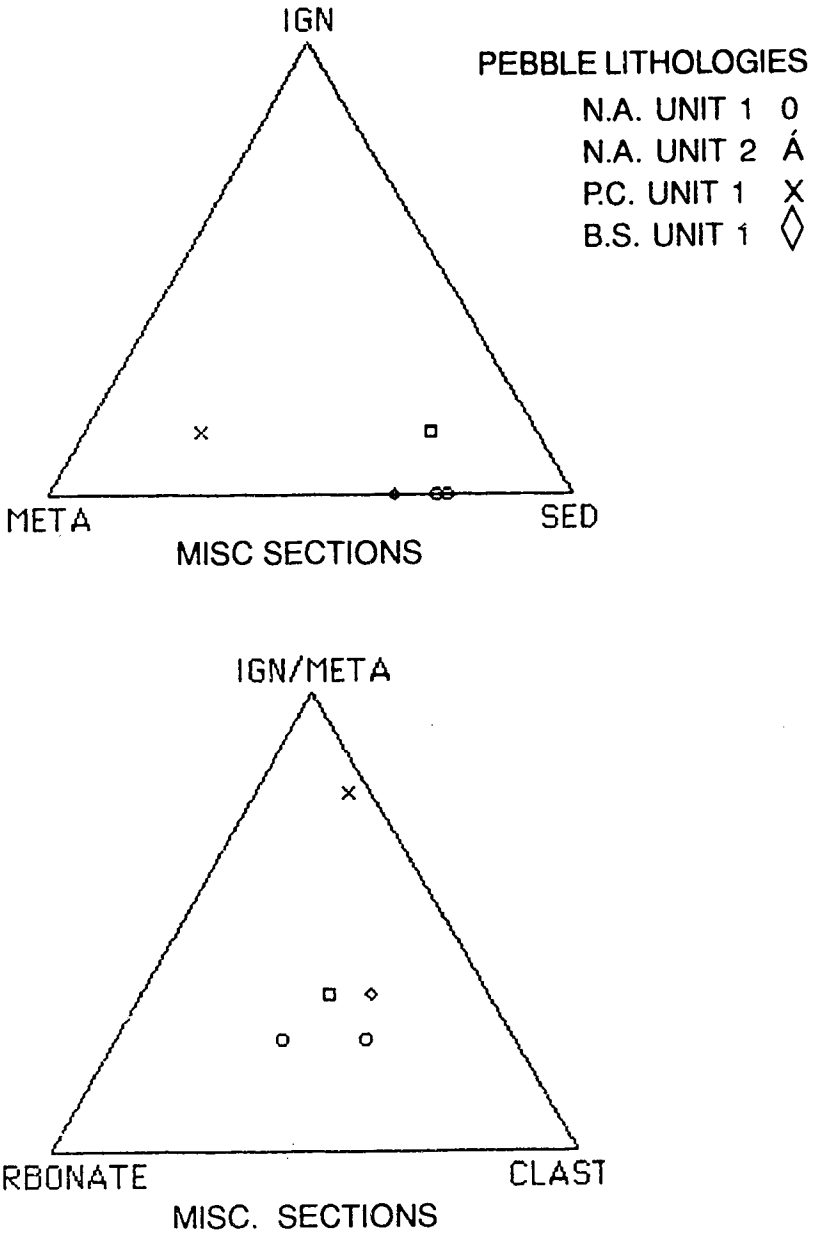

Ternary diagram comparing pebble lithologies for several units at the North Air, Paul Creek, and Bad Smell Section.

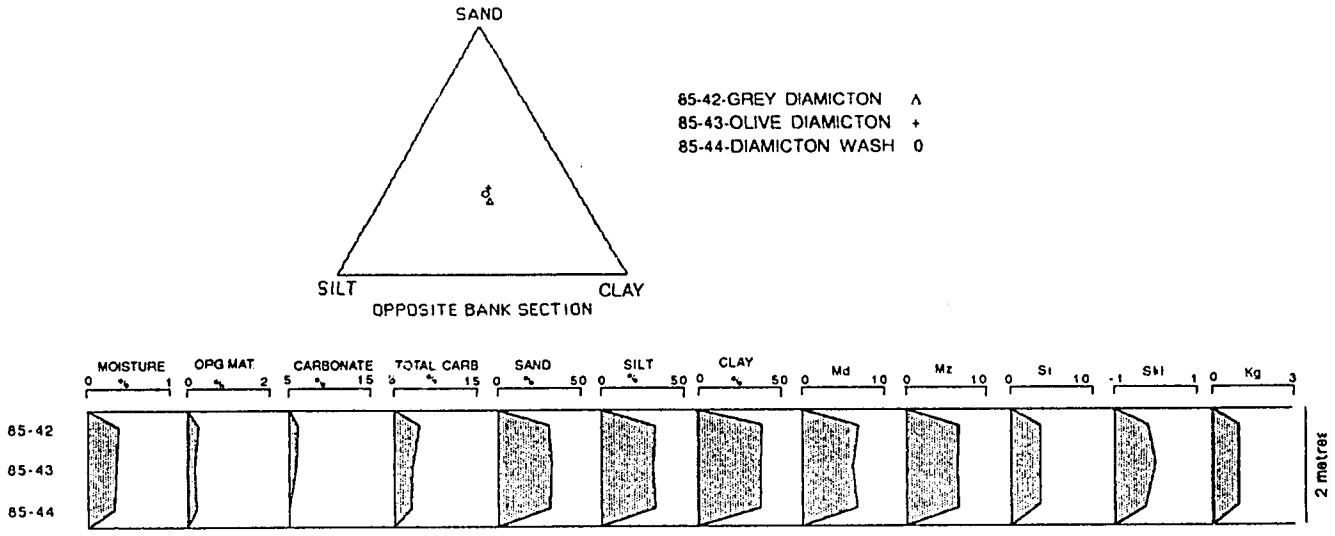

Compositional variation in three bulk samples of the same diamicton at the Opposite Bank Section.

Appendix 17. Laboratory methodology used in amino acid racemization analysis of wood samples at the University of Alberta, Amino Acid Laboratory, Department of Geology.

AMINO ACID RACEMIZATION METHODOLOGY

1. Wear disposable rubber gloves when handling all materials to avoid transfer of amino acids from hands onto samples. Label appropriate number of vials and caps with sample numbers.

2. Soak small beakers in chromic acid for 3 hours. Wash/rinse beakers with doubly distilled water 20 times. Also rinse small ceramic 4.25 cm Buchner funnels twice with HCl and 10 times with doubly distilled water.

3. Scrub wood samples with small brush and rinse with distilled water to remove adhered sediment.

4. Fill beaker with distilled water, place wood sample in beaker and sonicate for 3 minutes. Pour off water and repeat wash process 3 or 4 times.

5. Clean IKA automatic mill with HCl and rinse with distilled water. Remove wood sample from beaker and grind in mill until material is fine enough to pass through a 20 mesh sieve. Attach Buchner funnel to vacuum flask and place glass filters into Buchner funnels. Form fit filters with distilled water.

6. Place sample in clean, dry beaker and fill with 2N HCl to cover sample. Sonicate for 3 minutes. Pour sample liquid into funnel and rinse sample from beaker with 250-400 ml of distilled water pouring all liquid into funnel.

7. Remove filter paper and scrape wood sample from paper into a labelled snap top vial. Cover vial with tissue paper (Kim-wipe) and secure with elastic band. Allow sample to dry overnight before proceeding with hydrolization.

8. Clean culture test tubes with chromic acid. Weigh out 100-250 mg of sample and place into test tubes. Fill test tubes roughly two thirds full with 5.5N HCl. Line inside of test tube screw caps with teflon and screw tightly onto test tubes.

9. Preheat heating block to 108° C, place samples into heating block and leave in oven for 24 hours. Cool samples.

10. To separate the acid from the sample, first tape a wide mouth glass vial to the end of the Buchner funnel and pour sample into funnel. Alternatively, one can centrifuge the samples, decant the liquid and place sample into a clean culture tube.

11. Concentrate sample liquid by centrifuging with vacuum attachment or using a biodryer. Stop concentration process when sample is 0.5 ml or less. Proceed with desalting. Remove inorganic salts from sample liquid by ion exchange chromatography.

12. Obtain Dowex AG 50W-X8, 50-100 mesh resin and rinse three times in a beaker with distilled water. Prepare the ion exchange columns by filling the end of column with 1 cm of clean glass wool. Put stem in place and dampen wool with distilled water.

13. Using a felt pen, mark off points 7 and 14 and 21 cm from top of the glass wool. Make a slurry of the resin and distilled water and transfer slurry into column, covering glass wool up to the 7 cm mark.

14. Regenerate the resin samples by passing through 4 bed volumes of 2N NaOH. Rinse with 8 bed volumes of distilled water. Rinse with 4 bed volumes of 2N HCl and rinse with another 8 bed volumes of distilled water. Drain distilled water down to the top of the resin. Column is now ready for sample purification.

15. Dissolve the sample in 1 ml of distilled water and apply it very carefully to the top of the resin with a pipette. Drain the sample into the resin bed and wait for 15 seconds. Without disturbing the resin, filter column again with distilled water and rinse the sample through with 2 bed volumes of distilled water. Drain water down to the surface of the resin.

16. Very carefully fill the column with 1.5 bed volumes of 3M NH_4OH (ammonium hydroxide). Immediately begin draining the NH_4OH by dripping it slowly. Notice a front will appear in the resin producing heat. Follow this front down with fingers until approximately 2 cm above the glass wool. At this point place a clean culture tube under the column tip and collect the remaining NH_4OH. If the column does not feel cool at end of draining process, add a bit more NH_4OH and collect this amount as well into the culture tube. Dry the ammonium solution completely in the biodryer, then proceed with esterification.

17. To convert the non-volatile amino acids into volatile derivatives, add 0.1 ml (or 15 drops with a Pasteur disposable pipette) of anhydrous acidic alcohol reagent (isopropanol acidified to 3.5M with HCl) with a micro-pipette and dissolve completely in the sonicator. Heat mixture for 15 minutes at 100° C in a silicone oil bath. Place tube into biodryer and evaporate the excess alcohol completely. Proceed with acylation.

18. Acylate resulting amino acid esters in the fume hood by adding 0.1 ml (or 5 drops with a Pasteur disposable pipette) of pentafluoropropionic anhydride (PFPA) with a micro-pipette . NOTE: this solution must be stored in freezer, it is extremely volatile, so work quickly. Add approximately 0.3 ml of dichloromethylene to sample, mix well in sonicator for at least 10 minutes. Heat solution again in the silicone oil bath for 5 minutes at 100° C. Cool samples.

19. Remove the excess PFPA (PFPA can damage the GC column). Place the closed tubes into a small dewer flask which contains acetone and dry ice. Freeze the samples until they appear white on the outside. Freezing can also be accomplished with liquid nitrogen.

20. Evaporate the samples in a Buchi rotary evaporator until the sample is slightly damp at bottom. Add 1 ml of dichloromethylene and repeat the process. NOTE: do not allow the sample to completely dry during evaporation or all volatile amino acids will be lost.

21. Add 1 ml of dichloromethylene and mix well in the sonicator. Next add 10-30 grains of anhydrous potassium carbonate to the solution and leave sample at room temperature overnight.
NOTE: if samples are to be stored for any length of time, samples must be stored with anhydrous potassium carbonate in bottom of tube.

22. Filter sample into a clean autoinjector vial through a 0.2 micron filter which is compatible with methylene chloride. Proceed with Gas Chromatography (GC).

23. Separate the amino acids by injecting 1 microlitre of the sample into a Chirasil-val glass capillary column. If the sample is too weak or strong, alter the injection amount appropriately. Detect amino acid concentrations with a flame ionization detector. For each sample perform injection 3 times for 3 trial readings. Adjust the ratios against a standard solution which has been run through the GC on the same day.

Appendix 18. Laboratory methodology used in pollen processing at the University of Alberta, Paleoenvironmental Laboratory, Department of Anthropology.

POLLEN PROCESSING METHODOLOGY

1. Obtain 4-250 ml, clean, dry beakers. Weigh beakers and record weights.

2. Add approximately 25 ml of sample, less if highly organic.

3. Weigh beakers containing sediment and record.

4. Add 2 Lycopodium tablets to sample and record batch number.

5. Carefully add concentrated HCl to samples in small amounts to dissolve calcium carbonates. Where concentrations are high, the reaction may be violent- Use Caution. Continue adding, while stirring, up to 75 ml or to cover sample. Let sit for one hour or until reaction ceases. Add distilled water to 150 ml line. Samples may be left overnight at this point.

6. Find 16 clean Nalgene test tubes and label 4 tubes per sample.

7. Starting with Sample #1, stir vigorously with stirring rod for 60 seconds. Let settle for exactly 20 seconds and carefully but quickly pour liquid into the four tubes, leaving the thick sediment in the bottom of the beaker. Balance tubes and centrifuge for 3 minutes at 3/4 speed. After centrifuging combine the sediment from the bottom of all 4 tubes into one. Repeat for the remaining samples. Balance the 4 tubes, centrifuge and proceed with Heavy Liquid procedures.

8. Heavy Liquid Procedure. Pour clean heavy liquid ($ZnBr_2$) into a 100 ml graduated cylinder. Check specific gravity with hydrometer. It should be between 1.97 and 2.025. If too dense (>2.025) add a bit of distilled water and recheck. If reading is less than 1.95 boil to reduce volume, cool and measure again with hydrometer.

9. Distribute liquid between tubes containing sediment samples in volume at least equal to the amount of sediment. Balance the tubes and mix contents thoroughly with stirring rod. Cap the tubes and shake vigorously for 15 seconds holding tube firmly between thumb and baby finger. Slowly release thumb to check for release of pressure then continue to shake for another 45 seconds. Grip the tube tightly and gently ease off the caps with thumbs. Centrifuge samples for 20 minutes at 3/4 speed.

10. Obtain 4 small size white Buchner funnel tops and place glass filter papers, slightly larger in diameter, inside by pressing gently and evenly.

11. Clamp large sidearm flask to retort stand and connect with vacuum tube in fume hood. Use black suction ring between flask and tunnel bottom. Place funnel top with filter on funnel bottom and turn vacuum on. Pour supernatant slowly into filter, leaving heavy sediment in the bottom of tube. Sometimes supernatant will be very thick and filter very slowly. It is sometimes necessary to use more than one filter per sample if the filter paper gets clogged.

12. Carefully remove filter paper containing sample from funnel and place in clean Nalgene tube.

13. Add HF, using extreme caution. Samples may sit overnight if desired. Continue with HF procedure as explained in point 15.

14. Pour used heavy liquid into "used" bottle. This can be cleaned by filtering twice through 2 glass filters under vacuum and then place in "clean" bottle.

15. After "Heavy Liquid Procedure" add up to 25 ml of hydrofluoric acid (HF) to remove silicates. (USE EXTREME CAUTION! WEAR MASK, APRON AND GLOVES IN FUME HOOD!) Stir carefully with clean wooden stick being careful not to touch anything with the HF and to clean any drops which may spill. Dispose of stirring sticks in appropriate garbage can.

16. Leave samples overnight and/or heat in boiling water bath (hot plate setting at 6) for at least 1 hour. Stir occasionally. Centrifuge, decant.

17. The sediment may have greyish or whitish appearance due to colloids from the breakdown of the silica and it is important to get rid of this colloid. Add up to 25 ml of concentrated HCl, stir and place in hot water bath (setting at 4) for 5 minutes. Do not stir while heating or HCl will "pop". Centrifuge, decant. Repeat this process until sediment no longer appears greyish but should appear dark in colour and should no longer seem sticky.

18. At this point if sample contains large particles, wash through fine screen mech with distilled water. If sample is very rich in humates, these can be dissolved by boiling in 10% NaOH for 5 minutes, centrifuge decant and repeat this until supernatant is straw colored.

19. Wash sample in water, centrifuge, decant and proceed with "Acetolysis" which follows.

20. Samples at this stage should be in centrifuge tubes and should have been rinsed with distilled water.

21. Rinse pollen in glacial acetic acid, centrifuge.

22. Prepare acetolysis mixture by adding 1 part concentrated H_2SO_4 (sulfuric acid) into 9 parts acetic anhydride under a fume hood. Use caution as this mixture is corrosive. Add mixture to the samples and heat in a boiling water bath for approximately 5 minutes. Centrifuge and decant acetolysis mixture into a disposal container (this mixture reacts violently on contact with water).

23. Rinse with glacial acetic acid, centrifuge.

24. Rinse with distilled water.

25. Dehydrate samples by rinsing with 95% ethanol and undiluted tertiary butyl alcohol, centrifuging between each solvent.

26. Add a small amount of TBA to suspend the sample and transfer to a glass vial or to an Eppendorf micro-centrifuge tube, depending upon the amount of sample. Add a few drops of silicone oil to cover pollen and place, uncovered, in a drawer or cupboard overnight to allow the TBA to evaporate.

27. Mix pollen well with a toothpick and mount on glass slides.